This electronic thesis or dissertation has been downloaded from the King's Research Portal at https://kclpure.kcl.ac.uk/portal/

Characterisation of the impact of systemic insulin resistance and its reversal on human brain responses to meal ingestion and food cues: a functional magnetic resonance imaging study.

Cheah, Yee Seun

Awarding institution:
King's College London

The copyright of this thesis rests with the author and no quotation from it or information derived from it may be published without proper acknowledgement.

END USER LICENCE AGREEMENT

Unless another licence is stated on the immediately following page this work is licensed

under a Creative Commons Attribution-NonCommercial-NoDerivatives 4.0 International

licence. https://creativecommons.org/licenses/by-nc-nd/4.0/

You are free to copy, distribute and transmit the work

Under the following conditions:

- Attribution: You must attribute the work in the manner specified by the author (but not in any way that suggests that they endorse you or your use of the work).
- Non Commercial: You may not use this work for commercial purposes.
- No Derivative Works - You may not alter, transform, or build upon this work.

Any of these conditions can be waived if you receive permission from the author. Your fair dealings and other rights are in no way affected by the above.

Take down policy

If you believe that this document breaches copyright please contact librarypure@kcl.ac.uk providing details, and we will remove access to the work immediately and investigate your claim.

Download date: 09. Jan. 2025

Characterisation of the impact of systemic insulin resistance and its reversal on human brain responses to meal ingestion and food cues: a functional magnetic resonance imaging study.

Yee Seun Cheah

Diabetes Research Group
Diabetes and Nutritional Sciences
King's College London

Thesis for the degree of Doctor of Philosophy in
Diabetes, Endocrinology and Metabolism,
King's College London 2017

Acknowledgements

I first would like to express my thanks to my supervisors, Prof. Stephanie Amiel and Dr. Fernando Zelaya. I recall the very moment, soon after Prof. Amiel had examined me during my MSc viva, as we were walking up the stairs of the Golden Jubilee Wing at King's College Hospital to commence a ward round, that she suggested I see her about doing a little research project. Little did I know that the neuroimaging data I had discussed earlier would be something in which I could get first-hand experience. I thank Prof. Amiel for sparking off my interest in diabetes research, and for providing me with the opportunity to escape temporarily from the world of clinical medicine to one of academia. I thank Dr. Zelaya for making the daunting task of MRI physics, neuroimaging and statistics a little easier to digest and comprehend, whilst challenging me as I developed my skills and abilities in neuroimaging. I thank both of you for the many intellectual discussions, and for the endless encouragement, support and guidance you have provided me during this journey.

I am indebted to Dr. Sarah Lee for her patience in showing me the ropes of neuroimaging analysis, and the countless trips to the Proms! I also thank my colleague and PET-imaging partner in crime, Dr. Katharine Hunt, for the 4 years that we shared the fellows' office and the joys (and occasional pain) of neuroimaging. I thank both of you for your friendship and support.

I am grateful to Prof. Mick Brammer and Dr. Laurence Reed for their assistance in the early developmental stages of this project, and for their statistical and neurocognitive advice. I am also grateful to Tracy Dew for analysis of the hormones.

My predecessor, Dr. Yashica Nathan, and my successor, Dr. Munachiso Nwokolo, thank you for your friendship and encouragement, and for helping me come to terms with the fact that research is not a sprint but a long distance run. I am also obliged to Dr. Pratik Choudhary for his mentorship.

To the diabetes research team, I extend my gratitude to research nurses, Bula Wilson who kindly dedicated so much of her time in these MRI studies, even on her birthday,

and to Andrew Pernet, for his assistance and technical advice. I also thank Sophia Coker for her administrative support.

Diabetes specialist dietitians, Lucy Diamond, Anita Beckwith, Victoria Francis and Christopher Cheyette, and Clinical Trials Pharmacist Joanna Flanagan, without whom I would not have been able to treat the volunteers in this study.

Dr. Tyrell Evans and Paxton Green Group Practice, for all your help with volunteer recruitment and for the chance to practice diabetic medicine in the community.

I am grateful to all the radiographers at the Centre for Neuroimaging Studies for your patience, and for putting up with my "mixed meals".

I thank all the volunteers for their interest and participation, the NIHR Biomedical Research Centre at Guy's and St. Thomas' and King's College London and Diabetes UK for awarding me clinical training fellowships and King's College Hospital Charity for funding these projects, all without whom this research would not have been possible.

Lastly, I thank my mother, father, Elaine and Anthony for their unreserved understanding, endless support and for being there always, and to the new additions, Emma and Zoey, who joined in during my time in research, thank you for all the laughter.

Abstract

Altered corticolimbic regulation of appetite is implicated in the aetiology of obesity and type 2 diabetes, conditions more prevalent with age and associated with insulin resistance. This thesis characterises the impact of ageing, systemic insulin resistance before disease onset and, insulin sensitisation, on brain processing of satiation and satiety, furthering our understanding of the role of insulin in appetite control.

Brain responses to meal vs water ingestion, and the modulation of food image-evoked responses by a meal were examined using pseudo-continuous arterial spin labelling and blood oxygenation level dependent functional neuroimaging respectively, in healthy men/women aged 19.5-52.6 years, and insulin sensitive (IS) and resistant (IR) men. IR men were re-examined after 3-months lifestyle changes with metformin.

Ageing was associated with diminishing hunger-suppression and increasing insula, orbitofrontal (OFC) and anterior cingulate cortex activity after eating, and diminishing modulation of dorsolateral prefrontal cortex (DLPFC), OFC and striatal food image-evoked activity by the meal.

IR men had greater food restraint, weight/shape concern, and less hunger-suppression after eating. The insula activated in IR and deactivated in IS subjects after eating. IS, but not IR, subjects showed DLPFC, striatal and lingual gyrus activation increased to high- and decreased to low-calorie food images after eating, the opposite observed when fasted. Between-group comparisons revealed greater DLPFC activation to high- vs low-calorie food cues when fed, and low- vs high-calorie food cues when fasted in IR men. The intervention improved insulin sensitivity and glycaemic status, reduced post-prandial insula activity, and increased post-prandial low-calorie food cue-evoked activity.

Results indicate impaired satiation with exaggerated post-prandial interoceptive and reward centre activity, and diminishing sensitivity of inhibitory control and reward centre responses to external food cues to current nutritional status with ageing and systemic insulin resistance. Insulin sensitisation improves insulin resistant central processing of satiation and satiety, implicating insulin in appetite regulation.

Personal contribution

I was involved in all phases of the studies described in the insulin resistance and sensitisation studies. I developed the protocol and study design with my supervisors, Prof. Amiel and Dr. Zelaya. I developed the BOLD fMRI task, validating the photographs used for the local population, and with the centre for neuroimaging's programmer I developed the playlists used. After completing Good Clinical Practice training, I applied for Research Ethics and Research and Development approval, and obtained confirmation that the study was not a clinical trial of a medicinal product from the MHRA. I developed the Standard Operating Procedures for pharmacy dispensing of Metformin (Glucophage SR). I recruited and screened all potential subjects in the insulin resistant study, and half of the subjects in the ageing study, which included performing all oral glucose tolerance tests. I performed all the neuroimaging studies, and with the diabetes specialist dietitian, developed and implemented the insulin sensitisation intervention. I performed all analyses in this thesis, under the supervision of Prof. Amiel, Dr. Zelaya and Dr. Lee, and the interpretations of the results are my own.

Publications

Y.S. Cheah, S. Lee, G. Ashoor, Y. Nathan, L.J. Reed, F.O. Zelaya, M.J. Brammer, S.A. Amiel. "The impact of aging on the modulation of human brain responses to visual food cues by meal ingestion." International Journal of Obesity 2014; **38**, 1186-1192.

Y.-S. Cheah, S.A Amiel. "Metabolic neuroimaging of the brain in diabetes mellitus and hypoglycaemia." Nature Reviews Endocrinology 2012; **8** (10), 588-97.

Conference Presentations

Y.S. Cheah, S. Lee, F.O. Zelaya, S.A. Amiel. "Insulin sensitisation normalises brain processing of satiation in non-obese insulin resistant men." Oral presentation (139), 16th September 2015, Stockholm, Sweden, 51st Annual Meeting of the EASD. *Diabetologia* 2015; **58** (Suppl1)

Y.S. Cheah, S. Lee, B.M. Wilson, A. Pernet, L. Diamond, C. Cheyette, A. Beckwith, L.J. Reed, M.J. Brammer, F.O. Zelaya, S.A. Amiel. "Insulin sensitisation normalises the human brain response to high calorie visual food cues after meal ingestion in insulin resistant men." Guided audio poster presentation (1996-P), 23rd June 2014, San Francisco, USA, ADA 74th Scientific Sessions. *Diabetes* 2014; 63 (Suppl1) A511.

Y.S. Cheah, S. Lee, B.M. Wilson, L. Diamond, C. Cheyette, A. Beckwith, L.J. Reed, M.J. Brammer, F.O. Zelaya, S.A. Amiel. "Systemic insulin sensitisation selectively normalises altered high calorie food cue-evoked brain responses in insulin resistant men." Oral presentation, 3rd April 2014, Cambridge, Association of Physicians of Great Britain and Ireland, Annual Meeting.

Y.S. Cheah, S. Lee, B.M. Wilson, L. Diamond, C. Cheyette, A. Beckwith, L.J. Reed, M.J. Brammer, F.O. Zelaya, S.A. Amiel. "The impact of insulin sensitisation intervention on the brain response to meal ingestion in insulin resistant, non-diabetic, non-obese men: an arterial spin labelling magnetic resonance imaging study." Oral presentation, 6th March 2014, Liverpool, Diabetes UK APC. *Diabetic Medicine* 2014: 31 (S1).

Y.S. Cheah, S. Lee, B.M. Wilson, L.J. Reed, M.J. Brammer, F.O. Zelaya, S.A. Amiel. "Increasing HOMA-IR modulates brain responses to meal ingestion in insulin sensitive men: a continuous arterial spin labelling functional magnetic resonance imaging study." Facilitated poster presentation 25th September 2013, Barcelona, Spain, 49th Annual Meeting of the EASD. *Diabetologia* 2013; **56** (Suppl1).

Y.S. Cheah, S. Lee, L.J. Reed, F.O. Zelaya, S.A. Amiel. "Systemic insulin resistance modulates the brain response to food cues after consuming a high calorie meal in non-obese men." Guided audio poster presentation (2106-P), 23rd June 2013, Chicago, USA, ADA 73rd Scientific Sessions. *Diabetes* 2013; 62 (Suppl1)

Y.S. Cheah, S. Lee, B.M. Wilson, M.J. Brammer, F.O. Zelaya, S.A. Amiel. "The impact of meal ingestion on human brain responses to food cues is altered with systemic insulin resistance." Poster presentation, 19th April 2013, Vienna, Austria, Prediabetes and the Metabolic Syndrome 4th International Congress. *Journal of Diabetes* 2013.

Y.S. Cheah, S. Lee, B.M. Wilson, A. Pernet, M.J. Brammer, F.O. Zelaya, S.A. Amiel. "Impact of systemic insulin resistance on brain responses to eating in non-obese non-diabetic men: an arterial spin labelling functional magnetic resonance imaging study." Oral presentation, 13th March 2013, Manchester, Diabetes UK APC. *Diabetic Medicine* 2013: 30 (S1).

Y.S. Cheah, S. Lee, F.O. Zelaya, M.J. Brammer, S.A. Amiel. "Post-Prandial Brain Responses to High Calorie Visual Food Cues are Associated With Meal Induced GLP-1 Secretion." Guided audio poster presentation (1849-P), 9th June 2012, Philadelphia, USA, ADA 72nd Scientific Sessions. *Diabetes* 2012; 61 (Suppl1) A474.

Y.S. Cheah, S. Lee, Y. Nathan, L.J. Reed, M.J. Brammer, S.A. Amiel, F.O. Zelaya. "The effect of the GLP-1 receptor agonist exenatide on regional brain response to food ingestion in Type 2 diabetes: a functional magnetic resonance imaging arterial spin labelling study." Oral presentation 7th March 2012, Glasgow, Diabetes UK APC. *Diabetic Medicine* 2012; **29** (S1), 3.

Y.S. Cheah, S. Lee, Y. Nathan, G. Ashoor, B.M. Wilson, A.M. Pernet, F.O. Zelaya, M.J. Brammer, S.A. Amiel. "Both ageing and body mass modulate the human brain response to food cues." Oral presentation on 14th September 2011, 47th Annual Meeting of the EASD, Lisbon, Portugal. *Diabetologia* 2011; **54** (Suppl1), s62.

Y.S. Cheah, S. Lee, Y. Nathan, M. Brammer, B. Wilson, A. Pernet, F.O. Zelaya, S.A. Amiel. "Effect of ageing on the brain's response to food cues." Oral presentation, 7th April 2011, Madrid, Spain, Prediabetes and the Metabolic Syndrome 4th International Congress. *Journal of Diabetes* 2011; **3** (s1), 12.

Prizes

Diabetes UK Type 2 Diabetes Research Award for outstanding contribution to the advancement of the understanding of Type 2 diabetes and its treatment. 13th March 2013.

Diabetes UK Type 2 Diabetes Research Award for outstanding contribution to the advancement of the understanding of Type 2 diabetes and its treatment. 7th March 2012.

Prediabetes and the Metabolic Syndrome 4th International Congress, 6th-9th April 2011. Prize for best oral presentation.

King's College London School of Medicine Graduate Showcase, 17th June 2011. Prize for best poster.

TABLE OF CONTENTS

List of tables

List of figures

Abbreviations

ACC: anterior cingulate cortex
AEP: auditory evoked potentials
AgRP: agouti-related peptide
α-MSH: alpha-melanocyte stimulating hormone
ASL: arterial spin labelling
AMP-K: 5' adenosine monophosphate-activated kinase
AN(C)OVA: analysis of (co)variance
BBB: blood brain barrier
BMI: body mass index
BOLD: blood oxygenation level dependent
cASL: continuous arterial spin labelling
CSF: cerebrospinal fluid
$CMR_{glucose}$: cerebral metabolic rate for glucose
DLPFC: dorsolateral prefrontal cortex
DMN: default mode network
DMPFC: dorsomedial prefrontal cortex
EEG: electroencephalography
fALFF: fractional amplitude of low-frequency (0.01-0.08 Hz) fluctuation
[^{18}F]FDG: fluorodeoxyglucose
FWHM: Full-width at half maximum
fMRI: functional magnetic resonance imaging
GE EPI: gradient echo, echo planar image
GLP-1: glucagon-like peptide-1
Glx: composite glutamine/glutamate/GABA
HOMA-IR: homeostatic model assessment of insulin resistance
iAUC: incremental area under the curve
ICV: intracerebroventricular
IL-6: interleukin-6
INT: intermediate insulin sensitivity
IR: insulin resistant
IRS-PI3K: insulin receptor substrate-2 phosphatidylinositol 3-OH kinase
IS: insulin sensitive
LH: lateral hypothalamus
MAPK: mitogen-activated protein kinases
MEG: magnetoencephalography
mTOR: mammalian target of rapamycin
NAA: *N*-acetylaspartate
NAcc: nucleus accumbens
NPY: neuropeptide Y
NTS: nucleus tractus solitarius
OGTT: 75g oral glucose tolerance test
OFC: orbitofrontal cortex
pASL: pulsed arterial spin labelling
pCASL: pseudocontinuous arterial spin labelling
PCC: posterior cingulate cortex
PCOS: polycystic ovarian syndrome
PYY: peptide tyrosine-tyrosine
PET: positron emission tomography

PFC: prefrontal cortex
POMC: pro-opiomelancortin
PVN: paraventricular nucleus
rCBF: regional cerebral bloodflow
RFT: Random field theory
ROI: region of interest
RYGB: roux-en-y gastric bypass
rTMS: repetitive transcranial magnetic stimulation
SOCS3: suppressor of cytokine signalling
SPECT: single-photon emission computed tomography
SPM: statistical parametric mapping
SSQ: sum of squares
STAT3: signal transducer and activator of transcription 3
tDCS: transcranial direct current stimulation
VLPFC: ventrolateral prefrontal cortex
VMH: ventromedial hypothalamus
VLCD: very low calorie diet
VMPFC: ventromedial prefrontal cortex
VTA: ventral tegmental area
WSR: Wilcoxon signed rank test

1 Introduction

1.1 Central control of appetite: homeostatic vs hedonic processes.

Global predictions that approximately one-fifth of adults will be obese by 2025 (NCD Risk Factor Collaboration, 2016), with associated conditions such as cardiovascular disease, type 2 diabetes mellitus (T2DM), dementia and cancer, have huge implications on health care provision for our ageing population. The obesity pandemic is being driven by the consumption of readily available, highly palatable, energy-dense foods and reduced physical activity. Our genetic propensity to eat to excess when food is available and store surplus energy may have had evolutionary advantages in pre-agricultural lifestyles with intermittent food supply (Prentice, 2005), but appetite control systems that encourage eating are now detrimental if food is abundant. Common variants of genes associated with obesity being expressed in the brain (Chambers *et al*, 2008; Thorleifsson *et al*, 2009; Willer *et al*, 2009) provide support for a "thrifty genotype" operating through neural networks controlling appetite, predisposing to weight gain in our obesogenic environment.

Two aspects of appetite regulation have received much attention: satiation (the process of meal termination) and satiety (the effect of a meal to reduce the drive to eat again). Satiation and satiety signals arise from the gastrointestinal tract, although many are also produced within the brain. They include gut peptides cholecystokinin, proglucagon derived peptides (glucagon-like peptide-1 [GLP-1], oxyntomodulin), peptide tyrosine-tyrosine (PYY), digestion-related peptides (apolipoprotein A-IV and enterostatin), bombesin family peptides (gastrin-releasing peptide and neuromedin B), amylin (secreted from the pancreas) and ghrelin (Coll *et al*, 2007; Woods and D'Alessio, 2008). Levels of most of these signals increase during a meal to terminate eating, except ghrelin, which stimulates hunger, decreasing after meal ingestion. These peptides influence hypothalamic regulation of eating, either indirectly via paracrine actions on the vagal nerve which, combined with neural signals from the gastrointestinal tract, transmits to the nucleus tractus solitarius (NTS), or directly by crossing the blood-brain barrier (BBB), where receptors for these peptides have been identified and characterised by receptor blockade or through peripheral and

intracerebroventricular (ICV) peptide administration (Woods and D'Alessio, 2008). These peptides have been called "intermediate" satiation signals (Woods, 2009), being intimately involved in the physiological response to ingestion, whilst "proximal" cues, the ingested nutrients themselves, are also sensed by the hypothalamus to influence eating (Obici and Rossetti, 2003).

Food consumption in man is not just a matter of energy balance, but evokes feelings of anticipation and pleasure. The integration of neural networks involved in energy homeostasis and eating behaviour with those involved in reward, hedonism, mood and memory is now recognised (Berthoud and Morrison, 2008; Trinko *et al*, 2007). A recent meta-analysis of functional neuroimaging studies revealed a significant overlap in abnormal activation of neural networks involving striatal reward centres in drug addition, obesity and eating disorders (Tomasi and Volkow, 2013). Berridge and Robinson (2003) proposed three components of reward processing: learning stimulus-action-outcome relationships; motivation to learn and act and; the hedonic effects elicited by rewarding stimuli, which are implicit, unconscious processes (anticipatory, incentive salience or "wanting", and hedonic responses upon consumption of pleasurable rewards or "liking") and explicit cognitively experienced processes. Each has discrete but overlapping neural correlates: "Wanting" involves dopaminergic and opioid projections from ventral tegmental area (VTA) to nucleus accumbens (NAcc) shell and lateral hypothalamus (LH), and amygdala; "liking" involves opioid, endocannabinoid and GABAergic projections of NAcc core and shell (ventral striatum), ventral pallidum, amygdala and brainstem; whilst learning and maintaining reward representations and the conscious experience of reward involves orbitofrontal (OFC), prefrontal (PFC), anterior cingulate (ACC) and insula, hippocampus and amygdala. These reward circuits interact with homeostatic paraventricular nucleus (PVN) and LH to coordinate responses to stimuli of potential interest, modulated by bottom-up processes that signal the status of nutrient stores, including the circulating fuels themselves, humoral processes (e.g. leptin, insulin and incretin hormones) and those transmitted via vagal afferents, and regulated by top-down executive prefrontal control centres that integrate internal information with external stimuli to execute behavioural change (Berthoud, 2011; Berthoud and Morrison, 2008) (Figure 1.1).

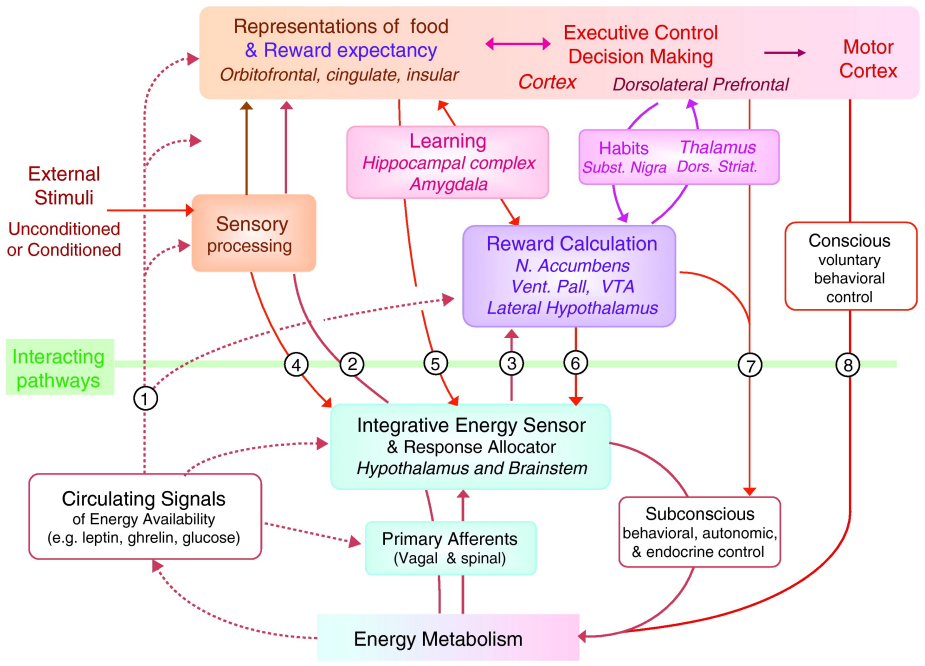

Figure 1.1

Model of interaction between homeostatic and hedonic networks involved in regulating food intake. From Berthoud (2011)

A natural progression of this framework is that altered activity within, or connections between, networks involved in motivation, affect, reward representation and executive control could lead to obesity. In the incentive salience model (Berridge and Robinson, 2003), a hypersensitive "wanting" and/or "liking" corticolimbic system activity could lead to addictive behaviours as exhibited in drug addiction, but towards food, with altered dopaminergic activity being either cause or consequence of weight gain (Berridge, 2009; Berridge *et al*, 2010). However, this model was based largely on animal models of drug addiction, and the separation of "wanting" and "liking" reward constructs may not be as easy to observe or as crucial in human obesity (Havermans, 2011, 2012). Earlier psychological models of human eating behaviour involved cognitive constructs of hunger, restraint and disinhibition of control (Stunkard and Messick, 1985). Situations of disinhibition, such as a previous meal or stress, are posited to promote overeating in individuals with otherwise high levels of restraint e.g. strict dieters (Polivy and Herman, 1985). However, this model may be simplistic: whilst high restraint, especially "rigid" all-or-nothing restraint, may lead to obesity, once obesity is established, more "flexible" restraint may improve the success of weight loss interventions (Johnson *et al*, 2012). A model of obesity combining defects in incentive salience, motivation, learning and inhibitory control networks has

thus been proposed. Stronger recall, conditioning and habit network involvement (hippocampus, amygdala, dorsal striatum [caudate, putamen]) formed from previous experience with food stimuli may strengthen neural reward representations of expected foods (medial OFC, NAcc, ventral pallidum), leading to diminished control and disinhibition (dorsolateral PFC [DLPFC], lateral OFC), resulting in an increased drive to respond to such stimuli (OFC, dorsal striatum, supplementary motor cortex), increasing food intake (Volkow *et al*, 2008a, 2011) (Figure 1.2). However, if reward signalling upon consumption of food is diminished, this may additionally stimulate further food intake in order to achieve sufficient reward. Evidence for both hypersensitive and hyporesponsive reward networks in human obesity are discussed.

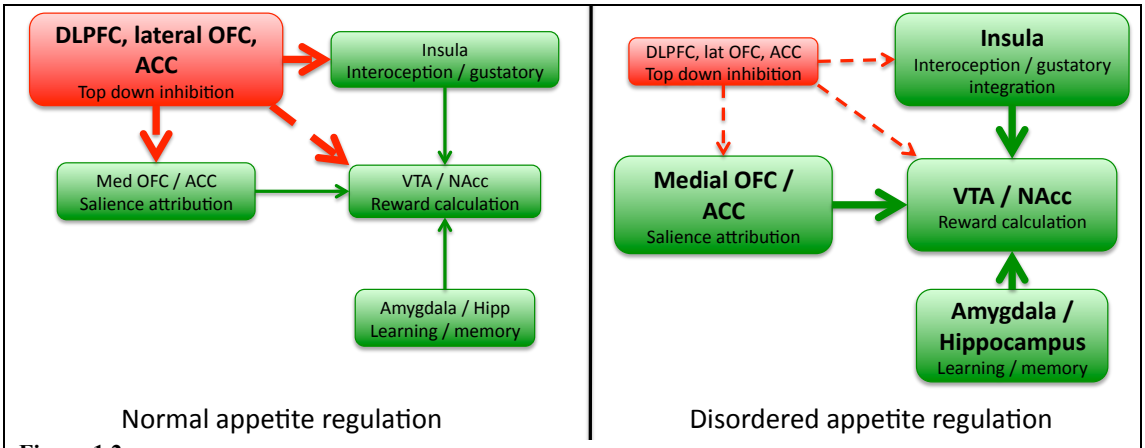

Figure 1.2

Model of obesity. Insufficient executive control with enhanced salience, conditioning and drive may dysregulate eating. Adapted from Volkow *et al* (2011)

1.2 Human brain responses to food and food cues

Functional neuroimaging has been used to explore central mechanisms of appetite regulation in health and disease in man. Studies can be broadly divided into those examining responses to food ingestion, and responses to food cues.

1.2.1 Normal brain response to food ingestion

Many functional neuroimaging studies have deliberately focussed on the role of the hypothalamus in sensing ingested nutrients. When non-obese volunteers consume glucose, hypothalamic blood oxygenation level dependent (BOLD) functional magnetic resonance imaging (fMRI) signal, a surrogate marker of regional brain

activity described further in Chapter 2, decreases (Flanagan *et al*, 2012; Matsuda *et al*, 1999), in a dose-response relationship (Smeets *et al*, 2005a), with higher fasting insulin levels associated with greater delays in signal changes (Liu *et al*, 2000). Responses are greater and more prolonged with oral than intravenous glucose (Smeets *et al*, 2007), accompanied with the "incretin effect" of more pronounced insulin secretion. This hypothalamic response appears to depend on the sweetness and energy content of glucose, given the lack of response with artificial sweeteners and non-sweet carbohydrates (Smeets *et al*, 2005b), possibly through interactions with reward networks, increasing hypothalamic functional connectivity of BOLD signal with thalamus and dorsal striatum and reducing regional cerebral blood flow (rCBF) in these centres, insula and ACC as demonstrated by pulsed arterial spin labelling (pASL) fMRI (Page *et al*, 2013). These latter findings are not observed with fructose, a sweetener that has been implicated in the recent rise in obesity, suggesting the brain is less able to sense this nutrient to evoke satiation (Page *et al*, 2013). The reward network response to energy loads may also depend on peripheral signals, as changes in insulin correlated with striatal rCBF changes after glucose, but not fructose ingestion, which stimulated a smaller insulin response. Together, these data suggest the hypothalamic response to ingested glucose is influenced by the degree of peripheral insulin resistance, the humoral response to nutrient ingestion, and its sensory effects, potentially through interactions with reward, interoceptive and inhibitory control networks.

The hypothalamus also responds to other macronutrients. A pASL fMRI study showed high but not low fat yoghurt reduced hypothalamic perfusion, where small post-prandial insulin increments were associated with decreases in rCBF, and larger increments with increases in rCBF (Frank *et al*, 2012). Greater insulin secretion occurred with low fat yoghurt, despite equivalent carbohydrate content in the two yoghurts, possibly due to potential delays in gastric emptying with high fat foods. The insula was also sensitive to changes in fat content, with an initial reduction in rCBF at 30 mins with both yoghurts, but greater increases in rCBF 120 mins after consuming low fat yoghurt. As the two yoghurts reduced hunger equally, and analyses adjusted for hunger, these changes in brain activity may represent homeostatic responses to meal ingestion independent of explicit hedonic responses. The ingestion of satiating isocaloric (1255 kJ) protein, fat or glucose compared to

water has each been shown to reduce BOLD signal in insula, thalamus, parahippocampal gyrus, caudate and lateral OFC (Li *et al*, 2012a). Post-fat insulin secretion was minimal and thus not associated with signal changes, whilst post-glucose insulin secretion was negatively associated with insula, thalamus, amygdala and lateral OFC signal changes, and the smaller post-protein insulin response was negatively associated with caudate signal changes. As overall corticolimbic network deactivation was similar for each macronutrient, but accompanied by different humoral responses, these central responses may have been to the caloric load *per se*. However, as high- compared to low-glycaemic index meals evoke greater insulin secretion and striatal and NAcc perfusion during continuous ASL (cASL) fMRI (described in Chapter 2), with NAcc rCBF correlating with post-prandial insulin (Lennerz *et al*, 2013), humoral responses to meal ingestion are likely to remain an important modulator of satiation processing in these reward centres. As orally consumed chocolate milk evokes greater putamen, amygdala, thalamus and precuneus activation than nasogastric infusion at similar rates of consumption, the sensory perception of food is also an important stimulus to these reward networks (Spetter *et al*, 2014).

This is exemplified in a pivotal [^{15}O]H_2O-PET (positron emission tomography) study where healthy subjects who crave chocolate, ate increasing amounts of chocolate, resulting in a transition from increased rCBF in medial OFC, insula, dorsal striatum when chocolate was pleasant, to lateral OFC, PFC and parahippocampal gyrus on reaching satiation (Small *et al*, 2001). Another [^{15}O]H_2O-PET study showed rCBF increased in left DLPFC and right ventrolateral PFC (VLPFC), thalamus and hippocampus, and decreased in medial PFC, when men tasted a flavoured liquid meal after a prolonged fast (Gautier *et al*, 1999). Once satiation was reached, rCBF increased in these lateral prefrontal centres, and decreased in OFC, ACC, dorsal striatum, insula, thalamus and parahippocampal and hippocampal gyri in both men (Tataranni *et al*, 1999) and women (Gautier *et al*, 2001). A similar study showed that when men tasted chocolate milk and tomato juice, before and after satiation by one of these drinks, OFC BOLD signal decreased specifically when the drink that was consumed to satiation was tasted, presumably as it became increasingly less pleasant, in keeping with OFC processing of reward salience (Kringelbach *et al*, 2003). The

insula, ACC and caudal OFC activated on tasting the drinks, irrespective of satiation, suggesting a sensory processing role.

The brain thus appears to respond to changes in nutritional state, with the activation of OFC and medial PFC during extreme hunger decreasing upon satiation, in keeping with its role in processing reward salience, accompanied by changes in activity of reward representation (striatum), interoception (insula), memory (hippocampus) and signal relay (thalamus) centres. The increasing lateral PFC activity during eating provides inhibitory regulation of these hedonic centres to reach satiation. As changes in post-prandial GLP-1 positively correlate with post-prandial changes in DLPFC and hypothalamic activity, it is possible that endogenous GLP-1 suppresses appetite through both higher executive and homeostatic centres (Pannacciulli *et al*, 2007b).

Gender may influence brain activity during meal ingestion. Using data from lean and obese subjects undergoing [^{15}O]H_2O-PET examination of responses to a liquid meal described above (Gautier *et al*, 2000, 2001; Tataranni *et al*, 1999), direct comparisons showed satiation induced greater rCBF decreases in left DLPFC and parahippocampal gyrus in men and greater rCBF increases in left DLPFC and attenuated rCBF increases in right VMPFC in women (Del Parigi *et al*, 2002). An fMRI study similarly showed that after eating chocolate to satiation, activation responses to tasting a chocolate drink increased in ventral striatum, insula and OFC (unlike the decreases observed in previous studies) in men, and increased in dorsal striatum and decreased in hypothalamus and amygdala in women, with significant differences in activity between sexes in hypothalamus, ventral striatum and medial PFC (Smeets *et al*, 2006). The greater hedonic network response in men, and greater homeostatic response in women during satiation could be due to potential differences in the enjoyment of eating chocolate and subsequent weight concern between the sexes. Given the above [^{15}O]H_2O-PET studies showed increasing post-prandial insulin excursions were associated with greater reductions in insula and OFC rCBF in men, whilst greater reductions in post-prandial free fatty acid were associated with diminishing DLPFC rCBF increments and ACC rCBF decrements in men (Tataranni *et al*, 1999), and smaller insula rCBF decrements in women (Gautier *et al*, 2001; Tataranni *et al*, 1999), it is also possible the central response to circulating hormones and fuels may also differ between men and women. Hence, the impact of gender was

controlled for in the studies reported in Chapters 5-8, by restricting the investigations to men.

PET radioligands can also be used to characterise changes in specific neurotransmitters signalling during feeding. For example, when eating a favourite meal following a prolonged fast, the post-prandial reduction in [^{11}C]raclopride binding to dorsal striatal dopaminergic D_2 receptors is correlated with meal pleasantness ratings, suggesting that meal-induced striatal dopamine release is a neural correlate of pleasure and reward (Small *et al*, 2003).

1.2.2 Brain response to food ingestion in obesity and diabetes

Obesity and diabetes appear to alter brain activity during meal ingestion. Using the same [^{15}O]H_2O-PET protocols described previously (Gautier *et al*, 1999; Tataranni *et al*, 1999), the rCBF increases in insula and decreases in PCC on tasting food, and decreases in hippocampus, PCC and amygdala once satiated in lean subjects were augmented in obesity (DelParigi *et al*, 2004). A direct comparison between groups showed rCBF increases in insula and midbrain and decreases in medial OFC on tasting the meal after the prolonged fast were augmented in obesity (DelParigi *et al*, 2005). Insulin resistance was not formally assessed, but implied in the obese group by higher insulin levels. Body fat and plasma glucose levels correlated with insula rCBF changes, supporting a role for insulin resistance in modulating post-prandial central interoception processing, resulting in exaggerated or hypersensitive consummatory responses to meal ingestion. Two further within-sex analyses of these data showed post-prandial increases in PFC and decreases in insula and hippocampus rCBF were exaggerated in both obese men and women than their lean counterparts, and hypothalamic rCBF decreases were attenuated in obese men (Gautier *et al*, 2000, 2001). However, these three initial analyses used single-level fixed-effects methods with lenient statistical thresholds. Re-analysis of these data from right-handed volunteers using random effects modelling now showed attenuated post-prandial increases in rCBF in left DLPFC in obesity (Le *et al*, 2006, 2007). These opposite findings were attributed to the original analyses not accounting for between-subject variability, invalidating the earlier reports. In keeping with a study showing increasing BMI was associated with diminishing frontal rCBF during a response

inhibition task (Willeumier *et al*, 2011), these data imply insufficient post-prandial recruitment of inhibitory control centres in obesity could attenuate satiation.

The hypothalamic responses to oral glucose in health described earlier, are increasingly delayed with increasing fasting glucose and insulin (Liu *et al*, 2000; Matsuda *et al*, 1999), and are diminished and delayed in obesity (Matsuda *et al*, 1999). In addition patients with T2DM treated with oral agents or diet alone do not show any reduction in hypothalamic response to glucose and actually show an activation response with water ingestion (Vidarsdottir *et al*, 2007). Together, these data are consistent not only with altered nutrient sensing in homeostatic centres, but also altered hedonic network responses to meal ingestion in conditions associated with systemic insulin resistance.

1.2.3 Normal brain response to visual food cues

Functional neuroimaging has also been used to examine responses to cues of food, such as touch (St-Onge *et al*, 2005), taste (Uher *et al*, 2006; Frank *et al*, 2003; Grabenhorst *et al*, 2008, 2010; De Araujo and Rolls, 2004; Kringelbach *et al*, 2003; Rolls, 2007), smell (Bragulat *et al*, 2010; Cerf-Ducastel and Murphy, 2001; O'Doherty *et al*, 2000; Small *et al*, 2005, 2008; Volkow *et al*, 2002), and imagery (Morris and Dolan, 2001; Hinton *et al*, 2004; Piech *et al*, 2009; Jastreboff *et al*, 2012), that engage homeostatic and non-homeostatic networks. Whilst PET studies of neurotransmitter activity or receptor availability can be used to examine such responses, such as food-cue evoked striatal dopamine release, signals are weak with low temporal resolution and may only be demonstrable after pharmacologically amplifying the signal (Volkow *et al*, 2002). Instead, task-driven BOLD signal changes under different physiological conditions are frequently examined in studies of appetite regulation, the most common paradigm being the viewing of food cues, which when compared to non-foods, elicit changes in activity of similar networks described upon food ingestion itself, including insula (Cornier *et al*, 2007; Frank *et al*, 2003; Fuhrer *et al*, 2008; Killgore *et al*, 2003; LaBar *et al*, 2001; Porubská *et al*, 2006; Schur *et al*, 2009; Siep *et al*, 2009; Simmons *et al*, 2005; St-Onge *et al*, 2005; Uher *et al*, 2006), OFC (Beaver *et al*, 2006; Frank *et al*, 2003; Fuhrer *et al*, 2008; Porubská *et al*, 2006; Schur *et al*, 2009; Siep *et al*, 2009; Simmons *et al*, 2005),

DLPFC (Cornier *et al*, 2007; Goldstone *et al*, 2009; Killgore *et al*, 2003; Schur *et al*, 2009; Siep *et al*, 2009; Uher *et al*, 2006), ACC (Goldstone *et al*, 2009; Passamonti *et al*, 2009; Siep *et al*, 2009; Simmons *et al*, 2005; St-Onge *et al*, 2005), striatum (Beaver *et al*, 2006; Passamonti *et al*, 2009; Porubská *et al*, 2006; Schur *et al*, 2009), parahippocampal gyrus (Goldstone *et al*, 2009; Siep *et al*, 2009; Simmons *et al*, 2005; St-Onge *et al*, 2005), amygdala (Goldstone *et al*, 2009; Killgore *et al*, 2003; LaBar *et al*, 2001; Passamonti *et al*, 2009; Schur *et al*, 2009; Siep *et al*, 2009), and thalamus (Fuhrer *et al*, 2008; Killgore *et al*, 2003; Schur *et al*, 2009; Uher *et al*, 2006).

Responses to food cues predict appetite and eating behaviour. For example, in a study of lean females, visual food cue-evoked NAcc activity predicted the quantity of food eaten during an ad libitum meal, whilst OFC activity predicted self-reported food craving (Lawrence *et al*, 2012). Manipulating the incentive value of food stimuli influences their motivational value or "wanting" of food. This can be achieved by using food images of different calorie content, assuming that pleasurable foods are more energy dense. For example, in a study of lean women, high-calorie food images elicited greater medial PFC, DLPFC, thalamic and hypothalamic activation, whilst low-calorie food images elicited insula, somatosensory cortex, medial OFC and hippocampal activation (Killgore *et al*, 2003). When high- and low-calorie food images were directly compared, the former evoked greater responses in medial PFC, DLPFC and thalamus, whilst the latter elicited greater medial OFC, lingual and middle temporal gyrus activation. Another study similarly showed greater DLPFC, OFC, insula, striatum, thalamus, VTA, hypothalamus and amygdala activation on viewing fattening food images compared to non-food or low-calorie food images in lean women (Schur *et al*, 2009). Furthermore, "high hedonic" food image-evoked DLPFC activation is negatively correlated with energy intake during an ad libitum meal in lean volunteers, supporting its role in inhibitory control of eating behaviour (Cornier *et al*, 2010). Changes in nutritional state, assuming foods are more "rewarding" when fasted, may also modify the incentive value of food cues. For example, food images elicit responses in amygdala, parahippocampal and fusiform gyri in fasted but not fed states (LaBar *et al*, 2001), and when compared directly, fasting elicits greater responses than fed states to food images in fusiform gyrus (Uher *et al*, 2006), amygdala and ACC (Fuhrer *et al*, 2008). Similarly, oral glucose reduces food image-evoked activation of striatum, ACC, medial frontal and middle temporal

gyri and increases activation in precuneus and visual cortex in lean volunteers (Kroemer *et al*, 2013b). The post-glucose rise in plasma insulin levels was associated with decreasing responses to food images in insula, striatum, cingulate, PFC, thalamus, amygdala and hippocampus, in keeping with a role for insulin in mediating the post-prandial suppression of food-evoked corticolimbic activity.

A meta-analysis of 14 studies in 207 non-satiated subjects revealed activation of amygdala, insula, lateral OFC, ventral striatum, fusiform gyrus, thalamus, ACC and medial frontal lobe on viewing food compared to non-food images (Tang *et al*, 2012). A larger meta-analysis of 18 studies in 246 lean subjects showed insula, lateral OFC and posterior fusiform gyrus activation on viewing food compared to non-food images, with feeding increasing parahippocampal-amygdala and lateral OFC responses, whilst high- compared to low-energy food images evoke greater ventral striatum-hypothalamus activation (van der Laan *et al*, 2011). Different inclusion criteria are likely to have produced the different findings, with the high degree of variation and low concurrence between individual studies being an effect of study design. For example, passive food image viewing compared to explicit tasks alters OFC engagement (Siep *et al*, 2009). Cognitive attributes, such as external eating behaviour, where food evokes the desire to eat even in the absence of hunger, may also affect food cue-evoked brain responses (Passamonti *et al*, 2009).

External (calorie content) and internal (hunger state) modifiers of "reward" may have interacting cerebral effects. A study of healthy female volunteers showed a 500 kcal meal following a prolonged fast decreased high-calorie food image-evoked activity in medial OFC, insula and striatum, and increased low-calorie food image-evoked activity in these regions (Siep *et al*, 2009). A similar study of lean men and women showed that fasting elicited greater OFC, ventral striatum, insula and amygdala responses to high- than low-calorie food images, without any differences in response to these different food stimuli when fed, and the change in "appeal bias" for high- over low-calorie food images between fasted and fed states positively correlated with the respective changes in OFC activity (Goldstone *et al*, 2009). This is in keeping with the OFC utilising information about internal states and food energy values to award their valence. Other studies show overfeeding attenuates hypothalamus and visual attention centre activation specifically to "high hedonic" compared to

"utilitarian" food images (Cornier *et al*, 2007), whilst increasing the interval between breakfast and subsequent fMRI increases the appeal of fattening food images, with such ratings predicting the volume of a post-scan ad libitum meal (Mehta *et al*, 2012). Moreover, the differential dorsal striatum response to fattening over non-fattening food images was associated with greater fullness, and that of medial OFC, amygdala, insula and NAcc predicted greater consumption of fatty food during the ad libitum meal. These data suggest homeostatic and reward networks are sensitive to internal and external cues of food and energy availability, integrating these signals to calculate the incentive salience of food and determine food choice.

As with the response to meal ingestion, gender may also influence brain responses to food cues. One study showed that women had greater responses to high- compared to low-calorie food images in middle frontal gyrus, inferior lateral and ventromedial OFC than men (Killgore and Yurgelun-Todd, 2010). Additional region of interest (ROI) analyses also demonstrated greater insula responses in women and greater amygdala responses in men. Greater DLPFC activation on viewing hedonic food images has similarly been shown in women in the fasted state, who ate significantly less during a subsequent ad libitum meal compared to the pre-scan eucaloric diet, reflecting greater self-reported dietary restraint, than in men (Cornier *et al*, 2010). Larger responses to visual food cues in fusiform gyrus and to food tastants in insula and medial PFC have also been shown in women (Uher *et al*, 2006). Whilst no differential effects of gender on the impact of prior meal ingestion on evoked responses were detected in this study, a subsequent analysis of responses to high-calorie food images alone showed women had greater responses in superior medial frontal lobe and fusiform gyrus when hungry, whilst there was no effect of meal ingestion in these brain regions in men (Frank *et al*, 2010a). Greater responses to high- compared to low-calorie food images in OFC during the luteal phase and in NAcc during the follicular phase is accompanied by greater food ingestion during the luteal phase (Frank *et al*, 2010b), whilst greater food image-evoked activity in insula and inferior frontal gyrus in fed than fasted states in the late follicular phase has also been shown (Alonso-Alonso *et al*, 2011) suggesting sex hormones, or other cycle-associated changes such as insulin sensitivity (Brown *et al*, 2015), influence reward network responses to food.

1.2.4 Brain response to visual food cues in obesity and diabetes

As with food ingestion *per se*, central processing of visual food cues appears to be altered by conditions associated with systemic insulin resistance. In one study, patients with T2DM had greater food image-evoked activity in insula, OFC and striatum than controls (Chechlacz *et al*, 2009). Patient self-reported dietary adherence correlated positively with food-related activity in lateral OFC and negatively in NAcc, putamen and amygdala, suggesting greater prefrontal inhibitory control and lower reward processing of food stimuli are linked to dietary changes in T2DM. However, diabetic subjects were older and many used insulin. Another study showed the food cue-evoked insula, OFC and amygdala activations when fasted and post-prandial reduction in insula and OFC activation were greater in overweight diabetic patients than lean controls (ten Kulve *et al*, 2015), whilst food cue-evoked activation during a somatostatin pancreatic-pituitary clamp in diabetic patients was greater in left insula than lean, insulin-sensitive subjects, but lower in right insula than BMI-matched insulin-resistant non-diabetic individuals (van Bloemendaal *et al*, 2014).

These studies cannot tease apart effects of diabetes, obesity, insulin resistance, and educational and medical interventions on the food cue-evoked responses in these interoceptive, reward and salience processing centres. However, studies in women with polycystic ovarian syndrome (PCOS) support an effect of systemic insulin resistance, with increasing insulin resistance (based on 2-hr post-75g oral glucose tolerance test (OGTT) glucose:insulin ratios) associated with smaller discriminatory responses to high- compared to low-calorie food images in OFC, DLPFC, insula, VTA, ventral pallidum and midbrain, and greater differential activation in dorsal striatum, 5-hrs post-breakfast (Van Vugt *et al*, 2013). These striatal discriminatory responses were *smaller* with increasing insulin resistance immediately after ingesting glucose (Van Vugt *et al*, 2014), suggesting diminished salience processing and hypersensitive reward processing of visual food cues during a period of fasting, the latter diminishing immediately after a caloric load, with increasing insulin resistance.

When divided into insulin sensitive and resistant groups, defined by homeostatic model assessment of insulin resistance (HOMA2%S)<60% (equivalent to HOMA-IR>1.7) and post-OGTT glucose:insulin<1.5 mg/cl/μU/ml, oral glucose immediately

attenuated the hunger observed after water ingestion equally (Van Vugt *et al*, 2014). However, oral glucose reduced the differential response to high- compared to low-calorie food images in DLPFC, insula, thalamus and midbrain in insulin sensitive women, but only in temporal lobe in insulin resistant women. Direct comparisons between groups showed that responses to viewing food images converted from activations after water ingestion to deactivations after glucose ingestion in insula, ACC, midbrain and precuneus in insulin sensitive women, the opposite occurring in insulin resistant women. These data are consistent with a corticolimbic network that is hypersensitive to external food cues with little discrimination for caloric content, and hyposensitive to internal cues of energy availability in states of peripheral insulin resistance, where the normal inhibitory effect of ingested glucose on these networks when exposed to further food converts to an activation that may impair satiety.

The effects of obesity have been more widely examined. A meta-analysis of 10 published studies showed the obese response to food compared to non-food images is attenuated in left DLPFC and insula and exaggerated in left DMPFC, right ACC, precentral and parahippocampal gyri, consistent with diminished inhibitory control (DLPFC) and interoceptive awareness (insula) and greater "wanting" (ACC) when exposed to food cues (Brooks *et al*, 2013). An impact of obesity on reward centre responses was not found, possibly due to differences in cue salience between studies.

When the energy content of the food cues is manipulated, non-fasted obese women have exaggerated activation of caudate, putamen, hippocampus and insula to high-calorie food cues, with such responses in these regions and lateral OFC positively correlating with BMI (Rothemund *et al*, 2007). Frontal responses to low-calorie food images were also exaggerated in this study, but as these images were rated as most appealing, there were no significant discriminatory responses between food cues classes. In another study, responses in fasted obese women to high compared to low-calorie food cues were exaggerated in OFC, ACC, insula, NAcc, caudate, amygdala, hippocampus and ventral pallidum (Stoeckel *et al*, 2008).

When feeding status is manipulated, a meta-analysis of published and unpublished fMRI studies showed the obese response to food cues is exaggerated in hippocampus and amygdala and attenuated in insula within the pre-meal state, whilst it is

exaggerated in caudate and medial PFC post-prandially (Kennedy and Dimitropoulos, 2014). An effect of obesity on DLPFC responses was not detected. However, in one study responses to food compared to object cues were exaggerated in anterior PFC pre-lunch and in DLPFC and OFC post-prandially, despite hunger falling equally in obese and lean groups (Dimitropoulos *et al*, 2012), which might be interpreted as an attempt to control the exaggerated post-prandial reward network activity observed in the meta-analysis by Kennedy and Dimitropoulos (2014). Pre-meal responses to high- compared to low-calorie food images in parahippocampal gyrus and insula were attenuated in obesity, suggesting interoceptive centres in obesity may be less discriminatory of energy value of food cues, when highly salient, pre-meal.

A limitation of the meta-analysis by Kennedy and Dimitropoulos (2014) is that data directly comparing differences in the change in food cue-evoked brain response from before to after eating, between obese and non-obese subjects, were excluded, instead only including data comparing groups within each nutritional state. However, one study showed lean subjects had activation responses to high-calorie food cues that attenuated post-prandially in OFC and deactivated in caudate and insula, whilst obese subjects showed opposite findings in insula, with OFC and caudate activation being insensitive to the meal (Dimitropoulos *et al*, 2012). Another study detected interactions between stimulus, feeding state and subject group in ACC and putamen, where lean subject responses to food images in ACC were deactivation when fasted and activation when fed, the opposite observed in overweight subjects (Martens *et al*, 2013). Analyses within the fed state also showed PFC activation to food cues in lean subjects, with deactivation in overweight subjects. Additionally, food cue-evoked activity was positively correlated with BMI in ACC when fasted and negatively correlated in PFC when fed. These data were interpreted as greater food-"wanting" ACC signalling in obesity in the fasted state when food is most salient, that falls after meal consumption, whilst post-prandial PFC inhibitory control of food-related behaviour is diminished in obesity. This is consistent with the attenuated DLPFC response to meal ingestion *per se* in obesity (Le *et al*, 2006, 2007).

Studies examining the neural correlates of cognitive processes such as imagery, inhibitory control and attention to food cues support this hypothesis. Overweight women have greater post-prandial activation of ACC, OFC, striatum, insula,

parahippocampal gyrus and DLPFC than lean women when imagining the taste of high-calorie foods, which may represent greater "wanting" (Frankort *et al*, 2012). Decreasing pre-prandial DLPFC and increasing post-prandial putamen responses to low-calorie food images are associated with self-reported impairment of satiety in obesity (Ho *et al*, 2012). Greater recruitment of corticolimbic reward centres is observed in obese than lean women when passively viewing high-calorie food images (Scharmüller *et al*, 2012). However, after consciously reducing the perceived value of these foods, activity in lateral OFC, DLPFC, insula and striatum increased above that elicited from passive food image viewing in lean subjects, whilst this was limited to OFC in obese volunteers, with appetite falling in lean subjects only. Similarly, when lean, overweight and obese adolescent females were instructed to press a button on viewing images of vegetables, but to inhibit responses to desserts, increasing BMI was associated with faster and more erroneous presses, and lesser OFC, medial PFC, VLPFC, superior and middle frontal gyri activation to desserts, consistent with diminished prefrontal inhibitory control of responses to appetising foods (Batterink *et al*, 2010). Greater insula activation during these inhibitory responses to desserts was also observed with increasing baseline BMI, suggestive of greater food salience and interoceptive awareness. At the same time, smaller opercula responses were associated with greater weight gain 1 year later, suggesting that diminished gustatory processing may be a risk factor for future weight gain. A visual attention study in the same subjects similarly demonstrated increasing BMI was associated with faster reaction times, and greater activity in insula, operculum and lateral OFC when attending to cues that signalled the imminent presentation of appetising foods, with OFC activation correlated with increases in BMI 1 year later (Yokum *et al*, 2011).

The observation that corticolimbic responses to food cues might predict future weight brings into debate whether reward network activity alterations play a causative role in obesity. In non-obese volunteers, increasing BMI is associated with decreasing PFC and cingulate cerebral metabolic rate for glucose ($CMR_{glucose}$) in fluorodeoxyglucose ([^{18}F]FDG)-PET (Volkow *et al*, 2009) and greater ventral striatal D_2 receptor availability (Caravaggio *et al*, 2013). One fMRI study showed meal ingestion reduced insula, inferior and medial PFC responses to food images only in "obesity resistant" subjects who maintain current weight with ease, whilst "obesity prone" subjects showed post-prandial activation in medial and anterior PFC (Cornier *et al*,

2013), similar to the studies in established obesity. However, the "obesity prone" had greater BMI, and the history of fluctuating weight that characterised the propensity to weight gain, itself may have affected PFC activity making it difficult to establish if differences in brain activation were altered prior to weight gain. Another study showed food cue-evoked NAcc responses in non-fasted women were associated with weight gain at 6 months, although baseline BMI was unreported (Demos *et al*, 2012).

Collectively these data are in keeping with a network of reward, incentive salience and interoceptive centres that is hyper-responsive to external food cues, responses to which are hyposensitive to the blunting effects of internal cues of recent meal ingestion, potentially through inadequate prefrontal inhibitory control, in established obesity and states of systemic insulin resistance, but may also provide a predilection to future weight gain and obesity through impaired satiation. Longitudinal studies of subjects who are initially of normal weight are required to confirm this hypothesis.

However, data consistent with a reward deficit or hyporesponsive model of obesity, where greater food consumption is proposed to be needed to evoke the same degree of reward, also exist. ^{123}I-iodobenzamide SPECT demonstrate lower striatal D_2/D_3 receptor availability in severely obese women (de Weijer *et al*, 2011). A [^{11}C]raclopride/[^{18}F]FDG-PET study also showed reduced striatal D_2 receptor availability in severely obese compared to lean subjects, with increasing BMI associated with reduced receptor availability in obesity (Wang *et al*, 2001). Whilst there were no global or regional $CMR_{glucose}$ differences in this study, striatal D_2 receptor availability was positively associated with $CMR_{glucose}$ in DLPFC, medial OFC, and ACC in obesity (Volkow *et al*, 2008b). This was interpreted as diminished bottom-up dopaminergic modulation of prefrontal inhibitory and reward salience centres in obesity, although impaired prefrontal regulation of striatal activity is also possible. Furthermore, a [^{18}F]fallypride-PET study has shown D_2 receptor availability in ventromedial striatum was negatively associated with BMI, consistent with a hyporesponsive reward model, but within dorsolateral striatum was positively associated with BMI and with measures of susceptibility to "opportunistic" or habitual eating (Guo *et al*, 2014). A limitation of all these studies is that low D_2 receptor availability could either represent a reward deficit system with low D_2 receptor levels, or a hypersensitive striatum with increased dopamine release in

obesity. In terms of food cue-evoked activity, one fMRI study has shown BMI to be negatively correlated with responses to both high- and low-calorie foods in inferior OFC, and to the former in ACC, suggesting diminishing prefrontal food salience processing with weight gain (Killgore and Yurgelun-Todd, 2005a). However, feeding status was not clearly controlled, with a minimum 90 mins duration of food abstinence, and scans were performed at night, which may have affected performance.

1.2.5 Brain anticipatory ("liking") and consummatory ("wanting") responses to food cues and food in health and obesity

The previous sections have shown that responses to meal ingestion and food cues, and the effect of the former on the latter, are altered in conditions associated with systemic insulin resistance. In a series of studies, based on the incentive motivation model (Berridge *et al*, 2010), Stice *et al* (2009) highlight the importance of distinguishing anticipatory ("liking") responses to food cues from consummatory ("wanting") responses to food ingestion, but in the context of the sight or smell of food increasing the anticipation for their subsequent consumption. Indeed, most fMRI studies described above did not follow food cue presentation by consumption of the same food. In healthy volunteers, cues alerting the imminent administration of an appetising glucose tastant elicited greater midbrain, NAcc and amygdala responses than to tasting glucose *per se*, whilst consummatory responses were greater than anticipatory responses in OFC (O'Doherty *et al*, 2002). Using odours to signal later tastant delivery, others have shown anticipatory responses were greater in lateral OFC, thalamus, midbrain, ventral pallidum and amygdala, whilst consummatory responses were greater in insula, conjunction analyses indicating insula/operculum and OFC to have both anticipatory and consummatory functions (Small *et al*, 2008).

Anticipatory and consummatory responses also appear to be altered in obesity. Obese compared to lean females show greater anticipatory responses in insula and ACC, and greater anticipatory and consummatory responses in operculum (Stice *et al*, 2008). Increasing BMI was associated with greater anticipatory responses in DLPFC, VLPFC and operculum and consummatory responses in operculum and insula, and falling consummatory responses in caudate. This was interpreted to suggest a *hypersensitive* anticipatory and consummatory reward network involving insula and

PFC, and a consummatory reward *deficit* in caudate in obesity. Women expressing high "food addiction" had greater anticipatory responses in DLPFC and caudate and lower consummatory responses in lateral OFC compared to low "food addiction" women, with increasing "food addition" associated with greater anticipatory responses in ACC, medial OFC and amygdala (Gearhardt *et al*, 2011). This could be interpreted as lateral PFC inhibitory activity increasing in an attempt to control the desire to eat (represented in medial OFC and ACC) when exposed to food cues. Naturally, not all obese people are "food addicted", as indicated by a lack of association between addiction scores and BMI, and the data are at odds with the PET study of chocolate cravers (Small *et al*, 2001), possibly due to differences in weight concern between the studies.

In a similar study, dorsal striatum and operculum consummatory responses were greater, without any differences in anticipatory responses to food cues, in adolescents at high risk of future obesity than those at low risk, where risk was based on parental weight (Stice *et al*, 2011). However, a longitudinal study in overweight and obese volunteers showed that weight gain reduced dorsal striatal consummatory responses (Stice *et al*, 2010). It was thus proposed that a dorsal striatum network hypersensitive to food consumption predisposes one to weight gain by overeating, but that once obesity has developed, diminishing dopaminergic reward processing leads to the need to consume more in order to achieve sufficient reward, similar to habituation models of drug addiction. However, the fact that subjects were already overweight in the longitudinal study, with baseline BOLD parameter estimates being activation in those who gained weight and deactivation in those who later lost weight, limits this hypothesis. In addition, tastant delivery rather than actual meal ingestion was used to elicit "consummatory" responses in all these studies, whilst some used arbitrary shapes as cues to which the association with subsequent "consummatory" tasks was learned (Stice *et al*, 2008). The studies in the previous section describing the effect of meal ingestion on responses to food cues may thus be more physiologically relevant, but the data in this section highlight the need to differentiate consumption and satiation, from anticipation and satiety.

1.2.6 Impact of weight reduction on brain response to food ingestion and visual food cues

Research examining whether changes in neural responses to food and food cues in obesity are persistent or amenable to therapy, potentially as a treatment target, is emerging. A [^{15}O]H_2O-PET study initially showed obese and "post-obese" subjects, the latter with phenotypes matching lean subjects after maintaining weight loss for at least 3 months through lifestyle changes, both had similarly greater increases in insula rCBF on tasting food, and decreases in hippocampal rCBF after a satiating meal, than lean subjects (DelParigi *et al*, 2004). However, as statistical methodology was suboptimal, subsequent random-effects re-analyses showed post-prandial DLPFC activity in "formerly obese" women did not differ from that of lean subjects, but was attenuated in obesity (Le *et al*, 2007). This suggests weight loss interventions may normalise impaired post-prandial prefrontal inhibitory control centre activity in obesity, improving satiation. An fMRI study of individuals achieving similar degrees of weight loss as the PET study showed greater visual food cue-evoked activity in frontal and temporal regions than lean and obese subjects (McCaffery *et al*, 2009). As "post-obese" subjects also have longer reaction times on Stroop colour naming tasks for high-calorie food words, a task dependent on response inhibition (Phelan *et al*, 2011), these data suggest greater engagement of inhibitory control centres on exposure to food in those who successfully lose weight.

In keeping with previous investigations (Small *et al*, 2001), a study of lean, non-dieting females showed less ventral striatal and greater amygdala food cue-evoked responses in those pre-fed milkshake than water, indicative of suppressed food reward and increased food aversion centre activity when satiated (Demos *et al*, 2011). Opposite findings in dieters suggestive of *greater* reward and *reduced* vigilance after a meal appear to conflict with the hypothesis that improved inhibitory control and suppression of food reward processing reduces weight through appetite suppression. However, these dieters may not reflect "post-obese" states as weight history was unknown, with the authors proposing this was an aversion response to violating usual dietary restraint. In another study, overfeeding reduced food cue-evoked hypothalamic and insula activity in lean subjects but not in individuals who had lost weight through dietary changes (Cornier *et al*, 2009). Diminished homeostatic and

hedonic centre responsiveness to excess food in this study may represent a persistent obesity-prone trait with risk of weight regain, but this apparent lack of normalisation of food-related brain activity may have been due to residual excess weight in the "reduced obese".

Food-related brain activity may also predict the efficacy of weight loss intervention. A recent study demonstrated that a 12-week structured dietary weight loss programme in obese volunteers reduced high-calorie food image-evoked activity in medial PFC, consistent with earlier cross sectional studies, but also that greatest weight loss was achieved in those with the smallest baseline ACC, operculum and insula responses (Murdaugh *et al*, 2012). Greater reductions in activity over the intervention period in VTA, putamen, insula and hippocampus were associated with greater weight loss maintenance 9 months later, consistent with earlier studies where lower food cue reactivity is associated with less weight gain (Yokum *et al*, 2011).

Neuroimaging has also demonstrated activity in corticolimbic networks that regulate eating may be consciously controlled to modulate food cue salience and reduce habitual eating tendencies. In healthy volunteers, evaluating the health and taste value of food images modulated VMPFC activity, whilst self-control when choosing foods engaged DLPFC (Hare *et al*, 2009). Active restraint towards appetising food images, by thinking about the long term consequences of eating such foods, engaged OFC, inferior frontal gyrus, insula and DLPFC in healthy females, with greater restraint associated with greater food-related DLPFC activity (Hollmann *et al*, 2012). In a similar study, "up-regulation" of thoughts about the pleasure of eating high-calorie foods increased reward network activity in ventral striatum, VTA, medial OFC, VMPFC, operculum and insula (Siep *et al*, 2012). Activity of these networks is less well developed in adolescence, where "cognitive appraisal" of appetising foods does evoke greater superior frontal gyrus and VLPFC activity, but "suppression" is less effective in engaging prefrontal control centres, instead increasing operculum activity (Yokum and Stice, 2013).

Physical activity may also have complementary effects on food-related brain activity. Observational studies show greater self-reported physical activity was associated with decreasing differential responses to high- compared to low-calorie food images in

medial OFC and anterior insula (Killgore *et al*, 2013). However the study included lean, overweight and obese subjects, which may have confounded the results, and whose feeding state was not well defined. Acute high intensity aerobic exercise in fasted lean volunteers reduced responses to food images in putamen, insula and operculum, post-central and supramarginal gyri (Evero *et al*, 2012). A 6 month exercise programme resulting in reduced food intake, fat mass and a trend towards a reduction in total body weight in overweight and obese volunteers, reduced food image-evoked activity in insula, parietal and visual cortex, with greater reduction in fat mass and body weight associated with greater attenuation of insula responses (Cornier *et al*, 2012). The collective findings may represent a reduction in food-salience and interoception encoding with both acute and chronic exercise.

The changes in activity of central homeostatic and hedonic networks after bariatric surgery are also of interest. PET/SPECT data are currently conflicting, with increases (Steele *et al*, 2010), decreases (Dunn *et al*, 2010), and no change (de Weijer *et al*, 2014) in post-bariatric surgery striatal dopamine receptor availability reported. However, current BOLD fMRI data are more consistent with each other. Longitudinal studies show that whilst differences in somatosensory cortex responses to ingested glucose in obese compared to lean individuals persisted despite Roux-en Y gastric bypass (RYGB), defective hypothalamic responses in obesity improved post-operatively, with hypothalamic functional connectivity with OFC and somatosensory cortex changing in pattern towards that of lean subjects (van de Sande-Lee *et al*, 2011). RYGB also reduced post-prandial DLPFC, precuneus, dorsal cingulate, lentiform nucleus and ventral striatum activation to visual and auditory cues of high- compared to low-calorie foods, such that there were no longer any differences in cue-evoked activation or desire to eat between the two food categories, due to greater reduction of responses to high-calorie food cues post-operatively (Ochner *et al*, 2011). These post-operative changes in lentiform nucleus, caudate, DLPFC, ACC, thalamus activity were associated with the post-operative reductions in "wanting" or desire to eat the presented stimuli, but not "liking" (Ochner *et al*, 2012b). Cross-sectional studies show high-calorie food images were less appealing and elicited lower OFC, striatum, hippocampus and cingulate gyrus activation in post-RYGB patients than post-gastric banding patients (Scholtz *et al*, 2014). Together these data are consistent with a corticolimbic network that is hypersensitive to food cues in obesity, which

normalises following bariatric surgery. Unlike weight-loss achieved via lifestyle interventions, the post-operative *reduction* in DLPFC activity suggests this is a direct reduction in reward network activity rather than being dependent on increased prefrontal inhibitory control, and may be less prone to disinhibition (Volkow *et al*, 2011).

To date, only one study has examined the effect of therapies in patients with T2DM on food related brain activity. As discussed earlier, the normal reduction in hypothalamic BOLD signal with oral glucose is absent in T2DM (Vidarsdottir *et al*, 2007). Men with early T2DM undergoing just 4 days of an insulin sensitising very low-calorie diet showed restitution of this response (Teeuwisse *et al*, 2012), which the authors suggest may represent an improvement in hypothalamic insulin sensitivity.

1.2.7 Impact of normal ageing on brain responses to food ingestion and food cues

In keeping with post-mortem data (Rinne *et al*, 1990), PET studies demonstrate reduced striatal dopamine D_1 and D_2 receptor availability with age, decreasing by 7.4% and 7.9% per decade of life passed respectively from young adulthood (Volkow *et al*, 1996; Wang *et al*, 1998). These studies mirror [^{18}F]FDG-PET data where ageing was associated with reduced fasting $CMR_{glucose}$ in regions including OFC and DLPFC in healthy volunteers, as well as insula in men and caudate in women (Kim *et al*, 2009). This is in keeping with an increasing deficit in dopaminergic reward processing with age that could explain the weight gain observed in middle age.

The post-prandial reduction in food cue-evoked corticolimbic BOLD signal in adults (van der Laan *et al*, 2011) has also been demonstrated in younger children in OFC, insula, parahippocampal gyrus, cingulate and fusiform gyri (Holsen *et al*, 2005). However, prefrontal responses to high-calorie food images appear to be significantly smaller in children and adolescents than young adults, with OFC responses increasing in strength as children get older (Killgore and Yurgelun-Todd, 2005b). This would suggest that responses to food in prefrontal cortical regions involved in processing reward salience and self control continue to develop and mature from adolescence through to young adulthood, with voxel based morphometry data showing associated structural changes in both PFC and striatum (Sowell *et al*, 1999).

The central effects of obesity have been examined in children. Non-fasted responses to food images were exaggerated in DLPFC and diminished in caudate in obese compared to lean children, in keeping with a reward deficit model (Davids *et al*, 2010). Another study showed that responses to food images in obese children were exaggerated in PFC when fasted and OFC when fed (Bruce *et al*, 2010). Whilst both groups of children showed post-prandial decreases in prefrontal and insula activation, the reduction in PFC activity was smaller in the obese, with post-prandial reductions in striatal, amygdala and parahippocampal responses observed in lean children only, in keeping with adult data. Fasting insulin concentrations positively correlated with post-prandial food cue-evoked hippocampal and insula activation, and negatively correlated with frontal gyrus and thalamus activation (Wallner-Liebmann *et al*, 2010). A study showing overweight children who lost weight after a 45 week diet and exercise programme had greater food image-evoked putamen activation than non-responders to the intervention (Kinder *et al*, 2014), contrary to adult data (Murdaugh *et al*, 2012), may suggest a restoration of dopaminergic striatal reward processing.

As obesity is most prevalent in older, middle aged adults (Flegal *et al*, 2010), it is prudent to investigate the impact of further ageing from young adulthood on such food-associated neural responses. One group investigated the effect of ageing when evaluating the pleasantness of a number of taste cues such as sucrose, caffeine, and citric acid, before and after a 700kcal meal with greater responses to such stimuli in older than younger adults, in both fasted (generally activation) and fed (generally "negative activation" or deactivation) states, in regions including OFC, superior, medial and inferior frontal gyri, caudate and parahippocampal gyrus (Jacobson *et al*, 2010). Significant negative associations between BMI or waist circumference and responses in dopaminergic reward centres including caudate, NAcc, and amygdala in older adults when fasted, but not when fed have been observed, with no such associations detected in younger adults when either fasted or fed (Green *et al*, 2011). However, these studies compared a group of young adults aged between 18-29 years, with a group of older adults aged between 65-87 years, using artificial tastants rather than food related stimuli. Examination of potential changes in corticolimbic regulation of satiety and satiation that may be observed during the intervening years when obesity is most prevalent is called for.

1.2.8 Interim summary

Functional neuroimaging has shown that whilst changes in nutritional status alter activity of homeostatic brain centres (hypothalamus), activity also changes in regions that process reward (striatum), food salience (OFC), interoceptive awareness (insula), memory (parahippocampal formation) and inhibitory control (DLPFC, lateral OFC). The response to external food cues in these centres depends on the energy value of the stimuli and an individual's current nutritional status, which modulate cue valence and its representation in these centres. Central homeostatic and hedonic network regulation of appetite appears to mature from childhood to adulthood, and is altered in obesity and T2DM, conditions associated with systemic insulin resistance. Indeed, many studies show associations between circulating insulin, insulin resistance, and neural responses to food and food cues. Whilst hyperinsulinaemic euglycaemic clamp measures of peripheral (predominantly skeletal muscle) insulin resistance do not predict future weight gain after adjusting for baseline BMI (Rebelos *et al*, 2011), studies using fasting surrogate markers that predominantly reflect hepatic insulin resistance under physiological conditions, do (Chen *et al*, 2015; Howard *et al*, 2004; Mosca *et al*, 2004). Evidence for the involvement of circulating insulin at physiological concentrations in appetite regulation via these brain networks, and how defects in these processes might promote overeating in man and thus explain this association between systemic insulin resistance and future weight gain are discussed.

1.3 Insulin modulates homeostatic and hedonic networks of appetite control

Pancreatic insulin, circulating concentrations of which are associated with increasing adiposity, modulates central responses to satiation signals (reviewed by (Woods and D'Alessio, 2008)). The majority of cerebral insulin derives from circulating insulin which crosses the BBB via saturable transporters, with highest transport rates in the olfactory bulb, hypothalamus and pons-medulla (Banks, 2004; Banks *et al*, 2012; Schwartz *et al*, 1992). As reviewed by Schwartz *et al* (1992), mathematical models suggest insulin crosses the BBB into brain interstitial fluid first, before reaching cerebrospinal fluid (CSF), consistent with observations that insulin concentrations in

CSF are only 5-10% that of plasma. However, recent data reviewed by Gray *et al* (2014) suggests a small proportion of insulin leaves the circulation via the ventricular choroid plexus directly into CSF before reaching the subarachnoid space, with a larger proportion crossing the BBB, the two admixing in the paravascular Vichow-Robin space before eventually entering brain interstitial fluid (Figure 1.3).

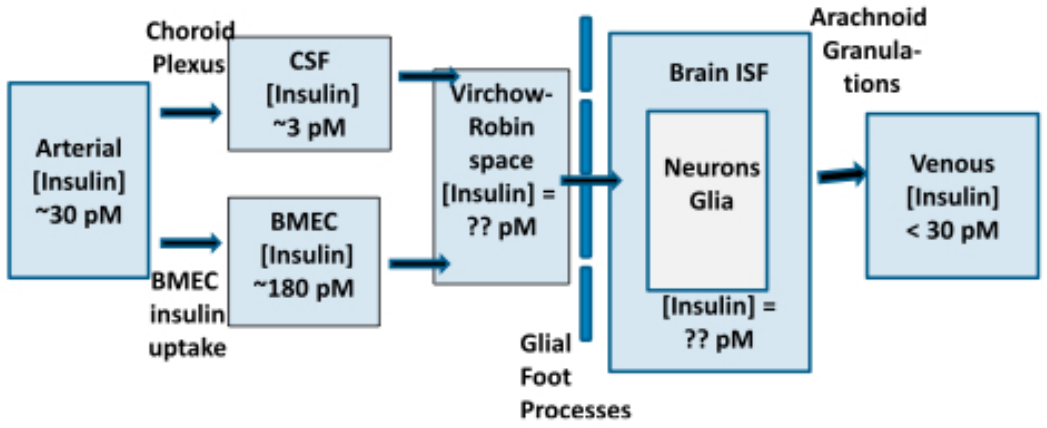

Figure 1.3

Insulin transport from circulation to brain interstitial fluid. BMEC = brain microvascular endothelial cell (BBB). From Gray *et al* (2014).

Whichever model is correct, the finding that whilst peripherally infused insulin reaches CSF relatively slowly (Wallum *et al*, 1987), insulin reaches brain tissue rapidly (Banks and Kastin, 1998), is in keeping with the hypothesis that circulating insulin may act as a satiety signal in the brain. Insulin receptors with intrinsic tyrosine kinase activity are located in hypothalamic arcuate nucleus, ventromedial hypothalamus (VMH), LH and PVN, VTA, olfactory bulb, hippocampus, cerebellum, cerebral cortex and NTS in rats (Havrankova *et al*, 1978), with post-mortem data suggesting similar patterns of distribution in humans (Hopkins and Williams, 1997). Whilst insulin up-regulates peripheral GLUT4 glucose transporters, glucose transport across the BBB (GLUT1) and into neurones (GLUT2/3), astrocytes (GLUT1) and glia (GLUT5) is largely insulin independent. Instead, activation of neuronal insulin receptor signal transduction pathways that involve mitogen-activated protein kinases (MAPK) and phosphatidylinositol 3-OH kinase (IRS-PI3K), modulate neural membrane potential by opening K_{ATP} channels, and neuropeptide production (Belgardt and Brüning, 2010; Plum *et al*, 2005, 2006). ICV injection (Air *et al*, 2002;

Brown *et al*, 2006; Chavez *et al*, 1995) or intranasal inhalation (Hallschmid *et al*, 2004a, 2012) of insulin or insulin mimetics, increasing brain insulin whilst avoiding systemic hypoglycaemia, reduces feeding and weight, presumably through altering such central signalling mechanisms. Insulin (and leptin) increases arcuate nucleus transcription of pro-opiomelanocortin (POMC), a precursor of α-melanocyte-stimulating hormone (α-MSH), which acts on melanocortin receptors (MC3R and MC4R) to reduce food intake, and decreases transcription of neuropeptide Y (NPY) and the melanocortin receptor antagonist, Agouti-related peptide (AgRP), which both directly inhibit POMC neuronal activity. Downstream actions on LH and PVN reduce food intake (Belgardt and Brüning, 2010; Plum *et al*, 2005, 2006).

As insulin receptors are located in VTA, prefrontal and insular cortices (Havrankova *et al*, 1978), circulating insulin may not only regulate food intake with respect to physiological requirements via the hypothalamus, but may modulate eating behaviour through higher motivational and reward networks (Figlewicz, 2003; Figlewicz and Benoit, 2009). In addition, the findings that (i) insulin activates peripheral nodose ganglion vagal afferent neurones in vitro (Iwasaki *et al*, 2013), and (ii) insulin administration into the dorsal vagal complex where these afferent neurones terminate within the area postrema reduces food intake in vivo (Filippi *et al*, 2014), may suggest the appetite suppressive effects of insulin are also mediated via vagal afferents to the brain. Parenthetically, centrally applied insulin, mediated through K_{ATP} channel activation, improves peripheral effects of meal-related insulin by decreasing hepatic gluconeogenesis in animal studies (Pocai *et al*, 2005), an important mechanism in post-prandial glucose control.

1.4 Defective central insulin signalling leads to obesity in animal models

Schwartz and Porte (2005) proposed that obesity and T2DM may develop through impaired processing of central adiposity- or nutrient-related signals, including insulin, leading to weight gain and further insulin resistance. Animal data support this model, showing impaired transport of insulin across the BBB in diet-induced obese dogs (Kaiyala *et al*, 2000) and obese Zucker *fa/fa* rats (Stein *et al*, 1987); development of

obesity and peripheral insulin resistance following knockout of brain insulin receptors or use of anti-insulin receptor antibodies (Brüning *et al*, 2000; Obici *et al*, 2002); and impairment of downstream hypothalamic insulin signalling, POMC expression, reduced weight loss and reduced suppression of feeding with ICV insulin in animals fed a high fat diet (Arase *et al*, 1988; Clegg *et al*, 2005, 2011). Additionally, other studies have shown obese IRS-2 knockout mice have intact suppressive responses to insulin in hypothalamic orexigenic ghrelin-responsive neurones, but impaired insulin responses within nodose ganglion afferents (Iwasaki *et al*, 2013), whilst high-fat fed rats failed to respond to insulin injected into the dorsal vagal complex (Filippi *et al*, 2014), suggesting that insulin resistance within the vagus may also contribute to the development of obesity. The finding that rats prone to diet-induced obesity have pre-existing impaired central insulin signalling, as do animals fed a high fat diet prior to weight gain, suggests that central insulin resistance may play a causative role in the development of obesity (Clegg *et al*, 2005, 2011). Insulin resistance may also affect reward networks that influence non-homeostatic eating behaviour and energy balance. Evidence to support a role of the diminished effects of insulin on the suppression of reward network activity and resultant hyper-responsiveness to food-related stimuli include the consumption of high fat diets that reduce ICV insulin- (or leptin-) mediated suppression of sucrose self-administration (Figlewicz *et al*, 2006) and loss of conditioned place preference to amphetamine (Davis *et al*, 2008). High fat diet-induced central insulin resistance could be a primary event leading to systemic metabolic dysfunction both directly, and through dysregulated eating, subsequent weight gain (Pagotto, 2009). The mechanisms involved in the development of neuronal insulin resistance continue to be investigated, but include altered availability of insulin receptors and IRS through overexpression of suppressor of cytokine signalling 3 (SOCS3) and protein phosphatase 1b, tumour necrosis factor-alpha and IL-6, which are involved in inflammation and induced by high fat diets, as well as saturated fatty acids directly (Belgardt and Brüning, 2010). However the finding that a change back to a low fat diet in rats with diet-induced obesity reduces weight, increases CSF insulin after peripheral administration of insulin, and regains the anorexic effects of centrally applied insulin, suggests that defects in cerebral insulin transport and action are reversible (Begg *et al*, 2013).

1.5 Insulin modifies brain activity in healthy humans

The following studies discussed show that intravenous insulin modulates spontaneous and task-driven brain activity, although none have primarily been studies of appetite regulation, unlike the studies of intranasal insulin.

1.5.1 DC potential, EEG and MEG studies of the effect of intravenous insulin

Electrophysiological techniques have demonstrated cerebral effects of circulating insulin. In one electroencephalographic (EEG) study, an intravenous insulin and glucose bolus produced a negative direct current (DC) potential shift in frontal brain regions that started within 7 mins of insulin administration and reached a maximum 40-50 mins post-injection, occurring concurrently with changes in plasma insulin, indicating a rapid effect of circulating insulin on brain activity (Hallschmid *et al*, 2004b). This was attenuated and delayed when hypoglycaemia was permitted, suggesting nutrient depletion may override central insulin signalling. In a magnetoencephalographic (MEG) study during a stepped hyperinsulinaemic euglycaemic clamp, high rate insulin infusions increased spontaneous global beta and theta activity, as well as activation of mismatch fields in the auditory cortex during auditory discriminant tasks to two different tones (Tschritter *et al*, 2006). Two further EEG studies have examined the effect of circulating insulin on brain activity during cognitive tasks. In one study, insulin infusion, under hyperinsulinaemic euglycaemic clamp conditions, altered auditory evoked potential (AEPs) responses specifically to target stimuli, presented amongst standard stimuli during an oddball vigilance task, increasing "P3" (positive deflection 280-700 ms post-stimulus, an indicator of target processing) latency in parietal, frontal and central leads and frontal slow negative potentials (280-700 ms) (Kern *et al*, 2001). Better performance during declarative memory word recall and Stroop attention tasks, improvements in mood and decreased hunger were also observed, which may have been facilitated by the changes in frontal brain activity. However, a second study failed to show an effect of intravenous euglycaemic insulin infusion, with concurrent somatostatin infusion, on occipital visual evoked potentials (VEPs) to viewing a reversing chequerboard, potentially due to this task being less cognitively demanding (Seaquist *et al*, 2007). However, these

studies are generally in keeping with an effect of circulating insulin on activity of attention and memory processing centres.

1.5.2 PET studies of the effect of intravenous insulin

Electrophysiology has good temporal, but poor spatial resolution, a limitation overcome by functional neuroimaging. Early studies employed PET. Peripheral insulin infusion to physiological concentrations, whilst suppressing endogenous insulin production using somatostatin, increased global $CMR_{glucose}$ by 15.3±12.5% in healthy men, measured using [^{18}F]FDG)-PET (Bingham *et al*, 2002). Regional analyses showed physiological concentrations of insulin had less effect on cerebellar and brainstem $CMR_{glucose}$, hypothesised to be a protective property, ensuring sufficient glucose uptake during starvation in these homeostatic centres at times when insulin levels are particularly low. In a subsequent study using the same protocol, insulin sensitive men showed a 17.4% insulin-induced global increase in $CMR_{glucose}$ (Anthony *et al*, 2006). With respect to global glucose uptake, insulin infusion was associated with relative local increases in glucose uptake in bilateral ventral striatum, and PFC (insula, ACC, retrosplenial cortex) and local decreases in cerebellar and bilateral amygdala/hippocampal regions. Such changes in $CMR_{glucose}$ reflect altered neuronal activity, either as a direct phenomenon of insulin on cellular metabolic processes, or by indirectly influencing neuronal activity, and suggest systemic insulin resistance is associated with regional brain resistance to circulating insulin. However, behavioural effects of these changes in brain activity were not examined.

1.5.3 BOLD fMRI studies of the effect of intravenous insulin

BOLD fMRI has been used to examine the effect of circulating insulin on brain activity during cognitive tasks. One of the first studies examined BOLD signals evoked by viewing a reversing chequerboard before and during hyperinsulinaemic euglycaemic clamp conditions, combined with somatostatin infusion (Seaquist *et al*, 2007). Insulin reduced visual cortex responses by 16%. However, with just 5 subjects, only subject-level analyses were performed, with no control for order effects. Another study examined temporal lobe BOLD responses to a picture encoding task during a baseline session followed by hyperinsulinaemic euglycaemic

clamp on one day, and on another day a baseline study followed by either saline infusion or a higher rate hyperinsulinaemic euglycaemic clamp (Rotte *et al*, 2005). The combined effect of insulin at all rates was reported to reduce reaction times compared to baseline, although direct comparisons between pairs of scans showed no effect of insulin. Compared to saline, low rate insulin infusion was associated with right fusiform gyrus activation, and when all 15 insulin infusion studies were grouped, bilateral fusiform gyrus activation was observed, a region involved in visual attention processing. The lack of significant findings with the high rate insulin infusion alone and thus lack of a dose-response relationship, makes the validity of these data questionable, but may be due to the study being underpowered. At present, the effects of intravenous insulin on BOLD fMRI measures of brain activity during studies of appetite have not been examined.

1.5.4 Behavioural / phenotypic studies of the effect of intranasal insulin

Intranasally applied insulin increases CSF insulin concentrations without significant effects on peripheral insulin or glucose concentrations (Born *et al*, 2002), reaching the brain rapidly via direct extracellular pathways (Balin *et al*, 1986). Groups in Germany have performed a series of investigations of the metabolic and neurological effects of intranasal insulin.

Intranasal insulin acutely has implicit effects on satiation in men, reducing energy intake during an ad-libitum meal without explicit effects on satiation or satiety as measured by subjective hunger ratings before or after a meal (Benedict *et al*, 2008). This was not observed in women, who instead showed acute cognitive improvements. Prolonged intranasal insulin therapy over 8 weeks also reduced total body weight and body fat in lean men, but not lean women (Hallschmid *et al*, 2004a). The weight loss may have been due, in part, to reduced hunger observed after acute drug administration, but also increased post-prandial thermogenesis (Benedict *et al*, 2011). Insulin also improved delayed word recall, mainly for emotional and neutral, rather than for food-related words at 8 weeks in men and women, and improved mood, implying insulin acted on hedonic brain networks (Benedict *et al*, 2004). A further study replicated the observation that intranasal insulin administered when fasted had no effect on satiation during a subsequent meal in women, but it did demonstrate an

effect on satiety when administered immediately after eating, curtailing the post-prandial rise in hunger and reducing the palatability of a subsequent pleasant snack (Hallschmid *et al*, 2012). Intranasal insulin thus appears to have differential effects in men and women on satiation and satiety. Such "resistance" to the satiation effects of cerebral insulin in women is consistent with observations in animal studies (Clegg *et al*, 2003). This may not be a sex hormone dependent phenomenon, given the lack of effect of intranasal insulin on hunger or food intake during a subsequent ad libitum meal in both pre-menopausal women (all on oral contraception) and post-menopausal women, of similar degree of insulin resistance (Krug *et al*, 2010).

In addition to these appetite effects, intranasal insulin also reduces pancreatic insulin secretion, pre- and post-meal ingestion, with either no effect or small but significant reductions in serum glucose (Benedict *et al*, 2008, 2011; Heni *et al*, 2012), which may be attributed to insulin-mediated activation of a central neural pathway, in keeping with animal data showing cerebral insulin reduces hepatic glucose production, interference of which reduces the suppressive effects of circulating insulin on hepatic gluconeogensis (Pocai *et al*, 2005). Furthermore, improvements in insulin sensitivity after an acute administration of intranasal insulin, quantified by HOMA-IR (mainly representing hepatic insulin sensitivity) (Heni *et al*, 2012) and hyperinsulinaemic euglycaemic clamp techniques (predominantly representing skeletal muscle insulin sensitivity) in lean, but not obese men, that were associated with changes in heart rate variability (Heni *et al*, 2014c), may provide evidence that the acute peripheral insulin sensitising effects of cerebrally-applied insulin are mediated by the parasympathetic nervous system, effects that are diminished in obesity

1.5.5 EEG studies of the effect of intranasal insulin

Intranasal insulin has been found to have similar effects to intravenous insulin, on resting brain activity during EEG studies of healthy men, inducing marked negative DC potential shifts in frontal brain regions (Hallschmid *et al*, 2004b). Repeated, pulses of intranasal insulin in healthy men alter AEPs to target stimuli during an oddball vigilance task, increasing P3 latency as found with intravenous insulin, and reducing "N1" (100 ms post-stimulus vertex negative deflection, a nonspecific cortical arousal response) and P3 AEP component amplitudes, being most pronounced

over frontal brain regions (Kern *et al*, 1999). Hunger was unaltered although this study was not designed to examine intranasal insulin effects on appetite.

1.5.6 BOLD fMRI studies of the effect of intranasal insulin

Functional neuroimaging studies of spontaneous, task-independent BOLD signal or "resting state" activity are now emerging. Two reports by the same group examined the effect of intranasal insulin in healthy females on the fractional amplitude of low-frequency fluctuation (fALFF) in spontaneous BOLD signal. Intranasal insulin improved markers of peripheral insulin sensitivity. Increasing insulin sensitivity 30 mins after intranasal insulin, was associated with concurrent decreasing hypothalamic, putamen and OFC activity, whilst at 120 mins, increasing insulin sensitivity was associated with greater insula activity (Heni *et al*, 2012). The authors suggested the improvements in peripheral insulin sensitivity were mediated by insulin signalling in brain reward networks. However, a transient rise in serum insulin concentrations was observed after insulin inhalation, before a subsequent fall in serum glucose, insulin and c-peptide during fMRI, suggesting intranasal insulin leaked into the systemic circulation. The reduction of glucose and endogenous insulin secretion puts the use of HOMA-IR as a measure of dynamic changes in insulin sensitivity into question and the placebo data were not included in the analyses. A reduction in resting OFC and hypothalamic activity between 30-90 mins after intranasal insulin compared to placebo administration was later reported, suggesting central insulin signalling might reduce spontaneous activity of homeostatic and reward processing centres in the fasted state (Kullmann *et al*, 2013). This suppressive effect of activity by insulin diminished with increasing body mass in ACC at 30 mins, and PFC at 90 mins, suggests a possible resistance to the effects of insulin, although all subjects were lean, precluding any conclusion about its effects in obesity. In addition, whilst subjective hunger in the fasted state was unaffected by intranasal insulin, the study was not designed to examine central appetite control mechanisms.

BOLD fMRI is more conventionally used to examine task-driven signal changes. One study investigated the effect of intranasal insulin during visual stimulus-evoked fMRI (Guthoff *et al*, 2010). Intranasal insulin increased blood insulin concentrations when the post-insulin fMRI commenced, returning to baseline concentrations by the

time fMRI was completed, without affecting glucose concentrations. Subjects identified blurred images that gradually became clear, faster if they were food than object images. Although intra-nasal insulin did not affect response times, it did attenuate the deactivation to food images in bilateral fusiform gyrus, right hippocampus, right superior temporal cortex and left post-central cortex for the "pop-out condition" between image presentation to recognition, and the right middle frontal cortex for the "response condition" between recognition to the end of stimulus presentation. These data suggest cerebral insulin may alter activity of regions involved in visual processing, recognition and decision making, with preferential effects towards food-related stimuli, and may imply a role for post-prandial insulin on appetite regulation when faced with food cues.

1.5.7 ASL fMRI studies of the effect of intranasal insulin

pASL fMRI has shown the acute administration of intranasal insulin does not affect visual cortical rCBF, nor concurrent BOLD signal, at rest and during visual stimulation (Grichisch *et al*, 2012). However, this study was small with a limited ROI analysis, such that effects of insulin elsewhere in the brain were not measured, nor its effect on appetite or weight.

A larger randomised control cASL study showed intranasal insulin acutely increases bilateral insula, opercula and left putamen and caudate rCBF in healthy men, regions that process interoception, gustatory sensation and reward (Schilling *et al*, 2013). Insulin did not alter subjective measures of appetite, which may have been due to the much lower doses of insulin used compared to previous studies, and may have been affected by the variable period of fasting prior to the scan, with subjects being studied either in the morning or afternoon. Previous studies also show lack of effect on subjective measures of appetite using visual analogue scales, despite reductions in food intake (Benedict *et al*, 2008; Jauch-Chara *et al*, 2012; Kern *et al*, 1999; Kullmann *et al*, 2013), suggesting intranasal insulin may induce satiation implicitly. Interestingly, a study of the cognitive effects of intranasal insulin in patients with non-insulin treated T2DM demonstrated increases in insula rCBF with intranasal insulin that were not observed in the non-diabetic control group (Novak *et al*, 2014). However, the use of the same low dose of insulin in a much older age group

compared to previous studies, the mixed gender and unreported BMI of both groups, and the use of oral hypoglycaemic agents that may potentially influence cerebral responsiveness to insulin, may explain the apparently greater effects of intranasal insulin in diabetic subjects and the apparent lack of effect in controls in this study.

As described earlier, intranasal insulin immediately improves peripheral insulin sensitivity, as indicated by an increase in glucose infusion rates during a concurrent hyperinsulinaemic euglycaemic clamp (Heni *et al*, 2014c). In a sub-section of subjects, pASL-measured changes in hypothalamic rCBF after intranasal insulin, were correlated with the accompanying changes in insulin sensitivity. Collectively, these ASL data are consistent with an effect of intranasal insulin, via homeostatic and reward processing centres, on peripheral insulin sensitivity and appetite, respectively.

1.5.8 Brain MR spectroscopy studies of the effect of intranasal insulin

The intraneuronal effects of insulin in man are now being examined through other MRI techniques. For example, the reduction in calorie intake during an ad-libitum meal by the preceding administration of intranasal insulin is associated with insulin-evoked increases in cortical ATP and phosphocreatinine concentrations measured by ^{31}P magnetic resonance spectroscopy (Jauch-Chara *et al*, 2012). The authors interpret these data to suggest that the availability of cerebral energy substrate *per se* influences eating behaviour, with less energy leading to greater food intake, and that insulin may manipulate brain energy levels. However, it is also possible that insulin may similarly increase ATP levels in brain networks that regulate appetite, reflecting changes in neuronal activity, in order to induce satiation.

1.5.9 Interim summary

By increasing cerebral insulin levels whilst avoiding hypoglycaemia, intranasal insulin acutely increases brain energy substrate (Jauch-Chara *et al*, 2012), post-prandial thermogenesis (Benedict *et al*, 2011) and satiation (Benedict *et al*, 2008) in healthy men, whilst chronic administration reduces body weight and fat (Hallschmid *et al*, 2004a). Cognitive effects of acute intranasal insulin are more apparent in women (Benedict *et al*, 2008; Krug *et al*, 2010), but subtle changes in satiety,

influencing post-prandial food choices, have been shown (Hallschmid *et al*, 2012). Physiological concentrations of circulating insulin increase global $CMR_{glucose}$ (Bingham *et al*, 2002) with local increases in $CMR_{glucose}$ in ventral striatum, insula, PFC and ACC and decreases in cerebellum, amygdala and hippocampus (Anthony *et al*, 2006), and reduce visual cortex responses to visual stimuli (Seaquist *et al*, 2007). Insulin administered intravenously with glucose, or intranasally, alters EEG (Hallschmid *et al*, 2004b; Kern *et al*, 1999, 2001) and MEG (Tschritter *et al*, 2006) measures of frontal brain activity, as well as resting state OFC and hypothalamic BOLD signal (Kullmann *et al*, 2013) in non-appetite studies, improves processing of food-related visual stimuli with changes in frontal and temporal cortical, fusiform gyrus and hippocampus BOLD signal (Rotte *et al*, 2005; Guthoff *et al*, 2010), and increases insula, operculum and ventral striatum perfusion (Schilling *et al*, 2013). Whilst acute improvements in peripheral insulin sensitivity associated with changes in hypothalamic resting state activity and perfusion following intranasal insulin are consistent with changes in homeostatic network activity by cerebral insulin (Heni *et al*, 2012, 2014c), these data support the hypothesis that insulin may suppress appetite by modulating dopaminergic "wanting" and opioid "liking" reward network activity.

1.6 Evidence of brain insulin resistance in man

CSF insulin levels are lower in obesity, and CSF:plasma insulin ratios are negatively associated with BMI, fat mass, waist and hip circumference, and positively associated with insulin sensitivity, the latter explaining 40% of the variance in this ratio (Kern *et al*, 2006), this relationship persisting after adjusting for age, gender and BMI (Heni *et al*, 2014b). Insulin transport across the BBB and brain insulin receptor expression diminish with age in animal (Frank *et al*, 1985) and human post-mortem studies (Frölich *et al*, 1998), and CSF:plasma insulin also falls with age (Sartorius *et al*, 2015). These data suggest that insulin transfer across the BBB falls with normal ageing, and is impaired in insulin resistant states.

1.6.1 fMRI studies of resting state activity

Increasing HOMA-IR is associated with increasing pASL measures of resting rCBF in somatosensory cortex, operculum and insula, DLPFC and posterior cingulate cortex (PCC) in healthy, fasted volunteers (Ryan *et al*, 2013). This suggests systemic insulin resistance modulates activity of regions considered to be part of the default mode network (DMN), which is active at rest and reflects spontaneous, non-task-driven activity, that are also regions involved in corticolimbic reward processing. Functional connectivity or synchronicity within neural networks is another measure of resting state brain activity. In a study of functional connectivity within five networks, some proposed to be involved in food processing, functional connectivity strength in the fasted state was greater in precuneus and PCC (DMN) and lower in right ACC (DMN) and left insula (temporal lobe network) in obesity (Kullmann *et al*, 2012). The authors proposed that this might indicate altered connections between regions involved in higher cognitive (PCC) and affective processing (ACC) and in orexigenic regions (insula) that regulate eating in obesity. Functional connectivity strength was also positively associated with BMI, independent of fasting insulin levels, in left OFC (prefrontal higher executive function network) and left precuneus (DMN) and negatively associated with BMI in right ACC (DMN) and left insula (temporal cortex network). Interestingly, fasting functional connectivity strength was negatively associated with the screening Matsuda index of insulin resistance, independent of BMI, in left OFC (prefrontal network) and right putamen (basal ganglia network), suggesting that increasing peripheral insulin resistance is associated with increasing activity in regions involved in reward processing and higher executive or inhibitory control. The impact of systemic insulin resistance on central appetite control mechanisms using functional connectivity techniques has yet to be explored.

1.6.2 EEG/MEG studies of the effect of intravenous insulin

Electrophysiological studies provide more conclusive evidence for cerebral resistance to insulin. For example, the insulin-induced increase in magnetic mismatch negativity and spontaneous beta and theta band cortical activity discussed earlier in lean subjects during hyperinsulinaemic euglycaemic clamp conditions, was either diminished or absent in obese subjects (Tschritter *et al*, 2006). When stratified by *Insulin Receptor Substrate-1* polymorphism, insulin-induced beta activity was greater in subjects

carrying wild-type Gly/Gly than Gly/Arg or Arg/Arg genotypes (Tschritter *et al*, 2006), the latter genotypes linked with reduced insulin signalling and peripheral insulin resistance (Marini *et al*, 2003). Similarly, when stratified by *FTO* genotype, reduced insulin-induced beta activity is observed in subjects carrying the obesity (AC or CC) than wild-type (AA) allele, independent of *IRS-1* polymorphism (Tschritter *et al*, 2007b). Whilst these earlier studies demonstrated a negative association between insulin-induced beta and theta activity with BMI (Tschritter *et al*, 2006, 2007b), more recent analyses suggest increasing BMI is independently negatively associated with theta activity, and ageing may reduce insulin-induced beta activity (Tschritter *et al*, 2009a). These also demonstrated an association between peripheral insulin sensitivity and beta and theta activity. Although these associations were no longer significant after adjusting for BMI and age, a subsequent study showed insulin-induced theta activity was inversely associated with fasting saturated NEFA, visceral fat and liver fat, independent of BMI, with the effect of fasting saturated NEFA remaining significant after correcting for the latter fat depots, suggesting dietary fat may play a role in the development of cerebral insulin resistance (Tschritter *et al*, 2009b).

In clinical practice, the use of detemir, a longer acting insulin analogue, compared to intermediate acting NPH insulins, has been associated with less weight gain. The long duration of action of detemir is achieved by a ^{14}C fatty acid side chain that binds to albumin. As albumin may reach the CSF via the choroid plexus epithelia, detemir may have greater access to the brain than human insulin. Indeed, healthy men undergoing a hyperinsulinaemic euglycaemic clamp showed more negative DC-potential shifts with intravenous detemir than human insulin, the degree to which was associated with differences in carbohydrate and protein intake during a post-clamp ad-libitum meal, with significantly lower total energy intake after infusion of detemir (Hallschmid *et al*, 2010). This was not associated with any differences in subjective appetite between the two clamp conditions, suggesting that the greater anorexigenic effects of detemir may by mediated by satiation signals that terminate meal ingestion, independent of the motivation driven by hunger or fullness. Much higher doses of detemir than human insulin were used to compensate for pharmacodynamic differences, in order to achieve comparable effects on peripheral glucose and glucose infusion rates during the clamp. However, whilst the peripheral effects may have been equipotent, animal data suggest the central pharmacodynamics of the two

insulins are not, detemir having greater central effects than human insulin, at doses of equal systemic glucose lowering effect (Hennige *et al*, 2006).

Nevertheless, if cerebral insulin resistance does occur at the BBB level, these studies may suggest that it can be overcome by insulin detemir. A recent study demonstrated beta activity was unaffected by human insulin during hyperinsulinaemic clamp conditions in overweight subjects, but increased when infused with detemir to levels observed in lean subjects receiving human insulin (Tschritter *et al*, 2007a). It should be noted that in overweight subjects the initial bolus of detemir was 5-fold greater and infusion rate double that of human insulin, resulting in 40-fold higher level of detemir than human insulin due to albumin binding with the former, whilst the glucose infusion rate to maintain euglycaemia was significantly greater with human insulin. However, the authors reported that this increase in beta activity persisted after correcting for differences in glucose infusion rate. Interestingly, in patients with type 1 diabetes, detemir compared to NPH insulin increases fullness and reduces weight, increases CSF levels of insulin, and increases rCBF in appetite-reward networks (insula, putamen, caudate, thalamus, ACC, PCC and right medial inferior frontal cortex) as measured with [^{15}O]H_2O-PET without any difference in cerebral glucose metabolism during [^{18}F]FDG-PET, and reduces visual food cue-evoked insula BOLD signal (van Golen *et al*, 2013, 2014).

1.6.3 PET studies of the effect of intravenous insulin

When compared to insulin sensitive subjects, insulin resistant subjects (HOMA-IR ≥2.77, representing the upper 20% distribution of HOMA-IR) infused with insulin reaching physiological concentrations, with endogenous insulin secretion inhibited by somatostatin, showed smaller increases in $CMR_{glucose}$ globally and locally in ventral striatum and PFC (including insula), with no difference in local reductions in amygdala, during [^{18}F]FDG-PET (Anthony *et al*, 2006). Although not directly examined, the authors interpret these data within the context of eating behaviour, hypothesising that greater post-prandial insulin responses to a meal are required to generate a pleasant experience in people with systemic insulin resistance, whilst a greater reduction in activity in regions involved in processing fear and anxiety from such an insulin response may exaggerate the sensation of comfort after a meal.

Supraphysiological concentrations of insulin under hyperinsulinaemic euglycaemic clamp conditions increase whole brain $CMR_{glucose}$ by 18% in patients with impaired glucose tolerance (IGT), with no significant effect in healthy volunteers during [^{18}F]FDG-PET (Hirvonen *et al*, 2011). This effect of insulin in IGT patients was maximal in insula, even after correcting for age. Whole brain blood flow measured by [^{15}O]H_2O-PET was not different between the two groups, and did not change with insulin infusion, although changes in rCBF were not assessed. Whilst the effects of hyperglycaemia, obesity and insulin resistance cannot be disentangled, the data from these two studies suggest there is a maximal effect of the lower physiological concentrations of insulin on brain metabolism in insulin sensitive subjects, whilst such responses to insulin are only observed at much higher concentrations in states of peripheral insulin resistance, especially in interoceptive processing centres.

A more recent study of people with newly diagnosed, untreated T2DM or prediabetes showed increasing insulin resistance was associated with decreasing fasted $CMR_{glucose}$, after correcting for fasting and 2 hour post-75g OGTT glucose levels, in OFC, precuneus, PCC, temporal and parietal cortices (Baker *et al*, 2011). Whilst this study's use of HOMA-IR to quantify insulin resistance in abnormal glucose states is questionable, the data are consistent with the earlier PET studies of diminished activity in brain regions involved in processing food salience.

1.6.4 MR spectroscopy studies of the effect of intravenous insulin

A ^{1}H-MRS study demonstrated no differences in baseline cerebral metabolite concentrations between healthy men with low and high insulin sensitivity defined by median whole-body glucose uptake during a subsequent hyperinsulinaemic euglycaemic clamp (Karczewska-Kupczewska *et al*, 2013). However, insulin during the clamp increased frontal concentrations of *N*-acetylaspartate (NAA), a marker of neuronal density, integrity and functionality, and in frontal and temporal regions insulin increased glutamine/glutamate/GABA (Glx) neurotransmitters, and decreased choline and *myo*-inositol, glial cell markers, in high insulin sensitive subjects only. Insulin sensitivity was also associated with insulin-mediated changes in frontal NAA and temporal *myo*-inositol and Glx across the groups. This suggests high concentrations of circulating insulin increase frontal metabolic activity, and alter

frontal and temporal synaptic plasticity, cellular signalling and membrane turnover, effects that are impaired in systemic insulin resistance. These results differ from the [^{18}F]FDG-PET studies that showed the increases in frontal and insula $CMR_{glucose}$ with physiological insulin concentrations in insulin sensitive subjects (Anthony *et al*, 2006), were only demonstrable in insulin resistant subjects during hyperinsulinaemic conditions (Hirvonen *et al*, 2011), but are consistent with a diminished effect of circulating insulin on prefrontal activity in systemic insulin resistance, the threshold for which being dependent on the metabolic process being measured.

1.6.5 Behavioural / phenotypic studies of the effect of intranasal insulin

In addition to characterising the effects of intranasal insulin in health, groups in Germany have used intranasal insulin to demonstrate diminished effects of cerebral insulin in conditions of, or associated with, peripheral insulin resistance. Obese men randomised to receive an 8-week course of intranasal insulin showed no significant change in hunger, body weight, fat or composition, compared to volunteers receiving placebo (Hallschmid *et al*, 2008), unlike the weight loss observed in non-obese men (Hallschmid *et al*, 2004a). This lack of effect in obesity supports the concept of cerebral insulin resistance, but unlike the intravenous insulin studies, at a post-BBB level, which may play a role in the development of obesity.

1.6.6 EEG / MEG studies of the effect of intranasal insulin

A MEG study showed that fasting resting state functional connectivity was no different between lean and overweight volunteers, but differences in insulin-induced theta band path length (a measure of global interconnectedness) became apparent 30 mins after intranasal insulin (Stingl *et al*, 2010). A positive relationship between BMI and theta band path length across the whole group was observed, which the authors interpret as worsening global network communication efficiency with obesity, and thus decreasing signalling between appetite regulatory centres in response to insulin.

Intranasal insulin did not affect performance for a visual memory task of food and non-food pictures, but selectively increased M2 (140-190ms) higher visual cortex-evoked potentials to food pictures in lean subjects only, without affecting MEG

responses to non-food pictures in either group (Guthoff *et al*, 2011). Higher fasting glucose, insulin and c-peptide in overweight subjects were suggestive of greater insulin resistance. This is consistent with subconscious effects of insulin on brain responses to food-related stimuli and satiety processing, effects to which the brain is "resistant", in systemic insulin resistance.

1.6.7 fMRI studies of the effect of intranasal insulin

In the study described earlier that examined the effect of intranasal insulin on resting state brain activity in healthy women, BMI was positively correlated with changes in fALFF 30 mins after drug administration in superior frontal gyrus, and with changes in fALFF 60 mins after drug administration in ACC (Kullmann *et al*, 2013). Thus increasing BMI in normal weight subjects is associated with increasing responses to centrally applied insulin in the fasted state in regions involved in functions such as decision-making and attention, which are implicated in regulating eating behaviour. As BMI is commonly associated with systemic insulin resistance, it is possible that the latter may be involved in mediating these findings, although these subjects were all of normal BMI, and measures of insulin resistance were not reported. These data contradict the reduced MEG responses to intranasal insulin in obesity, although the incongruence of BOLD vs MEG responses is recognised (Grummich *et al*, 2006).

As described earlier, acute improvements in peripheral insulin resistance, quantified by HOMA-IR, have been observed 120 mins post-intranasal insulin (Heni *et al*, 2012). Greater improvements in peripheral insulin sensitivity were associated with greater reductions in resting state activity, as defined by fALFF, in hypothalamus at 30 mins post-intranasal insulin and putamen and OFC at 120 mins, and greater increases in resting state insula activity at 120 mins. This may suggest impaired suppression of homeostatic and reward processing and impaired activation of interoceptive processing networks by acute central insulin administration results in diminished improvements in systemic insulin resistance. Given the involvement of these networks in appetite regulation, and the previously described lack of improvement in satiety and weight with longer-term intranasal insulin treatment in obesity, the relationship between peripheral and central insulin responsiveness and appetite regulation require further exploration.

1.6.8 PET/SPECT studies of neurotransmitter activity

Dopaminergic and opioid reward pathway signalling in insulin resistance-associated conditions are now being investigated. A [^{123}I]iodobenzamide SPECT study in obese women prior to bariatric surgery found a non-significant trend towards decreased resting striatal D_2/D_3 receptor availability with decreasing peripheral (but not hepatic) insulin sensitivity based on a two step hyperinsulinaemic euglycaemic clamp with stable glucose isotopes, suggesting impaired striatal dopaminergic reward processing in states of peripheral insulin resistance (de Weijer *et al*, 2014). A PET study showed that the insulin sensitivity index for glucose disposal using oral glucose minimal modelling, was negatively associated with ventral striatal [^{18}F]fallypride binding in a mixed group of lean and obese, fasted women (Dunn *et al*, 2012b). As [^{18}F]fallypride competes with endogenous dopamine, it is possible that increased extracellular dopamine and therefore striatal signalling occurs with increasing insulin sensitivity. However, the only relationship between [^{18}F]fallypride binding and peripheral hormones measured during the study to survive correction for BMI was ghrelin, where increasing fasting ghrelin levels were associated with reduced [^{18}F]fallypride binding in caudate, putamen, striatum and amygdala (Dunn *et al*, 2012b).

Lastly, a [^{11}C]carfentanil-PET study in obese, insulin resistant (based on HOMA-IR) women with PCOS had greater μ-opioid receptor availability than lean insulin sensitive non-PCOS controls in NAcc/ventral pallidum and amygdala (Berent-Spillson *et al*, 2011). Whilst effects of altered sex hormone secretion or obesity cannot be excluded, the authors interpreted this to represent a hyporesponsive reward network in insulin resistance with compensatory opioid receptor upregulation.

1.6.9 Insulin resistance and cerebral perfusion

Regional cerebral blood flow as measured by ASL correlates with BOLD fMRI measures of resting state activity (Li *et al*, 2012b; Viviani *et al*, 2011; Zhu *et al*, 2013). Based on the concept of neurovascular coupling, the haemodynamic responses detected with these neuroimaging techniques act as surrogate markers of neuronal activity. However it is conceivable that insulin resistance may elicit cerebrovascular effects *per se*. Early studies in T2DM demonstrated diminished cerebrovascular reactivity to inhaled carbon dioxide using ^{133}Xe-inhalation methods (Dandona *et al*,

1978) and transcranial Doppler ultrasonography (Novak *et al*, 2006). pASL MRI has detected lower global CBF in insulin resistant, non-diabetic volunteers, compared to insulin sensitive volunteers and patients with T2DM, decreasing with increasing waist circumference (Rusinek *et al*, 2015), although insulin resistant and diabetic groups were of greater BMI and had more female volunteers, and the diabetic group were generally taking antihypertensive therapies. Similarly, ^{99m}Tc-HMPAO SPECT measures of temporal, occipital and superior frontal CBF are lower in volunteers with metabolic syndrome (Efimova *et al*, 2014). pCASL measures of global grey matter CBF after a 4 hour fast in volunteers with metabolic syndrome was 15% lower than controls, with high waist circumference and triglycerides independently predicting CBF, with voxel-wise analysis demonstrating lower medial and lateral frontal parietal lobe and lateral temporal and occipital lobes rCBF (Birdsill *et al*, 2013).

1.6.10 Intervention studies

A 9-month lifestyle intervention study, adapted from the Diabetes Prevention Study (Tuomilehto *et al*, 2001), of healthy volunteers showed that whilst the 2.7±0.8 kg weight loss observed at 9 months was not sustained at 2 years follow-up, reductions in total and visceral adipose tissue and intrahepatic lipid were observed at 2 years (Tschritter *et al*, 2012). Baseline beta and theta MEG responses to insulin during a hyperinsulinaemic euglycaemic clamp were negatively associated with absolute total and visceral adipose tissue (adjusted for change in body weight) at both 9 months and 2 years. Baseline cerebral insulin sensitivity as defined by the insulin-stimulated theta responses did not predict final body weight, but was associated with lower self-reported fat and saturated fatty acid intake at the end of the study, as well as being associated with greater adherence to the dietary and physical activity changes of the intervention. These findings are compatible with inter-individual differences in cerebral insulin sensitivity contributing to the variance in success of lifestyle interventions in achieving weight loss and preventing diabetes, which may also play an aetiological role in the development of obesity. Unfortunately, the impact of the intervention itself on brain insulin sensitivity was not examined, bringing into question whether this may potentially be modifiable.

1.6.11 Interim summary

Obese humans have low CSF insulin concentrations (Kern *et al*, 2006) and are resistant to weight loss and satiety effects of intranasal insulin (Hallschmid *et al*, 2008). MEG studies show reduced responses to peripheral insulin infusion under euglycaemic conditions in obesity, carriers of obesity-related FTO genotype and diabetes-associated IRS-1 polymorphisms, which are restored by insulin detemir infusion (Tschritter *et al*, 2006, 2007b, 2007a, 2009b), whilst responses to intranasal insulin *per se* correlate with BMI (Stingl *et al*, 2010), with attenuated effects of intranasal insulin on food image-evoked responses in obesity (Guthoff *et al*, 2011). The diminished changes in ventral striatal and PFC glucose metabolism evoked by physiological levels of circulating insulin in systemic insulin resistance states (Anthony *et al*, 2006) only reach normality with supraphysiological insulin concentrations (Hirvonen *et al*, 2011), consistent with reduced dopaminergic reward signalling in systemic insulin resistance (Dunn *et al*, 2012b; de Weijer *et al*, 2011). Cerebral sensitivity to insulin predicts the success of lifestyle intervention in achieving sustained weight loss (Tschritter *et al*, 2012).

1.7 Other circulating hormones that may regulate weight and appetite modulate brain activity in man

Evidence that other circulating hormones involved in appetite regulation modulate brain homeostatic and hedonic networks activity are briefly reviewed.

1.7.1 Leptin

Leptin, an adipokine, reduces food intake and increases energy expenditure, resulting in weight loss in obese patients with congenital leptin deficiency, and has been used as a model to investigate the central effects of this hormone (Farr *et al*, 2015). Leptin therapy in three adults with congenital leptin deficiency reduced post-prandial BOLD fMRI signal responses to high- compared to low-calorie food images in insula, fusiform and parahippocampal gyri and increased medial, superior and middle frontal gyri responses (Baicy *et al*, 2007). In teenagers with congenital leptin deficiency,

leptin therapy reduced food cue-induced activation of striatum (Farooqi *et al*, 2007), amygdala, substantia nigra and VTA and increased OFC activation (Frank *et al*, 2011). Leptin deficiency is also observed in lipodystrophy, conditions associated with marked insulin resistance. Leptin analogue therapy reduced fasting caudate and post-prandial amygdala, hippocampus, insula, and striatal responses and increased OFC responses to food images in 10 lipodystrophic subjects (Aotani *et al*, 2012). These data support a role for leptin in suppressing food-related striatal reward activity in both fasted and fed states and the normal suppressive effect of meal ingestion on interoceptive processing in insula and increasing satiation processing within PFC.

In the absence of leptin deficiency, post-prandial leptin concentrations are positively associated with post-prandial visual food cue-induced ventral striatal activity suggesting a possible role in normal appetite regulation (Grosshans *et al*, 2012). However, leptin levels are generally *greater* in obesity, reflecting greater adiposity, which *falls* after weight loss (Considine *et al*, 1996), whilst leptin analogue therapies are not associated with weight loss, indicative of a resistance to the weight loss effects of leptin (Zelissen *et al*, 2005). The finding that increasing fasting leptin levels are associated with decreasing putamen and opercula grey matter volumes, regions involved in reward and gustatory processing, may reflect this resistance to the weight loss of effects of leptin in obesity (Pannacciulli *et al*, 2007a).

1.7.2 GLP-1 and GLP-1 receptor agonists

GLP-1, an incretin hormone secreted from L cells of the gastrointestinal tract upon food ingestion, stimulates insulin secretion and suppresses glucagon in a glucose dependent manner. As GLP-1 secretion is diminished in T2DM, GLP-1 receptor agonists are a treatment strategy, inducing glucose lowering and weight loss, the latter via appetite suppressive effects. In rodents, ICV injected GLP-1 binds to thalamic, hypothalamic and amygdala receptors to reduce food intake (Turton *et al*, 1996), whilst satiating effects of intraperitoneal GLP-1 receptor agonist injection are blocked by ICV injected GLP-1 receptor antagonists (Kanoski *et al*, 2011), implicating brain homeostatic and hedonic networks in mediating the satiety-inducing effects of circulating GLP-1. Human post-mortem data show GLP-1 binds to cerebral cortex, hypothalamus, thalamus, hippocampus, striatum and brainstem receptors (Alvarez *et*

al, 2005; Farr *et al*, 2016). Circulating post-prandial GLP-1 concentrations positively correlate with post-prandial changes in DLPFC and hypothalamic rCBF in healthy volunteers on [^{15}O]H_2O-PET (Pannacciulli *et al*, 2007b), and with changes in food-cue evoked OFC BOLD signal in lean and obese subjects (Heni *et al*, 2015), whilst GLP-1 receptor antagonist infusion blocked post-prandial reduction in hunger and meal-induced reduction in insula and OFC BOLD responses to visual food cues in overweight subjects with T2DM, but not lean controls (ten Kulve *et al*, 2015). This might suggest endogenous GLP-1 modulates post-prandial inhibitory control centre activity to initiate satiation, whist effects in the fasted state appear to be detectable in diabetic patients but not healthy controls when viewing food cues, potentially as the former started off with greater responses prior to GLP-1 blockade.

GLP-$1_{7\text{-}36}$ infusion reduces $CMR_{glucose}$ globally on [^{18}F]FDG-PET, with greatest effects in hypothalamus and brainstem (Alvarez *et al*, 2005; Lerche *et al*, 2008). Intravenous infusion of exenatide, a GLP-1 receptor agonist, increases hypothalamic functional connectivity with the rest of the brain specifically when viewing food images only in obese subjects who responded to the satiating effects of the drug (Schlögl *et al*, 2013). The differences in the effect of exenatide on eating behaviour were thus proposed to be driven by interindividual differences in the responsiveness to exenatide of homeostatic networks, but not hedonic ones given the lack of effect on subjective ratings of the visual stimuli and the meal, although the effects of exenatide on reward network connectivity was not specifically interrogated. Other studies have demonstrated potential effects on such reward systems. Intravenous exenatide infusion during a somatostatin pancreatic-pituitary clamp reduced food image-evoked activation of insula and amygdala in obese subjects, and insula, putamen and OFC in diabetic subjects, insula and caudate activity correlating with the reduction in food intake during a subsequent ad-libitum meal in both groups, all effects reduced by co-infusion of a GLP-1 receptor antagonist, whilst no significant neurological effect of exenatide was observed in lean subjects (van Bloemendaal *et al*, 2014). Additionally, exenatide decreased anticipatory responses to a chocolate tastant in OFC in lean subjects, and putamen, insula and amygdala in diabetic subjects, whilst increasing consummatory responses in caudate in lean subjects, OFC in obese subjects and putamen, insula and amygdala in diabetic subjects, effects all blocked by GLP-1 receptor antagonism (van Bloemendaal *et al*, 2015). A short course of the GLP-1

receptor agonist liraglutide reduced food-cue evoked insula and putamen activation prior to weight loss in diabetic patients (Farr *et al*, 2016). These data therefore suggest the clinical effects of GLP-1 receptor agonists on suppressing appetite are mediated centrally through interoceptive and reward processing centres.

1.7.3 PYY

Meal ingestion increases gastrointestinal L cell PYY secretion (Adrian *et al*, 1985). Obesity is associated with lower fasting and post-prandial PYY levels, but intact anorectic effects of exogenous PYY (Batterham *et al*, 2003). As reviewed by Simpson *et al* (2012), the appetite suppressive effects of PYY are mediated by inhibiting arcuate nucleus NPY activity, either directly after crossing the BBB, or via the vagus. Peripheral infusion of PYY to post-prandial concentrations that reduce subsequent food consumption, results in spontaneous BOLD signal changes in VTA, OFC, insula, ACC, globus pallidus, putamen, and hypothalamus that are positively associated with PYY concentrations (Batterham *et al*, 2007). Hypothalamic activity accounted for 59% of the variance in energy intake during an ad libitum meal following saline infusion, but after PYY infusion this decreased to 1%, whilst OFC activity predicted 77% of this variance. In another study, PYY infused alone or co-infused with GLP-1, reduced food-cue induced activation in insula, as did meal ingestion (De Silva *et al*, 2011). These data suggest the satiating effect of meal ingestion may in part be mediated by modulation of activity from homeostatic to reward and interoceptive processes by postprandial PYY.

1.7.4 Cholecystokinin

Protein and free fatty acid ingestion increases cholecystokinin (CCK) secretion from small intestinal I cells, which amongst other actions, slows gastric emptying and reduces food intake by acting on NTS through acting on the vagal nerve, but potentially directly in the brain, as reviewed by Simpson *et al* (2012). By using dexloxiglumide, a CCK-1 receptor antagonist, the activation of a number of regions including brain stem, hypothalamus, caudate, precuneus, cingulate gyrus, temporal gyrus and thalamus during ingestion of free fatty acids in healthy volunteers has been shown to be CCK dependent (Lassman *et al*, 2010). Whilst appetite did not change

with dexloxiglumide, given that that many of these brain regions are involved in homeostatic and reward processing, and such effects were found to occur rapidly after free fatty acid ingestion, the satiating effects of a meal may in part be mediated in these centres through CCK signalling in the vagal nerve.

1.7.5 Ghrelin

Ghrelin is the only known incretin hormone to date to initiate eating, its secretion from the stomach being greatest when fasted and declining after meal ingestion (Cummings *et al*, 2004). Ghrelin binds to receptors on NPY/AgRP hypothalamic neurones, increasing food intake, but such receptors are also distributed amongst reward centres including VTA, NAcc, amygdala and hippocampus (reviewed by Ferrini *et al* (2009)). Fasting ghrelin levels are positively associated with fasting food cue-evoked activity in striatum, operculum, amygdala, hypothalamus, thalamus and ACC (Kroemer *et al*, 2013a). In studies of food cue-evoked activity, a post-prandial intravenous ghrelin bolus increased OFC, amygdala, insula, VTA, caudate, and hippocampus activity, and OFC and amygdala activity was associated with the ghrelin-induced rise in hunger (Malik *et al*, 2008), whilst post-meal subcutaneous ghrelin administration attenuated the meal-induced reduction in high energy food salience and mimicked the fasted OFC and hippocampal responses (Goldstone *et al*, 2014). Resting fMRI studies show a post-prandial intravenous ghrelin bolus reduced BOLD signal in hypothalamus, insula, parahippocampal gyrus, thalamus, cerebellum, medulla and midbrain, whilst continuous ghrelin infusion in the pre-meal state increased BOLD signal in similar regions, and attenuated the subsequent BOLD signal increase after free fatty acid ingestion (Jones *et al*, 2012). Fasting endogenous ghrelin thus appears to increase food-salience by increasing reward centre activity, whilst supraphysiological ghrelin administration when fed replicates the fasted state.

Whilst fasting ghrelin levels are *lower* in hyper- than normoinsulinaemic obese individuals and highest in lean individuals, the post-prandial reduction in ghrelin secretion is attenuated in obesity (Erdmann *et al*, 2005). Central responses to ghrelin might confer an obesity risk: whilst low obesity risk TT genotype carriers of the *FTO* gene show a normal positive association between fasting ghrelin and food cue-evoked activity in NAcc, OFC, hypothalamus, thalamus, parahippocampal gyrus and

cingulate and a similar association between post-prandial ghrelin and caudate activity, this relationship is reversed in high risk obesity risk AA carriers, in whom the post-prandial suppression of ghrelin was also attenuated (Karra *et al*, 2013).

1.8 Improving brain insulin sensitivity pharmacologically

Reversing insulin resistance, by improving diet and exercise and pharmacologically using the insulin sensitising agent metformin, prevents the onset of T2DM and lowers weight in high-risk populations (Knowler *et al*, 2002, 2009). The predominant mode of action of metformin is hepatic AMP-kinase activation, reducing hepatic gluconeogenesis (Viollet *et al*, 2012). Animal studies show oral metformin crosses the BBB and is detectable in cerebellum, olfactory bulb, pituitary and hypothalamus, frontal cortex, hippocampus and striatum after acute administration, remaining detectable after chronic administration, although concentrations fall in the striatum, cerebellum, hypothalamus and olfactory bulb (Łabuzek *et al*, 2010; Lv *et al*, 2012). Lipopolysaccharide-induced inflammation increases pituitary, hypothalamic and striatal concentrations of metformin (Łabuzek *et al*, 2010). Metformin also increases hypothalamic leptin receptor expression (Aubert *et al*, 2011) and sensitivity (Kim *et al*, 2006) in vivo. It also restores insulin-stimulated tyrosine phosphorylation of the insulin receptor, IRS1 and PI3K activity in in vitro models of neuronal insulin resistance (Gupta *et al*, 2011). It increases AMP-K activity in the central nervous system in some (Duan *et al*, 2013; Gupta *et al*, 2011; Kim *et al*, 2013a; Ma *et al*, 2007; Nath *et al*, 2009), but not all studies (Chau-Van *et al*, 2007; Stevanovic *et al*, 2012), suggesting other mechanisms of action such as STAT3 (signal transducer and activator of transcription 3) and mTOR (mammalian target of rapamycin)/S6 kinase signalling (Kim *et al*, 2013a; Lv *et al*, 2012) are involved. Metformin reduces hypothalamic orexigenic NPY *in vitro* (Chau-Van *et al*, 2007), whilst ICV and oral metformin decrease NPY expression *in vivo* and reduces food intake (Duan *et al*, 2013; Lv *et al*, 2012). Oral metformin reduces AgRP (Lv *et al*, 2012) and ICV metformin increases hypothalamic POMC (Lee *et al*, 2012) and suppresses ghrelin-induced food intake through AMP-K inhibition (Stevanovic *et al*, 2012). The central effects of metformin may also be mediated via the vagal nerve, either directly or

through altering incretin and other peripheral hormone secretion, given that orally administered metformin decreases food intake and increases c-FOS expression in NTS of high fat diet-induced obese mice (Kim *et al*, 2013b).

In humans, metformin causes weight loss in childhood obesity (Brufani *et al*, 2013), and reduces weight gain in insulin treated patients with T2DM by reducing food intake (Yki-Järvinen *et al*, 1999). In a [^{11}C]carfentanil-PET study of women with insulin resistant PCOS, the increased availability of μ-opioid receptors in NAcc/ventral pallidum and amygdala normalised after 4 months metformin therapy (Berent-Spillson *et al*, 2011), although a later report did not show any accompanying change in BOLD signal evoked by negative emotional pictures (Marsh *et al*, 2013). Whilst improvements in HOMA-IR and weight after treatment did not reach statistical significance, pre-treatment HOMA-IR was correlated with baseline μ-opioid receptor availability (Berent-Spillson *et al*, 2011). Metformin may therefore be expected to reduce food intake and weight through direct pharmacological effects on hypothalamic homeostatic processes but also through neuronal insulin sensitisation in hedonic and higher executive function networks and may be a potential therapeutic target for preventing and treating both diabetes and obesity.

1.9 Conclusion

Hunger and satiation, and external food stimuli in these different energy states elicit detectable changes in activity in neural networks involved in homeostasis, reward, interoception, memory and inhibitory control that likely reflect changes in appetite regulation by the brain (Small *et al*, 2001; Siep *et al*, 2009; Goldstone *et al*, 2009). In obesity, T2DM and PCOS, conditions associated with systemic insulin resistance, inhibitory PFC activity after meal ingestion *per se* appears to be diminished (Le *et al*, 2006, 2007), whilst striatal reward and insular interoceptive responses to food cues that are highly salient when fasted are exaggerated, these centres being less sensitive to modulatory effects of meal ingestion (Dimitropoulos *et al*, 2012; ten Kulve *et al*, 2015; Martens *et al*, 2013; Van Vugt *et al*, 2013). Nasally applied cerebral insulin suppresses appetite, reduces weight, and modulates these brain network activities,

effects that are diminished in obesity, especially in men (Guthoff *et al*, 2011; Hallschmid *et al*, 2008). As circulating insulin has reduced effects on reward network activity in systemic insulin resistance (Anthony *et al*, 2006), this implies that the brain may become resistant to the anorexigenic and weight loss effects of insulin through defective modulation of reward and control networks.

It is however unclear if the apparent abnormal central mechanisms of appetite regulation in these networks are a cause or effect of these insulin resistant states, as the studies examining responses to food have largely been performed in established disease. The specific effects of systemic insulin resistance, in the absence of associated disease, on the central mechanisms of appetite regulation are yet to be determined. Furthermore, whether the normalisation of altered reward network responses to food and food cues after weight loss interventions is mediated through changes in insulin sensitivity is unknown (Le *et al*, 2007; McCaffery *et al*, 2009). Lastly, whilst developmental changes in these appetite networks have been demonstrated during the transition from adolescence to young adulthood (Killgore and Yurgelun-Todd, 2005b), any changes that might occur with further ageing into middle life, when obesity is most prevalent, needs further exploration.

1.10 Research approach

This thesis aimed to investigate whether (a) healthy ageing, (b) systemic insulin resistance in the absence of obesity and (c) improvements in insulin sensitivity influence how the brain processes satiation after meal ingestion using cASL fMRI, and the impact of a meal on viewing visual food cues using BOLD fMRI in man. Specifically, based on the data described above, I hypothesise that systemic insulin resistance is associated with diminished post-prandial prefrontal inhibitory centre activity (Le *et al*, 2006, 2007), and striatal reward and insular interoceptive responses to food cues are exaggerated when fasted and less sensitive to the effects of a meal (Dimitropoulos *et al*, 2012; ten Kulve *et al*, 2015; Martens *et al*, 2013; Van Vugt *et al*, 2013). In the first study, 24 healthy non-obese men and women (age range 19.5-52.6 years) were studied on two separate days, after water and meal ingestion in

random order, to examine the association between ageing and BMI with regional brain responses to meal ingestion, and the impact of a meal on brain responses to visual food cues. This provided the opportunity to assess and develop the experimental protocol for subsequent studies. In the second study, 16 insulin resistant and 17 insulin sensitive non-obese men underwent a modified version of the protocol used in the first study. Fourteen of the 16 insulin resistant men consented to take part in a 12-week insulin sensitisation programme involving lifestyle intervention and metformin therapy, before the experimental protocol was repeated.

2 Methods

2.1 Nuclear magnetic resonance and magnetic resonance imaging

The concepts behind MRI have been reviewed comprehensively Huettel *et al* (2008). I here summarise these as relevant to my studies. Atomic nuclei with odd numbered atomic mass and charge possess angular momentum as each nucleus rotates about its axis, creating a current that generates a magnetic field with a rotational force or torque (the magnetic moment) perpendicular to the spin's axis. These nuclear "spins" are oriented randomly. In an externally applied magnetic field, such as the static field (B_0) of an MRI scanner, these spins align and gyroscopically precess, like a spinning top, at a characteristic frequency around a precession axis that lies parallel with the longitudinal direction (*z* axis) of this external field. If an electromagnetic pulse oscillating at the same characteristic frequency is then applied, energy is transferred from the pulse to the spins, an effect called resonant absorption. The frequency at which maximum energy transfer is possible is termed the resonant frequency.

Hydrogen nuclei (protons) are most widely imaged in MRI, given their widespread presence and large magnetic moment. More spins precess in a lower energy state in the same longitudinal (*z*) direction of the scanner's static magnetic field, than in the higher energy state in the opposite direction, the net sum of all the magnetic moments producing a net magnetisation (M) (Figure 2.1). Increasing external field strength

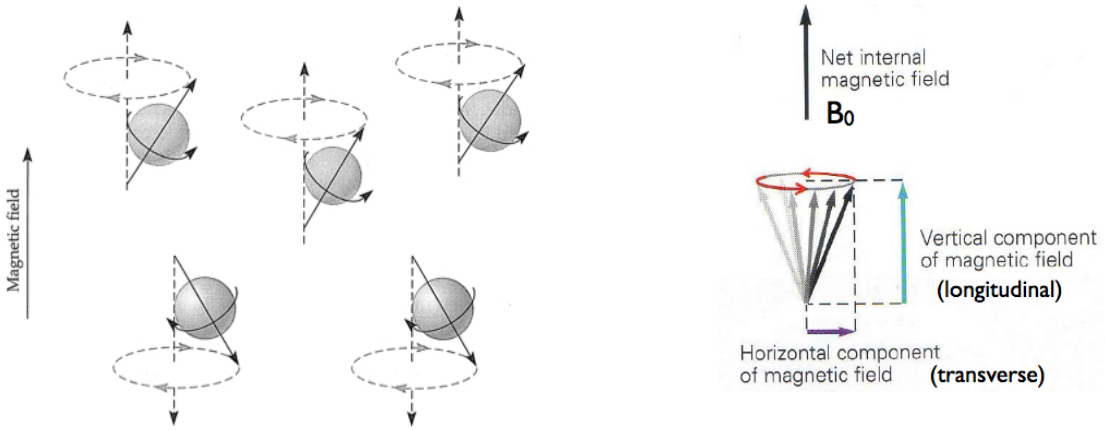

Figure 2.1

Proton "spins" precess, with more aligning in the direction of the magnetic field (B_0) than in the opposite direction (left), producing a net magnetisation with longitudinal (*z*) and transverse (*x*-*y*) components (right). Adapted from Huettel *et al* (2008) and Kandel *et al* (2013).

increases the net magnetisation, with more spins lying in the lower energy state. As the phase or rotational angle of precession (the starting point of rotation) about the direction of the external field is random for each spin, these effectively cancel each other out, resulting in no net magnetisation along the transverse (*x*-*y*) plane, 90º to B_0. The precession angle is determined by the frequency at which the spins precess, the Larmor frequency (ω), which in turn is dependent on the strength of the external magnetic field (B_0), scaled by a factor, the gyromagnetic ratio (γ):

$$\omega = \gamma B_0$$

Equation 1

This ratio is dependent on the spins' nuclear charge and mass. The Larmor frequency for a proton in the 1.5T field used in the present experiments is approximately 63.8 MHz. The Larmor frequency is also a spin's resonant frequency.

In MRI, the net magnetisation is perturbed by applying a radiofrequency pulse (B_1) oscillating at the Larmor frequency, to excite more spins held in the static external field (B_0) from the low to the higher energy state. When applied long enough for equal numbers of spins to exist in low and high energy states, the net longitudinal magnetisation falls to zero, with the spins spiralling or nutating to a new precession angle, the flip angle, 90º to B_0 along the transverse (*x*-*y*) plane (Figure 2.2).

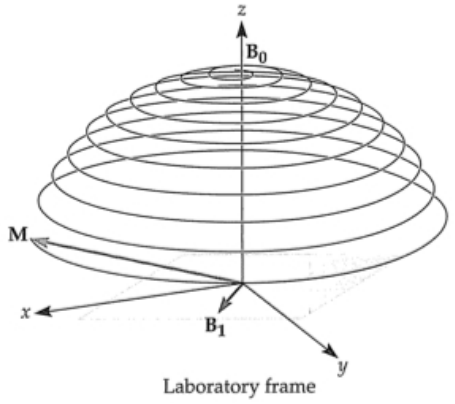

Figure 2.2

The application of a radiofrequency pulse (B_1) of Larmor frequency leads to nutation of the net magnetisation to a new precession angle (flip angle) in the transverse (*x*-*y*) plane. From Huettel *et al* (2008)

The flip angle (θ) is determined by the gyromagnetic ratio, the duration (T) and field strength (B_1) of the excitation pulse:

$$\theta = \gamma B_1 T$$

Equation 2

The change in net transverse magnetisation in turn elicits a current or "MR signal" in the detector coil that is used to construct MR images. The MR signal from the

transverse magnetisation will start to diminish, a process called free induction decay. Initially, spins within a spin system will undergo transverse relaxation along the *x*-*y* plane, precessing out of synchronicity or phase of each other (Figure 2.3).

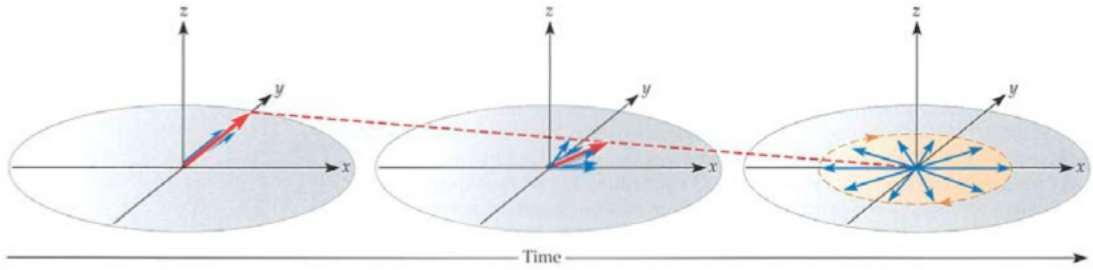

Figure 2.3

Dephasing of spins (blue arrows) in the transverse plane leads to decay of net magnetisation (red arrow) to zero in this plane (T2 decay). From Huettel *et al* (2008)

This dephasing is in part due to intrinsic spin-spin interactions, leading to irreversible MR signal loss known as T_2 decay, and due to inhomogeneity of the external magnetic field, the combination of which is termed T_2^* decay. This signal loss due to T_2* decay can be "re-focussed" by application of another 180º radiofrequency pulse, rephasing the spins to produce an "echo" signal (the time between the 90º radiofrequency pulse and the echo being the "echo time", TE).

Longitudinal relaxation along the *z* plane also occurs when spins in the high-energy anti-parallel state return back towards the lower energy parallel state (Figure 2.4), an effect termed T_1 relaxation. Despite the loss of longitudinal magnetisation, the instantaneous magnitude of magnetisation that remains available can be obtained again by application of a further excitation radiofrequency pulse. By changing the echo time and time to complete a pulse sequence, the repetition time (TR), the "weighting" of T_1 and T_2 relaxation can be optimised to control the MR image contrast between grey and white matter and CSF.

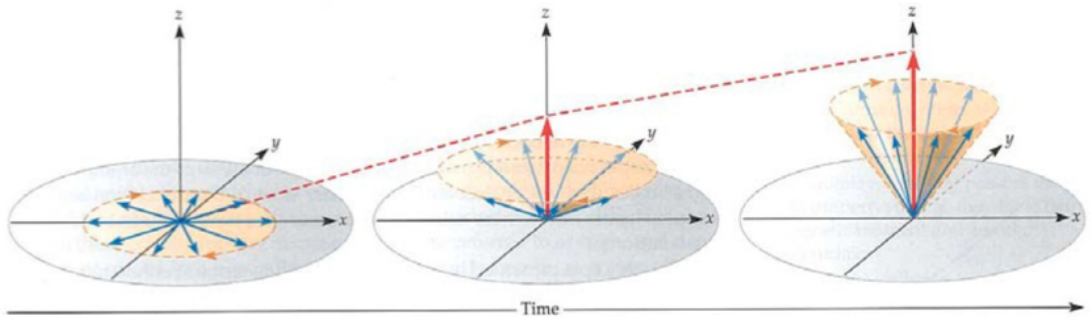

Figure 2.4

Longitudinal decay of spins (blue arrow), results in the net magnetisation (red arrow) returning to the longitudinal axis (T_1 relaxation). From Huettel *et al* (2008)

2.2 Blood Oxygenation Level Dependent (BOLD) fMRI

Infrared spectroscopic studies indicate that neural activity is associated with an early transient increase in deoxygenated haemoglobin concentrations in local brain tissue through a rise in oxidative metabolism, followed by a delayed nadir below baseline concentrations, whilst oxyhaemoglobin concentrations show a delayed gradual rise within a larger brain volume which is sustained for longer and with greater amplitude than the deoxyhaemoglobin rise (Malonek and Grinvald, 1996) (Figure 2.5A).

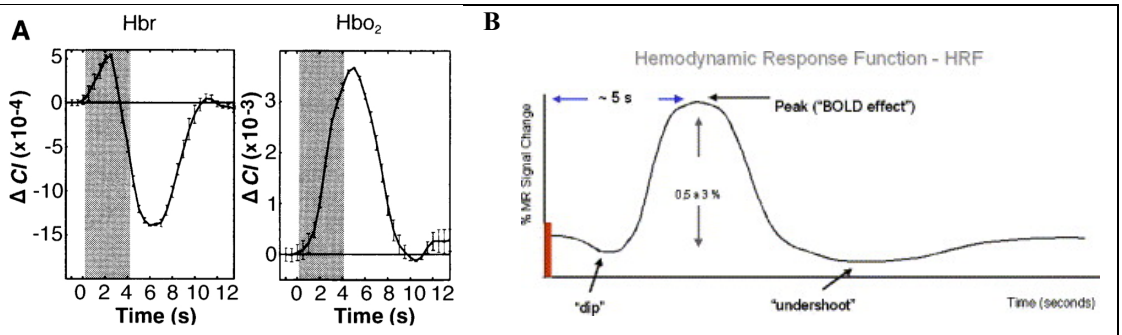

Figure 2.5

A: Changes in brain deoxyhaemoglobin (Hbr) and oxyhaemoglobin (Hbo_2) concentrations during visual stimulation (grey bar). From Malonek and Grinvald (1996). B: MR signal changes after a stimulus (red bar) modelled as a haemodynamic response function. From Amaro and Barker (2006).

This suggests neural activity elicits a haemodynamic response in the form of an increase in rCBF that supplies more oxygen to metabolically active brain regions with an overshoot in supply, and removal of deoxyhaemoglobin, which are thought to be

responsible for the change in MR signal that lags behind neural activity, modelled to a gamma-variate function (Figure 2.5B). Whilst oxyhaemoglobin is diamagnetic (no unpaired electrons, zero magnetic moment), deoxyhaemoglobin is paramagnetic (four unpaired electrons, magnetic moment of 5.46 μB) (Pauling and Coryell, 1936) and alters the local magnetic fields experienced by hydrogen spins, causing greater decay of transverse magnetisation, reducing T_2* (Thulborn *et al*, 1982) and MR signal detected on T_2* sensitive gradient echo sequences (Ogawa *et al*, 1990b). These different susceptibility effects of oxyhaemoglobin and deoxyhaemoglobin on gradient echo images were first demonstrated in vivo and in vitro by Ogawa and colleagues (Ogawa *et al*, 1990b; Ogawa and Lee, 1990), with greater MR signal occurring during neural activation (Ogawa *et al*, 1990a).

This BOLD signal, which continues beyond the duration of neuronal activity, is thus thought to represent a functional hyperaemia that takes place during such activation, although the exact mechanisms remain under debate (Kim and Ogawa, 2012; Steinbrink *et al*, 2006). The rate of regional delivery of oxygenated blood is linked to the level local of neuronal activity. As discussed by Attwell *et al* (2010), this 'neurovascular coupling' phenomenon is thought to be mediated by synaptic neurotransmitters including glutamate that in turn modulate astrocyte arachidonic acid derivatives including prostaglandins and epoxyeicosatrienoic acids, and neuronal nitric oxide (which also modulates astrocyte arachidonic acid signalling) and GABA leading to changes in rCBF by acting on arteriolar wall smooth muscle. In addition, ambient oxygen directly influences the rates of production of the vasoconstrictor 20-hydroxyeicosatetraenoic acid from arachidonic acid and vasodilatory nitric oxide, whilst oxygen consumption during neural activation may lead to a reduction in oxidative phosphorylation and increase in glycolysis, increasing adenosine and lactate, that cause vasodilatation.

The BOLD signal amplitude is influenced by stimulus duration, with longer durations producing greater BOLD signals, up to approximately 6-8s when the BOLD response reaches a maximum. Beyond this point, if the stimulus continues, the BOLD signal remains approximately constant. However, similar stimuli presented in succession will produce a BOLD signal of greater amplitude and duration. In the block design protocols used in the present BOLD fMRI studies, where stimuli of interest (food

images) are presented in groups or blocks, alternating with blocks of control stimuli (object images, blurred images), the BOLD signals evoked by individual stimuli within a block superimpose, with large responses sustained until the end of a block. Comparison of BOLD signals evoked by the stimulus of interest with that of a control stimulus permits correlation of specific neural responses to the experimental condition, in these studies the food-cue evoked response in specific satiety states.

2.3 Perfusion-weighted contrast imaging using pseudo-continuous flow-driven inversion arterial spin labelling (pCASL) fMRI

Perfusion, the volume of blood travelling through a unit of tissue volume over time, can be measured by invasive techniques such as the infusion of iodinated contrast agents during computerised tomography (CT), the detection of gamma photons following beta decay and annihilation of radioisotopes such as $[^{15}O]H_2O$ during PET, or tracers such as chelated gadolinium contrast agents that are detected during MRI. These techniques introduce exogenous agents into the circulation and in CT and PET expose individuals to ionising radiation that may prohibit repeated imaging. Arterial spin labelling (ASL) fMRI avoids this by using radio-frequency pulses to "label" arterial water spins selectively, and takes advantage of the ability of such spins to act as a freely diffusible endogenous tracer.

Continuous ASL (CASL), first described in 1992, applies a continuous adiabatic radiofrequency pulse (B_1) perpendicular to the scanner's main linearly varying gradient field (G) (Detre *et al*, 1992; Williams *et al*, 1992). Unlike conventional radiofrequency pulses that elicit flip angles that are proportional to the field strength of the pulse (Equation 2), the flip angles elicited by adiabatic pulses depend on how the size *and* frequency or phase of the pulse are modulated during the pulse, allowing the flip angle to remain constant at any pulse field strength once above a certain threshold. The resultant effective field (B_{eff}, the combined gradient field G and pulse field B_1) gradually rotates from a direction parallel to the main field (+z) to an anti-parallel (-z) direction. Arterial spins flowing along the direction of the gradient field experience this effective field, tracking the direction of the rotating effective field

whilst flowing past the labelling plane, and invert before entering the brain prior to image acquisition (Figure 2.6).

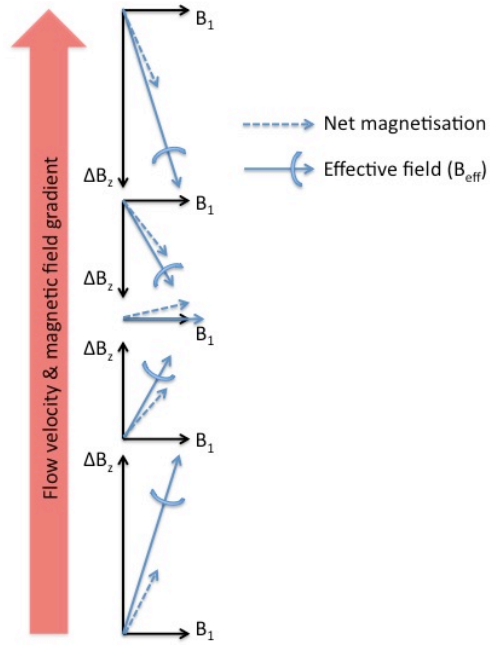

Figure 2.6

Spins flowing along the direction of the gradient magnetic field in the neck arteries during the continuous/pulsed radiofrequency (B_1), causing the net magnetisation (in rotating frame of the radiofrequency) to follow the effective field, and invert before entering the brain. Adapted from Detre and Alsop (1999).

The inverted spins continue to decay in magnetisation as they perfuse through tissue, limiting the magnitude of "labelling" that arterial spins have accumulated once a steady state has been reached. The radiofrequency pulse also causes off-resonance saturation (magnetisation inversion) of tissue-bound water distal to the labelling plane, transferring magnetisation from tissue to free water, reducing the signal and T_1 of free water. In early CASL studies a control scan, with radiofrequency pulses applied distal to the tagging plane outside the brain, was performed to correct for these magnetisation transfer effects. Subtracting labelled from control images creates a "perfusion weighted difference image", which is used to generate a CBF map in physiological units of tissue perfusion (*f*, [mL blood]/[100g tissue]/s) (Figure 2.7A), using a model that depends only on the magnitude of signal difference at each voxel and the sequence parameters, assuming that the entire labelled water is delivered to the brain with no outflow (which is generally valid as the pool of tissue water is greater than that of blood water), and that the relaxation of labelled water spins is determined by the T_1 of blood. Until recently, most scanners used pulsed radiofrequency amplifiers that cannot be used continuously. In addition, only single slices could be imaged using distal radiofrequency pulse control labelling, as it produces magnetisation transfer effects identical to that of the proximal tagging pulse

only at a level midway between control and tagging planes. Magnetisation transfer also reduces resting magnetisation and T_1 of the tissue imaged, decreasing signal-to-noise ratios (Detre and Alsop, 1999).

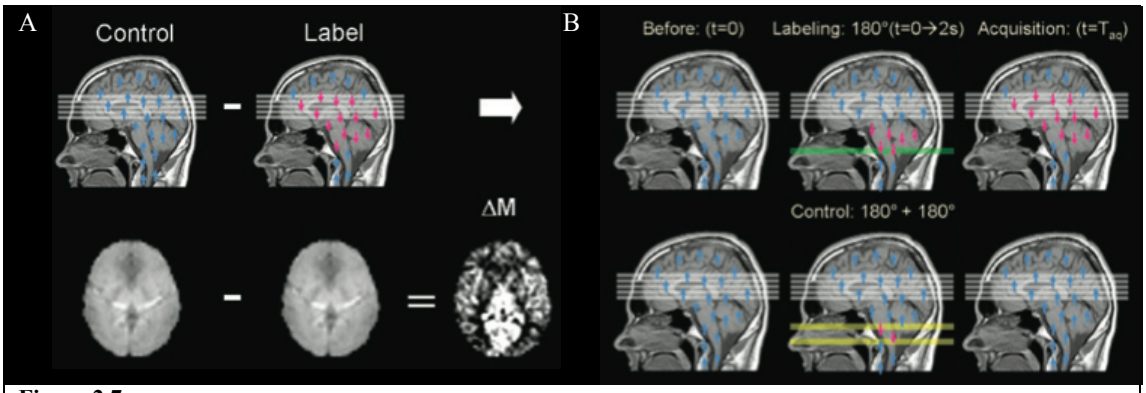

Figure 2.7

A: Subtraction of labelled from control images produces a perfusion weighted image, ΔM. B: Arterial water is tagged (label image: single inversion, green line = tagging plane; amplitude-modulated control: double inversion, yellow lines = tagging plane) before image acquisition (white lines). Arrows = arterial spins (blue: unlabelled; red: inverted). From Petersen *et al* (2006).

The recently developed amplitude-modulated control labelling, applied at the level of the tagging plane, effectively inverts the spins twice (Figure 2.7B), producing identical magnetisation transfer effects without tagging blood, permitting multi-slice imaging, although reduced signal strengths reduce the efficiency of spin inversion (O'Gorman *et al*, 2006). A more recent modification to the ASL pulse sequence is pseudo-CASL (pCASL). Instead of a continuous radiofrequency pulse, a train of pulses that are positive during the labelled scan, and alternate from positive to negative during the control so that the average gradient between pulses is zero, shifting the phase by 180º, is applied. A steady state in effective magnetisation B_{eff} comparable to that of a continuous pulse is achieved, but with greater efficiency, and therefore greater signal-to-noise ratios (Dai *et al*, 2008). The relationship between CBF and the signal intensity of labelled blood ($SI_{control} - SI_{label}$) that has entered brain tissue by perfusion, calculated from the perfusion weighted difference image, depends on the labelling efficiency (α, 95%) of the train of radiofrequency pulses, the labelling duration (τ, 1.5 s), the post-labelling delay (PLD, 1.5 s), during which labelled blood flows into the brain before image acquisition, and the longitudinal relaxation time of blood ($T_{1,\,blood}$, 1350 ms at 1.5T) at each voxel:

$$CBF = \frac{6000 \cdot \lambda \cdot (SI_{control} - SI_{label}) \cdot e^{\frac{PLD}{T_{1,blood}}}}{2 \cdot \alpha \cdot T_{1,blood} \cdot SI_{PD} \cdot (1 - e^{-\frac{\tau}{T_{1,blood}}})} \text{ (ml/100g/min)}$$

Equation 3

where λ is the blood:brain partition coefficient (0.9 ml/g) which scales the signal intensity of tissue to that of blood and SI_{PD} is the signal intensity of a proton density-weighted image, to estimate the signal intensity of fully relaxed blood spins to be used as a scaling factor (Alsop *et al*, 2015).

2.4 Clinical research application of BOLD and pCASL fMRI

ASL can be applied clinically to investigate cerebrovascular disease and other neurological conditions. Whilst functional neuroimaging has widely used BOLD fMRI, as discussed this does not measure an entity with physiological units, but a composite representing blood flow and volume, and oxygen extraction, unlike ASL which measures tissue perfusion in standard units. BOLD signals show greater sensitivity and temporal resolution, whilst ASL is more suitable for low frequency stimuli, since it is less sensitive to low-frequency sources of contamination. In order to overcome issues of low signal:noise ratios, the shorter duration BOLD signal is better suited to investigating neural responses of rapid onset and short duration to explicit stimuli such as briefly presented visual stimuli (e.g. food images). In contrast, ASL permits investigation of gradually changing neural activity over longer time frames, at rest and to explicit stimuli such as caffeine and alcohol (Detre *et al*, 2012). It is therefore well suited to delineate the neural responses that may occur during and after meal ingestion.

2.5 Quantification of insulin resistance

Insulin resistance is defined as a reduction in the ability of insulin to evoke a biological response on a target tissue. Whilst arguments have been put forward proposing that initial defects in insulin action lie in skeletal muscle (DeFronzo and

Tripathy, 2009), liver (Perseghin, 2009), adipose tissue (Iozzo, 2009) or brain (Pagotto, 2009) in T2DM and obesity, most in vivo studies refer to a diminution of insulin-mediated peripheral tissue glucose disposal and/or inhibition of hepatic glucose production. Insulin sensitivity, the reciprocal of insulin resistance, may be defined pharmacodynamically by the concentration at which insulin evokes half the maximal response, with a right-shift of the dose-response curve indicating greater insulin resistance, whilst the maximal evoked effect depicted by the height of the plateau of the curve indicates insulin responsiveness (Muniyappa *et al*, 2008). If an insulin-resistant body can adequately increase insulin concentration, through increased secretion and/or reduced clearance, normal glucose tolerance can be maintained (Jones *et al*, 2000). Thus at any given glucose concentration, insulin concentrations are greater in insulin resistant than insulin sensitive individuals.

In vivo methods of quantifying insulin sensitivity can be classified as either dynamic or static. Dynamic tests include those that examine responses to exogenous insulin, and those that detect endogenous insulin responses to exogenous glucose challenges. The hyperinsulinaemic euglycaemic clamp is considered as the gold standard method (DeFronzo *et al*, 1979). Insulin is infused intravenously at supraphysiological concentrations at which suppression of hepatic glucose production is assumed. The rate of concurrent glucose infusion required to maintain steady state euglycaemia reflects the rate of peripheral (predominantly skeletal muscle) glucose disposal (M), which if normalised for glucose concentration and change in insulin concentrations, produces the insulin sensitivity index (SI_{clamp}), the change in glucose clearance per unit change in insulin concentration. Hepatic glucose production may be estimated by infusing radiolabelled glucose tracers and construction of insulin dose-response curves can enhance accuracy of measurement of both hepatic and peripheral insulin sensitivity. Whilst highly reproducible, this method has limitations. It is labour intensive, time consuming and costly. It quantifies the sensitivity of peripheral tissues to insulin at supraphysiological concentrations, reverses the ratio of insulin concentration in portal compared to peripheral circulatory systems, and no longer reflects physiological hepatic insulin clearance nor the homeostatic effect of circulatory glucose on beta cell insulin secretion. The insulin suppression test (Harano *et al*, 1977) adds co-infusion of somatostatin or octreotide to suppress

endogenous insulin secretion, with similar practical limitations to hyperinsulinaemic euglycaemic clamp methods.

Modelling responses to exogenous glucose reflects both beta cell responsiveness to ambient glucose levels and secretory capacity, and insulin sensitivity. Intravenous glucose challenges such as the hyperglycaemic clamp (DeFronzo *et al*, 1979) and continuous infusion of glucose with model assessment (Hosker *et al*, 1985) model insulin sensitivity in the steady state, whilst the frequently sampled intravenous glucose tolerance test (Bergman *et al*, 1979) models dynamic changes in glucose and insulin. As with insulin clamp methods, intravenous glucose reverses the ratio of glucose concentrations in peripheral and portal circulatory systems.

Modelling responses to oral glucose is more physiological. The Matsuda (Matsuda and DeFronzo, 1999), Belfiore (Belfiore *et al*, 2001) and Gutt (Gutt *et al*, 2000) indices model insulin sensitivity from changes in glucose and insulin alone, whilst others such as the Stumvoll index (Stumvoll *et al*, 2000) include other factors such as BMI, based on linear regression models of population data. These models involve both a fasting steady state and dynamic changes that occur after glucose ingestion, thus reflecting hepatic and peripheral tissue insulin sensitivity more, respectively. These methods are less reproducible, in part due to varying gastric emptying and absorption. Furthermore, these tests not only reflect direct beta-cell responsiveness to glucose, but also incretin hormone secretory capacity and beta-cell responsiveness to such hormones. Meta-analyses have failed to show any consistent alteration in GLP-1 or GIP secretion in established diabetes (Calanna *et al*, 2013a, 2013b), and limited data indicate apparently normal effects of oral glucose on insulin, GLP-1 and GIP secretion in first-degree relatives of people with T2DM and controls (Nauck *et al*, 2004), whilst GLP-1 responses are diminished in prediabetic states (Færch *et al*, 2015). This makes comparisons between data from the different glycaemic control states more difficult to interpret.

Static tests use surrogate markers of insulin resistance in the fasted state. They assume steady state conditions, where rates of insulin secretion are sufficient to achieve steady state glucose concentrations by maintaining a balance between whole body glucose disposal and suppression of hepatic glucose production (DeFronzo *et al*,

1989), and provide an estimate of whole body insulin sensitivity from the fasting insulin and glucose concentrations. Such models are predominantly employed in population studies as they are simple to perform (requiring one fasting blood sample) and much less time consuming compared to dynamic tests. As insulin assays are not standardised, such tests should not be used for absolute quantification of insulin resistance in an individual, and as with oral glucose-based models, they are not suitable in established T2DM when insulin secretion is impaired. However, they have been used as indicators of comparative degrees of insulin resistance with reference to population data (Anthony *et al*, 2006), and may be appropriate for screening large numbers of individuals. In addition, fasting surrogate markers predicted 5-year weight gain in 424 5-year old children in the Da Qing study (Chen *et al*, 2015), 3-year weight gain in 3390 post-menopausal women in the Women's Health Initiative study (Howard *et al*, 2004), and 14-year weight gain when combined with dietary fat intake in 782 adults in the San Luis Valley (Mosca *et al*, 2004), unlike hyperinsulinaemic euglycaemic clamp measures of insulin resistance in 1028 adults in the Relationship Between Insulin Sensitivity and Cardiovascular Disease (RISC) study which did not predict 3-year weight changes (Rebelos *et al*, 2011). Surrogate markers of relative insulin resistance were therefore employed to identify potential volunteers in the present study of the effects of systemic insulin resistance.

Two commonly used surrogate static markers are the Quantitative insulin sensitivity check index (QUICKI) (Katz *et al*, 2000) and Homeostatic Model Assessment (HOMA) (Matthews *et al*, 1985), recently updated to the HOMA2 (Levy *et al*, 1998). QUICKI is the inverse sum of logarithmically transformed fasting insulin and glucose, whilst HOMA2 is based on non-linear relationships between fasting glucose and insulin, modelling homeostatic feedback between glucose-dependent beta cell secretion of insulin and insulin-mediated suppression of hepatic glucose production (Wallace *et al*, 2004). In one of the largest studies comparing methods of quantifying insulin resistance, the correlation between HOMA-IR and hyperinsulinaemic euglycaemic clamps was -0.82 (Bonora *et al*, 2000). However, in a recent meta-analysis the pooled correlation coefficient between HOMA-IR and hyperinsulinaemic euglycaemic clamp M values was only -0.53 (95% CI -0.6, -0.46), although this improved to -0.64 (95% CI -0.76, -0.48) when the M values were normalised for the steady state glucose achieved and the increment in insulin concentrations during the

clamp (Otten *et al*, 2014). This relatively low degree of correlation between surrogate markers and clamps is understandable given that each primarily reflect insulin sensitivity in different organs (liver in the static post-absorptive state when peripheral glucose uptake is minimised by virtue of being at rest; and peripheral tissues in the insulin stimulated state respectively), although degrees of insulin sensitivity between different organs are considered to correlate with each other.

In the present study, HOMA2-IR, rather than QUICKI, was used to differentiate insulin sensitive (IS) from insulin resistant (IR) subjects recruited from first-degree relatives of patients with T2DM. The former models glucose uptake in brain, muscle and fat, and accounts for renal glucose losses (Wallace *et al*, 2004). Furthermore, I was able to obtain non-diabetic population data for the distribution of both HOMA-IR (Bonora *et al*, 1998) and HOMA2-IR (personal communication, (Sierra-Johnson *et al*, 2007)) from which I was able to create a reference range.

2.6 Subjects with insulin resistance

Healthy first-degree relatives of people with T2DM are at high risk of future diabetes through increasing insulin resistance. While still normally glucose tolerant they have increased fasting hepatic glucose production measured using glucose isotopes, which Osei (1990) demonstrated at similar insulin levels, but higher fasting c-peptide levels compared to controls, suggesting higher portal insulin concentrations and therefore hepatic insulin resistance. Indeed, Henriksen *et al* (2000) also showed 25% less suppression of hepatic glucose production in first-degree relatives during euglycaemic near-normoinsulinaemic pancreatic clamp studies, as well as greater peripheral insulin resistance. Likewise, Nyholm *et al* (1996) and Eriksson *et al* (1989) showed reduced peripheral insulin sensitivity during hyperinsulinaemic euglycaemic clamp studies in first-degree relatives compared to controls, although they did not find a difference in hepatic glucose production either in the fasted or insulin stimulated state. More recently, clamp data from the European Group of Insulin Resistance database of 235 individuals with and 564 without a family history of T2DM showed greater peripheral insulin resistance based on reduced insulin-stimulated glucose disposal and lower

insulin sensitivity indices during the clamp after adjusting for BMI in the former, again with no significant differences in hepatic glucose production during basal and clamp conditions (Vaag *et al*, 2001). Thus whilst greater peripheral insulin resistance in relatives of people with T2DM is established, data regarding hepatic insulin resistance based on insulin-induced suppression of hepatic glucose production are inconsistent. However, similar to studies demonstrating cerebral brain insulin resistance (Anthony *et al*, 2006), it may be that hepatic insulin resistance is more reliably demonstrable at physiological insulin concentrations (Henriksen *et al*, 2000). HOMA-IR, which represents predominantly fasting hepatic insulin resistance, is greater in first-degree relatives (e.g. first-degree relatives vs controls: 2.1 [1.9-2.3] vs 1.7 [1.6-1.8] $p<0.005$, (Mansfield *et al*, 1996); pair-matched for age, BMI, waist:hip circumference ratio and sex 2.1 vs 1.8, $p=0.02$, (Humphriss *et al*, 1997); age and BMI-matched 2.03±0.5 vs 0.9±0.1, $p=0.003$, (Rudovich *et al*, 2004)), supporting the notion that first-degree relatives have greater hepatic insulin resistance. Increasing hepatic fat mass is associated with decreased suppression of hepatic glucose production during low dose hyperinsulinaemic euglycaemic clamp conditions (Kotronen *et al*, 2008), and high fat feeding increases hepatic fat mass and glucose production under fasting and hyperinsulinaemic euglycaemic clamp conditions in healthy individuals (Brøns *et al*, 2009; Seppälä-Lindroos *et al*, 2002) implicating current energy-dense diets in inducing hepatic insulin resistance, with the potential to be amenable to intervention. These data support the use of HOMA-IR in first-degree relatives of people with T2DM as an appropriate group in which to investigate the impact of insulin resistance in non-diabetic, non-obese individuals, who are also at high risk for the development of T2DM.

2.7 Methods of improving insulin sensitivity

Lifestyle interventions are fundamental in treating T2DM and obesity. Intensive changes in diet and physical activity reduced the incidence of T2DM in high risk individuals with either impaired fasting glucose or impaired glucose tolerance by 58% in both the diabetes prevention programme (DPP) (Knowler *et al*, 2002) and the Finnish diabetes prevention study (DPS) (Lindström *et al*, 2003), and by 31-46% in

the Da Qing study (Pan *et al*, 1997) and have persistent beneficial effects in preventing (or delaying) diabetes onset beyond the trial duration (Knowler *et al*, 2009; Lindström *et al*, 2006). Whilst such effects were detected after a relatively long follow up period (DPP: 2.8 years (Knowler *et al*, 2002); DPS: 3.2 years (Lindström *et al*, 2003); Da Qing: 6 years (Pan *et al*, 1997)), with greatest effect in those at greatest risk (Sussman *et al*, 2015), insulin sensitivity, although not specifically measured, is likely to have improved earlier. In a study of 438 overweight or obese, non-diabetic women, compared to no intervention (baseline vs follow-up HOMA-IR: 2.83 vs 2.78), insulin resistance improved in those randomised to receive either dietary advice alone (2.59 vs 1.96, $p<0.001$ compared to control) or combined with an intensive exercise (2.50 vs 1.84, $p<0.001$ compared to control), with accompanying reductions in fasting glucose, c-peptide and insulin over 12 months (Mason *et al*, 2011). The failure of exercise without dietary intervention to improve insulin sensitivity (2.55 vs 2.33, $p<0.19$ compared to control) is surprising. This might be explained by the intensity of exercise achieved, with one study observing an exercise intensity "threshold" in non-obese individuals, only above which improvements in insulin sensitivity are observed and are correlated with exercise intensity (Magkos *et al*, 2008). Mason *et al* (2011) also found insulin sensitivity only improved in those with impaired fasting glucose, in keeping with observations by Magkos *et al* (2008) that a single bout of aerobic exercise had greatest impact on insulin sensitivity in those with highest HOMA-IR.

In order to maximise the ability to improve systemic insulin sensitivity during the short timeframe of the present proof-of-concept study, lifestyle interventions, focussing particularly though not exclusively on dietary manipulation, were combined with pharmacological methods. Thiazolidinediones ("-glitazones") and biguanides (metformin) are classes of diabetes therapies that improve insulin sensitivity. Rosiglitazone (no longer in clinical use) reduces T2DM incidence by 62% (Gerstein *et al*, 2006), and metformin by 31% (Knowler *et al*, 2002) in high risk individuals. Thiazolidinediones were not considered in the present study due to concerns regarding weight gain, risk of heart failure and urological malignancy. However, the safety profile of metformin is well established. Metformin is weight neutral, is advocated by the American Diabetes Association for T2DM prevention in high risk groups (Inzucchi *et al*, 2012), and is used to treat PCOS, another condition associated with insulin resistance.

In a systematic review of hyperinsulinaemic euglycaemic clamp with glucose isotope studies of patients with T2DM, a 6±2% reduction in fasting basal (pre-clamp) endogenous glucose production was observed for every 1g of metformin used compared to placebo (Natali and Ferrannini, 2006). Whilst metformin suppresses hepatic glucose production during basal conditions, this action has not been consistently demonstrated during hyperinsulinaemic euglycaemic clamp conditions, likely due to the complete suppression of hepatic glucose production at supraphysiological insulin concentrations masking any effect of metformin. A stepped hyperinsulinaemic isoglycaemic clamp study performed after just two doses of metformin were administered (500 mg at 5 and 1 hour prior to the clamp), demonstrated a reduction in hepatic glucose production in both lean and obese subjects with T2DM during basal and low dose insulin infusion conditions (with greater glucose infusion rates needed to maintain isoglycaemia), but not during high dose insulin infusion (Perriello *et al*, 1994). The pooled analysis did not show an effect on peripheral insulin sensitivity, although some individual studies have shown this improves after metformin treatment in obese but not lean diabetic subjects, possibly due to weight loss rather than direct pharmacological effects (DeFronzo *et al*, 1991). Metformin therapy in people with T2DM does not appear to alter insulin signalling processes such as such as IRS-1 phoshorylation, PI3-kinase activity, and Akt phosphorylation in skeletal muscle biopsied following exposure to insulin during hyperinsulinaemic euglycaemic clamp conditions, although it increases atypical PKC activity (Karlsson *et al*, 2005; Luna *et al*, 2006; Musi *et al*, 2002). Therefore, the predominant insulin sensitising effect of metformin in diabetes is hepatic.

There are more hyperinsulinaemic euglycaemic clamp studies of the effect of metformin in established T2DM than in non-diabetic insulin resistance. Widén *et al* (1992) compared metformin against placebo during hyperinsulinaemic euglycaemic clamp studies with [3-^{3}H]-glucose and indirect calorimetry in insulin-resistant first-degree relatives with normal glucose tolerance. Prior to the clamp, hepatic glucose production and total body glucose metabolism did not differ between relatives after metformin or placebo therapy, and control subjects. This might initially be interpreted to suggest that hepatic insulin resistance was not different between controls and relatives, but basal insulin concentrations were higher in the latter, consistent with greater hepatic insulin resistance. Insulin-mediated total body glucose

disposal during the clamp was impaired in relatives due to a reduction in non-oxidative glucose metabolism, which improved after an acute dose of metformin. This may suggest metformin acutely had a predominant effect on peripheral insulin resistance. Lehtovirta *et al* (2001) found 6 months metformin therapy compared to placebo in impaired glucose tolerant, first-degree relatives did not alter fasting glucose metabolism during indirect calorimetry, but did improve total body glucose disposal by approximately 20%, due predominantly to improvements in glucose oxidation. Hepatic glucose production was not assessed in this study.

The insulin sensitising effect of metformin has also been quantified using surrogate markers of insulin resistance in insulin resistant, non-diabetic subjects. Two randomised placebo controlled studies of the impact 500 mg twice daily metformin have been performed: a three month treatment period reduced HOMA-IR by 26% in volunteers meeting the WHO definition of the metabolic syndrome (Metformin: 3.39 to 2.5, Placebo; 3.42 to 3.37, p=0.01 (Vitale *et al*, 2005)), whilst a six-month treatment period showed similar reductions in HOMA-IR in non-diabetic obese adolescent first-degree relatives (Metformin: 6.6±0.7 to 3.6±0.3; Placebo: 5.4±0.1 to 5.3±1.7, p<0.01, (Freemark and Bursey, 2001)). Jensterle *et al* (2008) showed improvements in HOMA-IR in non-diabetic women with PCOS either receiving 6 months treatment with metformin 1700 mg daily (2.98±3.17 vs 1.24±1.54), or rosiglitazone 4 mg daily (2.72±1.58 vs 1.64±1.93), with no significant difference between treatments. James *et al* (2005) also found non-diabetic obese insulin resistant volunteers (HOMA-IR>2.0) showed improvements in HOMA-IR when randomised to receive either 8 weeks' treatment with metformin 2g daily (4.0±0.7 vs 2.9±0.3) or rosiglitazone 8 mg daily (2.9±0.4 vs 1.9±0.3) compared to an untreated control group (3.6±0.4 vs 4.5±0.3). These studies had small sample sizes, but a meta-analysis of a pooled group of 320 non-diabetic obese children and adolescents showed treatment with at least 6 months with metformin, compared to placebo, reduced HOMA-IR by 2.01 (95% confidence interval 0.75-3.26, (Park *et al*, 2009)). In a study by Morel *et al* (1999), obese volunteers with impaired glucose tolerance underwent a cross-over study, with a 2 week run-in period with placebo, followed by 5 weeks of either placebo or metformin 1700 mg daily, and then 2 weeks placebo-based washout during which basal insulin sensitivity by HOMA-IR, and dynamic responses to insulin via a modified intravenous insulin tolerance test during somatostatin infusion

were assessed. HOMA-IR improved with metformin, compared to placebo, with lower levels of fasting glucose, insulin and c-peptide, whilst the intravenous insulin-stimulated glucose disposal was no different between treatment arms. The authors suggest that this discrepancy may be due to metformin having greatest effects at lower, basal insulin concentrations (consistent with the effect of basal insulin *per se* on brain activity described earlier (Anthony *et al*, 2006)), as opposed to the hyperinsulinaemic levels observed during the dynamic tests, with glucose disposal effects of metformin being masked by that of intravenous insulin.

I concluded that metformin evokes its main effect on improving hepatic insulin resistance, which can be quantified in non-diabetic insulin resistant subjects with surrogate markers of insulin resistance such as HOMA-IR.

2.8 General study design

As the design of the ageing and insulin resistance studies were similar, the general protocol methodology is described, and discrepancies between studies described.

2.8.1 Subject recruitment

Subjects were recruited by email advertisement to staff and students at King's Health Partners (King's College London, King's College Hospital NHS Foundation Trust, Guy's and St. Thomas' Hospital NHS Foundation Trust). For the insulin resistance study, leaflets were also given to patients attending diabetes clinics at the above hospitals and Lambeth and Southwark primary care sites, at a community diabetes clinic I held at Paxton Green GP Surgery, and patients taking part in the South London Diabetes (SOUL-D) study (REC reference 08/H0808/1), to pass on to non-diabetic male relatives. Advertisements were placed on the Diabetes UK website, the patient and public webpage for the comprehensive Biomedical Research Centre at Guy's and St. Thomas' NHS Foundation Trust and King's College London, and the Desang magazine (www.desang.net).

2.8.2 Inclusion/Exclusion criteria

Subjects were right-handed (Oldfield, 1971) healthy, non-obese (BMI 18-30 kg/m^2) adults, aged 18-65 years. Non-diabetic status was confirmed by self-report and HbA1c, and in the insulin resistance study by a 75g oral glucose tolerance test (OGTT) (World Health Organization, 2006a, 2011) (Section 2.8.3). All subjects understood English and had normal or corrected-to-normal vision. Exclusion criteria included any active medical illness or use of any medication, including treatments that could alter weight or appetite, blood glucose levels, brain activity or CBF (i.e. psychiatric or neurological disorders (including previous eating disorders), antidepressant, antipsychotic, anticonvulsant or antihypertensive agents, diabetes medication, oral, topical or inhaled glucocorticoids, orlistat), claustrophobia, or implants that could affect MRI signal or are MRI contraindications (e.g. pacemaker, tattoos in head and neck region, previous penetrating eye trauma, metal surgical clips, extensive dental work etc.).

HOMA2-IR was used to measure insulin resistance. One of the first [^{18}F]FDG PET studies to demonstrate altered central effects of circulating insulin at physiological concentrations in men with systemic insulin resistance (Anthony *et al*, 2006)) defined subjects as insulin resistant (IR) by HOMA-IR $\geq$ 2.77 or insulin sensitive (IS) by HOMA-IR < 1.55, based on the upper quintile and lower two quintiles, respectively, of the distribution of HOMA-IR in 888 volunteers aged 40-79 years, selected from the general population of Bruneck (Bonora *et al*, 1998). This study included people with non-insulin treated T2DM, with HOMA-IR validated by labelled hyperinsulinaemic clamp studies in 85 subjects (41 of whom had diabetes). In order to identify IR volunteers from a non-diabetic population, including adults aged below 40 years, and using the updated HOMA2-IR model, I contacted Dr. Justo Sierra-Johnson, author of a study investigating ApoB/ApoA-I ratio as a predictor of insulin resistance in non-diabetic men and non-pregnant women aged 20-90 years participating in the Third National Health and Nutrition Examination Survey (NHANES-III) (Sierra-Johnson *et al*, 2007). The cut-offs for the upper and lower quartiles of HOMA2-IR distribution in 6166 non-diabetic adults from NHANES-III were $\geq$ 1.47 and $\leq$ 0.76, respectively, and were used to identify IS and IR subjects. As HOMA2-IR has a lower cut-off of

0.4 (values below which continue to indicate IS status), the HOMA-IR was used (which has no lower limit) for correlation analyses.

2.8.3 Oral glucose tolerance test

All potential subjects for the insulin resistant study underwent a standard 75g OGTT following an overnight fast of at least 8 hours. A cannula was inserted in an antecubital vein, and after a 10 mins rest period, blood was sampled at time 0 mins for fasting plasma glucose, serum insulin, lipid profile, renal function, haemoglobin estimation and glycated haemoglobin (HbA1c). Subjects then consumed 75 g glucose (anhydrous preparation in 300 mL water or ready-to-consume 330 mL Glutole), with blood sampling for plasma glucose and serum insulin performed at 10, 30, 60, 90 and 120 mins. Participants meeting the criteria for diabetes (fasting glucose $\geq$ 7.0 mmol/L, 2 hour glucose $\geq$ 11.1 mmol/L (World Health Organization, 2006a), HbA1c $\geq$ 6.5% (World Health Organization, 2011)) were excluded.

2.8.4 Power calculation

A formal power calculation was not performed in the ageing study, which was performed to validate the protocol. For the insulin resistant study, power calculations were performed using G*power (version 3.1.9.2) using 0.05 two-side significance levels. Using data from the study by Anthony *et al* (2006), where changes in insulin-mediated ventral striatal metabolic rate for glucose were smaller in IR than IS subjects, 19 subjects in each group would be needed to provide 80% power to detect an effect size of 0.96, using a two-independent group t-test. Three studies of the effect of metformin on HOMA-IR measures of insulin sensitivity in non-diabetic subjects, showed effect sizes of 0.74 (Vitale *et al*, 2005), 1.80 (James *et al*, 2005) and 4.49 (Freemark and Bursey, 2001), the latter study differing from the others by the higher baseline HOMA-IR, and hence a greater impact of treatment. Using data from the study by Vitale *et al* (2005) in which 3 months of metformin was used, 17 subjects receiving metformin provides 80% power to detect an effect size of 0.74 in HOMA-IR, using a two sample matched paired t-test.

2.8.5 Randomisation procedures

Subjects in the ageing study, and IS subjects in the insulin resistance study, underwent MRI scanning procedures twice on two separate mornings at least one week apart, during which subjects either received water or a mixed meal. The order was block randomised using an online randomisation programme (www.randomization.com). As IR subjects repeated these two MRI scanning visits after the intervention, the order for water/mixed meal scans, pre-/post-intervention was block randomised by King's Clinical Trials Unit randomisation service. Subjects did not know whether they would receive water or the mixed meal until it was presented during the first visit.

2.8.6 fMRI study procedure

The general experimental procedures in both studies were similar (Figure 2.8). All studies were performed the morning after an overnight fast of at least 8 hours at the Centre for Neuroimaging Science, King's College London. Each visit was at least one week apart. An intravenous cannula was first inserted into a left antecubital vein, and kept patent with 0.9% saline. After at least 10 mins rest, fasting blood samples were drawn. Subjects were then positioned supine in the MRI scanner. The radiofrequency head coil was placed over the subject's immobilised head, and overhead mirrors positioned making the projector screen at the foot of the scanning table visible. After a localiser scan confirmed head position, a pCASL scan (pCASL1) measuring CBF was performed at -14 mins. Subjects were then withdrawn from the scanner and sat to consume either a mixed meal (Section 2.8.7) or 50mL water between -6 and 0 mins. Subjects were then repositioned in the scanner, and after another localiser scan, two further pCASL scans (pCASL2-3) were performed at 0 and +8 mins.

At +16 mins, subjects viewed alternating blocks of images of food (which in the insulin resistance study were divided into high- and low-calorie food blocks) and non-food related objects (and in the insulin resistance study, additional blocks of blurred images) presented on the projector screen during BOLD signal acquisition (Section 2.8.8). Subjects were instructed through headphones to "Imagine you are eating the following foods/using the following objects" before each food and object block, respectively (and to "Please look at the following images" before each blurred image

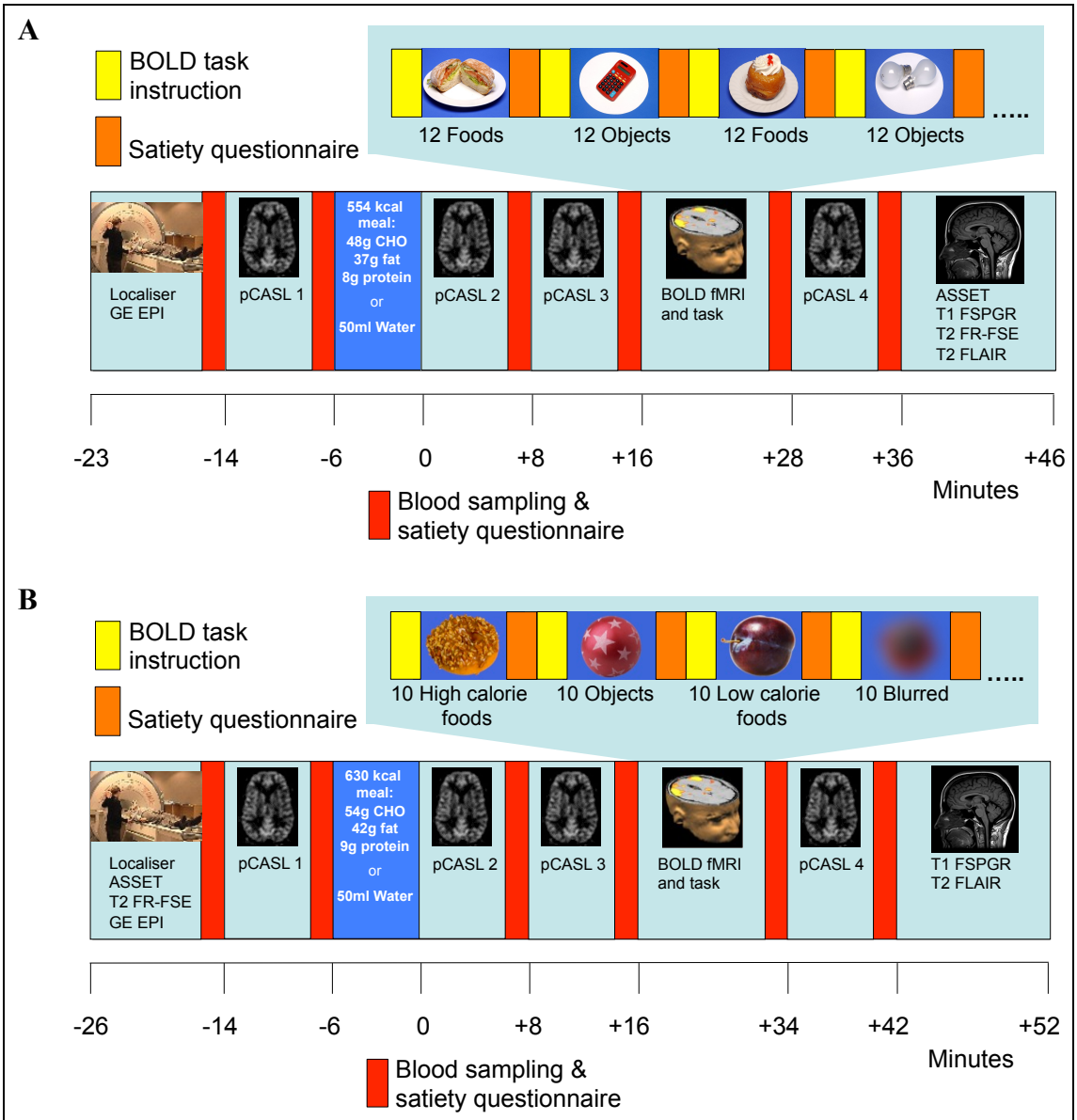

Figure 2.8

A: Ageing study protocol. B: Insulin resistance protocol. See text for abbreviations.

block in the insulin resistance study). After each block, subjects were asked "How hungry do you feel?" through the headphones, which was answered using a handheld keypad that moved a marker along a visual analogue scale that was anchored with "Not-at-all" and "Extremely" (Flint *et al*, 2000) projected on the screen. After BOLD fMRI, a final pCASL scan (pCASL4) was performed. Before pCASL1, after each pCASL1-4 scan, and after the image-viewing task, subjects answered the hunger question, and the questions "How sick to you feel?", "How full do you feel?" and, "How pleasant would it be to eat right now?" on the visual analogue scale (Flint *et al*, 2000), with concomitant blood sampling.

2.8.7 Mixed meal

The mixed meal consisted of partially melted Häagen-Dazs Belgian Chocolate ice cream (Uxbridge, Middlesex, UK), based on that used in previous non-neuroimaging studies investigating the role that PYY and bile acid secretion during meal ingestion may play in insulin resistance and obesity (Glicksman *et al*, 2010; le Roux *et al*, 2006). A fixed quantity of the mixed meal was chosen, rather than varying the amount according to a subject's weight or body-mass, as this would be equivalent to a subject consuming a fixed amount of food provided in a ready-meal or a single serving in a restaurant in the real world.

2.8.8 Visual images

In the ageing study, subjects viewed alternating blocks of photographs of food (Table 2.1) and non-food related objects (Table 2.2). Seventy-two different food and 72 non-food pictures provided by Prof. Janet Treasure, King's College London, that had previously been rated highly for recognition, pleasantness, appeal, visual complexity, colour and palatability in healthy volunteers (Uher *et al*, 2006) were viewed. T2*-weighted images were not acquired whilst instructions were being delivered and questions answered.

In the insulin resistance study, subjects viewed blocks of photographs of high calorie food (Table 2.3), low calorie food (Table 2.4), non-food related objects (Table 2.5), and a mixture of these images that were Gaussian blurred, presented in a block design in one of two pseudo-randomised orders at each visit. Foods of different energy densities were chosen, due to evidence that the neural response to high compared to low calorie food images are affected by feeding status (Goldstone *et al*, 2009). Photographs kindly provided by Prof. Michael Stumvoll, Leipzig, Germany, were first rated by a group of 13 healthy volunteers who did not take part in the neuroimaging study, for pleasantness and appeal on a 1-7 scale, with ratings summed for each picture, and whether they felt the food presented was easily recognisable and of high or low calorie content, based on whether they perceived the food was appropriate for a healthy diet (yes/no). Photographs with the highest scores were selected and only identifiable images that were correctly perceived to be of high or low calorie content were used. There were no significant differences in the combined

pleasantness and appeal scores between high (305.9±111.94 kcal/100g) and low (67.6±37.1 kcal/100g) calorie food images (8.62±0.58 vs 8.75±1.08, p=0.462). During BOLD signal acquisition, 50 images of each category were viewed. T2*-weighted images were acquired continuously.

2.8.9 MRI acquisition

Imaging was performed in a 1.5T MRI scanner (1.5T GE Signa HDx, General Electric, Milwaukee, WI, USA) equipped with echo-speed gradient coils and full fMRI capability.

2.8.9.1 Localiser scan

Performed to confirm head position (21 slices, slice thickness 5mm, slice gap 5.5mm, matrix 256x128, field of view [FoV] 240mm, flip angle 30º, TE 1.32 ms, TR 4.844 ms, duration 10 s).

2.8.9.2 pCASL image

pCASL images were acquired using 3D fast spin-echo "stack-of-spirals" readout (labelling duration 1.5s, post-labelling delay 1.5 s, slice location thickness 3mm, no slice gap, 512 points per spiral, 8 spiral arms per slice location, echo train length 64, FoV 240mm, flip angle 90º, TE 32 ms, TR 5.5 s; voxel size 2x2x3mm, duration 5.5 mins; 3 tag-control pairs and 2 reference images [fluid suppressed and combined fluid and white matter suppressed images] were acquired to derive a perfusion weighted difference image, together with a proton density image to compute CBF maps in physiological units (Equation 3), computed automatically by GE software), with background suppression pulses to minimise static signal.

2.8.9.3 BOLD image

In the ageing study, 108 T2*-weighted whole-brain images were acquired (41 slices, slice thickness 2.4mm, slice gap 0.3mm, matrix size 64 x 64, FoV 240mm, flip angle 90º, TE 40 ms, TR 4 s, duration 10 mins). As more stimuli were presented in the insulin resistance study, 320 T2*-weighted images were acquired (41 slices, slice

thickness 3mm, slice gap 0.3mm, matrix size 64 x 64, FoV 211mm, flip angle 90º, TE 40ms, TR 3s, duration 16 mins).

2.8.9.4 High-resolution GE EPI (gradient echo, echo planar image)

Structural images used for coregistration of BOLD images and spatial normalisation (43 slices acquired in the anterior commissure-posterior commissure plane, slice thickness 3mm, slice gap 0.3mm, matrix 128x128, FoV 240mm, flip angle 90º, TE 40ms, TR 3s, duration 3 mins).

2.8.9.5 Axial T1 FSPGR (Fast Spoiled Gradient-Recalled-Echo) image

Structural image used for coregistration of pCASL images and spatial normalisation (146 slices, slice thickness 1.1mm, no slice gap, matrix 256x160, FoV 280mm, flip angle 18º, TE 4.836ms, TR 11.16ms, inversion time 300ms, duration 6 mins).

2.8.9.6 ASSET (Array Spatial Sensitivity Encoding Technique) calibration image

Calibration scan for parallel imaging (49 slices, slice thickness 5mm, no slice gap, matrix 32x32, FoV 300mm, flip angle 70º, TE 1.672ms, TR 150ms, duration 1 min).

2.8.9.7 Axial T2 FR-FSE (Fast-Recovery Fast Spin-Echo) image

Anatomical image to exclude structural lesions (ageing study: 36 slices, slice thickness 4mm, no slice gap, matrix size 320 x 320, FoV 240mm, flip angle 90º, TE 87.104ms, TR 4380ms, duration 2 mins; Insulin resistant study: 72 slices, slice thickness 2mm, no slice gap, matrix size 320 x 320, FoV 240mm, flip angle 90º, TE 54.48ms, TR 3 s, duration 6 mins).

2.8.9.8 Axial T2 FLAIR (Fluid Attenuated Inversion Recovery) image

Anatomical image to exclude structural lesions (36 slices, slice thickness 4 mm, no slice gap, matrix size 256 x 128, FoV 240mm, flip angle 90º, TE 128ms, TR 8002ms, inversion time 2000ms, duration 4 mins).

2.8.10 Eating behaviour questionnaires

Eating behaviour was characterised to exclude eating disorders in the insulin resistance study. In the fasted state, volunteers completed the Questionnaire on Eating and Weight Patterns-Revised [QEWP-R] (Spitzer *et al*, 1993), the Dutch Eating Behaviour Questionnaire [DEBQ] (van Strien *et al*, 1986), and Eating Disorder Examination Questionnaire [EDE-Q 6.0] (Fairburn and Beglin, 2008). The DEBQ assesses restrained, emotional and external eating patterns, based on psychosomatic theory (Kaplan & Kaplan 1957) of eating in response to arousal states, externality theory (Schachter et al 1968) of eating in response to food-related stimuli irrespective of current state of hunger or satiety, and restraint theory (Herman and Polivy 1980) where diminution or impairment of self-control processes that control eating leads to disinhibited, external and emotional eating. The QEWP identifies DSM-IV diagnostic criteria for Binge Eating Disorder, Bulimia Nervosa and subclinical abnormal eating behaviours (episodic overeating, binge eating, binge eating syndrome and binge eating syndrome with distress), applied to patients attending weight control programmes, non-patient communities, and people attending overeaters anonymous (Spitzer *et al*, 1992). The EDE-Q is based on the Eating Disorders Examination, a 62 item semi-structured interview of eating behaviour over the preceding 4 weeks that was developed from review of eating disorder literature and unstructured interviews. Compared to the EDE semi-structured interview, the QEWP-R has a sensitivity of 0.85 (although a low specificity of 0.20) for identifying severe binge eating, whilst the frequency of binge eating identified by QEWP-R and EDE-Q correlate well with that identified by the EDE interview (Celio *et al*, 2004).

2.8.11 Insulin sensitisation

The insulin sensitisation intervention for IR subjects started after the initial two (meal and water) visits. A registered diabetes specialist dietitian reviewed self-reported three-day food diaries, and provided personal individual plans for each subject, setting SMART (specific, measurable, achievable, realistic, time-limited) goals. Diets high in fibre and low in glycaemic index carbohydrates were encouraged (National Institute for Health and Care Excellence, 2009). Face-to-face or telephone contact was made following the initial consultation to review progress. Slow-release metformin (Glucophage® SR, Merck Serono) was also initiated in a dose escalation

regimen, starting at 500 mg daily for the first two weeks, increasing by 500 mg every two weeks to a maximum of 2g daily or the maximum dose tolerated by the subject. Subjects were contacted every two weeks to supervise dose escalation and monitor for side effects. At the end of the intervention period, blood samples were collected for HbA1c and HOMA2-IR. Metformin was not taken on the morning of the scan.

2.8.12 Ethical approval

The research study protocol and participant recruitment material were approved by the London-Dulwich research Ethics Committee of the NHS National Research Ethics Service (Ageing study: reference 07/H0808/137; Insulin resistance study: reference 10/H0808/47). The Medicines and Healthcare Products Regulatory Agency confirmed the insulin sensitisation intervention was not a Clinical Trial of an Investigational Medicine Product as defined by the EU Directive 2001/20/EC. Participant recruitment materials were reviewed by the lay panel of the National Institute for Heath Research North East London Diabetes Research Network.

2.8.13 fMRI analysis

In order to compare data, pCASL and BOLD images are spatially normalised, correcting for anatomical differences between subjects, and spatially smoothed or blurred to meet Gaussian random field theory (described later) requirements, and improve coregistration and signal-to-noise ratios. Additionally, as BOLD fMRI collects runs of images, these are corrected for motion-artefacts before the "time-series" of changes in BOLD signal in 3D space over time are modelled to the experimental paradigm.

Pre-processed subject-level images are then entered into mixed-effects group-level models that assume subjects are randomly selected so that results are generalisable to a population. Three levels of statistical inference are available (Poldrack *et al*, 2011). Voxel-level inference examines whether activity in each voxel is significantly different to the null hypothesis at that voxel by determining whether each voxel's statistic passes a "height" threshold (Figure 2.9A). This method does not use spatial information, such as the likelihood that contiguous voxels co-activate due to anatomy

(brain regions being larger than individual voxels) and to the spatial normalisation and smoothing performed during pre-processing, which averages adjacent voxels. It is thus often used in studies of *a priori* regions of interest.

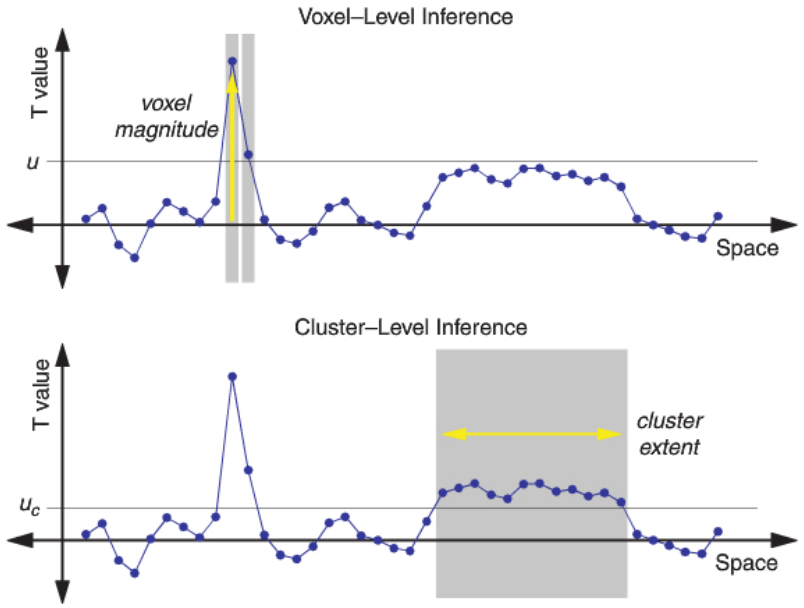

Figure 2.9

A: Left cluster passes the height threshold (u); B: Two clusters pass the cluster-forming threshold (u_c) but only the right one passes the cluster-extent threshold. From Poldrack *et al* (2011).

Cluster-level inference does take this into account, by first defining clusters as contiguous voxels passing an arbitrary voxel-level primary threshold, before ascertaining cluster significance by comparing their size to a critical cluster size (Figure 2.9B). This method is more sensitive but spatially less specific than voxel-wise inference, as the significance of individual voxels within a cluster cannot be inferred. Lastly, set-level inference establishes the number of clusters at an arbitrary cluster-defining threshold that are larger than an arbitrary cluster-size threshold, but does not identify which clusters are significant. Cluster-level inference is the most commonly used method (Woo *et al*, 2014), and is employed in this thesis.

As statistical tests are performed on each of the thousands of voxels of data contained in the volume of each brain map, the thresholds used in subject- and group-level analyses must correct for the number of tests to minimise type 1 errors that a voxel is falsely labelled as active. Bonferroni correction is considered overly conservative, as an alpha value (family-wise error rate, P_{FWE}) divided by the number of voxels within

the brain map would produce extremely low uncorrected voxel-level *p*-values. It also assumes that each statistical test is independent, an assumption that cannot be met as activity in adjacent voxels will be highly correlated as discussed earlier, reducing the number of independent observations. To account for this, two different approaches, Gaussian random field theory and permutation methods, were employed for pCASL and BOLD data respectively in this thesis.

2.8.13.1 Subject-level pCASL pre-processing

pCASL images were pre-processed using Statistical Parametric Mapping version 8 (SPM-8) (University College London, 2008) (Figure 2.10). Each perfusion map acquired through 3D pCASL fast spin-echo stack-of-spirals and the associated structural T1-weighted FSPGR scan for each subject were reoriented to the anterior commissure-posterior commissure line, with the origin changed to the anterior commissure. The segmentation function was then applied to the structural image, which spatially normalised the image into the standard space of the Montreal Neurological Institute (MNI, voxel size 2x2mm) and produced grey and white matter and CSF maps (Ashburner and Friston, 2004a). These segmentation parameters were used to remove the skull from the structural scan, and create a brain-only binary mask. Co-registration followed, where pCASL scans were superimposed onto the anatomically detailed skull-stripped structural image, permitting accurate normalisation and localisation of activation (Ashburner and Friston, 2004b). In the ageing study, pCASL scans were directly co-registered to the structural scan. However, as structurally less detailed (but more devoid of extra-cerebral signal) equilibrium magnetisation maps (M0) acquired in each pCASL scan were available in the insulin resistance study, each M0 image was co-registered to the structural scan first, with these transformations subsequently applied to the CBF map. The binary mask was then applied, removing extra-cerebral signal from the co-registered CBF map. The parameters used to normalise the structural scan during segmentation were applied to each co-registered CBF map, transforming them into standard space. Finally, the normalised CBF maps were spatially smoothed using a Gaussian filter (full-width at half maximum, FWHM kernel = 8 mm).

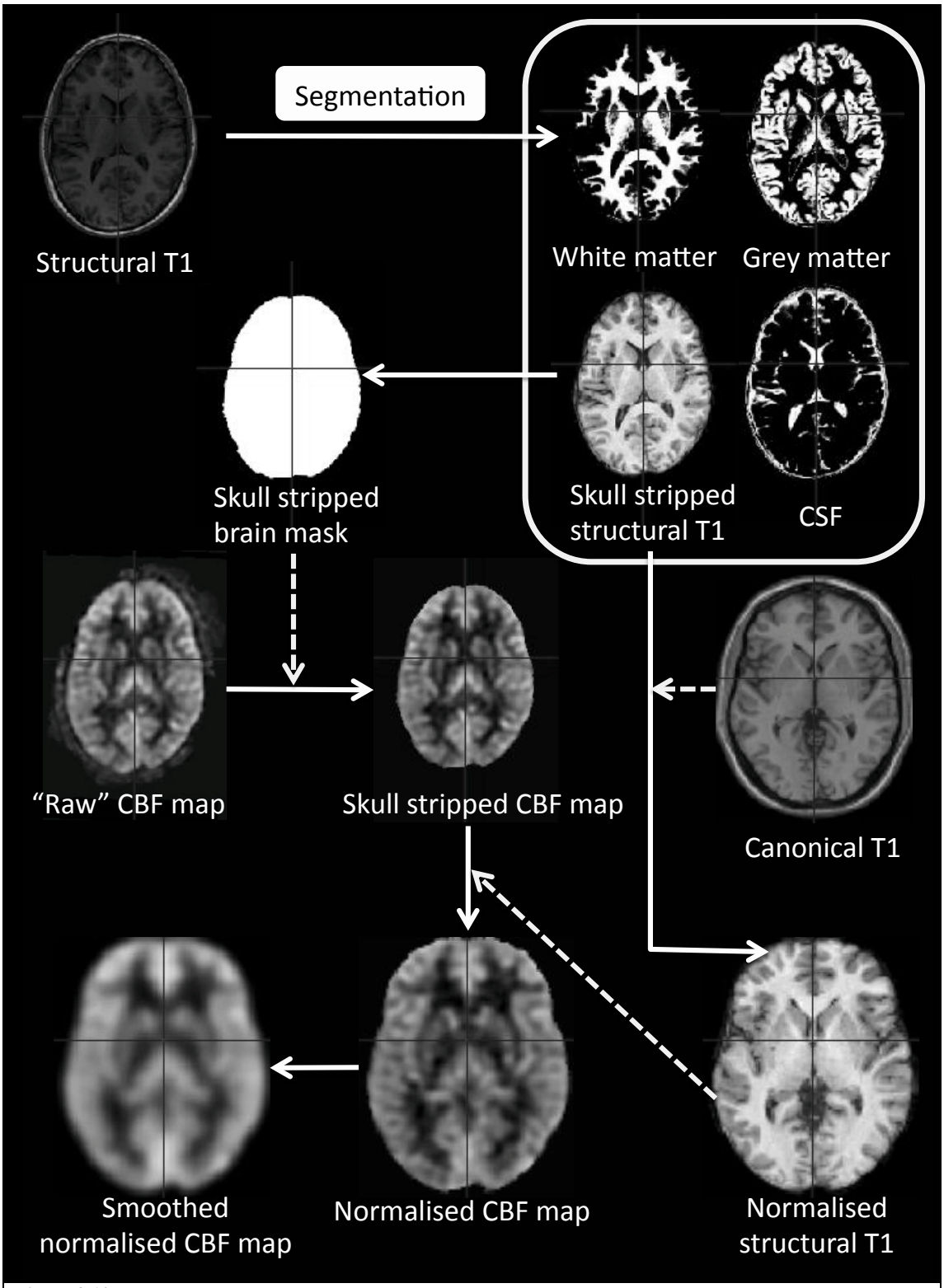

Figure 2.10

Pre-processing steps of CBF maps (described in main text). Solid arrow = transformation; dashed arrow = parameters used for transformation.

2.8.13.2 Group-level pCASL analysis

Statistical analyses in SPM-8 utilise the general linear model to examine the relationship (b) between independent predictors (X) and a continuous response (Y):

$$Y = \beta X + e$$

Equation 4

Where Y is the vector of observed data, X is the study design matrix of the explanatory variables investigated (e.g. feeding status, group, treatment), and β is a matrix parameter vector that describes the linear relationship between the explanatory variable (regressor) and observed data and is estimated by the restricted maximum likelihood method to minimise e, the vector of residual errors between the fitted model and the data. Whole brain voxel-wise group-level analyses were performed by entering each subject's CBF maps into group-level matrices, with each column representing either a main factor or an interacting factor of interest. The flexible factorial model was applied, which accounts for intra-subject variability, using subject, feeding status (2 levels: water vs meal) and time (4 levels: pCASL1-4) as factors, with independence and variance configured to the recommendations of Gläscher and Gitelman (2008), with subject as main effect and [feeding status x time] as an interaction effect. The full factorial model was used when three interacting factors (e.g. in the insulin resistant study, [group x meal x time] and [treatment x meal x time]) were interrogated, as the flexible factorial model only permits two interacting factors.

Analyses were restricted to grey matter using an explicit mask (created by making a binary mask image of SPM's grey matter template with a threshold of 0.25) and mean global grey matter CBF was used as a nuisance covariate in an analysis of covariance (ANCOVA). T-contrast vectors were defined to compare rCBF between different conditions or between groups, and voxel-wise multiple regression analyses were performed to examine potential relationships between age and BMI in the ageing study, and HOMA-IR in the insulin resistance study.

SPM-8 employs random field theory to approach the problem of multiple comparisons introduced earlier. First, the number of "resolution elements" (resels) is

estimated, the volume of each of these "virtual voxels" being dependent on the smoothness (FWHM) of the brain map (which in turn depends on the intrinsic smoothness of the data and the kernel applied), thus accounting for the topology of the map. Greater smoothness decreases the number of resels and the P_{FWE} correction needed (Worsley *et al*, 1992), but is not equivalent to the Bonferroni correction. The Euler characteristic, which can be thought to represent the number of activated clusters in a brain map at a given threshold, is next estimated based on the number of resels in a map, and approximates the probability of observing an activated cluster at that threshold. Thus a Euler characteristic of 0.05 determines the corrected voxel-extent threshold at which the likelihood that any clusters present are due to chance is 5% (Brett *et al*, 2011). Random field theory also determines cluster-extent thresholds based on cluster size (Friston *et al*, 1994). A corrected cluster-wise $P_{FWE} < 0.05$ was used in this thesis, with the cluster-forming voxel-wise thresholds and further details of the analyses performed for each study described in their respective chapters.

Anatomical identities of the regions of detected voxels were determined using the Wake Forest University PickAtlas (Maldjian *et al*, 2003, 2004) and anatomical automatic labelling (AAL) atlas (Tzourio-Mazoyer *et al*, 2002). Unsmoothed data were extracted using Marsbarr (Brett *et al*, 2002) to examine both global grey matter CBF (with statistical tests performed in SPSS) and from the functionally identified regions from these voxel-wise analyses to illustrate changes or differences in rCBF when further clarification was required.

2.8.13.3 Subject-level BOLD pre-processing and analysis

BOLD fMRI analysis involves fitting a BOLD signal time series to a model of the haemodynamic response function, and estimating the effect of the experimental conditions (e.g. picture viewing) on the signal. In the ageing study BOLD signal acquisition was interrupted whilst instructions were administered and hunger questionnaires answered. As pre-processing and first-level SPM analyses of BOLD signal are best suited to uninterrupted time-series, data were analysed using XBAM version 4.1 (Centre for Neuroimaging Sciences, Institute of Psychiatry, Psychology & Neuroscience, King's College London, 2012), a BOLD fMRI package which uses

non-parametric approaches to minimise assumptions of normality, median statistics to control the effects of outliers, permutation rather than normal theory-based inference, and standardises an individual's response sizes from the fitted model with respect to their variance, permitting mixed-effects group-level analyses whereby intra-subject residual error and inter-subject variability are modelled (Brammer *et al*, 1997; Bullmore *et al*, 1999). The same methods were used in the insulin resistance study for consistency.

T2*-weighted images were first pre-processed, minimising motion-related signal artefact (Bullmore *et al*, 1999), by calculating a 3D volume of the average intensity at each voxel of the images (108 in the ageing study, 320 in the insulin resistance study) collected during the picture-viewing task, to be used as a template to which each of the volumes was realigned. The data were then smoothed using a Gaussian filter (FWHM kernel=5 mm) to improve signal-to-noise characteristics, before responses to viewing the visual stimuli were detected by convolving each component of the experiment (the effect of the different pictures viewed) with each of two gamma variate functions (peak responses at 4 and 8 s). A weighted sum of these two convolutions that provided the best fit to the time-series at each voxel was then computed using a constrained BOLD effect model (Friman *et al*, 2003). A goodness of fit statistic, the sum of squares (SSQ) ratio was computed, comprising the ratio of the SSQ of deviations from the mean image intensity (over the whole time-series) due to the model, to the SSQ of deviations due to the residuals (analogous to T-scores for the β-parameter estimates of fitted GLMs of BOLD contrasts in subject-level SPM analyses). A data-driven null distribution of SSQ-ratios under the assumption of no experimentally determined response was formed by permutation by cyclic rotation with Donoho denosing of the wavelet-transformed time series (Bullmore *et al*, 2001), repeated 20 times at each voxel, and the critical value of SSQ-ratio needed to threshold the map at a type 1 error <1 was calculated. The size of the BOLD response, the effect size, was computed by expressing differences between maximum and minimum values of the fitted model at each voxel for each picture-stimulus condition, as a percentage of the mean image intensity over the whole time-series.

Observed and permuted effect size maps for each subject were transformed into the standard space of Talairach and Tournoux (1998), by computing the transformations

required to map the average image intensity map to the structural GE EPI image and then to the Talairach template, with these transformations applied to the SSQ-ratio and BOLD effect size maps (Brammer *et al*, 1997).

2.8.13.4 Group-level analyses

Group activation maps examining the BOLD signal contrast *within* each separate feeding state evoked by food or blurred vs object pictures were computed by determining the median SSQ-ratio and effect size at each voxel across the group in the observed and permuted data maps (permuted 20 times). The distribution of median SSQ-ratios and effect sizes over all intra-cerebral voxels from the permuted data was then used to derive the null distribution of SSQ-ratios and effect sizes. Cluster level maps were thresholded to yield <1 false positive cluster per brain map to the null distribution, and a voxel-wise threshold of $p<0.05$ (Bullmore *et al*, 1999).

After restricting analyses to grey matter using a mask, comparisons of the aforementioned BOLD contrasts *between* conditions (e.g. feeding state; treatment) or between groups were made by fitting the data at each voxel at which all subjects have non-zero data using a linear model, computing differences in median effect size between measurements at each voxel (b), whilst minimising the sum of absolute deviations to reduce outlier effects:

$$Y = a + bX + e$$

Equation 5

Where Y is the vector of BOLD effect size for each individual, X is the contrast matrix for inter-condition/group contrasts, a is the mean effect size across all individuals in all conditions/groups, b is the computed median difference between conditions/groups, and e is the vector of residual errors. The computed difference in median effect size between condition or groups at each voxel (b) was compared with the null distribution of b (computed by random wavelet permutation of condition membership [1000 times per voxel], assuming the null hypothesis of no effect of condition/group and refitting the model), using cluster-level thresholds yielding < 1 false positive cluster per map to the null distribution of b at a voxel-wise threshold p <

0.05 (Bullmore *et al*, 1999). Further details of the analyses performed in each study are described in the respective chapters.

Correlation analyses were also performed, to examine the relationship between age or BMI in the ageing study, and HOMA-IR measures in the insulin resistance study, with the above picture-evoked BOLD signal contrast were examined by computing voxel-level Pearson product moment correlation coefficients between the variable of interest and BOLD signal contrast (limited to grey matter by a mask) across all volunteers, to produce one correlation (r) per intra-cerebral voxel. A null distribution of r was formed by randomly permuting the variable of interest without replacement to recalculate the respective correlation coefficients, repeated 1000 times per voxel. The observed correlation coefficient could then be assessed under the null hypothesis of no associations, using cluster-level thresholds yielding <1 false positive cluster per map to the null distribution of effect sizes formed by the permuted data, at a voxel-wise threshold $p<0.05$ (Bullmore *et al*, 1999). Further details of the analyses performed are described in the respective results chapters.

The anatomical identities of the regions of detected voxels were determined using Talairach daemon (Lancaster *et al*, 1997, 2000). Data were extracted from the functionally identified regions from these voxel-wise analyses to illustrate changes or differences in BOLD signal when further clarification was required.

2.8.14 Biochemical analyses and non-imaging statistics

Blood samples for glucose were collected in sodium fluoride tubes, insulin, leptin and adiponectin in plain tubes, and gut peptides in aprotinin-treated tubes. Collected blood was kept on ice until the end of each session, then centrifuged for 10 min at 4ºC, before pipetting the supernatant to 2 mL cryogenic screw-to vials. Plasma glucose was analysed in duplicate using a glucose oxidase technique (Yellow Springs Glucose Analyser, Yellow Springs Inc, Arizona USA, coefficient of variation [CV] 2%) immediately after each experiment. Serum was stored at -20ºC for later measurement of insulin using two-site sandwich chemiluminence immunoassays. Initially, the Immulite-2000 assay (Siemens Healthcare Diagnostics Ltd, Surrey, UK), utilising bead-bound murine monoclonal antibodies and sheep polyclonal anti-insulin

antibodies conjugated to alkaline phosphatase, was used but with a reported sensitivity of 3.0 mU/L, it did not accurately quantify the low concentrations of insulin observed in the fasted state. The ADVIA-centaur assay (Siemens Healthcare Diagnostics Ltd, Surrey UK) which utilises two monoclonal murine anti-insulin antibodies, one acridinium ester-labelled in the Lite reagent, the other bound to paramagnetic particles, was subsequently used, as it had greater sensitivity (minimum detectable concentration 0.5 mU/L) and lower inter-assay coefficient of variation (Table 2.6). Serum was also stored for later measurement by sandwich ELISA assays at -80ºC for total GLP-1 and GIP (Millipore Corporation, Billerica, Massachusetts USA), and -20ºC for adiponectin and leptin (R&D Systems Europe, Abingdon, Oxon, UK). Stored samples were analysed in batches at Viapath, King's College Hospital NHS Foundation Trust, such that a complete data-set for each subject was analysed together.

Net incremental areas under the curves (iAUC) for data collected during the OGTT and during each MRI study visit (using the mean of the two pre-ingestion data collection points as baseline) were calculated using the trapezoidal method. Statistical tests were performed using IBM SPSS statistics for Mac version 21 (IBM Corp., Armonk, New York, USA). Data were assessed for normality using the Shapiro-Wilks test. Parametric data were analysed using t-tests, ANOVA and Pearson's correlation. Non-parametric data were analysed using Mann-Whitney U, Kruskall-Wallis and Spearman rank and Chi-square tests as indicated.

Table 2.1

Food images in ageing study

Almond croissant	Vanilla ice cream banana split
Biscuit selection	Pretzels
Chips (Fries)	Penne pasta with carbonara sauce
Chocolate éclair	Strawberry ice cream cornetto
Cheese and salad bread roll	Slice of chocolate cake
Mille-feuille	Bread with cheese spread
Tuna and salad bread roll	Cooked breakfast (fried eggs, baked beans, potato waffle, poached tomato)
Chocolate bar (mars bar)	Brie
Chocolate biscuits	Iced bun
Chicken and salad bread roll	Pasta shells with sauce
Cashew nuts	Marshmallows
Lindt chocolate bar	Slice of chicken, sweetcorn and pineapple topped pizza
Guylian chocolate shells	Crisps (potato chips)
Tinned spaghetti and bread slice	Chocolate éclair
Tortilla chips	Chicken and salad seeded bread roll
Chocolate covered hazelnuts	Cheese, lettuce and tomato bread roll
Iced chocolate cupcake	Marathon chocolate bar
Fruit cake	Sandwich selection (chicken salad and cheese salad)
Kitkat chocolate covered biscuit	Chocolate digestive biscuits
Quality street chocolates	Cheese, cucumber and tomato bread roll
Fish and chips with peas	Peanuts
Cooked breakfast (toast, fried eggs, mushrooms, baked beans)	Chocolate bar
Whole cheese and mushroom pizza	Chocolate pieces
Doughnut with cream	Cheese and crackers
Mashed potato, roast pork with gravy, broccoli and carrots	Salt and pepper crisps (potato chips)
Tortilla wrap with guacamole and potato wedges	Sliced iced chocolate cupcake
Spaghetti Bolognese	Chocolate kitkat
Pecan nuts	Boiled sweets (hard candy)
Egg custard tart	Breaded fish with salad
Chips (fries) with tomato sauce	Slice of cheese and mushroom pizza
Wine gums	Jam doughnuts
Bounty coconut chocolate bar	Chow mein
Danish pastry	Baked beans and jacket potato
Slice of Swiss roll	Penne pasta with tomato sauce and cheese
Scone	Almonds
Chocolate chip cookies	Raspberry tart

Table 2.2

Object images in ageing study

Roll of string	Bulldog clip
Matchbox	Purse
Scrubbing brush	Address book
Compass	Cassette tape
Stapler	Calculator
Mousetrap	Light bulbs
Bath sponge selection	Screws
Brush	Iron
Wrench and pliers	Black floppy disks
Corkscrews	Hairdryer
Spectacle case	Doorstop
Seashells	Flashlight
Cellotape	Chessboard and chess pieces
Plastic clothes pegs	Shoe brush
Necklace	Gaffer and masking tape
Ball of string	Coat hanger
Wallet	Drawing pins
Shoelaces	Hairgrip
Hairbands	Ball of string
Coloured pencils	Coloured plastic clothes pegs
Coloured rubber bands	Ballpoint pens
Rope	Measuring tape
Pencils and pens	Open purse
String	CD Walkman
Open box of matches	Dishwasher sponge
Pencils	Balloons
Selection of sewing thread	Coloured felt tip pens
Mobile/cell phone	Coloured paints and paintbrush
Shoe polish kit	Rubber ink stamp
Telephone	Hairdryer
Bath sponge	Comb
Open wallet	Envelopes
Wool	Coloured floppy disks
Wooden clothes pegs	Coloured key rings
Candle selection	Computer mouse
Candle	Swimming goggles

Table 2.3

High calorie food images in insulin resistant study

	Summed Appeal and Pleasantness	**Caloric Content** (kcal/100 g)		**Summed Appeal and Pleasantness**	**Caloric Content** (kcal/100 g)
Spring rolls 1	9.36	166.0	Pancakes with jam	8.64	376.7
Spring rolls 2	8.86	166.0	Crepes with blueberries	8.71	371.6
Challah bread	7.86	266.4	Crepes with mixed fruit	8.93	353.6
Croissant	7.93	425.0	Chocolate selection	9.36	535.1
Nachos	8.14	503.1	Chocolate bar (mars bar)	8.57	449.5
Pretzels	8.07	409.6	Chocolate bar (twix)	7.50	504.5
Mozerella and vegetables in bread roll	8.29	193.9	Chocolate bar (plain)	8.07	532.3
Jacket potato, prawns, steak	9.14	156.0	Chocolate cookies	8.29	494.0
Jacket potato, steak	9.50	160.6	Chocolate gateau	8.29	393.1
Fish and chips	8.57	176.2	Cheese cake	8.93	355.2
Ham, bread and cheese	7.93	259.5	Sponge cake	9.14	435.3
Cheese	8.43	334.2	Strawberry tart, cream	9.00	226.5
Chicken and tomato pizza	8.29	197.0	Apple turnover	9.64	402.9
Tomato and mushroom pizza	8.50	227.4	Bakewell slice	9.07	368.0
Cheese and tomato pizza	8.64	197.0	Cream slice	8.21	228.3
Chicken and olive pizza	8.14	197.0	Fruit cake	9.43	174.1
Smoked salmon, cream cheese roll	8.07	228.1	Apple pie	8.64	250.8
Cheese, ham and tomato bagel	8.00	206.2	Jelly babies	7.57	331.0
Cream cheese bagel	8.07	241.5	Doughnut	8.64	438.5
Croissant with jam	8.36	337.4	Ice cream cornetto	9.07	330.1
Salami and cheese roll	8.07	297.5	Ice cream cone 1	8.79	331.5
Fruit tart	9.79	297.7	Ice cream cone 2	8.50	258.2
Chocolate with strawberries	9.07	197.5	Strawberry tart	9.71	174.6
Belgian waffle	8.71	354.6	Strawberry meringue	9.86	169.0
Ice cream sundae	8.21	221.7	Cake	8.64	395.3

Table 2.4

Low calorie food images in insulin resistant study

	Summed Appeal and Pleasantness	**Caloric Content** (kcal/100 g)		**Summed Appeal and Pleasantness**	**Caloric Content** (kcal/100 g)
Banana	9.14	95.0	Kebab with rice	9.50	107.6
Blackberries	9.21	32.0	Ham platter	6.21	129.6
Blueberries	8.71	45.0	Turkey with vegetables	8.79	79.4
Chicken soup	7.57	51.0	steak with vegetables	8.21	113.5
Ice lolly	8.07	73.0	Broccoli and potatoes	6.57	84.4
Kiwi	10.07	55.0	Apple	9.14	52.0
Mango	9.93	66.0	Pear	9.21	52.0
Peach	10.29	38.0	Orange	8.71	50.0
Plum	10.07	42.0	Strawberries	10.07	32.0
Raspberries	10.29	32.0	Strawberries	9.93	32.0
Red grapes	9.14	66.0	Mixed fruit	10.29	45.6
Tomato soup	7.57	59.0	Plain popcorn	9.71	31.0
Watermelon	9.21	31.0	Vegetable salad 1	8.07	116.6
White grapes	8.71	66.0	Vegetable salad 2	8.71	147.7
Grilled chicken	9.79	108.0	Vegetable salad 3	8.43	37.1
Sushi	9.71	87.3	Vegetable salad 4	5.79	19.2
Fried rice and vegetables	9.71	109.7	Salad with cheese	9.36	72.5
Cured ham with pickle	6.71	107.0	Potato salad	8.07	110.0
Boiled egg	8.79	154.0	Vegetable salad 5	8.29	23.6
Mackerel with vegetables	8.21	59.2	Vegetable salad 6	8.00	19.5
Cod and potatoes	7.50	139.9	Vegetable salad, salad cream 1	8.36	30.4
Chicken and potatoes	9.43	109.7	Vegetable salad, salad cream 2	7.64	34.7
Roast chicken, vegetables	8.43	71.3	Vegetable salad 7	8.43	20.2
Noodles and chicken	9.07	109.5	Fruit and vegetable salad	9.29	23.2
Kebab	9.93	71.5	Cream of mushroom soup	7.57	40.0

Table 2.5

Object images in insulin resistant study

Gardening gloves	Woolly hat
Red ball	Dumbbell
Baseball	Glass bottle
Basket	Light bulb
Spectacles	Rubber duck
Books	Beads
Brush	Mobile phone
Toy aeroplane	Gardening sheers
Baubles	Shoes
Standing knife	Electric power tool
Straw hat	Comb
Telephone	Feather duster
Floppy discs	Dustpan
Iron	Wallpaper scraper
Electric shaver	Swiss army knife
Candle	Coat hanger
Paints	Wool
Shuttlecock	Headphones
Windscreen scraper	Chess piece
Lighter	Paint brush
Fisherman's hat	Calculator
Coins	Clothes pegs
Watch	Flashlight
Wallet	Tape measure
Hammer	Sponges

Table 2.6

Laboratory assays (information from manufacturer)

		Intra-assay precision				Inter-assay precision			
		Level 1	Level 2	Level 3	Level 4	Level 1	Level 2	Level 3	Level 4
Immulite-2000 insulin chemilluminence (Siemens)	Mean measured insulin (mU/L)	6.27	50.65	228.10		5.89	43.74	122.63	
	CV (%)	4.85	3.14	3.21		8.98	8.18	5.16	
ADVIA Centaur insulin chemilluminence (Siemens)	Mean measured insulin (mU/L)	14.68	45.72	124.51		14.68	45.72	124.51	
	CV (%)	4.6%	3.2%	3.3%		5.9%	2.6%	4.8%	
Millipore total GLP-1 ELISA	Mean measured total GLP-1 (pM)	32	216			39	220		
	CV (%)	1%	2%			<12%	<10%		
Millipore total GIP ELISA	Mean measured total GIP (ng/L)	15	21	185	269	26	50	134	166
	CV (%)	6.7	7.3	8.8	3.0	6.1	3.3	2.3	1.8
Quantikine Adiponectin ELISA	Mean measured adiponectin (mg/L)	1.98	6.99	14.30		2.05	7.44	15.70	
	CV (%)	2.5	3.4	4.7		6.8	5.8	6.9	
Leptin ELISA	Mean measured leptin (ng/L)	64.5	146	621		65.7	146	581	
	CV (%)	3.3	3.0	3.2		5.4	4.2	3.5	

3 Ageing and cerebral response to meal ingestion

3.1 Introduction

The global population aged above 60 years will soon outnumber the population aged under 15 years (UN Department of Economic and Social Affairs., 2009). Our obesity pandemic (World Health Organization, 2006b) is most prevalent in middle-aged adults (Flegal *et al*, 2010), driven by increasingly available, highly palatable, energy-dense foods and reduced physical activity. Through its exacerbation of conditions such as cardiovascular disease, diabetes, musculoskeletal problems and some cancers, obesity will have huge implications on health care provision for our ageing population.

As discussed in Chapter 1, brain networks involved in hedonics, mood and memory influence eating behaviour (Berthoud and Morrison, 2008; Trinko *et al*, 2007). Human functional neuroimaging has shown altered brain responses to food ingestion in obesity, which may persist despite weight loss, in corticolimbic appetitive motivational networks, and in higher executive regions involved in self-control of eating, e.g. dorsolateral prefrontal cortex (DLPFC) (Cornier *et al*, 2009; Le *et al*, 2006).

In this chapter, the impact of ageing on the brain's response to food consumption *per se* is examined, to determine whether brain appetite network processing of satiation when approaching middle age is altered using pseudo-continuous arterial spin labelling (pCASL) fMRI.

3.2 Methods

3.2.1 Subjects

Recruitment methods and inclusion criteria have been described (sections 2.8.1-2). Twenty-four (12 male) healthy right-handed subjects were recruited. Twelve subjects had participated as control subjects for a study of patients with T2DM by my

supervisors' group, whilst I recruited the remaining 12 subjects specifically to expand the age range.

3.2.2 Study protocol

The general experimental design and MRI acquisition details are described in full in section 2.8. All subjects underwent the same protocol (Figure 3.1), and the BOLD fMRI study is described in Chapter 4. With regard to the CBF study, in brief, subjects were studied on two separate mornings following an overnight fast of at least 8 hours. After intravenous cannulation, subjects were positioned in the scanner. Following a GE EPI structural scan used for BOLD image pre-processing, 3D pCASL scans each lasting 6 mins were performed before (pCASL1 at -14 mins) and after (pCASL2-4 at 0, +8 and +28 mins, respectively) subjects were sat up out of the scanner to consume a mixed-meal (200ml, 554kcal, 36.8g fat, 7.8g protein, 47.6g carbohydrate, 22.8±3.8kcal/kg•m^{-2}) or 50ml water between -6 to 0 mins, in random order across the two sessions. Before (-16 mins) and after (-8 mins) pCASL1, after each subsequent pCASL scan (+7, +14 and +34 mins) and after the BOLD fMRI task (+16 mins, Chapter 4) that took place between pCASL3-4, subjects rated appetite on a projected 1-10 visual analogue scale using a handheld keypad, with concurrent blood sampling. The visit was completed with ASSET (a calibration scan for parallel imaging), Axial T1-weighted Fast, Spoiled Gradient Recalled acquisition (FSPGR), Axial T2-weighted Fast Spin Echo (FR-FSE) and Axial T2-weighted Fluid Attenuated Inversion Recovery (FLAIR) scans.

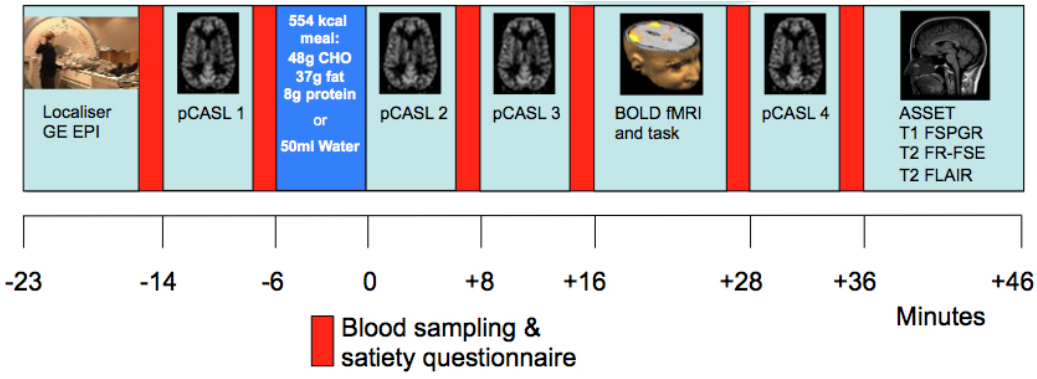

Figure 3.1

Study protocol

The order of the water/meal visits in the 12 subjects I had recruited was randomised with equal distribution (6 water first, 6 meal first). However pCASL data from two subjects who received the meal first were not saved or usable, and studies had to be repeated on another day.

3.2.3 Blood sampling

Failure of cannulation caused incomplete glucose sample collection in six of 24 subjects, and insulin samples were not obtained in all visits in a further three subjects.

3.2.4 Statistical analyses

General non-imaging statistical methods are described in section 2.8.14. Data are presented as mean±SEM or median with the interquartile range. pCASL image pre-processing and statistical analyses are described in sections 2.8.13.1-2. Smoothed, normalised CBF maps calculated for each subject, were entered into a flexible factorial mixed-effects GLM, with subject as a main factor, and an interaction factor of feeding status (2 levels: meal vs water) vs time (4 levels: pCASL1-4) (Figure 3.2). Analyses were restricted to grey matter, with mean global grey matter CBF used as a nuisance covariate. As the final pCASL image was not acquired for one subject, the model represents data from 23 subjects.

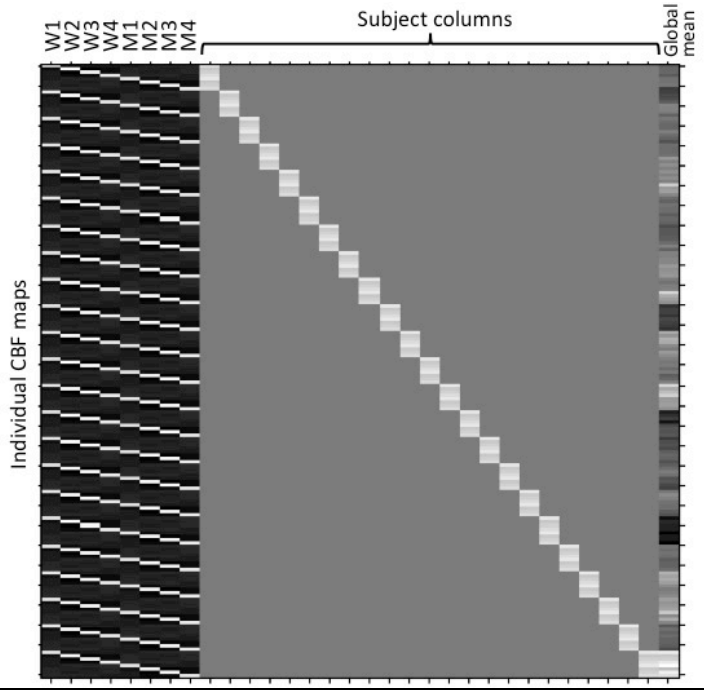

Figure 3.2
Flexible factorial model design matrix. Each row represents an individual CBF map, at a specific time poiont (pCASL1-4), within each feeding condition (Meal/Water) for an individual subject (the light coloured bar in the feeding status x time interaction columns: W1-4 = Water pCASL1-4; M1-4 = Meal pCASL1-4, respectively, [1=pre-ingestion; 2-4=post-ingestion]). The scans are grouped together for each subject, as indicated by the 23 subject main effect columns. The mean global grey matter CBF is used as a nuisance covariate in the global mean column.

T-contrast vectors were defined to: (a) exclude differences in rCBF pre-water compared to pre-meal (W1 vs M1); (b) examine the effect of the meal compared to water within each post-ingestion time point, pCASL2, 3 and 4 (i.e. W2 vs M2, W3 vs M3, W4 vs M4); (c) examine the main effect of the meal compared to water across the 3 post-ingestion time points, pCASL2-4 (i.e. W2-4 vs M2-4); (d) the interaction between feeding status and pre- vs post-ingestion (i.e. [meal vs water] x [pCASL1 vs pCASL2, 3 and 4, separately]).

Voxel-level multiple regression analyses were performed to examine the association between age, correcting for BMI (which was positively correlated with age (r_s=0.539, p=0.007), with pre-ingestion rCBF (W1 and M1) separately, using global grey matter CBF as a nuisance covariate (n=24). After creating maps of the difference in rCBF between post-meal and post-water states at each voxel within each time point ([M2-W2], [M3-W3] (n=24 each) and [M4-W4] (n=23)), similar analyses were performed with these "difference maps" using the respective difference in global grey matter CBF between feeding states as a nuisance covariate (Figure 3.3). The effect of ageing was the primary endpoint, but exploratory analyses for the effect of BMI were performed.

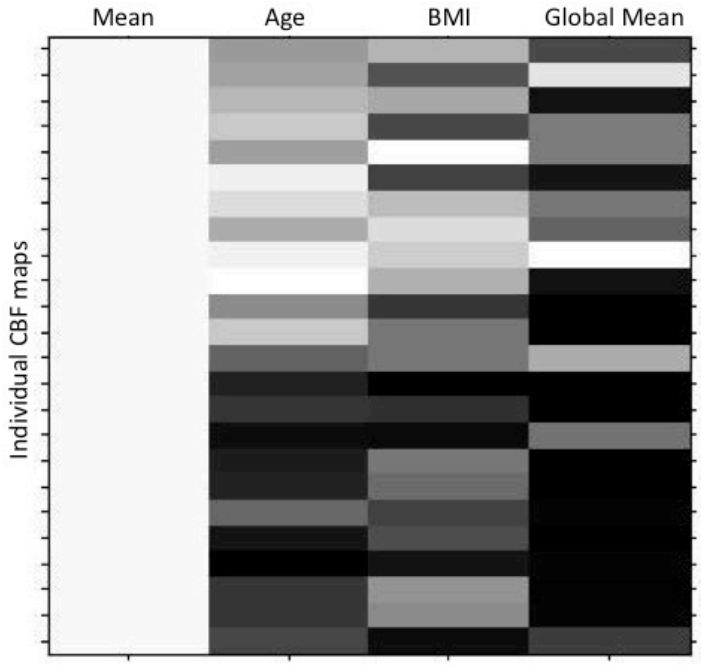

Figure 3.3

Multiple regression model. Global mean = global grey matter mean CBF

A cluster-forming uncorrected voxel-wise threshold of P<0.005 was employed, but only clusters that survived statistical significance ($P_{FWE\text{-}corrected}$<0.05) after correction for multiple comparisons are reported. Unsmoothed, normalised data were extracted from brain maps to examine global grey matter CBF (with statistical tests performed in SPSS) and functionally-defined regions from these voxel-wise analyses to quantify rCBF in physiological units and further characterise the regression analyses.

Exploratory analyses of a priori regions of interest, involved in appetite regulation (Berthoud and Morrison, 2008), were also performed. Anatomical masks of left and right insula, amygdala, caudate, putamen, thalamus, hippocampus and midline hypothalamus were created from the Automated Anatomical Labelling (AAL) atlas (Tzourio-Mazoyer *et al*, 2002) provided within the SPM analysis suite. In addition, masks of left and right medial and lateral orbitofrontal cortex (OFC) and DLPFC were created within the WFU PickAtlas (Maldjian *et al*, 2003, 2004) as follows: medial OFC by union of the gyrus rectus with the orbital parts of the medial and superior frontal gyri; lateral OFC by union of orbital parts of the middle and inferior frontal gyri and; DLPFC by union of Talairach daemon Brodmann areas 9, 10 and 46, inflated by 3 voxels, then using the interception of this mask with the middle frontal gyrus (Hutcherson *et al*, 2012), and subtracting the above OFC regions to ensure no overlap. Unsmoothed normalised data were extracted using these masks, and by using the time at which each ASL scan was completed, net incremental area under the curves (iAUC) for rCBF for each region was calculated. Paired t-tests were performed in SPSS, applying the Bonferroni correction for multiple comparisons (19 regions).

3.3 Results

3.3.1 Subjects

Subjects were aged 19.5-52.6 (median 35.9) years. None were obese (mean±SD BMI of 24.9±4.0 kg/m^2), or diabetic (mean±SD HbA1c 5.3±0.4%, fasting glucose 4.8±0.1 mmol/L) at screening (Table 3.1). Age was positively correlated with BMI (r_s=0.539, p=0.007).

3.3.2 Glucose and Insulin

Baseline glucose (pre-water vs pre-meal (mean±S.D.): 4.6±0.4 vs 4.4±0.4 mmol/L, t(17)=1.743, p=0.099) and insulin (pre-water vs pre-meal (median (interquartile range)): 4.7 (2.0) vs 6.1 (5.4) mU/L, WSR Z=-0.710, p=0.478) were similar between visits, but compared to water, meal ingestion evoked a small but significant increase in glucose (post-water vs post-meal net iAUC: 6.7±15.7 vs 28.7±30.5 mmol•min/L, t(17)=-3.434, p=0.003) and an increase in insulin (post-water vs post-meal net iAUC: -0.7(2.0) vs 2.2(8.9) mU•min/L, WSR Z = -3.237, p=0.001) (Figure 3.4).

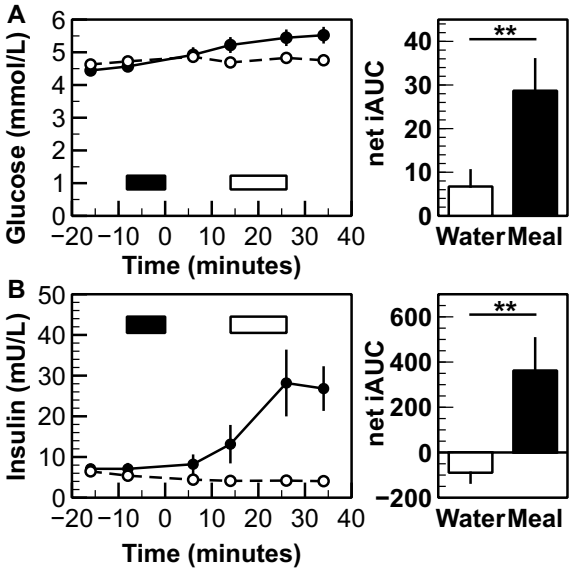

Figure 3.4

Glucose (A) and insulin (B) after the meal (solid line) and water (dashed line). Left: Mean (±SEM). Horizontal bars: black = time of water/meal; white = BOLD task. Right: net iAUC; ** $p < 0.01$.

3.3.3 Symptom scores

Analyses are based on 22 subjects, as data were incomplete for two. No differences in baseline symptoms were observed between visits (hunger: t(21)=1.23, p=0.228; fullness: WSR Z=−0.119, p=0.905; pleasantness to eat: WSR Z=−1.460, p=0.144; nausea: WSR Z=−1.091, p=0.275). Net iAUC analyses showed the meal, compared to water, induced greater fullness (t(21)=–4.826, p<0.001) and reduced hunger (WSR Z=−2.062, p=0.039) and pleasantness to eat (WSR Z=−1.460, p=0.144), without effect on nausea (WSR Z =−1.091, p=0.275) (Figure 3.5).

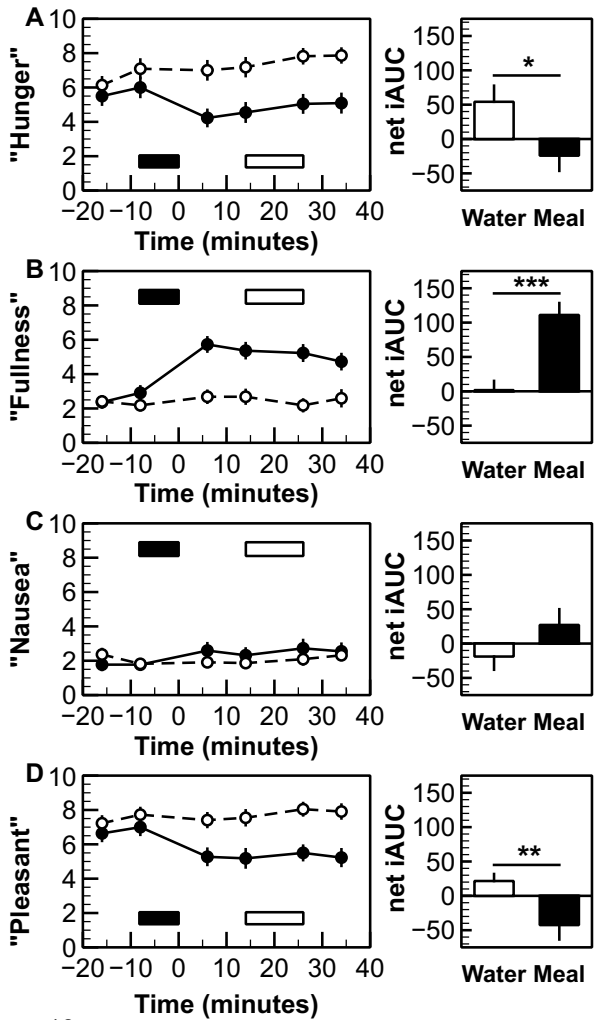

Figure 3.5

Hunger (A), fullness (B), nausea (C) and pleasantness to eat (D) scores after the meal (solid line) and water (dashed line). Left: Mean (±SEM). Horizontal bars: black: time of meal/water; white: BOLD task. Right: net iAUC; **p* = 0.039; ***p* = 0.002; ****p* < 0.001.

After correcting for BMI, age was positively associated with net iAUC for hunger after meal ingestion (r=0.449, p=0.041, Figure 3.6), with less suppression of hunger by the meal with increasing age. There were no significant associations between age and net iAUC for hunger post-water ingestion, nor with differences in net iAUC for hunger between feeding conditions. No other associations for the remaining symptoms with age/BMI reached statistical significance.

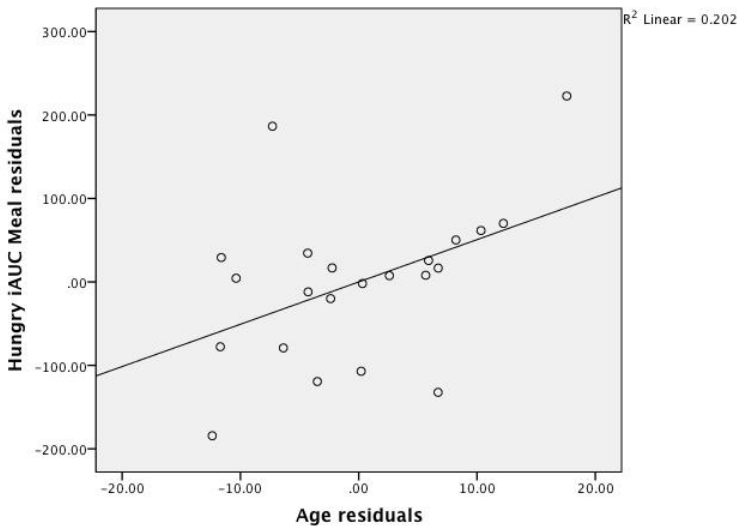

Figure 3.6

Partial correlation of post-meal hunger net iAUC with age, after adjusting for BMI.

3.3.4 Global grey matter CBF

The extracted global grey matter CBF during the study was subjected to repeated-measures ANOVA in SPSS. There was no significant main effect of the meal ($F(1,22)=0.131$, $p=0.721$) on global grey matter CBF, but there was a main effect of time, ($F(1.9,41.802)=8.818$, $p=0.001$), with a time x meal interaction ($F(3,66)=4.808$, $p<0.001$) (Figure 3.7). Post-hoc t-tests showed no significant difference at baseline (pre-ingestion) (paired t-test p=0.136 uncorrected) between the two visits, and that the time x meal interaction was due to a fall in global grey matter CBF after the meal over time (paired t-tests for pCASL2, pCASL3 and pCASL4 compared to pCASL1 post-meal ingestion: p=0.001, p=0.020, p<0.001 uncorrected, respectively). There were no significant relationships between age or BMI with global grey matter CBF at any time point in either meal or water studies on multiple linear regression analyses.

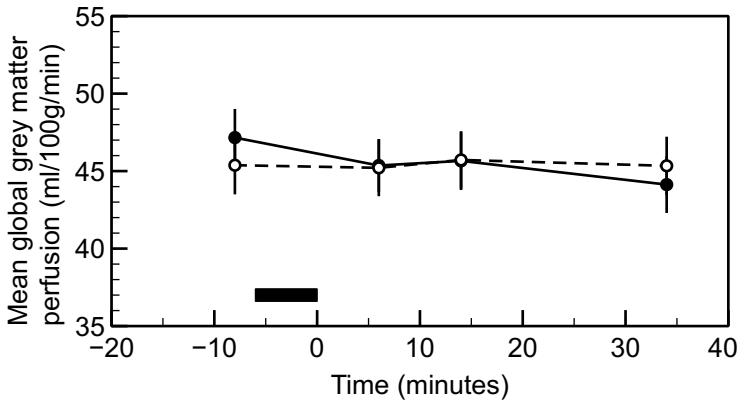

Figure 3.7

Global grey matter perfusion. Bars are S.E. Dashed line = water; solid line = mixed meal. Black bar = time of water/mixed meal.

3.3.5 Difference in pre-ingestion rCBF (pCASL1)

T-contrasts were created to compare rCBF within each time point between visits, adjusting for global grey matter CBF to ensure that any detected regional changes were not driven by post-prandial reduction in global CBF. No differences in pre-meal and pre-water rCBF were expected. However, whilst no regions showed greater rCBF pre-meal than pre-water ingestion, rCBF was lower in bilateral middle occipital-lingual gyrus pre-meal (Figure 3.8A, Table 3.2). To determine if this was due to an order effect, a paired t-test was performed showing that rCBF was lower in bilateral inferior occipital and cerebellum, and greater in bilateral insula and supplemental motor areas during the first than the second visit, irrespective of what was subsequently consumed (Figure 3.9, Table 3.3).

3.3.6 Difference in post-ingestion rCBF (pCASL2, 0 to +6 mins)

rCBF immediately after the meal, compared to water, was greater in bilateral insula and parahippocampal gyrus, and lower in right precuneus (Figure 3.8B, Table 3.2).

3.3.7 Difference in post-ingestion rCBF (pCASL3, +8 to +14 mins)

At +8 to +14 mins, rCBF after meal compared to water ingestion was greater in left inferior frontal gyrus (lateral PFC) and in a cluster extending from the cingulate gyrus to the supplementary motor area, and lower in right precuneus (inferior parietal lobule) and left lingual gyrus (Figure 3.8C, Table 3.2).

3.3.8 Difference in post-ingestion rCBF (pCASL4, +28 to +34 mins)

At +28 to +34 mins, rCBF after meal compared to water ingestion was greater in left insula, right operculum and anterior cingulate and lower in bilateral lingual gyrus, left precuneus and left cerebellum (Figure 3.8D, Table 3.2).

3.3.9 Difference in post-ingestion rCBF (main effect meal across pCASL2-4)

Given the similarity in changes in rCBF at each post-ingestion time point, T-contrasts were constructed to summarise the main effect of post-meal vs post-water ingestion. Meal ingestion was associated with greater rCBF in bilateral insula, right cingulate

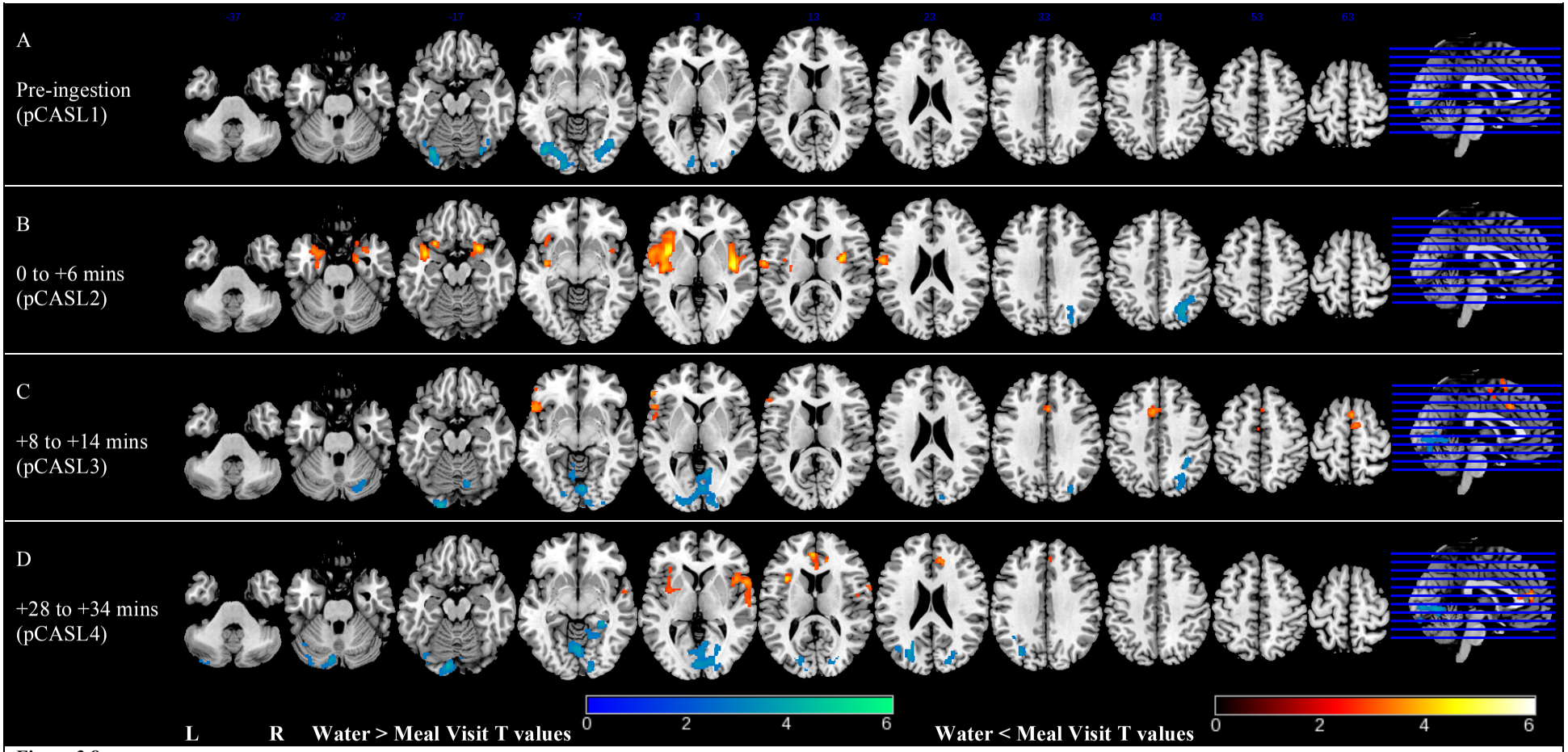

Figure 3.8

Group T-contrast brain maps of differences in rCBF, showing clusters with greater (red) or lesser (blue) rCBF on the meal than the water visit at (A) pre-ingestion and (B) 0 to +6, (C) +8 to +14 and (D) +28 to +34 mins post-ingestion time points. Voxel-threshold $P_{uncorrected} < 0.005$. Cluster-threshold $P_{FWE\text{-}corrected} < 0.05$.

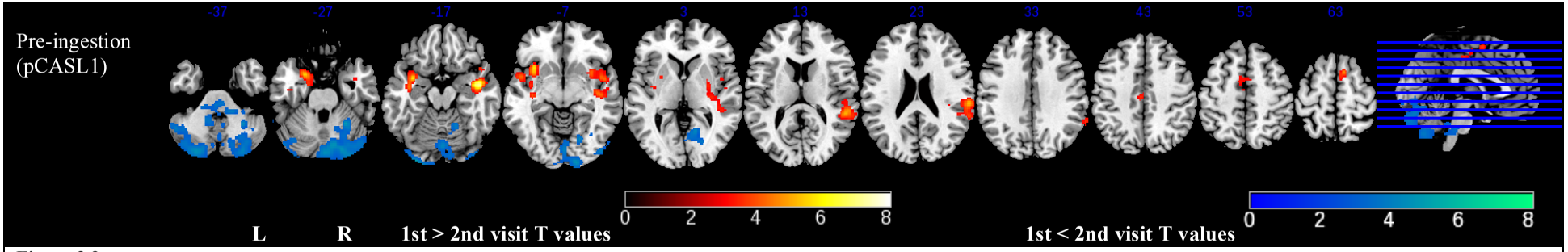

Figure 3.9

Group T-contrast brain maps of differences in rCBF during pCASL1 pre-ingestion scans, demonstrating an order effect, showing clusters with greater (red) or lesser (blue) rCBF on the first than second visit (both in the fasted state, irrespective of what would next be consumed). Voxel-threshold $P_{uncorrected} < 0.005$. Cluster-threshold $P_{FWE\text{-}corrected} < 0.05$.

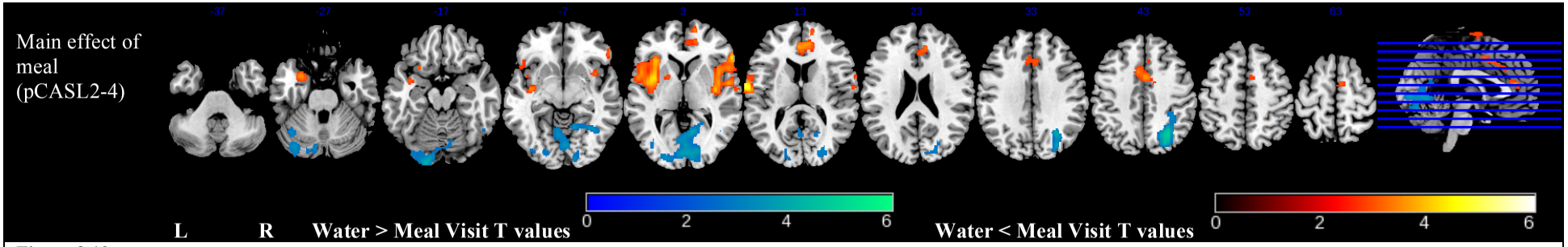

Figure 3.10

Group T-contrast brain maps of the main post-meal vs post-water differences in rCBF across the three post-ingestion time-points (pCASL2-4), showing clusters with greater (red) or lesser (blue) rCBF after meal, than after water ingestion. Voxel-threshold $P_{uncorrected} < 0.005$. Cluster-threshold $P_{FWE\text{-}corrected} < 0.05$.

gyrus and frontal gyrus/anterior cingulate, and lower rCBF in right precuneus and bilateral lingual gyrus, compared to water ingestion (Figure 3.10, Table 3.2).

3.3.10 Difference in change from pre- to post-ingestion rCBF between feeding conditions.

To confirm that the higher post-meal insular rCBF was not driven by the non-significant higher global CBF pre-meal compared to pre-water, three T-contrasts were calculated for the interaction between feeding status (meal vs water) and pre- vs each post-ingestion time point (pCASL1 vs pCASL2, 3 and 4 separately). The only interaction that revealed a significant change was from pre-ingestion to immediately post-ingestion (pCASL1 vs 2) in left insula (MNI coordinates X=−36, Y=2, Z=−18, T-value 4.30, 457 voxels, cluster $P_{FWE\text{-}corrected}$=0.018), the right insula failing to reach statistical significance (X=32, Y=−2, Z=12, T-value 5.22, 312 voxels, $P_{FWE\text{-}corrected}$ = 0.101). The mean rCBF data in this left insula cluster showed a post-meal rise from baseline compared to a post-water fall (Figure 3.11). There were no clusters that reached statistical significance when T-contrasts were constructed to examine differences in the main effect of meal vs water ingestion across the three post-ingestion time points (pCASL2,3 and 4) compared to baseline (pCASL1).

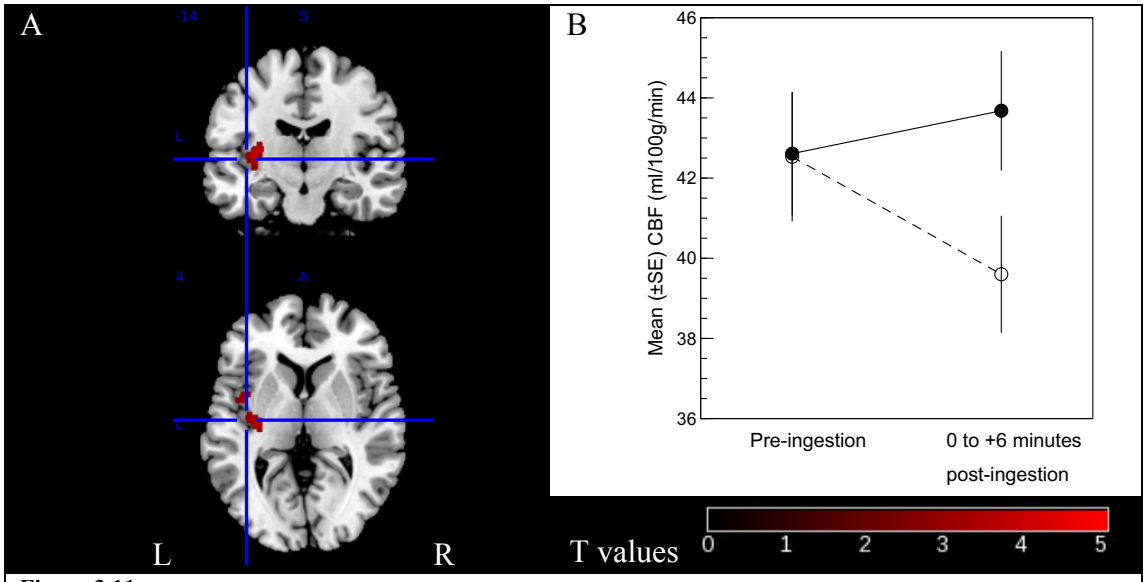

Figure 3.11

A: Group T-contrast brain CBF map of the feeding status x pre- vs immediately post-ingestion interaction; B: Extracted rCBF from cluster (insula) in (A). Dashed line = water; solid line = meal. Voxel-threshold $P_{uncorrected} < 0.005$. Cluster-threshold $P_{FWE\text{-}corrected} < 0.05$.

3.3.11 Multiple regression: Pre-ingestion pCASL1 (pre-water and pre-meal)

As there were differences in rCBF pre-meal compared to pre-water ingestion, separate multiple regression analyses were performed, with age and BMI as covariates, and global grey matter CBF as a nuisance covariate. For both visits, there were no regions where age was associated with rCBF after adjusting for BMI. However, after adjusting for age, BMI was positively associated with rCBF in right subcallosal gyrus-putamen, left medial OFC (superior orbital frontal gyrus), right lateral OFC (superior frontal and middle orbital frontal gyri) and bilateral supplemental motor areas, and negatively associated with rCBF in left posterior cingulate/precuneus, right middle occipital gyrus and left cerebellum pre-water ingestion, and positively associated with rCBF in superior frontal gyrus and negatively associated in cerebellum pre-meal ingestion (Figure 3.12, Table 3.4).

3.3.12 Multiple regression: Post-meal minus post-water pCASL2 (0 to +6 mins)

Similar multiple regression analyses were performed using [meal-minus-water] CBF difference maps at each post-ingestion time point (pCASL2, 3 and 4), with age and BMI as covariates and the respective difference in global grey matter CBF as a nuisance covariate.

Age was positively associated with the difference in rCBF immediately after meal compared to water ingestion (pCASL2) in the superior frontal gyrus (OFC) and negatively associated in the cerebellum after adjusting for BMI (Figure 3.13, Table 3.5). After plotting the linear regression lines for the extracted rCBF data, the intercept with the x-axis was 35.4 years for OFC (above which increasing age is associated with increasingly greater perfusion after meal compared to water ingestion) and 35.4 years for cerebellum (below which increasing age is associated with increasingly greater perfusion after the meal compared to water ingestion). There were no regions that demonstrated an association with BMI after adjusting for age.

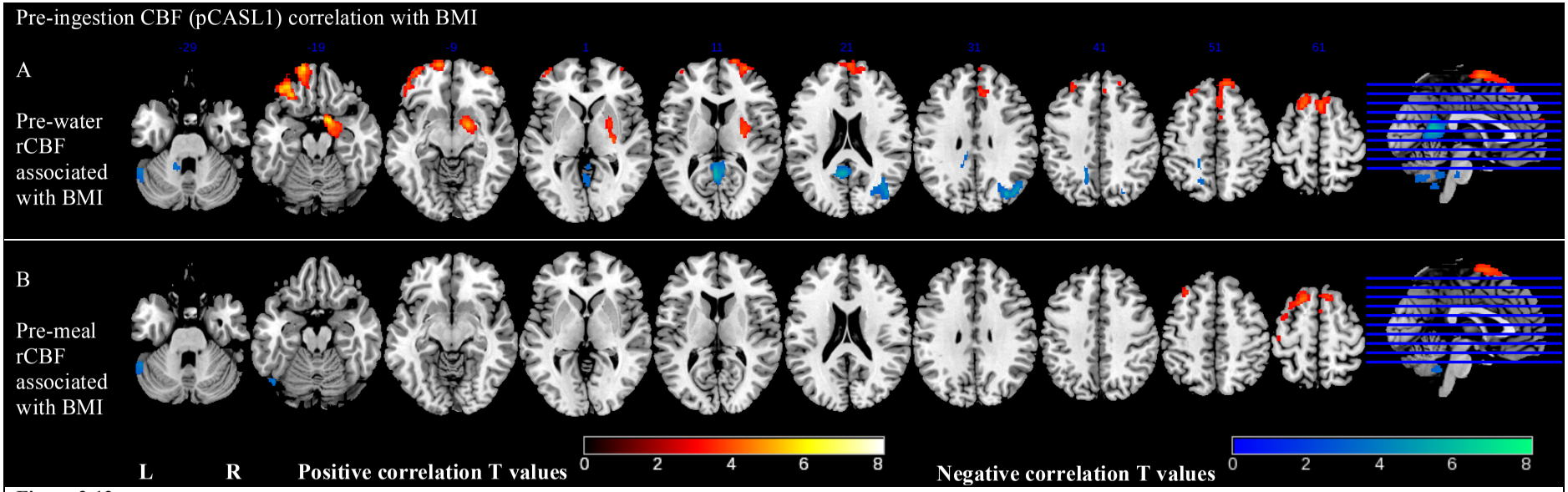

Figure 3.12

Group brain maps of voxel-wise multiple regression of fasted, pre-ingestion CBF (pCASL1) with BMI, showing clusters exhibiting positive (red) or negative (blue) associations between BMI and (A) pre-water and (B) pre-meal CBF, after correction for age. Voxel-threshold $P_{uncorrected} < 0.005$. Cluster-threshold $P_{FWE\text{-}corrected} < 0.05$.

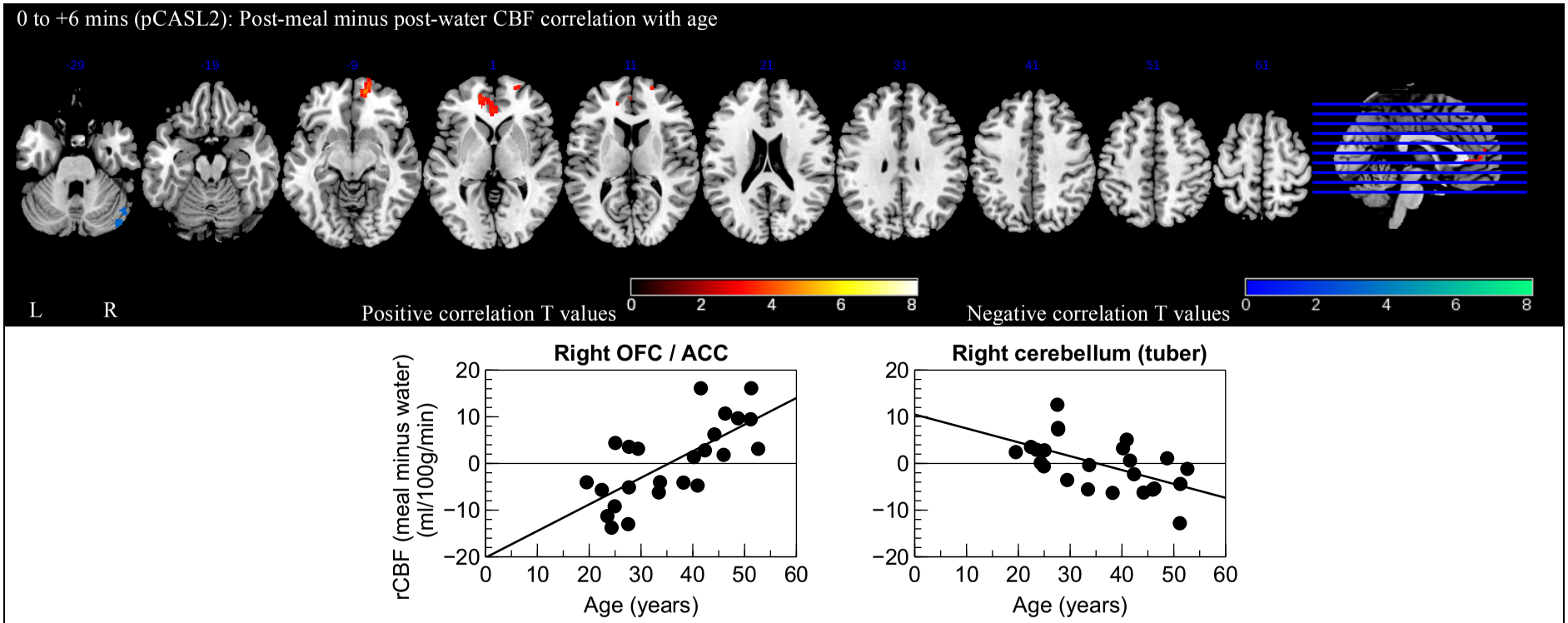

Figure 3.13

Group brain maps of voxel-wise multiple regression of differences in CBF between feeding states at 0 to +6 mins (pCASL2, post-meal minus post-water) with age, showing clusters with positive (red) or negative (blue) associations with age, after correction for BMI. Voxel-threshold $P_{uncorrected} < 0.005$. Cluster-threshold $P_{FWE\text{-}corrected} < 0.05$. Extracted mean rCBF from clusters identified, plotted for illustration. Positive values = rCBF greater after meal than water.

3.3.13 Multiple regression: Post-meal minus post-water pCASL3 (+8 to +14 mins)

There were no regions demonstrating an association between age and difference in rCBF between post-meal and post-water states after adjusting for BMI, whilst BMI was positively associated with the difference in rCBF in the cerebellum (Figure 3.14, Table 3.5). The plot of the linear regression line of the extracted rCBF data showed the intercept with the x-axis to be 26.44 kg/m^2 (above which increasing BMI is associated with increasingly greater perfusion of the cerebellum after meal compared to water ingestion).

3.3.14 Multiple regression: Post-meal minus post-water pCASL4 (+28 to +34 mins)

Age was positively associated with the difference in rCBF between post-meal and post-water states after adjusting for BMI in the precentral gyrus, inferior frontal gyrus, medial frontal gyrus and superior temporal gyrus (Figure 3.15, Table 3.5). The plots of the linear regression lines showed that increasing age was associated with increasingly greater perfusion of these regions after meal compared to water ingestion above the ages of 38.2 years, 35.9 years, 36.4 years and 35.9 years for the respective regions. There were no regions demonstrating an association between BMI and difference in CBF between feeding states.

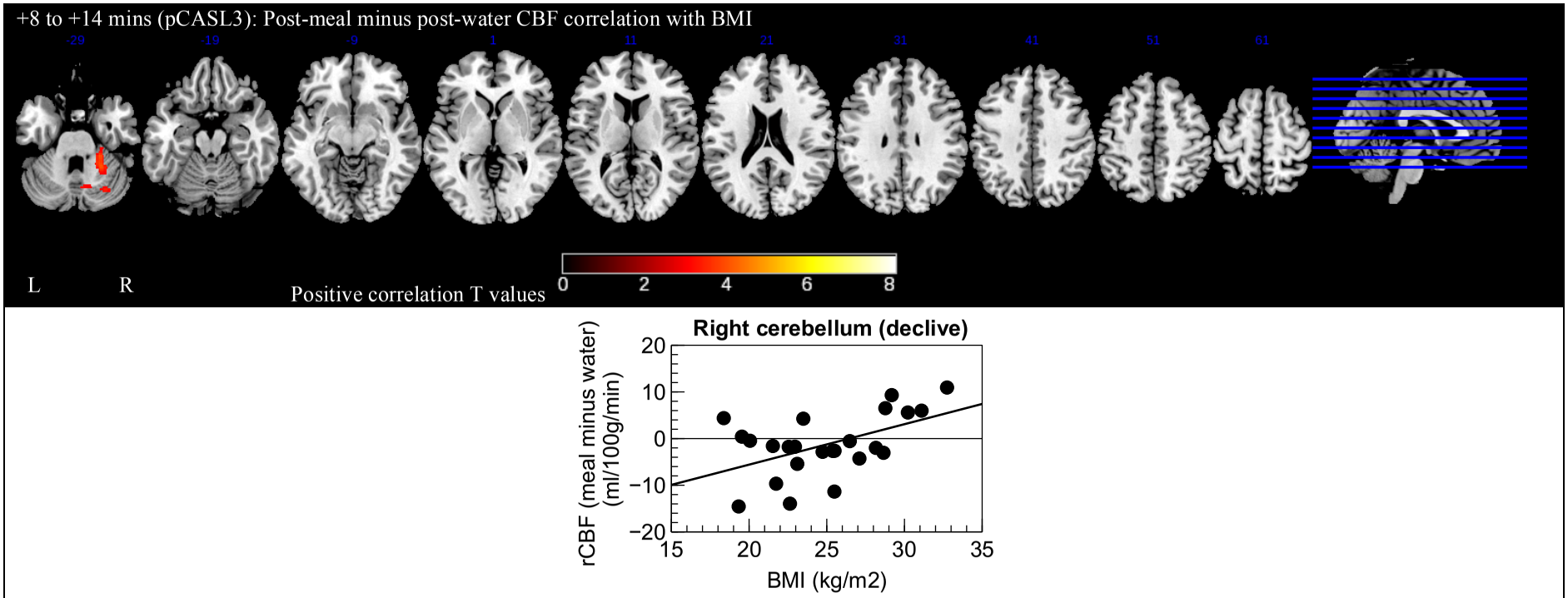

Figure 3.14

Group brain maps of voxel-wise multiple regression of differences in CBF between feeding states at +8 to +14 mins (pCASL3, post-meal minus post-water) with BMI, showing clusters exhibiting positive associations with BMI after correcting for age. Voxel-threshold $P_{uncorrected} < 0.005$. Cluster-threshold $P_{FWE\text{-}corrected} < 0.05$. Extracted mean rCBF from the cluster identified, plotted for illustration. Positive values = rCBF greater after meal than water.

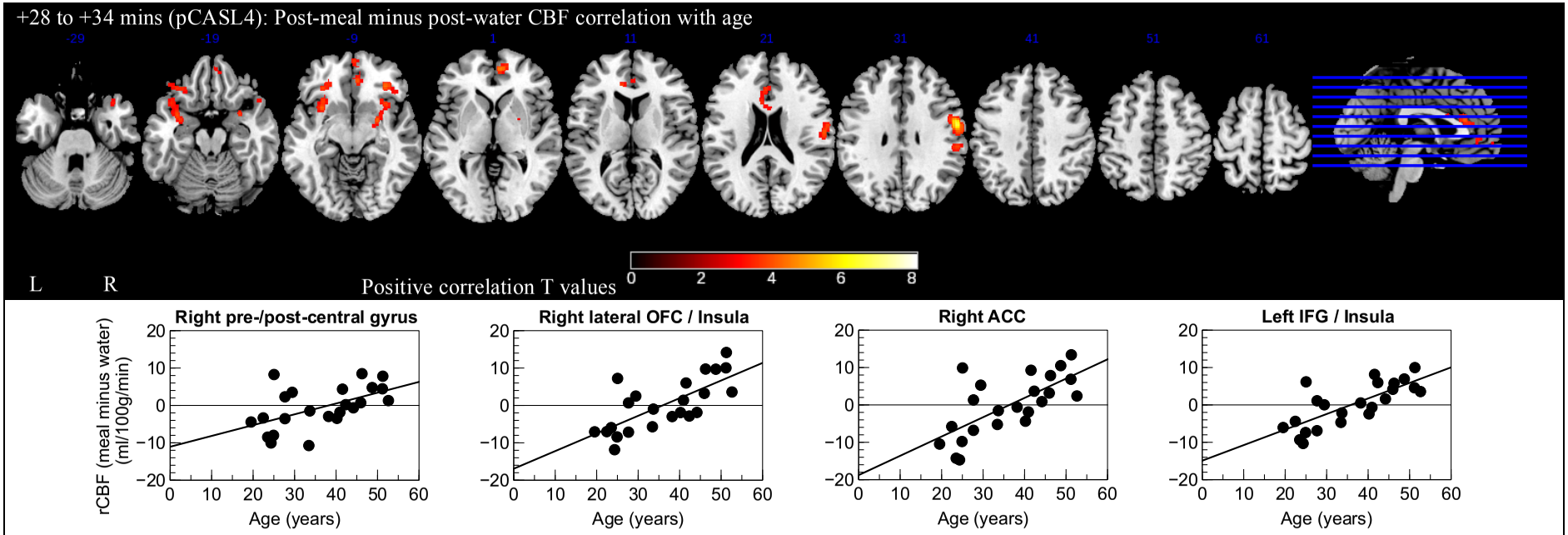

Figure 3.15

Group brain maps of voxel-wise multiple regression of differences in CBF between feeding states at +28 to +34 mins (pCASL4, post-meal minus post-water) with age, showing clusters exhibiting positive association with age after correcting for BMI. Voxel-threshold $P_{uncorrected} < 0.005$. Cluster-threshold $P_{FWE\text{-}corrected} < 0.05$. Extracted mean rCBF from clusters identified, plotted for illustration. Positive values = rCBF greater after meal than water.

3.3.15 Region of interest analyses

Given that there were regional differences in the pre-water and pre-meal rCBF, net iAUC for the extracted rCBF of 19 *a priori* regions of interest were calculated. The greater reduction in CBF from baseline after meal compared to water ingestion in the right lateral OFC, right thalamus and right hippocampus survived Bonferroni correction (p=0.0470, p=0.0125, p=0.0364 respectively) (Figure 3.16). There were no regions in which the difference in net iAUC-CBF between meal and water studies was associated with age or BMI.

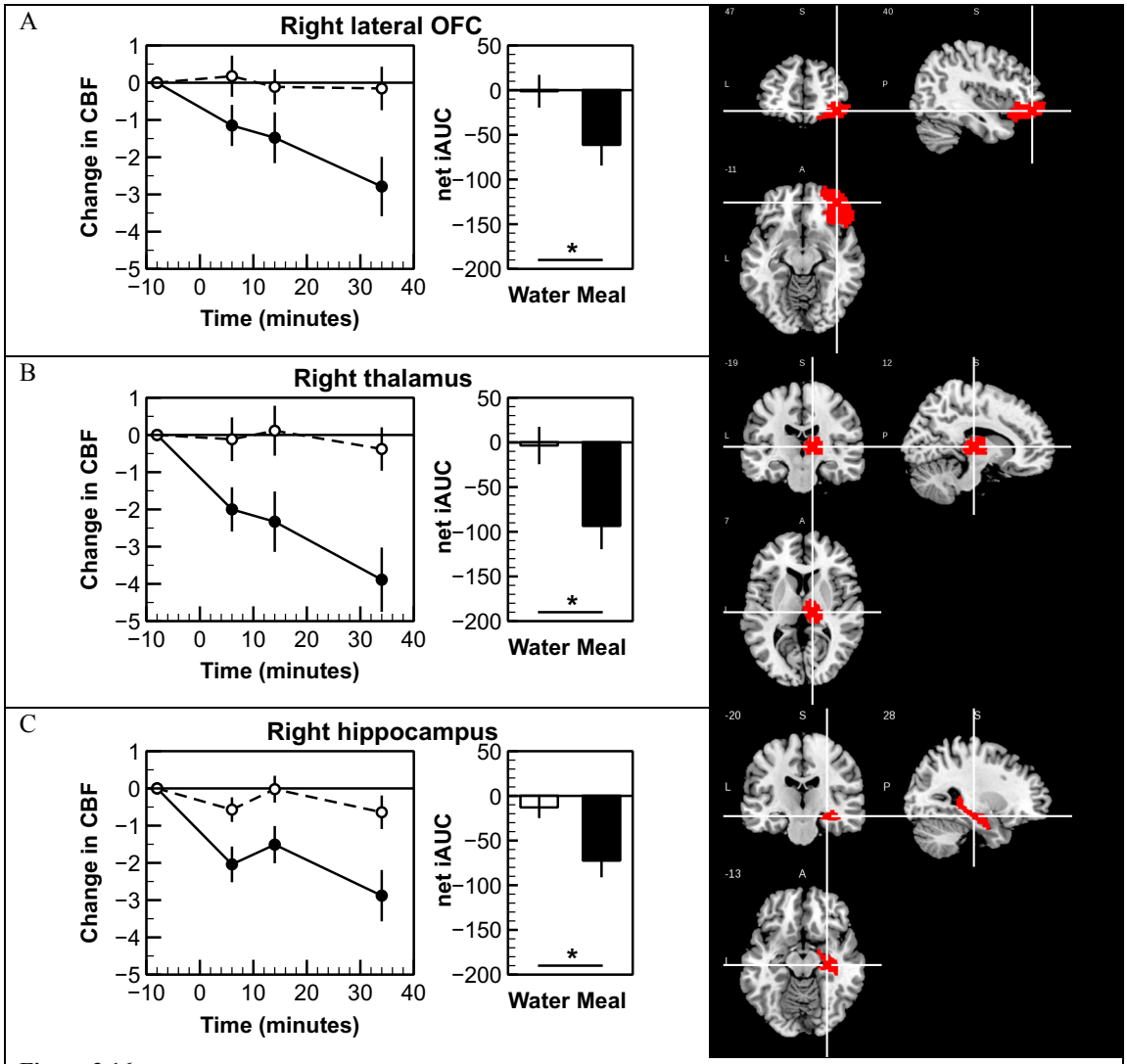

Figure 3.16

Change in rCBF (ml/100g/min) after water (dashed line) and meal ingestion (solid line) (left) and the respective net iAUC (ml/100g) (middle) for (A) right lateral OFC, (B) right thalamus and (C) right hippocampus anatomical regions of interest (masks depicted). *p < 0.05 Bonferonni corrected.

3.4 Discussion

This study aimed to characterise changes in normal human brain activity following meal ingestion, and how age and weight may influence such responses, using pCASL fMRI. Global grey matter CBF decreased during the 34 mins post-meal observation period, to a detectable degree that was surprising given the premise of cerebral haemodynamic autoregulation (Willie *et al*, 2014), and which to my knowledge has not previously been demonstrated. One possible explanation is a "steal" effect, with food ingestion diverting blood to the gastrointestinal tract. Post-prandial blood flow has been shown to increase rapidly in the coeliac artery and more gradually in the superior mesenteric artery, although common carotid, internal carotid and vertebral artery blood flow, as markers of global CBF, has not been shown to change post-prandially (Eicke *et al*, 2003; Someya *et al*, 2008; Totman *et al*, 2009; Xu *et al*, 2015). Potential reasons for the discrepancies between the current findings and these studies are that Totman *et al* (2009) and Xu *et al* (2015) investigated the response to oral glucose rather than a meal using MRI, whilst Eicke *et al* (2003) used duplex Doppler sonography to quantify CBF changes after a mixed-meal, a method that has lower reproducibility. Unfortunately, previous [^{15}O]H_2O-PET studies did not report post-meal changes in global CBF (Gautier *et al*, 2001; Tataranni *et al*, 1999). This diversion of blood may be accompanied by post-prandial hypotension, a phenomenon defined as a reduction in systolic blood pressure by 20 mmHg, that peaks 45 mins after eating and more commonly affects individuals with existing autonomic dysfunction (Trahair *et al*, 2014). Changes in blood pressure are likely to have been minimal in the present study, as subjects were healthy, and supine immediately after eating. Nevertheless, subtle changes in blood pressure may have resulted in small fluctuations in cerebral perfusion.

3.4.1 Effect of meal ingestion

Voxel-wise analyses were performed to investigate regional changes in brain activity, as reflected by changes in rCBF, upon meal compared to water ingestion, at each time point of the study, correcting for changes in global grey matter CBF. The observation that rCBF was greater pre-water compared to pre-meal ingestion in bilateral lingual and fusiform gyri, regions predominantly involved in visual processing, was

unexpected as subjects were fasted and had yet to consume the meal or water, with identical conditions at this point of each visit. This may have been due to an order effect of visits, as lower rCBF in bilateral inferior occipital and cerebellar regions was observed during the first compared to the second visit at this pre-ingestion (pCASL1) timepoint, irrespective of what was subsequently consumed. The imbalance in randomisation caused by re-acquiring lost data for two subjects, although minor, may have contributed to the greater activity of these occipital brain regions in the pre-water than pre-meal scan, as the two subjects repeating their first study would have known by default what they would be consuming during the repeat of their first visit and differences in expectation and spontaneous thought during this period would be expected to affect activation in brain regions involved in resting state activity. A recent meta-analysis has shown that the anterior insula and lingual gyrus play a role in this (Fox *et al*, 2015), in addition to the recognised "default mode network" described by Raichle (2015). The greater insular rCBF during the pre-ingestion scan of the very first visit compared to that of the second visit (irrespective of what was later consumed) is in keeping with this, but differences in activity were no longer observed when visit order was almost equally balanced across the water and meal visits, indicating the randomisation process controlled for this order effect in the insula well.

The increased activity within bilateral insula/opercula regions *after* meal compared to water ingestion (significant immediately after eating and during the final scan, with the non-significant change in the intermediate post-prandial scan accompanied by increased rCBF in part of the right lateral pre-frontal cortex that was spatially close to the insula), and the significantly greater rCBF in bilateral insula observed when the main effect of the meal was compared to water across the three post-ingestion studies, can be attributed to meal ingestion, especially in the absence of any regions where rCBF was greater pre-meal compared to pre-water. The effect was spatially greatest within bilateral insula immediately after meal ingestion. Furthermore, the rise in rCBF from pre-meal to immediately post-meal in the left insula was significantly greater than the decrease observed after water ingestion in the interaction analysis (water/meal vs pre-/immediately post-ingestion), with similar findings in the right insula not reaching statistical significance. This is consistent with the insula and operculum functioning as the primary gustatory cortex (de Araujo *et al*, 2012), processing taste and interoceptive awareness, with this early response likely to

represent both the taste of the meal but also the process of satiation, the immediate drive to terminate a meal, whilst later responses signal satiety, influencing subsequent eating behaviour, which is explored further in the next chapter. Interestingly, decreased rather than increased insular rCBF after meal (Gautier *et al*, 2001; Tataranni *et al*, 1999) and glucose ingestion (Page *et al*, 2013) have been shown with PET and pulsed ASL (pASL) fMRI respectively. The timing of meal ingestion and scanning in these studies may explain the disparity between these findings and those of the present study. In the PET studies, two 1 minute scans were performed "at baseline and two after feeding, with intervals of 10-15 mins between scans", which presumably refers to the time difference between the two scans, as feeding of the liquid meal was completed over a 25 mins period, whilst in the pASL study, CBF data were acquired every 5 mins during the hour following glucose/fructose drink, and it is not clear at what point changes in insula activity occurred. These studies therefore do not characterise the changes in insular activity observed immediately post-ingestion. Conversely, Frank *et al* (2012), using pASL fMRI, demonstrated a small decrease in insula rCBF at 30 mins, and a much larger increase in rCBF at 120 mins when low fat yoghurt was eaten, the latter observation being absent when high fat yoghurt was consumed. It is conceivable that a triphasic response may occur, with an immediate post-prandial increase in insular rCBF, followed by a decrease and a late increase, reflecting roles in processing taste, satiation and satiety.

The increases I observed in activity in the lingual gyrus, precuneus and cerebellum following meal ingestion are compatible with the PET findings by Gautier *et al* (2001) and Tataranni *et al* (1999), both in contrast to the pCASL studies post-fructose ingestion by Page *et al* (2013). Glucose ingestion was not found to affect activity in these regions in the latter study. Given that some of these regions comprise or interact with the default mode network discussed earlier, a possible interpretation is that the meal diverted the subjects' thoughts or attention towards how they felt after eating the meal.

The above voxel-wise analyses statistically accounted for any changes in brain activity that may have been driven by differences in global grey matter CBF during each scanning session. For the analysis of the data extracted from the *a priori* regions of interest, this was managed by calculating net incremental areas under the curve of

the changes in perfusion. Right lateral OFC, thalamus and hippocampus showed greater reduction in perfusion post-meal compared to post-water ingestion, surviving correction for multiple comparisons. Increasing BOLD signal in lateral OFC was observed by Small *et al* (2001) after subjects who identified themselves as chocolate cravers ate chocolate until it was no longer pleasant. In my study, the meal reduced pleasantness to eat, but it did not increase feelings of nausea, therefore the gradual reduction in perfusion I observed within the lateral OFC may reflect an intermediate stage of satiation before revulsion, "liking" but no longer "wanting" (Berridge and Robinson, 2003), which in turn influences satiety. The differences in the direction of change of activity (increase in BOLD signal in the study by Small *et al* (2001) and the reduction in rCBF in the present study) may be explained by the use of very different fMRI modalities, as well as differences in study design, as subjects in the present study and the mixed meal provided were not chosen to examine craving. The failure to see significant change in the insula with meal ingestion in these region of interest analyses is likely due to the size of the anatomical insula mask, extending well beyond the functional region identified in the voxel-wide analysis, encapsulating anterior and posterior insula which may have different functions. It is possible that using smaller defined masks may have avoided "dilution" from non-activated regions within the insula when calculating the mean voxel-wise rCBF from the mask and the discrepancy shows the value of using both methodologies.

3.4.2 Effect of ageing

The absence of association between resting global or regional grey matter CBF with age, after correcting for BMI, is consistent with a CASL fMRI study showing that after a rapid drop in global CBF during adolescence, CBF remains constant in adulthood (Biagi *et al*, 2007). Other CASL and PASL studies with subjects ranging in age from the 3rd to 9th decade, beyond the range of the current study, show a reduction in global CBF by 0.38-0.78% per year of life (Chen *et al*, 2011; Liu *et al*, 2012; Parkes *et al*, 2004). $^{15}[H_2O]$-PET and SPECT studies have shown reductions in rCBF with age may actually be an artefact of partial volume effects (a limitation of spatial resolution of brain imaging) that may be increased due to grey matter loss (Meltzer *et al*, 2000; Van Laere and Dierckx, 2001). It is important to note that the current study specifically focussed on changes between young and middle age

adulthood and my data do not rule out an effect of greater extremes of age (childhood and old age).

The relationship between increasing age, adjusted for BMI, with increasing differences in rCBF between the two feeding states immediately after meal ingestion in the anterior cingulate and orbital part of the superior frontal gyrus, and at +28 to +34 mins post-ingestion in the anterior cingulate/medial prefrontal gyrus, pre/post-central gyrus and bilateral insula, was found to have a critical age point in the mid-thirties, below which rCBF was greatest after water ingestion and above which rCBF was greater after meal ingestion.

The OFC processes food-related reward salience after receiving sensory inputs that include visual stimuli via the visual cortices, taste from the primary gustatory cortex (frontal operculum and insula), smell from the pyriform cortex and touch from primary somatosensory cortex, to influence appetite and subsequent eating behaviour through decision-making processes, goal-driven behaviour and habitual behaviour via the medial prefrontal cortex, anterior cingulate and striatum respectively (Rolls, 2015). [^{15}O]H_2O-PET studies have shown rCBF decreases in OFC, insula and striatal regions after meal ingestion following a prolonged fast, which may reflect the immediate increase in satiation that leads to meal termination (Gautier *et al*, 2001; Tataranni *et al*, 1999). I found similar data for the under 30s immediately after meal ingestion in the OFC/ACC, but as age increased, there was not only a diminution in the suppressive effects of eating on hunger, but an increase in food-related activity in these reward salience and goal-directed processing centres, which might be supposed to promote further eating. I am not aware of existing data that demonstrates how ageing to middle age may modify the brain response to meal ingestion per se. Green *et al* (2013) showed that young adults (aged 19-26 years) had greater insula and pre/post-central gyrus BOLD signal changes upon tasting sucrose compared to caffeine, with this sucrose response being greater than that observed in middle age adults (aged 45-54 years) who showed no differences in response between these stimuli, despite no differences in the reported pleasantness or intensity of the stimuli between the groups. This may suggest an age-dependent reduction in the responsiveness of interoceptive centres to rewarding stimuli that could encourage increased food intake in middle age in order to compensate for these deficits.

Jacobson *et al* (2010) showed young subjects (mean age 23.9 years) had lower BOLD signal than old subjects (mean age 72.2 years) to tastants in the anterior cingulate, PFC, OFC, caudate and amygdala in both fasted and fed states, although in this study, the effect of ageing on how feeding modulates the cerebral response to tastants was not examined. The authors suggest that the exaggerated responses in the older group may be compensatory for diminished food-related processes, although this requires further confirmation with other imaging modalities.

The association between age and the later response at +28 to +34 mins to the meal in the anterior cingulate/medial PFC demonstrates good internal consistency with the immediate post-prandial observations. The additional late post-prandial involvement of the bilateral insula in this relationship is of interest. GLP-$1_{7\text{-}36}$ amide reduces food image-evoked BOLD signal in the insula in a similar manner to that observed after meal ingestion (De Silva *et al*, 2011), and as does the GLP-1 receptor agonist, exenatide (van Bloemendaal *et al*, 2014). I did not collect sufficient GLP-1 samples during the present study to investigate the role incretin hormone secretion may have had, but we can expect a greater rise post-meal than post-water that has not been shown to be affected by ageing (Geloneze *et al*, 2014; MacIntosh *et al*, 1999) and, given their role in suppressing appetite possibly via the insula, it is possible that the insula becomes less sensitive to the post-prandial incretins beyond middle age, allowing it to be increasingly more active after a meal.

3.4.3 Effect of BMI

The positive association between BMI, independent of age, with rCBF in prefrontal (PFC) and orbitofrontal (OFC) cortices and putamen pre-water ingestion (not replicated pre-meal ingestion, again possibly due to an order effect) is inconsistent with data from Volkow *et al* (2009) where increasing BMI was associated with *decreased* activity in PFC and anterior cingulate gyrus, as quantified by [^{18}F]FDG-PET. In their study, cognitive function decreased with increasing BMI, with performance on cognitive function tests associated with resting prefrontal glucose metabolism, although not with task-related changes in activation. One reason for the discrepancies between those studies and the present study lies in the impact of my subjects knowing that they would either receive meal or water soon after the first

pCASL scan: it is conceivable that food-related cognitive processes such as the anticipation of a possible upcoming meal may have altered this relationship between BMI and resting cerebral activity. Indeed, changes in PFC activity during the anticipation of food, and how they may be influenced by body weight, have been demonstrated in a number of BOLD fMRI studies. For example, Yokum *et al* (2011) observed that increasing BMI in a group of adolescent girls was associated with greater BOLD signal responses in the lateral OFC, insula and ventrolateral prefrontal cortex (VLPFC) to arrows that signalled the presentation of food images. Frankort *et al* (2012) showed greater prefrontal, OFC and striatal activity in overweight than normal weight individuals whilst they imagined tasting food. Batterink *et al* (2010) also showed that when subjects explicitly inhibited responses to appetising food images during a go/no-go task, increasing BMI was associated with decreasing BOLD signal in superior and middle frontal gyri, VLPFC, medial PFC and OFC.

The only significant association between BMI and the difference in rCBF post-meal vs post-water was found during the intermediate +8 to+14 mins interval (during which no relationship with age was detected), was in the cerebellum, where in low BMI subjects, activity was greater post-water compared to post-meal, but that increasing body mass beyond overweight reversed this relationship. The cerebellum is often identified in neuroimaging studies of appetite, but its role in controlling food ingestion is not fully understood in humans. However, in animal studies, it has been shown to modulate intestinal motility and hypothalamic regulation of food-seeking behaviour and responses to glucose (Zhu and Wang, 2008).

3.4.4 Limitations and conclusions

The meal did not elicit complete satiation, nor completely suppress hunger and whilst caloric intake per BMI unit was similar for all subjects, energy intake was not adjusted for BMI, preventing us from establishing the impact of feeding to full satiation. Although subject preferences for ice cream were not examined, they were made aware of the nature of the mixed-meal prior to study, and we can assume people with an active distaste for it will have been self-excluded. Anecdotally, subjects reportedly enjoyed eating the ice cream but it is possible that differences in personal taste, including changes that might occur with age, could have influenced the results.

Nevertheless, the meal was sufficient to impact upon hunger, fullness and pleasantness to eat scores, suggesting it was adequate for our purposes. The subjects were fasted for at least 8 hours before scanning, but diet between scans was not controlled. We also need to consider the timing of the different scans performed in the present study, when comparing it to others, as this will affect the data. The effect of food (and non-food) image viewing during the BOLD fMRI task may have influenced brain activity during the final pCASL acquisition, by both placing demands on visual attention networks, but also bringing subjects thoughts and attentions to the food pictures viewed, rather than their internal feelings related to the meal consumed, although the response to such tasks is usually considered restricted to the actual performance and my own data described in the following chapter certainly showed instantaneous responses in terms of food-cue evoked hunger.

In summary, this study has validated the use of pCASL fMRI in the characterisation of the normal human brain response to meal ingestion, with the predominant response being an increase in insular activity, a region that processes taste and interoceptive awareness, which may then influence activity of prefrontal regions such as the OFC to induce satiation and alter later satiety. Multiple regression analyses did not demonstrate an effect of age on resting (fasting) brain activity in the age group studied, but increasing age was associated with increasingly greater OFC and insular responses to meal compared to water ingestion above a critical age during the mid-thirties, that is opposite to the suppression of activity that occurs below this age. Longitudinal studies would be optimal to establish whether this is cause or effect but it seems likely that changes in brain response to meal ingestion occurring with healthy ageing will facilitate the weight gain observed in middle age.

Table 3.1

Subject characteristics

	N=24
Age [median (range, interquartile range)]	35.9 (19.5-52.6, 19.84) years
Sex	12 males : 12 females
BMI [mean ± SD (range, interquartile range)]	24.9 ± 4.0 (19.4-23.7, 6.58) kg/m^2
HbA1c (mean ± SD)	5.3±0.4%
Fasting glucose (mean ± SD)	4.8±0.1 mmol/L

Table 3.2

Voxel-wise T-contrasts of differences in rCBF pre-water vs pre-meal, and post-water vs post-meal. Regions identified by AAL atlas (*talairach atlas*). Extracted rCBF is unadjusted for global grey matter CBF (Figure 3.8, Figure 3.10).

		MNI coordinates						Mean CBF (±SE)		% CBF change (with respect to water)
Contrast / Brain area	Hemi-sphere	X	Y	Z	T scores	No. voxels	$P_{FWE-corr}$	Water	Meal	
Pre-water > pre-meal ingestion (pCASL1)										
Inferior occipital gyrus / *middle occipital gyrus*	L	-38	-76	-4	4.42	930	< 0.001	44.71±3.32	41.44±2.56	-7.32
Fusiform / *Lingual gyrus*	R	28	-80	-10	3.97	632	0.003	38.07±3.11	35.22±1.99	-7.47
Post-water > post-meal at 0 to +6 minutes post-ingestion (pCASL2)										
Superior occipital gyrus / *Precuneus*	R	28	-66	42	3.80	627	0.003	61.53±3.32	57.30±3.11	-6.87
Post-Water > Post-Meal at +8 to +14 minutes post ingestion (pCASL3)										
Precuneus	R	36	-46	46	4.46	533	0.008	61.75±3.38	57.08±3.13	-7.57
Lingual gyrus	L	-20	-98	-16	4.44	2015	< 0.001	56.09±3.13	51.66±2.76	-7.89
Post-Water > Post-Meal +28 to +34 minutes post ingestion (pCASL4)										
Crus 2 Cerebellum / *Lingual gyrus*	L	-10	-90	-16	4.25	372	0.048	51.09±3.40	44.54±2.63	-12.81
Parahippocampal gyrus	R	0	-68	-4	4.07	1614	< 0.001	55.27±3.07	49.53±2.58	-10.39
Superior occipital gyrus / subgyral temporal lobe	L	-24	-70	24	3.95	521	0.009	58.59±3.42	52.47±2.77	-10.45
Crus 1 Cerebellum / *Pyramis*	L	-38	-86	-34	3.79	440	0.022	41.70±2.84	35.70±2.23	-14.39
Pre-Water < Pre-Meal pre-ingestion (pCASL1)										
No regions										
Post-Water < Post-Meal at 0 to +6 minutes post-ingestion (pCASL2)										
Insula	R	40	-10	6	5.57	796	0.001	45.90±1.45	50.28±1.69	9.53
Insula	L	-36	6	2	5.13	2322	< 0.001	44.91±1.48	49.18±1.64	9.50
Inferior frontal gyrus / Parahippocampal gyrus	R	28	8	-18	4.28	382	0.032	37.89±1.37	41.94±1.56	10.68

Table 3.2 continued

Contrast / Brain area	Hemi-sphere	MNI coordinates X	Y	Z	T scores	No. voxels	$P_{FWE-corr}$	Mean CBF (±SE) Water	Meal	% CBF change (with respect to water)
Post-Water < Post-Meal at +8 to +14 minutes post ingestion (pCASL3)										
Inferior frontal gyrus, triangular part / *inferior frontal gyrus*	L	-52	20	-2	3.95	377	0.046	50.93±1.88	55.34±2.12	8.66
Median cingulate and paracingulate gyri / *cingulate gyrus*	Mid/L	0	18	38	3.94	406	0.032	61.31±2.41	65.99±2.58	7.65
Post-Water < Post-Meal +28 to +34 minutes post ingestion (pCASL4)										
Insula	L	-32	14	12	4.95	387	0.04	38.78±1.65	41.90±1.74	8.05
Rolandic operculum / *Precentral gyrus*	R	62	8	8	4.03	581	0.005	50.23±1.76	53.46±2.16	6.43
Anterior cingulate and paracingulate gyri	Mid/L	-4	44	14	3.96	384	0.042	51.04±1.83	54.34±1.80	6.47

Contrast / Brain area	Hemis phere	MNI coordinates X	Y	Z	T scores	No. voxels	$P_{FWE-corr}$	Estimated marginal mean CBF (±SE) Water	Meal	% CBF change (with respect to water)
Main effect of post-water > post-Meal (pCASL2-4)										
Superior occipital gyrus / *precuneus*	R	28	-64	40	5.00	1223	< 0.001	58.54±3.25	54.51±3.01	-6.89
Lingual gyrus	R/mid	6	79	-12	4.19	3504	< 0.001	52.52±2.91	48.98±2.57	-6.73
Main effect of post-water < post-meal (pCASL2-4)										
Post-central gyrus / *transverse temporal gyrus* / Insula	L	-64	-8	14	4.92	1960	< 0.001	46.32±1.46	48.93±1.66	5.64
Insula	R	58	28	2	4.18	1262	< 0.001	48.23±1.67	50.78±1.88	5.30
Medial superior frontal gyrus / *Medial frontal gyrus*	R	14	58	10	4.13	695	0.001	48.45±1.81	51.19±1.79	5.65
Supplementary motor area / *Medial frontal gyrus*	R/mid	6	4	48	3.99	678	0.002	60.92±2.31	63.75±2.40	4.65

Table 3.3

Voxel-wise T-contrasts of differences in fasting rCBF (pCASL1) between first and second visits, irrespective of would later be consumed. Regions identified by AAL atlas (*talairach atlas*) (Figure 3.9).

		MNI coordinates					
Contrast / Brain area	Hemisphere	X	Y	Z	T scores	No. voxels	PFWE-corr
First pCASL1 > Second pCASL1							
Superior temporal gyrus; supra-marginal; insula	Right	46	-4	-16	7.89	2066	< 0.001
Insula / *superior temporal gyrus*	Left	-34	2	-18	5.84	1176	< 0.001
Supplementary motor area	Right	10	8	62	4.57	463	0.028
First pCASL1 < Second pCASL1							
Inferior occipital gyrus / cerebellum	Right	44	-86	-10	6.28	7640	<0.001

Table 3.4

Voxel-wise multiple regression of CBF with age and BMI pre-water and pre-meal ingestion (Figure 3.12).

Contrast / Brain area	Hemisphere	Direction of association	MNI coordinates X	Y	Z	T scores	No. voxels	$P_{FWE-corr}$
Pre-Water Ingestion								
Association of CBF with age after adjusting for BMI								
No regions								
Association of CBF with BMI after adjusting for age								
Subcallosal gyrus / putamen	R	Positive	12	4	-16	7.34	929	0.003
Superior orbital frontal gyrus	L	Positive	-16	60	-16	6.08	1147	0.001
Supplemental motor area / *Superior frontal gyrus*	R/mid	Positive	10	14	68	5.28	2414	< 0.001
Superior frontal gyrus / Middle orbital frontal gyrus	R	Positive	28	60	12	4.93	705	0.014
Precuneus / *posterior cingulate*	L	Negative	-6	-54	24	6.15	970	0.002
Middle occipital gyrus / *subgyral parietal*	R	Negative	34	-76	32	5.57	718	0.013
Crus 1 cerebellum / *culmen*	L	Negative	-50	-48	-36	4.68	2707	<0.001
Pre-Meal Ingestion								
Association of CBF with age after adjusting for BMI								
No regions								
Association of CBF with BMI after adjusting for age								
Superior frontal gyrus	L	Positive	-16	-10	74	6.59	1982	<0.001
Cerebellum crus 2 / tonsil	R	Negative	24	-56	36	3.73	538	0.047

Table 3.5

Voxel-wise multiple regression of (post-meal minus post-water) CBF with age and BMI (Figure 3.13, Figure 3.14, Figure 3.15).

Regression analysis / Brain area	Hemisphere	Direction of association	MNI coordinates X	Y	Z	T scores	No. voxels	$P_{FWE-corr}$
Meal minus Water CBF at 0 to +6 minutes post ingestion (pCASL2)								
Association of difference in CBF with age after adjusting for BMI								
Frontal superior gyrus, orbital part / *anterior cingulate*	R / mid	Positive	14	56	-12	4.95	493	0.021
Crus 1 cerebellum / *tuber*	R	Negative	42	-76	-36	4.39	466	0.028
Association of difference in CBF with BMI after adjusting for age								
No regions								
Meal minus Water CBF at +8 to +14 minutes post ingestion (pCASL3)								
Association of difference in CBF with age after adjusting for BMI								
No regions								
Association of difference in CBF with BMI after adjusting for age								
Hemispheric lobule VI cerebellum / *declive / culmen*	R	Positive	16	-62	-24	4.74	445	0.037
Meal minus Water CBF at +28 to +34 minutes post ingestion (pCASL4)								
Association of difference in CBF with age after adjusting for BMI								
Postcentral gyrus / *precentral gyrus*	R	Positive	58	-6	28	6.89	479	0.036
Inferior frontal gyrus, orbital part / Insula	L	Positive	-24	28	-22	5.44	558	0.017
Superior medial frontal gyrus / Anterior cingulate	R	Positive	6	52	0	3.9	583	0.014
Superior temporal pole / Inferior frontal gyrus, orbital part / insula	R	Positive	40	16	-26	4.71	472	0.039
Association of difference in CBF with BMI after adjusting for age								
No regions								

4 Ageing and the modulation of cerebral responses to food cues by meal ingestion

4.1 Introduction

The previous chapter described the impact of ageing and BMI on changes in post-prandial rCBF, a marker of cerebral processes of satiation. Functional neuroimaging has also demonstrated altered brain responses to food cues in obesity, which may persist despite weight loss, in corticolimbic appetitive motivational networks, and in higher executive regions involved in self-control of eating, e.g. dorsolateral prefrontal cortex (DLPFC) (Martin *et al*, 2010; Stoeckel *et al*, 2009). Such neural responses to visual food cues are present in childhood, with greater corticolimbic and paralimbic reward pathway responses in fasted compared to fed states (Holsen *et al*, 2005). These responses continue to develop from adolescence to young adulthood (Killgore and Yurgelun-Todd, 2005b), associated with structural changes in the brain during this period (Sowell *et al*, 1999). Given the increased prevalence of obesity in middle age (Flegal *et al*, 2010), this study aimed to examine the impact of ageing from young adulthood to middle age on brain responses to food cues in fed and fasted states using BOLD fMRI.

4.2 Methods

4.2.1 Subjects

The 24 subjects were the same as those in Chapter 3. Recruitment methods and inclusion criteria have been described (sections 2.8.1-2.8.2).

4.2.2 Study protocol

The general experimental design and MRI acquisition details are described in section 2.8 (Figure 3.1). The pCASL fMRI methods and results are described in Chapter 3. With regard to the BOLD fMRI study, in brief, subjects were studied on two separate mornings following an overnight fast of at least 8 hours. After intravenous cannulation, subjects were positioned in the scanner, and a high-resolution gradient echo, echo planar image (GE EPI) scan, and baseline pCASL1 scan were performed.

Between -6 and 0 mins, subjects were withdrawn from the scanner and sat up to consume a mixed meal (200ml, 554kcal, 36.8g fat, 7.8g protein, 47.6g carbohydrate) or 50ml water, in random order across the two sessions. After repositioning in the scanner and two further pCASL (pCASL2-3) scans, BOLD-fMRI data were acquired between +16 and +26 mins whilst subjects viewed 72 photographs each of food and non-food related objects that had previously been validated for recognition, pleasantness and appeal, visual complexity and colour, and for food images, palatability (Tables 2.1, 2.2) (Uher *et al*, 2006). These were shown in alternating blocks of 12 different pictures of either food or objects, each presented for 3 s (Figure 4.1). Subjects were asked to "Imagine you are eating the following foods/using the following objects" before viewing food and object blocks respectively. Subjects responded to the question "How hungry do you feel?" after each block, on a projected 1-10 visual analogue scale using a hand-held keypad. Subjects similarly rated appetite before and after pCASL1, after pCASL2-3, at the end of BOLD fMRI and the final pCASL4, with concurrent blood sampling.

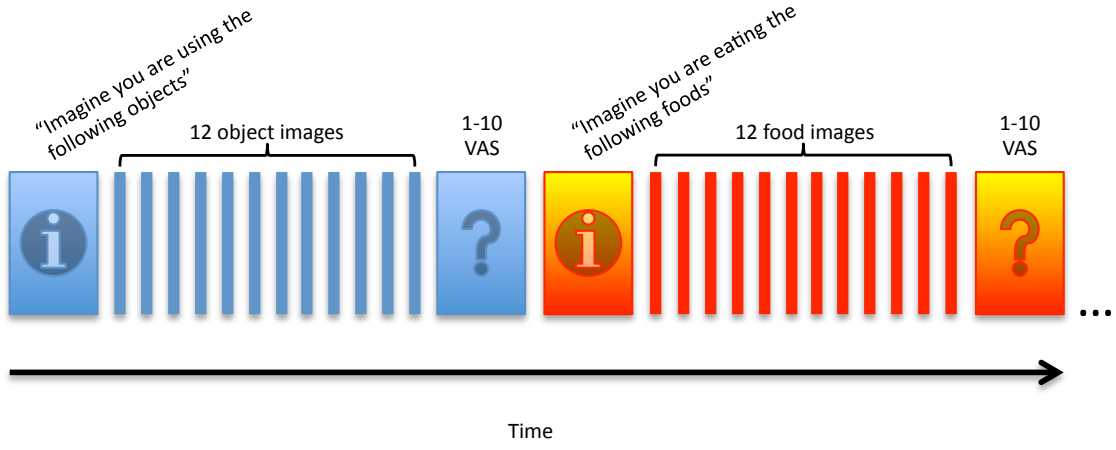

Figure 4.1

BOLD fMRI task (between pCASL3 and 4): Block design, each block consisted of auditory instructions, then 12 object or 12 food images, each image presented for 3 s with no inter-stimulus interval, and then the question "How hungry do you feel?" was answered using a 1-10 visual analogue scale. Food (n=6) and object (n=6) blocks alternated, in a pseudo-randomised playlist.

4.2.3 Statistical analyses

General non-imaging statistical methods are described in section 2.8.14. Each subject's mean hunger scores during image viewing for each stimulus-condition combinations (water-food, meal-food, water-object, meal-object) were submitted to

repeated measures ANOVA with feeding status (water/meal) and image (food/object) as factors. Associations between age with net symptom iAUC and hunger scores taken during image viewing, and between symptoms and BOLD signal, were assessed using Pearson's correlation coefficient/Spearman's rank test for normally/non-normally distributed data respectively (uncorrected *P*). Data are presented as mean±SEM or median with the interquartile range.

Subject-level BOLD image pre-processing and statistical methods using XBAM version 4.1 (Centre for Neuroimaging Sciences, Institute of Psychiatry, Psychology & Neuroscience, King's College London, 2012) are described in section 2.8.13.3. After normalised BOLD effect size maps of the response to food vs object images were calculated for each subject, group maps within each feeding state were generated to examine food vs object image-evoked BOLD signal contrast compared to a null distribution derived from the permuted data set (section 2.8.13.4). After restricting analyses to grey matter, differences in the median effect size of the food vs object signal contrast at each voxel between feeding states were computed and compared to a null distribution derived by permutation of feeding status. The direction of BOLD signal contrast (food > objects, food < objects) of the sub-clusters between feeding conditions was determined by phase clarification.

In separate analyses, the association between age and food vs object image-evoked BOLD signal contrast after water ingestion, and between age and the difference in food vs object BOLD signal contrast between feeding conditions, were examined by calculating voxel-wise Pearson product moment correlation coefficients compared to a null distribution derived by permutation of age. Correlation analyses were adjusted for BMI, which was positively correlated with age (r_s=0.539, p=0.007). The primary endpoint was the effect of ageing, but exploratory correlation analyses were performed for BMI after adjusting for age. All the above group maps were thresholded to yield <0.5 false positive clusters per map at a voxel-wise threshold p<0.05 (Bullmore *et al*, 1999) (section 2.11.4).

4.3 Results

4.3.1 Subjects, Glucose and Insulin

Subject characteristics, and changes in glucose and insulin during the study are described in sections 3.3.1-2.

4.3.2 Symptom scores

Analyses are based on 22 subjects, as symptom scores were incomplete for two. Responses to the four appetite questions collected at the defined time points before and after meal and water ingestion have been described (section 3.3). Hunger scores were collected after viewing each block of food and object pictures *during* BOLD fMRI. As expected, hunger scores were lower post-meal compared to post-water ingestion (main effect of feeding condition, $F(1,23)=30.268$, $p<0.001$), but more hunger was elicited after viewing pictures of foods than of objects (main effect of image type, $F(1,23)=13.024$, $p=0.001$) (Figure 4.2). There was no significant interaction between feeding status and image type ($F(1,23)=0.155$, $p=0.697$). However, when the mean hunger scores for each feeding status x image type combination in each subject were subjected to the following calculation:

$$\text{“net” hunger} = [\text{water-food} - \text{meal-food}]_{\text{hunger}} - [\text{water-object} - \text{meal-object}]_{\text{hunger}}$$

with negative numbers indicating greater suppression of hunger by the meal during food than object image-viewing, there was a trend towards a positive association between age and “net” hunger after adjusting for BMI (r=0.407, $p=0.054$), suggesting less meal-induced suppression of the hunger evoked by viewing food images with increasing age.

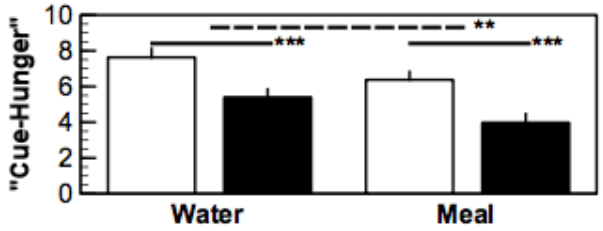

Figure 4.2

Mean (±SEM) hunger elicited by food (open bars) and object (solid bars) image viewing after water/meal ingestion. **main effect of meal, $p < 0.001$; ***main effect of image class, $p = 0.001$.

4.3.3 Effect of meal ingestion on brain responses to visual food cues

Food-vs-object picture-evoked BOLD signal contrast was greater after meal compared to water ingestion in a single cluster that was identified as precuneus, that included bilateral superior parietal lobule, and superior and middle temporal gyri (Figure 4.3, Table 4.1). Phase clarification showed this was largely due to greater deactivation on viewing food images (food < object) after drinking water, with activation (food > object) or a lesser degree of deactivation after the meal.

The BOLD signal contrast was lower after meal compared to water ingestion in a single cluster identified as right putamen that included right thalamus, amygdala and posterior insula. Phase clarification indicated that visual food image-evoked activation was greater after water ingestion in the right putamen, thalamus and posterior insula, whilst deactivation of the right amygdala was greater (BOLD signal contrast more negative) after the meal.

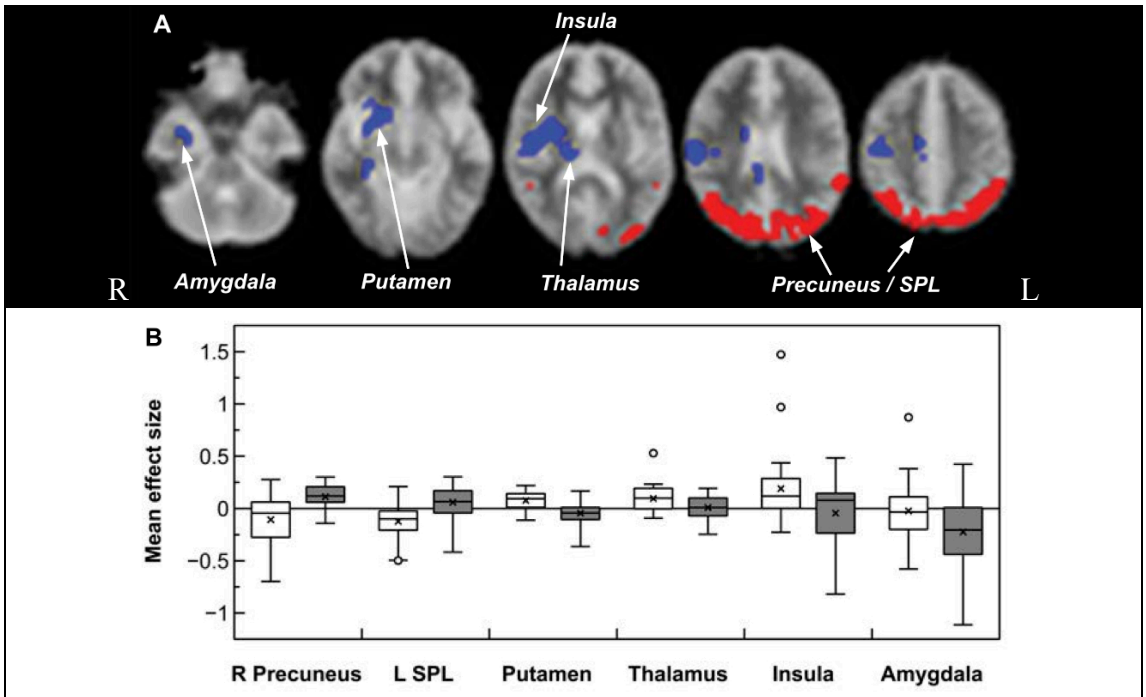

Figure 4.3

(A) Group map of the effect of meal compared to water on food-vs-object image-elicited BOLD signal contrast (voxel-wise $p < 0.05$, cluster-wise $p < 0.01$), showing clusters with greater (red) or lesser (blue) activity after meal than after water. (B) Extracted mean effect size from sub-clusters identified from phase clarification of clusters identified in (A), after water (open) and meal (grey) ingestion. Whiskers indicate lowest/highest datum within 1.5 IQR of lower/upper quartile. Positive effect size indicate greater BOLD signal elicited by food than object images. SPL: superior parietal lobule. Effect size units = % BOLD signal change.

Differences in net iAUC for symptoms of hunger, nausea, fullness, and pleasantness to eat, collected throughout the study visit, between feeding conditions were assessed for correlation with the respective differences in BOLD signal in these two clusters. Greater meal-induced reduction in hunger was associated with greater meal-induced suppression of the putamen cluster activity (r=0.483, p=0.023) (Figure 4.4). All other associations did not meet statistical significance. There was no association between BOLD signal changes and "net" hunger score (representing meal-induced suppression of the hunger evoked by viewing food images).

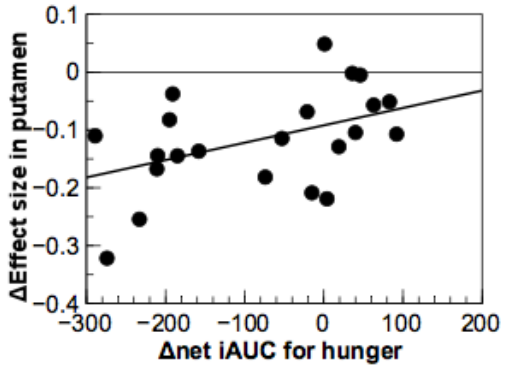

Figure 4.4

Correlation between the differences in net iAUC-hunger (from scores at predefined intervals during visit) and differences in effect size in right putamen (blue cluster, Figure 4.3) between meal and water conditions (r = 0.483, p = 0.023). Positive values: greater net iAUC hunger / BOLD signal after meal than after water; negative: greater net iAUC hunger / BOLD signal after water than after meal. Effect size = % BOLD signal change.

4.3.4 Effect of ageing on brain responses to visual food cues after water ingestion

Voxel-wise correlation analyses of the food-vs-object picture-evoked BOLD signal contrast after water ingestion with age, adjusting for BMI, were performed. Increasing age was positively correlated with BOLD signal contrast in left superior temporal gyrus and middle temporal gyrus bilaterally, posterior cingulate and cerebellum, and left anterior insula sub-region of the ventrolateral prefrontal cortex (VLPFC) after adjusting for BMI (Figure 4.5, Table 4.2). The extracted mean effect size (mean BMI-adjusted percentage BOLD signal change) indicated that the associations were largely due to a reduction in food image-evoked deactivations (less food < object), with increasing age. Ageing was negatively correlated with right fusiform gyrus, precuneus and DLPFC BOLD signal contrast, after adjusting for BMI, the latter due, conversely, to diminishing food image-evoked activation (less food > object), with increasing age. Fullness correlated with activation in culmen

(r=–0.501, p=0.018) and left posterior cingulate (r=0.440, p=0.041); pleasantness to eat correlated with right fusiform gyrus (r=–0.486, p=0.022).

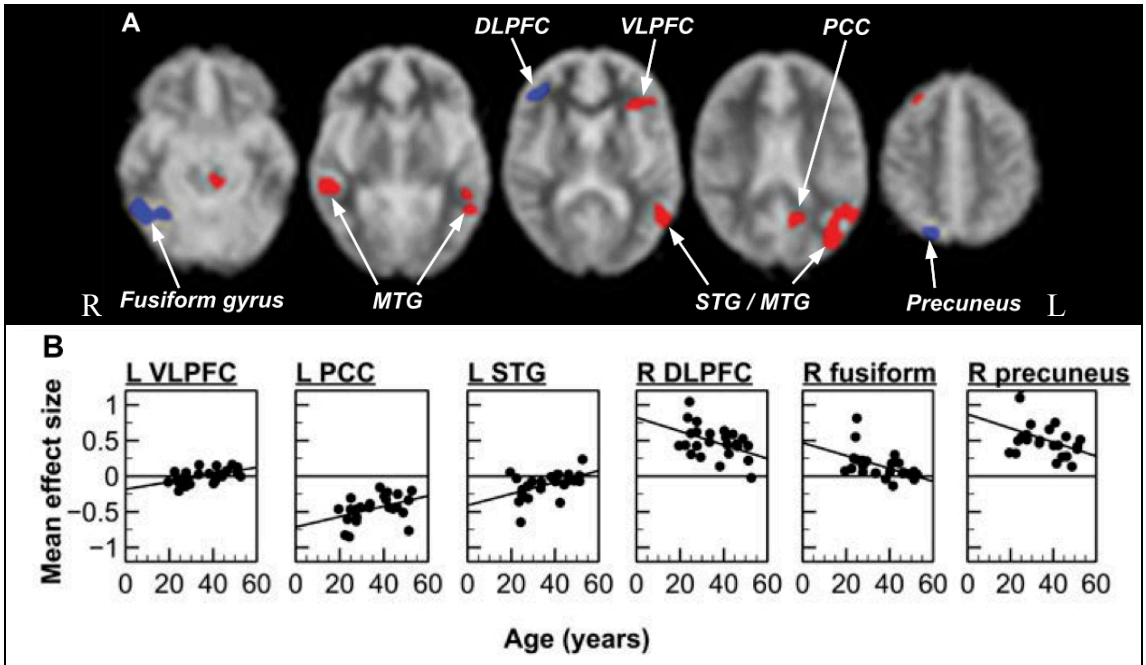

Figure 4.5

(A) Group map of whole-brain correlation of activation after water with age, showing clusters exhibiting linear positive (red) or negative (blue) correlation of age with food-vs-object picture-evoked BOLD signal contrast (corrected for BMI, voxel-wise $p < 0.05$, cluster-wise $p < 0.02$) (B) Mean BMI-adjusted effect size from clusters identified from (A) for each subject against age. Positive mean effect size: food > object. Effect size units = % BOLD signal change. Lines indicate linear regression. MTG, middle temporal gyrus; PCC, posterior cingulate cortex; STG superior temporal gyrus.

4.3.5 Effect of ageing on the modulation of brain responses to visual food cues by meal ingestion

Voxel-wise correlation analyses of the difference in food-vs-object picture-evoked BOLD signal contrast between feeding conditions with age, adjusting for BMI, were next performed. Increasing age was positively correlated with differences in magnitude of the BOLD signal contrast between feeding conditions in right DLPFC, amygdala and caudate body, a cluster extending from the right ventral (putamen) to dorsal (caudate head) striatum, and another cluster extending from the left dorsal striatum (caudate head) to left globus pallidus and left amygdala, after adjusting for BMI (Figure 4.6A, Table 4.2). The extracted mean effect size data indicated that this positive correlation in right DLPFC, right amygdala and left dorsal striatum/globus pallidus/amygdala clusters was largely due to the food vs object image-evoked BOLD

signal contrast being of greater magnitude after water than meal ingestion in younger subjects, with less differentiation between feeding conditions with increasing age, and that of the right ventral/dorsal striatum cluster being even greater after meal than water ingestion with increasing age (Figure 4.6B).

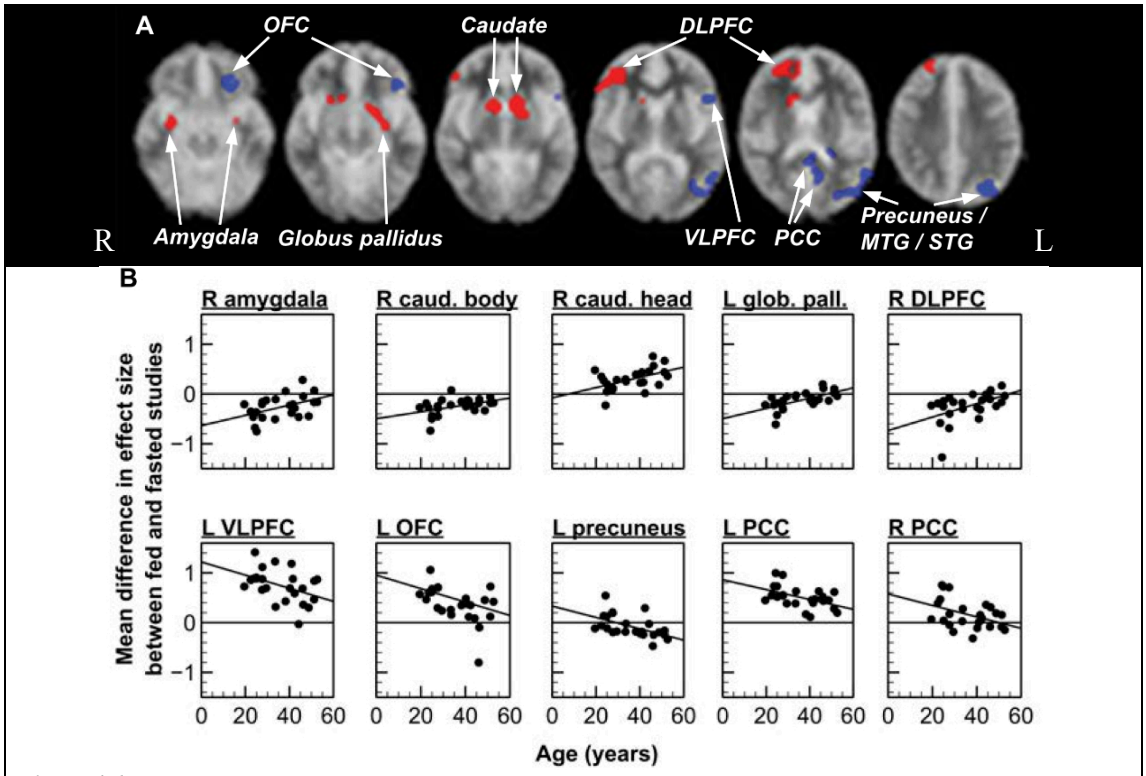

Figure 4.6

(A) Group map of whole-brain correlation of the difference in activation between feeding states with age, showing clusters exhibiting linear positive (red) or negative (blue) correlation of age with the difference in food-vs-object picture-elicited BOLD signal contrast between meal and water conditions (corrected for BMI, voxel-wise $p < 0.05$, cluster-wise $p < 0.02$). (B) Mean differences in BMI-adjusted effect size between meal and water conditions for clusters identified from (A) for each subject against age. Positive difference: meal > water. Effect size units = % BOLD signal change. Lines indicate linear regression. Caud, caudate; glob. pall., global pallidus; MTG, middle temporal gyrus; OFC, orbitofrontal cortex; PCC, posterior cingulate cortex; STG, superior temporal gyrus.

As the direction of signal contrast (food > object, or food < object) cannot be determined from these analyses, these clusters were used as masks from which mean effect size data from the activation maps within each feeding condition were extracted (Figure 4.7). These relationships with ageing appeared as driven predominantly by post-water activation and post-meal deactivation in the right DLPFC, right amygdala and left dorsal striatum/globus pallidus/amygdala cluster that diminished with age, whilst in the right ventral/dorsal striatal cluster, a deactivation response was observed after water ingestion, with progressive post-meal activation with increasing age.

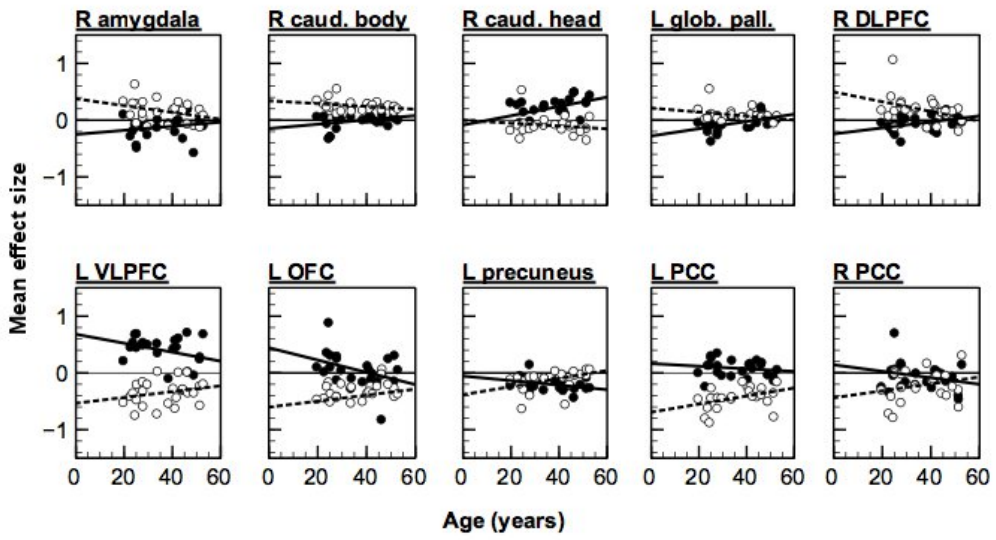

Figure 4.7

Mean BMI-adjusted effect size from each subject after meal (filled circles) and water (open circles), extracted from clusters identified in Figure 4.6. For illustrative purposes only, lines indicate linear regression (solid = meal, dashed = water). Positive effect size: food > object. Effect size units = % BOLD signal change. See Figure 4.6 for abbreviations.

Ageing was negatively correlated with differences in magnitude of the food vs object image-evoked BOLD signal contrast between feeding conditions in regions including the left inferior frontal gyrus, with VLPFC and orbitofrontal cortex (OFC), left superior frontal gyrus, left middle and superior temporal gyri, posterior cingulate cortex and left precuneus, after adjusting for BMI (Figure 4.6A, Table 4.2). The extracted mean effect size data indicated the negative correlation in the left VLPFC and inferior frontal gyrus/OFC to be due to greater magnitude of food vs object image-evoked BOLD signal contrast observed after meal than water ingestion in the younger adults, with less differentiation between feeding conditions with increasing age, although this was less clear in the precuneus, due to a transition from greater activity after meal than water ingestion in younger adults, to greater activity after water than meal ingestion in older adults. (Figure 4.6B). When the mean effect size data from the original activation maps within each feeding condition were extracted from these clusters further to determine the responses as activation/deactivation to food images (Figure 4.7), these relationships appeared as driven by post-meal activation and post-water deactivation in the left VLPFC and inferior frontal gyrus/OFC that both diminished with age.

There was no significant association between extracted effect size, reflecting differences in food vs object image-evoked BOLD signal contrast between feeding conditions, with the respective differences in net symptom iAUC, or with "net" hunger scores during image viewing.

4.3.6 Effect of BMI on brain responses to visual food cues after water ingestion

Voxel-wise correlation analyses of the food vs object image-evoked BOLD signal contrast after water ingestion with BMI, adjusting for age, were performed. Increasing BMI, independent of age, was positively correlated with BOLD signal contrast, predominantly in a cluster that included right post-central gyrus and insula, due to a reduction in the relative food image-evoked deactivation (less food < object) with increasing BMI, and decreasing BOLD signal contrast in left middle temporal gyrus and caudate tail, and right anterior cingulate, in the latter region due to a reduction in the relative food image-evoked activation (less food > object) with increasing BMI (Figure 4.8, Table 4.3).

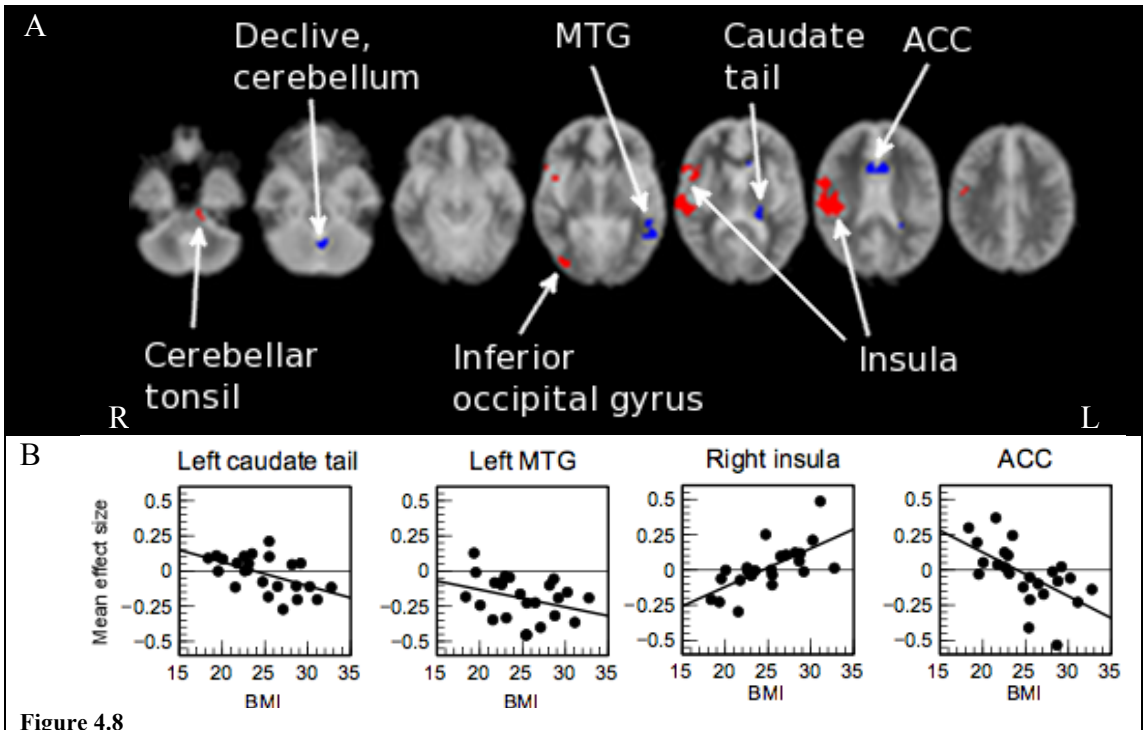

Figure 4.8

(A) Group map of whole-brain correlation of activation after water with BMI, showing clusters exhibiting linear positive (red) or negative (blue) correlation of BMI (kg/m^2) with food-vs-object picture-evoked BOLD signal contrast (corrected for age, voxel-wise $p < 0.05$, cluster-wise $p < 0.02$). (B) Mean age-adjusted effect size from four of the clusters identified from (A) for each subject, against BMI. Positive mean effect size: food > object. Effect size units = % BOLD signal change. Lines indicate linear regression. MTG, middle temporal gyrus; PCC, posterior cingulate cortex; STG, superior temporal gyrus.

4.3.7 Effect of BMI on the modulation of brain responses to visual food cues by meal ingestion

Voxel-wise correlation analyses of the difference in food vs object image-evoked BOLD signal contrast between feeding conditions with BMI, adjusting for age, were next performed. Increasing BMI, independent of age, was positively correlated with the difference in magnitude of the BOLD signal contrast between feeding conditions in regions including left VLPFC (inferior frontal gyrus), bilateral middle temporal gyri, anterior cingulate cortex, midbrain, precuneus and left superior parietal lobule (Figure 4.9A, Table 4.3).

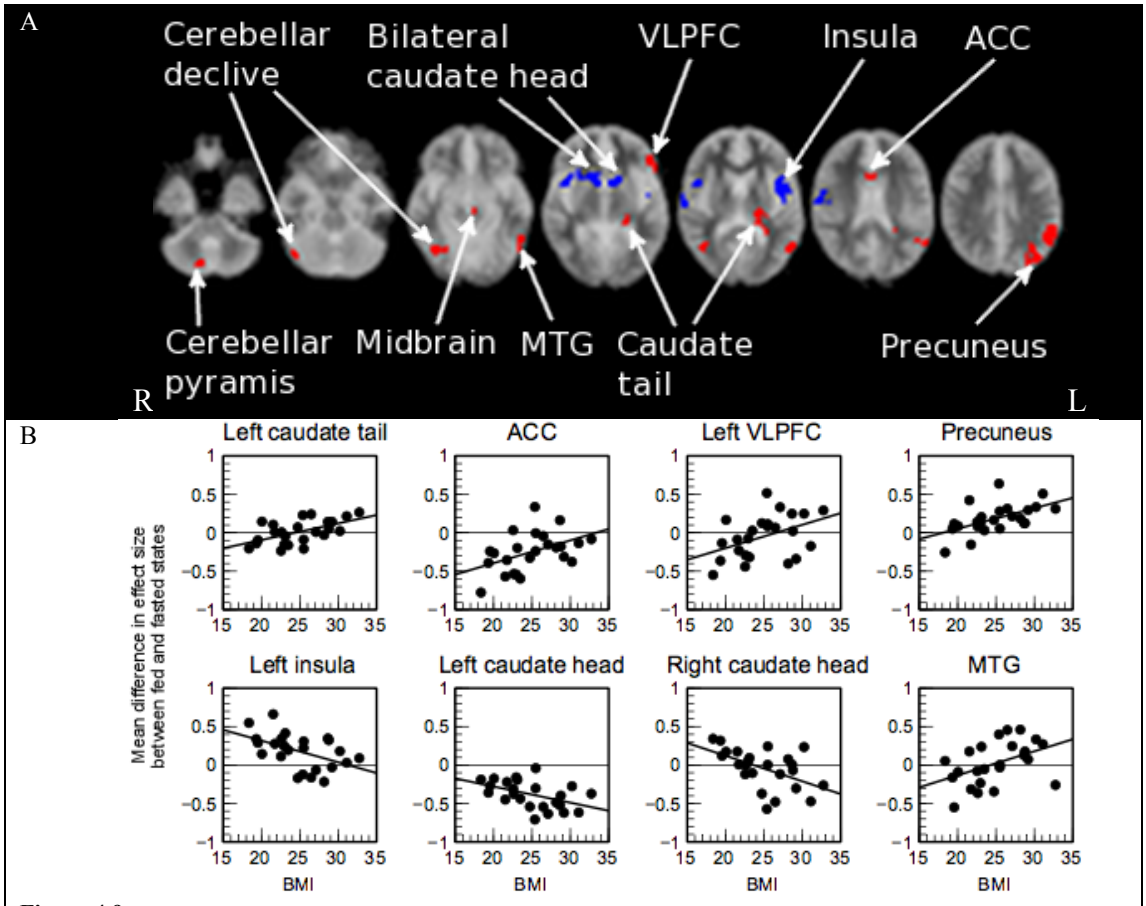

Figure 4.9

(A) Group map of whole-brain correlation of the difference in activation between feeding states with BMI, showing clusters exhibiting linear positive (red) or negative (blue) correlation of BMI (kg/m^2) with the difference in food-vs-object picture-evoked BOLD signal contrast between meal and water conditions (corrected for age, voxel-wise $p < 0.05$, cluster-wise $p < 0.01$). (B) Mean differences in age-adjusted effect size between feeding conditions for selected clusters identified from (A) for each subject, against BMI for visualisation. Positive difference: meal > water. Effect size units = % BOLD signal change. Lines indicate linear regression. ACC, anterior cingulate cortex; VLPFC, ventrolateral prefrontal cortex; MTG, middle temporal gyrus.

Extracted effect size data from the largest cluster, the precuneus, indicated this positive correlation to be due to the magnitude of BOLD signal contrast being increasingly greater after the meal as BMI increased, whilst the ACC and VLPFC showed a greater magnitude of BOLD signal contrast after water in thinner subjects, with decreasing differentiation between feeding states as BMI increased, and subsequently being greatest after meal ingestion in the latter structure in subjects with the highest BMI (Figure 4.9B).

As the direction of signal contrast (food > object, or food < object) cannot be determined from these analyses, these clusters were used as masks from which mean effect size data from the original activation maps within each feeding condition were extracted (Figure 4.10). These relationships appeared as driven predominantly by diminishing post-water activation in the ACC as BMI increased, whilst in the other structures, this appeared as an interaction effect of both meal and water, with increasing deactivation responses after water ingestion and diminishing deactivation after the meal with increasing BMI.

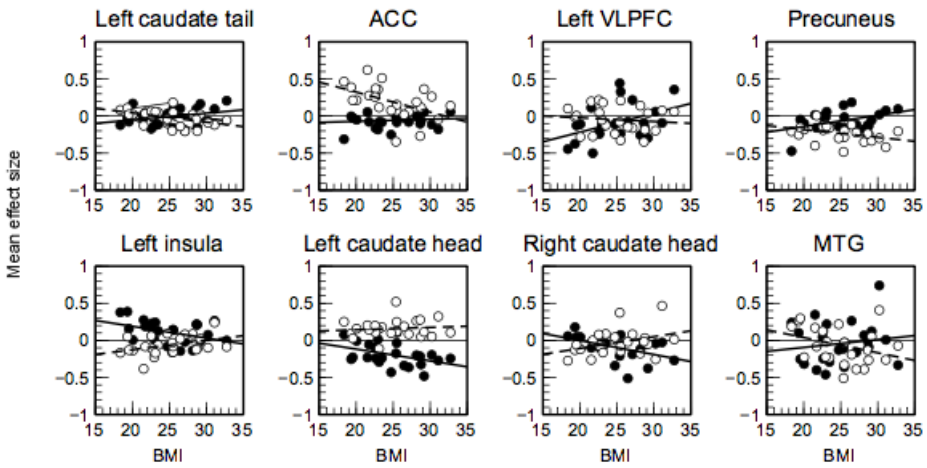

Figure 4.10

Mean age-adjusted effect size from each subject after meal (filled circles) and water (open circles), extracted from clusters identified in Figure 4.9. For illustrative purposes only, lines indicate linear regression (solid = meal, dashed = water). Positive effect size: food > object. Effect size units = % BOLD signal change. See Figure 4.9 for abbreviations.

Increasing BMI, independent of age, was negatively correlated with the difference magnitude of the BOLD signal contrast between feeding conditions in the bilateral caudate head, bilateral insula cortex and left cingulate gyrus (Figure 4.9A, Table 4.3). The extracted effect size data indicated this negative correlation to be due to greater

insula cortical BOLD signal contrast after meal than water ingestion observed in thinner volunteers, with less differentiation between the two feeding conditions as BMI increases, whilst in the caudate, BOLD signal contrast is of greater magnitude after water than meal ingestion with higher BMI (Figure 4.9B). When mean effect size data from the original activation maps within each feeding condition were extracted from these clusters further to determine the responses as activation or deactivation to food images, these relationships appeared as driven by post-meal activation and post-water deactivation in the insula that both diminished with increasing BMI, whilst in the caudate there was progressive post-meal deactivation with increasing BMI (Figure 4.10).

4.4 Discussion

This study has shown that visual food cue-evoked activation of striatal reward centres is converted to a deactivation by prior meal ingestion, consistent with existing BOLD fMRI research (Fuhrer *et al*, 2008; Goldstone *et al*, 2009). However, this study shows that increasing age from the 3rd to the 6th decade is associated with both a diminution of the satiety-inducing effects of a meal and of the modulatory effects of prior meal ingestion on visual food cue-evoked in striatal regions, as well as prefrontal centres involved in reward salience representation and inhibitory control. Increasing BMI was also associated with diminishing discriminatory responses to food images between feeding conditions in the centres involved in interoception, and greater post-prandial deactivation of the striatum.

4.4.1 Effect of meal ingestion

Meal compared to water ingestion reduced food image-evoked responses in dopaminergic corticolimbic structures in the network that subserves appetitive motivation and incentive saliency of cues and interoception (putamen, amygdala, thalamus and insula) (Berridge *et al*, 2010), the degree to which was significantly associated with suppression of subjective hunger experienced after eating. The early increase in insular rCBF after a meal described in the previous chapter likely

represents the processing of taste and satiation to terminate a meal, whilst the later increase in insular rCBF is accompanied by this meal-induced suppression of responses to visual food cues, which is consistent with existing BOLD fMRI data (Fuhrer *et al*, 2008; Goldstone *et al*, 2009), supporting the concept that neural representations of incentive salience or hedonic value of food are modulated by satiety states. The meal increased food cue-evoked neural activation (or decreased cue-evoked deactivation) in regions normally recruited in abstract visuospatial mental imagery tasks (precuneus, superior parietal lobule, superior and middle temporal gyri) (Cavanna and Trimble, 2006). As subjects were asked to imagine eating viewed food images, differential activation of precuneus and superior parietal lobule between nutritional states may reflect changes in imagined or anticipated taste of the food cues by the recent meal, which may in turn influence prospective eating. Imagining the smell of foods can modulate subsequent perception of such odours (Djordjevic *et al*, 2004). Conversely, it is possible that experiencing food may influence its imagery.

4.4.2 Effect of ageing

There is substantial evidence that elderly populations have lower energy intake, lower fasting and post-prandial hunger and greater post-prandial fullness compared to younger populations (Giezenaar *et al*, 2016). However, there is a paucity of research into the changes in appetite that occur from young adulthood to middle age. My subjects' ages ranged from 19.5-52.6 years, in order to allow the investigation of the hypothesis that altered appetite control mechanisms may contribute to the increased tendency to weight gain in middle age. Although the meal reduced hunger across the age spectrum, ageing was associated with greater hunger during and after meal ingestion, after adjusting for BMI, with a trend towards less suppression by meal ingestion of the hunger evoked by viewing food images. With increasing age, differences in magnitude of the food cue-evoked BOLD signal between fed (deactivation) and fasted (activation) states fell in the right DLPFC, bilateral amygdala and striatum (caudate body), as did the difference in food cue-evoked BOLD signal between fed (activation) and fasted (deactivation) states in left OFC and VLPFC/insula. These data are consistent with reduced sensitivity of corticolimbic networks to current nutritional states, when responding to food cues, with ageing from young adulthood to middle age.

DLPFC activation by stimuli representing high calorie (Goldstone *et al*, 2009; Killgore *et al*, 2003), "fattening" (Schur *et al*, 2009), highly appealing (Passamonti *et al*, 2009) and neutral hedonic foods (Cornier *et al*, 2007), its association with post-prandial secretion of anorexogenic incretin hormones (Pannacciulli *et al*, 2007b), and its engagement during attempts to control the desire to eat (Hollmann *et al*, 2012) have been described in human neuroimaging studies, as has the ability to reduce food cravings and hedonic valuation of food by transcranial direct current and magnetic stimulation of the DLPFC in healthy volunteers (Camus *et al*, 2009; Fregni *et al*, 2008). DLPFC is activated on eating to satiation *per se* (Small *et al*, 2001) and to food cues when satiated (Smeets *et al*, 2006) and its responses towards images of appealing foods are inversely associated with *ad libitum* food intake (Cornier *et al*, 2010). Furthermore, this effect is lost after a period of overfeeding (Cornier *et al*, 2007), with diminished post-prandial activity observed in obesity (Le *et al*, 2006). DLPFC responses to food cues are also increased in young adults compared to children and adolescents (Killgore and Yurgelun-Todd, 2005b) suggesting the role of the DLPFC in controlling eating behaviour continues to develop in youth. This is in keeping with laboratory studies of eating behaviour that show children are able to regulate food intake according to energy requirements, but that food "neophobia" diminishes and food preferences are formed as they get older (Tanofsky-Kraff *et al*, 2007). DLPFC activation by reward incentives during attention tasks also increases from childhood through to middle age (Smith *et al*, 2011), suggesting a general maturation of the function of this inhibitory control centre. We may speculate that weaker mechanisms of satiety in early childhood may ensure sufficient energy intake to support linear growth during this period of development. However, diminution of satiety mechanisms in middle age, when there is little benefit, and indeed positive disadvantage, to excess energy intake appears paradoxical and the observed reduced responsiveness of food cue-evoked activity in the DLPFC to meal ingestion with ageing to middle age is consistent with reduced engagement of these satiety mechanisms as a contributor to weight gain.

Functional connectivity fMRI analyses suggest that the DLPFC controls motivated behaviour, such as eating, by processing information on expected reward, modulating dopaminergic meso-cortical and -limbic networks (Ballard *et al*, 2011), including the OFC (Hare *et al*, 2009), which represents hedonic properties of food or associated

stimuli (Berridge *et al*, 2010; Kringelbach and Rolls, 2004). A recent BOLD fMRI meta-analysis showed consistent OFC activation upon viewing food images that was modulated by hunger (van der Laan *et al*, 2011). The present observation of decreasing modulation of food cue-evoked OFC activity by meal ingestion with ageing may represent reduced sensitivity to meal ingestion, possibly due to reduced dopamine D1 receptors (Jucaite *et al*, 2010) and glucose metabolism (Kim *et al*, 2009) in the OFC from adolescence to middle age which could promote continued eating.

The suppressive effects of meal ingestion in other dopaminergic structures that process incentive saliency of stimuli, including bilateral striatum (right caudate body, left globus pallidus) and right amygdala (Berridge *et al*, 2010), were also reduced with ageing due to diminishing post-water activation and post-meal deactivation responses to food images. Age-associated reductions in striatal dopamine transporter expression (Erixon-Lindroth *et al*, 2005), D_1 and D_2 receptor densities (Volkow *et al*, 1996; Wang *et al*, 1998) may explain the reduced responses to food cues with ageing in the present study in the fasted state, but the impact of ageing from young adulthood to middle age on striatal dopamine signalling in response to eating has not previously been investigated. However, significant differences in BOLD signal contrast to taste stimuli have been shown between the elderly and young adults in caudate, OFC and ACC, thalamus and hippocampus, in fed and fasted states which may represent changes in dopaminergic signalling (Jacobson *et al*, 2010). Negative associations between waist circumference and BMI with BOLD signal changes in the striatum to taste stimuli in older volunteers when fasted have been described that are not present when fed, or in younger volunteers (Green *et al*, 2011). Lower responses during hedonic evaluation of sweet tasting stimuli in middle age compared to young volunteers in regions including the putamen, globus pallidus and insula have been demonstrated, such regions showing discriminatory responses to sweet and bitter stimuli in younger subjects only (Green *et al*, 2013). These studies, together with the present findings, may suggest a mechanism for promoting further food intake, through deficient activation of dopaminergic reward pathways when encountering food-associated stimuli when fasted, requiring greater food exposure to elicit sufficient reward, and diminutions in deactivation and reduction reward value of food cues after eating, with increasing age to middle age. These regions may be potential therapeutic

targets with dopamine agonists (Pijl and Romijn, 2006). In addition, given the obesity-associated increase in functional connectivity between striatum, amygdala and insula on viewing appetising food cues may be secondary to impaired inhibitory control by the DLPFC (Nummenmaa *et al*, 2012), it is possible that the present findings may also represent altered regulation by the DLPFC in middle age with resultant downstream effects on corticolimbic networks. A further suggestion is that the attenuation of responses with age reflects an altered "hedonic set point", such that the amount of calorie intake or deprivation necessary to elicit a complete satiety response are larger than that required in younger adults (Egecioglu *et al*, 2011).

4.4.3 Effect of BMI

Increasing BMI, after adjusting for age, was associated with greater activation of the right insula on viewing food images after water ingestion. This is consistent with existing data showing greater food image-evoked insula responses in obesity (Scharmüller *et al*, 2012; Stoeckel *et al*, 2008), with regression analyses demonstrating similar positive associations between BMI and food-image evoked insula responses during passive viewing (Rothemund *et al*, 2007) and attention tasks (Yokum *et al*, 2011). The insula is involved in interoceptive awareness processing (Craig, 2009; Verdejo-Garcia *et al*, 2012), but is also part of the primary gustatory cortex processing not only consummatory responses to taste and texture of food, but also the anticipation of food, with such responses being greater in obesity (Stice *et al*, 2008), and with the OFC using this information to process the hedonic value of food (Rolls, 2015). The present findings that food image-evoked insula responses in the fasted state, when food is most appetising and rewarding, rise as BMI increases could be interpreted to represent increased attention and reward processes to food cues that promote food-seeking behaviour and facilitate greater food intake food when food is subsequently consumed, leading to further weight gain. The response to food images in the ACC decreased with increasing BMI after water ingestion. This is opposite to existing fMRI data showing greater ACC responses to food images in obese compared to lean individuals (Dimitropoulos *et al*, 2012; Martens *et al*, 2013; Martin *et al*, 2010; Stoeckel *et al*, 2008), although these studies were not designed to investigate the correlational relationships between BMI and food image-evoked responses in the non-obese weight range. Volkow *et al* (2009) demonstrated

decreasing activity of prefrontal cortices and ACC, with increasing BMI as quantified by [^{18}F]FDG-PET, which might provide a physiological explanation for the current findings, which the authors suggest may be a cause rather than a consequence of obesity, through reduced inhibitory self-control of eating behaviour.

Positive associations between BMI and the difference in magnitude of food cue-evoked BOLD signal between feeding states were observed in regions including the ACC, precuneus and VLPFC. In the ACC, this relationship was driven by the greater activation toward food images after water compared to meal ingestion in lean subjects diminishing with rising BMI as described previously, whilst the smaller post-meal responses were largely unaffected by BMI. In the precuneus, lean subjects showed little difference in activation responses to food images between feeding states, but greater post-water deactivation and less post-meal deactivation / greater activation were observed as BMI increased. Based on earlier discussions, this may suggest greater imagery of further eating in response to visual food cues with increasing BMI after consuming a meal. Indeed, explicit imagery instructions upon viewing images of high calorie palatable food, compared to passive viewing, appear to elicit greater responses in overweight compared to normal weight individuals in the precuneus, as well as in regions involved in reward processing and higher executive control (Frankort *et al*, 2012). In the left VLPFC, this positive association was driven by changes in responses to food images after meal ingestion, being predominantly deactivation responses in lean subjects, transitioning to activation responses as BMI increased. The lateral prefrontal and orbitofrontal cortices are implicated in inhibitory control of behaviour, including eating (Burger and Stice, 2011; Hollmann *et al*, 2012). Deficiencies in inhibitory control may be expected to lead to increased food intake, but excessive activity may infer excessive restraint, which through subsequent disinhibition has been implicated in increasing food intake, although others propose that rather being implicated in its causation, restraint is a marker of the tendency to overeat (Johnson *et al*, 2012).

Negative associations between BMI and the difference in magnitude of food cue-evoked BOLD signal between feeding states were observed in the left insula and bilateral caudate. In the left insula, this was driven by post-water deactivation and post-meal activation to food images (the opposite of the activity in the right insula)

that both diminished with increasing BMI. As previously discussed, the insula is involved in interoceptive awareness (Craig, 2009; Verdejo-Garcia *et al*, 2012) and in both anticipatory and consummatory responses to food (Stice *et al*, 2008). The present findings of smaller differences in response to food images between feeding states as BMI increases may suggest diminishing consummatory responses with lesser ability to differentiate cues of hunger from those of fullness, which could facilitate continued food intake. These result may appear to conflict with data of Stice *et al* (2008), showing greater anticipatory and consummatory responses in obesity, but in that study, the anticipatory responses were towards learned cues of subsequent food that would otherwise be meaningless, whilst consummatory responses represented the effects of tasting rather than eating food, and direct comparisons between pre- and post-consumption responses were not examined. The present findings are consistent with data showing lesser deactivation of the insula to food images after a period of overfeeding in individuals who had successfully lost weight, but at risk of weight regain, compared to those who had never been overweight (Cornier *et al*, 2009).

The difference in magnitude of food-image evoked striatal responses was negatively associated with BMI after adjusting for age, whilst it was positively associated with age after adjusting for BMI. As discussed above, the latter association was driven by diminishing activation post-water and deactivation post-meal to food images with age after adjusting for BMI. However, the former association was driven by increasingly greater deactivation responses to food images after eating as BMI increased, whilst activation responses after water appeared relatively stable across the range of BMI, after adjusting for age. Thus whilst these regions appear less responsive to the effects of meal ingestion when subsequently exposed to food cues with progressive age, increasing BMI is associated with increasing deactivation responses to food cues after eating. Stice *et al* (2008) have demonstrated decreased consummatory activation in the caudate in obesity, and others have shown obesity-associated reductions in striatal dopamine transporter (Chen *et al*, 2008) and dopamine receptor (de Weijer *et al*, 2011), which in turn is associated with prefrontal activity (Volkow *et al*, 2008b). However, reduced activation is not the same as increasing deactivation, which few fMRI studies report, and it is unclear if the present observation of greater deactivation to food cues infers "negative reward" after meal ingestion as BMI increases.

4.4.4 Limitations and conclusions

As noted in the previous chapter, the meal did not elicit complete satiation, nor completely suppress hunger, and it therefore does not establish the impact of maximal satiation on food cue-evoked BOLD signals. Nevertheless, the meal was sufficient to reduce scores of appetite during the 34 min observation period, and suppress the hunger elicited by food pictures, and thus the associated neural responses. The ability to detect associations between BOLD signal and symptoms may have been limited by assessing hunger after each image block rather than each image and not measuring food restraint. The group was of mixed gender, which is known to affect brain responses to food images (Frank *et al*, 2010a; Geliebter *et al*, 2013; Uher *et al*, 2006), and scans were not timed with menstrual cycles in women, a factor known to influence responses to food images (Frank *et al*, 2010b), due to logistical reasons.

The present findings and existing data may imply that satiety processing develops during childhood through to young adulthood, diminishes in middle age to coincide with the greater prevalence of obesity, but then increases in the later stages of life with the resultant reduced food intake that is observed in the elderly. However, my study was limited to recruiting subjects between 18-65 years of age, and future studies using similar experimental protocols beyond these age ranges are needed to confirm this proposal. As age and BMI are inextricably associated, as demonstrated both in the present study and in larger scale epidemiological studies, we are limited to controlling for BMI statistically when assessing independent effects of age, and vice versa. Differentiating cause from effect is not possible and there is the danger of making circuitous or even conflicting interpretations of the effect of age on central mechanisms of appetite regulation that may influence future weight, at the same time as the effect of current BMI on such neural processes. Future, longitudinal studies are therefore warranted to elaborate further the changes that occur in the central regulation of appetite. The BOLD signal response to visual food cues may either be positive or negative in direction, with respect to the control non-food related object images. Negative responses have been interpreted as deactivation, such that the correlation analyses may suggest a critical age or BMI at which neither activation or deactivation may occur, which should be interpreted with caution. Nevertheless, the present study suggests that physiological ageing into middle age has effects

independent of BMI on the impact of meal ingestion in response to unconditioned stimuli that promote further eating, which may be involved in the predilection to weight gain observed in middle age.

Table 4.1

Impact of meal compared to water ingestion on food-vs-object picture-evoked BOLD signal contrast (voxel-wise $P < 0.05$, cluster threshold < 0.5 false positive clusters/brain map on Figure 4.3).

Size	Talairach coordinates of voxel with peak effect size			$P \leq$	BA	Brain regions
	x	Y	z			
Meal > Water (cluster-wise $P < 0.007246$)						
1021	8	-77	41	0.000092	7	Precuneus
Phase clarification of Meal > Water*:						
Meal (activation) > Water (activation)						
13	*-4*	*-78*	*23*	*0.011858*	*18*	*Left cuneus*
6	*32*	*-60*	*36*	*0.023772*	*39*	*Right sub-gyral, parietal lobe*
Meal (activation) > Water (deactivation)						
163	*-22*	*-78*	*30*	*0.021284*	*6*	*Left cuneus*
365	*26*	*-71*	*37*	*0.008486*	*19*	*Right precuneus*
141	*-32*	*-59*	*43*	*0.018988*	*7*	*Left superior parietal lobule*
65	*-11*	*-63*	*53*	*0.01094*	*7*	*Left superior parietal lobule*
Meal (deactivation) > Water (deactivation)						
60	*42*	*-61*	*21*	*0.043656*	*39*	*Right middle temporal gyrus*
54	*-24*	*-73*	*34*	*0.052488*	*19*	*Left precuneus*
60	*-54*	*-41*	*20*	*0.052488*	*13*	*Left superior temporal gyrus*
Meal < Water (cluster-wise $P < 0.011905$)						
612	32	-22	0	0.002474	N/A	Right putamen
Phase clarification of Meal < Water*:						
Meal (activation) < Water (activation)						
8	*18*	*7*	*-7*	*0.026056*	*N/A*	*Right putamen*
33	*11*	*-19*	*13*	*0.098643*	*N/A*	*Dorsal nucleus of thalamus*
7	*58*	*-15*	*30*	*0.062388*	*3*	*Right postcentral gyrus*
Meal (deactivation) < Water (activation)						
26	*29*	*19*	*-10*	*0.012827*	*13*	*Right extra-nuclear sub-lobar*
63	*32*	*-22*	*0*	*0.051789*	*N/A*	*Right putamen*
6	*6*	*-36*	*27*	*0.12558*	*31*	*Right cingulate gyrus*
120	*61*	*-19*	*26*	*0.065915*	*2*	*Right postcentral gyrus*
40	*21*	*-17*	*38*	*0.099397*	*24*	*Right cingulate gyrus*
61	*47*	*-19*	*46*	*0.057949*	*3*	*Right postcentral gyrus*
36	*18*	*-26*	*63*	*0.039162*	*4*	*Right precentral gyrus*
Meal (deactivation) < Water (deactivation)						
21	*30*	*-2*	*-18*	*0.013288*	*N/A*	*Right amygdala*
17	*19*	*-24*	*38*	*0.117613*	*31*	*Right cingulate gyrus*

[1]Phase clarification of the parent cluster. Activation = Food > Objects; deactivation = Food < Objects. P values are the mean values of the cluster / sub-clusters. BA = Brodmann area.

Table 4.2

Whole brain linear correlation of age with food-vs-object picture-evoked BOLD signal contrast after water ingestion, and of difference in food-vs-object picture-evoked BOLD signal contrast between meal and water conditions after adjustment for BMI (voxel-wise $P < 0.05$, cluster threshold < 0.5 false positive clusters/brain map, Figure 4.5, Figure 4.6).

Size	Talairach coordinates of voxel with peak effect size			P ≤	BA	Brain regions
	X	Y	z			
Water						
Positive correlation with age, after correction for BMI *(cluster-wise P < 0.011364)*						
17	11	-67	-40	0.000347	N/A	Right inferior semi-lunar lobule, cerebellum
13	-13	-31	-10	0.001991	N/A	Left culmen, cerebellum
13	56	-31	2	0.000717	21	Right middle temporal gyrus
14	-31	25	5	0.000046	45	Left inferior frontal gyrus, VLPFC, anterior insula
16	-9	-55	22	0.002918	31	Left posterior cingulate
120	-41	-53	22	0.000001	39	Left superior temporal gyrus
11	-18	37	40	0.001464	8	Left superior frontal gyrus
22	33	29	41	0.000277	8	Right middle frontal gyrus
11	-11	23	57	0.005055	6	Left superior frontal gyrus
Negative correlation with age, after correction for BMI *(cluster-wise P < 0.016129)*						
41	39	-55	-12	0.000001	37	Right fusiform gyrus
18	44	34	14	0.001672	46	Right middle frontal gyrus (DLPFC)
14	21	-69	47	0.010973	7	Right precuneus
Meal-minus-water						
Positive correlation with age, after correction for BMI *(cluster-wise P < 0.017241)*						
9	30	-5	-15	0.008076	N/A	Right amygdala
76	-14	4	-3	0.000001	N/A	Left lateral globus pallidus
36	11	11	0	0.000001	N/A	Right caudate head
15	16	19	13	0.000075	N/A	Right caudate body
162	24	48	31	0.000001	9	Right superior frontal gyrus, including DLPFC
Negative correlation with age, after correction for BMI *(cluster-wise P < 0.009434)*						
22	-35	5	-32	0.000001	21	Left middle temporal gyrus
16	22	-59	-26	0.000173	N/A	Right culmen, cerebellum
9	-43	19	-26	0.000187	38	Left superior temporal gyrus
17	11	-73	-16	0.005403	N/A	Right declive, cerebellum
23	-36	-70	-23	0.000273	N/A	Left uvula, cerebellum
40	-42	28	-7	0.000001	47	Left inferior frontal gyrus, OFC
14	-47	19	3	0.001019	45	Left inferior frontal gyrus, VLPFC
12	4	-45	17	0.007732	29	Right posterior cingulate
17	-19	-32	14	0.000047	N/A	Left caudate tail
26	-5	57	22	0.000001	31	Left posterior cingulate
185	-28	-71	34	0.000001	19	Left precuneus, superior and middle temporal gyri
17	-13	23	57	0.00068	6	Left superior frontal gyrus

P values are the mean values of the clusters. BA = Brodmann area.

Table 4.3

Whole brain linear correlation of BMI with food-vs-object picture-evoked BOLD signal contrast after water ingestion, and of difference in food-vs-object picture-evoked BOLD signal contrast between meal and water conditions, after correction for age (voxel-wise $P < 0.05$, cluster threshold < 0.5 false positive clusters/brain map, Figure 4.8, Figure 4.9).

Size	Talairach coordinates of voxel with peak effect size			$P \leq$	BA	Brain regions
	x	y	z			
Water						
Positive correlation with BMI, after correction for age *(cluster-wise P < 0.015152)*						
24	-12	-38	-39	0.000035	30	Left cerebellar tonsil
14	40	-78	-3	0.000545	19	Right inferior occipital gyrus
245	52	-12	17	0.000001	43	Right postcentral gyrus, *Insula*
Negative correlation with BMI, after correction for age *(cluster-wise P < 0.015625)*						
13	-4	-59	-16	0.004697	N/A	Left declive, cerebellum
35	-54	-45	3	0.000026	22	Left middle temporal gyrus
21	-24	-38	13	0.000001	N/A	Left caudate tail
43	6	14	24	0.000001	24	Right anterior cingulate
Meal-minus-Water						
Positive correlation with BMI, after correction for age *(cluster-wise P < 0.011628)*						
13	11	-74	-26	0.001407	N/A	Right cerebellar pyramis
32	35	-62	-12	0.000001	N/A	Right cerebellar declive
10	-55	-51	0	0.006249	37	Left middle temporal gyrus
10	-4	-19	-7	0.00907	N/A	Red nucleus, midbrain
22	-49	35	2	0.00028	47	Left inferior frontal gyrus, *VLPFC*
12	41	-58	14	0.000175	19	Right middle temporal gyrus
48	-21	-35	15	0.000001	N/A	Left caudate tail
13	6	14	24	0.000071	24	Right anterior cingulate
211	-31	-73	34	0.000001	19	Left precuneus
18	-21	-59	54	0.000394	7	Left superior parietal lobule
24	-25	-4	56	0.000013	6	Left subgyral frontal lobe, *Putamen*
Negative correlation with BMI, after correction for age *(cluster-wise P < 0.012195)*						
8	-29	-52	-40	0.002695	N/A	Left cerebellar tonsil, *Hippocampus*
9	-7	7	0	0.008489	N/A	Left caudate head
42	-42	8	9	0.000001	44	Left precentral gyrus, *Insula*
77	11	15	0	0.000001	N/A	Right caudate head
34	62	-10	11	0.000001	42	Right transverse temporal gyrus
40	-5	-31	42	0.000001	31	Left cingulate gyrus

P values are the mean values of the clusters. BA = Brodmann area.

5 Systemic insulin resistance and central responses to meal ingestion

5.1 Introduction

Systemic insulin resistance is associated with a range of health disorders, including obesity, type 2 diabetes (T2DM) and cardiovascular disease. The rising prevalence of these conditions has been attributed to recent changes in lifestyle, with increased intake of energy-dense foods in the absence of increased energy expenditure. As discussed in Chapter 1, the main role of circulating insulin in the periphery is that of glucose homeostasis, but within the brain insulin is implicated in anorexigenic signalling, reducing food intake, decreasing weight and increasing peripheral insulin sensitivity, amongst other central functions that are still being elucidated (Belgardt and Brüning, 2010; Heni *et al*, 2012, 2014c, Plum *et al*, 2005, 2006).

Using changes in regional cerebral blood flow (rCBF) as a surrogate marker of regional brain activity, [^{15}O]H_2O-PET studies have demonstrated increased rCBF in the dorsolateral prefrontal cortex (DLPFC) after consumption of a satiating liquid meal in healthy volunteers, with diminished responses observed in obese men and women who, given their higher circulating fasting and post-prandial insulin levels, were presumably insulin resistant (Le *et al*, 2006, 2007). Whilst there are studies examining the response to tasting food in volunteers who appear to be prone to or at risk of obesity (Stice *et al*, 2011), as well as to visual food cues in systemic insulin resistance in the context of polycystic ovarian syndrome (Van Vugt *et al*, 2013), there are no studies to date investigating whether men, who are at risk for clinical conditions such as obesity and T2DM by virtue of family history and systemic insulin resistance, show altered central responses to a satiating meal per se, before overt clinical conditions ensue. Using pCASL fMRI, I have evidence for an early increase in rCBF in bilateral insula, right medial frontal gyrus/anterior cingulate cortex and cingulate gyrus, and a reduction in rCBF in lingual gyrus and precuneus after meal compared to water ingestion in healthy volunteers (Chapter 3), centres involved in processing food-related reward and salience, under the inhibitory control of the DLPFC (Hollmann *et al*, 2012; Siep *et al*, 2012). The present study therefore aimed

to establish whether systemic insulin resistance, *in the absence of obesity or diabetes,* is associated with altered satiation responses to meal ingestion in these brain regions.

5.2 Methods

5.2.1 Subjects

Recruitment methods and inclusion criteria have been described (sections 2.8.1-2). In brief, insulin sensitive (IS) and resistance (IR) status were defined by HOMA2-IR of ≤ 0.76 and ≥ 1.47 respectively, cut-offs derived from the upper and lower quartiles of distribution of HOMA2-IR in 6166 non-diabetic adults from the NHANES-III study (personal communication, (Sierra-Johnson *et al*, 2007)). Subjects were restricted to non-obese men to avoid effects of gender and menstrual cycle. As relatives of people with T2DM are an enriched population for identifying IR, (see section 2.6 for discussion), IR subjects were first-degree relatives of patients with T2DM (IS subjects having no first-degree diabetic relatives). Diabetes was excluded by 75g oral glucose tolerance test (OGTT) (World Health Organization, 2006a). Eating behaviours were assessed by completion of the Questionnaire on Eating and Weight Patterns-Revised (QEWP-R) (Spitzer *et al*, 1993), Dutch Eating Behaviour Questionnaire (DEBQ) (van Strien *et al*, 1986) and Eating Disorder Examination Questionnaire (EDE-Q-6.0) (Fairburn and Beglin, 2008) in the fasted state before the OGTT.

5.2.2 Study protocol

The general experimental design and MRI acquisition details are described in section 2.8. All subjects underwent the same protocol (Figure 5.1). The BOLD fMRI study is described in Chapter 6. With regard to the CBF study, in brief, subjects were studied on two separate mornings following an overnight fast of at least 8 hours. After intravenous cannulation, subjects were positioned in the scanner. Following ASSET calibration, Axial T2 FR-FSE and GE EPI scans, 3D pCASL scans each lasting 6 mins were performed before (pCASL-1 at -14 mins) and after (pCASL2-4 at 0, +8 and +34 mins, respectively) subjects were sat up out of the scanner to consume 630 kcal mixed-meal (225ml, 630kcal, 42g fat, 9g protein, 54g carbohydrate) or 50ml water (-6 to 0 mins) in random order across visits. A larger meal than in the ageing study was used to maximise satiation. Before pCASL1, after each pCASL1-4 and

after the BOLD fMRI task (+16 mins, Chapter 6) that took place between pCASL3-4, subjects rated appetite on a projected 1-100 visual analogue scale, marked at every 10th point, using a handheld keypad, with concurrent blood sampling. The visit was completed with T1 FSPGR and axial T2 FLAIR scans.

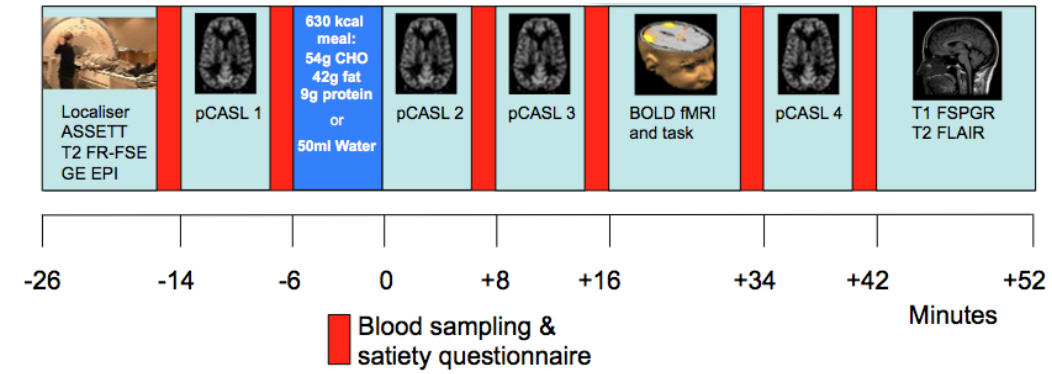

Figure 5.1

Study protocol

5.2.3 Biochemical analyses

Laboratory methods for quantifying plasma glucose, serum insulin, GLP-1, GIP, leptin and adiponectin are described in section 2.8.14. The first five subjects identified as IS were studied, but were found to have HOMA2-IR between IS and IR cut-offs when low sensitivity of the Immulite-2000 insulin assay was identified and therefore no longer used, and samples were re-analysed using the ADVIA-Centaur assay. These subjects formed a group of intermediate insulin sensitivity ("INT").

5.2.4 Statistical analyses

General non-imaging statistical methods are described in section 2.8.14. Data are presented as mean±SEM or median (with interquartile range). pCASL image pre-processing and statistical analyses are described in sections 2.8.13.1-2. Smoothed, normalised CBF maps calculated for each subject were entered into second-level group analyses. Within-group analyses were performed using a flexible factorial general linear model (GLM) as used in the ageing study (Figure 3.2). As flexible factorial GLMs in SPM do not permit more than two interacting factors, between-group analyses were performed using a full factorial mixed-effects GLM, with group (2 levels: IS, IR), feeding status (2 levels: meal, water) and time (4 levels: pCASL1-4)

as interaction factors (Figure 5.2). Analyses were restricted to grey matter, with mean global grey matter CBF used as a nuisance covariate. T-contrast vectors were defined to examine differences between IS and IR groups in (a) pre-ingestion rCBF (pCASL1); (b) post-water rCBF and (c) post-meal rCBF across three post-ingestion time points (pCASL2-4) and; (d) differences in the effect of meal compared to water ingestion across three post-ingestion time points (pCASL2-4). Separate multiple regression models using the combined IS, IR and INT dataset were also constructed to examine linear relationships between insulin resistance (using HOMA-IR which is continuous without a lower limit, unlike HOMA2-IR which has a lower limit of 0.4) and DEBQ-restraint scores with rCBF, using mean global grey matter CBF as a nuisance covariate. A cluster-forming uncorrected voxel-wise threshold of $P<0.01$ was employed, but only those clusters that survived statistical significance ($P_{FWE\text{-}corrected}<0.05$) after correction for multiple comparisons are reported. Mean CBF values were extracted from unsmoothed CBF maps to examine global grey matter CBF (with statistical tests performed in SPSS) and functionally identified regions from these voxel-wise analyses to quantify differences in rCBF in physiological units and for illustrative purposes to characterise the nature of the regression analyses.

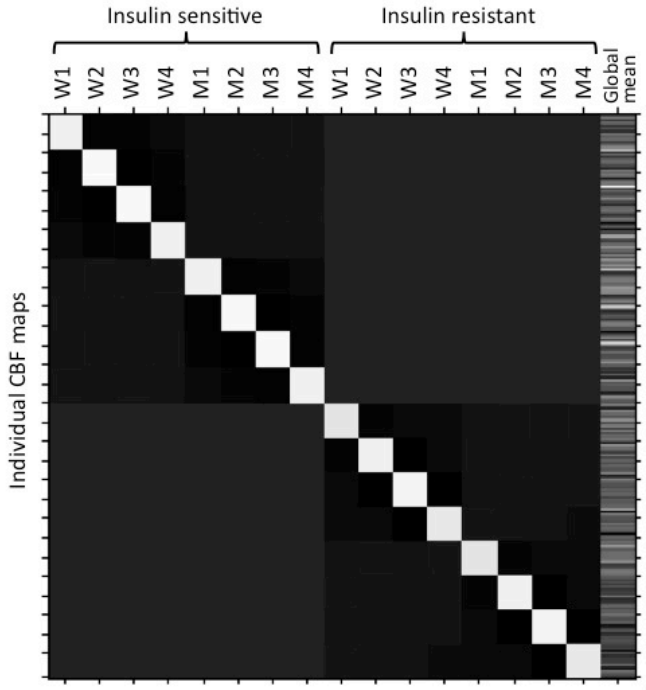

Figure 5.2

Full factorial GLM design matrix. W1-4 = pCASL1-4 on water visit; M1-4 = pCASL1-4 on meal visit. Global mean = mean global grey matter CBF.

5.3 Results

5.3.1 Subjects

A total of 125 men were screened until,16 IR and 17 IS subjects meeting the inclusion criteria (using the ADVIA-Centaur insulin assay) were identified and consented. The primary outcome of differences between IS and IR groups during fMRI was examined. However, with the additional five INT subjects, exploratory mixed model ANOVA was only applied to the baseline characteristics for the three groups. All subjects were matched for age, weight and neck circumference, although BMI, waist circumference and systolic blood pressure were lower in the IS group (Table 5.1). Fasting triglycerides were highest and HDL lowest in the IR group. The metabolic syndrome (International Diabetes Federation, 2006) was identified in three IR subjects and one INT subject.

5.3.2 Oral glucose tolerance test

Fasting plasma glucose during the OGTT did not differ between groups, but fasting insulin levels were greater in IR than IS subjects (Table 5.1). Two-hour glucose concentrations were higher in IR than IS, as were net iAUCs for glucose (Figure 5.3). Net iAUCs for insulin were significantly greater in IR than IS and INT. The Matsuda index was higher in IS than IR and INT groups, consistent with HOMA2-IR.

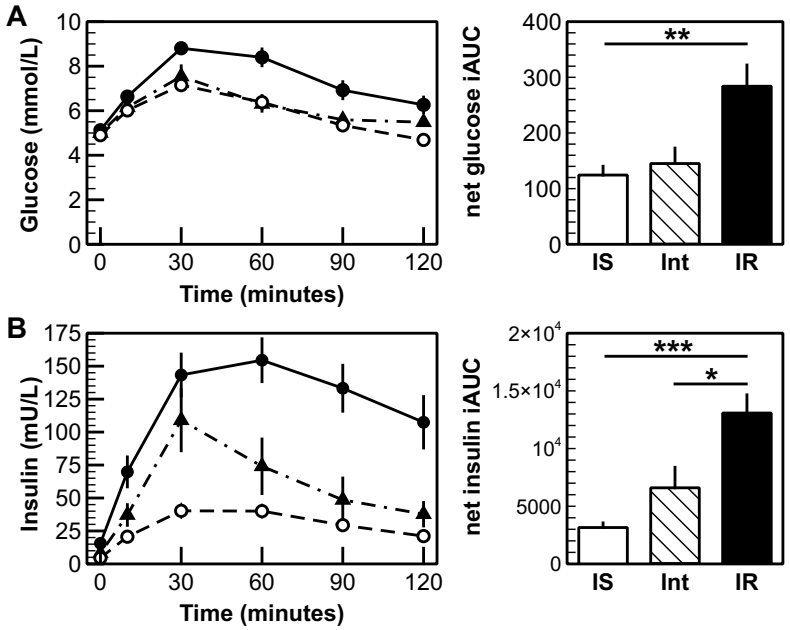

Figure 5.3

Plasma glucose (A) and serum insulin (B) during 75 g oral glucose tolerance test. Mean (± SE) (left) and net iAUC (right). White circle and dashed line = IS; triangle and dot/dashed line = INT; black circle and solid line = IR, insulin resistant. *p < 0.05; **p < 0.01, ***p < 0.001 (Bonferroni corrected).

5.3.3 Eating behaviour

None of the subjects exhibited binge-eating or purging behaviour. Food restraint was significantly greater in IR than IS subjects on the DEBQ (Table 5.2), with a trend to being greater on the EDE-Q (Table 5.3). IR subjects had significantly greater weight and shape concern and higher global scores on the EDE-Q. Weight and shape concern appeared to affect self-value, with a trend towards weight or shape being more important in how IR subjects evaluated themselves over the preceding 6 months compared to IS subjects based on the QEWP (Table 5.4). There were no differences in disinhibited eating based on DEBQ emotional and external scales. DEBQ-restraint, and EDE-Q-restraint, -shape concern, -weight concern and -global scores were positively associated with HOMA-IR. As a crude indicator of parental BMI, subject-reported build of mothers at their heaviest was greater in IR than IS subjects.

5.3.4 Symptom scores

Symptom scores were subjected to statistical tests in IS and IR subjects only (Figure 5.4 shows all data for completeness). Repeated measures ANOVA of the mean pre-meal/water (i.e. mean of pre- and post-ASL1) subjective scores indicated significantly less hunger (main effect of group, $F(1,31)=7.752$, $p=0.009$), greater fullness ($F(1,31)=11.501$, $p=0.002$) and less pleasantness to eat ($F(1,31)=6.561$, $p=0.016$) in IR than IS subjects, whilst there were no differences in pre-ingestion nausea ($F(1,31)=0.294$, $p=0.591$). To examine the effect of the meal compared to water, net iAUC for each symptom were calculated, using the mean pre-ingestion score as baseline to account for differences in baseline scores. The main effect of the meal across all groups was reduced hunger ($F(1,31)=24.993$, $p<0.001$) and pleasantness to eat ($F(1,31)=34.163$, $p<0.001$) and increased fullness ($F(1,31)=55.316$, $p<0.001$), without significant effect on nausea ($F(1,31)=1.888$, $p=0.179$), and no significant differences between groups, or group x meal interactions.

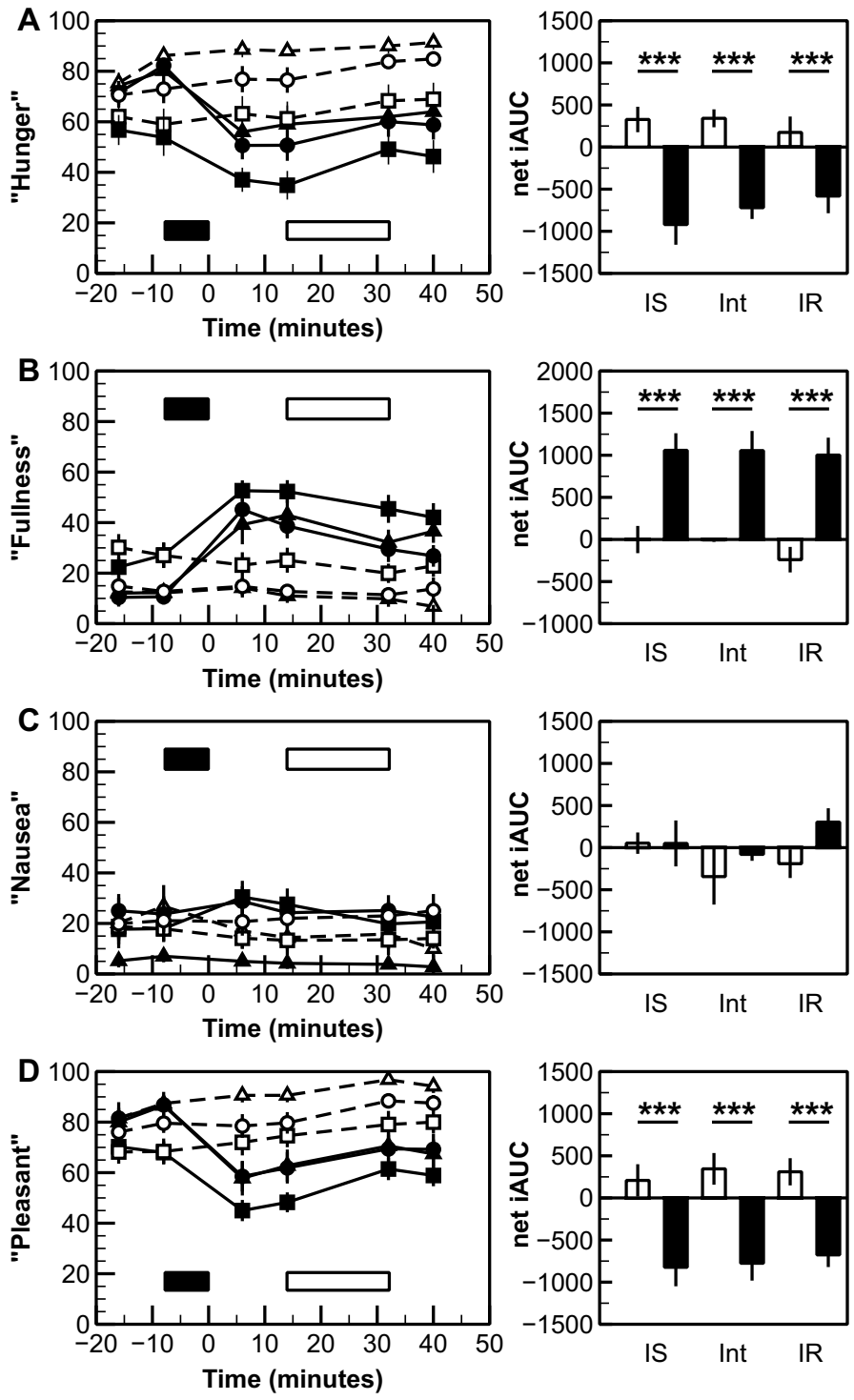

Figure 5.4

Hunger (A), fullness (B), nausea (C) and pleasantness to eat (D) scores after the meal (solid line) and water (dashed line) in IS (circle), IR (square) and INT (triangle) group. Left: Mean (± S.E.M); horizontal bars: black = time of meal/water; white = BOLD task. Right: net iAUC; white bars = water; black bars = meal; ***$p < 0.001$ main effect of meal.

5.3.5 Glucose, insulin, GLP-1 and GIP during MRI scan visits

Biochemical data were subjected to statistical tests in IS and IR groups only (Figure 5.5 shows all data for completeness).

5.3.5.1 Glucose

There was a small but significant difference in fasting glucose levels, being higher in IR than IS subjects (5.1±0.7 vs 4.9±0.8 mmol/L, p=0.034). The net iAUC data showed a small but significant post-prandial rise in glucose across all subjects (main effect $F(1,31)=46.286$, $p<0.001$), that was not significantly different between groups (meal x group interaction $F(1,31)=3.281$, $p=0.08$).

5.3.5.2 Insulin

Fasting insulin levels were greater in IR than IS subjects (13.6±0.8 vs 5.3±0.7 mU/L, $P<0.001$). The net iAUC data showed a post-prandial rise in insulin in both groups (main effect of meal $F(1,30)=64.193$, $p<0.001$), being greatest in IR subjects (meal x group interaction, $F(1,30)=14.087$, $p=0.001$).

5.3.5.3 GLP-1

Fasting GLP-1 levels were greater in IR than IS subjects (13.9±1.3 vs 8.6±1.4 pmol/L $p=0.01$). Net iAUC showed a post-prandial rise in GLP-1 in both groups (main effect of meal, $F(1,28)=6.743$, $p=0.015$), that was not significantly different between groups (meal x group interaction, $F(1,28)=0.158$, $p=0.694$).

5.3.5.4 GIP

The difference in baseline GIP levels between groups did not reach statistical significance (59.8±12.4 vs 30.951±13.3 ng/L, p=0.123). The net iAUC data showed a significant post-prandial rise in GIP across all subjects (main effect of meal, $F(1,28)=59.604$, $p<0.001$), being larger in IR subjects ($F(1,28)=9.626$, $p=0.004$).

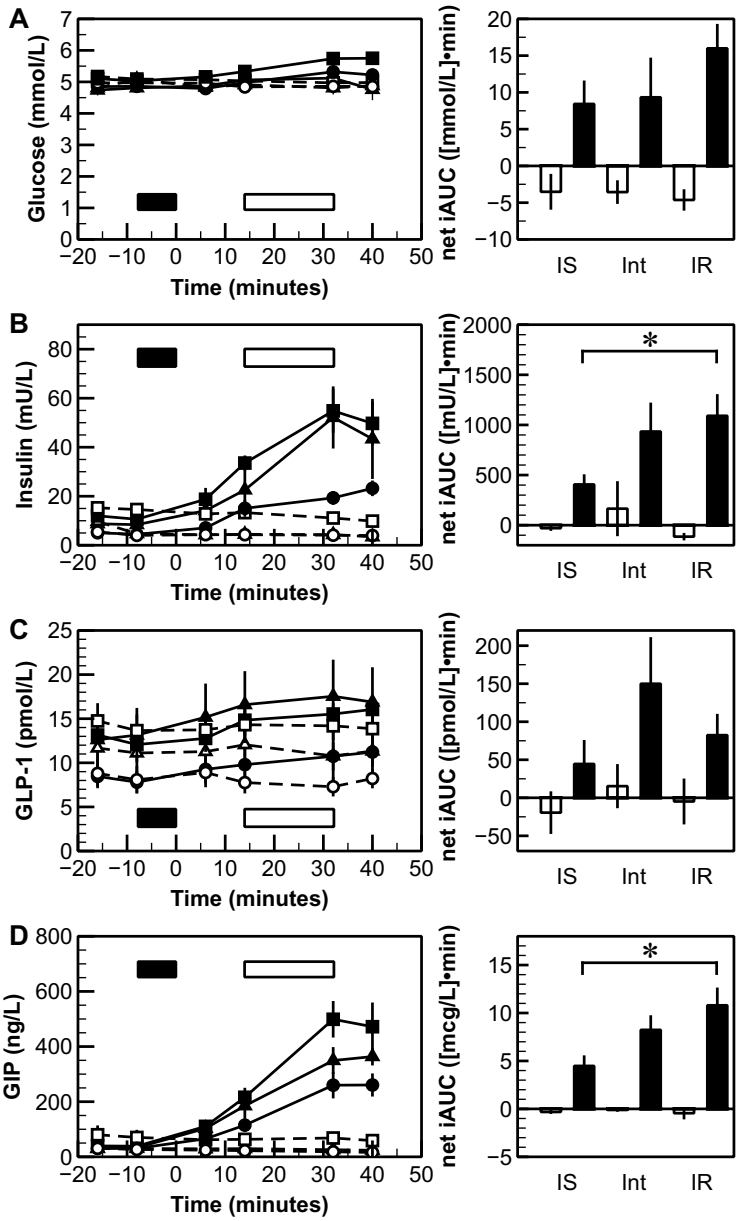

Figure 5.5

Glucose (A), insulin (B), total GLP-1 (C) and total GIP (D) after meal (solid line) and water (dashed line) in IS (circle), IR (square) and INT (triangle) groups. Left: Mean (± S.E.M.); horizontal bars: black = time of meal/water; white = BOLD task. Right: net iAUC; white bars = water; black bars = meal; all net iAUCs were significantly greater post-meal than post-water in all groups. *p < 0.01 for IR vs IS.

5.3.6 Impact of systemic insulin resistance on global grey matter CBF

The extracted global grey matter CBF from IS and IR subjects was subjected to repeated-measures ANOVA in SPSS. There were no significant differences between pre-water and pre-meal ingestion scans (pCASL1) from the two visits (p=0.297). During the course of each scan visit, there was a significant main effect of time ($F(1.68,52.18)=14.32$, $p<0.001$) and a meal x time interaction ($F(1.75,54.34)=3.997$,

p=0.029), due to greater reduction in global grey matter CBF after the meal. Differences between groups did not reach statistical significance (main effect, F(1,31)=3.102, p=0.088; all interactions also non-significant) (Figure 5.6). When the INT group was included, there was no significant association between the average pre-ingestion global grey matter CBF and HOMA-IR.

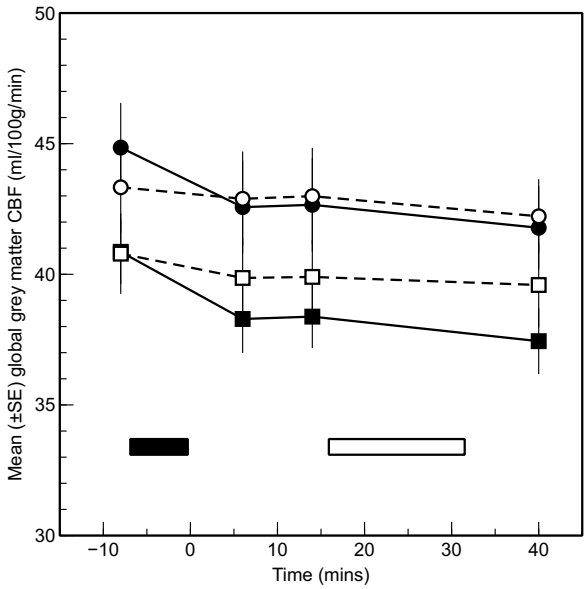

Figure 5.6

Global grey matter CBF after water (dashed lines) and meal (solid lines) in IS (circle) and IR (square) subjects. Black bar = meal / water ingestion; white bar = BOLD task.

5.3.7 Impact of meal ingestion on rCBF within insulin sensitive subjects

There were no differences in fasting, pre-ingestion rCBF (pCASL1) between planned meal and water visits. T-contrasts for the main effect of post-meal vs post-water ingestion (pCASL2-4) showed greater rCBF in right angular gyrus and less rCBF in bilateral lingual gyrus after the meal (Figure 5.7A, Table 5.5).

5.3.8 Impact of meal ingestion on rCBF within insulin resistant subjects

No differences in fasting, pre-ingestion rCBF (pCASL1) were observed between visits. Post-meal compared to post-water rCBF across the three time points (pCASL2-4) was significantly lower in right orbitofrontal cortex (OFC) (inferior frontal gyrus, triangular part) (Figure 5.7B, Table 5.5), with a cluster in left insula showing greater rCBF that did not reach statistical significance (MNI coordinates: X=-38, Y=0, Z=48, cluster $P_{FWEcorrected}$=0.065, T-value 4.53, 839 voxels, not shown).

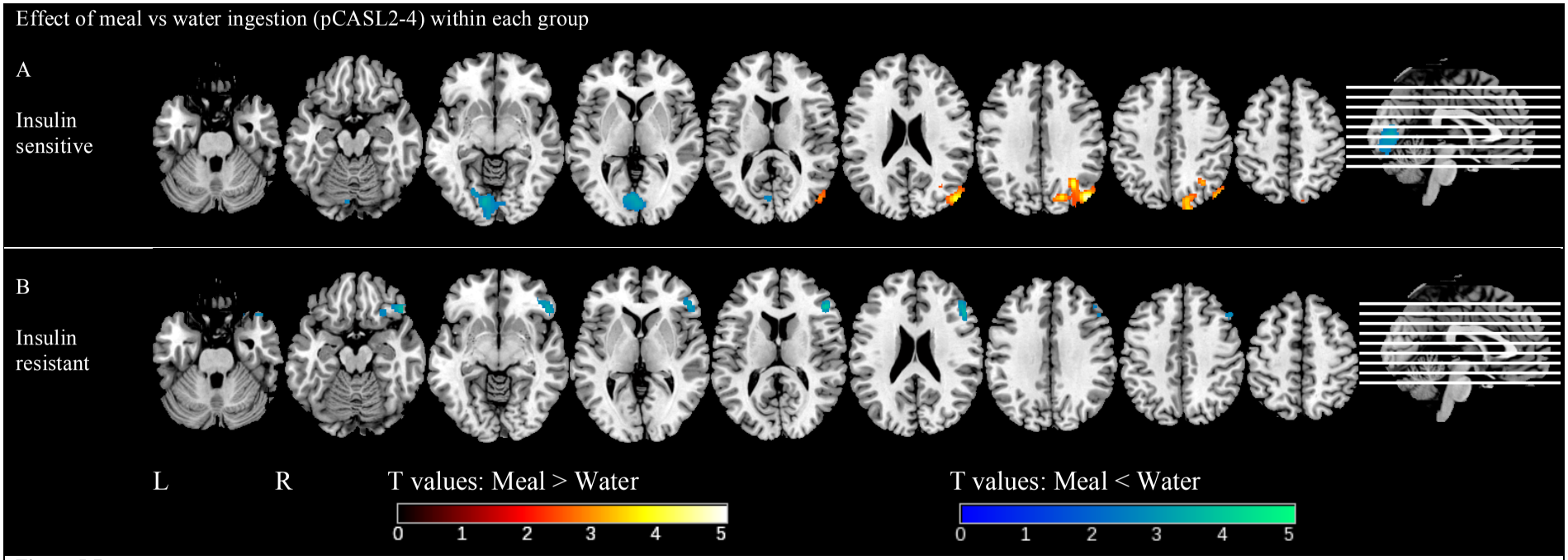

Figure 5.7

Within-group T-contrast brain maps of the main post-meal vs post-water differences in rCBF across the three post-ingestion time-points (pCASL2-4), showing clusters with greater (red) or lesser (blue) rCBF after meal, than after water ingestion in (A) IS and (B) IR groups (there were no differences in pre-meal and pre-water rCBF within each group). Voxel-threshold $P_{uncorrected} < 0.01$. Cluster-threshold $P_{FWE\text{-}corrected} < 0.05$.

5.3.9 Impact of systemic insulin resistance on fasting rCBF

T-contrasts of fasting rCBF showed IR subjects had lower rCBF in left precuneus/inferior parietal lobule and right cerebellum, and greater rCBF in right OFC (superior frontal gyrus, orbital part) than IS subjects (Figure 5.8A, Table 5.6).

5.3.10 Impact of systemic insulin resistance on post-water ingestion rCBF

T-contrasts of the main effect of group across all post-water time points (pCASL2-4), were similar to the differences in fasting rCBF, with IR subjects demonstrating lower rCBF in left inferior parietal lobule and right cerebellum, and greater rCBF in right OFC (triangular part, inferior frontal gyrus, Figure 5.8B, Table 5.6).

5.3.11 Impact of systemic insulin resistance on post-meal ingestion rCBF

T-contrasts of the main effect of group on rCBF across all post-meal time points (pCASL2-4) showed significantly lower rCBF in left mid frontal gyrus, left inferior parietal lobe and right cerebellum (Figure 5.8C, Table 5.6), and greater rCBF in left insula that failed to reach statistical significance (X=-28, Y=18, Z=-6, T-value 4.13, cluster $P_{FWE\text{-}corrected}$ =0.052, 920 voxels, not shown) in IR subjects.

5.3.12 Exploratory analysis of right orbitofrontal cortex CBF

Both fasting and post-water ingestion OFC CBF were greater in IR than IS subjects (Figure 5.8A, B), but there were no significant differences in CBF in this region when comparing IR and IS subjects after meal ingestion. This is likely due to the reduction in rCBF in IR subjects after meal compared to water ingestion (Figure 5.7B). To visualise this, a right OFC region of interest (ROI) was created (Figure 5.9A) by conjoining voxels present in both functional ROIs from the pCASL1: IR > IS (Figure 5.8A) and from pCASL2-4 (water): IR > IS (Figure 5.8B) contrasts. Unsmoothed rCBF data were extracted from this region but not subjected to statistical analyses to avoid inferential bias. As already known from earlier analyses, rCBF in right OFC was greater in the fasted, pre-ingestion state in IR than IS subjects, remaining so after water ingestion, being relatively static during the study period (Figure 5.9B). There was little difference in OFC rCBF between feeding conditions in IS subjects, with

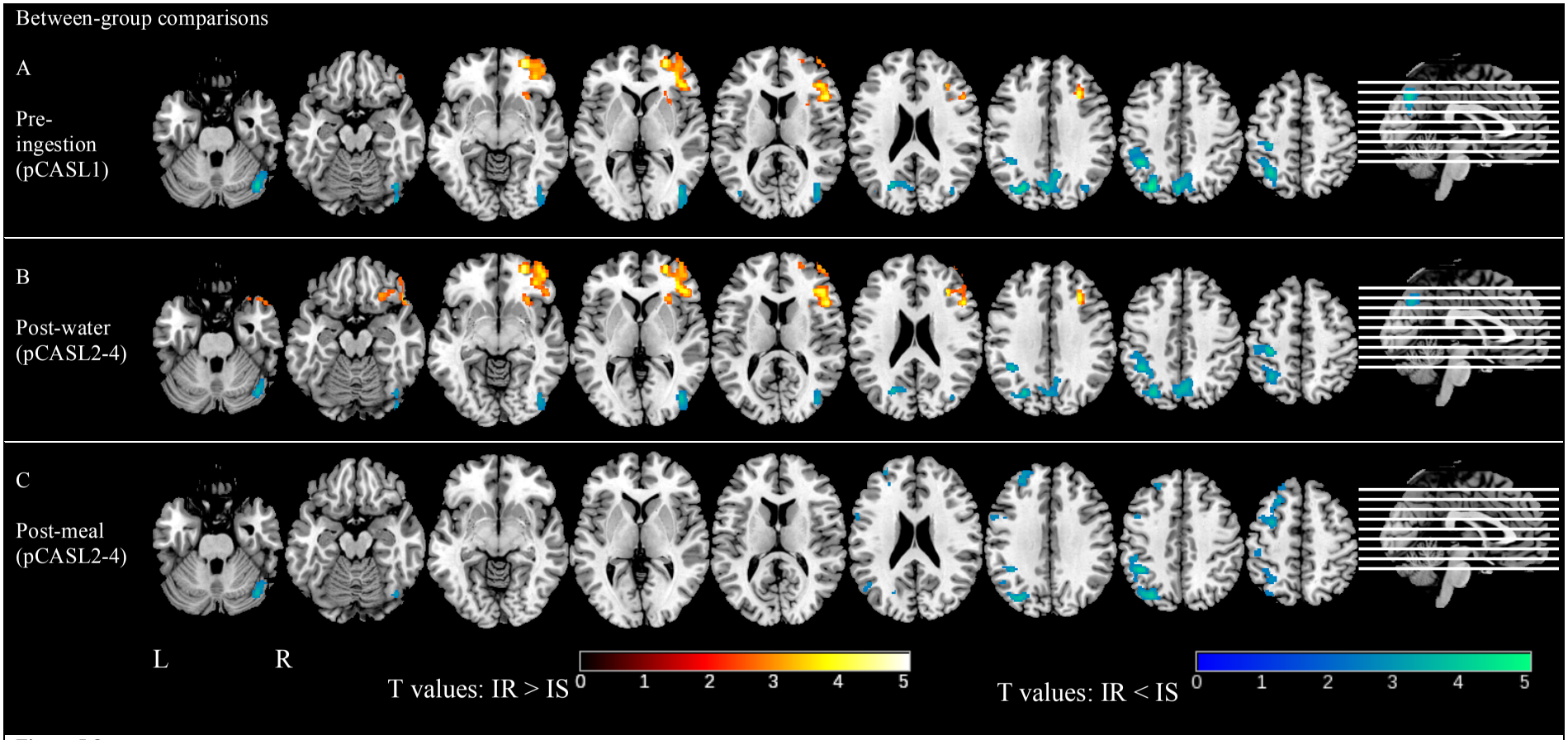

Figure 5.8

Between-group T-contrast brain maps of differences in rCBF, showing clusters with greater (red) or lesser (blue) rCBF in IR than IS groups (A) in the fasted pre-ingestion state (pCASL1), and across post-ingestion time points (pCASL2-4) after (B) water and (C) meal. Voxel-threshold $P_{uncorrected} < 0.01$. Cluster-threshold $P_{FWE\text{-}corrected} < 0.05$.

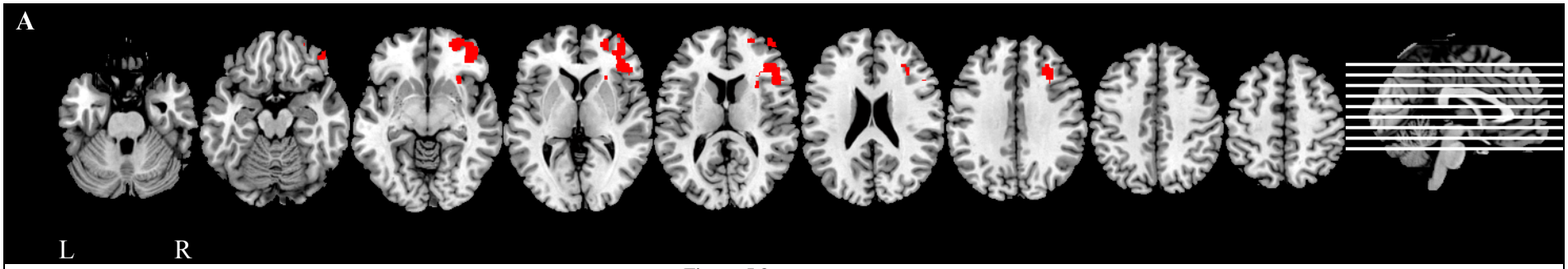

B

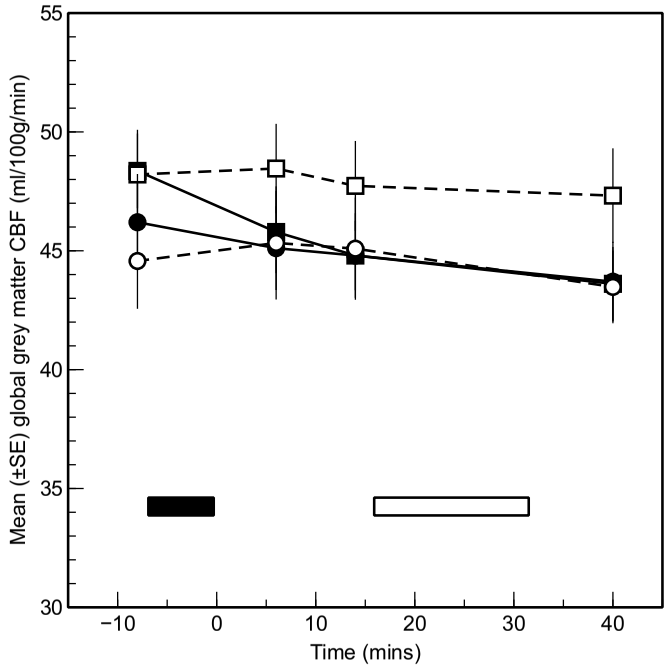

Figure 5.9

A: Region of interest (ROI) constructed from conjoining functional right OFC from fasting pCASL1 (IR > IR) contrast (Figure 5.8A) and Water ASL2-4 (IR > IR) (Figure 5.8B).
B: extracted unsmoothed CBF data from this ROI to explore changes in OFC rCBF post-meal (solid line) and post-water (dashed line) in IS (circle) and IR (square). Black bar = meal / water ingestion; White bar = BOLD task.

post-meal CBF also being relatively static. However, post-meal rCBF in IR subjects decreased from the higher baseline, to match that of the IS group.

5.3.13 Impact of systemic insulin resistance on post-meal vs post-water rCBF

In order to examine differences in rCBF between IS and IR subjects that specifically occur after meal compared to water ingestion, T-contrasts were constructed for the interaction of IS vs IR group with feeding status (post-meal vs post-water) across all post-ingestion time points (pCASL2-4). The IS[Water > Meal] vs IR[Water < Meal] contrast identified significant differences in rCBF within left insula (Figure 5.10, Table 5.6). There were no regions identified in which IS[Water < Meal] vs IR[Water > Meal] rCBF were significantly different. Separate exploratory analyses within each post-ingestion time point only identified a significant interaction during the second post-prandial scan (pCASL3), in the same left insula region (X=-36, Y=4, Z=-16, 1901 voxels, T-value 5.03, cluster $P_{FWE\text{-}corrected}$=0.001, not shown).

5.3.14 Association between HOMA-IR and fasting rCBF

As paired voxel-wise t-tests of all 38 IS, IR and INT subjects did not detect any regional differences in pre-water and pre-meal ingestion CBF (pCASL1), brain maps of the average CBF at each voxel from these two fasting scans were calculated for each subject and entered into a multiple regression model, to examine possible linear relationships between HOMA-IR and fasting CBF. The respective average global grey matter CBF for each subject was used as a nuisance covariate. No significant clusters were identified.

5.3.15 Association between HOMA-IR and differences in post-meal compared to post-water ingestion rCBF

In order to identify possible linear relationships between systemic insulin resistance and differences in brain activity after meal compared to water ingestion, brain maps of CBF post-water subtracted from CBF post-meal at each voxel, at each time point (pCASL2, 3 and 4) were calculated for each subject, and entered into individual multiple regression models, with HOMA-IR as a covariate of interest and global mean

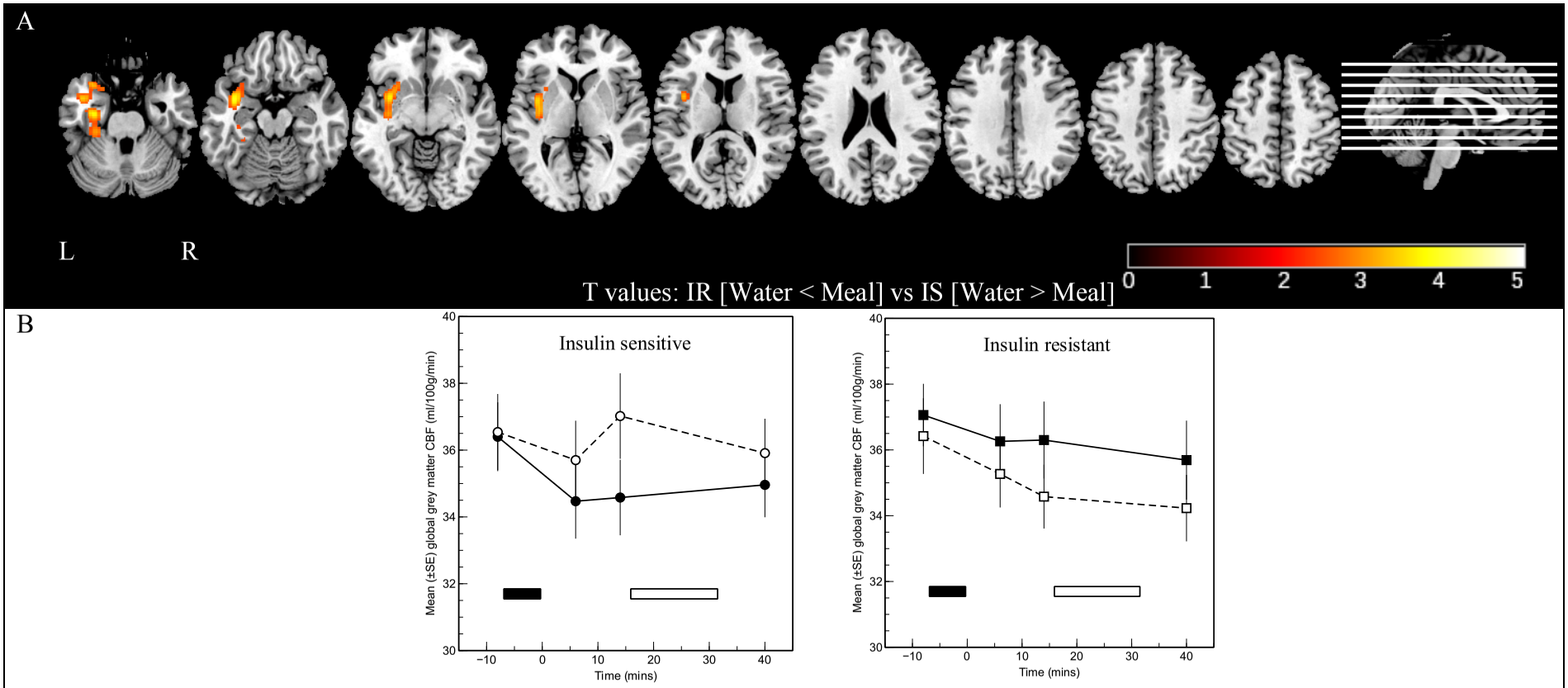

Figure 5.10

(A) T-contrast brain map of main interaction between group and feeding status on across post-ingestion time-points (pCASL2-4). Voxel-threshold $P_{uncorrected} < 0.01$. Cluster-threshold $P_{FWE\text{-}corrected} < 0.05$. (B) Extracted rCBF from left insula cluster in (A) shows lower rCBF after meal (solid line) than after water ingestion (dashed line) in IS (circles) with the opposite pattern of responses in IR (squares). Black bar = meal / water ingestion; white bar = BOLD task.

differences in CBF as nuisance covariate. There were no significant associations between HOMA-IR and differences in rCBF between feeding states immediately (pCASL2), nor at +34 to +40 mins (pCASL4) after the meal. However, between +8 to +14 mins (pCASL3), differences in rCBF between feeding states were positively associated with HOMA-IR in a left insula/inferior frontal operculum cluster (X=-28, Y=-16, Z=-30, T-value 5.0, 3272 voxels, cluster $P_{FWE\text{-}corrected}$=0.001) (Figure 5.11). The extracted rCBF showed an intercept of HOMA-IR at 2.37 (it is not possible to convert to HOMA2-IR, but based on the dataset, is approximately 1.4), above which greater rCBF was observed after meal than water ingestion.

5.3.16 Association between food restraint and fasting rCBF

Given that insulin resistance was positively associated with food restraint reported in the fasted state, a regression model of the average fasting (pCASL1) CBF maps with DEBQ-restraint as a covariate of interest and the respective global grey matter CBF as a nuisance covariate was performed. Restraint was positively associated with fasting rCBF in left insula and rolandic operculum and negatively associated with fasting rCBF in left cerebellum and right mid occipital gyrus (Figure 5.12, Table 5.7).

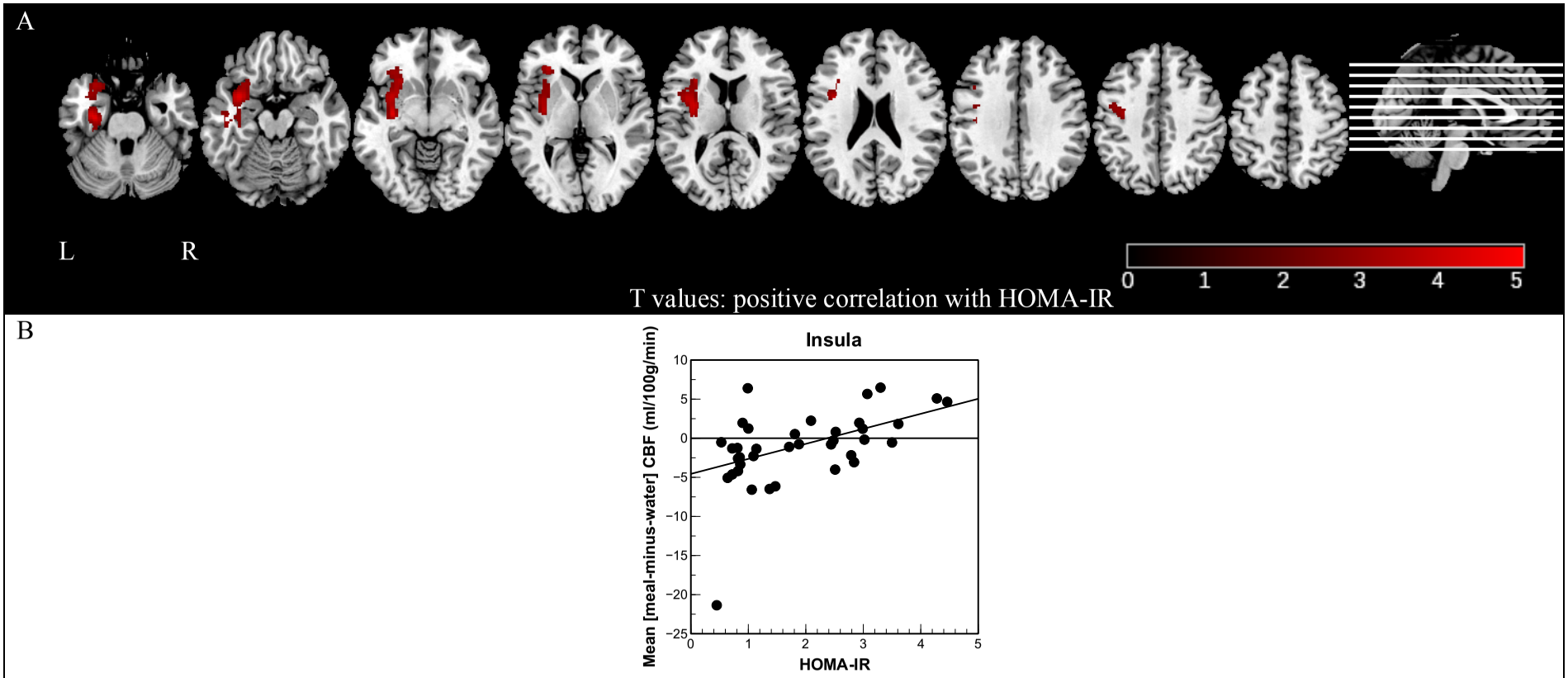

Figure 5.11

(A) Group (IS, IR, INT, n = 38) brain map of voxel-wise regression of HOMA-IR with differences in CBF between feeding states at +8 to +14 mins (pCASL2), adjusted for differences in respective global grey matter blood flow. Voxel-threshold $P_{uncorrected} < 0.01$. Cluster-threshold $P_{FWE\text{-}corrected} < 0.05$. (B) Extracted CBF from insula cluster shows increasing insulin resistance is associated with increasingly greater rCBF after meal. Positive values : meal > water CBF.

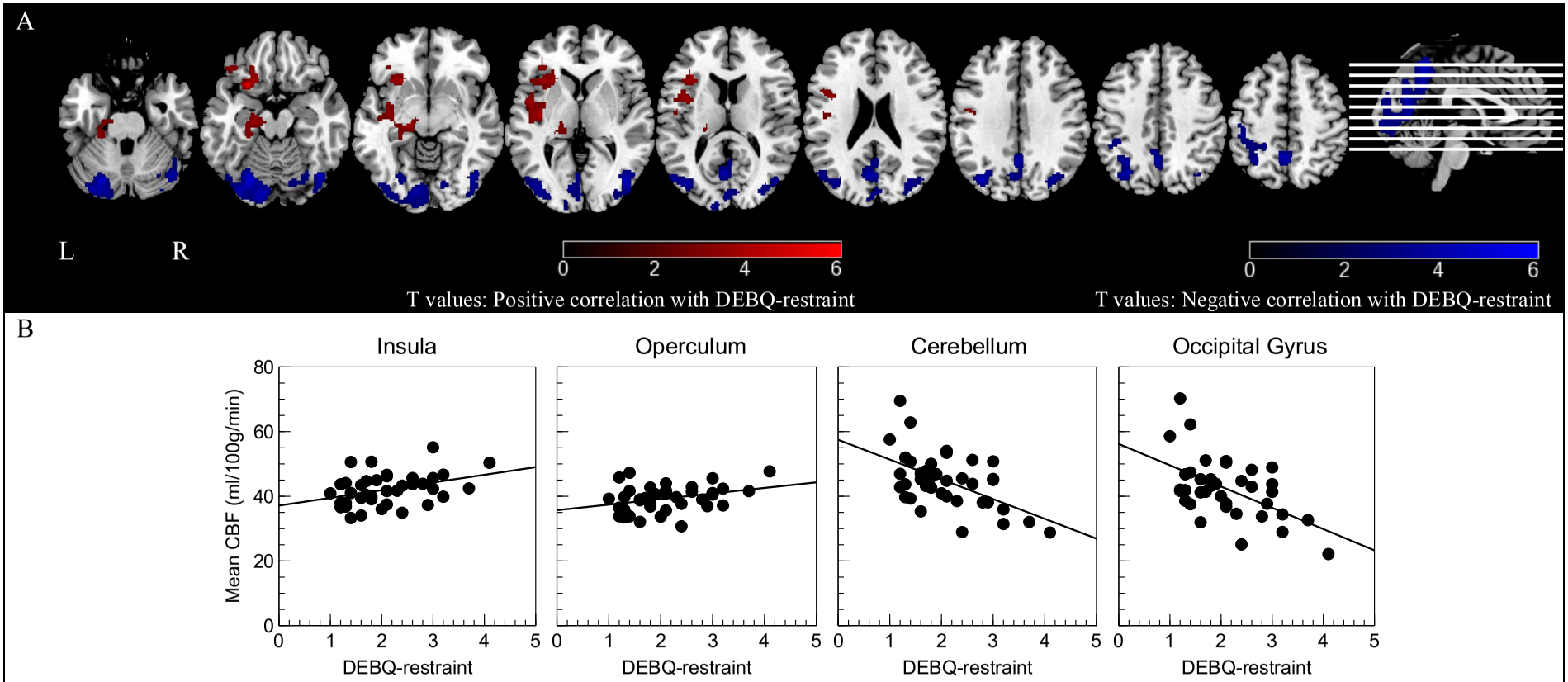

Figure 5.12

(A) Group (IS, IR, INT, n = 38) brain map of voxel-wise linear regression of DEBQ-restraint scores with mean fasting CBF (pCASL1), adjusted for mean global grey matter CBF, showing clusters with positive (red) and negative (blue) associations, as illustrated by the extracted rCBF in (B).

5.4 Discussion

This study set out to examine whether systemic insulin resistance in the absence of obesity or diabetes is associated with altered early central satiation responses to meal ingestion using pCASL fMRI. Age- and weight-matched IS and IR subjects were successfully recruited, with the lower Matsuda indices in the IR group in keeping their insulin resistant status as defined by HOMA2-IR.

5.4.1 Eating behaviour

The observation that our IR subjects had greater self-reported food restraint and weight and shape concern, and evidence for increasing insulin resistance as quantified by HOMA-IR being associated with increasing levels of these constructs is consistent with one published study showing that men, but not women, exhibit a positive association between food restraint as measured by DEBQ, and insulin resistance as measured by HOMA-IR (Jastreboff *et al*, 2014). Restraint theory suggests that eating behaviours driven by conscious restriction of eating will reduce sensitivity to internal satiety cues, lead to disinhibited eating if cognitive restraint is no longer sustained, and explains the failure of lifestyle interventions to maintain weight loss (Stunkard and Messick, 1985), but this concept is not universally agreed (Johnson *et al*, 2012), with evidence that although increasing restraint in normal weight populations is associated with higher weight and may be a marker of overeating tendencies, restraint in obese populations is associated with greater propensity to successful weight loss. Our subjects being non-obese, with a positive association between food restraint and fasting rCBF in left insula (see discussion below), may be consistent with the former. Our data cannot determine causality, but are consistent with the hypothesis that, in people with a family history for metabolic syndrome disease, insulin resistance evokes greater food restraint that is associated with overeating. However, we did not measure usual food intake and cannot rule out the possibility that overeating in high food restraint can induce greater insulin resistance.

5.4.2 Orbitofrontal cortex

The replication of our finding of greater rCBF in the right lateral OFC in IR than IS subjects before food and water ingestion and after water ingestion, indicates good internal consistency of our neuroimaging data. rCBF in the lateral OFC was no longer different between IR and IS subjects after meal ingestion, due to a post-prandial reduction in rCBF in IR subjects. Current neuropsychological models of eating behaviour suggest that the higher prefrontal regions including the lateral OFC provide top-down inhibitory control of surrounding cortical and subcortical reward networks, with diminished inputs from these prefrontal regions leading to dysregulation of reward network responses to meal ingestion that could enable excess eating (Volkow *et al*, 2008a, 2011). Our data suggest such a mechanism may be operating in our non-obese but high risk insulin resistant subjects. As reviewed by Elliott *et al* (2000), the lateral OFC is anatomically connected to the amygdala, thalamus, insula and temporal pole, with fMRI studies demonstrating recruitment of the lateral OFC when a response to a reward is suppressed. In studies of appetite regulation, the lateral OFC becomes increasingly active in cravers of chocolate, when chocolate becomes less pleasant when consumed to satiety (Small *et al*, 2001). Active control of the desire for foods depicted on viewed images increases BOLD signal in both OFC and DLPFC (Hollmann *et al*, 2012). The greater fasting lateral OFC activity in our IR subjects could thus be interpreted to represent the lower degrees of hunger and feelings of pleasantness to eat, and greater fullness observed in the fasted state, which could in turn be related to the greater degree of food restraint observed in IR subjects. Whilst the incremental effect of meal ingestion on the explicit responses to the appetite questionnaire during the MRI visit were no different between IS and IR subjects, the subsequent post-prandial reduction in lateral OFC activity may represent an implicit withdrawal of appetite control that could facilitate continued eating.

5.4.3 Insula

As mentioned above, I have demonstrated a positive association between fasting rCBF in left insula with food restraint. In response to meal compared to water ingestion, left insular rCBF decreased in IS subjects whilst it increased in IR subjects, with the difference in left insular rCBF between feeding conditions at +8 to +14 mins

increasing with progressive insulin resistance across IS, INT and IR subjects. As reviewed by Frank *et al* (2013) and Berthoud (2011), the insula, with the overlying operculum, is part of the primary taste cortex, but is also implicated in interoceptive processing of the bodily state, receiving sensory inputs from a number of different sources to influence processing of reward representation and motivation, including those related to food and eating. Pulsed ASL studies have demonstrated a reduction in insular CBF after oral glucose ingestion in healthy volunteers (Page *et al*, 2013), and early reductions in insular CBF after both low and high fat yoghurt ingestion (Frank *et al*, 2012). A reduction in insular CBF has also been demonstrated by [^{15}O]H_2O-PET imaging after a mixed meal was consumed to satiety following a prolonged 36 hour fast in healthy men, with greater increases in post-prandial insulin associated with greater reductions in post-prandial insular CBF (Tataranni *et al*, 1999). However, later studies showed obese individuals, who had higher fasting insulin levels in keeping with greater insulin resistance, also had significantly greater increases in post-prandial CBF in the left insula compared to lean subjects using the same protocol (DelParigi *et al*, 2005). Greater insular BOLD signal both in anticipation of and in response to tasting milkshake has been demonstrated in obese compared to lean adolescent girls (Stice *et al*, 2008), whilst non-obese adolescent girls at risk of future obesity based on parental obesity showed greater opercula BOLD signal activation in response to tasting milkshake, compared to a relative deactivation in these regions in those at low risk of obesity (Stice *et al*, 2011). The present study thus complements these findings, demonstrating a similarly abnormal increase in activity of brain regions that receive internal satiation signals, possibly due to diminished post-prandial inhibitory regulation by the lateral OFC, in otherwise healthy men with systemic insulin resistance, compared to the reduction in activity observed in insulin sensitive counterparts. Particularly, our data suggest that it is the insulin resistance, not the obesity, which drives the difference from health, supporting the view that insulin resistance may be the driver to obesity. Furthermore, in the ageing study (Chapter 3), an *increase* in bilateral insular rCBF after meal compared to water ingestion was observed, being most pronounced immediately after eating in the left insula, whilst the later response at +28 to +34 mins in bilateral insula was a deactivation in young adults, that converted from the 4th decade onwards to an activation, a period of life when obesity is most prevalent. Insulin resistance was not quantified and details of family history of T2DM were not captured, but based on the

present findings it is possible that these changes in response to meal ingestion are driven by systemic insulin resistance.

5.4.4 Mechanisms of the altered response to meal ingestion in systemic insulin resistance

The mechanisms involved in these altered satiation responses are worth considering. Whilst post-prandial GLP-1 responses were no different between IS and IR subjects, both post-prandial insulin and GIP were exaggerated in the latter group. Small intestinal K cells secrete GIP in response to intraluminal nutrients, which in turn evoke an incretin effect on beta cells to release insulin in a glucose-dependent manner. Greater GIP secretion in response to oral glucose has been observed in normoglycaemic overweight/obese subjects with compared to without metabolic syndrome (Calanna *et al*, 2012) and in subjects with impaired glucose tolerance (IGT) (Theodorakis *et al*, 2004). The present data are thus in keeping with these studies demonstrating a relationship between systemic insulin resistance and GIP secretion. Animal models of diet-induced obesity demonstrate hypersecretion of GIP, with blockade of GIP signalling ameliorating the weight gain and insulin resistance induced by high-fat diets (Miyawaki *et al*, 2002). As intracerebroventricular (ICV) insulin infusions in dogs reduce GIP secretion in response to intraduodenal glucose (Yavropoulou *et al*, 2009), it is also conceivable that cerebral resistance to insulin could facilitate GIP hypersecretion. However, further clarification is required given recent in vitro studies of human subcutaneous adipocytes that exposure to GIP improves their insulin sensitivity, and reduced GIP receptor expression in obesity (Ceperuelo-Mallafré *et al*, 2014). ICV administration of GIP in high-fat fed mice leads to weight loss comparable to that of dietary restriction, although probably through increased energy expenditure rather than reduced energy intake (Porter *et al*, 2011). Whether GIP has a significant role to play within the brain in weight and eating behaviour in humans is unknown, but it is possible that insulin resistance is associated with resistance to the weight loss effects of cerebral GIP.

An alternative mechanism could involve central responses to peripheral insulin secretion. As discussed in Chapter 1, insulin can modulate activity of both hypothalamic homeostatic (Belgardt and Brüning, 2010; Plum *et al*, 2005, 2006) and

corticolimbic reward networks (Figlewicz, 2003; Figlewicz and Benoit, 2009), directly via action on residing insulin receptors, or via vagal afferents (Filippi *et al*, 2014), to reduce food intake and weight. Few studies have looked at insulin signalling at specific cortical regions, but insulin has been shown to facilitate repetitive spike firing via PI3K cascades in the insula (Takei *et al*, 2010), whilst muscarinic modulation of the activity of prefrontal GABAergic inhibitory neurones is dependent on insulin signalling (Ma *et al*, 2003). Intravenous infusion of insulin at physiological concentrations, whilst endogenous insulin secretion is suppressed by co-infusion of somatostatin, increases glucose uptake, as quantified by [^{18}F]FDG-PET, in a number of prefrontal regions including the insula in insulin sensitive volunteers, an effect that is diminished in volunteers with peripheral insulin resistance (Anthony *et al*, 2006). Pharmacological doses of intranasal insulin have been reported to suppress appetite (Benedict *et al*, 2008; Jauch-Chara *et al*, 2012; Kullmann *et al*, 2015), increase post-prandial energy expenditure (Benedict *et al*, 2011), reduce weight (Hallschmid *et al*, 2004a) and improve peripheral insulin sensitivity (Heni *et al*, 2012, 2014c) in healthy volunteers without affecting peripheral insulin or glucose levels, an effect that is lost in obesity (Hallschmid *et al*, 2008). MR spectroscopy studies reveal intranasal insulin increases brain energy levels, the smaller the increase, the greater food intake observed during a subsequent ad libitum meal (Jauch-Chara *et al*, 2012). Intranasal insulin decreases resting state BOLD activity of the OFC in lean subjects (Kullmann *et al*, 2013), with greater improvements in insulin sensitivity (as measured by reductions in HOMA-IR) 2 hour later associated with greater insulin-induced decreases in OFC resting state activity (Schilling *et al*, 2013). Pulsed ASL studies also show intranasal insulin reduces CBF in lean and increases CBF in obese subjects in the prefrontal cortex (Kullmann *et al*, 2015). It is therefore conceivable that the greater fasting CBF in the lateral OFC observed in IR subjects in the present study is related to the higher levels of circulating insulin. Furthermore, greater improvements in insulin sensitivity 2 hours after application of intranasal insulin is associated with greater insulin-induced increases in insula CBF (Schilling *et al*, 2013). Whilst the validity of quantifying insulin resistance by HOMA-IR dynamically soon after application of intranasal insulin is speculative, it does suggest changes in insula activity in response to insulin are modulated by systemic insulin resistance, which could explain the differential insula response to meal ingestion observed in the present study.

5.4.5 Limitations and conclusions

There are some limitations in the present study. The appetite questions during the study did not specifically interrogate food restraint or disinhibition, which may have provided further strength to the interpretation of the changes in lateral OFC activity observed in the insulin resistant group. With regards to this brain region, significant differences in rCBF were not observed in the interaction of feeding status vs insulin sensitivity status, and were only demonstrated by an absence of difference in this region in the post-prandial state. However, interaction analyses may not be sensitive to such changes, as they model a relative increase caused by the meal (e.g. fed greater than fasted state) in one group being significantly different from the opposite observation (e.g. fed less than fasted state) in another group. We were unable to model the CBF changes with peripheral changes in important mediators of satiation, due to incomplete blood sampling. Lastly, given the cross-sectional nature of the study, it not possible to determine causality, in terms of whether these observations are a cause or effect of insulin resistance, or if these observations will indeed lead to worsening metabolic status and overt clinical disease, or whether these observations are a protective mechanism against future weight gain. However, rodent studies have shown reduced sensitivity to ICV insulin in animals that subsequently gain weight following a high fat diet, compared to animals that appear to be resistant to such diets, suggesting a primary role for central insulin resistance in the development of obesity (Clegg *et al*, 2005). Our data are consistent with a primary role for insulin resistance but longitudinal studies are needed to confirm this.

In conclusion, the present study demonstrates that even in the absence of obesity, systemic insulin resistance is associated greater levels of food restraint and weight and shape concern, hyperactivity of brain regions that are involved in inhibitory control of eating in the fasted state (left lateral OFC), with a subsequent post-prandial reduction in activity that may represent a reduction in inhibitory control food-related behaviour. Systemic insulin resistance is associated with meal-induced increases in insula activity, a region involved in taste perception and interoception not observed in insulin sensitive subjects, which may be a result of diminished control by the lateral OFC. These altered responses to meal ingestion may be mediated by altered cerebral responses to circulating insulin, and may facilitate continued eating after a meal,

providing a mechanism whereby insulin resistance may be a driver to obesity and obesity-related diseases.

Table 5.1

Subject characteristics. Data for adiponectin/leptin are for 13 IS, 15 IR and 4 INT subjects. Waist circumference measured midway between inferior margin of ribs and superior border of iliac crest.

	Mean ± SD			IS vs IR	3-way	Post hoc t tests p (Bonferroni corrected)		
	IS (n=17)	IR (n=16)	INT (n=5)	p	ANOVA p	IS vs IR	IS vs INT	IR vs INT
Age (years)	33.3±7.1	34.9±10.2	33.9±9.5	0.606	0.873			
Weight (kg)	78.2±6.7	82.3±10.5	84.8±6.8	0.194	0.221			
BMI (kg/m^2)	24.1±1.9	26.2±2.3	26.0±1.5	0.011	0.021	0.024	0.272	n.s.
Neck circumference (cm)	38.5±2.3	39.5±1.9	39.6±0.5	0.172	0.282			
Waist circumference (cm)	87.4±4.5	92.3±7.3	93.8±6.4	0.03	0.043	0.09	0.147	n.s.
SBP (mmHg)	117±12	127±13	131±23	0.023	0.058			
DBP (mmHg)	72±9	76±10	82±21	0.187	0.197			
HbA1c (%)	5.3±0.2	5.5±0.2	5.4±0.3	0.062	0.199			
Fasting glucose (mmol/L)	4.9±0.5	5.1±0.3	5.0±0.3	0.158	0.345			
2 hour glucose (mmol/L)	4.7±0.9	6.3±1.7	5.5±0.4	0.002	0.004	0.003	0.642	0.708
Fasting insulin (mU/L)	4.6±1.8	15.6±10.3	8.1±1.0	<0.001	<0.001	<0.001	0.966	0.115
HOMA2-IR	0.51±0.09	1.75±0.31	0.94±0.13	<0.001	<0.001	<0.001	0.001	<0.001
Matsuda index	9.8±3.9	2.5±1.1	5.0±1.5	<0.001	<0.001	<0.001	0.004	0.255
Net iAUC-OGTT glucose (mmol•min/L)	124.4±65.4	284.0±152.5	145.1±62.2	<0.001	0.001	0.001	n.s.	0.06
Net iAUC-OGTT insulin (mU•min/L)	3154±1646	13078±6302	6599±3969	<0.001	<0.001	<0.001	0.419	0.023
Total cholesterol (mmol/L)	4.5±0.5	4.9±1.4	4.8±0.7	0.283	0.515			
LDL (mmol/L)	2.8±0.5	3.2±1.1	3.0±0.7	0.156	0.317			
HDL (mmol/L)	1.3±0.2	1.1±0.2	1.3±0.4	0.046	0.149			
Triglycerides (mmol/L)	1.0±0.3	1.4±0.5	1.2±0.5	0.02	0.067			
Total cholesterol:HDL	3.6±0.9	4.4±0.9	3.8±0.7	0.018	0.046	0.043	n.s.	0.673
Adiponectin (mcg/L)	6773.4±3297.6	4979.4±1419.7	4896.3±2895.2	0.09	0.154			
Leptin (mcg/L)	3.9±2.1	6.1±3.2	5.5±2.4	0.36	0.095			

Table 5.2

DEBQ

				t-test	GLM	Post hoc t tests p (Bonferroni corrected)			Pearson's correlation with HOMA-IR	
DEBQ (mean ± SD)	**IS (n = 17)**	**IR (n = 16)**	**INT (n = 5)**	**p (IS vs IR)**	**p (3-way)**	**IS vs IR**	**IS vs INT**	**IR vs INT**	**r**	**p**
DEBQ-restraint	1.79±0.54	2.59±0.78	1.58±0.47	0.002	0.001	0.003	n.s.	0.013	0.516	0.002
DEBQ-emotional	1.70±0.77	1.72±0.60	1.45±0.37	0.920	0.710				-0.968	0.706
DEBQ-external	2.83±0.56	2.89±0.59	2.72±0.76	0.772	0.857				-0.032	0.861

Table 5.3

EDE-Q

				t-test	GLM	Post hoc t tests p (Bonferroni corrected)			Pearson's correlation with HOMA-IR	
EDE-Q (mean ± SD)	**IS (n = 16)**	**IR (n = 16)**	**INT (n = 5)**	**p (IS vs IR)**	**p (3-way)**	**IS vs IR**	**IS vs INT**	**IR vs INT**	**r**	**p**
EDE-Q-restraint	0.59±0.84	1.35±1.31	0.36±0.50	0.059	0.071				0.464	0.007
EDE-Q-eating concern	0.00±0.00	0.30±0.71	0.04±0.09	0.111	0.191				0.270	0.136
EDE-Q-shape concern	0.75±0.72	1.98±1.47	0.83±1.03	0.006	0.011	0.013	n.s.	0.168	0.632	< 0.001
EDE-Q-weight concern	0.29±0.53	1.50±1.37	0.64±0.83	0.004	0.007	0.005	n.s.	0.322	0.664	< 0.001
EDE-Q-global	0.41±0.41	1.28±0.95	0.47±0.58	0.003	0.004	0.004	n.s.	0.098	0.674	< 0.001

Table 5.4

QEWP

QEWP (selected questions) [Percentage or median (range)]	IS (n = 17)	IR (n = 16)	INT (n = 5)	p (IS vs IR)	p (3-way)	Post hoc t tests p(Bonf. corr.)		
						IS vs IR	IS vs INT	IR vs INT
Have you ever been overweight by at least 4.5 kg as a child or 7 kg as an adult?	29.41%	25.00%	0.00%	0.776	0.391			
Have you every lost 9 kg or more and then gained it back?	35.29%	25.00%	20.00%	0.52	0.723			
During the past 6 months, did you often eat within any 2 hour period what most people would regard as an unusually large amount of food?	17.65%	12.50%	0.00%	0.68	0.588			
In general, during the past 6 months, how upset were you by overeating (eating more than you think is best for you)? (1 [not at all] to 5 [extremely])	1 (1-4)	1 (1-3)	1 (1-2)	0.736	0.992			
In general, during the past 6 months, how upset were you by the feeling that you couldn't stop eating or control what or how much you were eating? (1 [not at all] to 5 [extremely])	1 (1-2)	1 (1-4)	1 (1)	0.51	0.259			
During the past 6 months, how important has your weight or shape been in how you feel about or evaluate yourself as a person - as compared to other aspects of your life, such as how you do at work, or as a parent, or how you get along with other people? (1 [not very important] to 4 [most important])	2 (1-2)	2 (1-4)	1 (1-3)	0.063	0.084			
Since you have been an adult, how much of the time have you been on a diet, been trying to follow a diet, or in some way been limiting how much you were eating in order to low weight or keep from regaining weight you had lost? (1 [none) to 5 (nearly all of the time])	1 (1-2)	1 (1-5)	1 (1)	0.455	0.292			
Build of father at his heaviest (1 [thinnest] to 9 [largest])	6 (3-8)	6.5 (3-8)	4 (2-6)	0.23	0.024	n.s.	0.063	0.021
Build of mother at her heaviest (1 [thinnest] to 9 [largest])	5 (4-7)	6 (4-8)	5.5 (5-7)	0.003	0.004	0.003	0.747	0.774

IS vs IR: Chi-squared / Mann-Whitney U test. Three-way comparison: Chi-squared / ANOVA.

Table 5.5

Voxel-wise T-contrasts of differences in rCBF between meal and water visits within IS and IR groups (Figure 5.7).

Contrast / Brain area	Hemisphere	MNI coordinates X	Y	Z	T scores	No. voxels	Cluster $P_{FWE-corr}$	Brodmann area
IS								
Pre-water > Pre-meal (pCASL1)								
No significant clusters								
Pre-water < Pre-meal (pCASL1)								
No significant clusters								
Post-water > Post-meal (pCASL2-4)								
Lingual gyrus	Left	-10	-80	-6	3.33	1094	0.045	18
Post-water < Post-meal (pCASL2-4)								
Angular gyrus	Right	48	-72	32	4.86	1180	0.013	39
IR								
Pre-water > Pre-meal (pCASL1)								
No significant clusters								
Pre-water < Pre-meal (pCASL1)								
No significant clusters								
Post-water > Post-meal (pCASL2-4)								
Inferior frontal gyrus, triangular part	Right	48	32	12	4.07	916	0.045	45
Post-water < Post-meal (pCASL2-4)								
No significant clusters								

Table 5.6

Voxel-wise T-contrasts of differences in rCBF pre- and post-water and meal ingestion between IS and IR subjects (Figure 5.8, Figure 5.10)

		MNI coordinates						
Contrast / Brain area	Hemisphere	X	Y	Z	T scores	No. voxels	Cluster $P_{FWE\text{-}corr}$	Brodmann area
Pre-water/meal: IS > IR								
Middle occipital gyrus, precuneus	Left	-30	-72	40	4.83	2877	<0.001	7, 40
Cerebellum crus 1	Right	42	-70	-32	4.67	2027	0.001	
Pre-water/meal: IS < IR								
Superior frontal gyrus, orbital part	Right	26	54	-2	5.00	1948	0.001	11, 48, 10, 47
ASL2-4 Water: IS > IR								
Inferior parietal	Left	-30	-56	50	4.33	2352	<0.001	7, 40, 3
Cerebellum crus 1	Right	48	-62	-38	4.28	1545	0.003	
ASL2-4 Water: IS<IR								
Inferior frontal gyrus, triangular part	Right	30	28	28	4.83	2952	<0.001	48, 11, 45, 38, 47
ASL2-4 Meal: IS > IR								
Inferior parietal	Left	-40	-46	40	4.21	1376	0.007	40, 7
Cerebellum crus 2	Right	46	-62	-34	4.14	1044	0.029	
Middle frontal gyrus	Left	-30	2	56	3.51	950	0.045	6, 46
ASL2-4 Meal: IS < IR								
No significant clusters								
ASL2-4 Meal x Group interaction: IS[Water > Meal] vs IR[Water < Meal]								
Fusiform gyrus, Insula	Left	-26	-30	-36	4.28	1814	0.001	36, 48
ASL2-4 Meal x Group Interaction: IS[Water < Meal] vs IR[Water > Meal]								
No significant clusters								

Table 5.7

Voxel-wise regression of DEBQ-restraint with fasting rCBF (Figure 5.12)

Contrast / Brain area	Hemisphere	MNI coordinates X	Y	Z	T scores	No. voxels	Cluster $P_{FWE\text{-}corr}$	Brodmann area
Positive association between DEBQ-restraint and fasting rCBF (pCASL1)								
Insula	Left	-26	16	-18	5.46	1195	0.018	13
Rolandic operculum	Left	-46	0	8	4.99	2008	0.001	44
Negative association between DEBQ-restraint and fasting rCBF (pCASL1)								
Cerebellum	Left	-24	-74	-22	5.66	6588	<0.001	
Mid occipital gyrus	Right	44	-76	4	4.38	1906	0.001	

6 Impact of systemic insulin resistance on central responses to food cues after meal and water ingestion

6.1 Introduction

In the last chapter, decreased post-prandial suppression of appetite was observed in non-obese insulin resistant men, accompanied by a post-prandial reduction in lateral orbitofrontal cortex (OFC) rCBF and increased left insula rCBF, as quantified by pCASL fMRI, the latter associated with the higher levels of food restraint. It is feasible that the observed changes in satiation processing in centres involved in inhibitory control and interoception could delay meal termination and facilitate weight gain. The neural processing of satiety (the effect of a prior meal on subsequent food intake) has also been investigated in insulin resistance-associated conditions such as polycystic ovarian syndrome (PCOS) (Van Vugt *et al*, 2013) and obesity (Dimitropoulos *et al*, 2012; Martens *et al*, 2013), as well as in the ageing study (Chapter 4), by examining the impact of a caloric pre-load on appetite brain network responses to visual food cues using BOLD fMRI. The altered influence that meal ingestion has on such corticolimbic activities in obesity, including the differential response to food cues of varying caloric content, has been suggested to promote intake of energy-dense foods in the post-prandial state, leading to weight gain. However, it is possible that such effects are a result, rather than a cause, of obesity. By investigating the impact of systemic insulin resistance on the modulation of responses to food cues by a meal in non-obese, non-diabetic men, this study aims to provide further evidence that dysregulated satiety processing by the brain, driven by insulin resistance, plays a role in the development of obesity.

6.2 Methods

6.2.1 Subjects

The 17 insulin sensitivity (IS), 16 insulin resistant (IR) and 5 subjects of intermediate sensitivity (INT) were described in Chapter 5.

6.2.2 Study protocol

The general experimental design and MRI acquisition details are described in section 2.8. All subjects underwent the same protocol. The pCASL fMRI study is described in Chapter 5. For the BOLD fMRI study, in brief, subjects were studied on two separate mornings following an overnight fast of at least 8 hours. After intravenous cannulation, subjects were positioned in the scanner. Following ASSET calibration, Axial T2 FR-FSE, GE EPI and the initial 3D pCASL (pCASL-1) scans, subjects were sat up out of the scanner to consume a 630 kcal mixed meal (225ml, 630kcal, 42g fat, 9g protein, 54g carbohydrate) or 50ml water between -6 to 0 mins. After re-positioning in the scanner, and two further pCASL (pCASL2-3) scans, BOLD fMRI data were acquired between +16 and +32 mins, whilst subjects viewed 50 photographs each of high-calorie (HiCal) and low-calorie (LoCal) foods, objects (OBJ) and Gaussian blurred images (BLU), that were validated for use (section 2.8.8). These were shown in blocks of 10 different pictures for each category, each block presented in one of two pseudo-randomised orders, each picture presented for 3 s (Figure 6.1). Subjects were instructed to "Imagine you are eating the following foods/using the following objects" or "Please view the following images", before viewing food, object and blurred images respectively. After each auditory instruction, but before the block of pictures was presented, an "X" placed in the centre of the screen was shown for 3 s, alerting the subject that they were about to be shown the pictures. After each block, subjects were asked, "How hungry do you feel?" which was answered on a projected 1-100 visual analogue scale, marked at every 10^{th} point, using a hand-held keypad. Subjects similarly rated appetite before and after pCASL1, after each pCASL2-3, at the end of BOLD fMRI and the final pCASL4, with concurrent blood sampling. The study visit was completed T1 FSPGR and axial T2 FLAIR scans.

6.2.3 Statistical analyses

General non-imaging statistical methods are described in section 2.8.14. Each subject's mean hunger scores during image viewing for each stimulus-condition combination (water-HiCal, water-LoCal, water-OBJ, water-BLU, meal-HiCal, meal-LoCal, meal-OBJ, meal-BLU) were submitted to mixed ANOVA with feeding status (water/meal) and image (HiCal/LoCal/OBJ/BLU) as within-subject factors, and group

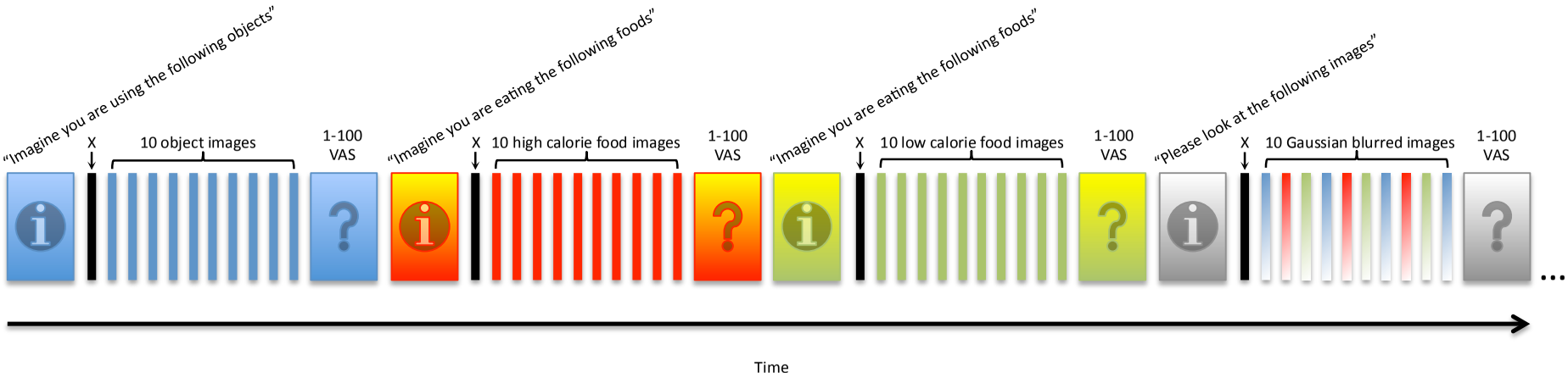

Figure 6.1

BOLD fMRI task (between pCASL3 and 4): Block design, each block consisted of auditory instructions, a 3 s cross followed 10 images of either objects, high calorie foods, low calorie foods, or Gaussian blurred images (each image presented for 3 s with no inter-stimulus interval) and then the question "How hungry do you feel?" was answered using a 1-10 visual analogue scale. There were five blocks of each stimulus category that were presented in a pseudo-randomised playlist.

(IS/IR) as between-subject factor. Estimated marginal means and standard errors were reported for significant effects.

Subject-level BOLD image pre-processing and statistical methods using XBAM version 4.1 (Centre for Neuroimaging Sciences, Institute of Psychiatry, Psychology & Neuroscience, King's College London, 2012) are described in section 2.8.13.3. After normalised BOLD effect size maps of the response to HiCal, LoCal and BLU images with the time-series for OBJ images used as the baseline ([HiCal/OBJ], [LoCal/OBJ] and [BLU/OBJ]) were calculated for each subject, group maps within each feeding state were generated for each contrast compared to a null distribution derived from the permuted data set (section 2.8.13.4). After restricting analyses to grey matter, the effect of feeding condition (meal vs water) on the median effect size for [HiCal/OBJ], [LoCal/OBJ] and [BLU/OBJ] image-evoked BOLD signal contrast at each voxel was computed separately and compared to a null distribution derived by permutation of feeding status using traditional repeated measures ANOVA, within each IS and IR group. The interaction effect of feeding status with [HiCal/OBJ] and [LoCal/OBJ] contrasts were computed using a complex factorial ANOVA within each group. The interaction effect of feeding condition and group (IS vs IR) on the median effect size for [HiCal/OBJ], [LoCal/OBJ], high vs low calorie food ([HiCal/LoCal], after voxel-wise subtractions of [LoCal/OBJ] from [HiCal/OBJ] effect size for each subject within each feeding condition) and [BLU/OBJ] image-evoked BOLD signal contrast at each voxel were computed and compared to a null distribution derived by permutation of feeding status and group using a traditional split-plot ANOVA.

Voxel-level Pearson product moment correlation coefficients were also calculated to examine the association between HOMA-IR and the above image contrasts after water ingestion, and between HOMA-IR and the difference in BOLD signal contrast between feeding conditions (after performing voxel-wise subtraction of post-water from post-meal effect size evoked by each contrast), compared to a null distribution derived by permutation of HOMA-IR for all 38 IS, INT and IR subjects. Talairach daemon was used to identify the regions of detected voxels anatomically (Lancaster *et al*, 2000). All group activation maps were thresholded to yield <1 false positive cluster per map (equivalent p values are listed in each results table), at a voxel-wise threshold of $p<0.05$ (Bullmore *et al*, 1999) (section 2.11.4).

6.3 Results

6.3.1 Hunger responses to visual stimuli

Mean hunger scores collected after each image block in IS and IR subjects (Figure 6.2) were greater after water than meal ingestion (main effect of feeding, $F(1,31)=24.873$, $p<0.001$, estimated marginal mean: Water: 73.7±3.0, Meal: 55.4±3.7). They were significantly different depending on the type of visual stimulus (main effect of stimulus $F(1.891,58.631)=24.221$, $p<0.001$). Post-hoc comparisons indicated hunger was greater after viewing both high- and low-calorie food images compared to both object (mean difference 9.5±1.7, $p<0.001$ and 10.0±1.7, $p<0.001$ respectively, Bonferroni corrected) and blurred images (8.7±1.7, $p<0.001$ and 9.2±1.9, $p<0.001$ respectively, Bonferroni corrected), with no significant difference in the hunger elicited between the two food image classes, nor between object and blurred images, irrespective of feeding status. There were no significant interactions between meal and stimulus ($F(2.079,64.449)=0.807$, $p=0.455$). The lower hunger scores evoked in the IR group did not reach statistical significance (main effect of group, $F(1,31)=3.508$, $p = 0.071$) and there were no significant interaction effects of

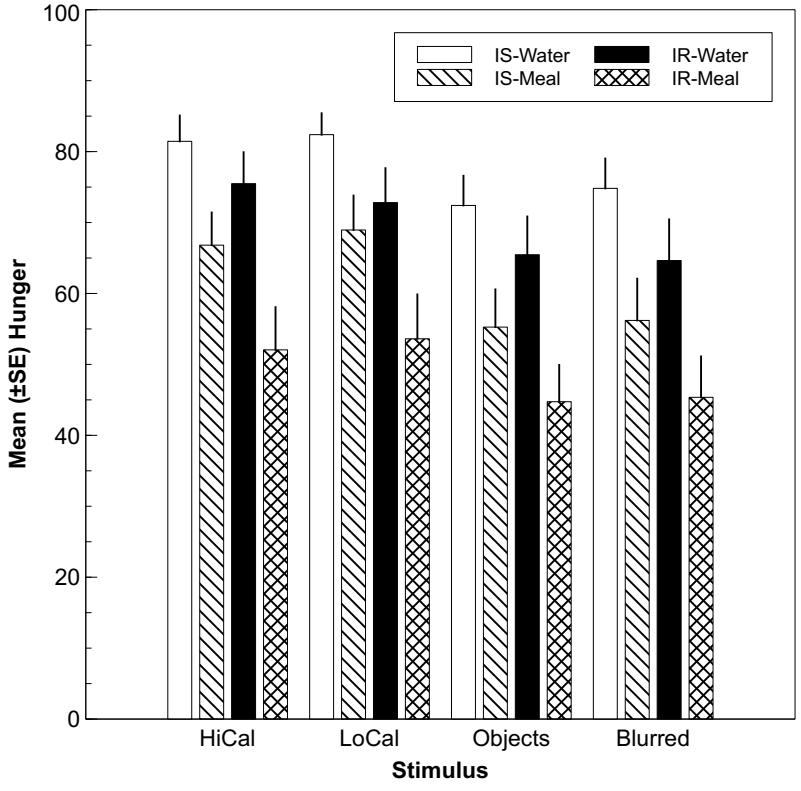

Figure 6.2

Hunger responses to visual stimuli. Mean hunger scores evoked after viewing blocks of high-calorie (HiCal) and low-calorie (LoCal) food images, object and blurred images.

insulin sensitivity status on image-evoked hunger scores (meal x group interaction, $F(1,31)=0.409$, $p=0.527$; stimulus x group interaction, $F(1.891,58.631)=0.482$, $p=0.610$; meal x stimulus x group interaction, $F(2.079,64.449)=1.354$, $p=0.266$).

6.3.2 Effect of meal ingestion on brain responses to food images in insulin sensitive subjects

Separate voxel-wise ANOVAs were performed to assess the impact of meal vs water ingestion on [HiCal/OBJ]-, [LoCal/OBJ]- and [BLU/OBJ]-evoked BOLD signal contrast in IS subjects (Table 6.1). Meal ingestion converted responses from deactivation to activation on viewing high-calorie food images in right precentral gyrus, extending down to right insula, and left postcentral gyrus (Figure 6.3A), and on viewing low-calorie food images in left postcentral gyrus (Figure 6.3B). The meal converted midbrain activation responses to blurred images to a deactivation (Figure 6.3C). A factorial ANOVA examining differences in the effect of feeding status on [HiCal/OBJ]- vs [LoCal/OBJ]-evoked BOLD signal contrast detected significant interaction effects in right lingual gyrus, left caudate, and dorsolateral prefrontal cortex (DLPFC, left middle frontal gyrus) (Figure 6.4). The extracted BOLD signal from these regions indicated a lower degree of activation in lingual gyrus, and deactivation in caudate and DLPFC when viewing low-calorie food images after water ingestion, that converted to greater activation after the meal, whilst high-calorie food images evoked greater activation after water ingestion that converted to lower activation in lingual gyrus and deactivation in caudate and DLPFC after the meal.

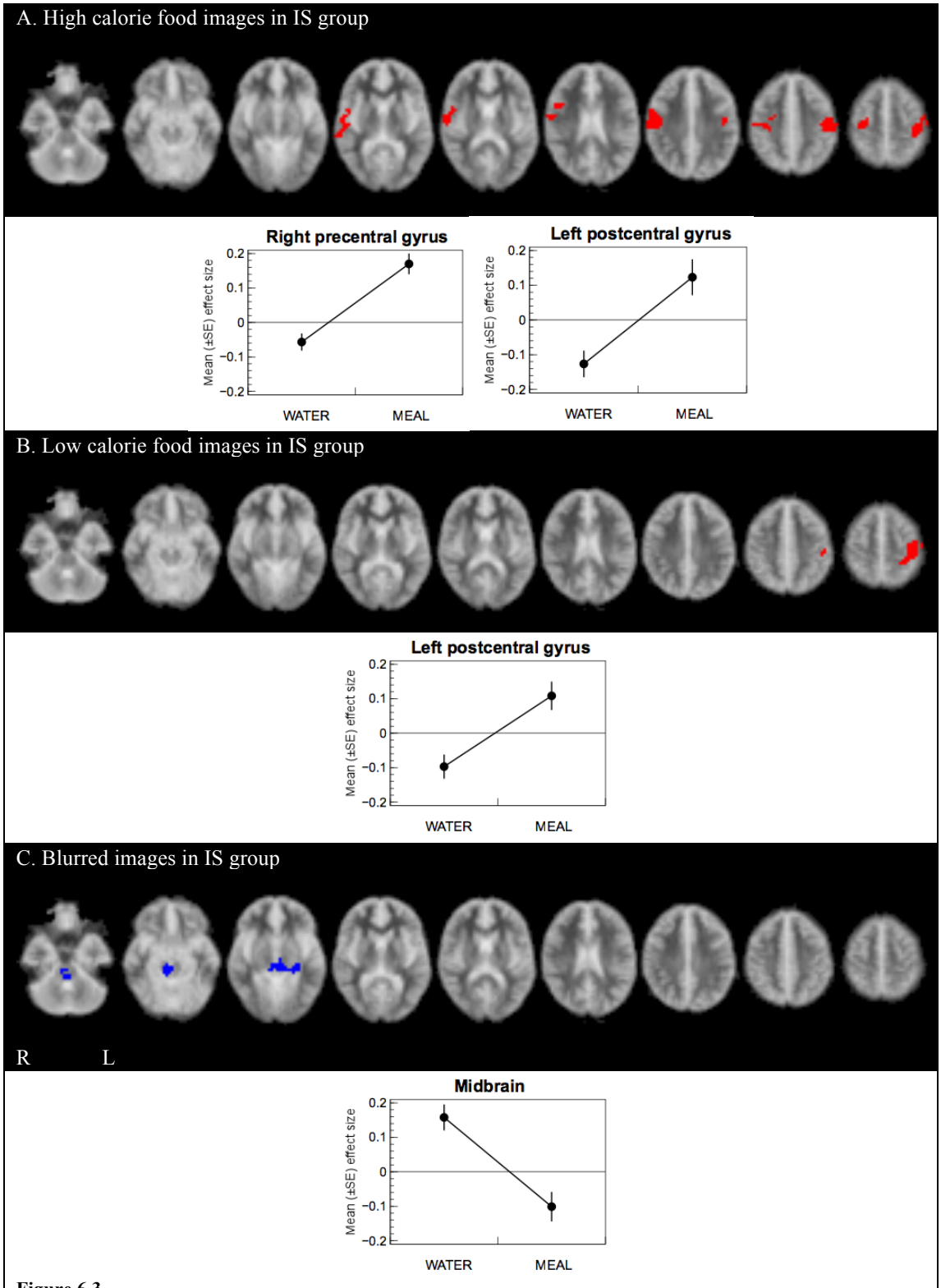

Figure 6.3

Voxel-wise ANOVA of the effect of meal ingestion on brain responses to visual cues in IS subjects. Group activation brain maps show clusters with greater (red) or lesser (blue) BOLD signal contrast evoked by (A) high- and (B) low-calorie food and (C) blurred images after meal compared to water ingestion (object image-evoked time series as baseline, voxel-wise $p < 0.05$, cluster-wise $p < 0.02$) with extracted effect size (% BOLD signal change) from each cluster (positive values: activation i.e. food or blurred images > object images).

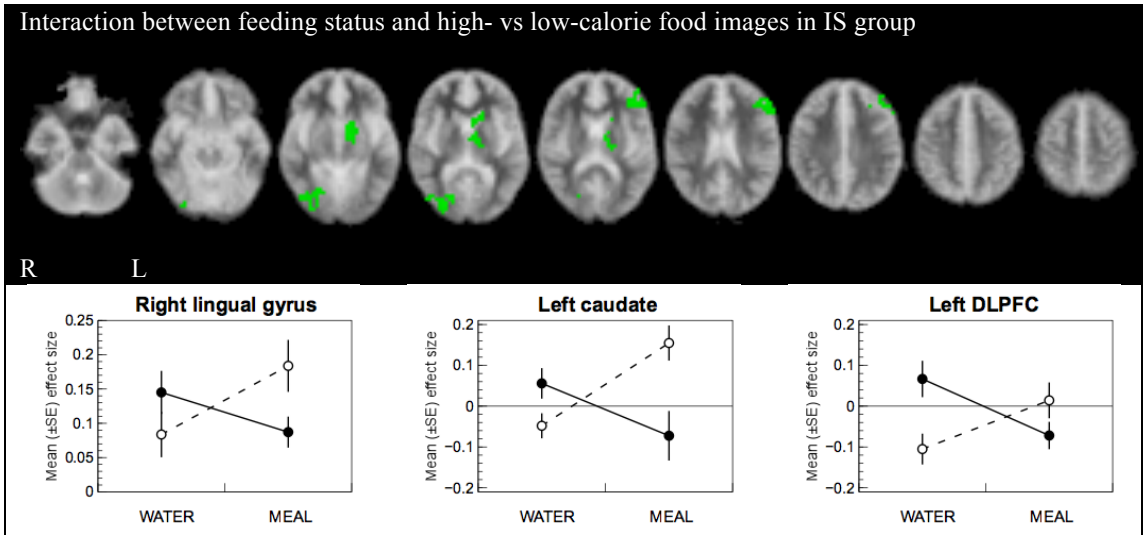

Figure 6.4

Voxel-wise ANOVA of effect of meal ingestion on brain responses to high- vs low-calorie food images in IS subjects. Group activation brain maps show clusters with significant interaction effect of feeding status (meal vs water) and stimulus (high- vs low-calorie food images (object image-evoked time series as baseline, voxel-wise $p < 0.05$, cluster-wise $p < 0.005$) with extracted effect size (% BOLD signal change) from each cluster [high- (solid line) and low- (dashed line) calorie food images]. Positive values: activation i.e. foods > objects. DLPFC = dorsolateral prefrontal cortex.

6.3.3 Effect of meal ingestion on brain responses to food images in insulin resistant subjects

Similar analyses were performed in IR subjects (Table 6.2). The meal converted responses to high-calorie food images to a deactivation in left inferior parietal lobule and right postcentral gyrus (Figure 6.5A). The meal also converted the responses to low-calorie food images to a deactivation in right precuneus and left DLPFC (middle frontal gyrus), reduced deactivation of left superior temporal gyrus and converted it to an activation in right middle frontal gyrus (Figure 6.5B). The meal converted responses to blurred images to a deactivation in right middle occipital gyrus and left precuneus, and an activation in right superior frontal gyrus (Figure 6.5C). The factorial ANOVA did not identify any regions where feeding status had significantly different effects on responses to high- compared to low-calorie food images.

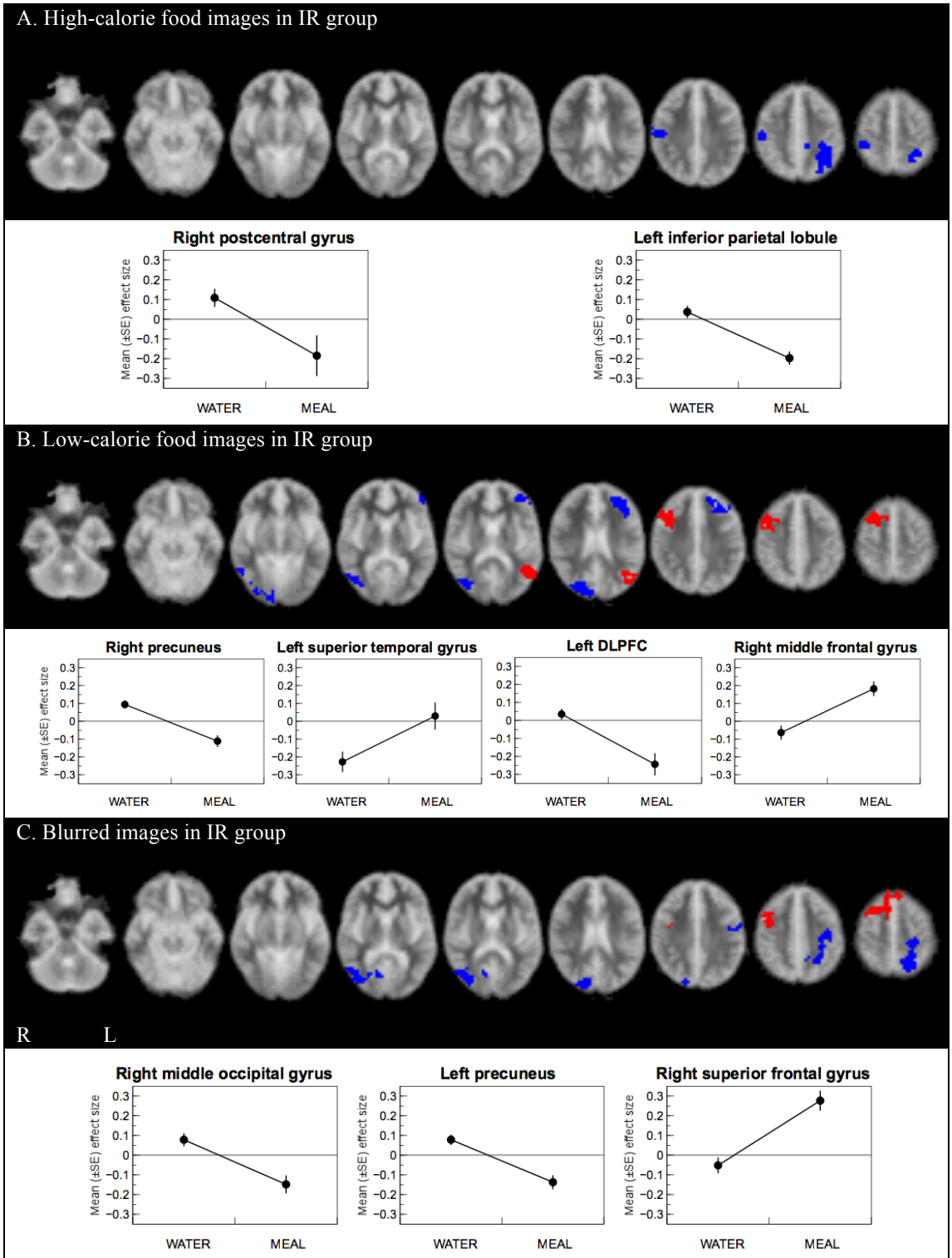

Figure 6.5

Voxel-wise ANOVA of the effect of meal ingestion on brain responses to visual cues in IR subjects. Group activation brain maps show clusters with greater (red) or lesser (blue) BOLD signal contrast evoked by (A) high- and (B) low-calorie food and (C) blurred images after meal compared to water ingestion (object image-evoked time series as baseline, voxel-wise $p < 0.05$, cluster-wise $p < 0.01$) with extracted effect size (% BOLD signal change) from each cluster (positive values: activation i.e. food or blurred images > object images).

6.3.4 Differences in brain response to food images in insulin sensitive compared to insulin resistant subjects after water ingestion

Separate voxel-wise non-repeated measures ANOVA were performed to examine differences in [HiCal/OBJ], [LoCal/OBJ] and [BLU/OBJ]-evoked BOLD signal contrasts between IR and IS subjects in the fasted (post-water ingestion) state (Table 6.3). Significant differences were observed between the two groups' responses to food cues in the continued fasted state, where high-calorie food images evoked deactivation in medial frontal gyrus and activation in right claustrum/insula whilst low-calorie food images evoked activation in right superior temporal gyrus in IS subjects, with the opposite occurring in IR subjects (Figure 6.6A-B). Differences in BOLD signal contrast on viewing blurred images were similar to that of high-calorie food images, with additional significant differences observed in right putamen, where blurred images evoked deactivation in IS and activation in IR subjects (Figure 6.6C).

A voxel-wise split-plot factorial ANOVA examining differences between [HiCal/OBJ]- and [LoCal/OBJ]-evoked BOLD signal contrasts in the fasted (post-water ingestion) state between the two groups (Figure 6.7) showed that within the left DLPFC, an activation response to high-calorie images converted to deactivation on viewing low-calorie food images in IS subjects, with an opposite pattern of activity observed in IR subjects. Conversely, within the right superior frontal gyrus and premotor cortex, deactivation responses to high-calorie food images converted to activation on viewing low-calorie food images in IS subjects, with an opposite pattern of activity observed in IR subjects.

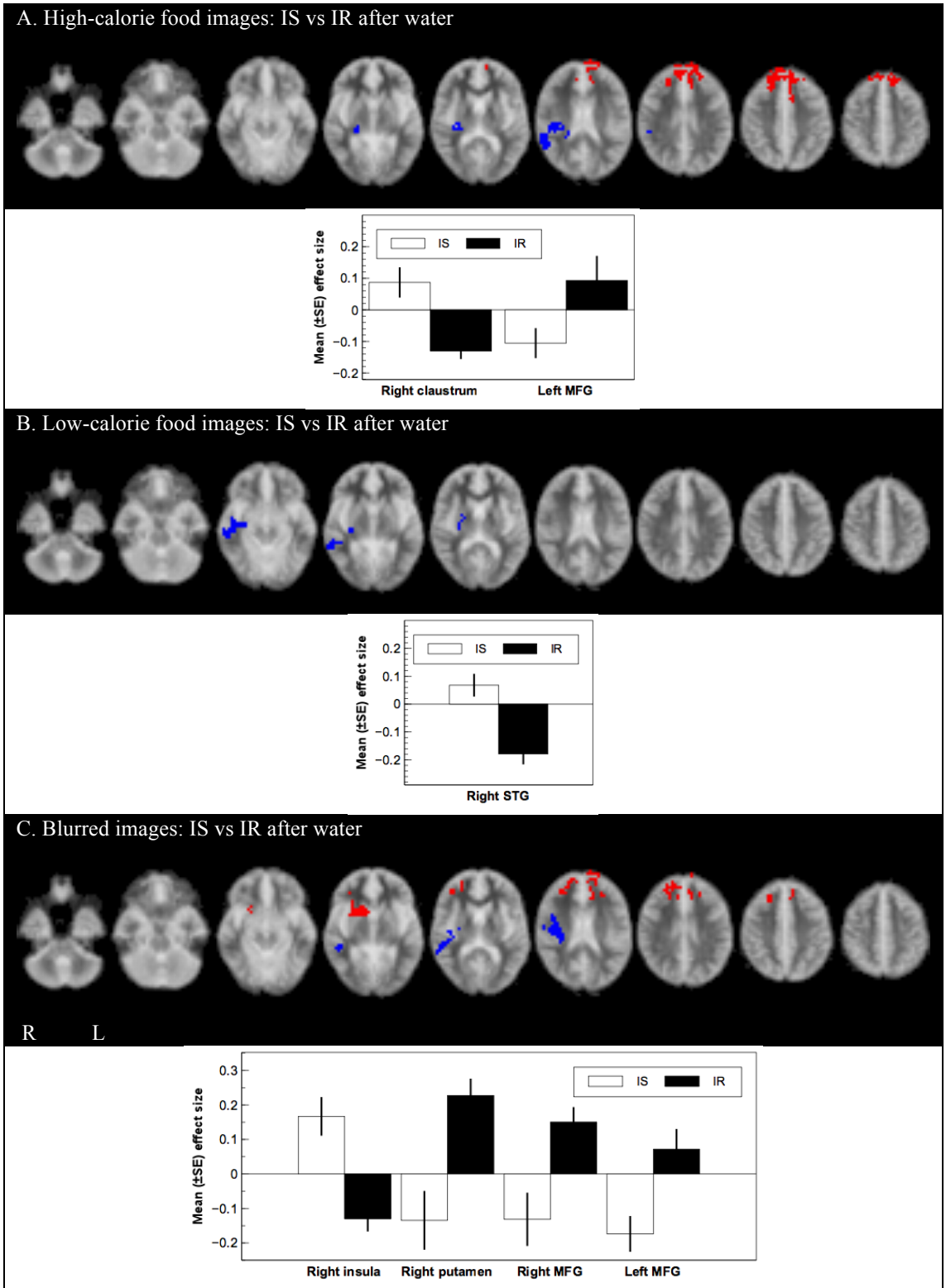

Figure 6.6

Voxel-wise ANOVA of brain responses to visual cues in IS vs IR subjects after water ingestion. Group activation brain maps show clusters where compared to IS, IR subjects had greater (red) or lesser (blue) BOLD signal contrast evoked by (A) high- and (B) low-calorie food and (C) blurred images (object image-evoked time series as baseline, voxel-wise $p < 0.05$, cluster-wise $p < 0.01$) with extracted effect size (% BOLD signal change) from each cluster (positive values: activation i.e. food or blurred images > object images). MFG = medial frontal gyrus. STG = superior temporal gyrus.

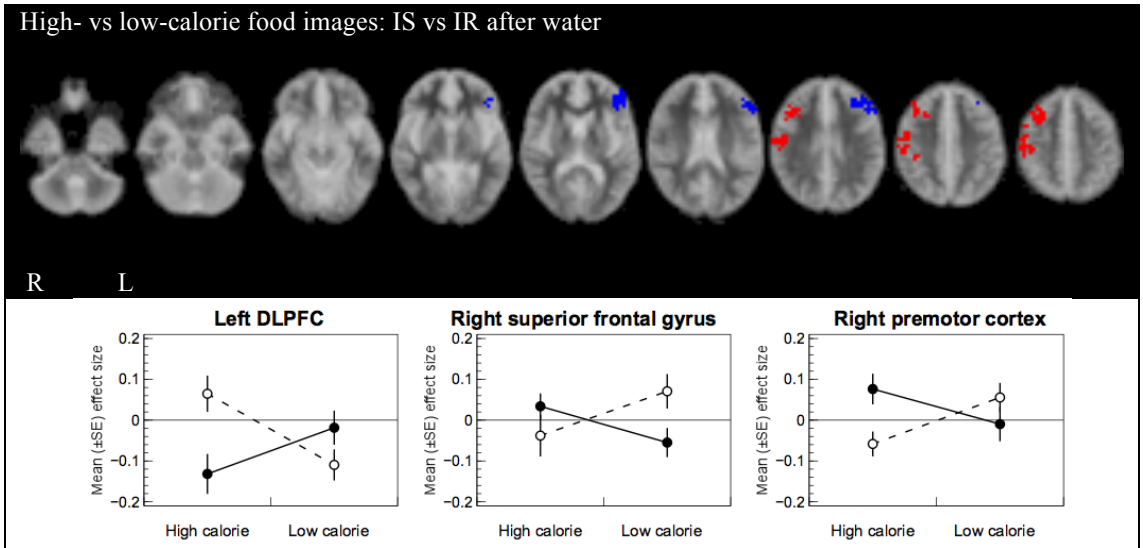

Figure 6.7

Voxel-wise ANOVA of brain responses to high- vs low-calorie food images in IS vs IR subjects. Group activation brain maps show significant [IS(HiCal > LoCal) vs IR(HiCal < LoCal)] (red clusters) and [IS(HiCal < LoCal) vs IR(HiCal > LoCal)] (blue clusters) interactions (object image-evoked time series as baseline, voxel-wise $p < 0.05$, cluster-wise $p < 0.005$) with extracted effect size (% BOLD signal change) from each cluster (positive values: activation i.e. food > object images) in IS (dashed line) and IR (solid line) subjects.

6.3.5 Differential effect of meal ingestion on brain responses to food images in insulin sensitive compared to insulin resistant subjects

Voxel-wise split-plot factorial ANOVAs for interaction effects between feeding status and group on [HiCal/OBJ], [LoCal/OBJ] and [BLU/OBJ]-evoked BOLD signal contrast were performed (Table 6.4). There were no regions where the meal had significantly different effects between IS and IR groups on responses to high-calorie food cues. On viewing low-calorie food images, deactivation responses decreased in IS subjects and increased in IR subjects in left insula/DLPFC, and activation responses decreased in IS subjects and increased in IR subjects in right DLPFC (middle frontal gyrus) after meal compared to water ingestion (Figure 6.8A). The meal converted responses to blurred images from deactivation to activation in IS and activation to deactivation in IR in right cuneus and left precentral gyrus (Figure 6.8B).

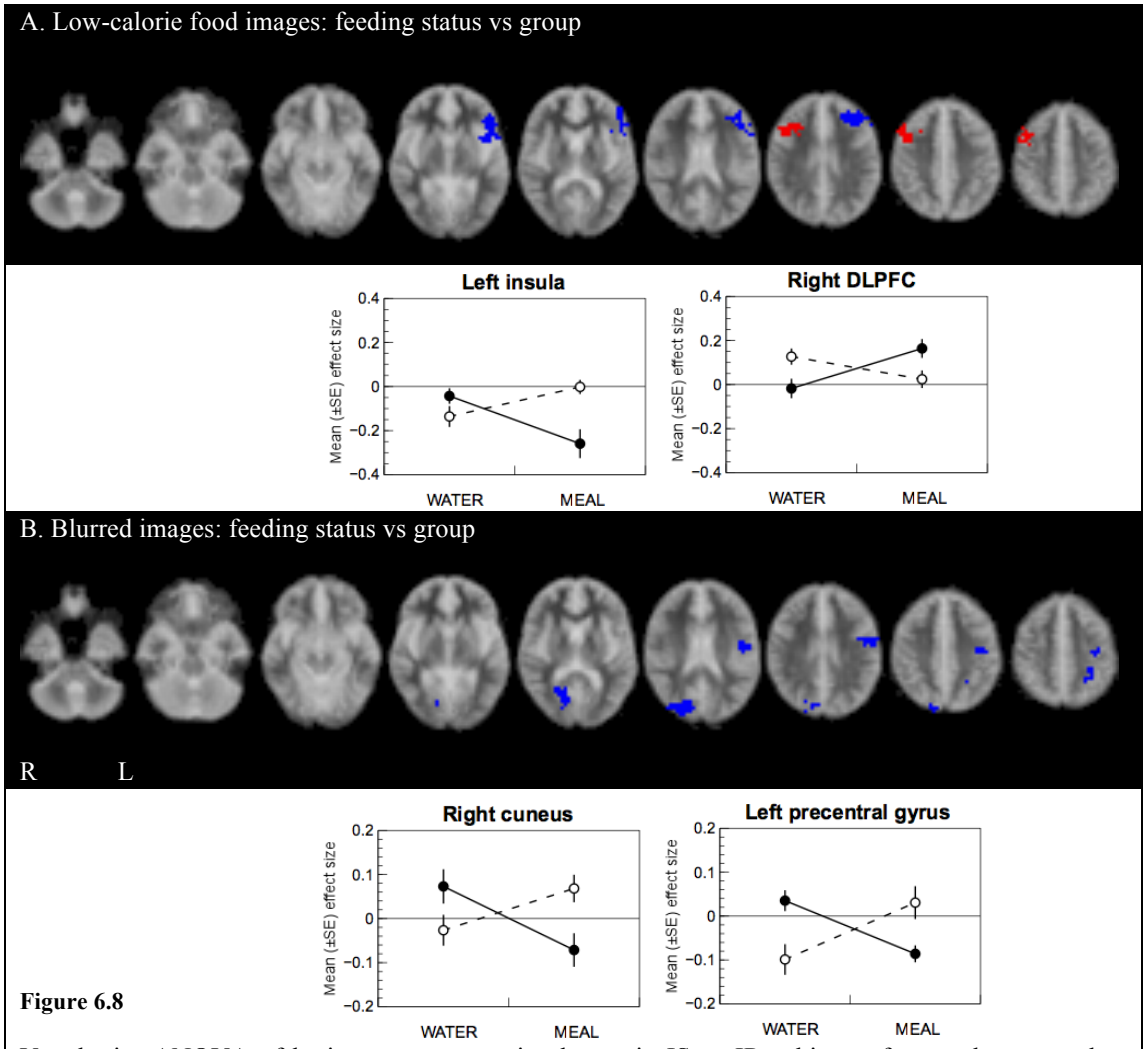

Figure 6.8

Voxel-wise ANOVA of brain responses to visual cues in IS vs IR subjects after meal compared to water ingestion. Group activation brain maps show [IS(water>meal) vs IR(water<meal)] (red) and [IS(water<meal) vs IR (water>meal)] (blue) interactions in BOLD signal contrast evoked by (A) low-calorie food and (B) blurred images (object image-evoked time series as baseline, voxel-wise $p < 0.05$, cluster-wise $p < 0.01$) with extracted effect size (% BOLD signal change) from each cluster (positive values: activation [food/blurred images>object images]) in IS (dashed line) and IR (solid line) subjects.

Split-plot ANOVA of [HiCal/LoCal] contrast maps (constructed from voxel-wise subtraction of [LoCal/OBJ] from [HiCal/OBJ]-BOLD signal contrast in each feeding state for each subject), examining the meal's impact on differential responses to high- vs low-calorie food cues, identified in left DLPFC a greater activation to images of high-calorie foods after water and low-calorie foods after the meal in IS subjects, whilst IR subjects showed a greater activation to images of low-calorie foods after water and high-calorie foods after the meal (Figure 6.9). Conversely, in right middle frontal gyrus, greater activation to low-calorie food images after water diminished after the meal in IS subjects, whilst IR subjects had greater activation to images of high-calorie foods after water and low-calorie foods after the meal.

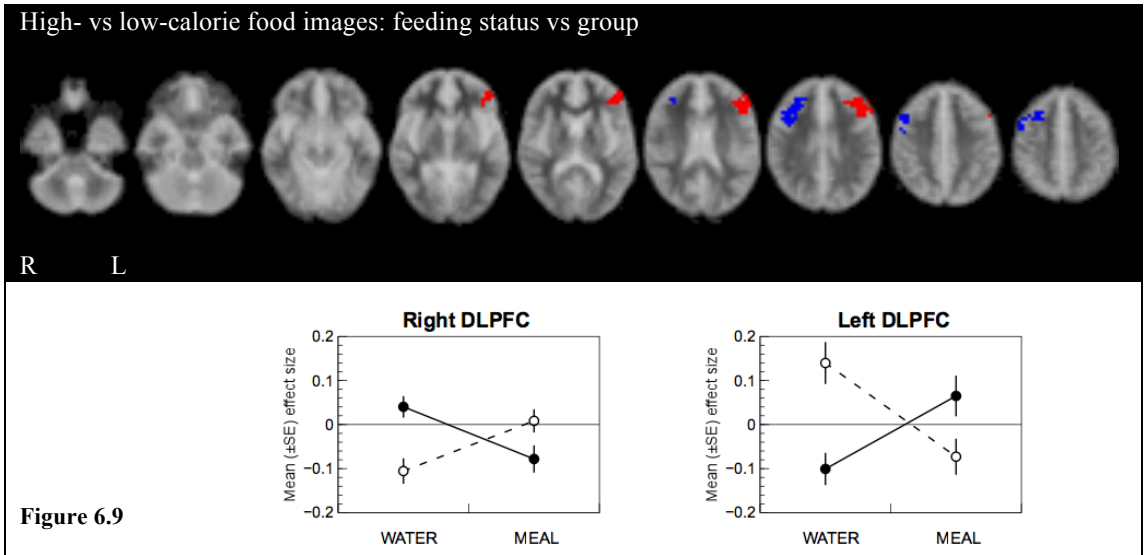

Figure 6.9

Voxel-wise ANOVA of brain responses to high- vs low-calorie food images in IS vs IR subjects after meal and water. Group activation brain maps show significant [IS(water > meal] vs IR(water < meal)] (red clusters) and [IS(water < meal) vs IR(water > meal)] (blue clusters) interactions (voxel-wise $p < 0.05$, cluster-wise $p < 0.005$) with extracted effect size (% BOLD signal change) from each cluster (positive values: high > low calorie food images) in IS (dashed line) and IR (solid line) subjects.

6.3.6 Correlation between insulin resistance and brain responses to food images after water ingestion

Voxel-wise Pearson correlation coefficients were calculated to examine linear associations between HOMA-IR and [HiCal/OBJ]-, [LoCal/OBJ]-, [BLU/OBJ]- and [HiCal/LoCal]-evoked BOLD signal contrasts in all 38 IS, INT and IR subjects in the fasted (post-water ingestion) state (Table 6.5). Insulin resistance correlated positively with responses to high-calorie food images in right putamen and precentral gyrus, and negatively in right thalamus (Figure 6.10A), and correlated negatively with responses to low-calorie food images in right middle temporal gyrus and left inferior parietal lobule (Figure 6.10B). Insulin resistance correlated positively with responses to blurred images in left medial frontal gyrus and negatively in right insula (Figure 6.10C). Insulin resistance correlated positively with differential responses to high- compared to low-calorie food images in right precentral gyrus, and negatively in left DLPFC (inferior frontal gyrus) and right middle occipital gyrus (Figure 6.11).

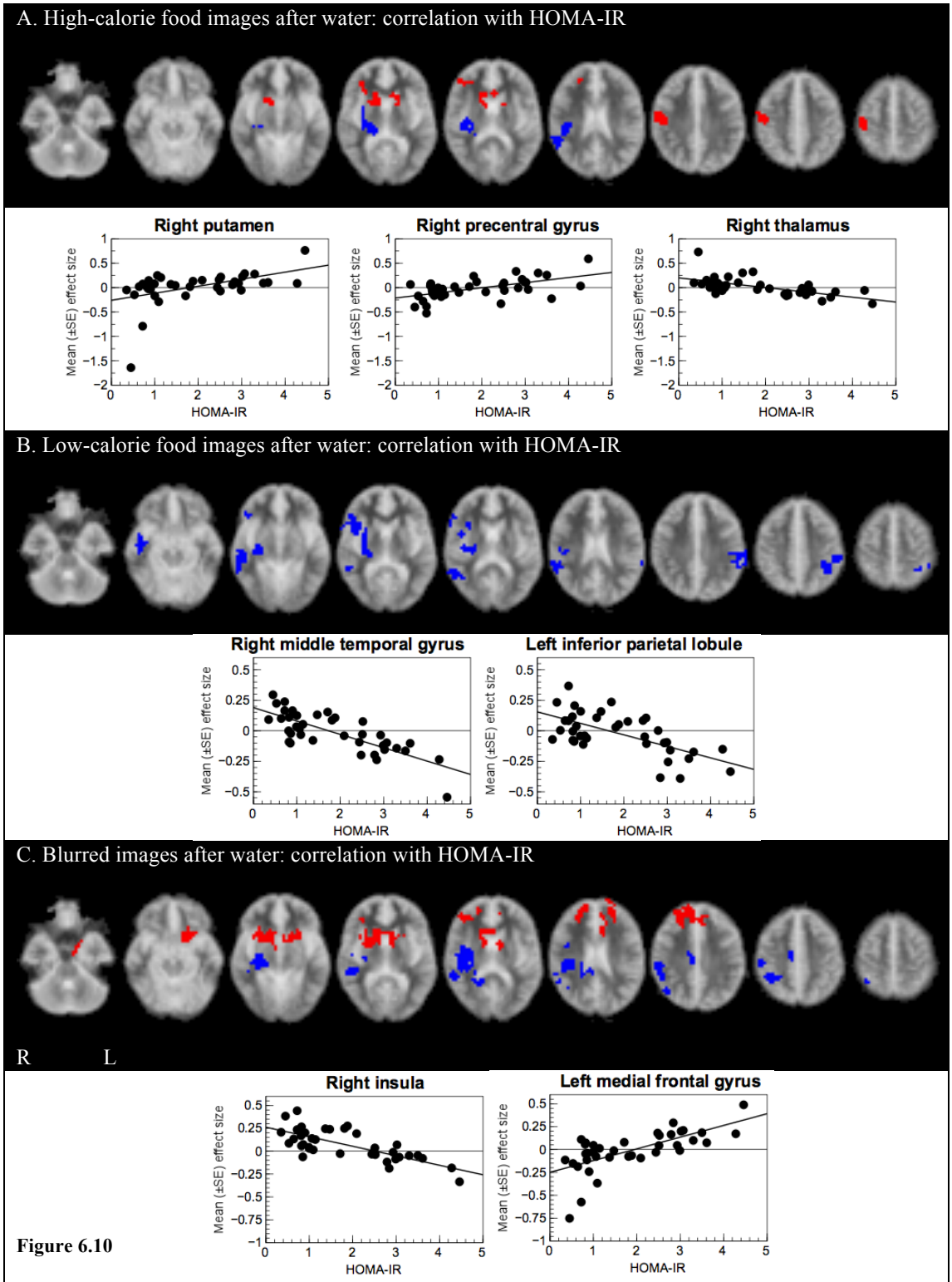

Figure 6.10

Group map of whole-brain correlation of activation after water with HOMA-IR, showing clusters exhibiting linear positive (red) or negative (blue) correlation of HOMA-IR with BOLD signal evoked by (A) high- and (B) low-calorie food and (C) blurred images (object image time series as baseline, voxel-wise $p < 0.05$, cluster-wise $p < 0.02$) and extracted effect size (% BOLD signal change, positive values: food/blurred>object).

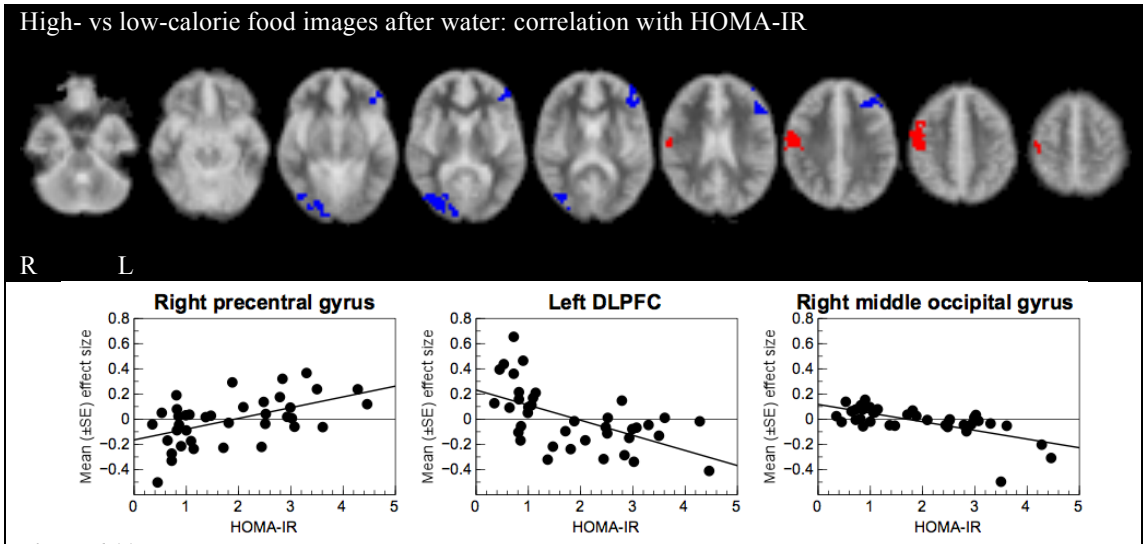

Figure 6.11

Group map of whole-brain correlation of activation after water with HOMA-IR, showing clusters exhibiting linear positive (red) or negative (blue) correlation of HOMA-IR with high- vs low-calorie food image-evoked BOLD signal (voxel-wise $p < 0.05$, cluster-wise $p < 0.01$) and extracted effect size (% BOLD signal change, positive values: high-calorie > low-calorie food).

6.3.7 Correlation between insulin resistance and difference in brain responses to food images after meal compared to water ingestion

Voxel-wise subtractions of BOLD signal after water from the respective signal after the meal for each image contrast in each subject, produced maps of the difference in BOLD signal contrast between feeding states. Voxel-wise Pearson correlation coefficients were calculated from these "difference" maps to examine linear associations between HOMA-IR and changes in brain response to visual images after meal compared to water ingestion in all 38 subjects studied (Table 6.6). Increasing insulin resistance was negatively associated with differences in [HiCal/OBJ]-evoked BOLD signal contrast in right precentral gyrus after the meal compared to water (Figure 6.12A). Insulin resistance was also negatively associated in left insula (extending to left DLPFC) and positively associated in right DLPFC (middle frontal gyrus) with the differences in [LoCal/OBJ]-evoked BOLD signal contrast after the meal compared to water (Figure 6.12B). Differences in [BLU/OBJ]-evoked BOLD signal contrast between feeding conditions were associated positively in right superior temporal gyrus and negatively in right middle occipital gyrus and precentral gyrus with insulin resistance (Figure 6.12C). The differential response to high- compared to low-calorie food images after meal compared to water were associated positively in left DLPFC (middle frontal gyrus) and negatively in right middle frontal gyrus with

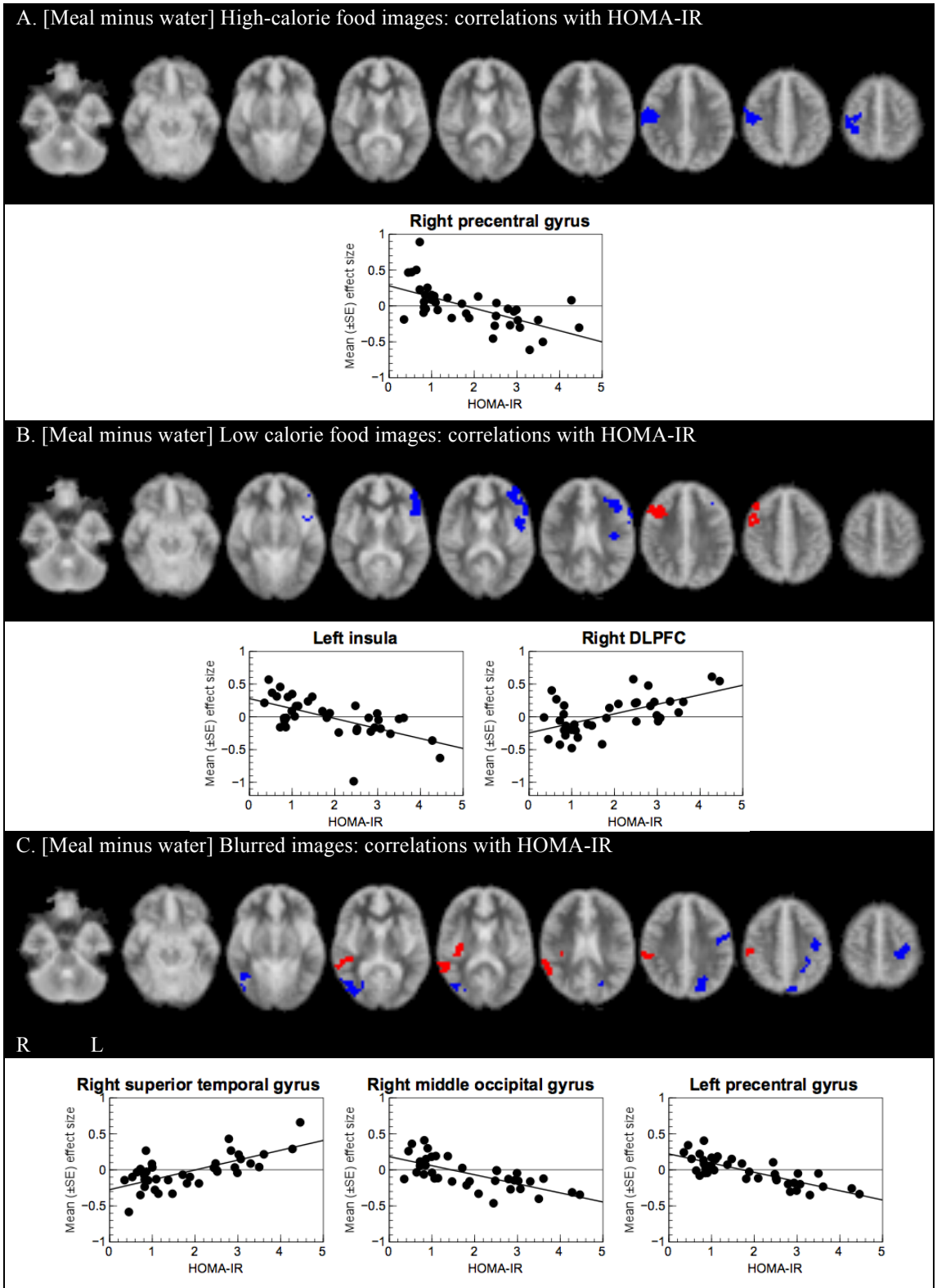

Figure 6.12

Group map of whole-brain correlation of differences in activation after meal compared to water with HOMA-IR, showing clusters exhibiting linear postive (red) or negative (blue) correlation of HOMA-IR with differences in BOLD signal evoked by (A) high- and (B) low-calorie food and (C) blurred images between feeding conditions (object image time series as baseline, voxel-wise $p < 0.05$, cluster-wise $p < 0.02$) and extracted effect size (% BOLD signal change, positive values: meal > water).

increasing insulin resistance (Figure 6.13A-B). The respective [HiCal/LoCal] image evoked-BOLD signal contrast from each feeding state were extracted from these two regions (Figure 6.13C), showing these associations were due to larger responses to high- than low-calorie food images after the meal and the reverse after water in left DLPFC, and larger responses to low- than high-calorie food images after the meal and the reverse after water in right middle frontal gyrus, with increasing insulin resistance.

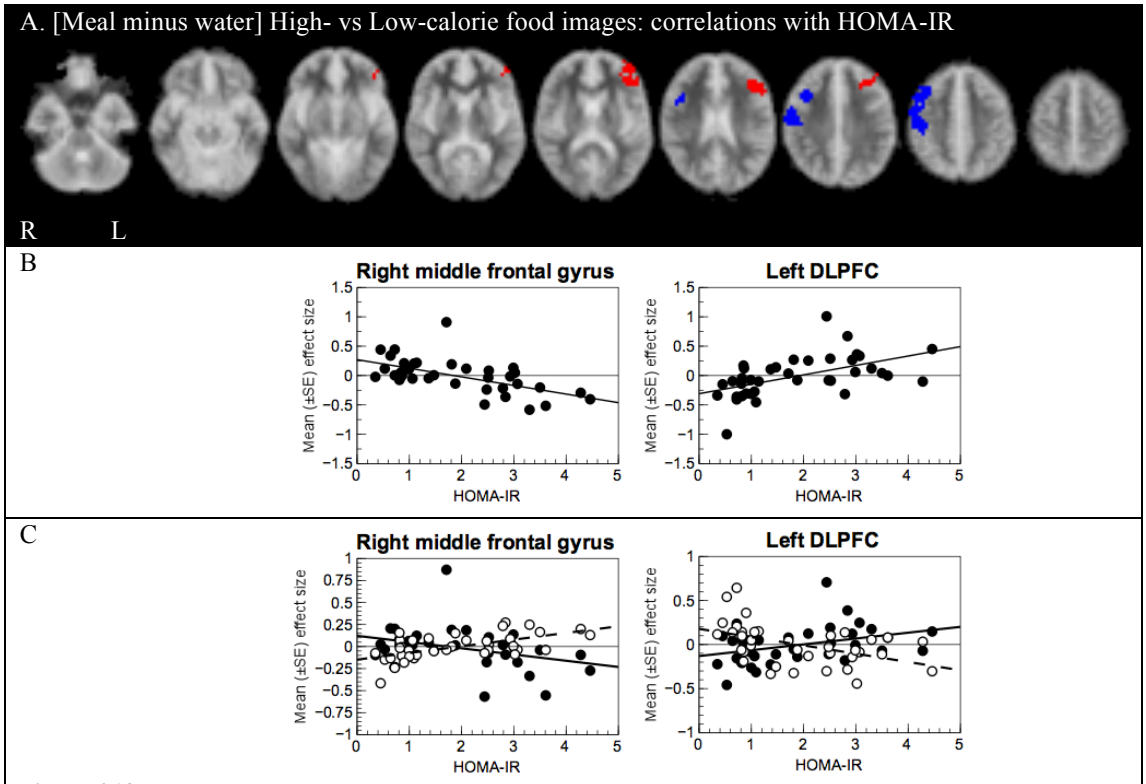

Figure 6.13

A: Group map of whole-brain correlation of differences in activation after meal vs water with HOMA-IR, showing clusters exhibiting linear postive (red) or negative (blue) correlation of HOMA-IR with differences in BOLD signal evoked by high- vs low-calorie food images between feeding conditions (voxel-wise $p < 0.05$, cluster-wise $p < 0.02$). B: extracted effect size (% BOLD signal change, positive values: meal > water) from (A). C: extracted water (white circles, dashed line) and meal (black circles, solid line) effect size from masks from (A) (positive values: high > low calorie food images).

6.4 Discussion

The present study set out to establish whether systemic insulin resistance influences the modulatory effects of meal ingestion on the subsequent brain response to visual food cues, using a BOLD fMRI paradigm that is commonly employed in the study of central appetite regulatory mechanisms (van der Laan *et al*, 2011; Tang *et al*, 2012). The paradigm used in this study was a development of the paradigm used to study the

effect of ageing (Chapter 4) to allow further manipulation of the incentive salience of the cues by altering the calorie content of the food images, as well as nutritional state.

6.4.1 Effect of meal ingestion on responses to food images

The normal response was first established by examining IS subjects. High- and low-calorie food images evoked greater subjective measures of hunger than object and blurred images equally. Food images are routinely used as surrogates for food itself in studies of appetite regulation, through the recognition that they create an anticipation and desire to eat, in contrast to the expected response from food consumption. Many studies select high-calorie food images that are more appealing or "motivationally salient" than low-calorie cues, their salience manipulated further by feeding status (Goldstone *et al*, 2009; Killgore *et al*, 2003), but there are studies employing high- and low-calorie food images of equal palatability (Siep *et al*, 2009). The lack of difference in hunger evoked by high- compared to low-calorie food images we observed may be due to a real lack of difference in the desire to eat, a lack of sensitivity to detect difference in the paradigm or be due to the fact that images were chosen in each class that had equal salience in a separate group of volunteers not involved in the neuroimaging study, and that food salience may have influenced hunger more than caloric content in the two feeding states in this study. Meal ingestion reduced such evoked hunger in response to all visual cues equally, compatible, given the timing relative to the meal, with satiation.

In contrast to the uniformity of the subjective response, there was an effect of feeding status and food-cue group on the central responses to their viewing, with meal ingestion increasing BOLD signal contrast evoked by images of high-calorie foods compared to objects in IS subjects in a region that included the right insula, involved in processing interoceptive awareness (Craig, 2009), a response not observed when viewing low-calorie food images. In the earlier study (Chapter 4), there was a *reduction* in BOLD signal in this region when observing mixed-calorie food images. The difference is likely to be due to differences in stimuli and the volunteers studied, with the earlier study examining responses in male and female volunteers with a wide age range.

Interaction analyses directly comparing responses to the different classes of food images in the two feeding states, showed the meal had differential effects depending on the energy density of the food cues, converting a deactivation on viewing low-calorie food images after water ingestion (effectively continued fasting) to an activation in the striatum and no response in the DLPFC. In contrast, meal ingestion converted the high-calorie food image-evoked activation observed in these regions in the continued fasted state, to a deactivation. The DLPFC is implicated in providing higher executive control, in terms of inhibition and initiation of motivated behaviours including eating behaviour (Ballard *et al*, 2011; Camus *et al*, 2009), through modulation of the activity of dopaminergic reward centres (Cho and Strafella, 2009; Fregni *et al*, 2008; Lowe *et al*, 2014), including the striatum (Staudinger *et al*, 2011). These responses are therefore consistent with meal consumption acting on these corticolimbic centres to reduce the drive to eat high-calorie foods during a post-prandial, energy-replete state. Meal compared to water ingestion also increased activation to low-calorie food images and reduced it to high-calorie food images in the right lingual gyrus, extending down to the right fusiform gyrus. The lingual and fusiform gyri are implicated in visual processing and attention to visual food cues, relaying such information to prefrontal regions (Frank *et al*, 2010a; Siep *et al*, 2009), activity in which also appear to be sensitive to current nutritional status. My findings are consistent with the observation by Goldstone *et al* (2009) that fasting "biases" reward networks to high-calorie food cues, increasing activation responses to high-calorie food images and reducing activation or evoking deactivation responses to low-calorie food images in ventral striatum, amygdala, insula and medial and lateral OFC in non-obese healthy volunteers. Siep *et al* (2009) similarly showed that responses to high-calorie food images were greatest after 18 hour fasting and to low-calorie food images after meal ingestion in OFC, insula, ventral striatum, posterior cingulate and fusiform gyrus in healthy female volunteers. Frank *et al* (2010) also showed superior medial frontal lobe and fusiform gyrus responses to high calorie food images were greater in the fasted state and to low calorie food images in the fed state in female subjects only, but their study may have been underpowered to show similar findings in men given the small sample size (6 male and 6 female subjects) and short, 3 hour period of fasting, unlike the present study. My data extend these findings by demonstrating in insulin sensitive men, that internal satiety signals following a meal influence the way we react to potential external sources of further food by modulating

the activity of corticolimbic networks involved in regulating eating behaviour, "calorically biasing" responses towards food cues that are concordant with current nutritional needs.

6.4.2 Effect of systemic insulin resistance

Systemic insulin resistance did not affect the subjective hunger evoked by the food images, nor the reduction in such evoked hunger by prior meal ingestion. In addition, unlike IS subjects, the meal did not alter reward network responses to high-calorie food images, and decreased responses to low-calorie food images in left DLPFC. Importantly, the interaction analyses in IR subjects failed to show the "caloric biasing" effects of greater reward network responses to low- than high-calorie food cues when fed and high- than low-calorie food cues when fasted that was observed in IS subjects. In fact, direct comparisons between groups indicated that this "caloric bias" effect observed in left DLPFC in IS subjects, is the direct opposite to that observed in IR subjects, with greater responses to high- than low-calorie food cues when fed, and low- than high-calorie food cues when fasted, discordant with current nutritional status.

This is the first study to explore the impact of non-obese, non-diabetic insulin resistance on the modulation of brain's response to food cues by feeding. However, impaired modulatory effects of meal ingestion on reward network responses to external food cues of differing nutritional value has been demonstrated in established obesity, where the high calorie food cue-evoked OFC, caudate and insula activation before lunch, decreased or deactivated after consuming lunch in lean subjects, similar to our data, whilst obese subjects showed opposite patterns of activity in the insula, and lack of any modulatory effects of the meal on food cue-evoked OFC and caudate responses (Dimitropoulos *et al*, 2012). Insulin sensitivity was not reported but insulin resistance is common in obesity. In contrast, Van Vugt *et al* (2013) failed to find a difference in brain responses to high- or low-calorie food images 5-6 hours following breakfast between insulin sensitive and resistant women with PCOS, possibly due to the use of metformin in some of the insulin resistant women, the relatively short period of fasting, and did not examine the impact of the meal on such evoked responses.

My data are also consistent with a similarly designed study, that demonstrated precuneus and fusiform gyrus activation to images of high-calorie foods and deactivation to low-calorie foods after water ingestion following an overnight fast, with the opposite pattern observed after a 75 g oral glucose load in lean subjects (Heni *et al*, 2014a). Conversely, deactivation to images of high-calorie foods and activation to low-calorie foods in these regions after water ingestion, without any difference between responses to the two food image classes following the glucose load was observed in overweight/obese subjects, who were significantly more insulin resistant. The lack of involvement of more typical reward processing centres in producing discriminatory responses to food cues of differing energy content, depending on current nutritional status, may have been due to the lack of other macronutrients consumed, such as fat, which has been shown to influence insular activity (Frank *et al*, 2012), or to smaller hedonic effects of consuming glucose compared to a meal, as used in the present study.

The above interpretations are supported by our voxel-wise regression analyses of the combined IS/INT/IR groups. Increasing insulin resistance was associated with greater striatal responses to high-calorie food cues and decreasing responses to low-calorie food cues in right insula after water ingestion and diminishing discriminatory responses between fed and fasted states to low-calorie food cues in left DLPFC/insula. However, the relationship between HOMA-IR and response to high calorie food images after water was similar to that for blurred images. Interestingly, differences in response to blurred images after water between the two groups shared similarities with the differences in response to both high and low calorie food images. Anecdotally, some subjects reported that they were actively trying to identify original food items in the blurred images, increasing the interest or salience of these images on a par to that of high-calorie foods, which may have driven the accompanying neural responses, but alternatively they could have been driven by the response to the object images, the time-series for which was used as the baseline.

The differential response to high- compared to low-calorie food images may be more physiologically meaningful. Increasing insulin resistance was positively associated with the difference in the response to this contrast between feeding conditions in left DLPFC, with greater responses to images of high-calorie foods after water and to

low-calorie foods after the meal in the more insulin sensitive subjects, converting to greater responses to low-calorie foods after water and high-calorie foods after the meal as insulin resistance increased. Thus, the strength of the normal "caloric bias" effect in this inhibitory control centre diminishes with increasing insulin resistance. (Van Vugt *et al*, 2013) showed in women with PCOS that decreasing insulin sensitivity (defined by 2 hour glucose:insulin ratio, post-75g oral glucose) was associated with increasing activation in DLPFC, anterior cingulate and midbrain to high-calorie food images and in OFC, ventral pallidum, substantia nigra, ventral tegmental area (VTA) and thalamus to low-calorie food images in the pre-lunch state. They also found that as insulin sensitivity decreased, the greater response to high- vs low-calorie food images diminished in OFC, DLPFC, insula, ventral pallidum and VTA, whilst the greater response to low- compared to high-calorie food images in the caudate also fell. However, these findings could not be replicated when the more validated HOMA-IR was used a covariate of interest

6.4.3 Limitations and conclusion

There is therefore mounting evidence that in conditions of systemic insulin resistance, such as obesity and PCOS, the neural networks that regulate hedonic responses to external cues of food and control food-seeking behaviour are insensitive to the modulatory effects of homeostatic signals of energy balance, with the present study compatible with a disruption to such networks in early insulin resistance, prior to weight gain. Indeed, (Cornier *et al*, 2013) have shown that subjects who self-identify as being prone to weight gain demonstrate less meal-induced reduction of responses to food images in the insula, inferior and medial prefrontal cortex than those who identify as being resistant to obesity, with greater meal induced reduction in activity associated with greater suppression of hunger, supporting an aetiological role for altered corticolimbic activity in future obesity risk.

As discussed in Chapter 1, cerebral resistance to insulin could explain the present findings. Kroemer *et al* (2013) showed that the endogenous peripheral insulin response to an oral glucose load is associated with the glucose-evoked reduction in corticolimbic responses to food images, in regions including the insula, inferior prefrontal cortex and striatum. Exogenous insulin applied at physiological

concentrations during euglycaemic clamps with somatostatin suppression of endogenous insulin secretion increases striatal and prefrontal glucose uptake less effectively in insulin resistant than insulin sensitive volunteers (Anthony *et al*, 2006). Increasing cerebral insulin by intranasal inhalation, effects evokes anorexia (Benedict *et al*, 2008), reduces body fat (Hallschmid *et al*, 2004a), enhances post-prandial thermogenesis (Benedict *et al*, 2011) and increases satiety and reduces food intake (Hallschmid *et al*, 2012) with increased brain energy levels (Jauch-Chara *et al*, 2012), selectively reducing responses to food images in the fusiform gyrus, hippocampus, middle frontal cortex and temporal lobe (Guthoff *et al*, 2010). These effects of weight loss and modulation of neural responses to food cues with intranasal insulin are impaired in obesity (Guthoff *et al*, 2011; Hallschmid *et al*, 2008), with recent studies indicating increasing peripheral insulin resistance is associated with diminishing intranasal insulin-evoked reductions in prefrontal cortical activity (Kullmann *et al*, 2015). Decreasing DLPFC responses to high calorie food cues predict greater food intake (Cornier *et al*, 2010), with responses to meal ingestion *per se* being diminished in established obesity (Le *et al*, 2006). Striatal reactivity to food ingestion is also diminished in established obesity (Stice *et al*, 2008), and decreases concurrently with weight gain (Stice *et al*, 2010). It is therefore conceivable that the impaired modulatory effects of meal ingestion on the corticolimbic responses to high- and low-calorie food cues observed in insulin resistant individuals, at high risk of future diabetes and obesity by family history, is mediated by an impaired response to post-prandial insulin, altering satiety processing and increasing obesity risk.

There are some limitations to the present study. There was no effect of systemic insulin resistance on the food image-evoked hunger. Although this may relate to the reduced power of the symptomatic study, it is also likely that the observed differences in neural activity influence eating behaviour through subconscious mechanisms. Objective measures of eating behaviour, such as the use of an ad-libitum meal following the first mixed meal, were not collected to support this hypothesis but it is supported by existing evidence discussed earlier. As systemic insulin resistance influenced responses to blurred images, perhaps because these evoked hedonic, food-related responses, an alternative comparator such as prolonged viewing of a fixation cross may help to confirm a food-specific effect of systemic insulin resistance on reward network activity. Nevertheless, the present study has demonstrated that early

systemic insulin resistance is associated with a reversal of the normal “caloric bias” in prefrontal executive control centres that direct eating behaviour towards food cues appropriate to current energy status, which may permit continued eating and weight gain.

Table 6.1

Impact of meal compared to water ingestion on BOLD signal contrasts listed in insulin sensitive subjects (voxel-wise $P < 0.05$, cluster-wise threshold < 1 false positive cluster/brain map as listed, Figure 6.3, Figure 6.4). BA = Brodmann area.

	Talairach coordinates of voxel with peak effect size					
Size	**X**	**Y**	**Z**	**P ≤**	**BA**	**Brain regions**
High calorie food / object contrast: Water > Meal *(cluster-wise P ≤ 0.010309)*						
No significant clusters						
High calorie food / object contrast: Water < Meal *(cluster-wise P ≤ 0.014286)*						
253	47	-11	33	0.006132	6	Right precentral gyrus (with insula)
164	-46	-18	47	0.006711	3	Left postcentral gyrus
Low calorie food / object contrast: Water > Meal *(cluster-wise P ≤ 0.011364)*						
No significant clusters						
Low calorie food / object contrast: Water < Meal *(cluster-wise P ≤ 0.012821)*						
188	-40	-22	53	0.005268	3	Left postcentral gyrus
Blurred image / object contrast: Water > Meal *(cluster-wise P ≤ 0.016393)*						
145	2	-20	-3	0.009702	N/A	Right midbrain
Blurred image / object contrast: Water < Meal *(cluster-wise P ≤ 0.010417)*						
No significant clusters						
[High calorie food / object vs Low calorie food / object contrasts] vs [Water vs Meal] *(cluster-wise P ≤ 0.007752)*						
143	25	-69	2	0.002296	18	Right lingual gyrus
124	-7	15	3	0.004745	N/A	Left caudate head
157	-45	32	21	0.002799	46	Left middle frontal gyrus (DLPFC)

Table 6.2

Impact of meal compared to water ingestion on BOLD signal contrasts listed in insulin resistant subjects (voxel-wise $P < 0.05$, cluster-wise threshold < 1 false positive cluster/brain map as listed, Figure 6.5). BA = Brodmann area.

	Talairach coordinates of voxel with peak effect size					
Size	**X**	**Y**	**Z**	**P ≤**	**BA**	**Brain regions**
High calorie food / object contrast: Water > Meal *(cluster-wise P ≤ 0.012346)*						
227	-36	-55	47	0.006733	40	Left inferior parietal lobule
187	40	-33	56	0.011497	40	Right postcentral gyrus
High calorie food / object contrast: Water < Meal *(cluster-wise P ≤ 0.013889)*						
No significant clusters						
Low calorie food / object contrast: Water > Meal *(cluster-wise P ≤ 0.010753)*						
216	23	-74	25	0.009793	31	Right precuneus
225	-27	36	28	0.004721	9	Left middle frontal gyrus (DLPFC)
Low calorie food / object contrast: Water < Meal *(cluster-wise P ≤ 0.013158)*						
124	-47	-56	16	0.011727	22	Left superior temporal lobe
237	30	14	57	0.003722	6	Right middle frontal gyrus
Blurred image / object contrast: Water > Meal *(cluster-wise P ≤ 0.010753)*						
222	41	-69	9	0.003974	19	Right middle occipital gyrus
285	-17	-55	57	0.002377	7	Left precuneus
Blurred image / object contrast: Water < Meal *(cluster-wise P ≤ 0.014286)*						
267	6	40	52	0.001370	8	Right superior frontal gyrus
[High calorie food / object vs Low calorie food / object] vs [Water vs Meal] *(cluster-wise P ≤ 0.007634)*						
No significant clusters						

Table 6.3

Differences in BOLD signal contrasts listed between insulin sensitive (IS) and resistant (IR) subjects after water (voxel-wise $P < 0.05$, cluster-wise threshold < 1 false positive cluster/brain map as listed, Figure 6.6, Figure 6.7). BA = Brodmann area.

	Talairach coordinates of voxel with peak effect size					
Size	**X**	**Y**	**Z**	**P ≤**	**BA**	**Brain regions**
Water: High calorie food / object contrast: IS > IR *(cluster-wise P ≤ 0.005525)*						
156	32	-19	13	0.004423	N/A	Right claustrum
Water: High calorie food / object contrast: IS < IR *(cluster-wise P ≤ 0.008065)*						
361	-4	52	16	0.000186	9	Left medial frontal gyrus
Water: Low calorie food / object contrast: IS > IR *(cluster-wise P ≤ 0.006024)*						
149	47	-15	-6	0.003028	22	Right superior temporal gyrus
Water: Low calorie food / object contrast: IS < IR *(cluster-wise P ≤ 0.006211)*						
No significant clusters						
Water: Blurred images / object contrast: IS > IR *(cluster-wise P ≤ 0.006289)*						
178	40	-7	16	0.002366	13	Right insula
Water: Blurred images / object contrast: IS < IR *(cluster-wise P ≤ 0.006211)*						
96	24	16	1	0.003993	N/A	Right putamen
157	12	54	13	0.005604	10	Right medial frontal gyrus
116	-6	41	24	0.006169	9	Left medial frontal gyrus
Water: [IS: High calorie food/object > Low calorie food/object] vs [IR: High calorie food/object < Low calorie food/object] *(cluster-wise P ≤ 0.004425)*						
154	-40	34	14	0.000986	46	Left middle frontal gyrus (DLPFC)
Water: [IS: High calorie food/object < Low calorie food/object] vs [IR: High calorie food/object > Low calorie food/object] *(cluster-wise P ≤ 0.004202)*						
110	41	21	48	0.003105	8	Right superior frontal gyrus
143	29	-7	53	0.003496	6	Right middle frontal gyrus (pre-motor/supplementary motor cortex)

Table 6.4

Differences in impact of meal compared to water ingestion on BOLD signal contrasts listed between insulin sensitive (IS) and resistant (IR) subjects (voxel-wise $P < 0.05$, cluster-wise threshold < 1 false positive cluster/brain map as listed, Figure 6.8, Figure 6.9). BA = Brodmann area.

	Talairach coordinates of voxel with peak effect size					
Size	**X**	**Y**	**Z**	**P ≤**	**BA**	**Brain regions**
High calorie food / object contrast: IS (Water > Meal) vs IR (Water < Meal) *(cluster-wise P ≤ 0.006494)*						
No significant clusters						
High calorie food / object contrast: IS (Water < Meal) vs IR (Water > Meal) *(cluster-wise P ≤ 0.005814)*						
No significant clusters						
Low calorie food / object contrast: IS (Water > Meal) vs IR (Water < Meal) *(cluster-wise P ≤ 0.005848)*						
130	41	19	33	0.002531	9	Right middle frontal gyrus (DLPFC)
Low calorie food / object contrast: IS (Water < Meal) vs IR (Water > Meal) *(cluster-wise P < 0.005051)*						
261	-43	11	0	0.001125	13	Left insula (DLPFC)
Blurred image / object contrast: IS (Water > Meal) vs IR (Water < Meal) *(cluster-wise P < 0.004950)*						
No significant clusters						
Blurred image / object contrast: IS (Water < Meal) vs IR (Water < Meal) *(cluster-wise P < 0.006061)*						
170	22	-74	20	0.003179	18	Right cuneus
193	-36	-11	43	0.003156	6	Left precentral gyrus
[**High calorie food / object] - [Low calorie food / object] contrast: IS (Water > Meal) vs IR (Water < Meal)** *(cluster-wise P ≤ 0.005208)*						
206	-36	30	30	0.000849	9	Left middle frontal gyrus (DLPFC)
[**High calorie food / object] - [Low calorie food / object] contrast: IS (Water < Meal) vs IR (Water > Meal)** *(cluster-wise P ≤ 0.005263)*						
139	43	19	33	0.00417	9	Right middle frontal gyrus (DLPFC)

Table 6.5

Voxel-wise Pearson product moment correlation of HOMA-IR with BOLD signal contrasts listed after water in 38 (IS, INT, IR) subjects (voxel-wise $P < 0.05$, cluster-wise threshold < 1 false positive cluster/brain map as listed, Figure 6.10, Figure 6.11). BA = Brodmann area.

	Talairach coordinates of voxel with peak effect size					
Size	**X**	**Y**	**Z**	**P ≤**	**BA**	**Brain regions**
Water: High calorie food / object contrast: positive association with HOMA-IR *(cluster-wise P ≤ 0.013699)*						
226	19	15	2	0.011940	N/A	Right putamen
178	50	-10	47	0.007466	4	Right precentral gyrus
Water: High calorie food / object contrast: negative association with HOMA-IR *(cluster-wise P ≤ 0.013286)*						
204	25	-26	3	0.007633	N/A	Right thalamus
Water: Low calorie food / object contrast: positive association with HOMA-IR *(cluster-wise P ≤ 0.011628)*						
No significant clusters						
Water: Low calorie food / object contrast: negative association with HOMA-IR *(cluster-wise P ≤ 0.014925)*						
454	56	-38	3	0.002697	22	Right middle temporal gyrus
205	-51	-30	33	0.004490	40	Left inferior parietal lobule
Water: Blurred images / object contrast: positive association with HOMA-IR *(cluster-wise P ≤ 0.015625)*						
761	-41	11	-16	0.000127	25	Left medial frontal gyrus
Water: Blurred images / object contrast: negative association with HOMA-IR *(cluster-wise P ≤ 0.017857)*						
665	36	-22	13	0.000239	13	Insula
Water: [High calorie food / object] - [Low calorie food / object] contrast: positive association with HOMA-IR *(cluster-wise P ≤ 0.013699)*						
164	51	-7	43	0.010703	4	Right precentral gyrus
Water: [High calorie food / object] - [Low calorie food / object] contrast: negative association with HOMA-IR *(cluster-wise P ≤ 0.014925)*						
171	35	-82	9	0.003979	19	Right middle occipital gyrus
152	-45	46	5	0.013206	46	Left inferior frontal gyrus (DLPFC)

Table 6.6

Voxel-wise Pearson product moment correlation of HOMA-IR with the difference in BOLD signal contrasts listed between meal and water in 38 (IS, INT, IR) subjects (voxel-wise $P < 0.05$, cluster-wise threshold < 1 false positive cluster/brain map as listed, Figure 6.12, Figure 6.13). BA = Brodmann area.

	Talairach coordinates of voxel with peak effect size					
Size	**X**	**Y**	**Z**	**P ≤**	**BA**	**Brain regions**
Meal minus water: High calorie food / object contrast: positive association with HOMA-IR *(cluster-wise P ≤ 0.014706)*						
No significant clusters						
Meal minus water: High calorie food / object contrast: negative association with HOMA-IR *(cluster-wise P ≤ 0.011236)*						
287	53	-13	38	0.00233	4	Right precentral gyrus
Meal minus water: Low calorie food / object contrast: positive association with HOMA-IR *(cluster-wise P ≤ 0.016393)*						
131	40	22	30	0.011417	9	Right middle frontal gyrus
Meal minus water: Low calorie food / object contrast: negative association with HOMA-IR *(cluster-wise P ≤ 0.011765)*						
374	-43	11	0	0.003075	13	Insula
Meal minus water: Blurred images / object contrast: positive association with HOMA-IR *(cluster-wise P ≤ 0.019231)*						
237	57	-47	13	0.010473	22	Right superior temporal gyrus
Meal minus water: Blurred images / object contrast: negative association with HOMA-IR *(cluster-wise P ≤ 0.017857)*						
121	48	-69	4	0.006884	37	Right middle occipital gyrus
244	-36	-11	43	0.006066	6	Left precentral gyrus
Meal minus water: [High calorie food / object] – [Low calorie food / object] contrast: positive association with HOMA-IR *(cluster-wise P ≤ 0.010638)*						
185	-36	30	30	0.008237	9	Left middle frontal gyrus (DLPFC)
Meal minus water: [High calorie food / object] - [Low calorie food / object] contrast: negative association with HOMA-IR *(cluster-wise P ≤ 0.013889)*						
255	51	11	43	0.006164	6	Right middle frontal gyrus

7 Impact of systemic insulin sensitisation on central responses to meal ingestion in insulin resistance

7.1 Introduction

In Chapter 5, systemic insulin resistance in non-obese, non-diabetic men was associated with greater degrees of food restraint and greater resting activity of the right lateral orbitofrontal cortex (OFC) in the fasted state. Meal ingestion reduced activity in this inhibitory control centre of eating behaviour to lower levels observed in both fasted and fed states in insulin sensitive (IS) men, and increased activity in the left insula in insulin resistant (IR) subjects, potentially due to reduced top-down regulation of this interoceptive region by the lateral OFC, in contrast to the post-prandial reduction in insula activity observed in IS men. I hypothesised that post-prandial insulin may modulate the activity of these corticolimbic reward networks to invoke satiation and satiety in health, and that central insulin resistance could explain the current observations. Functional neuroimaging studies have shown that these networks in obesity may be receptive to lifestyle changes, pharmacological therapies or weight loss surgery, but whether changes in activity of these appetite control centres are a cause or a consequence of these interventions is uncertain. The aim of the present study was to investigate the effect of improving systemic insulin sensitivity on the function of these corticolimbic centres, specifically in the insula and lateral OFC, during meal ingestion in non-clinical insulin resistance, hypothesising an aetiological role of central insulin resistance in altered satiation processing, and seeking evidence of its reversibility.

7.2 Methods

7.2.1 Subjects

The IR subjects recruited for the study described in Chapters 5 and 6 also consented to participate in a double-blind randomised control trial of insulin sensitisation using metformin with lifestyle advice, compared to placebo, with lifestyle advice offered on completion of the study. This was rendered impractical by regulatory delays (in confirming the study did not constitute a clinical trial of an investigational medicinal

product and in delivery and repackaging of the study medication sourced successfully from Merck-Serono), as well as by insufficient numbers of participants to ensure an adequately powered study. Instead, the protocol was converted to a proof-of-concept study and re-designed as a single-arm, open-label study of the effect of insulin sensitisation on the responses of interest. Of the 16 original IR subjects, one subject withdrew consent due to lack of free time to continue with the study and one subject emigrated, after completing the pre-intervention studies. In addition, two IR subjects originally screened as IS controls, but found to be insulin resistant, consented to lifestyle intervention but declined to consent to medical therapy. Thus 14 subjects consented to a 3-month intervention of insulin sensitisation (two subjects through lifestyle changes alone), before repeating the original neuroimaging protocols.

7.2.2 Study protocol

Once initial MRI studies, described in Chapters 5-6, were completed, subjects entered the insulin sensitisation intervention phase of the study as described in section 2.8.11. In brief, consenting subjects received 3 months of open-label metformin (Glucophage SR, Merck Serono) in an escalating dose of 500mg *od* for 2 weeks, 1g *od* for 2 weeks, 1.5g *od* for 2 weeks, and 2g *od* for the remaining 6 weeks or the maximum tolerated dose. Subjects could take the metformin in divided doses if they wished. Subjects also received a consultation with a registered diabetes specialist dietitian, providing dietary advice according to NICE guidance for the prevention and management of type 2 diabetes (T2DM), with personalised individual plans made, setting specific, measurable, achievable, realistic and timely (SMART) goals after assessment of a 3-day food diary (National Institute for Health and Care Excellence, 2009). Written information was also provided ("Get active, stay active", (British Heart Foundation, 2014)). Subjects could see the dietitian as many times as they wished during the 3 month study period following the initial consultation: the majority of subjects kept in contact via email and telephone, rather than in person.

At the end of the intervention period, subjects underwent the same study protocol as described in Chapters 5-6, with MRI acquisition details as described in section 2.8, the order of the total 4 scan visits balanced across the group through block randomisation on study entry.

The measures of insulin sensitivity, HOMA2-IR and HOMA-IR, were calculated from fasting blood taken at the screening visit, and after the intervention on the morning of the follow-up scan, after an initial 15 mins rest period, followed by a further 15 mins rest after intravenous cannulation.

7.2.3 Biochemical analysis

Laboratory methods for quantifying plasma glucose, serum insulin, GLP-1, GIP, leptin and adiponectin are described in section 2.8.14.

7.2.4 Statistical analysis

General non-imaging statistical methods are described in section 2.8.14. Data are presented as mean±SEM or median with the interquartile range. pCASL image pre-processing and statistical analyses are described in sections 2.8.13.1-2. Smoothed, normalised CBF maps calculated for each subject were entered into second-level group analyses. Post-intervention data were submitted to a flexible factorial model as used in the ageing study (Figure 3.2). The complete pre- and post-intervention data set were submitted to a full factorial repeated measures general linear model (GLM), with intervention (2 levels: pre- and post-insulin sensitisation ("Rx")), feeding status (2 levels: meal vs water) and time (4 levels: pre-ingestion and three post-ingestion time points, pCASL1-4 respectively) as factors. Analyses were restricted to grey matter, with mean global grey matter CBF used as nuisance covariates in the GLM (Figure 7.1). A full rather than a flexible factorial model was used, as the latter only permits interrogation of 2 interacting factors. T-contrast vectors were defined to examine (a) the impact of the intervention on pre-ingestion rCBF (pCASL1) and (b) the impact of the intervention on the effect of meal compared to water ingestion (interaction of pre-Rx/post-Rx with feeding status across the three post-ingestion time points, ASL2-4). However, as the latter assumes that the intervention may have different central effects dependent on feeding status, which may not necessarily be the case, and to avoid a type II error, T-contrast vectors were constructed to examine the effect of the intervention within each feeding state. If insulin sensitisation were to normalise the pre- and post-ingestion brain activity, based on the results in Chapter 5, one would hypothesise that the intervention would reduce right lateral OFC rCBF in

the fasted state, and left insula rCBF in the post-prandial state. *A priori* regions of interest analyses were not performed to avoid inferential bias, as the regions identified from Chapter 5 are based on the same pre-intervention data used in this chapter.

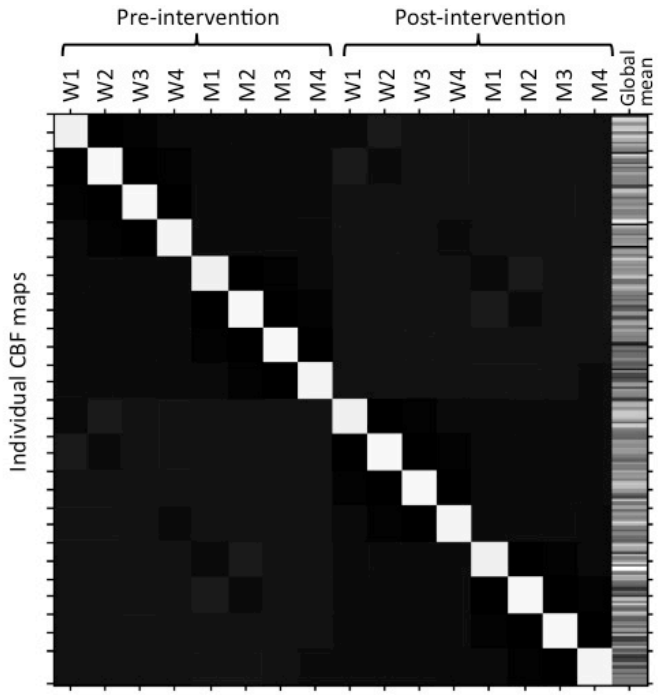

Figure 7.1

Full factorial GLM design matrix. W1-4 = pCASL1-4 on water visit; M1-4 = pCASL1-4 on meal visit. Global mean = mean global grey matter CBF.

rCBF data at each voxel pre-intervention were also subtracted from the respective voxel post-intervention, within each feeding state and respective time point (e.g. post-Rx meal pCASL4 minus pre-Rx-meal pCASL4 etc.) creating "difference" CBF maps. These were submitted to separate multiple regression models to examine linear relationships between changes in insulin sensitivity (difference in HOMA-IR) with changes in rCBF within each feeding condition from pre-Rx to post-Rx, at each post-ingestion time point, using the respective change in mean global grey matter CBF after the intervention as a nuisance covariate. A cluster-forming uncorrected voxel-wise threshold of $P<0.01$ was employed, but only those clusters that survived statistical significance ($P_{FWE\text{-}corrected}<0.05$) after correction for multiple comparisons are reported. Mean CBF values were extracted from unsmoothed CBF maps to examine global grey matter CBF (with statistical tests performed in SPSS) and functionally identified regions from these voxel-wise analyses, to quantify differences

in rCBF in physiological units and for illustrative purposes to characterise the nature of the regression analyses.

7.3 Results

7.3.1 Subject characteristics

The mean (±SD) age of the 14 subjects at baseline was 34.0±10.6 years. There was a mean interval of 35.6±22.1 weeks between the second pre-intervention and first post-intervention MRI visits. HbA1c, HOMA-IR and HOMA2-IR significantly improved after the intervention (Table 7.1). There were no significant differences in fasting leptin or adiponectin, suggesting that whilst indices of glycaemic index and insulin sensitivity improved, there were no significant changes in fat mass, consistent with absence of a significant change in the physically examined characteristics after the intervention. Eight of the 12 subjects receiving metformin returned the medication packaging and any remaining tablets at the end of the study (mean number of tablets consumed 230±32 out of 252 supplied). The two subjects who followed dietary advice only, showed the following pre- and post-intervention observations, respectively: Subject #SCN023: HOMA-IR 2.52 vs 2.78, HOMA2-IR 1.50 vs 1.55, HbA1c 5.5% vs 4.8%, Weight 99 vs 93.6 kg, BMI 24.75 vs 23.4 kg/m^2; Subject #SIR075: HOMA-IR 2.99 vs 1.88; HOMA2-IR 1.50 vs 1.05; HbA1c 5.2% vs 4.9%; BMI 20.26 vs 20.29 kg/m^2.

7.3.2 Appetite scores

There was no significant effect of the intervention on fasting measures of hunger (main effect $F(1,13)=0.297$, $p=0.154$) or nausea ($F(1,13)=1.321$, $p=0.271$), whilst it decreased sensations of fullness (main effect $F(1,13)=6.623$, $p=0.023$, estimated mean difference -9.48±3.69) and increased pleasantness to eat ($F(1,13)=5.682$, $p=0.033$, estimated mean difference=-7.93±3.33) (Figure 7.2). Using net incremental areas under the curves (iAUC), allowed for the differences in baseline symptom scores. The main effect of meal compared to water ingestion was to reduce hunger ($F(1,13)=5.439$, $p=0.036$) and pleasantness to eat ($F(1,13)=17.129$, $p=0.001$) and increase fullness ($F(1,13)=33.071$, $p<0.001$), without affecting nausea ($F(1,13)=1.874$,

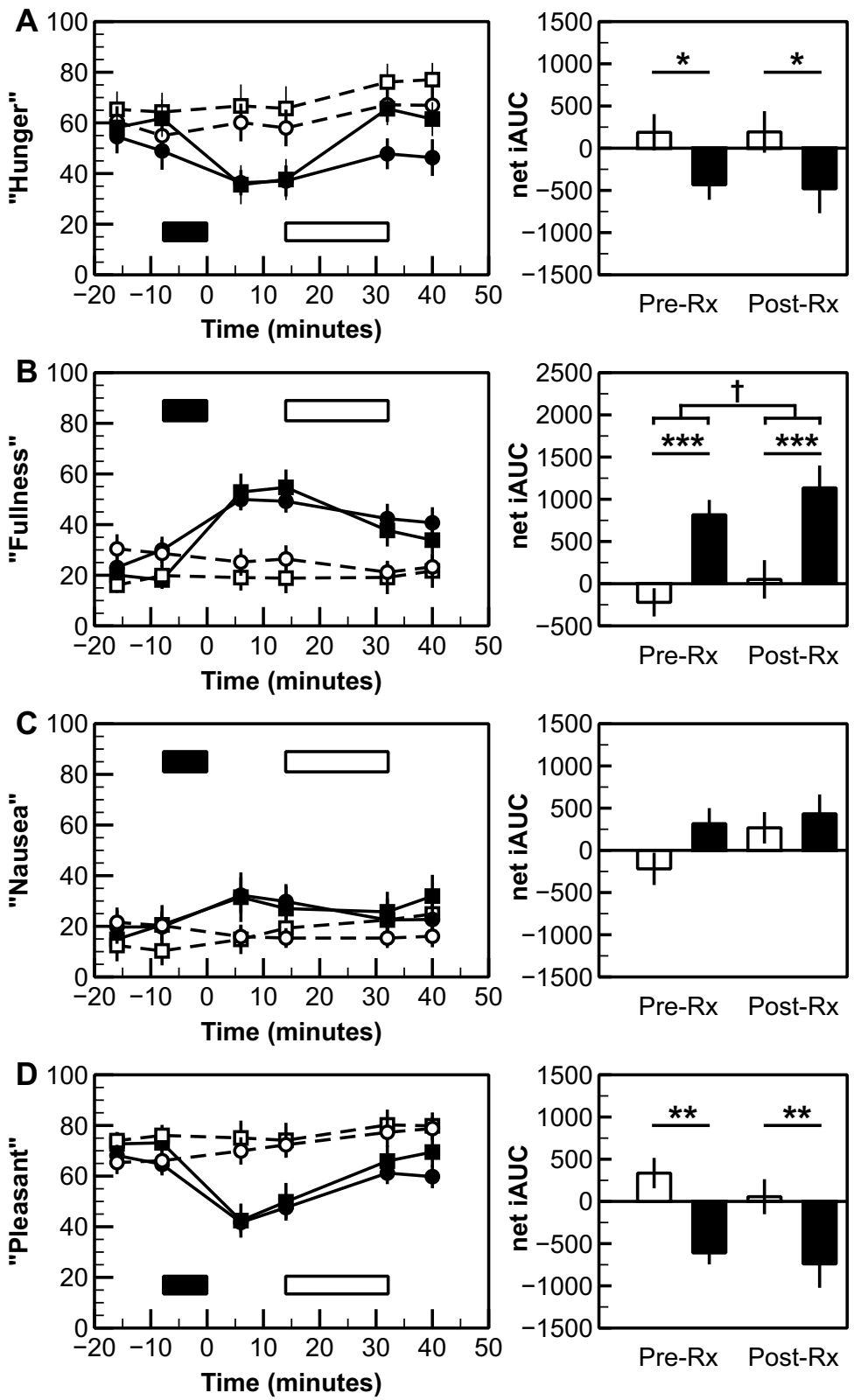

Figure 7.2

Hunger (A), fullness (B), nausea (C) and pleasantness to eat (D) scores after the meal (solid line) and water (dashed line) pre-intervention (Pre-Rx, circle) and post-intervention (Post-Rx, square). Left: Mean (± S.E.M); horizontal bars: black = time of meal/water; white = BOLD task. Right: net iAUC; white bars = water; black bars = meal; Main effect of meal: *p < 0.05, **p < 0.01 ***p < 0.001; main effect of intervention: †p < 0.05.

p=0.194), irrespective of the intervention. There were no main or interaction effects of the intervention on incremental changes in hunger (main effect F(1,13)=0.17, p=0.897; interaction F(1,13)=0.019, p=0.894), nausea (main effect F(1,13)=4.006, p=0.067; interaction F(1,13)=1.331, p=0.269) or pleasantness to eat (main effect F(1,13)=2.284, p=0.155); interaction F(1,13)=0.150, p=0.705) after meal / water ingestion. However there was a main effect of the intervention to increase the incremental change in fullness after meal or water ingestion (main effect of intervention F(1,13)=7.017, p=0.02, mean estimated difference 297.4±100.6 pre-Rx vs 592.9±144.1 post-Rx), an effect independent of feeding status (meal x intervention interaction F(1,13)=0.010, p=0.922).

7.3.3 Glucose, Insulin, GLP-1 and GIP during MRI scan visits

Whilst there was a significant reduction in HOMA2-IR and HOMA-IR from the screening visit to post-intervention, after calculating the mean fasting glucose and insulin levels across the two pre- and two post-intervention scanning visits, there were no significant changes in fasting glucose (mean difference -0.05±0.08 mmol/L, p=0.558), insulin (mean difference -1.65±1.14 mU/L, p=0.171), GLP-1 (mean difference -0.49±1.17 pmol/L, p=0.682) or GIP levels (mean difference -20.1±18.2 ng/L, p=0.289) (n=14).

Based on the net iAUC, post-meal glucose (n=8) and insulin (n=6) levels increased across the four scan visits (main effect of meal: glucose F(1,7)=82.540, p<0.001; insulin F(1,5)=27.246, p=0.002), and were unaffected by the intervention (main effect of intervention: glucose F(1,7)=0.620, p=0.457; insulin: F(1,5)=1.529, p=0.271; meal x intervention interaction: glucose F(1,7)=0.132, p=0.727, insulin F(1,5)=1.487, p=0.277). Post-ingestion GLP-1 levels (n=4) were unaffected by the meal (main effect of meal: F(1,3)=0.459, p=0.546) or intervention (main effect of intervention F(1,3)=0.049, p=0.840; meal x intervention F(1,3)=0.021, p=0.893), whilst post-meal GIP levels (n=3) increased across the four visits (main effect of meal F(1,2)=19.643, p=0.047), but were unaffected by the intervention (main effect of intervention (F1,2)=1.43, p=0.742; meal x intervention interaction F(1,2)=0.036, p=0.868), although post-ingestion sample collection was incomplete.

7.3.4 Effect of insulin sensitisation therapy on global grey matter CBF

Pre-ingestion (pCASL1) global grey matter CBF across the four visits were analysed in SPSS, showing no significant differences between pre-water or pre-meal scans (main effect of meal-allocation $F(1,13)=0.001$, $p=0.979$), nor any effect of the intervention (main effect of intervention $F(1,13)=0.050$, $p=0.826$). When all the global grey matter CBF maps (pCASL1-4) were entered into a repeated-measures ANOVA, there was a significant main effect of time ($F(3,39)=13.118$, $p<0.001$) and meal x time interaction ($F(1.643, 21.356)=4.648$, $p=0.027$), due to the fall in global grey matter CBF during each visit being greater after the meal (Figure 7.3). Insulin sensitisation had no significant impact on global grey matter CBF (main effect of intervention, $F(1,13)=0.107$, $p=0.749$; intervention x meal interaction, $F(1,13)=0.042$, $p=0.841$; intervention x time interaction, $F(1.597, 20.767)=0.238$, $p=0.741$; intervention x meal x time interaction, $F(1,964, 25.536)=0.522$, $p=0.596$).

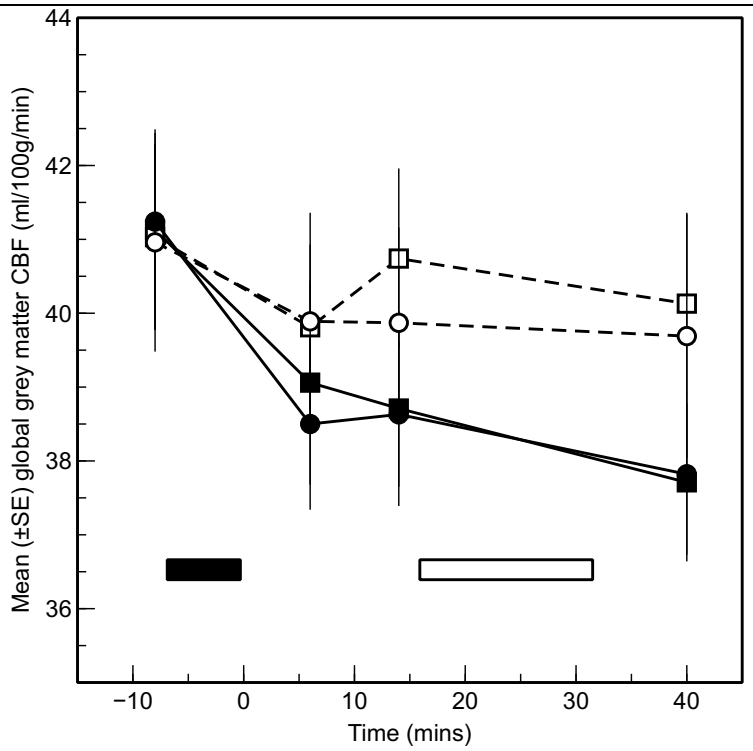

Figure 7.3

Global grey matter CBF after water (dashed lines) and meal (solid lines) before (circle) and after (square) insulin sensitisation. Black bar = meal / water ingestion; white bar = BOLD task.

7.3.5 Effect of meal ingestion on rCBF within the post-intervention state

Post-intervention CBF maps were first examined in isolation. There were no differences in fasting rCBF (pCASL1) between meal and water visits. T-contrasts of post-meal vs post-water rCBF across the three time points (pCASL2-4) revealed a fall in right lateral OFC rCBF that did not meet statistical significance (MNI coordinates X=40, Y=32, Z=-4, cluster $P_{FWEcorrected}$=0.054, T-value 4.95, 953 voxels, not shown).

7.3.6 Effect of insulin sensitisation therapy on fasting rCBF

Pre- and post-intervention data were next directly compared. T-contrasts of fasting rCBF (pCASL1) showed after the intervention, rCBF was lower in a cluster in the right inferior temporal gyrus, extending to angular gyrus of the inferior parietal lobule and hippocampus, and greater in bilateral fusiform gyrus (Figure 7.4A, Table 7.2).

7.3.7 Effect of insulin sensitisation therapy on post-water ingestion rCBF

T-contrasts of the main effect of the intervention on rCBF across all post-water time points (pCASL2-4, pre-Rx vs post-Rx) showed rCBF was lower in bilateral angular gyri and bilateral mid-frontal gyri, with the right cluster extending to right lateral orbitofrontal cortex (OFC) / dorsolateral prefrontal cortex (DLPFC), and greater in left post-central gyrus after the intervention (Figure 7.4B, Table 7.2).

7.3.8 Effect of insulin sensitisation therapy on post-meal ingestion rCBF

Similar T-contrasts of the main effect of the intervention on rCBF across all post-meal time points (pCASL2-4, pre-Rx vs post-Rx) showed rCBF was lower in left insula after the intervention (Figure 7.4C, Table 7.2).

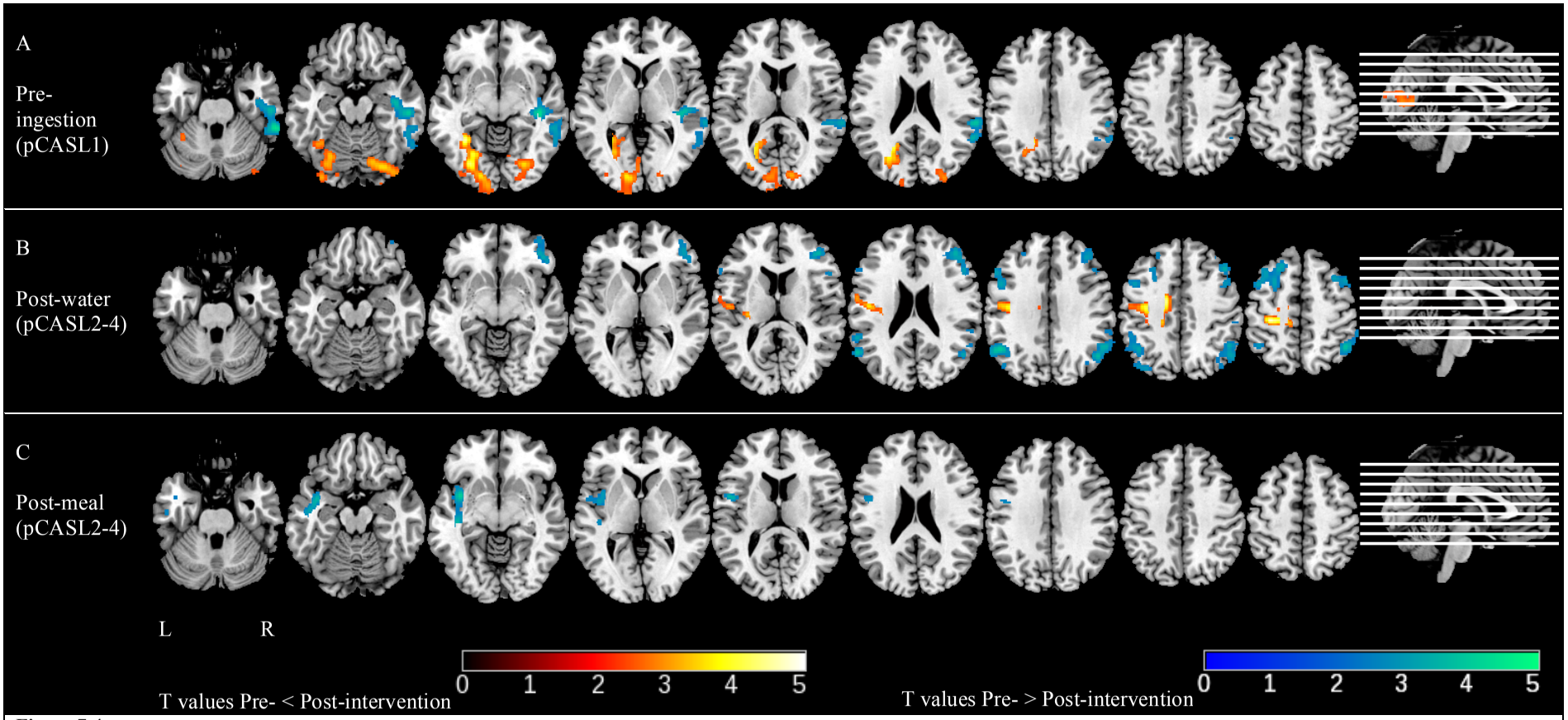

Figure 7.4

T-contrast brain maps of differences in rCBF, showing clusters with greater (red) or lesser (blue) rCBF post- than pre-intervention (A) in the fasted pre-ingestion state (pCASL1), and across post-ingestion time points (pCASL2-4) after (B) water and (C) meal. Voxel-threshold $P_{uncorrected} < 0.01$. Cluster-threshold $P_{FWE\text{-}corrected} < 0.05$.

7.3.9 Exploration of the right OFC/DLPFC and left insula rCBF

The regions identified in the preceding analyses showing reductions in rCBF following the intervention after water (right lateral OFC/DLPFC) and meal (left insula) were reminiscent of those identified to be different in the cross-sectional study between IS and pre-intervention IR subjects (post-water right lateral OFC/DLPFC rCBF greater in pre-intervention IR than IS subjects, and post-meal insular rCBF increased in pre-intervention IR and decreased in IS subjects). In order to explore the effect of the intervention in these centres further, two regions of interest were constructed from voxels spatially present in these [IS vs pre-intervention IR] and [pre- vs post-intervention IR] water/meal contrasts, from which unsmoothed rCBF data were extracted for illustrative purposes (Figure 7.5). Statistical analyses were not performed on these data, to avoid inferential bias. The intervention appeared to reduce post-water ingestion CBF in the right lateral OFC/DLPFC and post-meal ingestion CBF in the left insula in IR subjects towards rates observed in IS subjects.

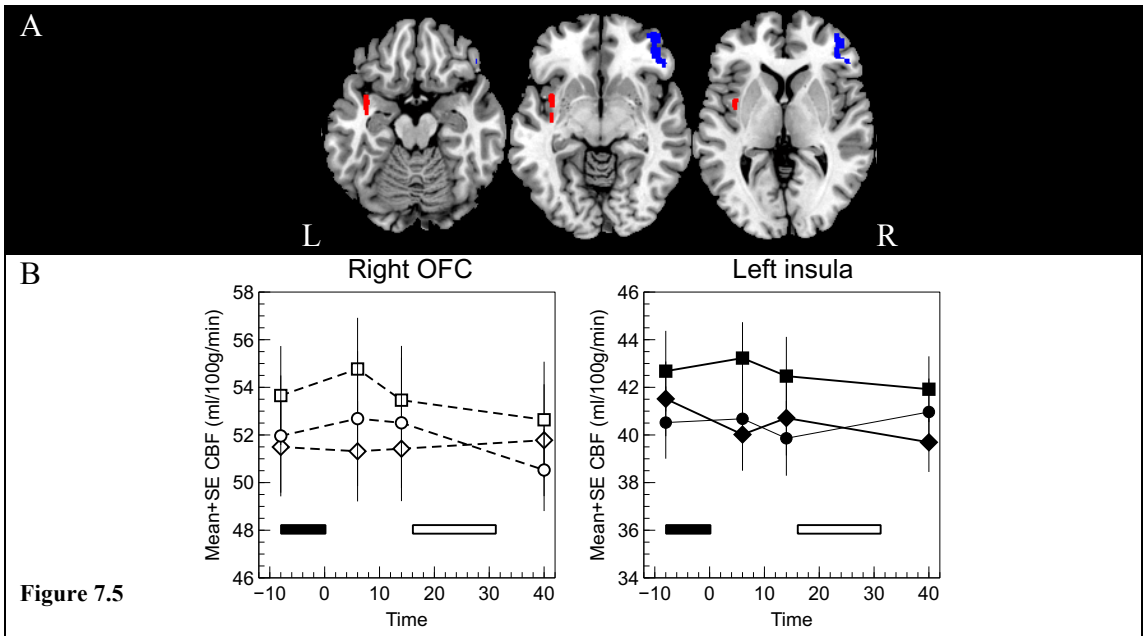

Figure 7.5

A: Right lateral OFC (blue) constructed from significant voxels in [water pCASL2-4: pre-Rx IR>IS] and [water pCASL2-4: pre-Rx>post-Rx IR] analyses and left insula (red) from significant voxels in [pCASL2-4: (meal vs water) vs (pre-Rx IR vs IS)] and [post-meal pCASL2-4: pre-Rx IR>post-Rx IR]. B: extracted rCBF data from (A). Dashed line = water; solid line = meal. Circle = IS (n = 17); square = pre-Rx IR (n=16); diamond = post-Rx IR (n=14); black bar = water/meal; white bar = BOLD task.

7.3.10 Effect of insulin sensitisation therapy on post-meal vs post-water ingestion rCBF

When T-contrasts for the interaction of intervention (pre-Rx vs post-Rx) and feeding status (post-meal vs post-water) across all post-ingestion time points (pCASL2-4) were constructed to examine effects of the intervention that were significantly different between feeding conditions, no significant clusters were identified. When these interactions were examined within each time point (pCASL2, 3, 4), a significant cluster in left mid-frontal gyrus, extending from left lateral OFC, through the left DLPFC to left ventrolateral prefrontal cortex, was identified immediately after ingestion (pCASL2), where post-prandial rCBF decreased before, and increased after the intervention (Figure 7.6).

The extracted rCBF data from this region in the IR subjects showed post-prandial rCBF decreased before, and increased after the intervention. Data were also extracted in this functional region of interest from the independent group of IS subjects, and compared with the IR group using unpaired t-tests. There were no significant differences in post-water rCBF between IR subjects, either before or after the intervention, and IS subjects. However, post-meal rCBF in IR subjects prior to the intervention was significantly lower than that of the IS subjects ($p = 0.038$, uncorrected), increasing to levels after the intervention that were no longer significantly different from the IS group.

No other significant clusters were identified on the interaction analysis at the later post-ingestion time points (pCASL3 [+8 to +14 mins] or pCASL4 [+34 to +40 mins]).

7.3.11 Correlation between post-intervention changes in insulin sensitivity and fasting rCBF

The mean fasting CBF at each voxel was calculated from the pCASL1 scans of the water and meal visits, at both pre- and post-intervention visits in each IR subject. These were then subtracted from each other, to produce maps of the change in fasting CBF after the intervention, which were entered into a voxel-wise multiple regression model with HOMA-IR as a covariate of interest, and the respective post-intervention change in mean fasting global grey matter CBF used as a nuisance covariate. No

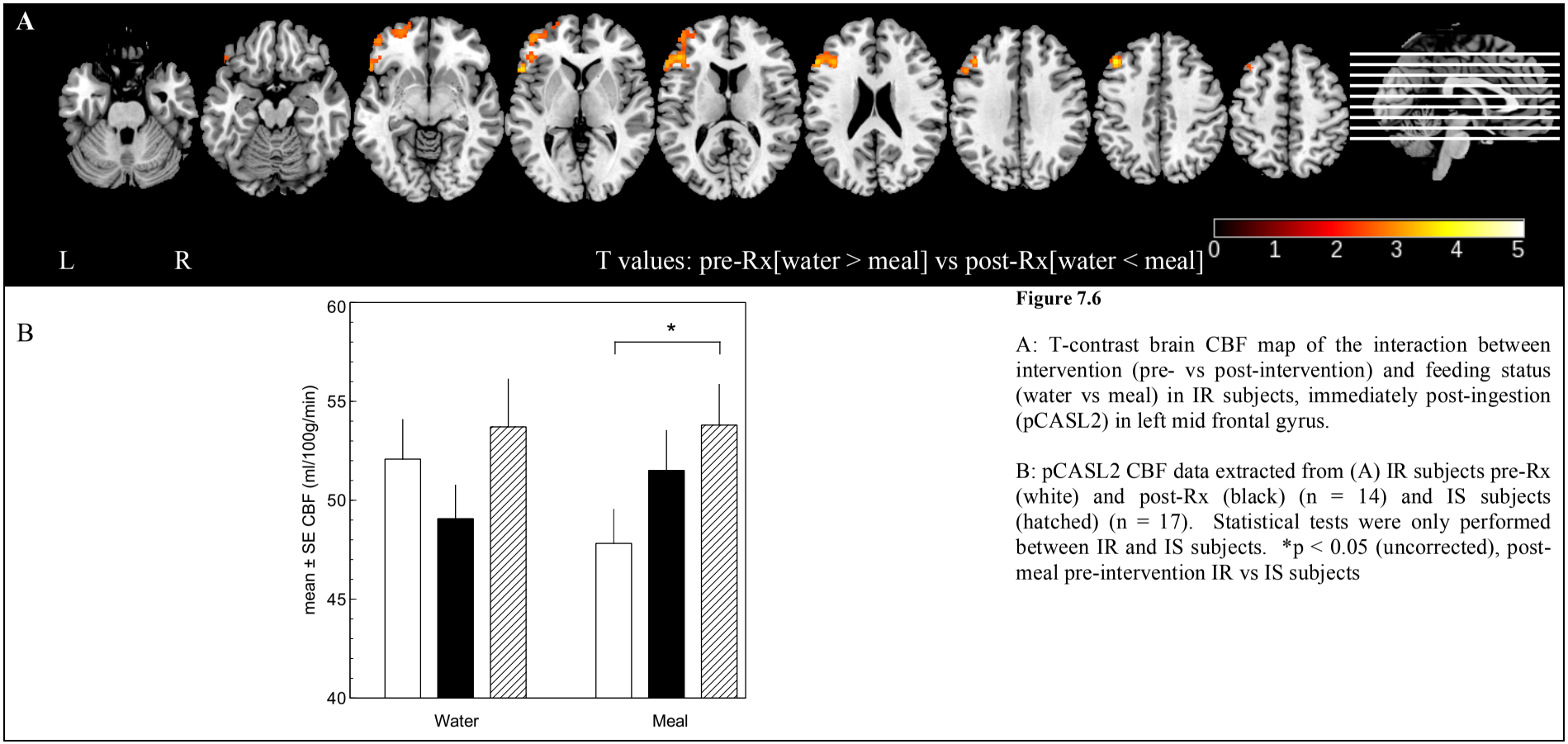

Figure 7.6

A: T-contrast brain CBF map of the interaction between intervention (pre- vs post-intervention) and feeding status (water vs meal) in IR subjects, immediately post-ingestion (pCASL2) in left mid frontal gyrus.

B: pCASL2 CBF data extracted from (A) IR subjects pre-Rx (white) and post-Rx (black) (n = 14) and IS subjects (hatched) (n = 17). Statistical tests were only performed between IR and IS subjects. *p < 0.05 (uncorrected), post-meal pre-intervention IR vs IS subjects

clusters demonstrating a significant association between change in HOMA-IR and change in fasting CBF were detected.

7.3.12 Correlation between post-intervention changes in insulin sensitivity and changes in post-water rCBF

Voxel-wise differences in pre- from post-intervention CBF within each time point (pCASL2, 3 and 4) after water ingestion were calculated for each subject, to produce maps of the change in post-water CBF after the intervention. These were submitted to similar separate voxel-wise multiple regression models, with HOMA-IR as a covariate of interest, and the respective post-intervention change in post-water global grey matter CBF at each time point used as a nuisance covariate. No clusters demonstrating a significant association between change in HOMA-IR and change in post-water CBF at any time point were detected.

7.3.13 Correlation between post-intervention changes in insulin sensitivity and changes in post-meal rCBF

Similar CBF maps representing the change in post-meal ingestion CBF at each time point following the intervention in each subject were constructed, and submitted to multiple regression analyses. Changes in the immediate post-meal ingestion rCBF (pCASL2) were positively associated with the change in HOMA-IR in right cerebellum (X=22, Y=-60, Z=-42, T-value 10.12, 1688 voxels, cluster $P_{FWE\text{-}corrected}$ =0.001) and negatively associated in left anterior cingulate (ACC) (X =-2, Y=34, Z=6, T-value 7.0, 1143 voxels, cluster $P_{FWE\text{-}corrected}$=0.01) (Figure 7.7A). There were no clusters showing significant associations between change in post-meal ingestion CBF at +8 to +14 mins (pCASL3) and change in HOMA-IR. However, the change in post-meal ingestion CBF at +34 to +40 mins (pCASL4) was negatively associated with the change in HOMA-IR in a cluster that included the right globus pallidum, putamen, caudate and hippocampus (X=20, Y=2, Z=0, T-value 12.8, 1588 voxels, cluster $P_{FWE\text{-}corrected}$=0.001) (Figure 7.7B). The rCBF data were extracted from these regions to examine the relationship between changes in rCBF and HOMA-IR after the intervention (Figure 8.7C), demonstrating that greater improvements in insulin sensitivity were associated with greater decreases in cerebellar rCBF and greater

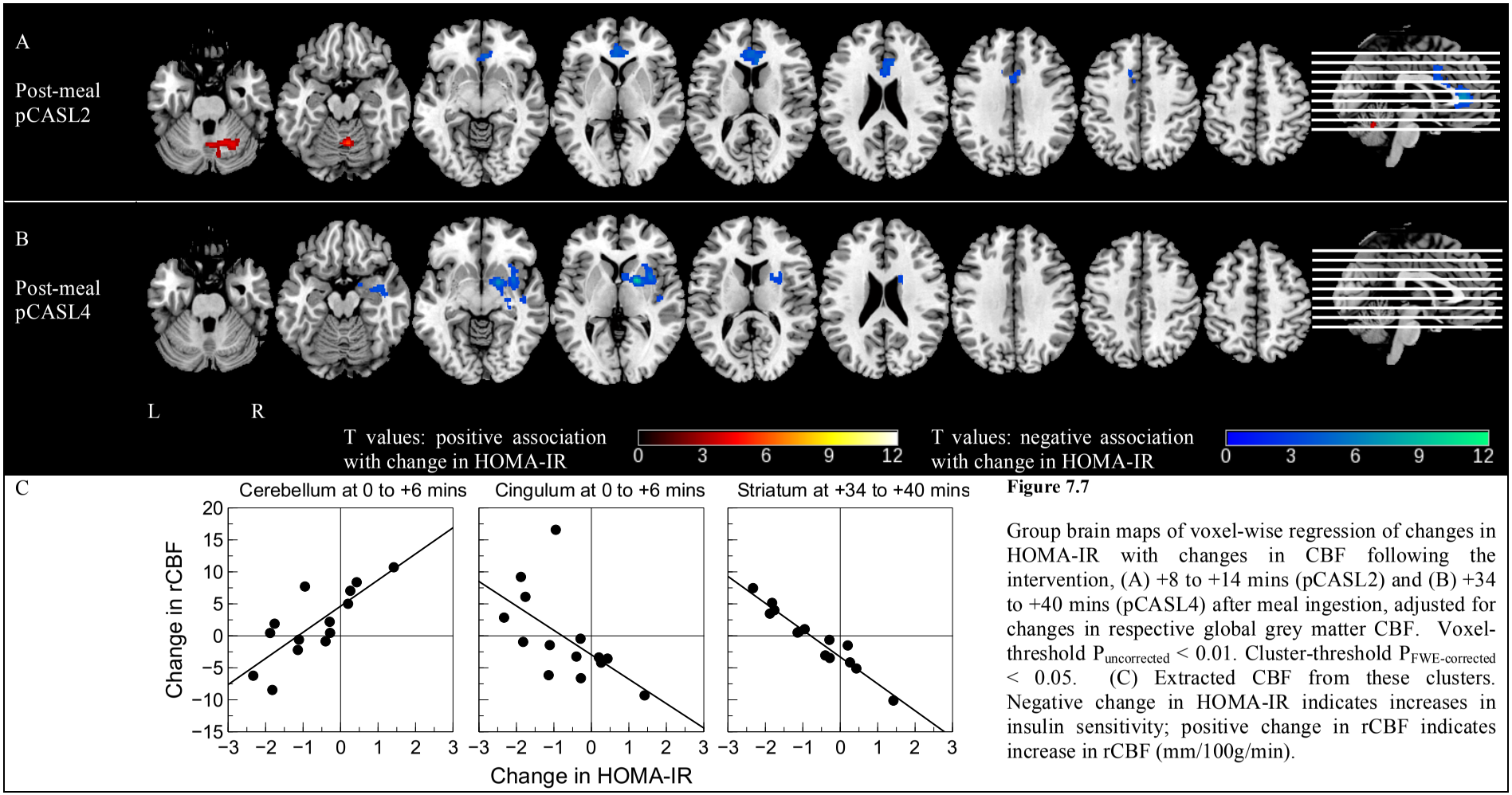

Figure 7.7

Group brain maps of voxel-wise regression of changes in HOMA-IR with changes in CBF following the intervention, (A) +8 to +14 mins (pCASL2) and (B) +34 to +40 mins (pCASL4) after meal ingestion, adjusted for changes in respective global grey matter CBF. Voxel-threshold $P_{uncorrected} < 0.01$. Cluster-threshold $P_{FWE\text{-}corrected} < 0.05$. (C) Extracted CBF from these clusters. Negative change in HOMA-IR indicates increases in insulin sensitivity; positive change in rCBF indicates increase in rCBF (mm/100g/min).

increases in anterior cingulate rCBF immediately after meal ingestion, and greater increases in later post-prandial (+34 to +40 mins) right striatal rCBF.

7.4 Discussion

This study set out to investigate the impact of an insulin sensitisation intervention, involving standard lifestyle advice as used in routine clinical practice in combination with metformin therapy, on brain responses to meal ingestion in healthy but insulin-resistant non-obese men. The intervention successfully improved glycaemic status and fasting indices of insulin sensitivity, without affecting body weight (consistent with the selection of insulin resistant participants of healthy body habitus), and changed regional brain responses to food ingestion.

7.4.1 Effect of insulin sensitisation on appetite

Surprisingly, *decreased* fullness sensation and *increased* desire for prospective eating in the fasted state were observed after the intervention. The incremental increase in the sensation of fullness occurred after the intervention period, irrespective of whether water or meal was consumed, suggesting an increase in satiation. This is in keeping with a previous study showing a three-day course of metformin therapy in women with diet controlled T2DM reduced subjective hunger and food consumption during an ad libitum meal (Lee and Morley, 1998).

7.4.2 Insulin sensitisation and fasting brain activity

These were accompanied by decreases in fasting activity of inferior temporal gyrus and increases in posterior fusiform gyrus activity at follow-up. These regions are implicated in visual processing but, as reviewed by Rosazza and Minati (2011) they are also recognised to be part of one of at least seven recognised "resting state networks" that have been identified in functional connectivity studies of BOLD fMRI to be spontaneously active at rest. Whilst the present study did not investigate the functional connectivity of brain regions, "static" measures of rCBF relative to the global mean CBF show spatial similarities to functional connectivity analyses of CBF

data in ASL studies (Zou *et al*, 2009). Given that the subjects did not have any specific tasks to perform during data collection, it is possible that the changes in activity as represented by changes in CBF after the intervention may reflect changes in the connectivity of these resting state visual processing networks.

7.4.3 Insulin sensitisation and post-water lateral OFC activity

Cortical activity increased in post-central gyrus and decreased in angular and mid-frontal regions including right lateral OFC after water ingestion following the intervention, with exploratory analyses suggesting the changes in activity in the latter region were towards that observed in IS men. In Chapter 5, greater food restraint was reported in IR than IS subjects and was positively associated with HOMA-IR, a construct that has been proposed to aid weight loss in obesity (Johnson *et al*, 2012), but may be detrimental in normal weight through disinhibited eating if cognitive restraint is no longer sustained (Stunkard and Messick, 1985). The lateral OFC and DLPFC provide inhibitory control of eating behaviour (Hollmann *et al*, 2012; Small *et al*, 2001); whilst data on eating behaviours were not re-collected following the intervention, the reduction in lateral OFC activity during a continued fasted state may represent a reduction in active food restraint. Unlike the data from the cross-sectional study (Chapter 5), where the cerebral effects of systemic insulin resistance were similar in the fasted state and after water ingestion, the effect of the intervention on cerebral activity in the fasted state and after water ingestion were different. It was originally assumed that water ingestion represents a continued fasted state, with static effects on cerebral activity during the post-ingestion observation period as observed pre-intervention, so the above observations may represent a dynamic effect of the intervention on continued fasting, or be a response to the consumption of water. However, no regions were identified in which changes in fasting (or post-water) activity were associated with changes in insulin sensitivity following the intervention. This may have been due to lack of power, with two subjects from the original IR cohort not taking part in the interventional arm of the study, or due to the intervention having greatest impact on post-prandial brain activity, when insulin secretion increases.

7.4.4 Insulin sensitisation and post-meal insula, lateral OFC, ACC and striatal activity

The main effect of insulin sensitisation on post-prandial brain activity was a reduction in left insula activity across the post-meal observation period, approaching that of the IS subjects. This may reflect an improvement in interoceptive processing of the sensation of fullness and satiation (Frank *et al*, 2013), supported by the greater post-ingestion fullness observed after the intervention. The differential effects of the intervention to increase left mid-frontal gyrus (lateral OFC, DLPFC and ventrolateral prefrontal cortex) activity immediately after meal compared to water ingestion were not sustained during the remainder of the observation period, which may reflect an immediate and short-lived response to terminate meal ingestion (Hollmann *et al*, 2012; Small *et al*, 2001). Correlation analyses indicated that larger decrements in HOMA-IR were associated with greater increments in activity in the immediate post-prandial period in ACC and ~30 mins later in the striatum following insulin sensitisation. Post-prandial ACC activity has been shown to correlate with fullness, independent of oral stimulation from a chocolate milk drink (Spetter *et al*, 2014), and this early relationship between improvements in insulin sensitivity and post-prandial activity may also reflect greater satiation. Unlike the ACC, post-prandial striatal activity appears to be more dependent on the oral stimulation from meal (Spetter *et al*, 2014). Thus, the later association between improvements in insulin sensitivity and post-prandial striatal activity may reflect greater meal-related reward processing derived from the act of eating.

My data are compatible with studies in other insulin resistant states. As discussed in Chapter 1, a series of BOLD fMRI studies in adolescent females showed consummatory responses to food are positively correlated with BMI in insula and operculum, and negatively correlated in caudate (Stice *et al*, 2008), and that weight gain over a 6 month period is associated with a concurrent fall in caudate responses to milkshakes (Stice *et al*, 2010). Elevating circulating insulin changes MR-spectroscopic estimates of frontal and temporal metabolites in insulin sensitive but not insulin resistant men (Karczewska-Kupczewska *et al*, 2013), whilst [^{18}F]FDG-PET studies have shown diminished increases in glucose metabolism in ventral striatal and prefrontal cortex (including insula and ACC) evoked by physiological concentrations

of circulating insulin in insulin resistant men, with similar diminution of insulin-evoked increases in global cerebral glucose metabolism (Anthony *et al*, 2006). A [^{18}F]FDG-PET study of elderly volunteers with pre-diabetes or established T2DM also showed increasing insulin resistance, as defined by HOMA-IR, was associated with reduced fasting cerebral glucose metabolism in posterior cingulate, precuneus, parietal cortex, temporal/angular gyri and anterior and inferior prefrontal cortex (Baker *et al*, 2011), whilst greater availability of striatal D2 receptors with decreasing insulin sensitivity has been shown in a combined group of lean and obese volunteers with [^{18}F]fallypride-PET, thought to be in response to diminished dopamine availability (Dunn *et al*, 2012b). The results of the present study extend these observations by demonstrating in younger, healthy, non-obese men with systemic insulin resistance, at high risk of future T2DM, improvements in satiation with a reversal of the exaggerated consummatory responses in regions that process interoceptive awareness, and an augmentation of post-prandial reward centre activity following metformin therapy and lifestyle changes, suggesting that altered satiation processing in these dopaminergic networks exists and is receptive to insulin sensitisation interventions in insulin resistant conditions, before obesity ensues.

Few studies to date have investigated the effect of insulin sensitisation interventions on brain activity in man. In an observational [^{18}F]FDG-PET study, glucose metabolism in metformin-treated patients with T2DM was greater in the white matter of the right temporal, right frontal and left occipital lobes and lower in left parahippocampal gyrus, left fusiform gyrus and right ventromedial prefrontal cortex and medial frontal gyrus, compared to metformin-naïve patients following a 6 hour fast (Huang *et al*, 2014). However, measures of insulin resistance were not reported and circulating glucose levels were not controlled for during data acquisition. As HbA1c levels were non-significantly lower in the metformin naïve group, differences in ambient glucose may have affected cerebral glucose metabolic rates. A cross-sectional [^{15}O]H_2O-PET study showed lean women and women who were previously obese but now lean following lifestyle changes had significantly greater post-prandial rCBF in left DLPFC than obese women, consistent with my observations immediately after meal ingestion (Le *et al*, 2007). Although insulin resistance was not formally measured, fasting insulin levels were significantly greater in the obese compared to comparable levels observed in the two lean groups, fasting glucose levels being

similar in the three groups, in keeping with normalised insulin sensitivity and cerebral metabolism following lifestyle intervention. Recent functional connectivity BOLD fMRI studies suggest increasing insulin resistance, independent of BMI, is associated with increasing fasting connectivity of the left OFC in a prefrontal resting state network, in the right putamen in a basal ganglia resting state network (Kullmann *et al*, 2012) and in the left ventral striatum with the left anterior insula and anterior mid-cingulate cortex (Ryan *et al*, 2012). Six months exercise intervention in overweight and obese adults reduced fasting connectivity of the precuneus part of the default mode network (McFadden *et al*, 2013), whilst obese children undertaking 8 months aerobic exercise intervention compared to sedentary attention control activities reduced connectivity of the occipital gyrus, superior temporal gyrus and posterior cingulate cortex parts of the default mode network, the cingulate and precuneus parts of the cognitive control resting state network, and within the motor resting state network decreased cuneus connectivity and increased medial, superior and middle frontal gyri connectivity (Krafft *et al*, 2014). Insulin sensitivity was not reported in these intervention studies but it is likely to have improved. Interestingly, the acute effects of a single 25 minute session of aerobic exercise in healthy adults include reductions in hippocampal and insula rCBF as measured by pCASL MRI (MacIntosh *et al*, 2014). Together, these studies may suggest in the fasted state there is a greater recruitment of corticolimbic reward networks including OFC, striatum and insula in insulin resistant conditions, which normalise with interventions that improve systemic insulin sensitivity. The post-prandial responses in reward processing (striatum) and inhibitory control (DLPFC, lateral OFC) centres that may be necessary for satiation signalling may be diminished in insulin resistance, and the effect of insulin sensitisation strategies on such responses have not been characterised until now.

As discussed in Chapters 1 and 2, haemodynamic responses detected with pCASL fMRI and other neuroimaging techniques act as surrogate markers of neuronal activity and changes in rCBF observed following the intervention in the present study are assumed to represent changes in neuronal activity, but may also reflect current cerebrovascular status, and it is conceivable that insulin sensitisation may elicit circulatory effects. A study of patients with T2DM randomised to receive 12 months pioglitazone and gliclazide therapy showed significant improvements in insulin resistance and transcranial Doppler pulsatility indices of middle cerebral and basilar

arteries, unlike those receiving gliclazide alone, despite equivalent improvements in HbA1c (Park *et al*, 2007). This suggests that the improvements in vascular resistance with pioglitazone may have been due to improved insulin sensitivity rather than glycaemic status, although effects on regional cerebral perfusion were not examined. Obese Zucker rat models of the metabolic syndrome have demonstrated reduced density of cortical microcirculation, which is improved with insulin sensitisation by either metformin or rosiglitazone (Chantler *et al*, 2015). Experimental pre-clinical models of cerebral ischaemia have shown metformin reduces post-ischaemic inflammatory responses and disruption of the blood brain barrier, increases neuronal autophagy and neurogenesis, enhances neuronal firing, decreases reactive hyperaemia and blood flow during post-ischaemic reperfusion, increases cerebral angiogenesis and reduces infarct size through mechanisms dependent on AMP-kinase activation (Farbood *et al*, 2015; Jiang *et al*, 2014; Jin *et al*, 2014; Liu *et al*, 2014; Venna *et al*, 2014), suggesting protective effects at both neuronal and vascular levels, with observational data from population-based registries showing metformin may prevent stroke (Cheng *et al*, 2014) and reduce 30 day mortality in diabetic patients compared to sulphonylureas (Horsdal *et al*, 2012) providing early clinical support. Although these latter findings are in the context of hypoxia-driven neurocirculatory changes, similar effects may be at play in the preclinical models of the central effects of insulin sensitisation in metabolic syndrome (Chantler *et al*, 2015), and in the present study. It is not possible to determine if the observations from the present study represent changes in neuronal activity alone, changes in cortical vascularity and/or vascular responsiveness to meal ingestion with insulin sensitisation. Longitudinal studies after withdrawal of such interventions and pre-clinical studies are therefore needed to characterise the mechanisms involved.

7.4.5 Limitations and conclusions

The intervention was successful in improving measures of systemic insulin sensitivity in the group as a whole. As expected, the response to the intervention as measured by HOMA-IR showed considerable inter-individual variation, but the limitations of HOMA-IR as an individual measure of insulin sensitivity have been discussed. However, the significant improvement in HbA1c is indicative of the efficacy of the intervention, and the observation that the magnitude of improvements in insulin

sensitivity was associated with changes in post-prandial striatal activity following the intervention circumvents to some extent the limitation of the lack of a placebo, and supports the hypothesis that the activity of central reward pathways in early insulin resistance may respond to attempts to improve early systemic insulin resistance. Incomplete blood sampling prevents further interrogation of the neurohumoral effect of the intervention. The eating behaviour questionnaires used during the screening process were not used again after the intervention, which may have helped deconstruct the changes in attitudes and eating behaviour constructs following insulin sensitisation. Nevertheless, the present study provides early evidence that an insulin sensitisation intervention in healthy men with systemic insulin resistance can improve appetite and change corticolimbic network processing of satiation towards that observed in insulin sensitive men.

Table 7.1

Subject characteristics

Mean±SD	Pre-Rx	Post-Rx	p
Weight (kg)	82.52±10.92	81.04±10.79	0.203
BMI (kg/m2)	25.99±2.45	25.53±2.48	0.197
Waist circumference (cm)	91.79±7.58	90.79+7.37	0.364
Neck circumference (cm)	39.57±2.06	39.21±1.85	0.431
SBP (mmHg)	128.5+12.3	130.0±11.8	0.656
DBP (mmHg)	76.9±10.0	79.9±6.1	0.201
HbA1c (%)	5.5±0.3	5.3±0.3	0.010
Leptin (mcg/L)	5.61±2.50	5.58±2.70	0.948
Adiponectin (mcg/L)	5052.84±1443.45	5514.96±2133.69	0.335
HOMA-IR	2.98±0.67	2.33±0.89	0.045
HOMA2-IR	1.72±0.33	1.34±0.46	0.020

Table 7.2

Voxel-wise T contrasts comparing pre-intervention (Pre-Rx) with post-intervention (Post-Rx) CBF in insulin resistant subjects (Figure 7.4)

		MNI coordinates						
Contrast / Brain area	Hemisphere	X	Y	Z	T scores	No. voxels	Cluster $P_{FWE\text{-}corr}$	Brodmann area
ASL1 Pre-water/meal: Pre-Rx > Post-Rx								
Inferior temporal gyrus	Right	60	-40	-26	4.47	2984	< 0.001	20, 21
ASL1 Pre-water/meal: Pre-Rx < Post-Rx								
Fusiform gyrus	Left	-32	-52	-2	4.73	3314	< 0.001	37, 19
Fusiform gyrus	Right	28	-78	-10	3.87	1284	0.015	19, 18
ASL2-4 Post-water: Pre-Rx > Post-Rx								
Angular gyrus	Left	-56	-60	26	4.18	1077	0.035	39, 42
Middle frontal gyrus	Left	-26	12	60	3.87	1608	0.004	8, 6
Angular gyrus	Right	58	-54	30	3.86	1308	0.014	40, 39
Middle frontal gyrus	Right	44	42	8	3.73	1770	0.002	45, 47
ASL2-4 Post-water: Pre-Rx < Post-Rx								
Post-central gyrus, Rolandic operculum	Left	-30	-28	50	5.12	1248	0.017	3
ASL2-4 Post-meal: Pre-Rx > Post-Rx								
Insula	Left	-40	2	-6	4.00	1041	0.041	48, 20
ASL2-4 Post-meal: Pre-Rx < Post-Rx								
No significant clusters								

Table 7.2 continued

Contrast / Brain area	Hemisphere	MNI coordinates X	Y	Z	T scores	No. voxels	Cluster $P_{FWE\text{-}corr}$	Brodmann area
ASL2-4 Feeding status x Treatment interaction								
No significant clusters in either direction								
ASL2 Feeding status x Treatment interaction [Pre-Rx: Post-water > Post-meal] vs [Post-Rx: Post-water < Post-meal]								
Middle frontal gyrus	Left	-40	28	40	3.97	1765	0.002	46, 37, 38
ASL2 Feeding status x Treatment interaction [Pre-Rx: Post-water < Post-meal] vs [Post-Rx: Post-water > Post-meal]								
No significant clusters								
ASL3 Feeding status x Treatment interaction								
No significant clusters in either direction								
ASL4 Feeding status x Treatment interaction								
No significant clusters in either direction								

8 Impact of insulin sensitisation on central responses to food cues after meal and water ingestion in systemic insulin resistance

8.1 Introduction

In Chapter 6, I described modulatory effects of recent meal ingestion on corticolimbic responses to external food cues, reducing neuronal activation to high-calorie food images and increasing activation to low-calorie food images in insulin sensitive (IS) men, which were absent in insulin resistant (IR), non-obese, non-diabetic men. The brain regions exhibiting these effects of systemic insulin resistance were left dorsolateral prefrontal cortex (DLPFC), which provides higher executive control of eating behaviour, striatum, implicated in processing the motivational salience and reward of food, and lingual gyrus, which directs visual attention to food cues. I hypothesised that the inability of these regions to modify their responses appropriately to external sources of food in the context of current nutritional and energy status may predispose the IR individual to future weight gain through dysregulated eating patterns, permitting continued eating beyond current physiological requirements. My hypothesis is supported by other human and animal data that suggest systemic insulin resistance is associated with cerebral resistance to potential satiety-inducing effects of circulating insulin, and may provide a mechanistic explanation for this hypothesis. In Chapter 7, I showed that systemic insulin sensitisation of IR subjects reduced hunger and altered the insula response to satiation, a region that processes interoceptive awareness, striatal reward centres, and lateral OFC and anterior cingulate centres which provide inhibitory control to terminate a meal. This chapter describes the cerebral effects of the intervention on the modulatory effects of meal ingestion on cerebral responses to food cues, to investigate the potential reversibility of the abnormal responses seen in systemic insulin resistance.

8.2 Methods

8.2.1 Subjects

The IR subjects are described in section 7.2.1.

8.2.2 Study protocol

The intervention has been described in section 7.2.2. In brief, consenting subjects received 3 months of open-label metformin (Glucophage SR, Merck Serono) in an escalating dose regimen, combined with personalised dietary advice from a registered specialist dietitian. At the end of the intervention period, subjects underwent the same study protocol described in Chapters 5-6, with MRI acquisition details as described in section 2.8, the order of scan visits balanced across the group by block randomisation. The order of the playlists of images (each containing pseudorandomised order of high calorie (HiCal), low calorie (LoCal), object (OBJ) and blurred (BLU) images) was also randomised. HOMA2-IR and HOMA-IR were calculated from fasting blood taken at the screening visit, and after the intervention on the morning of the follow-up scan, after an initial 15 mins rest period, followed by a further 15 mins rest after intravenous cannulation.

8.2.3 Biochemical analysis

Laboratory methods are described in sections 2.8.14 and 7.2.3.

8.2.4 Statistical analyses

General non-imaging statistical methods are described in section 2.8.14. Mean hunger scores for each feeding status/image class combination were calculated as described in section 6.2.3 and analysed using a 3-way repeated-measures ANOVA, with intervention (2 levels: pre-Rx vs post-Rx), feeding status (2 levels: meal vs water) and image class (4 levels: high calorie foods [HiCal], low calorie foods [LoCal], objects [OBJ] and blurred [BLU] images) as factors.

Subject-level BOLD image pre-processing and statistical methods, and within-group analyses used to examine the post-intervention data in isolation are described in detail

in section 2.8.13.3 and section 6.2.3. The interaction effect of feeding condition and intervention (pre-treatment vs post-treatment) on the median effect size for high-calorie and low-calorie food images and blurred images with the time series for object images as the baseline ([HiCal/OBJ], [LoCal/OBJ], [BLU/OBJ]) and HiCal vs LoCal [HiCal/LoCal] BOLD signal contrasts at each voxel were computed and compared to a null distribution derived by permutation of feeding status and treatment using factorial ANOVA. Voxel-level Pearson product moment correlation coefficients were calculated to examine the association between change in HOMA-IR and change in post-water BOLD signal for the above image contrasts pre- vs post-intervention (after performing voxel-wise subtraction of pre-intervention from post-intervention effect size evoked by each contrast), and between the change in HOMA-IR and change in incremental post-meal BOLD signal contrast pre- vs post-intervention (after performing voxel-wise subtraction of post-water from post-meal effect size evoked by each contrast within each intervention phase, which are then subtracted from each other), compared to a null distribution derived by permutation of the change in HOMA-IR. All group activation maps were thresholded to yield <1 false positive cluster per map (equivalent *p* values are listed in each results table), at a voxel-wise threshold of $p<0.05$ (Bullmore *et al*, 1999) (section 2.11.4). Talairach daemon was used to identify the regions of detected voxels anatomically (Lancaster *et al*, 2000).

8.3 Results

8.3.1 Subject characteristics

The effect of insulin sensitisation on subject biometric parameters is described in section 7.3.1.

8.3.2 Hunger responses to visual stimuli

The repeated-measures ANOVA of all pre- and post-intervention hunger scores in the 14 IR subjects showed a significant main effect of feeding on the mean hunger scores collected after viewing each class of visual images (main effect of feeding, $F(1,13)=17.571$, $p=0.001$, estimated marginal mean: Water: 70.1±4.5, Meal: 47.5±4.7), with the meal reducing hunger (Figure 8.1). There was also a significant difference in the hunger evoked by each class of images (main effect of visual image,

F(1.150, 14.951)=14.357, p=0.001). Post-hoc (Bonferroni corrected) comparisons showed no differences in hunger elicited by high- and low-calorie food images, which were both greater than that elicited by object (mean difference 11.1±2.9, p=0.011 and 11.5±2.7, p=0.005, respectively) and blurred images (9.4±2.8, p=0.03 and 9.8±2.7, p=0.014, respectively), with hunger elicited by blurred images being slightly greater than that after object images (1.7±0.5, p=0.022), irrespective of the intervention. There were no significant interactions between meal and stimulus (feeding status x stimulus, F(1.764, 22.928)=1.367, p=0.273). Insulin sensitisation did not alter hunger responses to any of the images (main effect of intervention, F(1,13)=0.030, p=0.866); intervention x feeding, F(1,13)=2.169, p=0.165; intervention x stimulus, F(1.5,19.3)=0.418, p=0.604; intervention x feeding x stimulus, F(1.6,20.2)=0.211, p=0.756), with no significant associations between the respective changes after the intervention in HOMA-IR and in hunger scores evoked by the different image categories in any condition.

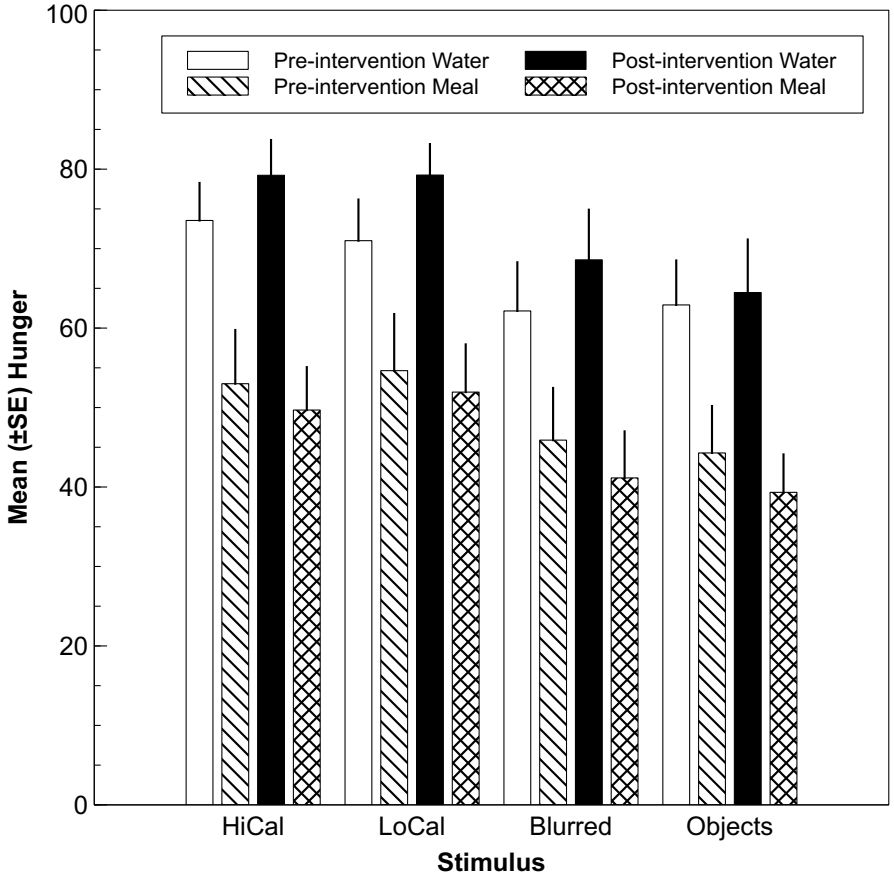

Figure 8.1

Hunger responses to visual stimuli. Mean hunger scores evoked after viewing blocks of high-calorie (HiCal) and low-calorie (LoCal) food images, object and blurred images.

8.3.3 Effect of meal ingestion on brain responses to visual food stimuli in insulin resistant subjects post-intervention

Voxel-wise ANOVAs examining the impact of meal vs water ingestion on [HiCal/OBJ]-, [LoCal/OBJ]- and [BLU/OBJ]-evoked BOLD signal contrasts in IR subjects within the post-intervention state were performed (Table 8.1). The meal converted a deactivation to an activation response in a cluster that included left DLPFC and insula on viewing high-calorie food images (Figure 8.2A), in the left ventrolateral prefrontal cortex (VLPFC) to low-calorie food images (Figure 8.2B) and a similar region that extended to the left orbitofrontal cortex (OFC) to blurred images (Figure 8.2C), with some spatial overlap in these three inferior frontal gyrus clusters identified for each contrast. A factorial ANOVA examining differences in the effect of feeding status on [HiCal/OBJ] vs [LoCal/OBJ]-evoked BOLD signal contrasts did not show a significant effect of meal ingestion on the differential response to high- compared to low-calorie food images.

8.3.4 Effect of systemic insulin sensitisation on brain responses to food images in insulin resistant subjects after water ingestion

Next, voxel-wise ANOVAs examining the effect of the intervention compared to the pre-intervention state on [HiCal/OBJ]-, [LoCal/OBJ]- and [BLU/OBJ]-evoked BOLD signal contrasts in the fasted (post-water ingestion) state were performed (Table 8.2). The intervention converted similar activation responses to both high- (Figure 8.3A) and low-calorie (Figure 8.3B) food images to a deactivation in a cluster in the right insula that extended to right lateral OFC, whilst it converted the activation response to blurred images to a deactivation in right precuneus (Figure 8.3C). A two-way repeated measures factorial ANOVA examining differences between [HiCal/OBJ]- and [LoCal/OBJ]-evoked BOLD signal contrasts, before and after the intervention, did not identify any significant clusters where the intervention altered the differential response to high- compared to low-calorie food images.

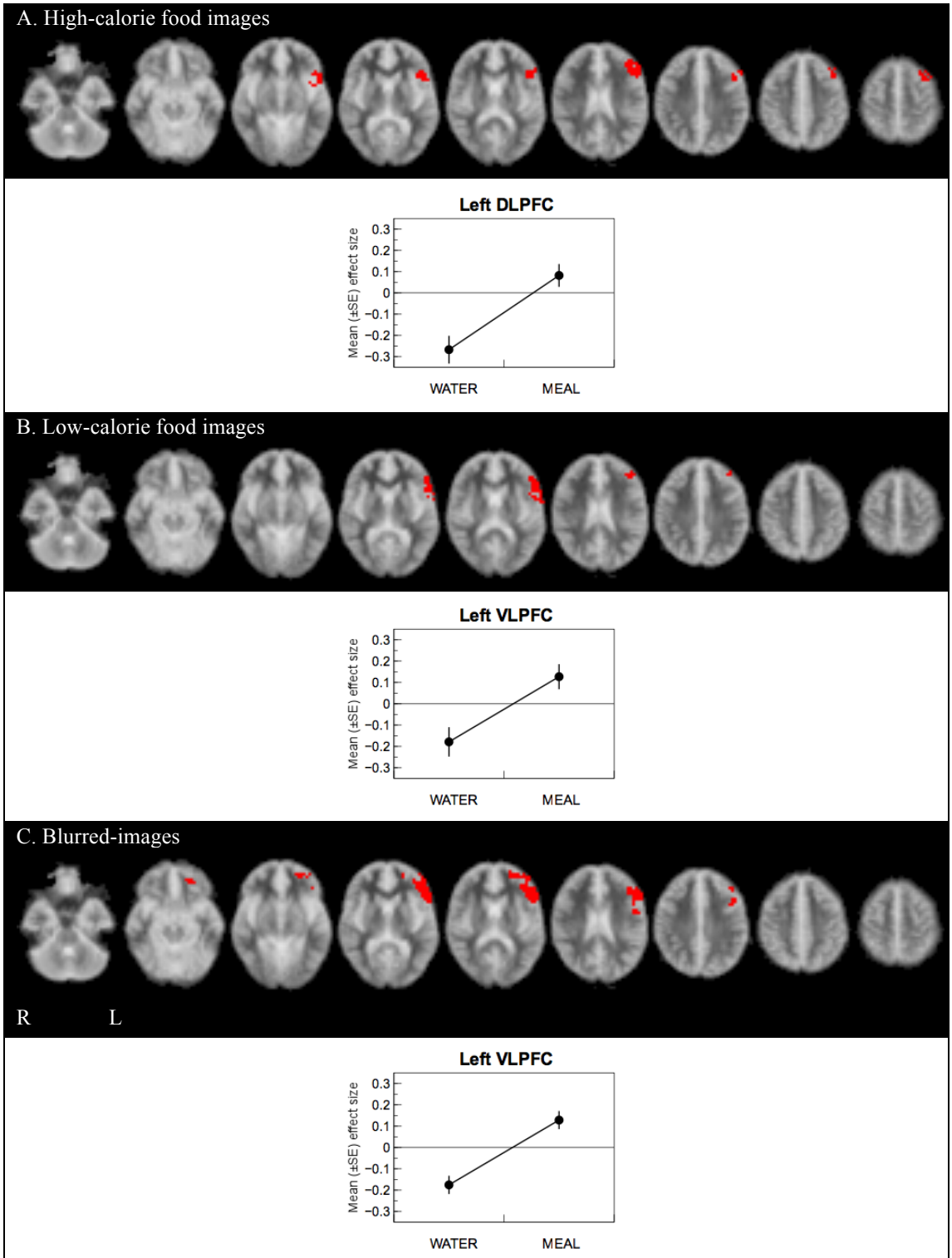

Figure 8.2

Voxel-wise ANOVA of the effect of meal ingestion on brain responses to visual cues in IR subjects after the intervention. Group activation brain maps show clusters with greater (red) or lesser (blue) BOLD signal contrast evoked by (A) high- and (B) low-calorie food and (C) blurred images after meal compared to water ingestion (object image-evoked time series as baseline, voxel-wise $p < 0.05$, cluster-wise $p < 0.02$) with extracted effect size (% BOLD signal change) from each cluster (positive values: activation i.e. food or blurred images > object images).

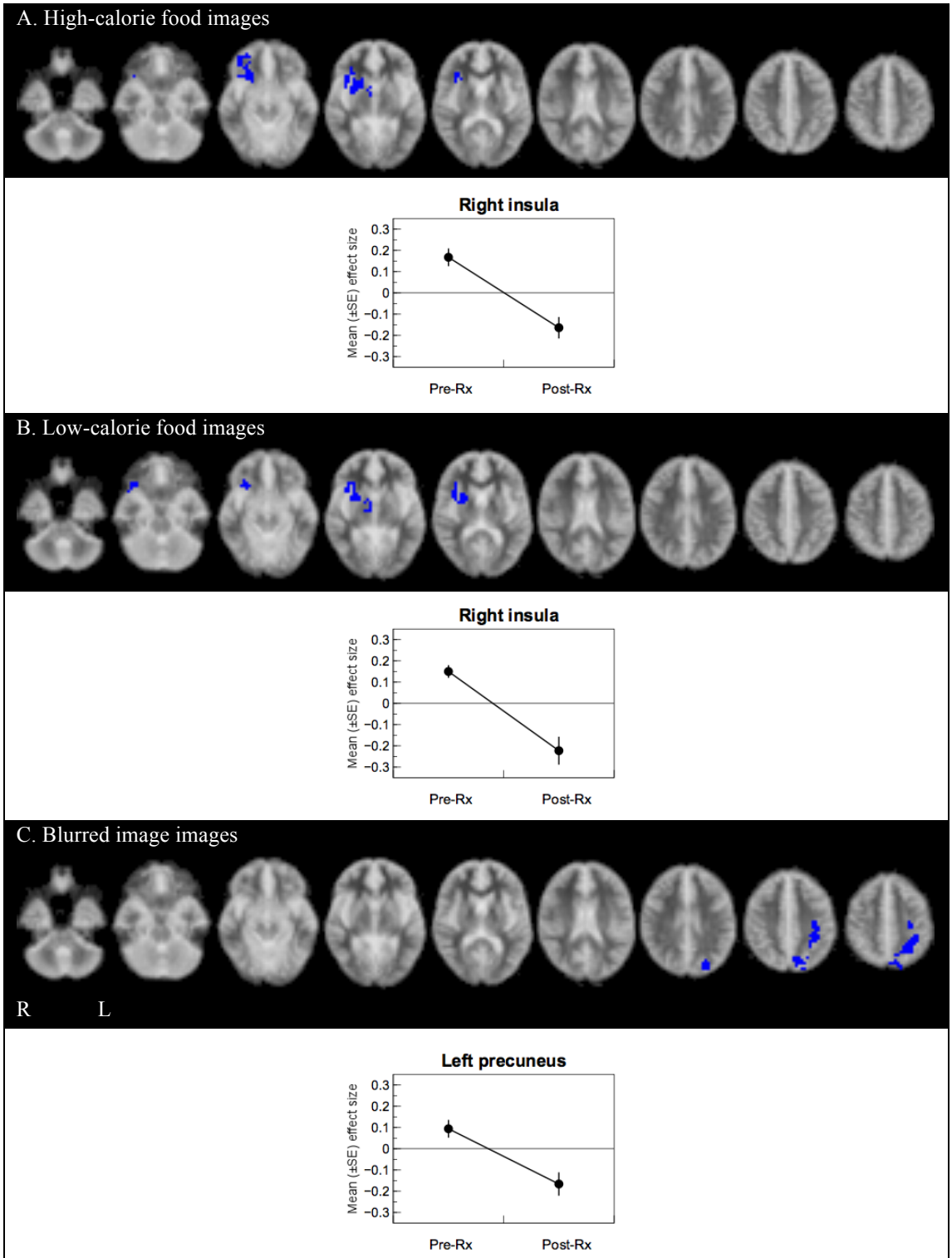

Figure 8.3

Voxel-wise ANOVA of brain responses to visual cues after water ingestion, before (Pre-Rx) vs after (Post-Rx) insulin sensitisation in IR subjects. Group activation brain maps show clusters where BOLD signal contrast evoked by (A) high and (B) low calorie food and (C) blurred images decreased after the intervention (object image-evoked time series as baseline, voxel-wise $p < 0.05$, cluster-wise $p < 0.01$) with extracted effect size (% BOLD signal change) from each cluster (positive values: activation i.e. food or blurred images > object images).

8.3.5 Effect of systemic insulin sensitisation on the modulatory impact of meal ingestion on brain responses to food images in insulin resistant subjects

Voxel-wise factorial ANOVAs examining the interaction between the intervention and feeding status were then performed for [HiCal/OBJ]-, [LoCal/OBJ]- and [BLU/OBJ]-evoked BOLD signal contrasts to determine whether there were specific changes following the intervention in the effect of meal compared to water ingestion on the cerebral response to the visual stimuli (Table 8.3). After the intervention, meal ingestion converted a deactivation to an activation response to high-calorie food images in left inferior parietal lobule (Figure 8.4A), and to low-calorie foods in left VLPFC (inferior frontal gyrus) and DLPFC (middle frontal gyrus) (Figure 8.4B), opposite to the deactivating effect of the meal before the intervention. Conversely, a relatively activating effect of the meal was converted to a deactivating effect after the intervention on the response to low-calorie foods in left middle temporal gyrus and right pre-motor cortex (middle frontal gyrus) (Figure 8.4B). The intervention also converted an activating effect of the meal to one of deactivation in left cerebellum, and a deactivating effect of the meal to one of relative activation in right middle temporal gyrus on the response to blurred images (Figure 8.4C). In order to examine possible changes following the intervention of the impact of meal ingestion on differential responses to high- compared to low-calorie food images, the evoked [LoCal/OBJ] BOLD signal contrast was subtracted at each voxel from that of the [HiCal/OBJ], before being entered into a two-way repeated measures factorial ANOVA. No significant interaction effects were observed.

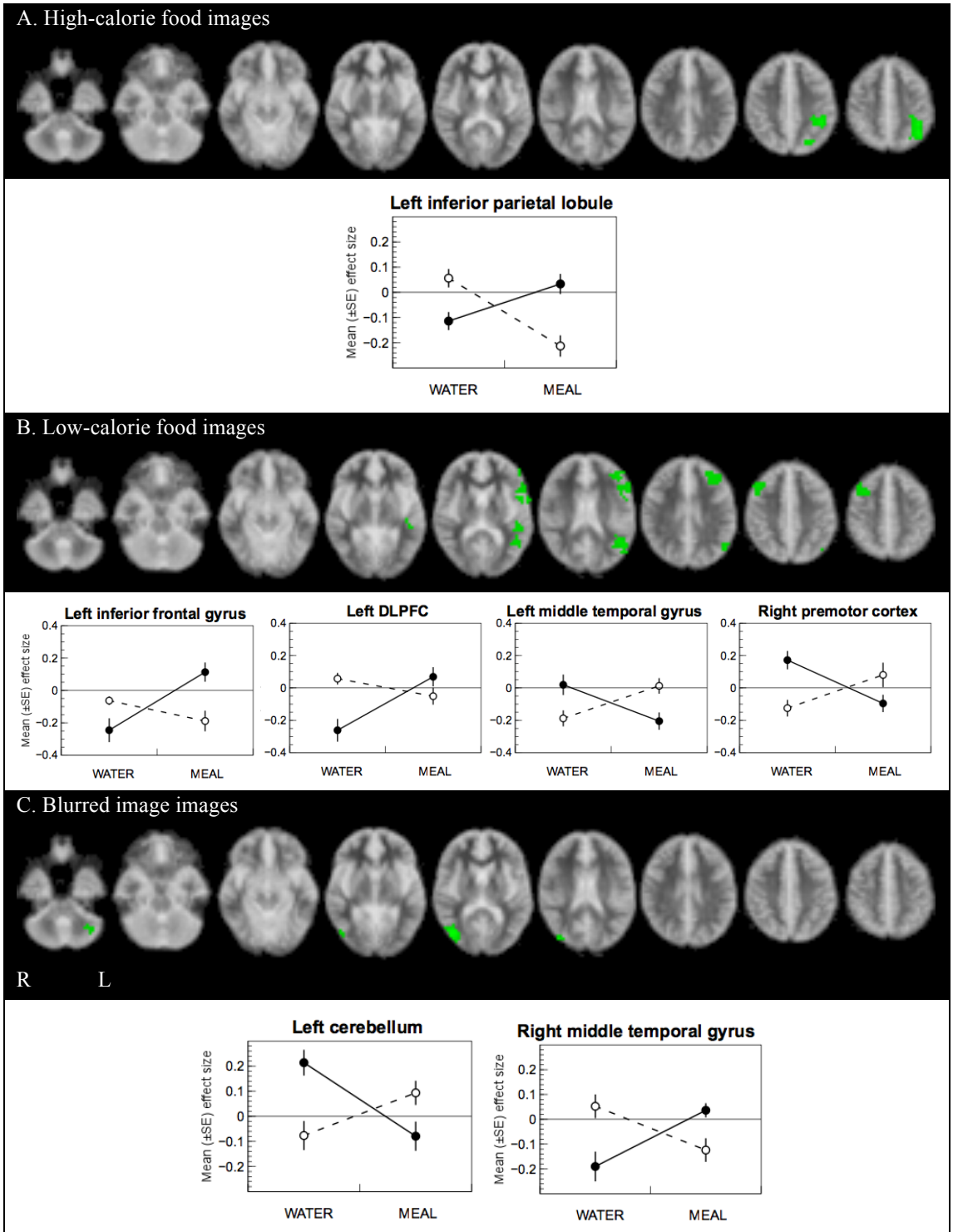

Figure 8.4

Voxel-wise ANOVA of brain responses to visual cues after meal compared to water ingestion, before compared to after systemic insulin sensitisation in IR subjects. Group activation maps show meal status x intervention interactions in BOLD signal contrast evoked by (A) high and (B) low calorie food and (C) blurred images (object image-evoked time series as baseline, voxel-wise $p < 0.05$, cluster-wise $p < 0.02$) with extracted effect size (% BOLD signal change) from each cluster (positive values: activation [food/blurred images > object images]) before (dashed line) and after (solid) the intervention. DLPFC = dorsolateral prefrontal cortex.

8.3.6 Association between changes in insulin sensitivity and in post-water ingestion brain responses to food images after insulin sensitisation intervention

Maps of the change in fasted (post-water) [HiCal/OBJ]-, [LoCal/OBJ]-, [BLU/OBJ]- and [HiCal/LoCal]-evoked BOLD signal contrasts following the intervention were produced by voxel-wise subtractions of BOLD signal pre-intervention from the respective signal post-intervention for each subject. Voxel-level Pearson product moment correlation coefficients of these "difference" maps were then calculated to examine possible linear associations between respective changes in HOMA-IR and fasting (post-water ingestion) BOLD signal for each contrast following the intervention (Table 8.4). There were no significant associations between changes in insulin sensitivity and changes in response to high-calorie food or blurred images after the intervention. However, changes in HOMA-IR were correlated with changes in response to low-calorie food images in left thalamus and left lateral OFC (inferior frontal gyrus) following the intervention, with greater improvements in insulin sensitivity associated with reductions in [LoCal/OBJ]-evoked BOLD signal contrast in the former and increases in signal contrast in the latter (Figure 8.5A). The differential response to high- compared to low-calorie food images was found to decrease as insulin sensitivity improved in the left medial OFC after the intervention (Figure 8.5B).

A. Low-calorie foods images after water: correlation between changes in BOLD signal with changes in HOMA-IR

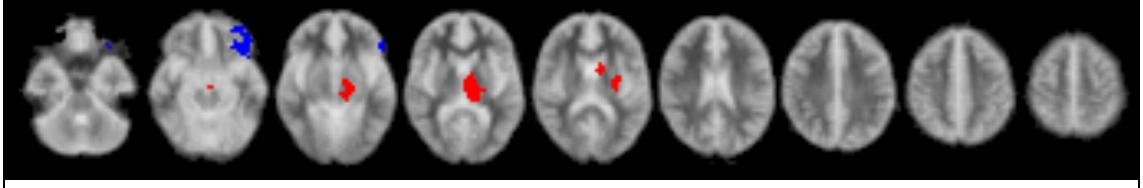

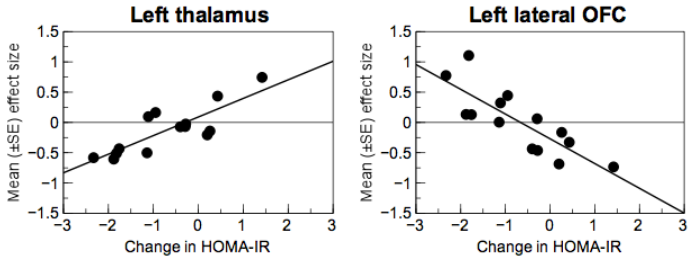

B. High- vs low-calorie food images after water: correlation between changes in BOLD signal with changes in HOMA-IR

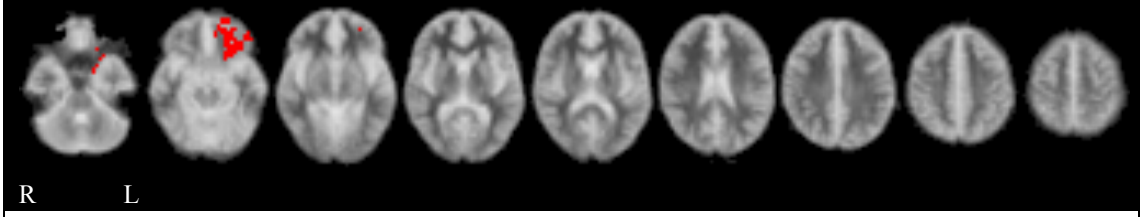

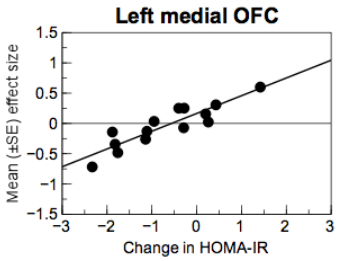

Figure 8.5

Group map of whole-brain correlation of changes in post-water activation with changes in HOMA-IR after systemic insulin sensitisation, showing clusters exhibiting linear positive (red) or negative (blue) correlation of respective changes in HOMA-IR with changes in BOLD signal after the intervention evoked by (A) low-calorie food images (object image time series as baseline) and (B) high- vs low-calorie food image-evoked BOLD signal (voxel-wise $p < 0.05$, cluster-wise $p < 0.01$) with extracted effect size (% BOLD signal change, positive values: post- > pre-intervention). OFC = orbitofrontal cortex. Negative change in HOMA-IR indicates improvements in insulin sensitivity.

8.3.7 Association between changes in insulin sensitivity and in incremental brain responses to food images after meal ingestion following the intervention

Voxel-wise subtractions of BOLD signal after water from the respective signal after the meal, within pre- and post-intervention states, were calculated for each subject, to produce maps of the difference in BOLD signal for each stimulus contrast between feeding states, with the resultant pre- and post-intervention "difference" maps then subtracted from each other. Voxel-wise Pearson correlation coefficients of these "difference of differences" maps were then calculated to examine possible linear

associations between the respective changes in HOMA-IR and BOLD signal evoked by the visual stimuli after meal compared to water ingestion, following the intervention compared to baseline (Table 8.5). There were no significant associations between the respective changes after the intervention in insulin sensitivity and in post-meal (compared to post-water) [HiCal/OBJ]- or [BLU/OBJ]-evoked BOLD signal contrasts. However, greater improvements in insulin sensitivity were associated with greater differences in the differential [LoCal/OBJ]-evoked BOLD signal contrast after the meal compared to water ingestion following the intervention, compared to baseline in the cerebellum (Figure 8.6A-B). To characterise this relationship further, the respective pre- and post-intervention differences in BOLD signal after meal compared to water ingestion were extracted from this cluster, showing that the change in evoked BOLD signal after the meal compared to water decreased pre-intervention and increased post-intervention, with greater improvements in insulin sensitivity (Figure 8.6C).

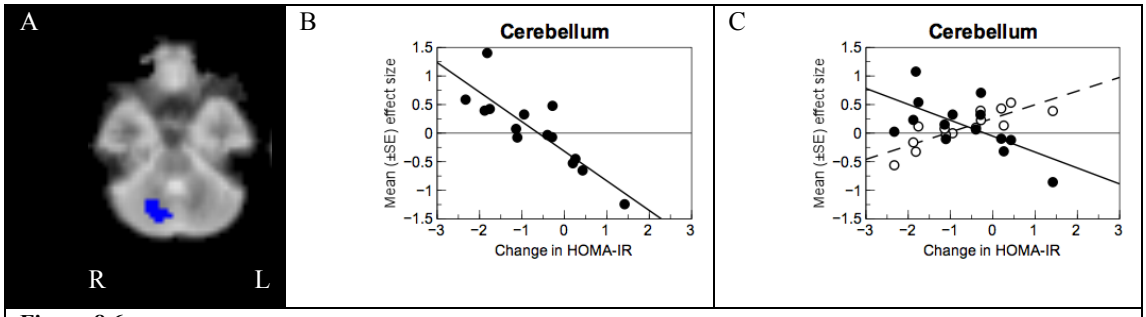

Figure 8.6

Group map of whole-brain correlation of changes in post-meal vs post-water activation with changes in HOMA-IR after systemic insulin sensitisation, showing clusters exhibiting linear negative correlation of changes in HOMA-IR with changes in incremental BOLD signal after meal compared to water after the intervention, evoked by (A) low-calorie food images (object image time series as baseline) (voxel-wise $p<0.05$, cluster-wise $p<0.01$) with (B) extracted differences in effect size (%BOLD signal change, positive values: post->pre-intervention) before vs after intervention and (C) extracted differences in effect size (%BOLD signal change, positive values: meal>water) between meal and water states in pre- (dashed line) and post-intervention (solid line) conditions. Negative change in HOMA-IR = improvements in insulin sensitivity.

8.4 Discussion

The present study aimed to establish the impact of insulin sensitisation on the cerebral response to visual food cues, and on the modulatory effects of prior meal ingestion on such responses, in insulin resistant, non-diabetic, non-obese men. I observed an improvement in insulin sensitivity following the intervention (Chapter 7), with significant changes in regional evoked BOLD signal in regions involved in appetite regulation and in ways that would be expected to change eating behaviour.

8.4.1 Effect of insulin sensitisation on food-cue evoked hunger

Whilst meal ingestion reduced hunger, and viewing high- and low-calorie food cues equally stimulated it, there was no significant effect of insulin sensitisation of IR subjects on the hunger evoked by viewing any of the stimuli. In Chapter 6, there were similarly no differences in evoked hunger between IR and IS groups. As discussed previously, the lack of difference in hunger evoked by the different classes of food images may be related to the high- and low-calorie food images being of equal salience, which may have influenced hunger more than food energy content. The absence of an effect of insulin resistance or its reversal on food-cue evoked hunger, despite differences in food-cue evoked neurological activity, may be due to a relative insensitivity of the paradigm on explicit symptoms.

8.4.2 Effect of insulin sensitisation on food-cue evoked brain activity

As discussed in Chapter 6, discriminatory responses or "caloric bias" towards high- over low-calorie food images when fasted, and low- over high-calorie food images when fed, in brain regions involved in the top-down regulation of eating behaviour (DLPFC), interoceptive processing (insula) and visual attention to food cues (lingual gyrus) were demonstrated in IS subjects only, with such differential responses in the DLPFC being significant different from that observed in IR subjects. When the post-insulin sensitisation IR responses were examined in isolation (i.e. not compared to pre-intervention), there again was no demonstrable "caloric bias" effect. However, the deactivation response to low-calorie food image, after meal ingestion in the left DLPFC pre-intervention converted to activation responses in the nearby VLPFC, to

both high- and low-calorie food images may be in keeping with a partial normalisation of this "bias effect" for low-calorie cues. A similar effect seen with blurred image viewing does not undermine this hypothesis, as discussed earlier.

The more powerful direct comparison between pre- and post- intervention, in a continued fasting (post-water ingestion) when food cues are most salient, were next performed to examine the effects of the intervention on the cerebral representation of the drive to eat. Responses to both high- and low-calorie food images in the right insula/caudate decreased after the intervention, consistent with the reduction in fasting insula responses to food cues observed after overweight/obese individuals completed a 6 month exercise programme (Cornier *et al*, 2012). Interaction analyses of the effect of insulin sensitisation on the modulatory effects of the meal on responses to food cues, detected the intervention had converted a deactivating effect of meal compared to water ingestion to one of activation effect on responses to low-calorie food images in left DLPFC and inferior frontal gyrus, including left insula, with more posterior cerebral effects to high-calorie food and blurred images. There were no significant effects of the intervention on the relative response to high- compared to low-calorie food images, compared to pre-intervention. Despite the lack of detectable effect on hunger, the present findings demonstrate a period of insulin sensitisation in non-obese but insulin resistant subjects at high risk of future T2DM, reduced activity of regions involved in interoceptive awareness and food-reward representation on exposure to food cues of any energy density, in the fasted state when food would normally be highly salient, which may reduce the drive to eat when exposed to food. Although post-prandial corticolimbic "appeal bias" against high-calorie food cues remained impaired, greater activity towards low-calorie food cues in the fed state of higher executive control centres that direct eating behaviour and food choice and of regions processing interoceptive awareness after systemic insulin sensitisation, may improve satiety and lead to healthier eating patterns.

Whilst the impact of systemic insulin sensitisation per se on food-cue evoked brain activity has not previously been investigated, there are a number of studies examining the effect of weight loss through lifestyle interventions. Cornier *et al* (2009) showed that, while overfeeding reduced insula and hypothalamic BOLD responses to food cues in thin subjects, it did not in individuals who had achieved 8% weight loss

through dietary changes. Demos *et al* (2011) found female dieters randomised to receive a milkshake had subsequently greater ventral striatal responses to food images compared to those receiving only water, whilst the opposite was detected in non-dieters. This might suggest an insensitivity of brain regions involved in signalling current nutritional status and processing reward when viewing food cues in those who successfully lose weight. McCaffery *et al* (2009) demonstrated that individuals who were no longer obese after lifestyle changes had greater visual food cue-evoked BOLD contrast changes in frontal and middle temporal regions compared to normal weight and obese subjects, which they interpreted as a greater engagement of inhibitory control mechanisms when exposed to food that is needed to successfully maintain weight loss. These findings being cross-sectional, it is possible that they relate to individual differences in brain responses to food cues that are pre-determined and not susceptible to change. In contrast, my study looking longitudinally within the same individuals is describing brain responses that are amenable to manipulation.

There are fewer longitudinal fMRI studies examining the effect of a weight-reducing intervention and those mostly involve dietary restriction. Murdaugh *et al* (2012) showed that a structured dietary weight loss programme in obese volunteers reduced high-calorie food image-evoked activity in the medial prefrontal cortex (region of interest analysis), involved in reward representation, and inferior parietal lobule and precuneus (whole brain analysis), involved in sensory processing and imagery, in the fasted state. The reduction in high- and low-calorie food cue-evoked activity observed after insulin sensitisation in the insula/caudate, involved in interoceptive awareness and reward processing, observed in the present study, is consistent with this. In contrast to my data, their weight loss programme did not alter the response to low-calorie food cues, but Murdaugh's use of intensive cognitive behavioural interventions to achieve their primary end-point of weight loss may have increased the discriminatory faculties of the participants in assessing different food types. Interestingly, the authors were unable to detect significant differences in the relative response to high-calorie compared to low-calorie food images in the obese group, before or after the weight loss intervention, which is consistent with the present study. Differential responses to high- compared to low-calorie food cues were also not detected in their normal weight subjects, which contrasts with my findings in insulin sensitive subjects (Chapter 6). Murdaugh did not report insulin sensitivity, so it is

possible their normal weight subjects included those with some degree of insulin resistance. In another fMRI study, striatal activation 4 hours after meal ingestion to high-calorie food images fell, whilst rising with low-calorie food images, in eight overweight subjects after a 24-week weight loss programme of dietary restriction, a pattern of changes in activation that was significantly different from that observed in five subjects randomised to receive delayed intervention (Deckersbach *et al*, 2014). These data should be interpreted with caution, given the analysis being limited to a striatal region of interest and the small numbers of participants. However, it is conceivable that changes in insulin sensitivity could have driven the changes in reward system responses to visual food cues observed following weight loss, as observed in the present study.

Data from longitudinal fMRI studies of the effect of weight-loss surgery have been inconsistent between studies. Ochner et al, studying people 1 month after gastric bypass surgery, showed greater reductions in striatum and DLPFC evoked responses to high calorie food than low calorie food cues in the post-prandial state (Ochner *et al*, 2011, 2012b), whilst other reports demonstrated a reduction in food cue activity in insula, medial frontal gyrus and DLPFC in the pre-meal state only (Ochner *et al*, 2012a). Bruce *et al* (2012) have demonstrated food cue-evoked activity to increase in middle and superior frontal gyri and decrease in medial frontal gyrus pre-meal, and decrease in middle and inferior frontal gyri, parahippocampal gyri and insula post-meal 3 months after gastric band insertion. Whilst these studies had different numbers of subjects and used different statistical analyses, the biggest challenge may be that both the dietary or bariatric surgery studies examined pre- and post-meal responses in isolation, rather than directly comparing the responses in fed and fasted conditions, which may explain the differences in findings in the present study. However, the findings that the greatest DLPFC activity when explicitly suppressing food cue-evoked hunger is observed in those who successfully lose and maintain lower body weight after gastric bypass (Goldman *et al*, 2013), and that transcranial stimulation of DLPFC decreases food craving (Fregni *et al*, 2008; Goldman *et al*, 2011), support the interpretation of the present conversion from DLPFC deactivation to activation after a meal following insulin sensitisation represents greater involvement of executive control centres to direct eating behaviour, in this case towards low-calorie foods, when insulin resistance is improved by lifestyle and

metformin. In another study, greater cerebral insulin sensitivity, as defined by insulin-evoked theta activity during hyperinsulinaemic euglycaemic clamp conditions, predicted subsequent reductions in adipose tissue mass through lifestyle changes (Tschritter *et al*, 2012). Thus my observation of changes in post-prandial food cue evoked activity following systemic insulin sensitisation may well be expected to facilitate weight loss through changes in appetite regulation.

8.4.3 Limitations and conclusions

There are limitations to the present study. As discussed in Chapter 7, the eating behaviour questionnaires at screening were not used after the intervention. The subjects had completed a three-day food diary that was reviewed by the dietitian, but quantification of portions and in turn estimation of caloric intake was unreliable. Robust data on changes in diet and eating behaviours during the intervention period would have been useful, both for interpretation of neuroimaging data, but also for implementation in clinical practice. The absence of a placebo control arm is also a limitation, although the significant association between the change in insulin sensitivity and changes in the differential response to high- compared to low-calorie food cues in OFC in the fasted state following the intervention provide validity to a proposed effect of systemic insulin sensitisation on the cerebral processing of food cue valence.

In summary, a short period of systemic insulin sensitisation through lifestyle changes with/without metformin in non-obese men with systemic insulin resistance, reduces food-cue evoked activity in brain regions that process reward and interoception in the fasted state, and alters the food-cue evoked activity in higher executive control centres from the fasted to the fed state, in ways that may be expected to prevent future weight gain and facilitate weight loss.

Table 8.1

Impact of meal compared to water ingestion on BOLD signal contrasts listed, in insulin resistant subjects after insulin sensitisation intervention (voxel-wise $P < 0.05$, cluster-wise threshold < 1 false positive cluster/map as listed, Figure 8.2). BA = Brodmann area; DLPFC = dorsolateral prefrontal cortex; VLPFC = ventrolateral prefrontal cortex.

	Talairach coordinates of voxel with peak effect size					
Size	**X**	**Y**	**Z**	**P ≤**	**BA**	**Brain regions**
High calorie food / object contrast: Water > Meal *(cluster-wise P ≤ 0.011236)*						
No significant clusters						
High calorie food / object contrast: Water < Meal *(cluster-wise P < 0.011364)*						
270	-43	19	0	0.002819	47	Left inferior frontal gyrus (DLPFC)
Low calorie food / object contrast: Water > Meal *(cluster-wise P ≤ 0.011628)*						
No significant clusters						
Low calorie food / object contrast: Water < Meal *(cluster-wise P ≤ 0.013889*						
148	-51	15	10	0.012120	44	Left inferior frontal gyrus (VLPFC)
Blurred image / object contrast: Water < Meal *(cluster-wise P ≤ 0.015873)*						
No significant clusters						
Blurred image / object contrast: Water > Meal *(cluster-wise P ≤ 0.010417)*						
379	-48	25	9	0.001863	45	Left inferior frontal gyrus (VLPFC)
[High calorie food / object vs Low calorie food / object] vs [Water vs Meal] *(Cluster-wise P ≤ 0.006944)*						
No significant clusters						

Table 8.2

Differences in BOLD signal contrasts listed, in insulin resistant subjects before vs after insulin sensitisation intervention after water (voxel-wise $P < 0.05$, cluster-wise threshold < 1 false positive cluster/brain map as listed, Figure 8.3). BA = Brodmann area.

	Talairach coordinates of voxel with peak effect size					
Size	**X**	**Y**	**Z**	**P ≤**	**BA**	**Brain regions**
High calorie food / object contrast: Pre-intervention > Post-intervention *(cluster-wise P ≤ 0.010870)*						
243	38	17	2	0.003449	N/A	Right insula
High calorie food / object contrast: Pre-intervention < Post-intervention *(cluster-wise P ≤ 0.013333)*						
No significant clusters						
Low calorie food / object contrast: Pre-intervention > Post-intervention *(cluster-wise P ≤ 0.0121821)*						
222	30	5	14	0.002801	N/A	Right claustrum (insula)
Low calorie food / object contrast: Pre-intervention < Post-intervention *(cluster-wise P ≤ 0.010989)*						
No significant clusters						
Blurred image / object contrast: Pre-intervention > Post intervention *(cluster-wise P ≤ 0.010417)*						
363	-17	-55	57	0.003274	7	Left precuneus
Blurred image / object contrast: Pre-intervention < Post intervention *(cluster-wise P ≤ 0.012500)*						
No significant clusters						
[High calorie food / object vs Low calorie food / object] vs [Pre- vs Post-intervention] *(cluster-wise P ≤ 0.008547)*						
No significant clusters						

Table 8.3

Differences in impact of meal compared to water ingestion on BOLD signal contrasts listed, in insulin resistant subjects before vs after insulin sensitisation intervention (voxel-wise $P < 0.05$, cluster-wise threshold < 1 false positive cluster/brain map as listed). BA = Brodmann area. The extracted effect size data in Figure 8.4 shows the direction of the interaction.

	Talairach coordinates of voxel with peak effect size					
Size	**X**	**Y**	**Z**	**P ≤**	**BA**	**Brain regions**
High calorie food / object contrast *(cluster-wise P ≤ 0.008772)*						
164	-36	-36	42	0.002497	40	Left inferior parietal lobule
Low calorie food / object contrast *(cluster-wise P ≤ 0.009346)*						
100	-51	11	13	0.00895	44	Left inferior frontal gyrus
102	-30	38	28	0.008915	9	Left middle frontal gyrus (DLPFC)
193	-47	-63	26	0.01653	39	Left middle temporal gyrus
116	32	18	53	0.002646	6	Right middle frontal gyrus (pre-motor cortex)
Blurred image / object contrast *(cluster-wise P ≤ 0.009709)*						
113	-22	-67	-3	0.003316		Left semi-lunar lobule, cerebellum
82	44	-69	11	0.00231	39	Right middle temporal gyrus
[**High calorie food / object] minus [Low calorie food / object] contrast** *(cluster-wise P ≤ 0.007463)*						
No significant clusters						

Table 8.4

Voxel-wise Pearson product moment correlation of the change in HOMA-IR with change in post-water BOLD signal contrasts listed, in insulin resistant subjects before compared to after insulin sensitisation intervention (voxel-wise $P < 0.05$, cluster-wise threshold < 1 false positive cluster/brain map as listed, Figure 8.5). BA = Brodmann area.

	Talairach coordinates of voxel with peak effect size					
Size	**X**	**Y**	**Z**	**P ≤**	**BA**	**Brain regions**
WATER						
High calorie food/object contrast: (post- minus pre-intervention) positively associated with change in HOMA-IR *(cluster-wise P ≤ 0.010417)*						
No significant clusters						
High calorie food/object contrast: (post- minus pre-intervention) negatively associated with change in HOMA-IR *(cluster-wise P ≤ 0.011236)*						
No significant clusters						
Low calorie food/object contrast: (post- minus pre-intervention) positively associated with change in HOMA-IR *(cluster-wise P ≤ 0.011905)*						
179	-7	-7	3	0.008407	N/A	Left ventral anterior nucleus, thalamus
Low calorie food/object contrast: (post- minus pre-intervention) negatively associated with change in HOMA-IR *(cluster-wise P ≤ 0.010309)*						
156	-34	28	-8	0.008223	47	Left inferior frontal gyrus
Blurred images/object contrast: (post- minus pre-intervention) positively associated with change in HOMA-IR *(cluster-wise P ≤ 0.012821)*						
No significant clusters						
Blurred images/object contrast: (post- minus pre-intervention) negatively associated with change in HOMA-IR *(cluster-wise P ≤ 0.012821)*						
No significant clusters						
([**High calorie food/object] - [Low calorie food/object]): (post- minus pre-intervention) pos. association with HOMA-IR** *(cluster-wise P ≤ 0.011364)*						
204	-25	22	-20	0.006284	47	Left inferior frontal gyrus
([**High calorie food/object] - [Low calorie food/object]): (post- minus pre-intervention) neg. association with HOMA-IR** *(cluster-wise P ≤ 0.011628)*						
No significant clusters						

Table 8.5

Voxel-wise Pearson product moment correlation of the change in HOMA-IR with changes in the difference in BOLD signal contrasts listed between meal and water in insulin resistant subjects, before vs after insulin sensitisation intervention (voxel-wise $P < 0.05$, cluster-wise threshold < 1 false positive cluster/brain map as listed, Figure 8.6). BA = Brodmann area.

	Talairach coordinates of voxel with peak effect size					
Size	**X**	**Y**	**Z**	**P ≤**	**BA**	**Brain regions**
MEAL MINUS WATER						
High calorie food/object contrast: (post- minus pre-intervention) positively associated with change in HOMA-IR *(cluster-wise P ≤ 0.011905)*						
No significant clusters						
High calorie food/object contrast: (post- minus pre-intervention) negatively associated with change in HOMA-IR *(cluster-wise P ≤ 0.010417)*						
No significant clusters						
Low calorie food/object contrast: (post- minus pre-intervention) positively associated with change in HOMA-IR *(cluster-wise P ≤ 0.011905)*						
No significant clusters						
Low calorie food/object contrast: (post- minus pre-intervention) negatively associated with change in HOMA-IR *(cluster-wise P ≤ 0.009524)*						
140	22	-70	-36	0.007825	N/A	Right inferior semi-lunar lobule, cerebellum
Blurred images/object contrast: (post- minus pre-intervention) positively associated with change in HOMA-IR *(cluster-wise P ≤ 0.015625)*						
No significant clusters						
Blurred images/object contrast: (post- minus pre-intervention) negatively associated with change in HOMA-IR *(cluster-wise P ≤ 0.010638)*						
No significant clusters						
([**High calorie food/object] - [Low calorie food/object]): (post- minus pre-intervention) pos. association with HOMA-IR** *(cluster-wise P ≤ 0.009901)*						
No significant clusters						
([**High calorie food/object] - [Low calorie food/object]): (post- minus pre-intervention) neg. association with HOMA-IR** *(cluster-wise P ≤ 0.012195)*						
No significant clusters						

9 Conclusion

9.1 Overview and summary of principal findings

This thesis aimed to examine the impact of systemic insulin resistance *per se,* in the absence of associated conditions, and its treatment on the human neural representation of two appetite constructs: satiation, the process of meal termination; and satiety, the effect of a meal on hunger and subsequent food intake. Based on evidence discussed in Chapter 1 that brain responses to food ingestion (satiation) and food cues (a surrogate for food in appetite and satiety research) are altered in obesity and type 2 diabetes (T2DM), conditions associated with insulin resistance, and that anorexigenic and weight loss effects of cerebral insulin with accompanying changes in brain activity are defective in obesity, I hypothesised that prior to disease onset, systemic insulin resistance is associated with diminished post-prandial prefrontal inhibitory centre activity, and that striatal reward and insular interoceptive responses to food cues are exaggerated when fasted and less sensitive to the effects of a meal. These changes would increase obesity and diabetes risk, by altering appetite regulation and eating behaviour, but may be amenable to intervention. To prove these hypotheses, brain responses to meal ingestion and food cues in insulin resistant (IR) and sensitive (IS) healthy non-obese men were examined using pCASL and BOLD fMRI respectively, after first examining the effect of healthy ageing up to middle age on these parameters to validate the research protocols.

9.1.1 The impact of ageing (Chapters 3-4)

Whilst other studies have examined the effect of food or food cues in childhood and in the elderly (Green *et al*, 2011; Jacobson *et al*, 2010; Killgore and Yurgelun-Todd, 2005b), this is the first study to examine the changes that occur with ageing to middle age, a period in life when obesity is most prevalent (Flegal *et al*, 2010). Post-prandial responses to a meal *per se* in insula (interoceptive awareness), orbitofrontal cortex (OFC) and anterior cingulate (ACC) increased with healthy ageing. Decreasing dorsolateral prefrontal cortex (DLPFC) inhibitory control centre responses to food cues whilst fasted, when cues are expected to be most salient, and diminishing differences in responses to food cues between fed and fasted states in DLPFC, OFC

and striatum were seen with ageing. These neural responses are in keeping with the observed diminishing suppression of hunger by the meal, and trends toward less suppression of food image-evoked hunger by a meal, with age. Thus, reward and interoceptive responses to a meal become more exaggerated, and responses to food cues in centres that direct eating behaviour and process reward become less sensitive to current nutritional status, consistent with existing neuroimaging data in established obesity (DelParigi *et al*, 2005; Dimitropoulos *et al*, 2012).

9.1.2 The impact of systemic insulin resistance (Chapters 5-6)

Using protocols based on the ageing study, the central effect of systemic insulin resistance in the absence of obesity or associated diseases was examined. IR men, who had first-degree relatives with T2DM, had greater food restraint, weight and shape concern than weight-matched insulin sensitive (IS) controls, these constructs increasing with worsening insulin resistance after including men of intermediate sensitivity, in keeping with recent data (Jastreboff *et al*, 2014). IR men had greater fasting (and post-water) right lateral OFC (inhibitory control) resting activity, which decreased after eating to levels observed in IS men in fasted and fed states. Compared to fasted (post-water) states, left insula (interoceptive) activity increased in IR and decreased in IS men after eating, in keeping with similar observations in established obesity (DelParigi *et al*, 2005; Stice *et al*, 2008).

IS men also demonstrated "caloric bias" effects in left DLPFC (inhibitory control), striatum (reward) and lingual gyrus (visual attention): post-prandial responses decreased to high- and increased to low-calorie food cues, the reverse observed in the fasted (post-water) state, consistent with similar findings in women (Siep *et al*, 2009). Direct comparisons with IS men showed the opposite pattern of greater left DLPFC responses to high- than low-calorie food cues when fed, and low- than high-calorie food cues when fasted in IR men, the strength of the "caloric bias" effect diminishing with increasing insulin resistance across all subjects. This is in keeping with similar observations of "caloric biasing" in lean but not in obese volunteers (Dimitropoulos *et al*, 2012) and in IS, but not in IR overweight/obese women with polycystic ovarian syndrome (Van Vugt *et al*, 2014).

Thus, systemic insulin resistance *per se* is associated with abnormal interoceptive centre activation responses to meal ingestion, whilst inhibitory control centre responses to the energy content of food cues are discordant with current energy requirements, observations that have not previously been demonstrated in established or at risk groups for obesity.

9.1.3 The impact of insulin sensitisation (Chapters 7-8)

Consenting IR men then undertook lifestyle advice with metformin, which improved insulin sensitivity and glycaemic status, without affecting weight. Fasting (post-water) right lateral OFC (inhibitory control) and post-prandial left insula (interoceptive) resting activity decreased after the intervention. Interaction analyses also showed the intervention converted a previous reduction, to an increase, in activity immediately after the meal in left DLPFC (inhibitory control), consistent with the greater post-prandial DLPFC activity observed in previously-obese women after weight loss compared to obese women (Le *et al*, 2007).

The intervention also reduced right insula (interoceptive) responses to all food cues in the fasted state, when they would be expected to be most salient, in keeping with the effect of exercise in obesity (Cornier *et al*, 2012). The full "caloric bias" effect towards low- over high-calorie food cues when fed and the reverse when fasted remained impaired. However, compared to pre-intervention, left DLPFC showed a normalisation of responses to low-calorie foods after the intervention, decreasing in activity in the fasted state and increasing in the fed state, with greater improvements in insulin sensitivity associated with greater DLPFC responses to high- compared to low-calorie foods in the fasted state.

Therefore, the rise in interoceptive centre activity after eating, and the discordance in inhibitory control centre responses to low-calorie food cues and current energy requirements in IR men changed towards a pattern of responses observed in IS men after a three-month period of insulin sensitisation.

9.1.4 Overarching summary

These findings are generally in keeping with the original hypothesis. However, the expected changes in activity were detected in the opposite imaging modalities with exaggerated insular interoceptive responses to the meal *per se* both with ageing and systemic insulin resistance in the pCASL fMRI studies, whilst prefrontal higher executive responses to food cues were less sensitive to the effects of meal ingestion with ageing, and discordant with current feeding status in systemic insulin resistance, in the BOLD fMRI studies. This may be due to the results reflecting a spectrum from satiation to satiety, rather than a dichotomy, given the relatively short period of time between meal consumption and food picture viewing. These data collectively are consistent with the hyper-responsive reward model of obesity put forward by (Volkow *et al*, 2011) in which insufficient prefrontal executive control and enhanced salience, conditioning and drive, may promote excess eating. Crucially, these effects of insulin resistance were observed in the absence of obesity and improved with insulin sensitisation.

9.2 Implications

Whilst obesity studies have demonstrated altered brain responses to meals (DelParigi *et al*, 2005; Stice *et al*, 2008) and the effect of such meals on responses to food cues (Dimitropoulos *et al*, 2012; Martens *et al*, 2013), my data are the first to show systemic insulin resistance *per se*, in the absence of established obesity or other insulin resistance-associated conditions, similarly alters central processes of appetite regulation, with concurrent increases in food restraint behaviour. These data support the notion that, rather than being a consequence of weight gain, the changes observed in functional neuroimaging of appetite regulation in obesity represent a mechanism by which the brain may promote continued eating and contribute to the aetiology of future obesity and T2DM, but which is amenable to intervention, in a presently healthy but high-risk population.

It is conceivable that the effects of systemic insulin resistance observed in this thesis are a result of cerebral resistance to circulating insulin, given that: systemic insulin resistance is associated with greater food restraint, a construct associated with weight

gain (Jastreboff *et al*, 2014); insulin receptors are present in corticolimbic centres involved in appetite regulation (Hopkins and Williams, 1997); the majority of cerebral insulin is derived from circulating insulin (Banks, 2004; Banks *et al*, 2012; Schwartz *et al*, 1992); circulating insulin at physiological concentrations alter brain activity (Bingham *et al*, 2002) (effects that are altered in systemic insulin resistance (Anthony *et al*, 2006)); IRS-1 genotypes associated with peripheral insulin resistance are associated with altered neural responses to circulating insulin (Tschritter *et al*, 2006) (effects that may also be affected by ageing (Tschritter *et al*, 2009a)) and; central application of insulin in man can suppress appetite (Hallschmid *et al*, 2004a, 2012) (effects that are diminished in obesity (Hallschmid *et al*, 2008)). Based on my data and the more extensive discussions of the role of cerebral insulin signalling and its defects on weight and appetite regulation and obesity in Chapter 1, I propose a model in which circulating insulin modulates the activity of brain appetite control networks, enhancing the top-down inhibitory control provided by prefrontal brain regions over reward and salience attribution centres on exposure to high calorie food cues, and suppresses post-prandial interoceptive and primary gustatory centre activity, effects that are diminished in states of systemic insulin resistance (Volkow *et al*, 2011), which may then facilitate over-eating beyond current energy requirements, and in turn leading to obesity (Figure 9.1). Conversely, improving cerebral insulin sensitivity may be a therapeutic target for the prevention and treatment of obesity.

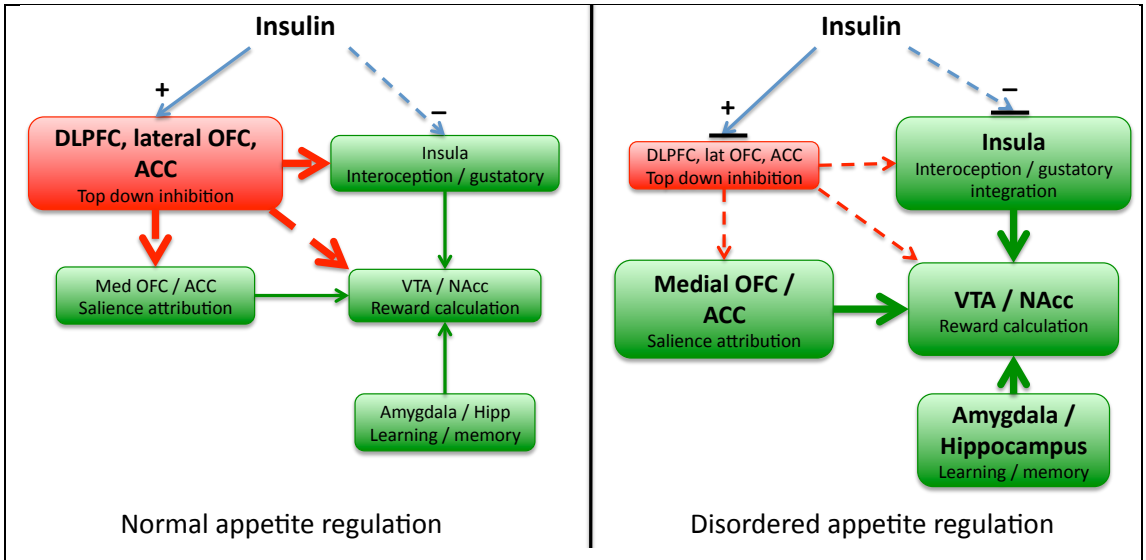

Figure 9.1

Proposed model of the modulatory effects of cerebral insulin on brain appetite control centres. Insulin enhances DLPFC activity (solid blue arrows, +) and suppresses insula activity (dashed blue arrows, –), these cerebral insulin effects being diminished in conditions of systemic insulin resistance (solid lines at end of blue arrows). Adapted from Volkow *et al* (2011).

Previous studies examining the effect of weight loss through lifestyle changes on brain responses to food or food-cues have been inconsistent, either showing normalisation (Le *et al*, 2007) or a persistence of activity observed in obesity (Cornier *et al*, 2009; DelParigi *et al*, 2004). The latter findings might be explained by the duration of established obesity, and hence insulin resistance, with defects in central appetite network activity potentially being less responsive to lifestyle interventions over time, the persistence of which would hypothetically increase risk of weight regain. However, evidence that lifestyle changes which lead to weight loss, also improve brain responses to circulating insulin (Tschritter *et al*, 2012) and the way the brain responds to food (Cornier *et al*, 2012), are in keeping with my observations of the susceptibility of the changes in brain appetite network activity in early systemic insulin resistance to insulin sensitisation, without necessarily requiring weight loss. Regular exercise, even without weight loss, has cardiovascular and musculoskeletal benefits, and is effective at preventing diabetes by improving insulin sensitivity peripherally (Kitabchi *et al*, 2005), but presumably also centrally in ways that may improve and maintain healthy satiation and satiety.

The changes in eating behaviour and brain responses to food following bariatric surgery are likely to be due to changes in gastrointestinal anatomy and incretin secretion, but given the early improvements in hepatic insulin sensitivity observed after such surgery in both diabetic and non-diabetic patients (Dunn *et al*, 2012a; Promintzer-Schifferl *et al*, 2011), improved cerebral insulin sensitivity after bariatric surgery may also play a role, identification of which may aid the development of future non-surgical interventions that achieve equivalent degrees of sustainable weight loss. In addition, one mechanism that has been proposed to explain the surplus weight gain and often hunger that is attributed to insulin therapy in people with diabetes is that of cerebral insulin resistance, with insufficient satiation and satiety effects of exogenous insulin within the brain, which to a limited extent might be overcome by using analogue insulins such as detemir, that have greater access to the brain (van Golen *et al*, 2013, 2014; Hallschmid *et al*, 2010; Tschritter *et al*, 2007a). Systemic insulin sensitisation might therefore limit the weight gain observed with insulin therapy through improvements in insulin satiety signalling within the brain.

The use of BOLD fMRI in the study of responses to food cues is well established. However, there are comparatively fewer studies examining the responses to meal ingestion by measurement of regional cerebral blood flow, and most have involved the use of $^{15}[O]H_2O$-PET, or more recently pulsed ASL (pASL) fMRI. This thesis has validated a protocol that applies pCASL fMRI to the examination of satiation, with the effect of meal ingestion *per se* producing similar findings to that observed with pASL fMRI (Frank *et al*, 2012) and $^{15}[O]H_2O$-PET (Gautier *et al*, 2001; Tataranni *et al*, 1999). pCASL fMRI can also detect post-treatment changes in regional brain activity, and may therefore be used to characterise the effect of weight loss or dietary interventions on brain appetite regulation networks, and predict their efficacy, in early phase studies in man.

9.3 Limitations and future research

Limitations specific to each study were described in the respective chapters. However, there are limitations that are common to all the studies performed which should be addressed in future investigations.

9.3.1 Power calculations

The present study was powered on the numbers of subjects required to show improvements in HOMA-IR, rather than differences in cerebral activity following the intervention, as standard methods of calculating power are difficult to apply to each of the thousands of voxels of data in each subject's MRI map and guidelines for calculating power were not available when my research commenced (Mumford, 2012). However, as simulation studies suggest 12 subjects are needed to achieve 80% power at a single voxel level (Desmond and Glover, 2002), this thesis should be sufficiently powered.

9.3.2 Satiation and satiety

Fixed quantities of the mixed meal were used in these studies to elicit satiation. This approach, a commonly used paradigm in functional imaging studies, was used to mimic real-life situations in which portions are fixed e.g. ready-meals, eating in

restaurants. However, the self-reported measures of satiation were not as high as expected in the insulin resistance studies compared to the ageing studies, despite the small increase in the volume of the meal. Personalised quantities of food as directed by the individual may have maximised satiation signals further, although there is evidence that gastric distension by different volumes produces different cerebral responses (Tomasi *et al*, 2009) which would need to be taken into account. As previously noted, different macronutrients and glycaemic indices of food have different effects on glucose and insulin excursions, satiation and brain activity (Frank *et al*, 2012; Lennerz *et al*, 2013; Li *et al*, 2012a), should be considered in future research. The mixed meal used in the present study consisted mainly of fat and carbohydrate, reflecting common Western diets, and was sufficient to evoke changes in appetite and cerebral activity.

Food image viewing is a common paradigm in neuroimaging studies, and has been used in this thesis to investigate the process of satiety. However, whilst systemic insulin resistance and sensitisation had significant effects on the BOLD fMRI signal contrasts evoked by the food cues, it did not have any detectable effect on the concurrent evoked hunger, unlike the subjective changes in appetite to the meal *per se*. This might be due to an insensitivity of self-reported hunger evoked by viewing images, or it could be due to systemic insulin resistance and sensitisation having less explicit, and more subtle effects on satiety, that can only be detected by methods that do not rely on self-reports, such as the use of an ad-libitum meal (Adeyemo *et al*, 2015). Such objective measures can be used in future neuroimaging studies and correlated with food-picture viewing tasks.

9.3.3 Effect of systemic insulin resistance and sensitisation in women and obesity

This thesis examined the effect of systemic insulin resistance in non-obese men only, in order to maximise the ability to observe effects of insulin resistance, given that weight loss and increased satiation have been observed with acute and prolonged intranasal insulin administration in men, but not in women, in whom enhancements in satiety and cognition are observed (Benedict *et al*, 2008; Hallschmid *et al*, 2004a, 2012). As discussed in Chapter 1, there is evidence that the cerebral response to food (Del Parigi *et al*, 2002) and food cues (Cornier *et al*, 2010; Frank *et al*, 2010a;

Killgore and Yurgelun-Todd, 2010; Uher *et al*, 2006) is different between genders. It is recognised from women with type 1 diabetes, that insulin sensitivity decreases in the early luteal phase (Brown *et al*, 2015), during which appetite increases in healthy women (Gorczyca *et al*, 2016), and DLPFC responses are evoked by high- but not low-calorie food images and are not modulated by feeding status (Alonso-Alonso *et al*, 2011; Frank *et al*, 2010b), unlike during the follicular phase. I would therefore hypothesise that during the menstrual cycle, the brain response to food cues and meal ingestion in premenopausal women fluctuates between patterns of activity observed in IS and IR men in the present study, which may affect risk of future weight gain. In addition, future studies are needed to determine whether the effects of systemic insulin sensitisation on brain processing of satiation and satiety observed in this thesis in non-obese men, can be replicated in obesity, and in pre-menstrual women with significant fluctuations in weight. The research protocols used in this thesis could be used to address these areas, with longitudinal studies to establish the efficacy of insulin sensitisation on the prevention and treatment of obesity.

9.3.4 Mechanism of action of insulin sensitisation on changes in brain responses to food and food cues

The mechanisms behind the changes I observed in food and food-cue evoked activity with my insulin-sensitising protocol are speculative. As discussed in chapter 1, actively devaluing or inhibiting thoughts of pleasure from foods increases DLPFC activity (Scharmüller *et al*, 2012). The subjects were asked to imagine they were eating the foods presented, which has been shown to alter corticolimbic activity (Frankort *et al*, 2012), so it is possible that the increase in prefrontal responses to low calorie foods after the intervention was due to changes in thoughts and feelings towards such food following dietary intervention. However, as the strength of the "caloric bias" was associated with baseline insulin sensitivity, the changes observed after the intervention, which may still represent conscious cognitive responses, may have been facilitated by changes in insulin sensitivity, given that cerebral insulin sensitivity predicts the success of lifestyle intervention in sustaining weight loss (Tschritter *et al*, 2012).

Diabetes prevention studies have shown that longer term lifestyle changes are more effective than metformin therapy in preventing diabetes (Knowler *et al*, 2002), but metformin was used to expedite improvements in insulin sensitivity over the defined period of intervention. A limitation of this thesis is that it is not possible to differentiate the effects of lifestyle changes from those of drug treatment, which should be compared in future studies. Metformin increases satiety in non-diabetic obese children (Adeyemo *et al*, 2015) and satiation in obese adults with T2DM (Lee and Morley, 1998), with meta-analyses showing weight loss benefits in non-diabetic obese children and adults, and either weight-loss or weight-neutrality in diabetic obese adults (Brufani *et al*, 2013; Golay, 2007). Whilst metformin predominantly acts by improving hepatic insulin sensitivity, animal studies also show oral and subcutaneous metformin is detectable in CSF, hypothalamus and corticolimbic brain regions and reduces food intake (Łabuzek *et al*, 2010; Lv *et al*, 2012; Rouru *et al*, 1995). In rodent studies, metformin reverses models of neuronal insulin resistance by improving insulin receptor signalling (Gupta *et al*, 2011). Although metformin may suppress appetite by improving cerebral responses to insulin, changes in eating behaviour may also due to other effects, independent of changing insulin sensitivity. Preclinical studies show metformin restores hypothalamic leptin receptor expression and leptin sensitivity in obesity (Aubert *et al*, 2011; Kim *et al*, 2006), suppresses orexigenic effects of ghrelin (Stevanovic *et al*, 2012), with inconsistent effects on orexigenic NPY (Aubert *et al*, 2011; Chau-Van *et al*, 2007; Lv *et al*, 2012). In humans, metformin may reduce striatal μ-opioid receptors (Berent-Spillson *et al*, 2011), and also affect secretion of gut hormones that regular appetite, such as GLP-1 (Mannucci *et al*, 2004), PYY (Tsilchorozidou *et al*, 2008) and ghrelin (English *et al*, 2007). Insufficient blood sample collection during the present studies prevented further examination of these incretin effects with metformin therapy.

I have interpreted the cerebral effects of an insulin sensitisation intervention in this thesis to be due to improvements in the action of circulating insulin in the brain, but further research is necessary to confirm this. For example, following on from the studies showing that circulating insulin at physiological concentrations (whilst suppressing endogenous insulin secretion by somatostatin infusion) changes regional cerebral glucose metabolism (Bingham *et al*, 2002), an effect that is altered in systemic insulin resistance (Anthony *et al*, 2006), a natural progression would to be

perform these ^{18}[F]FDG-PET studies in insulin resistant non-obese subjects, measuring the effect of circulating insulin on appetite and brain activity, after a period of insulin sensitisation. Improvements in the regional cerebral glucose metabolism would demonstrate reversibility of cerebral insulin resistance *per se*. In order to determine whether cerebral insulin resistance and its reversal lies at the level of the blood brain barrier (Heni *et al*, 2014b; Kern *et al*, 2006) or at the neuronal insulin receptor and beyond, the impact of insulin sensitisation on the effects of intranasal ("post-blood brain barrier" applied) insulin in systemic insulin resistance (Hallschmid *et al*, 2008) could be examined, employing for example the BOLD and pCASL protocols used in this thesis.

9.3.5 The role of cerebral insulin in mental and cognitive health

This thesis referred only to healthy and excessive eating and excluded the spectrum of eating disorders. Understanding the central mechanisms of appetite regulation in health and metabolic disease may provide insight into conditions such as binge eating disorder, which is prevalent in obesity and type 2 diabetes (Gorin *et al*, 2008) and shows similar patterns of activity in functional neuroimaging studies (Schienle *et al*, 2009). Insulin resistance is thought to be involved in the aetiology of Alzheimer's dementia, and there is interest in insulin sensitisation strategies to treat or prevent this disease (Cholerton *et al*, 2013). As depression is associated with systemic insulin resistance (Pearson *et al*, 2010), it is possible that cerebral insulin resistance may also play a role in mood disorders, and the improvements in depression with the thiazolidinedione class of insulin sensitising agents support this hypothesis (Colle *et al*, 2017). Similar paradigms discussed above could be used to confirm the presence of regional cerebral insulin resistance, and if found, the present study may be informative of the potential effects and mechanisms of action of insulin sensitisation therapies in mental health.

9.4 Final conclusions

The coordinated interplay of hypothalamic homeostatic circuits and hedonic corticolimbic networks will regulate food intake with respect to current physiological needs but also for pleasure. The peripheral effect of circulating insulin on glucose metabolism is well known, but its effects on brain activity are gaining greater recognition. The interactions between these networks are modulated by cerebral insulin, defects of which may lead to dysregulated eating behaviours. This thesis has contributed to our understanding of the impact of insulin resistance on the appetite regulation in the premorbid state, and demonstrated the potential for reversing these defects through interventions that improve systemic insulin sensitivity.

References

Adeyemo MA, McDuffie JR, Kozlosky M, Krakoff J, Calis KA, Brady SM, *et al* (2015). Effects of metformin on energy intake and satiety in obese children. *Diabetes Obes Metab* **17**: 363–370.

Adrian TE, Ferri GL, Bacarese-Hamilton AJ, Fuessl HS, Polak JM, Bloom SR (1985). Human distribution and release of a putative new gut hormone, peptide YY. *Gastroenterology* **89**: 1070–1077.

Air EL, Strowski MZ, Benoit SC, Conarello SL, Salituro GM, Guan X-M, *et al* (2002). Small molecule insulin mimetics reduce food intake and body weight and prevent development of obesity. *Nat Med* **8**: 179–183.

Alonso-Alonso M, Ziemke F, Magkos F, Barrios FA, Brinkoetter M, Boyd I, *et al* (2011). Brain responses to food images during the early and late follicular phase of the menstrual cycle in healthy young women: relation to fasting and feeding. *Am J Clin Nutr* **94**: 377–384.

Alsop DC, Detre JA, Golay X, Günther M, Hendrikse J, Hernandez-Garcia L, *et al* (2015). Recommended Implementation of Arterial Spin Labeled Perfusion MRI for Clinical Applications: A consensus of the ISMRM Perfusion Study Group and the European Consortium for ASL in Dementia. *Magn Reson Med* **73**: 102–116.

Alvarez E, Martínez MD, Roncero I, Chowen JA, García-Cuartero B, Gispert JD, *et al* (2005). The expression of GLP-1 receptor mRNA and protein allows the effect of GLP-1 on glucose metabolism in the human hypothalamus and brainstem. *J Neurochem* **92**: 798–806.

Amaro E, Barker GJ (2006). Study design in fMRI: basic principles. *Brain Cogn* **60**: 220–232.

Anthony K, Reed LJ, Dunn JT, Bingham E, Hopkins D, Marsden PK, *et al* (2006). Attenuation of Insulin-Evoked Responses in Brain Networks Controlling Appetite and Reward in Insulin Resistance. *Diabetes* **55**: 2986–2992.

Aotani D, Ebihara K, Sawamoto N, Kusakabe T, Aizawa-Abe M, Kataoka S, *et al* (2012). Functional Magnetic Resonance Imaging Analysis of Food-Related Brain Activity in Patients with Lipodystrophy Undergoing Leptin Replacement Therapy. *J Clin Endocrinol Metab* **97**: 3663–3671.

Arase K, Fisler JS, Shargill NS, York DA, Bray GA (1988). Intracerebroventricular infusions of 3-OHB and insulin in a rat model of dietary obesity. *Am J Physiol* **255**: R974-981.

Araujo I de, Geha P, Small D (2012). Orosensory and Homeostatic Functions of the Insular Taste Cortex. *Chemosens Percept* **5**: 64–79.

Ashburner JT, Friston KJ (2004a). Chapter 35 - Image Segmentation. *Hum Brain Funct Second Ed* 695–706.

Ashburner JT, Friston KJ (2004b). Chapter 32 - Rigid Body Registration. *Hum Brain Funct Second Ed* 635–653.

Attwell D, Buchan AM, Charpak S, Lauritzen M, Macvicar BA, Newman EA (2010). Glial and neuronal control of brain blood flow. *Nature* **468**: 232–243.

Aubert G, Mansuy V, Voirol M, Pellerin L, Pralong F (2011). The anorexigenic effects of metformin involve increases in hypothalamic leptin receptor expression. *Metabolism* **60**: 327–34.

Baicy K, London ED, Monterosso J, Wong M-L, Delibasi T, Sharma A, *et al* (2007). Leptin replacement alters brain response to food cues in genetically leptin-deficient adults. *Proc Natl Acad Sci U S A* **104**: 18276–18279.

Baker LD, Cross DJ, Minoshima S, Belongia D, Watson GS, Craft S (2011). Insulin resistance and Alzheimer-like reductions in regional cerebral glucose metabolism for cognitively normal adults with prediabetes or early type 2 diabetes. *Arch Neurol* **68**: 51–57.

Balin BJ, Broadwell RD, Salcman M, El-Kalliny M (1986). Avenues for entry of peripherally administered protein to the central nervous system in mouse, rat, and squirrel monkey. *J Comp Neurol* **251**: 260–280.

Ballard IC, Murty VP, Carter RM, MacInnes JJ, Huettel SA, Adcock RA (2011). Dorsolateral Prefrontal Cortex Drives Mesolimbic Dopaminergic Regions to Initiate Motivated Behavior. *J Neurosci* **31**: 10340–10346.

Banks WA (2004). The source of cerebral insulin. *Eur J Pharmacol* **490**: 5–12.

Banks WA, Kastin AJ (1998). Differential permeability of the blood-brain barrier to two pancreatic peptides: insulin and amylin. *Peptides* **19**: 883–889.

Banks WA, Owen JB, Erickson MA (2012). Insulin in the brain: There and back again. *Pharmacol Ther* **136**: 82–93.

Batterham RL, Cohen MA, Ellis SM, Le Roux CW, Withers DJ, Frost GS, *et al* (2003). Inhibition of food intake in obese subjects by peptide YY3-36. *N Engl J Med* **349**: 941–948.

Batterham RL, ffytche DH, Rosenthal JM, Zelaya FO, Barker GJ, Withers DJ, *et al* (2007). PYY modulation of cortical and hypothalamic brain areas predicts feeding behaviour in humans. *Nature* **450**: 106–109.

Batterink L, Yokum S, Stice E (2010). Body mass correlates inversely with inhibitory control in response to food among adolescent girls: an fMRI study. *NeuroImage* **52**: 1696–1703.

Beaver JD, Lawrence AD, Ditzhuijzen J van, Davis MH, Woods A, Calder AJ (2006). Individual Differences in Reward Drive Predict Neural Responses to Images of Food. *J Neurosci* **26**: 5160–5166.

Begg D, Mul J, Liu M, Reedy B, D'Alessio D, Seeley R, *et al* (2013). Reversal of diet-induced obesity increases insulin transport into cerebrospinal fluid and restores sensitivity to the anorexic action of central insulin in male rats. *Endocrinology* **154**: 1047–54.

Belfiore F, Iannello S, Camuto M, Fagone S, Cavaleri A (2001). Insulin sensitivity of blood glucose versus insulin sensitivity of blood free fatty acids in normal, obese, and obese-diabetic subjects. *Metabolism* **50**: 573–582.

Belgardt BF, Brüning JC (2010). CNS leptin and insulin action in the control of energy homeostasis. *Ann N Y Acad Sci* **1212**: 97–113.

Benedict C, Brede S, Schiöth HB, Lehnert H, Schultes B, Born J, *et al* (2011). Intranasal Insulin Enhances Postprandial Thermogenesis and Lowers Postprandial Serum Insulin Levels in Healthy Men. *Diabetes* **60**: 114–118.

Benedict C, Hallschmid M, Hatke A, Schultes B, Fehm HL, Born J, *et al* (2004). Intranasal insulin improves memory in humans. *Psychoneuroendocrinology* **29**: 1326–1334.

Benedict C, Kern W, Schultes B, Born J, Hallschmid M (2008). Differential sensitivity of men and women to anorexigenic and memory-improving effects of intranasal insulin. *J Clin Endocrinol Metab* **93**: 1339–1344.

Berent-Spillson A, Love T, Pop-Busui R, Sowers M, Persad CC, Pennington KP, *et al* (2011). Insulin resistance influences central opioid activity in polycystic ovary syndrome. *Fertil Steril* **95**: 2494–2498.

Bergman RN, Ider YZ, Bowden CR, Cobelli C (1979). Quantitative estimation of insulin sensitivity. *Am J Physiol* **236**: E667-677.

Berridge KC (2009). "Liking" and "wanting" food rewards: brain substrates and roles in eating disorders. *Physiol Behav* **97**: 537–550.

Berridge KC, Ho C-Y, Richard JM, DiFeliceantonio AG (2010). The tempted brain eats: pleasure and desire circuits in obesity and eating disorders. *Brain Res* **1350**: 43–64.

Berridge KC, Robinson TE (2003). Parsing reward. *Trends Neurosci* **26**: 507–513.

Berthoud H-R (2011). Metabolic and hedonic drives in the neural control of appetite: who is the boss? *Curr Opin Neurobiol* **21**: 888–896.

Berthoud H-R, Morrison C (2008). The Brain, Appetite, and Obesity. *Annu Rev Psychol* **59**: 55–92.

Biagi L, Abbruzzese A, Bianchi MC, Alsop DC, Del Guerra A, Tosetti M (2007). Age dependence of cerebral perfusion assessed by magnetic resonance continuous arterial spin labeling. *J Magn Reson Imaging JMRI* **25**: 696–702.

Bingham EM, Hopkins D, Smith D, Pernet A, Hallett W, Reed L, *et al* (2002). The Role of Insulin in Human Brain Glucose Metabolism. *Diabetes* **51**: 3384–3390.

Birdsill AC, Carlsson CM, Willette AA, Okonkwo OC, Johnson SC, Xu G, *et al* (2013). Low cerebral blood flow is associated with lower memory function in metabolic syndrome. *Obesity* **21**: 1313–1320.

Bloemendaal L van, IJzerman RG, Ten Kulve JS, Barkhof F, Konrad RJ, Drent ML, *et al* (2014). GLP-1 receptor activation modulates appetite- and reward-related brain areas in humans. *Diabetes* **63**: 4186–4196.

Bloemendaal L van, Veltman DJ, Ten Kulve JS, Groot PFC, Ruhé HG, Barkhof F, *et al* (2015). Brain reward-system activation in response to anticipation and consumption of palatable food is altered by glucagon-like peptide-1 receptor activation in humans. *Diabetes Obes Metab* **17**: 878–886.

Bonora E, Kiechl S, Willeit J, Oberhollenzer F, Egger G, Targher G, *et al* (1998). Prevalence of insulin resistance in metabolic disorders: the Bruneck Study. *Diabetes* **47**: 1643–1649.

Bonora E, Targher G, Alberiche M, Bonadonna RC, Saggiani F, Zenere MB, *et al* (2000). Homeostasis model assessment closely mirrors the glucose clamp technique in the assessment of insulin sensitivity: studies in subjects with

various degrees of glucose tolerance and insulin sensitivity. *Diabetes Care* **23**: 57–63.

Born J, Lange T, Kern W, McGregor GP, Bickel U, Fehm HL (2002). Sniffing neuropeptides: a transnasal approach to the human brain. *Nat Neurosci* **5**: 514–516.

Bragulat V, Dzemidzic M, Bruno C, Cox CA, Talavage T, Considine RV, *et al* (2010). Food-related odor probes of brain reward circuits during hunger: a pilot FMRI study. *Obes Silver Spring Md* **18**: 1566–1571.

Brammer MJ, Bullmore ET, Simmons A, Williams SC, Grasby PM, Howard RJ, *et al* (1997). Generic brain activation mapping in functional magnetic resonance imaging: a nonparametric approach. *Magn Reson Imaging* **15**: 763–770.

Brett M, Anton J-L, Valabregue R, Poline J-B (2002). Region of interest analysis using an SPM toolbox [abstract]. *Neuroimage* **16**: Abstract 497.

Brett M, Penny WD, Kiebel SJ (2011). Parametric procedures. *Stat Parametr Mapp Anal Funct Brain Images* 223–231.

British Heart Foundation (2014). Get active, stay active - physical activity into your daily routine. at <https://www.bhf.org.uk/-/media/files/publications/being-active/g12_get_active_stay_active.pdf>.

Brøns C, Jensen CB, Storgaard H, Hiscock NJ, White A, Appel JS, *et al* (2009). Impact of short-term high-fat feeding on glucose and insulin metabolism in young healthy men. *J Physiol* **587**: 2387–2397.

Brooks SJ, Cedernaes J, Schiöth HB (2013). Increased Prefrontal and Parahippocampal Activation with Reduced Dorsolateral Prefrontal and Insular Cortex Activation to Food Images in Obesity: A Meta-Analysis of fMRI Studies. *PLOS ONE* **8**: e60393.

Brown LM, Clegg DJ, Benoit SC, Woods SC (2006). Intraventricular insulin and leptin reduce food intake and body weight in C57BL/6J mice. *Physiol Behav* **89**: 687–691.

Brown SA, Jiang B, McElwee-Malloy M, Wakeman C, Breton MD (2015). Fluctuations of Hyperglycemia and Insulin Sensitivity Are Linked to Menstrual Cycle Phases in Women With T1D. *J Diabetes Sci Technol* **9**: 1192–1199.

Bruce AS, Holsen LM, Chambers RJ, Martin LE, Brooks WM, Zarcone JR, *et al* (2010). Obese children show hyperactivation to food pictures in brain

networks linked to motivation, reward and cognitive control. *Int J Obes* **34**: 1494–1500.

Bruce JM, Hancock L, Bruce A, Lepping RJ, Martin L, Lundgren JD, *et al* (2012). Changes in brain activation to food pictures after adjustable gastric banding. *Surg Obes Relat Dis Off J Am Soc Bariatr Surg* **8**: 602–608.

Brufani C, Crinò A, Fintini D, Patera PI, Cappa M, Manco M (2013). Systematic Review of Metformin Use in Obese Nondiabetic Children and Adolescents. *Horm Res Paediatr* **80**: 78–85.

Brüning JC, Gautam D, Burks DJ, Gillette J, Schubert M, Orban PC, *et al* (2000). Role of brain insulin receptor in control of body weight and reproduction. *Science* **289**: 2122–2125.

Bullmore E, Long C, Suckling J, Fadili J, Calvert G, Zelaya F, *et al* (2001). Colored noise and computational inference in neurophysiological (fMRI) time series analysis: Resampling methods in time and wavelet domains. *Hum Brain Mapp* **12**: 61–78.

Bullmore ET, Brammer MJ, Rabe-Hesketh S, Curtis VA, Morris RG, Williams SC, *et al* (1999). Methods for diagnosis and treatment of stimulus-correlated motion in generic brain activation studies using fMRI. *Hum Brain Mapp* **7**: 38–48.

Burger KS, Stice E (2011). Relation of dietary restraint scores to activation of reward-related brain regions in response to food intake, anticipated intake, and food pictures. *NeuroImage* **55**: 233–239.

Calanna S, Christensen M, Holst JJ, Laferrère B, Gluud LL, Vilsbøll T, *et al* (2013a). Secretion of glucagon-like peptide-1 in patients with type 2 diabetes mellitus: systematic review and meta-analyses of clinical studies. *Diabetologia* **56**: 965–972.

Calanna S, Christensen M, Holst JJ, Laferrère B, Gluud LL, Vilsbøll T, *et al* (2013b). Secretion of glucose-dependent insulinotropic polypeptide in patients with type 2 diabetes: systematic review and meta-analysis of clinical studies. *Diabetes Care* **36**: 3346–3352.

Calanna S, Urbano F, Piro S, Zagami RM, Di Pino A, Spadaro L, *et al* (2012). Elevated plasma glucose-dependent insulinotropic polypeptide associates with hyperinsulinemia in metabolic syndrome. *Eur J Endocrinol Eur Fed Endocr Soc* **166**: 917–922.

Camus M, Halelamien N, Plassmann H, Shimojo S, O'Doherty J, Camerer C, *et al* (2009). Repetitive transcranial magnetic stimulation over the right dorsolateral prefrontal cortex decreases valuations during food choices. *Eur J Neurosci* **30**: 1980–1988.

Caravaggio F, Raitsin S, Gerretsen P, Nakajima S, Wilson A, Graff-Guerrero A (2013). Ventral Striatum Binding of a Dopamine D2/3 Receptor Agonist But Not Antagonist Predicts Normal Body Mass Index. *Biol Psychiatry* **77**: 196–202.

Cavanna AE, Trimble MR (2006). The precuneus: a review of its functional anatomy and behavioural correlates. *Brain* **129**: 564–583.

Celio AA, Wilfley DE, Crow SJ, Mitchell J, Walsh BT (2004). A comparison of the binge eating scale, questionnaire for eating and weight patterns-revised, and eating disorder examination questionnaire with instructions with the eating disorder examination in the assessment of binge eating disorder and its symptoms. *Int J Eat Disord* **36**: 434–444.

Centre for Neuroimaging Sciences, Institute of Psychiatry, Psychology & Neuroscience, King's College London (2012). XBAM version 4.1. at <http://www.kcl.ac.uk/ioppn/depts/neuroimaging/research/imaginganalysis/Software/XBAM.aspx>.

Ceperuelo-Mallafré V, Duran X, Pachón G, Roche K, Garrido-Sánchez L, Vilarrasa N, *et al* (2014). Disruption of GIP/GIPR axis in human adipose tissue is linked to obesity and insulin resistance. *J Clin Endocrinol Metab* **99**: E908-919.

Cerf-Ducastel B, Murphy C (2001). fMRI activation in response to odorants orally delivered in aqueous solutions. *Chem Senses* **26**: 625–637.

Chambers JC, Elliott P, Zabaneh D, Zhang W, Li Y, Froguel P, *et al* (2008). Common genetic variation near MC4R is associated with waist circumference and insulin resistance. *Nat Genet* **40**: 716–718.

Chantler PD, Shrader CD, Tabone LE, Audiffret AC d', Huseynova K, Brooks SD, *et al* (2015). Cerebral cortical microvascular rarefaction in metabolic syndrome is dependent on insulin resistance and loss of nitric oxide bioavailability. *Microcirc N Y N 1994* **22**: 435–445.

Chau-Van C, Gamba M, Salvi R, Gaillard RC, Pralong FP (2007). Metformin inhibits adenosine 5'-monophosphate-activated kinase activation and prevents

increases in neuropeptide Y expression in cultured hypothalamic neurons. *Endocrinology* **148**: 507–511.

Chavez M, Kaiyala K, Madden LJ, Schwartz MW, Woods SC (1995). Intraventricular insulin and the level of maintained body weight in rats. *Behav Neurosci* **109**: 528–531.

Cheah YS, Lee S, Ashoor G, Nathan Y, Reed LJ, Zelaya FO, *et al* (2014). Ageing diminishes the modulation of human brain responses to visual food cues by meal ingestion. *Int J Obes 2005* **38**: 1186–1192.

Chechlacz M, Rotshtein P, Klamer S, Porubská K, Higgs S, Booth D, *et al* (2009). Diabetes dietary management alters responses to food pictures in brain regions associated with motivation and emotion: a functional magnetic resonance imaging study. *Diabetologia* **52**: 524–533.

Chen JJ, Rosas HD, Salat DH (2011). Age-associated reductions in cerebral blood flow are independent from regional atrophy. *NeuroImage* **55**: 468–478.

Chen PS, Yang YK, Yeh TL, Lee I-H, Yao WJ, Chiu NT, *et al* (2008). Correlation between body mass index and striatal dopamine transporter availability in healthy volunteers--a SPECT study. *NeuroImage* **40**: 275–279.

Chen YY, Wang JP, Jiang YY, Li H, Hu YH, Lee KO, *et al* (2015). Fasting Plasma Insulin at 5 Years of Age Predicted Subsequent Weight Increase in Early Childhood over a 5-Year Period-The Da Qing Children Cohort Study. *PloS One* **10**: e0127389.

Cheng Y-Y, Leu H-B, Chen T-J, Chen C-L, Kuo C-H, Lee S-D, *et al* (2014). Metformin-inclusive therapy reduces the risk of stroke in patients with diabetes: a 4-year follow-up study. *J Stroke Cerebrovasc Dis Off J Natl Stroke Assoc* **23**: e99-105.

Cho SS, Strafella AP (2009). rTMS of the Left Dorsolateral Prefrontal Cortex Modulates Dopamine Release in the Ipsilateral Anterior Cingulate Cortex and Orbitofrontal Cortex. *PLoS ONE* **4**: e6725.

Cholerton B, Baker LD, Craft S (2013). Insulin, cognition, and dementia. *Eur J Pharmacol* **719**: 170–179.

Clegg DJ, Benoit SC, Reed JA, Woods SC, Dunn-Meynell A, Levin BE (2005). Reduced anorexic effects of insulin in obesity-prone rats fed a moderate-fat diet. *Am J Physiol Regul Integr Comp Physiol* **288**: R981-986.

Clegg DJ, Gotoh K, Kemp C, Wortman MD, Benoit SC, Brown LM, *et al* (2011). Consumption of a high-fat diet induces central insulin resistance independent of adiposity. *Physiol Behav* **103**: 10–16.

Clegg DJ, Riedy CA, Smith KAB, Benoit SC, Woods SC (2003). Differential sensitivity to central leptin and insulin in male and female rats. *Diabetes* **52**: 682–687.

Coll A, Farooqi I, Orahilly S (2007). The Hormonal Control of Food Intake. *Cell* **129**: 251–262.

Colle R, Larminat D de, Rotenberg S, Hozer F, Hardy P, Verstuyft C, *et al* (2017). PPAR-γ Agonists for the Treatment of Major Depression: A Review. *Pharmacopsychiatry* **50**: 49–55.

Considine RV, Sinha MK, Heiman ML, Kriauciunas A, Stephens TW, Nyce MR, *et al* (1996). Serum immunoreactive-leptin concentrations in normal-weight and obese humans. *N Engl J Med* **334**: 292–295.

Cornier M-A, McFadden KL, Thomas EA, Bechtell JL, Eichman LS, Bessesen DH, *et al* (2013). Differences in the neuronal response to food in obesity-resistant as compared to obesity-prone individuals. *Physiol Behav* **110–111**: 122–128.

Cornier M-A, Melanson EL, Salzberg AK, Bechtell JL, Tregellas JR (2012). The effects of exercise on the neuronal response to food cues. *Physiol Behav* **105**: 1028–1034.

Cornier M-A, Salzberg AK, Endly DC, Bessesen DH, Rojas DC, Tregellas JR (2009). The effects of overfeeding on the neuronal response to visual food cues in thin and reduced-obese individuals. *PloS One* **4**: e6310.

Cornier M-A, Salzberg AK, Endly DC, Bessesen DH, Tregellas JR (2010). Sex-based differences in the behavioral and neuronal responses to food. *Physiol Behav* **99**: 538–543.

Cornier M-A, Von Kaenel SS, Bessesen DH, Tregellas JR (2007). Effects of overfeeding on the neuronal response to visual food cues. *Am J Clin Nutr* **86**: 965–971.

Craig ADB (2009). How do you feel--now? The anterior insula and human awareness. *Nat Rev Neurosci* **10**: 59–70.

Cummings DE, Frayo RS, Marmonier C, Aubert R, Chapelot D (2004). Plasma ghrelin levels and hunger scores in humans initiating meals voluntarily

without time- and food-related cues. *Am J Physiol - Endocrinol Metab* **287**: E297–E304.

Dai W, Garcia D, Bazelaire C de, Alsop DC (2008). Continuous Flow-Driven Inversion for Arterial Spin Labeling Using Pulsed Radio Frequency and Gradient Fields. *Magn Reson Med* **60**: 1488–1497.

Dandona P, James IM, Newbury PA, Woollard ML, Beckett AG (1978). Cerebral blood flow in diabetes mellitus: evidence of abnormal cerebrovascular reactivity. *Br Med J* **2**: 325–326.

Davids S, Lauffer H, Thoms K, Jagdhuhn M, Hirschfeld H, Domin M, *et al* (2010). Increased dorsolateral prefrontal cortex activation in obese children during observation of food stimuli. *Int J Obes 2005* **34**: 94–104.

Davis JF, Tracy AL, Schurdak JD, Tschöp MH, Lipton JW, Clegg DJ, *et al* (2008). Exposure to elevated levels of dietary fat attenuates psychostimulant reward and mesolimbic dopamine turnover in the rat. *Behav Neurosci* **122**: 1257–1263.

De Araujo IE, Rolls ET (2004). Representation in the human brain of food texture and oral fat. *J Neurosci Off J Soc Neurosci* **24**: 3086–3093.

De Silva A, Salem V, Long CJ, Makwana A, Newbould RD, Rabiner EA, *et al* (2011). The gut hormones PYY 3-36 and GLP-1 7-36 amide reduce food intake and modulate brain activity in appetite centers in humans. *Cell Metab* **14**: 700–706.

Deckersbach T, Das SK, Urban LE, Salinardi T, Batra P, Rodman AM, *et al* (2014). Pilot randomized trial demonstrating reversal of obesity-related abnormalities in reward system responsivity to food cues with a behavioral intervention. *Nutr Diabetes* **4**: e129.

DeFronzo RA, Barzilai N, Simonson DC (1991). Mechanism of metformin action in obese and lean noninsulin-dependent diabetic subjects. *J Clin Endocrinol Metab* **73**: 1294–1301.

DeFronzo RA, Ferrannini E, Simonson DC (1989). Fasting hyperglycemia in non-insulin-dependent diabetes mellitus: contributions of excessive hepatic glucose production and impaired tissue glucose uptake. *Metabolism* **38**: 387–395.

DeFronzo RA, Tobin JD, Andres R (1979). Glucose clamp technique: a method for quantifying insulin secretion and resistance. *Am J Physiol* **237**: E214-223.

DeFronzo RA, Tripathy D (2009). Skeletal Muscle Insulin Resistance Is the Primary Defect in Type 2 Diabetes. *Diabetes Care* **32**: S157–S163.

Del Parigi A, Chen K, Gautier J-F, Salbe AD, Pratley RE, Ravussin E, *et al* (2002). Sex differences in the human brain's response to hunger and satiation. *Am J Clin Nutr* **75**: 1017–1022.

DelParigi A, Chen K, Salbe AD, Hill JO, Wing RR, Reiman EM, *et al* (2004). Persistence of abnormal neural responses to a meal in postobese individuals. *Int J Obes Relat Metab Disord J Int Assoc Study Obes* **28**: 370–377.

DelParigi A, Chen K, Salbe AD, Reiman EM, Tataranni PA (2005). Sensory experience of food and obesity: a positron emission tomography study of the brain regions affected by tasting a liquid meal after a prolonged fast. *NeuroImage* **24**: 436–443.

Demos KE, Heatherton TF, Kelley WM (2012). Individual Differences in Nucleus Accumbens Activity to Food and Sexual Images Predict Weight Gain and Sexual Behavior. *J Neurosci* **32**: 5549–5552.

Demos KE, Kelley WM, Heatherton TF (2011). Dietary restraint violations influence reward responses in nucleus accumbens and amygdala. *J Cogn Neurosci* **23**: 1952–1963.

Desmond JE, Glover GH (2002). Estimating sample size in functional MRI (fMRI) neuroimaging studies: statistical power analyses. *J Neurosci Methods* **118**: 115–128.

Detre JA, Alsop DC (1999). Perfusion magnetic resonance imaging with continuous arterial spin labeling: methods and clinical applications in the central nervous system. *Eur J Radiol* **30**: 115–24.

Detre JA, Leigh JS, Williams DS, Koretsky AP (1992). Perfusion imaging. *Magn Reson Med Off J Soc Magn Reson Med Soc Magn Reson Med* **23**: 37–45.

Detre JA, Rao H, Wang DJJ, Chen YF, Wang Z (2012). Applications of arterial spin labeled MRI in the brain. *J Magn Reson Imaging* **35**: 1026–1037.

Dimitropoulos A, Tkach J, Ho A, Kennedy J (2012). Greater corticolimbic activation to high-calorie food cues after eating in obese vs. normal-weight adults. *Appetite* **58**: 303–312.

Djordjevic J, Zatorre RJ, Jones-Gotman M (2004). Effects of perceived and imagined odors on taste detection. *Chem Senses* **29**: 199–208.

Duan Y, Zhang R, Zhang M, Sun L, Dong S, Wang G, *et al* (2013). Metformin inhibits food intake and neuropeptide Y gene expression in the hypothalamus. *Neural Regen Res* **8**: 2379–2388.

Dunn JP, Abumrad NN, Breitman I, Marks-Shulman PA, Flynn CR, Jabbour K, *et al* (2012a). Hepatic and Peripheral Insulin Sensitivity and Diabetes Remission at 1 Month After Roux-en-Y Gastric Bypass Surgery in Patients Randomized to Omentectomy. *Diabetes Care* **35**: 137–142.

Dunn JP, Cowan RL, Volkow ND, Feurer ID, Li R, Williams DB, *et al* (2010). Decreased dopamine type 2 receptor availability after bariatric surgery: preliminary findings. *Brain Res* **1350**: 123–130.

Dunn JP, Kessler RM, Feurer ID, Volkow ND, Patterson BW, Ansari MS, *et al* (2012b). Relationship of Dopamine Type 2 Receptor Binding Potential With Fasting Neuroendocrine Hormones and Insulin Sensitivity in Human Obesity. *Diabetes Care* **35**: 1105–1111.

Efimova I, Efimova N, Lishmanov Y (2014). Cerebral blood flow and cognitive function in patients with metabolic syndrome: effect of antihypertensive therapy. *J Clin Hypertens Greenwich Conn* **16**: 900–906.

Egecioglu E, Skibicka KP, Hansson C, Alvarez-Crespo M, Friberg PA, Jerlhag E, *et al* (2011). Hedonic and incentive signals for body weight control. *Rev Endocr Metab Disord* **12**: 141–151.

Eicke BM, Seidel E, Krummenauer F (2003). Volume flow in the common carotid artery does not decrease postprandially. *J Neuroimaging Off J Am Soc Neuroimaging* **13**: 352–355.

Elliott R, Dolan RJ, Frith CD (2000). Dissociable Functions in the Medial and Lateral Orbitofrontal Cortex: Evidence from Human Neuroimaging Studies. *Cereb Cortex* **10**: 308–317.

English PJ, Ashcroft A, Patterson M, Dovey TM, Halford JCG, Harrison J, *et al* (2007). Metformin prolongs the postprandial fall in plasma ghrelin concentrations in type 2 diabetes. *Diabetes Metab Res Rev* **23**: 299–303.

Erdmann J, Lippl F, Wagenpfeil S, Schusdziarra V (2005). Differential Association of Basal and Postprandial Plasma Ghrelin With Leptin, Insulin, and Type 2 Diabetes. *Diabetes* **54**: 1371–1378.

Eriksson J, Franssila-Kallunki A, Ekstrand A, Saloranta C, Widén E, Schalin C, *et al* (1989). Early metabolic defects in persons at increased risk for non-insulin-dependent diabetes mellitus. *N Engl J Med* **321**: 337–343.

Erixon-Lindroth N, Farde L, Wahlin T-BR, Sovago J, Halldin C, Bäckman L (2005). The role of the striatal dopamine transporter in cognitive aging. *Psychiatry Res* **138**: 1–12.

Evero N, Hackett LC, Clark RD, Phelan S, Hagobian TA (2012). Aerobic exercise reduces neuronal responses in food reward brain regions. *J Appl Physiol Bethesda Md 1985* **112**: 1612–1619.

Færch K, Torekov SS, Vistisen D, Johansen NB, Witte DR, Jonsson A, *et al* (2015). GLP-1 Response to Oral Glucose Is Reduced in Prediabetes, Screen-Detected Type 2 Diabetes, and Obesity and Influenced by Sex: The ADDITION-PRO Study. *Diabetes* **64**: 2513–2525.

Fairburn CG, Beglin SJ (2008). Eating Disorder Examination Questionnaire (EDE-Q 6.0). *Cogn Behav Ther Eat Disord* 309–314.

Farbood Y, Sarkaki A, Khalaj L, Khodagholi F, Badavi M, Ashabi G (2015). Targeting AMPK by metformin adjusts post-ischemic hyperemia and extracellular neuronal discharge in transient global cerebral ischemia. *Microcirculation* **22**: 534–541.

Farooqi IS, Bullmore E, Keogh J, Gillard J, O'Rahilly S, Fletcher PC (2007). Leptin regulates striatal regions and human eating behavior. *Science* **317**: 1355.

Farr OM, Gavrieli A, Mantzoros CS (2015). Leptin applications in 2015: what have we learned about leptin and obesity? *Curr Opin Endocrinol Diabetes Obes* **22**: 353–359.

Farr OM, Sofopoulos M, Tsoukas MA, Dincer F, Thakkar B, Sahin-Efe A, *et al* (2016). GLP-1 receptors exist in the parietal cortex, hypothalamus and medulla of human brains and the GLP-1 analogue liraglutide alters brain activity related to highly desirable food cues in individuals with diabetes: a crossover, randomised, placebo-controlled trial. *Diabetologia* **59**: 954–965.

Ferrini F, Salio C, Lossi L, Merighi A (2009). Ghrelin in Central Neurons. *Curr Neuropharmacol* **7**: 37–49.

Figlewicz DP (2003). Adiposity signals and food reward: expanding the CNS roles of insulin and leptin. *Am J Physiol Regul Integr Comp Physiol* **284**: R882-892.

Figlewicz DP, Bennett JL, Naleid AM, Davis C, Grimm JW (2006). Intraventricular insulin and leptin decrease sucrose self-administration in rats. *Physiol Behav* **89**: 611–616.

Figlewicz DP, Benoit SC (2009). Insulin, leptin, and food reward: update 2008. *AJP Regul Integr Comp Physiol* **296**: R9–R19.

Filippi BM, Bassiri A, Abraham MA, Duca FA, Yue JTY, Lam TKT (2014). Insulin signals through the dorsal vagal complex to regulate energy balance. *Diabetes* **63**: 892–899.

Flanagan D, Fulford J, Krishnan B, Benattayallah A, Watt A, Summers I (2012). Functional MRI of the hypothalamic response to an oral glucose load. *Diabetologia* **55**: 2080–2082.

Flegal KM, Carroll MD, Ogden CL, Curtin LR (2010). Prevalence and trends in obesity among US adults, 1999-2008. *JAMA J Am Med Assoc* **303**: 235–241.

Flint A, Raben A, Blundell JE, Astrup A (2000). Reproducibility, power and validity of visual analogue scales in assessment of appetite sensations in single test meal studies. *Int J Obes Relat Metab Disord J Int Assoc Study Obes* **24**: 38–48.

Fox KCR, Spreng RN, Ellamil M, Andrews-Hanna JR, Christoff K (2015). The wandering brain: Meta-analysis of functional neuroimaging studies of mind-wandering and related spontaneous thought processes. *NeuroImage* **111**: 611–621.

Frank GK, Kaye WH, Carter CS, Brooks S, May C, Fissell K, *et al* (2003). The evaluation of brain activity in response to taste stimuli--a pilot study and method for central taste activation as assessed by event-related fMRI. *J Neurosci Methods* **131**: 99–105.

Frank H, Jankovi-Vokes T, Pardridge W, Morris W (1985). Enhanced insulin binding to blood-brain barrier in vivo and to brain microvessels in vitro in newborn rabbits. *Diabetes* **34**: 728.

Frank S, Heni M, Moss A, Schnurbein J von, Fritsche A, Häring H-U, *et al* (2011). Leptin therapy in a congenital leptin-deficient patient leads to acute and long-term changes in homeostatic, reward, and food-related brain areas. *J Clin Endocrinol Metab* **96**: E1283-1287.

Frank S, Kullmann S, Veit R (2013). Food related processes in the insular cortex. *Front Hum Neurosci* **7**: 499.

Frank S, Laharnar N, Kullmann S, Veit R, Canova C, Hegner YL, *et al* (2010a). Processing of food pictures: influence of hunger, gender and calorie content. *Brain Res* **1350**: 159–166.

Frank S, Linder K, Kullmann S, Heni M, Ketterer C, Çavuşoğlu M, *et al* (2012). Fat intake modulates cerebral blood flow in homeostatic and gustatory brain areas in humans. *Am J Clin Nutr* **95**: 1342–1349.

Frank TC, Kim GL, Krzemien A, Van Vugt DA (2010b). Effect of menstrual cycle phase on corticolimbic brain activation by visual food cues. *Brain Res* **1363**: 81–92.

Frankort A, Roefs A, Siep N, Roebroeck A, Havermans R, Jansen A (2012). Reward activity in satiated overweight women is decreased during unbiased viewing but increased when imagining taste: an event-related fMRI study. *Int J Obes* **36**: 627–637.

Freemark M, Bursey D (2001). The effects of metformin on body mass index and glucose tolerance in obese adolescents with fasting hyperinsulinemia and a family history of type 2 diabetes. *Pediatrics* **107**: E55.

Fregni F, Orsati F, Pedrosa W, Fecteau S, Tome FAM, Nitsche MA, *et al* (2008). Transcranial direct current stimulation of the prefrontal cortex modulates the desire for specific foods. *Appetite* **51**: 34–41.

Friman O, Borga M, Lundberg P, Knutsson H (2003). Adaptive analysis of fMRI data. *NeuroImage* **19**: 837–845.

Friston KJ, Worsley KJ, Frackowiak RSJ, Mazziotta JC, Evans AC (1994). Assessing the significance of focal activations using their spatial extent. *Hum Brain Mapp* **1**: 210–220.

Frölich L, Blum-Degen D, Bernstein H-G, Engelsberger S, Humrich J, Laufer S, *et al* (1998). Brain insulin and insulin receptors in aging and sporadic Alzheimer's disease. *J Neural Transm* **105**: 423–438.

Fuhrer D, Zysset S, Stumvoll M (2008). Brain Activity in Hunger and Satiety: An Exploratory Visually Stimulated fMRI Study. *Obesity* **16**: 945–950.

Gautier JF, Chen K, Salbe AD, Bandy D, Pratley RE, Heiman M, *et al* (2000). Differential brain responses to satiation in obese and lean men. *Diabetes* **49**: 838–846.

Gautier J-F, Chen K, Uecker A, Bandy D, Frost J, Salbe AD, *et al* (1999). Regions of the human brain affected during a liquid-meal taste perception in the fasting state: a positron emission tomography study. *Am J Clin Nutr* **70**: 806–810.

Gautier J-F, Del Parigi A, Chen K, Salbe AD, Bandy D, Pratley RE, *et al* (2001). Effect of Satiation on Brain Activity in Obese and Lean Women. *Obesity* **9**: 676–684.

Gearhardt AN, Yokum S, Orr PT, Stice E, Corbin WR, Brownell KD (2011). Neural Correlates of Food Addiction. *Arch Gen Psychiatry* **68**: 808–816.

Geliebter A, Pantazatos SP, McOuatt H, Puma L, Gibson CD, Atalayer D (2013). Sex-based fMRI differences in obese humans in response to high vs. low energy food cues. *Behav Brain Res* **243**: 91–96.

Geloneze B, Oliveira M da S de, Vasques ACJ, Novaes FS, Pareja JC, Tambascia MA (2014). Impaired incretin secretion and pancreatic dysfunction with older age and diabetes. *Metabolism* **63**: 922–929.

Gerstein HC, Yusuf S, Bosch J, Pogue J, Sheridan P, Dinccag N, *et al* (2006). Effect of rosiglitazone on the frequency of diabetes in patients with impaired glucose tolerance or impaired fasting glucose: a randomised controlled trial. *Lancet* **368**: 1096–1105.

Giezenaar C, Chapman I, Luscombe-Marsh N, Feinle-Bisset C, Horowitz M, Soenen S (2016). Ageing Is Associated with Decreases in Appetite and Energy Intake--A Meta-Analysis in Healthy Adults. *Nutrients* **8**: 28.

Gläscher J, Gitelman D (2008). Contrast weights in flexible factorial design with multiple groups of subjects. at <http://www.sbirc.ed.ac.uk/cyril/download/Contrast_Weighting_Glascher_Gitelman_2008.pdf>.

Glicksman C, Pournaras DJ, Wright M, Roberts R, Mahon D, Welbourn R, *et al* (2010). Postprandial plasma bile acid responses in normal weight and obese subjects. *Ann Clin Biochem* **47**: 482–484.

Golay A (2007). Metformin and body weight. *Int J Obes* **32**: 61–72.

Goldman RL, Borckardt JJ, Frohman HA, O'Neil PM, Madan A, Campbell LK, *et al* (2011). Prefrontal cortex transcranial direct current stimulation (tDCS) temporarily reduces food cravings and increases the self-reported ability to resist food in adults with frequent food craving. *Appetite* **56**: 741–746.

Goldman RL, Canterberry M, Borckardt JJ, Madan A, Byrne TK, George MS, *et al* (2013). Executive control circuitry differentiates degree of success in weight loss following gastric-bypass surgery. *Obesity* **21**: 2189–2196.

Goldstone AP, Hernandez CGP de, Beaver JD, Muhammed K, Croese C, Bell G, *et al* (2009). Fasting biases brain reward systems towards high-calorie foods. *Eur J Neurosci* **30**: 1625–1635.

Goldstone AP, Prechtl CG, Scholtz S, Miras AD, Chhina N, Durighel G, *et al* (2014). Ghrelin mimics fasting to enhance human hedonic, orbitofrontal cortex, and hippocampal responses to food. *Am J Clin Nutr* **99**: 1319–1330.

Golen LW van, IJzerman RG, Huisman MC, Hensbergen JF, Hoogma RP, Drent ML, *et al* (2013). Cerebral blood flow and glucose metabolism in appetite-related brain regions in type 1 diabetic patients after treatment with insulin detemir and NPH insulin: a randomized controlled crossover trial. *Diabetes Care* **36**: 4050–4056.

Golen LW van, Veltman DJ, Ijzerman RG, Deijen JB, Heijboer AC, Barkhof F, *et al* (2014). Effects of Insulin Detemir and NPH Insulin on Body Weight and Appetite-Regulating Brain Regions in Human Type 1 Diabetes: A Randomized Controlled Trial. *PloS One* **9**: e94483.

Gorczyca AM, Sjaarda LA, Mitchell EM, Perkins NJ, Schliep KC, Wactawski-Wende J, *et al* (2016). Changes in macronutrient, micronutrient, and food group intakes throughout the menstrual cycle in healthy, premenopausal women. *Eur J Nutr* **55**: 1181–1188.

Gorin AA, Niemeier HM, Hogan P, Coday M, Davis C, DiLillo VG, *et al* (2008). Binge eating and weight loss outcomes in overweight and obese individuals with type 2 diabetes: results from the Look AHEAD trial. *Arch Gen Psychiatry* **65**: 1447–1455.

Grabenhorst F, Rolls ET, Bilderbeck A (2008). How cognition modulates affective responses to taste and flavor: top-down influences on the orbitofrontal and pregenual cingulate cortices. *Cereb Cortex N Y N 1991* **18**: 1549–1559.

Grabenhorst F, Rolls ET, Parris BA, Souza AA d' (2010). How the brain represents the reward value of fat in the mouth. *Cereb Cortex N Y N 1991* **20**: 1082–1091.

Gray SM, Meijer RI, Barrett EJ (2014). Insulin regulates brain function, but how does it get there? *Diabetes* **63**: 3992–3997.

Green E, Jacobson A, Haase L, Murphy C (2011). Reduced nucleus accumbens and caudate nucleus activation to a pleasant taste is associated with obesity in older adults. *Brain Res* **1386**: 109–117.

Green E, Jacobson A, Haase L, Murphy C (2013). Can age-related CNS taste differences be detected as early as middle age? Evidence from fMRI. *Neuroscience* **232**: 194–203.

Grichisch Y, Cavuşoğlu M, Preissl H, Uludağ K, Hallschmid M, Birbaumer N, *et al* (2012). Differential effects of intranasal insulin and caffeine on cerebral blood flow. *Hum Brain Mapp* **33**: 280–287.

Grosshans M, Vollmert C, Vollstadt-Klein S, Tost H, Leber S, Bach P, *et al* (2012). Association of Leptin With Food Cue-Induced Activation in Human Reward Pathways. *Arch Gen Psychiatry* **69**: 529–537.

Grummich P, Nimsky C, Pauli E, Buchfelder M, Ganslandt O (2006). Combining fMRI and MEG increases the reliability of presurgical language localization: a clinical study on the difference between and congruence of both modalities. *NeuroImage* **32**: 1793–1803.

Guo J, Simmons WK, Herscovitch P, Martin A, Hall KD (2014). Striatal dopamine D2-like receptor correlation patterns with human obesity and opportunistic eating behavior. *Mol Psychiatry* **19**: 1078–1084.

Gupta A, Bisht B, Dey CS (2011). Peripheral insulin-sensitizer drug metformin ameliorates neuronal insulin resistance and Alzheimer's-like changes. *Neuropharmacology* **60**: 910–920.

Guthoff M, Grichisch Y, Canova C, Tschritter O, Veit R, Hallschmid M, *et al* (2010). Insulin modulates food-related activity in the central nervous system. *J Clin Endocrinol Metab* **95**: 748–755.

Guthoff M, Stingl KT, Tschritter O, Rogic M, Heni M, Stingl K, *et al* (2011). The insulin-mediated modulation of visually evoked magnetic fields is reduced in obese subjects. *PloS One* **6**: e19482.

Gutt M, Davis CL, Spitzer SB, Llabre MM, Kumar M, Czarnecki EM, *et al* (2000). Validation of the insulin sensitivity index (ISI(0,120)): comparison with other measures. *Diabetes Res Clin Pract* **47**: 177–184.

Hallschmid M, Benedict C, Schultes B, Born J, Kern W (2008). Obese men respond to cognitive but not to catabolic brain insulin signaling. *Int J Obes* **32**: 275–282.

Hallschmid M, Benedict C, Schultes B, Fehm H-L, Born J, Kern W (2004a). Intranasal Insulin Reduces Body Fat in Men but not in Women. *Diabetes* **53**: 3024–3029.

Hallschmid M, Higgs S, Thienel M, Ott V, Lehnert H (2012). Postprandial Administration of Intranasal Insulin Intensifies Satiety and Reduces Intake of Palatable Snacks in Women. *Diabetes* **61**: 782–789.

Hallschmid M, Jauch-Chara K, Korn O, Mölle M, Rasch B, Born J, *et al* (2010). Euglycemic infusion of insulin detemir compared with human insulin appears to increase direct current brain potential response and reduces food intake while inducing similar systemic effects. *Diabetes* **59**: 1101–1107.

Hallschmid M, Schultes B, Marshall L, Mölle M, Kern W, Bredthauer J, *et al* (2004b). Transcortical direct current potential shift reflects immediate signaling of systemic insulin to the human brain. *Diabetes* **53**: 2202–2208.

Harano Y, Ohgaku S, Hidaka H, Haneda K, Kikkawa R, Shigeta Y, *et al* (1977). Glucose, insulin and somatostatin infusion for the determination of insulin sensitivity. *J Clin Endocrinol Metab* **45**: 1124–1127.

Hare TA, Camerer CF, Rangel A (2009). Self-control in decision-making involves modulation of the vmPFC valuation system. *Science* **324**: 646–648.

Havermans R (2012). How to tell where 'liking' ends and 'wanting' begins. *Appetite* **58**: 252–255.

Havermans RC (2011). "You Say it's Liking, I Say it's Wanting …". On the difficulty of disentangling food reward in man. *Appetite* **57**: 286–294.

Havrankova J, Roth J, Brownstein M (1978). Insulin receptors are widely distributed in the central nervous system of the rat. *Nature* **272**: 827–829.

Heni M, Kullmann S, Gallwitz B, Häring H-U, Preissl H, Fritsche A (2015). Dissociation of GLP-1 and insulin association with food processing in the brain: GLP-1 sensitivity despite insulin resistance in obese humans. *Mol Metab* **4**: 971–976.

Heni M, Kullmann S, Ketterer C, Guthoff M, Bayer M, Staiger H, *et al* (2014a). Differential effect of glucose ingestion on the neural processing of food stimuli in lean and overweight adults. *Hum Brain Mapp* **35**: 918–928.

Heni M, Kullmann S, Ketterer C, Guthoff M, Linder K, Wagner R, *et al* (2012). Nasal insulin changes peripheral insulin sensitivity simultaneously with altered

activity in homeostatic and reward-related human brain regions. *Diabetologia* **55**: 1173–1782.

Heni M, Schöpfer P, Peter A, Sartorius T, Fritsche A, Synofzik M, *et al* (2014b). Evidence for altered transport of insulin across the blood-brain barrier in insulin-resistant humans. *Acta Diabetol* **51**: 679–681.

Heni M, Wagner R, Kullmann S, Veit R, Mat-Husin H, Linder K, *et al* (2014c). Central insulin administration improves whole-body insulin sensitivity via hypothalamus and parasympathetic outputs in men. *Diabetes* **63**: 4083–4088.

Hennige AM, Sartorius T, Tschritter O, Preissl H, Fritsche A, Ruth P, *et al* (2006). Tissue selectivity of insulin detemir action in vivo. *Diabetologia* **49**: 1274–1282.

Henriksen JE, Levin K, Thye-Rønn P, Alford F, Hother-Nielsen O, Holst JJ, *et al* (2000). Glucose-mediated glucose disposal in insulin-resistant normoglycemic relatives of type 2 diabetic patients. *Diabetes* **49**: 1209–1218.

Hinton EC, Parkinson JA, Holland AJ, Arana FS, Roberts AC, Owen AM (2004). Neural contributions to the motivational control of appetite in humans. *Eur J Neurosci* **20**: 1411–1418.

Hirvonen J, Virtanen KA, Nummenmaa L, Hannukainen JC, Honka M-J, Bucci M, *et al* (2011). Effects of insulin on brain glucose metabolism in impaired glucose tolerance. *Diabetes* **60**: 443–447.

Ho A, Kennedy J, Dimitropoulos A (2012). Neural correlates to food-related behavior in normal-weight and overweight/obese participants. *PloS One* **7**: e45403.

Hollmann M, Hellrung L, Pleger B, Schlögl H, Kabisch S, Stumvoll M, *et al* (2012). Neural correlates of the volitional regulation of the desire for food. *Int J Obes* **36**: 648–655.

Holsen LM, Zarcone JR, Thompson TI, Brooks WM, Anderson MF, Ahluwalia JS, *et al* (2005). Neural mechanisms underlying food motivation in children and adolescents. *NeuroImage* **27**: 669–676.

Hopkins DF, Williams G (1997). Insulin receptors are widely distributed in human brain and bind human and porcine insulin with equal affinity. *Diabet Med J Br Diabet Assoc* **14**: 1044–1050.

Horsdal HT, Mehnert F, Rungby J, Johnsen SP (2012). Type of preadmission antidiabetic treatment and outcome among patients with ischemic stroke: a

nationwide follow-up study. *J Stroke Cerebrovasc Dis Off J Natl Stroke Assoc* **21**: 717–725.

Hosker JP, Matthews DR, Rudenski AS, Burnett MA, Darling P, Bown EG, *et al* (1985). Continuous infusion of glucose with model assessment: measurement of insulin resistance and beta-cell function in man. *Diabetologia* **28**: 401–411.

Howard BV, Adams-Campbell L, Allen C, Black H, Passaro M, Rodabough RJ, *et al* (2004). Insulin resistance and weight gain in postmenopausal women of diverse ethnic groups. *Int J Obes* **28**: 1039–1047.

Huang Y-C, Hsu C-C, Lin W-C, Yin T-K, Huang C-W, Wang P-W, *et al* (2014). Effects of metformin on the cerebral metabolic changes in type 2 diabetic patients. *ScientificWorldJournal* **2014**: 694326.

Huettel SA, Song AW, McCarthy G (Sinauer Associates: Sunderland, Mass., 2008). *Functional magnetic resonance imaging*. .

Humphriss DB, Stewart MW, Berrish TS, Barriocanal LA, Trajano LR, Ashworth LA, *et al* (1997). Multiple metabolic abnormalities in normal glucose tolerant relatives of NIDDM families. *Diabetologia* **40**: 1185–1190.

Hutcherson CA, Plassmann H, Gross JJ, Rangel A (2012). Cognitive regulation during decision making shifts behavioral control between ventromedial and dorsolateral prefrontal value systems. *J Neurosci Off J Soc Neurosci* **32**: 13543–13554.

International Diabetes Federation (2006). IDF Worldwide Definition of the Metabolic Syndrome. at <http://www.idf.org/webdata/docs/IDF_Meta_def_final.pdf>.

Inzucchi SE, Bergenstal RM, Buse JB, Diamant M, Ferrannini E, Nauck M, *et al* (2012). Management of hyperglycaemia in type 2 diabetes: a patient-centered approach. Position statement of the American Diabetes Association (ADA) and the European Association for the Study of Diabetes (EASD). *Diabetologia* **55**: 1577–1596.

Iozzo P (2009). Viewpoints on the Way to the Consensus Session Where does insulin resistance start? The adipose tissue. *Diabetes Care* **32**: S168–S173.

Iwasaki Y, Shimomura K, Kohno D, Dezaki K, Ayush E-A, Nakabayashi H, *et al* (2013). Insulin Activates Vagal Afferent Neurons Including those Innervating Pancreas via Insulin Cascade and Ca(2+) Influx: Its Dysfunction in IRS2-KO Mice with Hyperphagic Obesity. *PloS One* **8**: e67198.

Jacobson A, Green E, Murphy C (2010). Age-related functional changes in gustatory and reward processing regions: An fMRI study. *NeuroImage* **53**: 602–610.

James AP, Watts GF, Mamo JCL (2005). The effect of metformin and rosiglitazone on postprandial lipid metabolism in obese insulin-resistant subjects. *Diabetes Obes Metab* **7**: 381–389.

Jastreboff AM, Gaiser EC, Gu P, Sinha R (2014). Sex differences in the association between dietary restraint, insulin resistance and obesity. *Eat Behav* **15**: 286–290.

Jastreboff AM, Sinha R, Lacadie C, Small DM, Sherwin RS, Potenza MN (2012). Neural Correlates of Stress- and Food- Cue-Induced Food Craving In Obesity: Association with insulin levels. *Diabetes Care* **36**: 394–402.

Jauch-Chara K, Friedrich A, Rezmer M, Melchert UH, Scholand-Engler HG, Hallschmid M, *et al* (2012). Intranasal Insulin Suppresses Food Intake via Enhancement of Brain Energy Levels in Humans. *Diabetes* **61**: 2261–2268.

Jensterle M, Sebestjen M, Janez A, Prezelj J, Kocjan T, Keber I, *et al* (2008). Improvement of endothelial function with metformin and rosiglitazone treatment in women with polycystic ovary syndrome. *Eur J Endocrinol Eur Fed Endocr Soc* **159**: 399–406.

Jiang T, Yu J-T, Zhu X-C, Wang H-F, Tan M-S, Cao L, *et al* (2014). Acute metformin preconditioning confers neuroprotection against focal cerebral ischaemia by pre-activation of AMPK-dependent autophagy. *Br J Pharmacol* **171**: 3146–3157.

Jin Q, Cheng J, Liu Y, Wu J, Wang X, Wei S, *et al* (2014). Improvement of functional recovery by chronic metformin treatment is associated with enhanced alternative activation of microglia/macrophages and increased angiogenesis and neurogenesis following experimental stroke. *Brain Behav Immun* **40**: 131–142.

Johnson F, Pratt M, Wardle J (2012). Dietary restraint and self-regulation in eating behavior. *Int J Obes* **36**: 665–674.

Jones CNO, Abbasi F, Carantoni M, Polonsky KS, Reaven GM (2000). Roles of insulin resistance and obesity in regulation of plasma insulin concentrations. *Am J Physiol - Endocrinol Metab* **278**: E501–E508.

Jones RB, McKie S, Astbury N, Little TJ, Tivey S, Lassman DJ, *et al* (2012). Functional neuroimaging demonstrates that ghrelin inhibits the central nervous system response to ingested lipid. *Gut* **61**: 1543–1551.

Jucaite A, Forssberg H, Karlsson P, Halldin C, Farde L (2010). Age-related reduction in dopamine D1 receptors in the human brain: from late childhood to adulthood, a positron emission tomography study. *Neuroscience* **167**: 104–110.

Kaiyala KJ, Prigeon RL, Kahn SE, Woods SC, Schwartz MW (2000). Obesity induced by a high-fat diet is associated with reduced brain insulin transport in dogs. *Diabetes* **49**: 1525–1533.

Kandel ER, Schwartz JH, Jessell TM, Siegelbaum SA, Hudspeth AJ (McGraw-Hill Education: 2013). *Principles of Neural Science*. .

Kanoski SE, Fortin SM, Arnold M, Grill HJ, Hayes MR (2011). Peripheral and central GLP-1 receptor populations mediate the anorectic effects of peripherally administered GLP-1 receptor agonists, liraglutide and exendin-4. *Endocrinology* **152**: 3103–3112.

Karczewska-Kupczewska M, Tarasów E, Nikołajuk A, Stefanowicz M, Matulewicz N, Otziomek E, *et al* (2013). The Effect of Insulin Infusion on the Metabolites in Cerebral Tissues Assessed With Proton Magnetic Resonance Spectroscopy in Young Healthy Subjects With High and Low Insulin Sensitivity. *Diabetes Care* **36**: 2787–2793.

Karlsson HKR, Hällsten K, Björnholm M, Tsuchida H, Chibalin AV, Virtanen KA, *et al* (2005). Effects of metformin and rosiglitazone treatment on insulin signaling and glucose uptake in patients with newly diagnosed type 2 diabetes: a randomized controlled study. *Diabetes* **54**: 1459–1467.

Karra E, O'Daly OG, Choudhury AI, Yousseif A, Millership S, Neary MT, *et al* (2013). A link between FTO, ghrelin, and impaired brain food-cue responsivity. *J Clin Invest* **123**: 3539–3551.

Katz A, Nambi SS, Mather K, Baron AD, Follmann DA, Sullivan G, *et al* (2000). Quantitative insulin sensitivity check index: a simple, accurate method for assessing insulin sensitivity in humans. *J Clin Endocrinol Metab* **85**: 2402–2410.

Kennedy J, Dimitropoulos A (2014). Influence of feeding state on neurofunctional differences between individuals who are obese and normal weight: a meta-analysis of neuroimaging studies. *Appetite* **75**: 103–109.

Kern W, Benedict C, Schultes B, Plohr F, Moser A, Born J, *et al* (2006). Low cerebrospinal fluid insulin levels in obese humans. *Diabetologia* **49**: 2790–2792.

Kern W, Born J, Schreiber H, Fehm HL (1999). Central nervous system effects of intranasally administered insulin during euglycemia in men. *Diabetes* **48**: 557–563.

Kern W, Peters A, Fruehwald-Schultes B, Deininger E, Born J, Fehm HL (2001). Improving influence of insulin on cognitive functions in humans. *Neuroendocrinology* **74**: 270–280.

Killgore WDS, Kipman M, Schwab ZJ, Tkachenko O, Preer L, Gogel H, *et al* (2013). Physical exercise and brain responses to images of high-calorie food. *Neuroreport* **24**: 962–967.

Killgore WDS, Young AD, Femia LA, Bogorodzki P, Rogowska J, Yurgelun-Todd DA (2003). Cortical and limbic activation during viewing of high- versus low-calorie foods. *NeuroImage* **19**: 1381–1394.

Killgore WDS, Yurgelun-Todd DA (2005a). Body mass predicts orbitofrontal activity during visual presentations of high-calorie foods. *Neuroreport* **16**: 859–863.

Killgore WDS, Yurgelun-Todd DA (2005b). Developmental changes in the functional brain responses of adolescents to images of high and low-calorie foods. *Dev Psychobiol* **47**: 377–397.

Killgore WDS, Yurgelun-Todd DA (2010). Sex differences in cerebral responses to images of high versus low-calorie food. *Neuroreport* **21**: 354–358.

Kim H-J, Park E-Y, Oh M-J, Park S-S, Shin K-H, Choi S-H, *et al* (2013a). Central administration of metformin into the third ventricle of C57BL/6 mice decreases meal size and number and activates hypothalamic S6 kinase. *Am J Physiol Regul Integr Comp Physiol* **305**: R499-505.

Kim H-J, Zhang X-H, Park E-Y, Shin K-H, Choi S-H, Chun B-G, *et al* (2013b). Metformin decreases meal size and number and increases c-Fos expression in the nucleus tractus solitarius of obese mice. *Physiol Behav* **110–111**: 213–220.

Kim I-J, Kim S-J, Kim Y-K (2009). Age- and sex-associated changes in cerebral glucose metabolism in normal healthy subjects: statistical parametric mapping

analysis of F-18 fluorodeoxyglucose brain positron emission tomography. *Acta Radiol Stockh Swed 1987* **50**: 1169–1174.

Kim S-G, Ogawa S (2012). Biophysical and physiological origins of blood oxygenation level-dependent fMRI signals. *J Cereb Blood Flow Metab Off J Int Soc Cereb Blood Flow Metab* **32**: 1188–1206.

Kim Y-W, Kim J-Y, Park Y-H, Park S-Y, Won K-C, Choi K-H, *et al* (2006). Metformin restores leptin sensitivity in high-fat-fed obese rats with leptin resistance. *Diabetes* **55**: 716–724.

Kinder M, Lotze M, Davids S, Domin M, Thoms K, Wendt J, *et al* (2014). Functional imaging in obese children responding to long-term sports therapy. *Behav Brain Res* **272**: 25–31.

Kitabchi AE, Temprosa M, Knowler WC, Kahn SE, Fowler SE, Haffner SM, *et al* (2005). Role of insulin secretion and sensitivity in the evolution of type 2 diabetes in the diabetes prevention program: effects of lifestyle intervention and metformin. *Diabetes* **54**: 2404–2414.

Knowler WC, Barrett-Connor E, Fowler SE, Hamman RF, Lachin JM, Walker EA, *et al* (2002). Reduction in the incidence of type 2 diabetes with lifestyle intervention or metformin. *N Engl J Med* **346**: 393–403.

Knowler WC, Fowler SE, Hamman RF, Christophi CA, Hoffman HJ, Brenneman AT, *et al* (2009). 10-year follow-up of diabetes incidence and weight loss in the Diabetes Prevention Program Outcomes Study. *The Lancet* **374**: 1677–1686.

Kotronen A, Seppälä-Lindroos A, Bergholm R, Yki-Järvinen H (2008). Tissue specificity of insulin resistance in humans: fat in the liver rather than muscle is associated with features of the metabolic syndrome. *Diabetologia* **51**: 130–138.

Krafft CE, Pierce JE, Schwarz NF, Chi L, Weinberger AL, Schaeffer DJ, *et al* (2014). An eight month randomized controlled exercise intervention alters resting state synchrony in overweight children. *Neuroscience* **256**: 445–455.

Kringelbach ML, O'Doherty J, Rolls ET, Andrews C (2003). Activation of the human orbitofrontal cortex to a liquid food stimulus is correlated with its subjective pleasantness. *Cereb Cortex N Y N 1991* **13**: 1064–1071.

Kringelbach ML, Rolls ET (2004). The functional neuroanatomy of the human orbitofrontal cortex: evidence from neuroimaging and neuropsychology. *Prog Neurobiol* **72**: 341–372.

Kroemer NB, Krebs L, Kobiella A, Grimm O, Pilhatsch M, Bidlingmaier M, *et al* (2013a). Fasting levels of ghrelin covary with the brain response to food pictures. *Addict Biol* **18**: 855–862.

Kroemer NB, Krebs L, Kobiella A, Grimm O, Vollstädt-Klein S, Wolfensteller U, *et al* (2013b). (Still) longing for food: insulin reactivity modulates response to food pictures. *Hum Brain Mapp* **34**: 2367–2380.

Krug R, Benedict C, Born J, Hallschmid M (2010). Comparable sensitivity of postmenopausal and young women to the effects of intranasal insulin on food intake and working memory. *J Clin Endocrinol Metab* **95**: E468-472.

Kullmann S, Frank S, Heni M, Ketterer C, Veit R, Häring H-U, *et al* (2013). Intranasal insulin modulates intrinsic reward and prefrontal circuitry of the human brain in lean women. *Neuroendocrinology* **97**: 176–182.

Kullmann S, Heni M, Veit R, Ketterer C, Schick F, Häring H, *et al* (2012). The obese brain: Association of body mass index and insulin sensitivity with resting state network functional connectivity. *Hum Brain Mapp* **33**: 1052–1061.

Kullmann S, Heni M, Veit R, Scheffler K, Machann J, Häring H-U, *et al* (2015). Selective Insulin Resistance in Homeostatic and Cognitive Control Brain Areas in Overweight and Obese Adults. *Diabetes Care* **38**: 1044–1050.

Kulve JS ten, Veltman DJ, Bloemendaal L van, Barkhof F, Deacon CF, Holst JJ, *et al* (2015). Endogenous GLP-1 mediates postprandial reductions in activation in central reward and satiety areas in patients with type 2 diabetes. *Diabetologia* **58**: 2688–2698.

Laan LN van der, Ridder DTD de, Viergever MA, Smeets PAM (2011). The first taste is always with the eyes: A meta-analysis on the neural correlates of processing visual food cues. *NeuroImage* **55**: 296–303.

LaBar KS, Gitelman DR, Parrish TB, Kim YH, Nobre AC, Mesulam MM (2001). Hunger selectively modulates corticolimbic activation to food stimuli in humans. *Behav Neurosci* **115**: 493–500.

Łabuzek K, Suchy D, Gabryel B, Bielecka A, Liber S, Okopień B (2010). Quantification of metformin by the HPLC method in brain regions, cerebrospinal fluid and plasma of rats treated with lipopolysaccharide. *Pharmacol Rep PR* **62**: 956–965.

Lancaster JL, Rainey LH, Summerlin JL, Freitas CS, Fox PT, Evans AC, *et al* (1997). Automated labeling of the human brain: a preliminary report on the

development and evaluation of a forward-transform method. *Hum Brain Mapp* **5**: 238–242.

Lancaster JL, Woldorff MG, Parsons LM, Liotti M, Freitas CS, Rainey L, *et al* (2000). Automated Talairach atlas labels for functional brain mapping. *Hum Brain Mapp* **10**: 120–131.

Lassman DJ, McKie S, Gregory LJ, Lal S, D'Amato M, Steele I, *et al* (2010). Defining the role of cholecystokinin in the lipid-induced human brain activation matrix. *Gastroenterology* **138**: 1514–1524.

Lawrence NS, Hinton EC, Parkinson JA, Lawrence AD (2012). Nucleus accumbens response to food cues predicts subsequent snack consumption in women and increased body mass index in those with reduced self-control. *NeuroImage* **63**: 415–422.

Le DSN, Pannacciulli N, Chen K, Salbe AD, Del Parigi A, Hill JO, *et al* (2007). Less activation in the left dorsolateral prefrontal cortex in the reanalysis of the response to a meal in obese than in lean women and its association with successful weight loss. *Am J Clin Nutr* **86**: 573–579.

Le DSNT, Pannacciulli N, Chen K, Del Parigi A, Salbe AD, Reiman EM, *et al* (2006). Less activation of the left dorsolateral prefrontal cortex in response to a meal: a feature of obesity. *Am J Clin Nutr* **84**: 725–731.

Lee A, Morley JE (1998). Metformin decreases food consumption and induces weight loss in subjects with obesity with type II non-insulin-dependent diabetes. *Obes Res* **6**: 47–53.

Lee CK, Choi YJ, Park SY, Kim JY, Won KC, Kim YW (2012). Intracerebroventricular injection of metformin induces anorexia in rats. *Diabetes Metab J* **36**: 293–299.

Lehtovirta M, Forsén B, Gullström M, Häggblom M, Eriksson JG, Taskinen MR, *et al* (2001). Metabolic effects of metformin in patients with impaired glucose tolerance. *Diabet Med J Br Diabet Assoc* **18**: 578–583.

Lennerz BS, Alsop DC, Holsen LM, Stern E, Rojas R, Ebbeling CB, *et al* (2013). Effects of dietary glycemic index on brain regions related to reward and craving in men. *Am J Clin Nutr* **98**: 641–7.

Lerche S, Brock B, Rungby J, Bøtker HE, Møller N, Rodell A, *et al* (2008). Glucagon-Like Peptide-1 Inhibits Blood-Brain Glucose Transfer in Humans. *Diabetes* **57**: 325–331.

Levy JC, Matthews DR, Hermans MP (1998). Correct homeostasis model assessment (HOMA) evaluation uses the computer program. *Diabetes Care* **21**: 2191–2192.

Li J, An R, Zhang Y, Li X, Wang S (2012a). Correlations of macronutrient-induced functional magnetic resonance imaging signal changes in human brain and gut hormone responses. *Am J Clin Nutr* **96**: 275–282.

Li Z, Zhu Y, Childress AR, Detre JA, Wang Z (2012b). Relations between BOLD fMRI-Derived Resting Brain Activity and Cerebral Blood Flow. *PLoS ONE* **7**: e44556.

Lindström J, Ilanne-Parikka P, Peltonen M, Aunola S, Eriksson JG, Hemiö K, *et al* (2006). Sustained reduction in the incidence of type 2 diabetes by lifestyle intervention: follow-up of the Finnish Diabetes Prevention Study. *The Lancet* **368**: 1673–1679.

Lindström J, Louheranta A, Mannelin M, Rastas M, Salminen V, Eriksson J, *et al* (2003). The Finnish Diabetes Prevention Study (DPS): Lifestyle intervention and 3-year results on diet and physical activity. *Diabetes Care* **26**: 3230–3236.

Liu Y, Gao J-H, Liu H-L, Fox PT (2000). The temporal response of the brain after eating revealed by functional MRI. *Nature* **405**: 1058–1062.

Liu Y, Tang G, Li Y, Wang Y, Chen X, Gu X, *et al* (2014). Metformin attenuates blood-brain barrier disruption in mice following middle cerebral artery occlusion. *J Neuroinflammation* **11**: 177.

Liu Y, Zhu X, Feinberg D, Guenther M, Gregori J, Weiner MW, *et al* (2012). Arterial spin labeling MRI study of age and gender effects on brain perfusion hemodynamics. *Magn Reson Med Off J Soc Magn Reson Med Soc Magn Reson Med* **68**: 912–922.

Lowe CJ, Hall PA, Staines WR (2014). The Effects of Continuous Theta Burst Stimulation to the Left Dorsolateral Prefrontal Cortex on Executive Function, Food Cravings, and Snack Food Consumption. *Psychosom Med Sept 2014* **76**: 503–511.

Luna V, Casauban L, Sajan MP, Gomez-Daspet J, Powe JL, Miura A, *et al* (2006). Metformin improves atypical protein kinase C activation by insulin and phosphatidylinositol-3,4,5-(PO4)3 in muscle of diabetic subjects. *Diabetologia* **49**: 375–382.

Lv W-S, Wen J-P, Li L, Sun R-X, Wang J, Xian Y-X, *et al* (2012). The effect of metformin on food intake and its potential role in hypothalamic regulation in obese diabetic rats. *Brain Res* **1444**: 11–19.

Ma TC, Buescher JL, Oatis B, Funk JA, Nash AJ, Carrier RL, *et al* (2007). Metformin therapy in a transgenic mouse model of Huntington's disease. *Neurosci Lett* **411**: 98–103.

Ma X-H, Zhong P, Gu Z, Feng J, Yan Z (2003). Muscarinic potentiation of GABA(A) receptor currents is gated by insulin signaling in the prefrontal cortex. *J Neurosci Off J Soc Neurosci* **23**: 1159–1168.

MacIntosh BJ, Crane DE, Sage MD, Rajab AS, Donahue MJ, McIlroy WE, *et al* (2014). Impact of a single bout of aerobic exercise on regional brain perfusion and activation responses in healthy young adults. *PloS One* **9**: e85163.

MacIntosh CG, Andrews JM, Jones KL, Wishart JM, Morris HA, Jansen JB, *et al* (1999). Effects of age on concentrations of plasma cholecystokinin, glucagon-like peptide 1, and peptide YY and their relation to appetite and pyloric motility. *Am J Clin Nutr* **69**: 999–1006.

Magkos F, Tsekouras Y, Kavouras SA, Mittendorfer B, Sidossis LS (2008). Improved insulin sensitivity after a single bout of exercise is curvilinearly related to exercise energy expenditure. *Clin Sci Lond Engl 1979* **114**: 59–64.

Maldjian JA, Laurienti PJ, Burdette JH (2004). Precentral gyrus discrepancy in electronic versions of the Talairach atlas. *NeuroImage* **21**: 450–455.

Maldjian JA, Laurienti PJ, Kraft RA, Burdette JH (2003). An automated method for neuroanatomic and cytoarchitectonic atlas-based interrogation of fMRI data sets. *NeuroImage* **19**: 1233–1239.

Malik S, McGlone F, Bedrossian D, Dagher A (2008). Ghrelin modulates brain activity in areas that control appetitive behavior. *Cell Metab* **7**: 400–409.

Malonek D, Grinvald A (1996). Interactions between electrical activity and cortical microcirculation revealed by imaging spectroscopy: implications for functional brain mapping. *Science* **272**: 551–554.

Mannucci E, Tesi F, Bardini G, Ognibene A, Petracca MG, Ciani S, *et al* (2004). Effects of metformin on glucagon-like peptide-1 levels in obese patients with and without Type 2 diabetes. *Diabetes Nutr Metab* **17**: 336–342.

Mansfield MW, Heywood DM, Grant PJ (1996). Circulating levels of factor VII, fibrinogen, and von Willebrand factor and features of insulin resistance in first-degree relatives of patients with NIDDM. *Circulation* **94**: 2171–2176.

Marini MA, Frontoni S, Mineo D, Bracaglia D, Cardellini M, De Nicolais P, *et al* (2003). The Arg972 variant in insulin receptor substrate-1 is associated with an atherogenic profile in offspring of type 2 diabetic patients. *J Clin Endocrinol Metab* **88**: 3368–3371.

Marsh CA, Berent-Spillson A, Love T, Persad CC, Pop-Busui R, Zubieta J-K, *et al* (2013). Functional neuroimaging of emotional processing in women with polycystic ovary syndrome: a case-control pilot study. *Fertil Steril* **100**: 200–207.e1.

Martens MJ, Born JM, Lemmens SG, Karhunen L, Heinecke A, Goebel R, *et al* (2013). Increased sensitivity to food cues in the fasted state and decreased inhibitory control in the satiated state in the overweight. *Am J Clin Nutr* **97**: 471–479.

Martin LE, Holsen LM, Chambers RJ, Bruce AS, Brooks WM, Zarcone JR, *et al* (2010). Neural mechanisms associated with food motivation in obese and healthy weight adults. *Obes Silver Spring Md* **18**: 254–260.

Mason C, Foster-Schubert KE, Imayama I, Kong A, Xiao L, Bain C, *et al* (2011). Dietary weight loss and exercise effects on insulin resistance in postmenopausal women. *Am J Prev Med* **41**: 366–375.

Matsuda M, DeFronzo RA (1999). Insulin sensitivity indices obtained from oral glucose tolerance testing: comparison with the euglycemic insulin clamp. *Diabetes Care* **22**: 1462–1470.

Matsuda M, Liu Y, Mahankali S, Pu Y, Mahankali A, Wang J, *et al* (1999). Altered hypothalamic function in response to glucose ingestion in obese humans. *Diabetes* **48**: 1801–1806.

Matthews DR, Hosker JP, Rudenski AS, Naylor BA, Treacher DF, Turner RC (1985). Homeostasis model assessment: insulin resistance and beta-cell function from fasting plasma glucose and insulin concentrations in man. *Diabetologia* **28**: 412–419.

McCaffery JM, Haley AP, Sweet LH, Phelan S, Raynor HA, Del Parigi A, *et al* (2009). Differential functional magnetic resonance imaging response to food

pictures in successful weight-loss maintainers relative to normal-weight and obese controls. *Am J Clin Nutr* **90**: 928–934.

McFadden KL, Cornier M-A, Melanson EL, Bechtell JL, Tregellas JR (2013). Effects of exercise on resting-state default mode and salience network activity in overweight/obese adults. *Neuroreport* **24**: 866–871.

Mehta S, Melhorn SJ, Smeraglio A, Tyagi V, Grabowski T, Schwartz MW, *et al* (2012). Regional brain response to visual food cues is a marker of satiety that predicts food choice. *Am J Clin Nutr* **96**: 989–999.

Meltzer CC, Cantwell MN, Greer PJ, Ben-Eliezer D, Smith G, Frank G, *et al* (2000). Does Cerebral Blood Flow Decline in Healthy Aging? A PET Study with Partial-Volume Correction. *J Nucl Med* **41**: 1842–1848.

Miyawaki K, Yamada Y, Ban N, Ihara Y, Tsukiyama K, Zhou H, *et al* (2002). Inhibition of gastric inhibitory polypeptide signaling prevents obesity. *Nat Med* **8**: 738–742.

Morel Y, Golay A, Perneger T, Lehmann T, Vadas L, Pasik C, *et al* (1999). Metformin treatment leads to an increase in basal, but not insulin-stimulated, glucose disposal in obese patients with impaired glucose tolerance. *Diabet Med J Br Diabet Assoc* **16**: 650–655.

Morris JS, Dolan RJ (2001). Involvement of Human Amygdala and Orbitofrontal Cortex in Hunger-Enhanced Memory for Food Stimuli. *J Neurosci* **21**: 5304–5310.

Mosca CL, Marshall JA, Grunwald GK, Cornier MA, Baxter J (2004). Insulin resistance as a modifier of the relationship between dietary fat intake and weight gain. *Int J Obes* **28**: 803–812.

Mumford JA (2012). A power calculation guide for fMRI studies. *Soc Cogn Affect Neurosci* **7**: 738–742.

Muniyappa R, Lee S, Chen H, Quon MJ (2008). Current approaches for assessing insulin sensitivity and resistance in vivo: advantages, limitations, and appropriate usage. *Am J Physiol Endocrinol Metab* **294**: E15-26.

Murdaugh DL, Cox JE, Cook EW, Weller RE (2012). fMRI reactivity to high-calorie food pictures predicts short- and long-term outcome in a weight-loss program. *NeuroImage* **59**: 2709–2721.

Musi N, Hirshman MF, Nygren J, Svanfeldt M, Bavenholm P, Rooyackers O, *et al* (2002). Metformin increases AMP-activated protein kinase activity in skeletal muscle of subjects with type 2 diabetes. *Diabetes* **51**: 2074–2081.

Natali A, Ferrannini E (2006). Effects of metformin and thiazolidinediones on suppression of hepatic glucose production and stimulation of glucose uptake in type 2 diabetes: a systematic review. *Diabetologia* **49**: 434–441.

Nath N, Khan M, Paintlia MK, Singh I, Hoda MN, Giri S (2009). Metformin attenuated the autoimmune disease of the central nervous system in animal models of multiple sclerosis. *J Immunol Baltim Md 1950* **182**: 8005–8014.

National Institute for Health and Care Excellence (2009). Type 2 diabetes: The management of type 2 diabetes | Guidance and guidelines | NICE. at <https://www.nice.org.uk/guidance/cg87>.

Nauck MA, El-Ouaghlidi A, Gabrys B, Hücking K, Holst JJ, Deacon CF, *et al* (2004). Secretion of incretin hormones (GIP and GLP-1) and incretin effect after oral glucose in first-degree relatives of patients with type 2 diabetes. *Regul Pept* **122**: 209–217.

NCD Risk Factor Collaboration (2016). Trends in adult body-mass index in 200 countries from 1975 to 2014: a pooled analysis of 1698 population-based measurement studies with 19·2 million participants. *The Lancet* **387**: 1377–1396.

Novak V, Last D, Alsop DC, Abduljalil AM, Hu K, Lepicovsky L, *et al* (2006). Cerebral blood flow velocity and periventricular white matter hyperintensities in type 2 diabetes. *Diabetes Care* **29**: 1529–1534.

Novak V, Milberg W, Hao Y, Munshi M, Novak P, Galica A, *et al* (2014). Enhancement of vasoreactivity and cognition by intranasal insulin in type 2 diabetes. *Diabetes Care* **37**: 751–759.

Nummenmaa L, Hirvonen J, Hannukainen JC, Immonen H, Lindroos MM, Salminen P, *et al* (2012). Dorsal Striatum and Its Limbic Connectivity Mediate Abnormal Anticipatory Reward Processing in Obesity. *PLoS ONE* **7**: e31089.

Nyholm B, Mengel A, Nielsen S, Skjaerbaek C, Møller N, Alberti KG, *et al* (1996). Insulin resistance in relatives of NIDDM patients: the role of physical fitness and muscle metabolism. *Diabetologia* **39**: 813–822.

Obici S, Feng Z, Karkanias G, Baskin DG, Rossetti L (2002). Decreasing hypothalamic insulin receptors causes hyperphagia and insulin resistance in rats. *Nat Neurosci* **5**: 566–572.

Obici S, Rossetti L (2003). Minireview: nutrient sensing and the regulation of insulin action and energy balance. *Endocrinology* **144**: 5172–5178.

Ochner CN, Kwok Y, Conceição E, Pantazatos SP, Puma LM, Carnell S, *et al* (2011). Selective reduction in neural responses to high calorie foods following gastric bypass surgery. *Ann Surg* **253**: 502–507.

Ochner CN, Laferrère B, Afifi L, Atalayer D, Pantazatos SP, Geliebter A, *et al* (2012a). Neural Responsivity to Food Cues in Fasted and Fed States Pre and Post Gastric Bypass Surgery. *Neurosci Res* **74**: 138–143.

Ochner CN, Stice E, Hutchins E, Afifi L, Geliebter A, Hirsch J, *et al* (2012b). Relation between changes in neural responsivity and reductions in desire to eat high-calorie foods following gastric bypass surgery. *Neuroscience* **209**: 128–135.

O'Doherty J, Rolls ET, Francis S, Bowtell R, McGlone F, Kobal G, *et al* (2000). Sensory-specific satiety-related olfactory activation of the human orbitofrontal cortex. *Neuroreport* **11**: 893–897.

O'Doherty JP, Deichmann R, Critchley HD, Dolan RJ (2002). Neural responses during anticipation of a primary taste reward. *Neuron* **33**: 815–826.

Ogawa S, Lee TM (1990). Magnetic resonance imaging of blood vessels at high fields: in vivo and in vitro measurements and image simulation. *Magn Reson Med Off J Soc Magn Reson Med Soc Magn Reson Med* **16**: 9–18.

Ogawa S, Lee TM, Kay AR, Tank DW (1990a). Brain magnetic resonance imaging with contrast dependent on blood oxygenation. *Proc Natl Acad Sci U S A* **87**: 9868–9872.

Ogawa S, Lee TM, Nayak AS, Glynn P (1990b). Oxygenation-sensitive contrast in magnetic resonance image of rodent brain at high magnetic fields. *Magn Reson Med* **14**: 68–78.

O'Gorman RL, Summers PE, Zelaya FO, Williams SCR, Alsop DC, Lythgoe DJ (2006). In vivo estimation of the flow-driven adiabatic inversion efficiency for continuous arterial spin labeling: A method using phase contrast magnetic resonance angiography. *Magn Reson Med* **55**: 1291–1297.

Oldfield RC (1971). The assessment and analysis of handedness: the Edinburgh inventory. *Neuropsychologia* **9**: 97–113.

Osei K (1990). Increased basal glucose production and utilization in nondiabetic first-degree relatives of patients with NIDDM. *Diabetes* **39**: 597–601.

Otten J, Ahrén B, Olsson T (2014). Surrogate measures of insulin sensitivity vs the hyperinsulinaemic-euglycaemic clamp: a meta-analysis. *Diabetologia* **57**: 1781–1788.

Page KA, Chan O, Arora J, Belfort-Deaguiar R, Dzuira J, Roehmholdt B, *et al* (2013). Effects of fructose vs glucose on regional cerebral blood flow in brain regions involved with appetite and reward pathways. *JAMA J Am Med Assoc* **309**: 63–70.

Pagotto U (2009). Where does insulin resistance start? The brain. *Diabetes Care* **32 Suppl 2**: S174-177.

Pan XR, Li GW, Hu YH, Wang JX, Yang WY, An ZX, *et al* (1997). Effects of diet and exercise in preventing NIDDM in people with impaired glucose tolerance. The Da Qing IGT and Diabetes Study. *Diabetes Care* **20**: 537–544.

Pannacciulli N, Le DSNT, Chen K, Reiman EM, Krakoff J (2007a). Relationships between plasma leptin concentrations and human brain structure: a voxel-based morphometric study. *Neurosci Lett* **412**: 248–253.

Pannacciulli N, Le DSNT, Salbe AD, Chen K, Reiman EM, Tataranni PA, *et al* (2007b). Postprandial glucagon-like peptide-1 (GLP-1) response is positively associated with changes in neuronal activity of brain areas implicated in satiety and food intake regulation in humans. *NeuroImage* **35**: 511–517.

Park JS, Cho MH, Lee KY, Kim CS, Kim HJ, Nam JS, *et al* (2007). The effects of pioglitazone on cerebrovascular resistance in patients with type 2 diabetes mellitus. *Metabolism* **56**: 1081–1086.

Park MH, Kinra S, Ward KJ, White B, Viner RM (2009). Metformin for obesity in children and adolescents: a systematic review. *Diabetes Care* **32**: 1743–1745.

Parkes LM, Rashid W, Chard DT, Tofts PS (2004). Normal cerebral perfusion measurements using arterial spin labeling: reproducibility, stability, and age and gender effects. *Magn Reson Med Off J Soc Magn Reson Med Soc Magn Reson Med* **51**: 736–743.

Passamonti L, Rowe JB, Schwarzbauer C, Ewbank MP, Hagen E von dem, Calder AJ (2009). Personality predicts the brain's response to viewing appetizing foods:

the neural basis of a risk factor for overeating. *J Neurosci Off J Soc Neurosci* **29**: 43–51.

Pauling L, Coryell CD (1936). The Magnetic Properties and Structure of Hemoglobin, Oxyhemoglobin and Carbonmonoxyhemoglobin. *Proc Natl Acad Sci U S A* **22**: 210–216.

Pearson S, Schmidt M, Patton G, Dwyer T, Blizzard L, Otahal P, *et al* (2010). Depression and Insulin Resistance. *Diabetes Care* **33**: 1128–1133.

Perriello G, Misericordia P, Volpi E, Santucci A, Santucci C, Ferrannini E, *et al* (1994). Acute antihyperglycemic mechanisms of metformin in NIDDM. Evidence for suppression of lipid oxidation and hepatic glucose production. *Diabetes* **43**: 920–928.

Perseghin G (2009). Viewpoints on the Way to a Consensus Session Where does insulin resistance start? The liver. *Diabetes Care* **32**: S164–S167.

Petersen ET, Zimine I, Ho Y-CL, Golay X (2006). Non-invasive measurement of perfusion: a critical review of arterial spin labelling techniques. *Br J Radiol* **79**: 688–701.

Phelan S, Hassenstab J, McCaffery JM, Sweet L, Raynor HA, Cohen RA, *et al* (2011). Cognitive interference from food cues in weight loss maintainers, normal weight, and obese individuals. *Obes Silver Spring Md* **19**: 69–73.

Piech RM, Lewis J, Parkinson CH, Owen AM, Roberts AC, Downing PE, *et al* (2009). Neural Correlates of Appetite and Hunger-Related Evaluative Judgments. *PLoS ONE* **4**: e6581.

Pijl H, Romijn JA (2006). Obesity, dopamine and the metabolic syndrome: potential of dopaminergic agents in the control of metabolism. *Curr Opin Endocrinol Diabetes* **13**: 179–184.

Plum L, Belgardt BF, Brüning JC (2006). Central insulin action in energy and glucose homeostasis. *J Clin Invest* **116**: 1761–1766.

Plum L, Schubert M, Brüning JC (2005). The role of insulin receptor signaling in the brain. *Trends Endocrinol Metab TEM* **16**: 59–65.

Pocai A, Lam TKT, Gutierrez-Juarez R, Obici S, Schwartz GJ, Bryan J, *et al* (2005). Hypothalamic K(ATP) channels control hepatic glucose production. *Nature* **434**: 1026–1031.

Poldrack RA, Mumford JA, Nichols TE (Cambridge University Press: 2011). *Handbook of Functional MRI Data Analysis*. .

Polivy J, Herman CP (1985). Dieting and binging. A causal analysis. *Am Psychol* **40**: 193–201.

Porter DW, Irwin N, Flatt PR, Hölscher C, Gault VA (2011). Prolonged GIP receptor activation improves cognitive function, hippocampal synaptic plasticity and glucose homeostasis in high-fat fed mice. *Eur J Pharmacol* **650**: 688–693.

Porubská K, Veit R, Preissl H, Fritsche A, Birbaumer N (2006). Subjective feeling of appetite modulates brain activity: an fMRI study. *NeuroImage* **32**: 1273–1280.

Prentice AM (2005). Early influences on human energy regulation: thrifty genotypes and thrifty phenotypes. *Physiol Behav* **86**: 640–645.

Promintzer-Schifferl M, Prager G, Anderwald C, Mandl M, Esterbauer H, Shakeri-Leidenmuhler S, *et al* (2011). Effects of Gastric Bypass Surgery on Insulin Resistance and Insulin Secretion in Nondiabetic Obese Patients. *Obesity* **19**: 1420–1426.

Raichle ME (2015). The Brain's Default Mode Network. *Annu Rev Neurosci* **38**: 433–447.

Rebelos E, Muscelli E, Natali A, Balkau B, Mingrone G, Piatti P, *et al* (2011). Body weight, not insulin sensitivity or secretion, may predict spontaneous weight changes in nondiabetic and prediabetic subjects: the RISC study. *Diabetes* **60**: 1938–1945.

Rinne JO, Lönnberg P, Marjamäki P (1990). Age-dependent decline in human brain dopamine D1 and D2 receptors. *Brain Res* **508**: 349–352.

Rolls ET (2007). Understanding the mechanisms of food intake and obesity. *Obes Rev Off J Int Assoc Study Obes* **8 Suppl 1**: 67–72.

Rolls ET (2015). Taste, olfactory, and food reward value processing in the brain. *Prog Neurobiol* **127–128C**: 64–90.

Rosazza C, Minati L (2011). Resting-state brain networks: literature review and clinical applications. *Neurol Sci Off J Ital Neurol Soc Ital Soc Clin Neurophysiol* **32**: 773–785.

Rothemund Y, Preuschhof C, Bohner G, Bauknecht H-C, Klingebiel R, Flor H, *et al* (2007). Differential activation of the dorsal striatum by high-calorie visual food stimuli in obese individuals. *NeuroImage* **37**: 410–421.

Rotte M, Baerecke C, Pottag G, Klose S, Kanneberg E, Heinze H-J, *et al* (2005). Insulin Affects the Neuronal Response in the Medial Temporal Lobe in Humans. *Neuroendocrinology* **81**: 49–55.

Rouru J, Pesonen U, Koulu M, Huupponen R, Santti E, Virtanen K, *et al* (1995). Anorectic effect of metformin in obese Zucker rats: lack of evidence for the involvement of neuropeptide Y. *Eur J Pharmacol* **273**: 99–106.

Roux CW le, Batterham RL, Aylwin SJB, Patterson M, Borg CM, Wynne KJ, *et al* (2006). Attenuated peptide YY release in obese subjects is associated with reduced satiety. *Endocrinology* **147**: 3–8.

Rudovich NN, Rochlitz HJ, Pfeiffer AFH (2004). Reduced hepatic insulin extraction in response to gastric inhibitory polypeptide compensates for reduced insulin secretion in normal-weight and normal glucose tolerant first-degree relatives of type 2 diabetic patients. *Diabetes* **53**: 2359–2365.

Rusinek H, Ha J, Yau PL, Storey P, Tirsi A, Tsui WH, *et al* (2015). Cerebral perfusion in insulin resistance and type 2 diabetes. *J Cereb Blood Flow Metab Off J Int Soc Cereb Blood Flow Metab* **35**: 95–102.

Ryan JP, Sheu LK, Critchley HD, Gianaros PJ (2012). A neural circuitry linking insulin resistance to depressed mood. *Psychosom Med* **74**: 476–482.

Ryan JP, Sheu LK, Verstynen TD, Onyewuenyi IC, Gianaros PJ (2013). Cerebral blood flow links insulin resistance and baroreflex sensitivity. *PloS One* **8**: e83288.

Sande-Lee S van de, Pereira FRS, Cintra DE, Fernandes PT, Cardoso AR, Garlipp CR, *et al* (2011). Partial Reversibility of Hypothalamic Dysfunction and Changes in Brain Activity After Body Mass Reduction in Obese Subjects. *Diabetes* **60**: 1699–1704.

Sartorius T, Peter A, Heni M, Maetzler W, Fritsche A, Häring H-U, *et al* (2015). The brain response to peripheral insulin declines with age: a contribution of the blood-brain barrier? *PloS One* **10**: e0126804.

Scharmüller W, Übel S, Ebner F, Schienle A (2012). Appetite regulation during food cue exposure: A comparison of normal-weight and obese women. *Neurosci Lett* **518**: 106–110.

Schienle A, Schäfer A, Hermann A, Vaitl D (2009). Binge-eating disorder: reward sensitivity and brain activation to images of food. *Biol Psychiatry* **65**: 654–661.

Schilling TM, Ferreira de Sá DS, Westerhausen R, Strelzyk F, Larra MF, Hallschmid M, *et al* (2013). Intranasal insulin increases regional cerebral blood flow in the

insular cortex in men independently of cortisol manipulation. *Hum Brain Mapp* **35**: 1944–1956.

Schlögl H, Kabisch S, Horstmann A, Lohmann G, Müller K, Lepsien J, *et al* (2013). Exenatide-Induced Reduction in Energy Intake Is Associated With Increase in Hypothalamic Connectivity. *Diabetes Care* **36**: 1933–1940.

Scholtz S, Miras AD, Chhina N, Prechtl CG, Sleeth ML, Daud NM, *et al* (2014). Obese patients after gastric bypass surgery have lower brain-hedonic responses to food than after gastric banding. *Gut* **63**: 891–902.

Schur EA, Kleinhans NM, Goldberg J, Buchwald D, Schwartz MW, Maravilla K (2009). Activation in brain energy regulation and reward centers by food cues varies with choice of visual stimulus. *Int J Obes 2005* **33**: 653–661.

Schwartz MW, Figlewicz DP, Baskin DG, Woods SC, Porte D Jr (1992). Insulin in the brain: a hormonal regulator of energy balance. *Endocr Rev* **13**: 387–414.

Schwartz MW, Porte D (2005). Diabetes, obesity, and the brain. *Science* **307**: 375–379.

Seaquist ER, Chen W, Benedict LE, Ugurbil K, Kwag J-H, Zhu X-H, *et al* (2007). Insulin reduces the BOLD response but is without effect on the VEP during presentation of a visual task in humans. *J Cereb Blood Flow Metab Off J Int Soc Cereb Blood Flow Metab* **27**: 154–160.

Seppälä-Lindroos A, Vehkavaara S, Häkkinen A-M, Goto T, Westerbacka J, Sovijärvi A, *et al* (2002). Fat accumulation in the liver is associated with defects in insulin suppression of glucose production and serum free fatty acids independent of obesity in normal men. *J Clin Endocrinol Metab* **87**: 3023–3028.

Siep N, Roefs A, Roebroeck A, Havermans R, Bonte M, Jansen A (2012). Fighting food temptations: The modulating effects of short-term cognitive reappraisal, suppression and up-regulation on mesocorticolimbic activity related to appetitive motivation. *NeuroImage* **60**: 213–220.

Siep N, Roefs A, Roebroeck A, Havermans R, Bonte ML, Jansen A (2009). Hunger is the best spice: an fMRI study of the effects of attention, hunger and calorie content on food reward processing in the amygdala and orbitofrontal cortex. *Behav Brain Res* **198**: 149–158.

Sierra-Johnson J, Romero-Corral A, Somers VK, Lopez-Jimenez F, Walldius G, Hamsten A, *et al* (2007). ApoB/apoA-I ratio: an independent predictor of insulin resistance in US non-diabetic subjects. *Eur Heart J* **28**: 2637–2643.

Simmons WK, Martin A, Barsalou LW (2005). Pictures of Appetizing Foods Activate Gustatory Cortices for Taste and Reward. *Cereb Cortex* **15**: 1602–1608.

Simpson K, Parker J, Plumer J, Bloom S (2012). CCK, PYY and PP: The Control of Energy Balance. *Appetite Control* 209–230doi:10.1007/978-3-642-24716-3_9.

Small DM, Gerber JC, Mak YE, Hummel T (2005). Differential neural responses evoked by orthonasal versus retronasal odorant perception in humans. *Neuron* **47**: 593–605.

Small DM, Jones-Gotman M, Dagher A (2003). Feeding-induced dopamine release in dorsal striatum correlates with meal pleasantness ratings in healthy human volunteers. *NeuroImage* **19**: 1709–1715.

Small DM, Veldhuizen MG, Felsted J, Mak YE, McGlone F (2008). Separable Substrates for Anticipatory and Consummatory Food Chemosensation. *Neuron* **57**: 786–797.

Small DM, Zatorre RJ, Dagher A, Evans AC, Jones-Gotman M (2001). Changes in brain activity related to eating chocolate: from pleasure to aversion. *Brain J Neurol* **124**: 1720–1733.

Smeets PAM, Graaf C de, Stafleu A, Osch MJP van, Grond J van der (2005a). Functional MRI of human hypothalamic responses following glucose ingestion. *NeuroImage* **24**: 363–368.

Smeets PAM, Graaf C de, Stafleu A, Osch MJP van, Grond J van der (2005b). Functional magnetic resonance imaging of human hypothalamic responses to sweet taste and calories. *Am J Clin Nutr* **82**: 1011–1016.

Smeets PAM, Graaf C de, Stafleu A, Osch MJP van, Nievelstein RAJ, Grond J van der (2006). Effect of satiety on brain activation during chocolate tasting in men and women. *Am J Clin Nutr* **83**: 1297–1305.

Smeets PAM, Vidarsdottir S, Graaf C de, Stafleu A, Osch MJP van, Viergever MA, *et al* (2007). Oral glucose intake inhibits hypothalamic neuronal activity more effectively than glucose infusion. *Am J Physiol - Endocrinol Metab* **293**: E754–E758.

Smith AB, Halari R, Giampetro V, Brammer M, Rubia K (2011). Developmental effects of reward on sustained attention networks. *NeuroImage* **56**: 1693–1704.

Someya N, Endo MY, Fukuba Y, Hayashi N (2008). Blood flow responses in celiac and superior mesenteric arteries in the initial phase of digestion. *Am J Physiol Regul Integr Comp Physiol* **294**: R1790-1796.

Sowell ER, Thompson PM, Holmes CJ, Jernigan TL, Toga AW (1999). In vivo evidence for post-adolescent brain maturation in frontal and striatal regions. *Nat Neurosci* **2**: 859–861.

Spetter MS, Graaf C de, Mars M, Viergever MA, Smeets PAM (2014). The sum of its parts--effects of gastric distention, nutrient content and sensory stimulation on brain activation. *PloS One* **9**: e90872.

Spitzer R, Yanovski SZ, Marcus MD (1993). The Questionnaire on Eating and Weight Patterns-Revised (QEWP-R). (New York State Psychiatric Institute: New York).

Spitzer RL, Devlin M, Walsh BT, Hasin D, Wing R, Marcus M, *et al* (1992). Binge eating disorder: A multisite field trial of the diagnostic criteria. *Int J Eat Disord* **11**: 191–203.

Staudinger MR, Erk S, Walter H (2011). Dorsolateral Prefrontal Cortex Modulates Striatal Reward Encoding during Reappraisal of Reward Anticipation. *Cereb Cortex* **21**: 2578–2588.

Steele KE, Prokopowicz GP, Schweitzer MA, Magunsuon TH, Lidor AO, Kuwabawa H, *et al* (2010). Alterations of central dopamine receptors before and after gastric bypass surgery. *Obes Surg* **20**: 369–374.

Stein LJ, Dorsa DM, Baskin DG, Figlewicz DP, Porte D Jr, Woods SC (1987). Reduced effect of experimental peripheral hyperinsulinemia to elevate cerebrospinal fluid insulin concentrations of obese Zucker rats. *Endocrinology* **121**: 1611–1615.

Steinbrink J, Villringer A, Kempf F, Haux D, Boden S, Obrig H (2006). Illuminating the BOLD signal: combined fMRI–fNIRS studies. *Magn Reson Imaging* **24**: 495–505.

Stevanovic D, Janjetovic K, Misirkic M, Vucicevic L, Sumarac-Dumanovic M, Micic D, *et al* (2012). Intracerebroventricular administration of metformin inhibits

ghrelin-induced Hypothalamic AMP-kinase signalling and food intake. *Neuroendocrinology* **96**: 24–31.

Stice E, Spoor S, Bohon C, Veldhuizen MG, Small DM (2008). Relation of reward from food intake and anticipated food intake to obesity: a functional magnetic resonance imaging study. *J Abnorm Psychol* **117**: 924–935.

Stice E, Spoor S, Ng J, Zald DH (2009). Relation of obesity to consummatory and anticipatory food reward. *Physiol Behav* **97**: 551–560.

Stice E, Yokum S, Blum K, Bohon C (2010). Weight gain is associated with reduced striatal response to palatable food. *J Neurosci Off J Soc Neurosci* **30**: 13105–13109.

Stice E, Yokum S, Burger KS, Epstein LH, Small DM (2011). Youth at Risk for Obesity Show Greater Activation of Striatal and Somatosensory Regions to Food. *J Neurosci* **31**: 4360–4366.

Stingl KT, Kullmann S, Guthoff M, Heni M, Fritsche A, Preissl H (2010). Insulin modulation of magnetoencephalographic resting state dynamics in lean and obese subjects. *Front Syst Neurosci* **4**: 157.

Stoeckel LE, Kim J, Weller RE, Cox JE, Cook EW, Horwitz B (2009). Effective connectivity of a reward network in obese women. *Brain Res Bull* **79**: 388–395.

Stoeckel LE, Weller RE, Cook EW, Twieg DB, Knowlton RC, Cox JE (2008). Widespread reward-system activation in obese women in response to pictures of high-calorie foods. *NeuroImage* **41**: 636–647.

St-Onge M-P, Sy M, Heymsfield SB, Hirsch J (2005). Human cortical specialization for food: a functional magnetic resonance imaging investigation. *J Nutr* **135**: 1014–1018.

Strien T van, Frijters JER, Bergers GPA, Defares PB (1986). The Dutch Eating Behavior Questionnaire (DEBQ) for assessment of restrained, emotional, and external eating behavior. *Int J Eat Disord* **5**: 295–315.

Stumvoll M, Mitrakou A, Pimenta W, Jenssen T, Yki-Järvinen H, Haeften TV, *et al* (2000). Use of the oral glucose tolerance test to assess insulin release and insulin sensitivity. *Diabetes Care* **23**: 295–301.

Stunkard AJ, Messick S (1985). The three-factor eating questionnaire to measure dietary restraint, disinhibition and hunger. *J Psychosom Res* **29**: 71–83.

Sussman JB, Kent DM, Nelson JP, Hayward RA (2015). Improving diabetes prevention with benefit based tailored treatment: risk based reanalysis of Diabetes Prevention Program. *BMJ* **350**: h454.

Takei H, Fujita S, Shirakawa T, Koshikawa N, Kobayashi M (2010). Insulin facilitates repetitive spike firing in rat insular cortex via phosphoinositide 3-kinase but not mitogen activated protein kinase cascade. *Neuroscience* **170**: 1199–1208.

Talairach J, Tournoux P (Thieme: 1998). *Co-planar stereotaxic atlas of the human brain: 3-D Proportional System: An Approach to Cerebral Imaging*. .

Tang DW, Fellows LK, Small DM, Dagher A (2012). Food and drug cues activate similar brain regions: a meta-analysis of functional MRI studies. *Physiol Behav* **106**: 317–324.

Tanofsky-Kraff M, Haynos AF, Kotler LA, Yanovski SZ, Yanovski JA (2007). Laboratory-Based Studies of Eating among Children and Adolescents. *Curr Nutr Food Sci* **3**: 55–74.

Tataranni PA, Gautier J-F, Chen K, Uecker A, Bandy D, Salbe AD, *et al* (1999). Neuroanatomical correlates of hunger and satiation in humans using positron emission tomography. *Proc Natl Acad Sci U S A* **96**: 4569–4574.

Teeuwisse WM, Widya RL, Paulides M, Lamb HJ, Smit JWA, Roos A de, *et al* (2012). Short-Term Caloric Restriction Normalizes Hypothalamic Neuronal Responsiveness to Glucose Ingestion in Patients With Type 2 Diabetes. *Diabetes* **61**: 3255–9.

Theodorakis MJ, Carlson O, Muller DC, Egan JM (2004). Elevated plasma glucose-dependent insulinotropic polypeptide associates with hyperinsulinemia in impaired glucose tolerance. *Diabetes Care* **27**: 1692–1698.

Thorleifsson G, Walters GB, Gudbjartsson DF, Steinthorsdottir V, Sulem P, Helgadottir A, *et al* (2009). Genome-wide association yields new sequence variants at seven loci that associate with measures of obesity. *Nat Genet* **41**: 18–24.

Thulborn KR, Waterton JC, Matthews PM, Radda GK (1982). Oxygenation dependence of the transverse relaxation time of water protons in whole blood at high field. *Biochim Biophys Acta* **714**: 265–270.

Tomasi D, Volkow ND (2013). Striatocortical pathway dysfunction in addiction and obesity: differences and similarities. *Crit Rev Biochem Mol Biol* **48**: 1–19.

Tomasi D, Wang G-J, Wang R, Backus W, Geliebter A, Telang F, *et al* (2009). Association of body mass and brain activation during gastric distention: implications for obesity. *PloS One* **4**: e6847.

Totman JJ, Marciani L, Foley S, Campbell E, Hoad CL, Macdonald IA, *et al* (2009). Characterization of the time course of the superior mesenteric, abdominal aorta, internal carotid and vertebral arteries blood flow response to the oral glucose challenge test using magnetic resonance imaging. *Physiol Meas* **30**: 1117–1136.

Trahair LG, Horowitz M, Jones KL (2014). Postprandial hypotension: a systematic review. *J Am Med Dir Assoc* **15**: 394–409.

Trinko R, Sears RM, Guarnieri DJ, DiLeone RJ (2007). Neural mechanisms underlying obesity and drug addiction. *Physiol Behav* **91**: 499–505.

Tschritter O, Hennige AM, Preissl H, Grichisch Y, Kirchhoff K, Kantartzis K, *et al* (2009a). Insulin effects on beta and theta activity in the human brain are differentially affected by ageing. *Diabetologia* **52**: 169–171.

Tschritter O, Hennige AM, Preissl H, Porubska K, Schäfer SA, Lutzenberger W, *et al* (2007a). Cerebrocortical beta activity in overweight humans responds to insulin detemir. *PloS One* **2**: e1196.

Tschritter O, Preissl H, Hennige AM, Sartorius T, Grichisch Y, Stefan N, *et al* (2009b). The insulin effect on cerebrocortical theta activity is associated with serum concentrations of saturated nonesterified Fatty acids. *J Clin Endocrinol Metab* **94**: 4600–4607.

Tschritter O, Preissl H, Hennige AM, Sartorius T, Stingl KT, Heni M, *et al* (2012). High cerebral insulin sensitivity is associated with loss of body fat during lifestyle intervention. *Diabetologia* **55**: 175–182.

Tschritter O, Preissl H, Hennige AM, Stumvoll M, Porubska K, Frost R, *et al* (2006). The cerebrocortical response to hyperinsulinemia is reduced in overweight humans: a magnetoencephalographic study. *Proc Natl Acad Sci U S A* **103**: 12103–12108.

Tschritter O, Preissl H, Yokoyama Y, Machicao F, Häring H-U, Fritsche A (2007b). Variation in the FTO gene locus is associated with cerebrocortical insulin resistance in humans. *Diabetologia* **50**: 2602–2603.

Tsilchorozidou T, Batterham RL, Conway GS (2008). Metformin increases fasting plasma peptide tyrosine tyrosine (PYY) in women with polycystic ovarian syndrome (PCOS). *Clin Endocrinol (Oxf)* **69**: 936–942.

Tuomilehto J, Lindström J, Eriksson JG, Valle TT, Hämäläinen H, Ilanne-Parikka P, *et al* (2001). Prevention of type 2 diabetes mellitus by changes in lifestyle among subjects with impaired glucose tolerance. *N Engl J Med* **344**: 1343–1350.

Turton MD, O'Shea D, Gunn I, Beak SA, Edwards CM, Meeran K, *et al* (1996). A role for glucagon-like peptide-1 in the central regulation of feeding. *Nature* **379**: 69–72.

Tzourio-Mazoyer N, Landeau B, Papathanassiou D, Crivello F, Etard O, Delcroix N, *et al* (2002). Automated anatomical labeling of activations in SPM using a macroscopic anatomical parcellation of the MNI MRI single-subject brain. *NeuroImage* **15**: 273–289.

Uher R, Treasure J, Heining M, Brammer MJ, Campbell IC (2006). Cerebral processing of food-related stimuli: effects of fasting and gender. *Behav Brain Res* **169**: 111–119.

UN Department of Economic and Social Affairs. (2009). World Population Ageing 2009. *ESA/P/WP/212* 4–14.

University College London (2008). Statistical Parametric Mapping (SPM-8). at <http://www.fil.ion.ucl.ac.uk/spm/software/>.

Vaag A, Lehtovirta M, Thye-Rönn P, Groop L, European Group of Insulin Resistance (2001). Metabolic impact of a family history of Type 2 diabetes. Results from a European multicentre study (EGIR). *Diabet Med J Br Diabet Assoc* **18**: 533–540.

Van Laere KJ, Dierckx RA (2001). Brain perfusion SPECT: age- and sex-related effects correlated with voxel-based morphometric findings in healthy adults. *Radiology* **221**: 810–817.

Van Vugt DA, Krzemien A, Alsaadi H, Frank TC, Reid RL (2014). Glucose-induced inhibition of the appetitive brain response to visual food cues in polycystic ovary syndrome patients. *Brain Res* **1558**: 44–56.

Van Vugt DA, Krzemien A, Alsaadi H, Palerme S, Reid RL (2013). Effect of insulin sensitivity on corticolimbic responses to food picture in women with polycystic ovary syndrome. *Obes Silver Spring Md* **21**: 1215–1222.

Venna VR, Li J, Hammond MD, Mancini NS, McCullough LD (2014). Chronic metformin treatment improves post-stroke angiogenesis and recovery after experimental stroke. *Eur J Neurosci* **39**: 2129–2138.

Verdejo-Garcia A, Clark L, Dunn BD (2012). The role of interoception in addiction: a critical review. *Neurosci Biobehav Rev* **36**: 1857–1869.

Vidarsdottir S, Smeets PAM, Eichelsheim DL, Osch MJP van, Viergever MA, Romijn JA, *et al* (2007). Glucose Ingestion Fails to Inhibit Hypothalamic Neuronal Activity in Patients With Type 2 Diabetes. *Diabetes* **56**: 2547–2550.

Viollet B, Guigas B, Sanz Garcia N, Leclerc J, Foretz M, Andreelli F (2012). Cellular and molecular mechanisms of metformin: an overview. *Clin Sci Lond Engl 1979* **122**: 253–270.

Vitale C, Mercuro G, Cornoldi A, Fini M, Volterrani M, Rosano GMC (2005). Metformin improves endothelial function in patients with metabolic syndrome. *J Intern Med* **258**: 250–256.

Viviani R, Messina I, Walter M (2011). Resting state functional connectivity in perfusion imaging: correlation maps with BOLD connectivity and resting state perfusion. *PloS One* **6**: e27050.

Volkow ND, Wang G-J, Baler RD (2011). Reward, dopamine and the control of food intake: implications for obesity. *Trends Cogn Sci* **15**: 37–46.

Volkow ND, Wang GJ, Fowler JS, Logan J, Gatley SJ, MacGregor RR, *et al* (1996). Measuring age-related changes in dopamine D2 receptors with 11C-raclopride and 18F-N-methylspiroperidol. *Psychiatry Res* **67**: 11–16.

Volkow ND, Wang G-J, Fowler JS, Logan J, Jayne M, Franceschi D, *et al* (2002). "Nonhedonic" food motivation in humans involves dopamine in the dorsal striatum and methylphenidate amplifies this effect. *Synap N Y N* **44**: 175–180.

Volkow ND, Wang G-J, Fowler JS, Telang F (2008a). Overlapping neuronal circuits in addiction and obesity: evidence of systems pathology. *Philos Trans R Soc Lond B Biol Sci* **363**: 3191–3200.

Volkow ND, Wang G-J, Telang F, Fowler JS, Goldstein RZ, Alia-Klein N, *et al* (2009). Inverse association between BMI and prefrontal metabolic activity in healthy adults. *Obes Silver Spring Md* **17**: 60–65.

Volkow ND, Wang G-J, Telang F, Fowler JS, Thanos PK, Logan J, *et al* (2008b). Low dopamine striatal D2 receptors are associated with prefrontal metabolism in obese subjects: Possible contributing factors. *NeuroImage* **42**: 1537–1543.

Wallace TM, Levy JC, Matthews DR (2004). Use and abuse of HOMA modeling. *Diabetes Care* **27**: 1487–1495.

Wallner-Liebmann S, Koschutnig K, Reishofer G, Sorantin E, Blaschitz B, Kruschitz R, *et al* (2010). Insulin and Hippocampus Activation in Response to Images of High-Calorie Food in Normal Weight and Obese Adolescents. *Obes Silver Spring Md* **18**: 1552–7.

Wallum BJ, Taborsky GJ, Porte D, Figlewicz DP, Jacobson L, Beard JC, *et al* (1987). Cerebrospinal fluid insulin levels increase during intravenous insulin infusions in man. *J Clin Endocrinol Metab* **64**: 190–194.

Wang GJ, Volkow ND, Logan J, Pappas NR, Wong CT, Zhu W, *et al* (2001). Brain dopamine and obesity. *Lancet* **357**: 354–357.

Wang Y, Chan GL, Holden JE, Dobko T, Mak E, Schulzer M, *et al* (1998). Age-dependent decline of dopamine D1 receptors in human brain: a PET study. *Synap N Y N* **30**: 56–61.

Weijer BA de, Giessen E van de, Amelsvoort TA van, Boot E, Braak B, Janssen IM, *et al* (2011). Lower striatal dopamine D2/3 receptor availability in obese compared with non-obese subjects. *EJNMMI Res* **1**: 37.

Weijer BA de, Giessen E van de, Janssen I, Berends FJ, Laar A van de, Ackermans MT, *et al* (2014). Striatal dopamine receptor binding in morbidly obese women before and after gastric bypass surgery and its relationship with insulin sensitivity. *Diabetologia* **57**: 1078–1080.

Widén EI, Eriksson JG, Groop LC (1992). Metformin normalizes nonoxidative glucose metabolism in insulin-resistant normoglycemic first-degree relatives of patients with NIDDM. *Diabetes* **41**: 354–358.

Willer CJ, Speliotes EK, Loos RJF, Li S, Lindgren CM, Heid IM, *et al* (2009). Six new loci associated with body mass index highlight a neuronal influence on body weight regulation. *Nat Genet* **41**: 25–34.

Willeumier KC, Taylor DV, Amen DG (2011). Elevated BMI Is Associated With Decreased Blood Flow in the Prefrontal Cortex Using SPECT Imaging in Healthy Adults. *Obesity* **19**: 1095–1097.

Williams DS, Detre JA, Leigh JS, Koretsky AP (1992). Magnetic resonance imaging of perfusion using spin inversion of arterial water. *Proc Natl Acad Sci U S A* **89**: 212–216.

Willie CK, Tzeng Y-C, Fisher JA, Ainslie PN (2014). Integrative regulation of human brain blood flow. *J Physiol* **592**: 841–859.

Woo C-W, Krishnan A, Wager TD (2014). Cluster-extent based thresholding in fMRI analyses: pitfalls and recommendations. *NeuroImage* **91**: 412–419.

Woods SC (2009). The control of food intake: behavioral versus molecular perspectives. *Cell Metab* **9**: 489–498.

Woods SC, D'Alessio DA (2008). Central Control of Body Weight and Appetite. *J Clin Endocrinol Metab* **93**: s37-50.

World Health Organization (2006a). Definition and diagnosis of diabetes mellitus and intermediate hyperglycaemia. A report of a WHO/IDF consultatation. at <http://www.who.int/diabetes/publications/Definition%20and%20diagnosis%20of%20diabetes_new.pdf>.

World Health Organization (2006b). WHO | Obesity and overweight. at <http://www.who.int/mediacentre/factsheets/fs311/en/index.html>.

World Health Organization (2011). Use of glycated haemoglobin (HbA1c) in the diagnosis of diabetes mellitus. at <http://www.who.int/diabetes/publications/diagnosis_diabetes2011/en/>.

Worsley KJ, Evans AC, Marrett S, Neelin P (1992). A Three-Dimensional Statistical Analysis for CBF Activation Studies in Human Brain. *J Cereb Blood Flow Metab* **12**: 900–918.

Xu F, Liu P, Pascual JM, Xiao G, Huang H, Lu H (2015). Acute effect of glucose on cerebral blood flow, blood oxygenation, and oxidative metabolism. *Hum Brain Mapp* **36**: 707–716.

Yavropoulou MP, Kotsa K, Anastasiou O, O'Dorisio TM, Pappas TN, Yovos JG (2009). Effect of intracerebroventricular infusion of insulin on glucose-dependent insulinotropic peptide in dogs. *Neurosci Lett* **460**: 148–151.

Yki-Järvinen H, Nikkilä K, Mäkimattila S (1999). Metformin prevents weight gain by reducing dietary intake during insulin therapy in patients with type 2 diabetes mellitus. *Drugs* **58 Suppl 1**: 53-54; discussion 75-82.

Yokum S, Ng J, Stice E (2011). Attentional bias to food images associated with elevated weight and future weight gain: an FMRI study. *Obes Silver Spring Md* **19**: 1775–1783.

Yokum S, Stice E (2013). Cognitive regulation of food craving: effects of three cognitive reappraisal strategies on neural response to palatable foods. *Int J Obes* **37**: 1575–1570.

Zelissen PMJ, Stenlof K, Lean MEJ, Fogteloo J, Keulen ETP, Wilding J, *et al* (2005). Effect of three treatment schedules of recombinant methionyl human leptin on body weight in obese adults: a randomized, placebo-controlled trial. *Diabetes Obes Metab* **7**: 755–761.

Zhu J-N, Wang J-J (2008). The cerebellum in feeding control: possible function and mechanism. *Cell Mol Neurobiol* **28**: 469–478.

Zhu S, Fang Z, Hu S, Wang Z, Rao H (2013). Resting state brain function analysis using concurrent BOLD in ASL perfusion fMRI. *PloS One* **8**: e65884.

Zou Q, Wu CW, Stein EA, Zang Y, Yang Y (2009). Static and dynamic characteristics of cerebral blood flow during the resting state. *NeuroImage* **48**: 515–524.

Appendix

King's College Hospital NHS
NHS Foundation Trust

KING'S College LONDON
University of London

A functional magnetic resonance imaging study of brain responses to food image viewing and food ingestion in insulin resistance: Information Sheet (Insulin Sensitive Subjects)

Information for research volunteers

You are invited to participate in a research study. Before you decide, it is important for you to understand why the research is being done and what it will involve. Please take time to read the following information carefully and discuss it with friends, relatives, and your GP if you wish. Please ask us if there is anything that is not clear, or you would like more information. Take time to decide whether or not you wish to take part.

Thank you for reading this

The purpose of the research
Obesity and related health problems including Type 2 diabetes are becoming more common causing long-term ill health. As yet, we do not understand why some people are particularly prone to weight gain and diabetes. One possibility is a malfunction in the brain mechanisms that stop our desire to eat more after a meal in people predisposed to obesity and diabetes. Gaining further knowledge of the way the brain controls eating will help the development of new ways to prevent and treat these diseases.

Our study is interested in looking at the way the brain responds to food by using functional magnetic resonance imaging (fMRI). fMRI is a method of taking images of the brain using strong magnets, without using any form of radiation (e.g. "X-rays"). This will allow us to see the activity of regions of the brain that control eating. We are interested in seeing whether these brain responses after eating in healthy volunteers with insulin-resistance are different to those who are insulin-sensitive. Insulin-resistance is a common condition where the body is less responsive to insulin, a hormone normally produced by the body to control glucose (sugar) levels. The presence of insulin-resistance puts people at risk of developing diabetes, high blood pressure and heart disease and is associated with obesity. Using fMRI will allow us to see if insulin-resistance also alters the way the brain responds to food, and may allow the development of treatments that can alter such brain responses to a healthier pattern.

Why have I been chosen?
We are looking for male volunteers aged between 18-65 years to participate in our study. You are being invited to take part because you are healthy with no known medical problems. We would like to compare your results with those of people with insulin-resistance. Taking part in this research may help lead to the possibility of preventing obesity and Type 2 diabetes in the future. Your contribution will be highly valued by those working in this important field of research as it will enable us to find out more about the causes of obesity and diabetes, how to predict who may develop it, and ways of preventing it altogether.

Do I have to take part?
No, taking part is voluntary. It is up to you to decide whether or not to take part. If you do decide to take part we will ask you to sign a consent form and give you a copy of this information sheet and the consent form to keep. If you decide to take part you are still free to withdraw at any time. If you decide not to take part you do not have to give a reason, nobody will be upset and the standard of care you receive will not be affected.

What you will be asked to do

Screening visits
On the first visit (before you enter the study), we will check your general health, which will also include a questionnaire about your eating habits. You will undergo a blood test (10 mls / 2 teaspoonfuls of blood) for your blood glucose and insulin after fasting overnight for 8 hours, to check your sensitivity to insulin.

If the blood tests confirm that you are sensitive to insulin, you will be invited for a second visit, to accurately ensure you do not have diabetes by undergoing an "Oral Glucose Tolerance Test". After fasting overnight you will drink a glucose drink, having blood taken before the drink, and every 30 minutes afterwards for 2 hours (i.e. before and 30 minutes, 1, 1.5 and 2 hours after the drink), for blood glucose and insulin levels. We will also measure your cholesterol, blood count, kidney and liver function once, at the beginning of this test. We will also show you a "dummy" or mock-up of the MRI scanning machine, to ensure you a happy to have the scans before starting the study.

Blood taking
This will be performed by experienced doctors and nurses from the research team. On the first screening visit, blood will be taken from your arm. On the second visit and during the scanning studies, a single thin plastic tube or "cannula" will be inserted into your arm or back of the hand, to allow blood to be taken without multiple needle injections with approximately a total of half a teacup of blood taken. To ensure that the cannula does not become blocked, a small amount of salt water (saline) will drip through the cannula.

Urine sample
You will be asked to provide a urine sample collected first thing in the morning.

fMRI Scanning Visits
The MRI scanner is located at the Centre for Neuroimaging Sciences, at the Institute of Psychiatry, which is opposite King's College Hospital, and will be used to take images of your brain. This is performed using strong magnets; therefore, if you have any metallic implants (e.g. pacemaker, surgical clips etc.) you will not be able to take part in the MRI scans.

You will be invited to attend for the scans on 2 separate visits. Each visit will take up a whole morning of your time, after an overnight fast. A cannula will be inserted into your arm and blood taken to measure glucose and insulin levels, as well as levels of hormones that control your appetite and hunger. You will then lie within the scanner. As the MRI scanner is noisy, a set of earphones will be fitted so that you may hear music, and the nurses, doctors and scanning staff. A nurse will accompany you at all times in the scanning room. A series of scans lasting approximately 1 hour altogether will be

performed at each visit. After the first scan you will be given either a drink of water or ice cream to eat (you will be given the alternative option on the second visit). You will also be shown pictures of various foods and everyday household items during one of the scans. You will also be asked questions about how hungry you feel, and will have blood taken to measure your hormone response to the food/water during the scans.

Genetic Tests
No genetic tests will be performed on any blood or urine samples provided.

What are the possible disadvantages and risks of taking part?
MRI is a safe way of taking images of parts of the body, in this case the brain. However, the scanner is narrow. If you suffer from claustrophobia you may not wish to participate, but we can show you a "dummy scanner" to ensure you are familiar with the scanner first.

What are the possible benefits in taking part?
If we discover that you have a medical condition that you did not know about before, we will tell you about it and discuss how this should be dealt with. For example, if we found you to have diabetes or high blood pressure, we might suggest informing your GP to ensure you receive the appropriate care and follow-up.

This research study is designed to allow a greater understanding of the way the brain responds to food and is not designed primarily to benefit your own health. However, you will be assessed for your risk of developing diabetes before starting the study and will be given advice about healthy living. By participating in the study, you will improve our knowledge of the risk factors for developing diabetes and obesity.

Remuneration
After each study is complete, you will be given a meal or the equivalent cash sum for you to buy your own meal and you will then be able to go home. Any travel expenses incurred by you in participating in this study will be reimbursed on provision of receipts, and we will offer a £10 for the Oral Glucose Tolerance Test visit, and £75 payment per MRI scanning visit, in recognition of your time.

What if something goes wrong?
If you are harmed by someone else's negligence, then you may have grounds for legal action and you are free to complain through normal NHS complaints services. However if you are harmed accidentally whilst taking part in this research study, there are no special compensation arrangements.

If you have concerns about any aspect of the way you have been approached or treated during the course of this study you may wish to contact the hospital's Patient Advice and Liaison Service (PALS) on 020 3299 3625 or 020 3299 360, or write to PALS, King's College Hospital, Denmark Hill, London SE5 9RS.

What about the results?
The results of this study will not be known until some time after the last patient has finished. The research doctor will let you know the results of study when it is completed. The results may be reported in professional publications or meetings but you will not be identified by name.

Who has reviewed the study?
This study has been approved by the South East London Research Ethics Committee 3 (formerly King's College Hospital Research Ethics Committee).

What if you wish to withdraw from the study?
Participation in this study is entirely voluntary, and you are free to withdraw at any point in time, and will not affect the treatment you receive from King's College Hospital NHS Foundation Trust.

Confidentiality
The study is confidential and all data collected will be secured against any unauthorised access. Confidential information regarding identity from volunteers will be destroyed after the trial unless we inform you otherwise, in which case we will ask for your consent to retain such information. We will normally inform your GP about your involvement in the study unless you request otherwise.

Any Questions:
Professor Stephanie Amiel, RD Lawrence Professor of Diabetic Medicine and members of her research group are leading this study. If you have any further questions please do not hesitate to contact us:

Contact: Dr. Yee Seun Cheah, Clinical Research Fellow
Diabetes Research Group
King's College London School of Medicine
Room 3.35, Weston Education Centre
Cutcombe Road
London SE5 9RJ
Telephone: 020 7848 5654 or 5653
Email: yee.cheah@kcl.ac.uk or andrew.pernet@kcl.ac.uk

King's College Hospital NHS
NHS Foundation Trust

KING'S College LONDON
University of London

A functional magnetic resonance imaging study of brain responses to food image viewing and food ingestion in insulin resistance: Information Sheet (Insulin Resistant Subjects)

Information for research volunteers.

You are invited to participate in a research study. Before you decide, it is important for you to understand why the research is being done and what it will involve. Please take time to read the following information carefully and discuss it with friends, relatives, and your GP if you wish. Please ask us if there is anything that is not clear, or you would like more information. Take time to decide whether or not you wish to take part.

Thank you for reading this

The purpose of the research

Obesity and related health problems including Type 2 diabetes are becoming more common causing long-term ill health. As yet, we do not understand why some people are particularly prone to weight gain and diabetes. One possibility is a malfunction in the brain mechanisms that stop our desire to eat more after a meal in people predisposed to obesity and diabetes. Gaining further knowledge of the way the brain controls eating will help the development of new ways to prevent and treat these diseases.

Our study is interested in looking at the way the brain responds to food by using functional magnetic resonance imaging (fMRI). fMRI is a method of taking images of the brain using strong magnets, without using any form of radiation (e.g. "X-rays"). This will allow us to see the activity of regions of the brain that control eating. We are interested in seeing whether these brain responses after eating in healthy volunteers with insulin-resistance are different to those who are insulin-sensitive. Insulin-resistance is a common condition where the body is less responsive to insulin, a hormone normally produced by the body to control glucose (sugar) levels. The presence of insulin-resistance puts people at risk of developing diabetes, high blood pressure and heart disease and is associated with obesity. Using fMRI will allow us to see if insulin-resistance also alters the way the brain responds to food. We will then study whether the use of treatment that will improve the body's sensitivity or response to insulin (described below), to see if we can improve the brain responses to food to a healthier pattern.

Why have I been chosen?

We are looking for male volunteers aged between 18-65 years to participate in our study. You are being invited to take part because you are healthy with no known medical problems, but as you are a relative of someone with Type 2 Diabetes mellitus, this increases the likelihood of you being insulin-resistant. Taking part in this research may help lead to the possibility of preventing obesity and Type 2 diabetes in the future. Your contribution will be highly valued by those working in this important field of research as it will enable us to find out more about the causes of obesity and diabetes, how to predict who may develop it, and ways of preventing it altogether.

Do I have to take part?
No, taking part is voluntary. It is up to you to decide whether or not to take part. If you do decide to take part we will ask you to sign a consent form and give you a copy of this information sheet and the consent form to keep. If you decide to take part you are still free to withdraw at any time. If you decide not to take part you do not have to give a reason, nobody will be upset and the standard of care you receive will not be affected.

What you will be asked to do

Screening visits
On the first visit (before you enter the study), we will check your general health, which will also include a questionnaire about your eating habits. You will undergo a blood test (10 mls / 2 teaspoonfuls of blood) for your blood glucose and insulin after fasting overnight for 8 hours, to check your sensitivity to insulin.

If the blood tests confirm that you are insulin-resistant, you will be invited for a second visit, to accurately ensure you do not have diabetes by undergoing an "Oral Glucose Tolerance Test". After fasting overnight you will drink a glucose drink, having blood taken before the drink, and every 30 minutes afterwards for 2 hours (i.e. before and 30 minutes, 1, 1.5 and 2 hours after the drink), for blood glucose and insulin levels. We will also measure your cholesterol, blood count, kidney and liver function once, at the beginning of this test. We will also show you a "dummy" or mock-up of the MRI scanning machine, to ensure you a happy to have the scans before starting the study.

Blood taking
This will be performed by experienced doctors and nurses from the research team. On the first screening visit, blood will be taken from your arm. On the second visit and during the scanning studies, a single thin plastic tube or "cannula" will be inserted into your arm or back of the hand, to allow blood to be taken without multiple needle injections with approximately a total of half a teacup of blood taken. To ensure that the cannula does not become blocked, a small amount of salt water (saline) will drip through the cannula.

Urine sample
You will be asked to provide a urine sample collected first thing in the morning.

fMRI Scanning Visits
The MRI scanner is located at the Centre for Neuroimaging Sciences, at the Institute of Psychiatry, which is opposite King's College Hospital, and will be used to take images of your brain. This is performed using strong magnets; therefore, if you have any metallic implants (e.g. pacemaker, surgical clips etc.) you will not be able to take part in the MRI scans.

You will be invited to attend for the scans on 4 separate visits. Each visit will take up a whole morning of your time, after an overnight fast. A cannula will be inserted into your arm and blood taken to measure glucose and insulin levels, as well as levels of hormones that control your appetite and hunger. You will then lie within the scanner. As the MRI scanner is noisy, a set of earphones will be fitted so that you may hear music, and the nurses, doctors and scanning staff. A nurse will accompany you at all times in the scanning room. A series of scans lasting approximately 1 hour altogether will be performed at each visit. For the first two visits you will either be given a drink of water or ice cream to eat during the visit at random (you will be given the alternative option on the second visit). You will also be shown pictures of various foods and everyday household items during one of the scans. You will also be asked questions about how hungry you feel, and will have blood taken to measure your hormone response to the food/water during the scans.

After the first two scans you will be given Metformin (Glucophage SR). We will ask you to take the tablets for 3 months.

Metformin (Glucophage SR) is a medication that is used as first line treatment of Type 2 diabetes. It is also commonly used for treating "pre-diabetes" and polycystic ovarian syndrome, which are both conditions caused by insulin-resistance. Although it is not licensed for use in these two latter conditions, it is advocated by many medical bodies and has also been shown to prevent the onset of diabetes in people with insulin resistance and at risk of developing diabetes, by improving the body's response to insulin. In this research study, the starting dose will be one tablet a day for the first week, increasing by an extra tablet per day every two weeks to a maximum of 4 tablets per day or as tolerated for the remainder of the 3 months. For further information please see the "Metformin: Information for Research Participants" leaflet and the "Metformin: Guide to Doses for Research Participants" leaflet.

After 3 months treatment you will then repeat the 2 MRI scanning visits as described above.

You will also receive healthy living advice on your diet and physical activity from our specialist dietitians, at the same time as the medication. If you are unable to tolerate the metformin (Glucophage SR) tablets, you may continue to follow the advice provided by the dietitians, but only those who show an improvement in insulin resistance will be able to undergo the last 2 MRI scans, in order for us to be able to look at the effect of improving insulin resistance on brain responses to food.

Genetic Tests
No genetic tests will be performed on any blood or urine samples provided.

What are the possible side-effects of taking part?
Some people experience altered taste, nausea, an upset stomach and loose stool with this Metformin (Glucophage SR). However, these symptoms are short-lived and usually resolve within a few weeks of starting treatment. A "slow-release" form of the tablet will be used so that the risk of developing these problems is reduced. For further information please see the "Metformin: Information for Research Participants" leaflet. During this time, you will be asked to fill in a diary of your physical activity and the number of tablets you have taken each week.

What are the possible disadvantages and risks of taking part?
MRI is a safe way of taking images of parts of the body, in this case the brain. However, the scanner is narrow. If you suffer from claustrophobia you may not wish to participate, but we can show you a "dummy scanner" to ensure you are familiar with the scanner first.

What are the possible benefits in taking part?
If we discover that you have a medical condition that you did not know about before, we will tell you about it and discuss how this should be dealt with. For example, if we found you to have diabetes or high blood pressure, we might suggest informing your GP to ensure you receive the appropriate care and follow-up.
This research study is designed to allow a greater understanding of the way the brain responds to food and is not designed primarily to benefit your own health. However, you will be assessed for your risk of developing diabetes before starting the study and will be given advice about healthy living. By participating in the study, you will improve our knowledge of the risk factors for developing diabetes and obesity.

Remuneration
After each study is complete, you will be given a meal or the equivalent cash sum for you to buy your own meal and you will then be able to go home. Any travel expenses incurred by you in participating in this study will be reimbursed on provision of receipts, and we will offer £10 for the Oral Glucose Tolerance Test visit, and £75 payment per MRI scanning visit, in recognition of your time.

What if something goes wrong?
If you are harmed by someone else's negligence, then you may have grounds for legal action and you are free to complain through normal NHS complaints services. However if you are harmed accidentally whilst taking part in this research study, there are no special compensation arrangements.

If you have concerns about any aspect of the way you have been approached or treated during the course of this study you may wish to contact the hospital's Patient Advice and Liaison Service (PALS) on 020 3299 3625 or 020 3299 360, or write to PALS, King's College Hospital, Denmark Hill, London SE5 9RS.

What about the results?
The results of this study will not be known until some time after the last participant has finished. The research doctor will let you know the results of the study when it is completed. The results may be reported in professional publications or meetings but you will not be identified by name.

Who has reviewed the study?
This study has been approved by the Research Ethical Committee at King's College Hospital NHS Foundation Trust.

What if you wish to withdraw from the study?
Participation in this study is entirely voluntary, and you are free to withdraw at any point in time, and will not affect the treatment you receive from King's College Hospital NHS Foundation Trust.

Confidentiality
The study is confidential and all data collected will be secured against any unauthorised access. Confidential information regarding identity from volunteers will be destroyed after the trial unless we inform you otherwise, in which case we will ask for your consent to retain such information. We will normally inform your GP about your involvement in the study unless you request otherwise.

Any Questions?
Professor Stephanie Amiel, RD Lawrence Professor of Diabetic Medicine and members of her research group are leading this study. If you have any further questions please do not hesitate to contact us:

Contact: Dr. Yee Seun Cheah, Clinical Research Fellow
Diabetes Research Group
King's College London School of Medicine
Room 3.35, Weston Education Centre
Cutcombe Road
London SE5 9RJ
Telephone: 020 7848 5654 or 5653
Email: yee.cheah@kcl.ac.uk or andrew.pernet@kcl.ac.uk

Diabetes Research Group
Division of Gene & Cell Based Therapy
King's College London School of Medicine
King's College Hospital Campus
Bessemer Road
London
SE5 9PJ

The effects of food ingestion on the regional brain responses in healthy volunteers.

Information for Healthy volunteers

You are invited to participate in a research study. Before you decide, it is important for you to understand why the research is being done and what it will involve. Please take time to read the following information carefully and discuss it with friends, relatives, and your GP if you wish. Ask us if there is anything that is not clear, or you would like more information. Take time to decide whether or not you wish to take part.

Consumers for Ethics in Research (CERES) publish a leaflet entitled 'Medical Research and You'. This leaflet gives more information about medical research and looks at some of the questions you may want to ask. A copy may be obtained from CERES, PO Box 1365, London N16 0BW.

Thank you for reading this.

The purpose of the research

This study looks at how the brain responds to food ingestion (eating) in healthy volunteers, using a technique called functional magnetic resonance imaging (fMRI). Therefore we will eventually be able to compare this response between healthy volunteers and patients with Type 2 diabetes.

fMRI uses magnetic fields to create pictures of the brain which show the parts that are active during particular activities. In this case, we are hoping to identify those parts of the brain that are active when a person swallows a meal, in this case, melted ice cream, comparing it to a small drink of water.

Why have I been chosen?

We intend to look at this activity in healthy volunteers who are 40-65 years of age with no significant medical history and not taking regular medications. Since you are not resistant to insulin your central responses to food ingestion should be normal and we can therefore compare them to insulin resistant patients.

What will you be asked to do

Screening 1st visit

In the first instance you will be asked to attend at King's College Hospital for a test to measure your body's insulin sensitivity. You will be asked to come up one morning having had nothing to eat or drink for 8 hours overnight.

You will also be asked to give a full medical history and undergo a brief physical examination to make sure that you are fit and healthy and baseline blood tests for kidney, liver, thyroid function, lipids and blood count are normal.

MRI scanning

You will then be asked to attend for an fMRI brain scan on 2 occasions. These scans will each be done in the morning after an 8 hour period of not eating or drinking anything (sips of water allowed). There will be at least a day's separation between scans. Scans are done in the Centre for Neuroimaging Sciences in the Institute of Psychiatry, King's College Hospital. You will be asked to lie down on a trolley that will slide into the scanner tunnel. Your head will rest on a pillow that helps hold it still and a rest and a headband will maintain your head position. Headphones will be provided through which we can talk to you and a microphone for you to reply. You will be asked to lie still while the scans are made. The scans are made by creating a moving magnetic field around your head. This is rather noisy and you will hear banging sounds, muted by the headphones. Although you will be on your own in the scanner, you will be able to talk to the people running the scan (and they will talk to you) throughout.

The first scan will take about ten minutes. You will then be slid out of the scanner and asked to swallow a drink that may contain glucose or water. You will then be returned to the scanner for the next fifty minutes.

Expenses and payments

For the scanning procedures we offer a £75 payment per scan in recognition of the time and effort. Any travel expenses incurred by you in participating in this project will be re-imbursed if you provide the receipts.

Safety Measures

Safety is not an endpoint for this study but it is clearly important that safety is monitored. The risk of the study is negligible as fMRI does not cause harmful radiation.

Safety Data

Any adverse events reported spontaneously by the subject, as well as those noted by the investigator or study site staff, will be recorded and reported to the Local Ethical committee. The clinical course of the adverse event will be followed according to accepted standards of medical practice, even after the end of the observation period, until a satisfactory explanation for the adverse event is found or the investigator considers it medically justifiable to terminate follow-up.

Data Analysis

DATA MANAGEMENT PLAN
Subjects in the study will receive a unique identifier number. Data from several sources will be entered into computer spreadsheets for analysis using the identifier number only. Some data (e.g. laboratory results) will be stored by patient name either on the clinical NHS IT systems of King's College Hospital and neuroimaging data will be stored on the systems of the Institute of Psychiatry and processed by our research team using the Institute's IT systems. These systems are protected by the 2 clinical institutions in accordance with usual procedures. Data removed from these clinical systems for analysis into spreadsheets will use the study identifier number only. The code of identifier numbers will be kept by the Principle Investigator, Professor Stephanie Amiel and, the clinical investigating team only.

STUDY TIMELINE
Data collection for the study should be completed by August 2010, with data analysis completed in the ensuing 3 months.

Special note for women

Functional magnetic resonance imaging is not known to be damaging in pregnancy. However because pregnancy alters the body's chemistry, we will not be studying pregnant women. If you are pregnant, or trying to become pregnant, we would suggest that you do not take part but as these are not harmful to pregnancy, we will not be taking special precautions to check for pregnancy.

How participating might help you

This research study is designed to investigate how the brain responds to glucose ingestion in healthy volunteers and is not designed to benefit your own health for the duration of this study. We hope that the information we gain from the study may help us localise the brain regions altered in insulin resistant individuals, predisposing them to obesity.

What are the side effects of any treatment received when taking part?

You are not exposed to any radiation with MRI scanning, only a strong magnetic field, so it is imperative that any metal you may have is removed

prior to entering the scanner. The scanner is also quite snug fitting around your body, so it is not best suited for people with a fear of tight spaces.

What if something goes wrong?

If you are harmed by someone else's negligence, then you may have grounds for legal action and you are free to complain through normal NHS complaints service. However, if you are harmed accidentally whilst taking part in this research project, there are no special compensation arrangements.

What about the results?

The results of the study will be presented to all volunteers when it is complete. The information will also be presented at scientific and medical meetings and written up as one or more papers in scientific and medical publications. No one will be able to identify you in any of these public statements of the results. The study is funded by a charitable organisation and fully approved by the ethical committee of King's College Hospital.

What if you wish to withdraw from the study?

This study is completely voluntary at any time. You are free to withdraw at any time and this will not affect your future treatment at King's in any way.

Confidentiality

The study is confidential and all data collected will be secured against any unauthorised access. Although the overall results will be published in medical journals, no individual subjects will be identifiable from this.

Confidential information regarding identity from subjects will be destroyed after the trial unless we inform you otherwise, in which case we will ask for your consent to retain such information.

We will normally inform your general practitioner about your involvement in the study, unless you request otherwise.

Any questions?

Professor Stephanie Amiel, Professor of Diabetic Medicine at King's, is ultimately responsible for the study. The day to day running of the study will be run by Dr. Yee Cheah (Clinical Research Fellow and Specialist Registrar in Diabetes & Endocrinology), Dr Pratik Choudhary (Lecturer in Diabetes) and the research nurses on the team, Mr. Andrew Pernet and Ms. Bula Wilson. All will be happy to answer any questions you may have and they can be contacted on:

Tel: 020 7737 4000 ext 2311/4161/2054 during working hours or via the King's switchboard on 020 7737 4000 after hours.
Email: yee.cheah@kcl.ac.uk or pratik.choudhary@kcl.ac.uk or andrew.pernet@kcl.ac.uk. **August 2007**

King's College Hospital NHS
NHS Foundation Trust

KING'S College LONDON
University of London

Diabetes Research Group,
King's College London School of Medicine,

PARTICIPANT CONSENT FORM

A functional magnetic resonance imaging study of brain responses to food image viewing and food ingestion in insulin resistance: Insulin Sensitive Participants

Please read the following statements and initial the box if you agree:

1. I confirm that I have read and understand the information sheet (dated ……..., version……) for the above study. I have had the opportunity to consider the information, ask questions and have had these answered satisfactorily. ☐

2. I understand that my participation is voluntary. I understand that if I agree to take part in the study I can change my mind at any time without affecting my medical care or legal rights. ☐

3. I understand that sections of my medical notes relevant to my taking part in this research and data collected during the study may be looked at by individuals from regulatory authorities or from the NHS Trusts. I give permission for these individuals to have access to my records. ☐

4. I agree to have my blood tested. ☐

5. I agree to my GP being informed of my participation in the study. ☐

6. I agree to take part in the above study. ☐

…….	……..	……..
Participant's name	Signature	Date
…….	……...	……..
Name of person taking consent	Signature	Date

When completed, 1 copy for participant; 1 copy for research site file; 1 copy to be kept in medical notes.

King's College Hospital NHS
NHS Foundation Trust

KING'S College LONDON
University of London

Diabetes Research Group,
King's College London School of Medicine,

PARTICIPANT CONSENT FORM

A functional magnetic resonance imaging study of brain responses to food image viewing and food ingestion in insulin resistance: Insulin Resistant Participants

Please read the following statements and initial the box if you agree:

1. I confirm that I have read and understand the information sheet (dated ……..., version……) for the above study. I have had the opportunity to consider the information, ask questions and have had these answered satisfactorily. ☐

2. I understand that my participation is voluntary. I understand that if I agree to take part in the study I can change my mind at any time without affecting my medical care or legal rights. ☐

3. I understand that sections of my medical notes relevant to my taking part in this research and data collected during the study may be looked at by individuals from regulatory authorities or from the NHS Trusts. I give permission for these individuals to have access to my records. ☐

4. I agree to have my blood tested. ☐

5. I understand that I will be offered metformin (Glucophage SR) with advice on diet and exercise. ☐

6. I agree to my GP being informed of my participation in the study. ☐

7. I agree to take part in the above study. ☐

…….	……..	……..
Participant's name	Signature	Date
…….	……...	……..
Name of person taking consent	Signature	Date

When completed, 1 copy for participant; 1 copy for research site file; 1 copy to be kept in medical notes.

Brain Imaging Responses to Food Images & Food in Insulin Resistance
REC Reference: 10/H0808/47

WHO SHOULD NOT TAKE METFORMIN?

People with the following conditions should not take metformin:

- Previous reactions to metformin.
- Active kidney or liver problems.
- Alcoholism.
- Recent heart attack.
- Other scans involving the injection of contrast "dyes"

The physical examination and blood tests performed during the screening visit have confirmed the absence of the above, and that it is safe for you to take metformin.

However, if you do fall ill or develop any of the above problems, or if you are prescribed any other medication, **please show this form to the doctors treating you, and contact us as soon as possible.**

FURTHER INFORMATION

For further information please contact:

Dr. Yee Seun Cheah

Clinical Research Fellow & Specialist Registrar in Diabetes & Endocrinology

Diabetes Research Group, King's College London

Room 3.35, Weston Education Centre

Cutcombe Road

London SE5 9RJ

Telephone: 020 7848 5654

Email: yee.cheah@kcl.ac.uk

King's College Hospital NHS
NHS Foundation Trust

King's Diabetes Research Group

KING'S College LONDON
University of London

Metformin leaflet Version 1.2 (24.07.2012)

A functional magnetic resonance imaging study of brain responses to food image viewing and food ingestion in insulin resistance.

Metformin

Information for Research Volunteers

WHAT IS INSULIN RESISTANCE?

Thank you for taking part in our research study.

You have been asked to take part in our research study, as you are healthy with no known medical problems, but are a relative of someone with Type 2 diabetes mellitus, which increases the likelihood of you being insulin resistant.

Insulin resistance is a common condition where the body is less responsive than usual to insulin, a hormone normally produced by the body to control glucose (sugar) levels. The presence of insulin resistance increases the risk of developing diabetes, high blood pressure, heart disease and obesity. Part of this study will involve taking Metformin (Glucophage SR) This leaflet explains the tablets.

The information provided in this leaflet is specifically for volunteers participating in our research study (**"A functional magnetic resonance imaging study of brain responses to food image viewing and food ingestion in insulin resistance"**).

It is not for people taking the same or similar medication for medical reasons – please contact your GP for such advice and information.

Further information about this study in general is available in the **"Information for Research Volunteers"** pamphlet.

WHAT IS METFORMIN?

Metformin (Glucophage SR) is a medication that is used as first line treatment of Type 2 diabetes. It is also commonly used for treating "pre-diabetes" and polycystic ovarian syndrome, which are both conditions caused by insulin resistance.

Although it is not licenced for use in these two latter conditions, it is advocated by many medical bodies[1,2] and has been shown to prevent the onset of diabetes in people with insulin resistance and a risk of developing diabetes[3].

HOW DOES METFORMIN WORK?

Metformin prevents and treats diabetes by improving the body's ability to respond to insulin. By improving the body's sensitivity to its own insulin, glucose and insulin levels are brought back down to the normal range. It does not reduce glucose levels below normal.

1. Nathan, D.M. et al. *Diabetes Care* **30**, 753-759 (2007).
2. Garber, A.J. et al. *Endocr Pract* **14**, 933-946 (2008).
3. Knowler, W.C. et al. *N. Engl. J. Med* **346**, 393-403 (2002).

WHAT ARE THE POSSIBLE SIDE EFFECTS OF TAKING PART?

Some people experience altered taste, nausea, loss of appetitte, an upset stomach and/or loose stools with metformin. These symptoms are short-lived and usually resolve within a few weeks of starting treatment. To minimise them, a "slow-release form" form of the tablet will be used (Glucophage SR), and the dose will be increased gradually from one tablet (500 mg) daily, taken with your main meal of the day for a week, to **four** tablets (**2g**) daily for the remainder of the 3 month period. Very rare side effects include skin reactions, low vitamin B12 levels and build up of lactic acid.

WHO SHOULD NOT TAKE METFORMIN?

People with the following conditions should not take metformin:

- Previous reactions to metformin.
- Active kidney or liver problems.
- Alcoholism
- Recent heart attack.
- Other scans involving the injection of contrast "dyes"

The physical examination and blood tests performed during the screening visit have confirmed the absence of the above, and that it is safe for you to take metformin.

However, if you do fall ill or develop any of the above problems, or if you are prescribed any other medication, **please show this form to the doctors treating you, and contact us as soon as possible.**

FURTHER INFORMATION

For further information please contact:

Dr. Yee Seun Cheah

Clinical Research Fellow & Specialist Registrar in Diabetes & Endocrinology

Diabetes Research Group, King's College London

Room 3.35, Weston Education Centre

Cutcombe Road

London SE5 9RJ

Telephone: 020 7848 5654

Email: yee.cheah@kcl.ac.uk

King's College Hospital NHS
NHS Foundation Trust

King's Diabetes Research Group

KING'S College LONDON
University of London

A functional magnetic resonance imaging study of brain responses to food image viewing and food ingestion in insulin resistance.

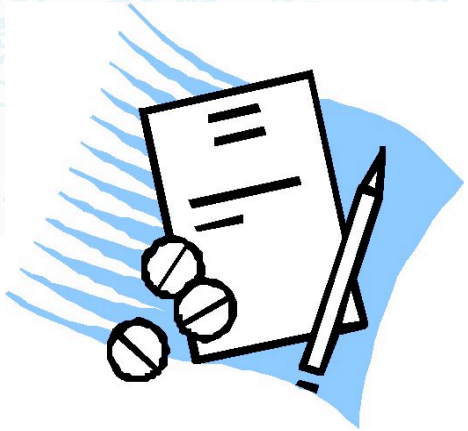

Metformin

Guide to Doses for Research Volunteers

Participant Study Number:_____

Participant Initials: _____

MEDICATION USED IN THIS STUDY

Thank you for taking part in our research study.

You will be given a course of Metformin SR (also known as Glucophage SR) for 3 months (12 weeks).

This leaflet is about the doses of medication used in this study.

For further information about these medications, please refer to the "Metformin: Information for Research Volunteers" leaflet.

The information provided in this leaflet is specifically for volunteers participating in our research study (**"A functional magnetic resonance imaging study of brain responses to food image viewing and food ingestion in insulin resistance"**).

It is not for people taking the same or similar medication for medical reasons – please contact your GP for such advice and information.

Further information about this study in general is available in the **"Information for Research Volunteers"** pamphlet.

DOSES:

All tablets should all be taken at the same time with your main meal of the day.

The number of tablets to be taken are shown in the table below.

If you are unable to tolerate the tablet at a higher dose, stay on the dose that you were able to tolerate and contact us for further advice.

WHAT DO I DO WITH ANY TABLETS THAT I HAVEN'T TAKEN?

Any remaining tablets should be returned to the research team or to the pharmacy department at King's College Hospital.

We would like to know how many tablets you were able to take, and would be grateful if you could complete the table below.

Week	Date	No. tablets to take	No. taken per day	No. days taken this week
1		**1 tablet per day**		
2				
3		**2 tablets per day**		
4				
5		**3 tablets per day**		
6				
7		**4 tablets per day**		
8				
9				
10				
11				
12				

King's College Hospital NHS
NHS Foundation Trust

KING'S College LONDON
University of London

A functional magnetic resonance imaging study of brain responses to food image viewing and food ingestion in insulin resistance.

Eating Behaviour Questionnaire Panel

For Research Volunteers[1]

[1]Adapted from:
- Questionnaire on Eating and Weight Patterns-Revised© (QEWP-R©) [selected questions].
- Dutch Eating Behaviour Questionnaire (DEBQ).
- Eating Disorder Examination Questionnaire© (EDE-Q 6.0©) [selected questions].

Thank your for completing these questionnaires. Please circle the appropriate number or response, or write in information where asked. You may skip any question you do not understand or do not wish to answer.

Screening Number: _____

Participant Study Number: _____

Participant Initials: _____

Date: __ __ / __ __ __ / __ __ __ __

Questionnaire on Eating and Weight Patterns-Revised© (QEWP-R©) [selected questions]

R.S. Spitzer, S.Z. Yanovski, & M.D. Marcus. (1993).

Thank you for completing this questionnaire. Please circle the appropriate number or response, or write in information where asked. You may skip any question you do not understand or do not wish to answer.

1. Age: _____ years

2. How tall are you? _____ft_____in / _____metres

3. How much to you weigh now? _____st_____lbs / _____kg

4. What has been your highest weight ever? _____st_____lbs / _____kg

5. Have you ever been overweight by at least 10 lbs (¾ st / 4.5 kg) as a child or 15 lbs (1 st 1 lbs / 7kg) as an adult?

   1. Yes 2. No or not sure

   IF YES: How old were you when you were first overweight (at least 10 lbs (¾ st / 4.5 kg) as child or 15 lbs (1 st 1 lbs / 7 kg) as an adult)? If you are not sure, what is your best guess?

   _____years

6. How many times (approximately) have you lost 20 lbs (1½ st / 9 kg) or more – when you weren't sick – and then gained it back?

   1. Never
   2. Once or twice
   3. Three of four times
   4. Five times or more

7. During the past ***six*** months, did you often eat within any two hour period what most people would regard as an unusually large amount of food?

   1. Yes 2. No **IF NO: SKIP TO QUESTION 11**

8. During the times when you ate this way, did you often feel you couldn't stop eating or control what or how much you were eating?

   1. Yes 2. No **IF NO: SKIP TO QUESTION 11**

9. During the past ***six*** months, how often, on average, did you have times when you ate this way – that is, large amounts of food ***plus*** the feeling that your eating was out of control? (There may have been some weeks when it was not present – just average those in.)

   1. Less than one day a week
   2. One day a week
   3. Two or three days a week
   4. Four or five days a week
   5. Nearly every day

10. Did you ***usually*** have any of the following experiences during these occasions?

a. Eating much more rapidly than usual? Yes_____ No_____

b. Eating until you felt uncomfortably full? Yes_____ No_____

c. Eating large amounts of food when you didn't feel physically hungry? Yes_____ No_____

d. Eating alone because you were embarrassed by how much you were eating? Yes_____ No_____

e. Feeling disgusted with yourself, depressed, or feeling very guilty after overeating? Yes_____ No_____

11. In general, during the past ***six*** months, how upset were you by overeating (eating more than you think is best for you)?

1. Not at all
2. Slightly
3. Moderately
4. Greatly
5. Extremely

12. In general, during the past ***six*** months, how upset were you by the feeling that you couldn't stop eating or control what or how much you were eating?

1. Not at all
2. Slightly
3. Moderately
4. Greatly
5. Extremely

13. During the past ***six*** months, how important has your weight or shape been in how you feel about or evaluate yourself as a person – as compared to other aspects of your life, such as how you do at work, as a parent, or how you get along with other people?

1. Weight and shape were ***not very important***
2. Weight and shape ***played a part*** in how you felt about yourself
3. Weight and shape ***were among the main things*** that affected how you felt about yourself
4. Weight and shape ***were the most important things*** that affected how you felt about yourself

14. During the past ***three*** months, did you ever make yourself vomit in order to avoid gaining weight after binge eating?

1. Yes 2. No

IF YES: How often, ***on average***, was that?

1. Less than once a week
2. Once a week
3. Two or three times a week
4. Four or five times a week
5. More than five times a week

15. During the past ***three*** months, did you ever take more than twice the recommended dose of laxatives in order to avoid gaining weight after binge eating?

IF YES: How often, ***on average***, was that?

1. Less than once a week
2. Once a week
3. Two or three times a week
4. Four or five times a week
5. More than five times a week

16. During the past ***three*** months, did you ever take more than twice the recommended dose of diuretics (water pills) in order to avoid gaining weight after binge eating?

IF YES: How often, ***on average***, was that?

1. Less than once a week
2. Once a week
3. Two or three times a week
4. Four or five times a week
5. More than five times a week

17. During the past ***three*** months, did you ever fast – not eating anything at all for at least 24 hours – in order to avoid gaining weight after binge eating?

IF YES: How often, ***on average***, was that?

1. Less than once a week
2. One day a week
3. Two or three days a week
4. Four or five days a week
5. Nearly every day

18. During the past ***three*** months, did you ever exercise for more than an hour specifically in order to avoid gaining weight after binge eating?

IF YES: How often, ***on average***, was that?

1. Less than once a week
2. Once a week
3. Two or three times a week
4. Four or five times a week
5. More than five times a week

19. During the past ***three*** months, did you ever take more than twice the recommended dose of a diet pill in order to avoid gaining weight after binge eating?

IF YES: How often, ***on average***, was that?

1. Less than once a week
2. Once a week
3. Two or three times a week
4. Four or five times a week
5. More than five times a week

20. During the past ***six*** months, did you go to any meetings of an organised weight control program? (e.g. Weight Watchers, Optifast, Jenny Craig) or a self-help groups (e.g. TOPS, Overeaters Anonymous)?

1. Yes 2. No

IF YES: Name of program:_____

21. Since you have been an adult – 18 years old – how much of the time have you been on a diet, been trying to follow a diet, or in some way been limiting how much you were eating in order to lose weight or keep from regaining weight you had lost? Would you say…?

1. None or hardly any of the time
2. About a quarter of the time
3. About half of the time
4. About three-quarters of the time
5. Nearly all of the time

22. **SKIP THIS QUESTION IF YOU NEVER LOST AT LEAST 10 LBS (¾ st / 4.5 Kg) BY DIETING**: How old were you the first time you lost at least 10 lbs (¾ st / 4.5 kg) by dieting, or in some way limiting how much you ate? If you are not sure, what is your best guess?

_____years

23. **SKIP THIS QUESTION IF YOU'VE NEVER HAD EPISODES OF EATING UNUSUALLY LARGE AMOUNTS OF FOOD ALONG WITH THE SENSE OF LOSS OF CONTROL**: How old were you when you first had times when you ate large amounts of food and felt that your eating was out of control? If you are not sure, what is your best guess?

_____years

24. Please take a look at the following silhouettes. Put a circle around the silhouettes that most resemble the body build of your natural father and mother ***at their heaviest***. If you have no knowledge of your biological father and/or mother, don't circle anything for that parent.

Dutch Eating Behaviour Questionnaire (DEBQ).

T. van Strien, J.E.R. Frijters, G.P.A. Bergers, P.B. Defares (1986).

Please circle the answer that apply to you

1. If you have put on weight, do you eat less than you usually do?

Never Seldom Sometimes Often Very Often Not Relevant

2. Do you try to eat less at mealtimes than you would like to eat?

Never Seldom Sometimes Often Very Often

3. How often do you refuse food or drink offered because you are concerned about your weight?

Never Seldom Sometimes Often Very Often

4. Do you watch exactly what you eat?

Never Seldom Sometimes Often Very Often

5. Do you deliberately eat foods that are slimming?

Never Seldom Sometimes Often Very Often

6. When you have eaten too much, do you eat less than usual the following days?

Never Seldom Sometimes Often Very Often Not Relevant

7. Do you deliberately eat less in order not to become heavier?

Never Seldom Sometimes Often Very Often

8. How often do you try not to eat between meals because you are watching your weight?

Never Seldom Sometimes Often Very Often

9. How often in the evening do you try not to eat because you are watching your weight?

Never Seldom Sometimes Often Very Often

10. Do you take into account your weight with what you eat?

Never Seldom Sometimes Often Very Often

11. Do you have the desire to eat when you are irritated?

Never Seldom Sometimes Often Very Often Not Relevant

12. Do you have a desire to eat when you have nothing to do?

Never Seldom Sometimes Often Very Often Not Relevant

13. Do you have a desire to eat when you are depressed or discouraged?

Never Seldom Sometimes Often Very Often Not Relevant

14. Do you have a desire to eat when you are feeling lonely?

Never Seldom Sometimes Often Very Often Not Relevant

15. Do you have desire to eat when somebody lets you down?

Never Seldom Sometimes Often Very Often Not Relevant

16. Do you have a desire to eat when you are cross?

Never Seldom Sometimes Often Very Often Not Relevant

17. Do you have a desire to eat when you are approaching something unpleasant to happen?

Never Seldom Sometimes Often Very Often

18. Do you get the desire to eat when you are anxious, worried or tense?

Never Seldom Sometimes Often Very Often

19. Do you have a desire to eat when things are going against you or when things have gone wrong?

Never Seldom Sometimes Often Very Often

20. Do you have a desire to eat when you are frightened?

Never Seldom Sometimes Often Very Often Not Relevant

21. Do you have a desire to eat when you are disappointed?

Never Seldom Sometimes Often Very Often Not Relevant

22. Do you have a desire to eat when you are emotionally upset?

Never Seldom Sometimes Often Very Often Not Relevant

23. Do you have a desire to eat when you are bored or restless?

Never Seldom Sometimes Often Very Often Not Relevant

24. If food tastes good to you, do you eat more than usual?

Never Seldom Sometimes Often Very Often

25. If food smells and looks good, do you eat more than usual?

Never Seldom Sometimes Often Very Often

26. If you see or smell something delicious do you have a desire to eat it?

Never Seldom Sometimes Often Very Often

27. If you have something delicious to eat, do you eat it straight away?

Never Seldom Sometimes Often Very Often

28. If you walk past the baker do you have the desire to buy something delicious?

Never Seldom Sometimes Often Very Often

29. If you walk past a snackbar or café, do you have the desire to buy something delicious?

Never Seldom Sometimes Often Very Often

30. If you see others eating, do you also have the desire to eat?

Never Seldom Sometimes Often Very Often

31. Can you resist eating delicious foods?

Never Seldom Sometimes Often Very Often

32. Do you eat more than usual, when you see others eating?

Never Seldom Sometimes Often Very Often

33. When preparing a meal are you inclined to eat something?

Never Seldom Sometimes Often Very Often

Eating Disorder Examination Questionnaire© (EDE-Q 6.0©) [selected questions]

C.G. Fairburn, S. Beglin (2008).

The following questions are concerned with the *past four weeks (28 days)* only. Please read each question carefully and circle the appropriate response. Please note that for these questions the term "binges" means eating what others would regard as an unusually large amount of food for the circumstances, accompanied by a sense of having lost control over eating.

	On how many of the past 28 days…							
1	Have you been deliberately ***trying*** to limit the amount of food you eat to influence your shape or weight (whether or not you have succeeded)?	**No days**	**1-5 days**	**6-12 days**	**13-15 days**	**16-22 days**	**23-27 days**	**Every day**
2	Have you gone for long periods of time (8 waking hours or more) without eating anything at all in order to influence you shape or weight?	**No days**	**1-5 days**	**6-12 days**	**13-15 days**	**16-22 days**	**23-27 days**	**Every day**
3	Have you ***tried*** to exclude from your diet any foods that you like in order to influence your shape or weight (whether or not you have succeeded)?	**No days**	**1-5 days**	**6-12 days**	**13-15 days**	**16-22 days**	**23-27 days**	**Every day**
4	Have you ***tried*** to follow definite rules regarding your eating (for example, a calorie limit) in order to influence your shape or weight (whether or not you have succeeded)?	**No days**	**1-5 days**	**6-12 days**	**13-15 days**	**16-22 days**	**23-27 days**	**Every day**
5	Have you had a definite desire to have an ***empty*** stomach with the aim of influencing your shape or weight?	**No days**	**1-5 days**	**6-12 days**	**13-15 days**	**16-22 days**	**23-27 days**	**Every day**
6	Have you had definite desire to have a ***totally flat*** stomach?	**No days**	**1-5 days**	**6-12 days**	**13-15 days**	**16-22 days**	**23-27 days**	**Every day**
7	Has thinking about ***food, eating or calories*** made it very difficult to concentrate on things you are interested in (for example, working, following a conversation, or reading)?	**No days**	**1-5 days**	**6-12 days**	**13-15 days**	**16-22 days**	**23-27 days**	**Every day**
8	Has thinking about ***shape or weight*** made it very difficult to concentrate on things you are interested in (for example, working, following a conversation, or reading)?	**No days**	**1-5 days**	**6-12 days**	**13-15 days**	**16-22 days**	**23-27 days**	**Every day**
9	Have you had a definite fear of losing control over eating?	**No days**	**1-5 days**	**6-12 days**	**13-15 days**	**16-22 days**	**23-27 days**	**Every day**
10	Have you had a definite fear that you might gain weight?	**No days**	**1-5 days**	**6-12 days**	**13-15 days**	**16-22 days**	**23-27 days**	**Every day**
11	Have you felt fat?	**No days**	**1-5 days**	**6-12 days**	**13-15 days**	**16-22 days**	**23-27 days**	**Every day**
12	Have you had a strong desire to lose weight?	**No days**	**1-5 days**	**6-12 days**	**13-15 days**	**16-22 days**	**23-27 days**	**Every day**
13	Over the past 28 days, on how many days have you eaten in secret (i.e. furtively)? [Do not count binges]	**No days**	**1-5 days**	**6-12 days**	**13-15 days**	**16-22 days**	**23-27 days**	**Every day**
14	On what proportion of the times that you have eaten have you felt guilty (felt that you've done wrong) because of its effect on your shape or weight? [Do not count binges]	**None of the times**	**A few of the times**	**Less than half**	**Half of the times**	**More than half**	**Most of the time**	**Every Time**

	Over the past 28 days…	Not at all		Slightly		Moderately		Markedly
15	How concerned have you been about other people seeing you eat? [Do not count binges]	**0**	**1**	**2**	**3**	**4**	**5**	**6**
16	Has your ***weight*** influenced how you think about (judge) yourself as a person?	**0**	**1**	**2**	**3**	**4**	**5**	**6**
17	Has you ***shape*** influenced how you think about (judge) yourself as a person?	**0**	**1**	**2**	**3**	**4**	**5**	**6**
18	How much would it have upset you if you had been asked to weigh yourself once a week (no more, or less, often) for the next four weeks?	**0**	**1**	**2**	**3**	**4**	**5**	**6**
19	How dissatisfied have you been with your ***weight***?	**0**	**1**	**2**	**3**	**4**	**5**	**6**
20	How dissatisfied have you been with your ***shape***?	**0**	**1**	**2**	**3**	**4**	**5**	**6**
21	How uncomfortable have you felt seeing your body (for example, seeing your shape in the mirror, in a shop window reflection, while undressing or taking a bath or shower)?	**0**	**1**	**2**	**3**	**4**	**5**	**6**
22	How uncomfortable have you felt about others seeing your shape or figure (for example, in communal changing rooms, when swimming, or wearing tight clothes)?	**0**	**1**	**2**	**3**	**4**	**5**	**6**

THANK YOU FOR COMPLETING THESE QUESTIONNAIRES

A functional magnetic resonance imaging study of brain responses to food image viewing and food ingestion in insulin resistance.

Meal & Activities Diary for Research Volunteers.

RESEARCH DIARY

Thank you for taking part in our study.

We will invite you to see a specialist dietitian during the study. In order for them to provide you with appropriate advice, it would be very useful to know more about the food you eat and your daily activities.

We would therefore like you to complete this diary over 3 consecutive days.

Here are some tips on completing it:

ALWAYS CARRY THE DIARY WITH YOU & WRITE DOWN WHAT YOU HAVE EATEN IMMEDIATELY AFTERWARDS.

Don't do it later or write things down on a scrap of paper and enter it into the diary later that day. It will be more accurate if you write in the diary as you go along; the longer you wait, the more likely it is that you will underestimate or forget what you ate.

WRITE DOWN EVERYTHING THAT YOU EAT OR DRINK AND BE SPECIFIC.

Every little bit counts and it is much more useful to know exactly what you have had to eat and drink and how much. For example, if you ate a sandwich, write exactly what was inside (e.g. cheese, mayonnaise, tomato etc.) and how many you ate.

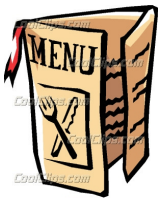

BE COMPLETE.

Don't limit your entries in the diary to what you ate. Include how much you ate, how quickly you ate and how you felt at the time.

DON'T FORGET YOUR PHYSICAL ACTIVITIES.

Follow the same tips for recording your physical activities.

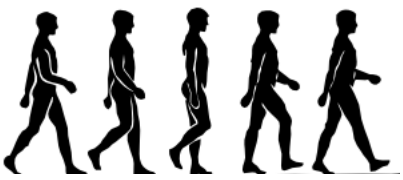

Subject No: _____ **Date:_____**

Time	**Food & drink consumed / Activities performed**	**Amount consumed / Duration of Activities**	**How you felt**	Office use only

THINK BEFORE YOU DRINK!

1 pint of beer = 180 calories
1 small glass of wine = 85 calories
1 medium cappuccino = 180 calories
200 ml glass of fruit juice = 100 calories
380 ml bottle of lucozade = 277 calories
330 ml can of cola = 160 calories
Water = 0 calories!

SLOW DOWN!

- Chew each mouthful slowly.
- Eat at a table and focus on your food, not whilst watching TV or on the move.
- Try to leave a mouthful of food on your plate at the end of each meal (but not vegetables!)

OTHER SUPPORT AND INFORMATION:
Walking for Health: www.whi.org.uk
British Heart Foundation: www.bhf.org.uk
Diabetes UK: www.diabetes.org.uk
NHS Choices: www.nhs.uk/LiveWell/Fitness
Eatwell (Food Standards Agency): www.eatwell.gov.uk/healthydiet

GOAL SETTING

Make you goals specific e.g. instead of saying "I want to become more active," set yourself a specific goal e.g. "I will walk for 15 minutes at lunchtime and another 15 minutes in the evening."

Be realistic set yourself a realistic goal that you can achieve

Write your routine Make a note of what activites you have done, and what and how you feel when eating. This will help you to review your progress, to see where things are going well and to identify any changes that might make things better. Those who are the most successful at changing habits do!

Don't give up! Some days you'll find you have the best intentions but they may not quite go to plan. The occasional laspe into unhealthier lifestyle activities are normal. It doesn't mean things are all downhill from here! Think back to why this happened and plan how you could prevent this happening if you were in the same situation again.

LOCAL SUPPORT

Southwark: www.southwarkpct.nhs.uk/952
- **Fusion Leisure** www.fusion-lifestyle.com 020 7740 7500
- **Southwark Healthy Walks** 020 7525 2253

Lambeth: email healthylifestyles@lambeth.gov.uk
- www.lambeth.gov.uk/sports 020 7926 0396
- **Active Walks Programme** 020 7926 0761

A functional magnetic resonance imaging study of brain responses to food image viewing and food ingestion in insulin resistance.

Healthy Living

Information for Research Volunteers

King's College Hospital NHS
NHS Foundation Trust

King's Diabetes Research Group

KING'S College LONDON

WHY BOTHER?

Physical activity combined with a healthy balanced diet can:

- **Improve mental and physical health**
- **prevent coronary heart disease, stroke, Type 2 diabetes, weight problems and high blood presure.**

HOW ACTIVE SHOULD I BE?

At least 30 minutes of moderate-intensity physical activity a day, on five or more days a week.

Moderate-intensity physical activity means working hard enough to make you breathe more heavily than normal and become slightly warmer.

If you are not used to doing 30 minutes day, start by doing 5 minutes at least three times a day and **build up gradually**.

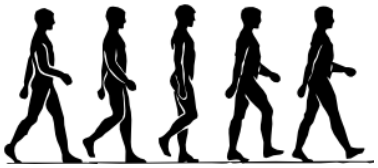

TOP TIPS ON BEING MORE ACTIVE

Fit activities into your daily routine! Reduce the time you spend sitting and free up some time to be active.

Cut couch time e.g. do some chores whilst watching TV – e.g. 30 mins of:

- Dusting = 75 calories
- Painting & decorating = 90 calories
- Vacuuming = 105 calories

Go for a walk e.g. get off the bus a few stops early and walk the rest of the way; walking groups; use stairs instead of lift.

Time out! Choose activities you find fun that you can do with friends e.g. dancing, swimming, gym, activity class, cycling, play ball.

Speed up! Set yourself goals and increase intensity and duration of each activity regularly. 30 mins of:

- Strolling = 75 calories
- Brisk walk = 150 calories
- Running = 300-400 calories
- Swimming – 600-700 calories

A pedometer may help: build up to 10,000 steps per day = 2500 calories over a week

WHAT IS A HEALTHY DIET?

Caution with your portions! Make sure at least half of your plate is vegetables/salads. Switch to a smaller plate.

Five a day! Eat at least 5 portions of fruit and veg a day.

Forget the fat! Use semi-skimmed/skimmed milk & low fat cheese; choose lean cuts of meat and eat less processed meats eg burgers, sausages

Oily fish: Eat at least 1 portions of oily fish a week e.g. mackerel, trout, salmon.

Less Salt: look for hidden salt in ready-made foods; use herbs to season food.

Per 100g	A Lot	A Little
Sugars	10 g	2 g
Fats	20 g	3 g
Salt	1.5 g	0.3 g
Sodium	0.6 g	0.1 g

Fat facts: All fats contain the same amount of calories whether good or bad, so you need to reduce your total fat intake even if using good fats (e.g. vegetable/nut/see based oils).

King's College Hospital NHS
NHS Foundation Trust

Do you have Type 2 diabetes ?

If so, your relatives may be interested in our research.

Close relatives of people with Type 2 diabetes are at increased risk of developing diabetes themselves.

The Diabetes Research Team at King's College Hospital are researching this using brain scanning to investigate appetite control. We are currently looking for male volunteers to participate in our studies.

If you have diabetes and you think one of your relatives (son or brother without diabetes themselves) may be interested in our studies, please give them this flyer. The study starts with a health check, in which we will measure:

- ✓Body Mass Index
- ✓Blood Pressure
- ✓Fasting blood sugar (glucose)

Willing volunteers may then take part in the brain scanning studies. Screening will take place at King's College Hospital. Results are strictly confidential. Responding to this flyer does not mean one has to take part in the research, which is entirely voluntary.

If you or your relative would like further information, please contact: Dr. Yee Seun Cheah, Clinical Research Fellow.

Telephone: 020 7848 5654 **Email: y.cheah@nhs.net**

KING'S HEALTH PARTNERS

EMIR. Flyer to prospective insulin resistant subjects. Version 1.1 01.09.2010

King's College Hospital NHS
NHS Foundation Trust

Do your parents, brothers or sisters have diabetes?

If so, you may be interested in our research.

Close relatives of people with Type 2 diabetes are at increased risk of developing diabetes themselves.

The Diabetes Research Team at King's College Hospital are researching this using brain scanning to investigate appetite control. We are currently looking for male volunteers without diabetes themselves, but with parents, brothers or sisters who do have diabetes, to participate in our studies.

The study starts with a health check, in which we will measure:

- ✓Body Mass Index
- ✓Blood Pressure
- ✓Fasting blood sugar (glucose)

Willing volunteers may then take part in the brain scanning studies. Screening will take place at King's College Hospital. Results are strictly confidential. Responding to this flyer does not mean one has to take part in the research, which is entirely voluntary.

If you would like further information, please contact:

Dr. Yee Seun Cheah, Clinical Research Fellow.

Telephone: 020 7848 5654 **Email: y.cheah@nhs.net**

KING'S HEALTH PARTNERS

Brain imaging responses to Food Images & Food in Insulin Resistance.
REC reference: 10/H0808/47

Pioneering better health for all

Volunteers needed for appetite research

King's College London

We invite people who don't have diabetes, but have family members with Type 2 diabetes, to take part in research looking at how our brains respond to food, to help find out why conditions like diabetes develop. A health check is included and volunteers will be reimbursed for their time. For more information please contact Dr. Yee Cheah on

020 7848 5654 or **yee.cheah@kcl.ac.uk**
Diabetes & Nutritional Sciences, King's College London

Subject heading: Effects of food ingestion on brain activation - circular

Circular email for use for recruitment of insulin sensitive volunteers for study ref: 10/H0808/47, approved by King's College Hospital Research Ethics Committee. This project contributes to the College's role in conducting research, and teaching research methods. You are under no obligation to reply to this email, however if you choose to, participation in this research is voluntary and you may withdraw at anytime.

We are looking for healthy male volunteers to participate in our study of the effect of eating on brain activity. This will build on current research on the way the brain controls our appetite and eating, which will help us understand why some people are more prone to weight gain, and may potentially allow the development of new ways to prevent and treat obesity and diabetes in the future.

Volunteers will attend a total of four visits. You will initially attend a screening visit at King's College Hospital (KCH), where you will provide a full medical history and undergo a brief physical examination by a doctor. You will also be asked to provide a sample of urine, and a sample of blood (approximately 10 ml / 2 tsp) after an overnight fast of 8 hours. This will take approximately 1 hour. The second visit to KCH will involve taking blood samples at 30 minute intervals over two hours (total 48 mls / 10 tsp) after a glucose drink to measure your body's chemical response and exclude the presence of diabetes.

Volunteers will then attend the Centre for Neuroimaging Science at the Institute of Psychiatry on two separate mornings. On each visit, after an overnight fast, you will have a small plastic tube or "drip" inserted into a vein in the arm or back of the hand to allow blood to be taken for measurements of glucose (sugar) and hormones that control appetite at 10 minute intervals during the scan (total 48 mls / 10 tsp each visit). You will then undergo a series of 5 functional magnetic resonance imaging (fMRI) scans. This will involve lying in the scanner for approximately 45 minutes in total. As this can be noisy, a microphone and headphones will be fitted with music being played, whilst allowing us to ask questions about your hunger and appetite during the scans. Images will be taken to detect the areas of the brain that are active after eating ice cream on one visit, compared to drinking water on another visit, given during the scan. fMRI will also be used to detect the brain's responses whilst being shown pictures of foods, compared to pictures of everyday household objects during both visits. This will allow us to look at the way the brain responds to the sight and eating of food.

We are looking for male volunteers aged between 18-65 years (inclusive) with a clear understanding of written and spoken English. As there are other factors that may affect the way the brain responds to food, you will need to be right-handed, healthy with no significant medical illnesses (e.g. diabetes, stroke, kidney or liver problems), not taking any regular medication. The scans will involve lying on a trolley that will slide into the scanner tunnel using strong magnets (no radiation) to produce pictures of the brain. You will therefore not be able to participate if you have any contraindications to MRI scanning e.g. cardiac pacemaker, extensive dental work, history of penetrating eye trauma, presence of certain metal surgical clips, claustrophobia. Full details about the study will be provided in a Participant Information Sheet.

Participation is completely voluntary and you are free to withdraw at any time. Participation will end on completion of the second scan visit. You will be compensated for your time and inconvenience, and any travel expenses will be reimbursed.

This study is being run by the Diabetes Research Team led by Prof. Stephanie Amiel, King's College London School of Medicine and has been approved by the King's College Hospital NHS Foundation Trust Research Ethics and Research & Development Committees.

For further information please contact Dr. Yee Seun Cheah, Clinical Research Fellow and Specialist Registrar in Diabetes & Endocrinology, telephone 020 7848 5654 or email yee.cheah@kcl.ac.uk

Thank you for reading this message.

Dr. Yee Seun Cheah
Diabetes Research Group, King's College London, Room 3.35 Weston Education Centre, Cutcombe Road, London SE5 9RJ

Subject heading: Effects of food ingestion on brain activation - circular

Circular email for use for recruitment of insulin resistant volunteers for study ref: 10/H0808/47, approved by King's College Hospital Research Ethics Committee. This project contributes to the College's role in conducting research, and teaching research methods. You are under no obligation to reply to this email, however if you choose to, participation in this research is voluntary and you may withdraw at anytime.

We are looking for healthy male volunteers, aged 18-65 years who are 1st degree relatives of people with Type 2 diabetes, to participate in our study of the effect of eating on brain activity. This will help us understand why some people are more prone to diabetes and weight gain, and may potentially allow the future development of new ways to prevent and treat obesity and diabetes.

Volunteers will attend a total of 6 visits. You will initially attend a screening visit at King's College Hospital (KCH), where you will provide a full medical history and undergo a brief physical examination by a doctor. You will also be asked to provide a sample of urine, and a sample of blood (approximately 10ml/2 tsp) after an overnight fast of 8 hours. This will take approximately 1 hour. The 2nd visit to KCH will involve taking blood samples at 30 minute intervals over 2 hours (total 48mls/10 tsp) after a glucose drink to exclude the presence of diabetes.

Volunteers will then attend the Centre for Neuroimaging Science (Institute of Psychiatry) on 2 separate mornings, where functional magnetic resonance imaging (MRI) brain scans will be performed. On each visit, after an overnight fast, a small plastic tube or "drip" will be inserted into a vein in the arm to allow blood to be taken for measurements of glucose (sugar) and hormones that control appetite at 10 minute intervals during the scan (total 48mls/10 tsp each visit). Each scan will involve lying on a trolley that will slide into the scanner tunnel using strong magnets (no radiation) for approximately 1 hour in total, to produce pictures of the brain. As this can be noisy, a microphone and headphones will be fitted with music being played, whilst allowing us to ask questions about your hunger and appetite during the scans. Images will be taken to detect the areas of the brain that are active after eating ice cream on one visit, compared to drinking water on another visit, given during the scan, as well as the responses to pictures of foods and everyday household objects shown during both visits. This will allow us to look at the way the brain responds to the sight and eating of food.

After these initial scans, each volunteer will be given a 3 month course of either Metformin or a placebo, allocated randomly. Metformin is an oral medication that improves the body's response to insulin, a hormone that is produced naturally to control glucose levels. The placebo has no active ingredients. After 2 further scans performed after this period, your participation ends.

You will need to be right-handed, healthy with no significant medical illnesses (e.g. diabetes, stroke, kidney or liver problems) and not be taking any regular medication that can influence glucose levels or the brain. You will not be able to participate if you have any contraindications to MRI scanning e.g. cardiac pacemaker, extensive dental work, history of penetrating eye trauma, presence of certain metal surgical clips, claustrophobia. Full details about the study, including further details on any risks involved in the procedures, and possible side effects of the medication, will be provided in a Participant Information Sheet. Participation is completely voluntary and you are free to withdraw at any time. You will be compensated for your time and inconvenience, and any travel expenses will be reimbursed.

This study is being run by the Diabetes Research Team led by Prof. Stephanie Amiel, King's College London School of Medicine and has been approved by the King's College Hospital NHS Foundation Trust Research Ethics and Research & Development Committees. For further information please contact Dr. Yee Seun Cheah, Clinical Research Fellow, tel: 020 7848 5654 / email: yee.cheah@kcl.ac.uk. Thank you for reading this message.

Diabetes Research Group
Division of Gene & Cell Based Therapy
King's College London School of Medicine
Denmark Hill Campus
c/o James Black Centre
Coldharbour Lane
London SE5 9RS
Tel: 020 3299 2311
Email: yee.cheah@kcl.ac.uk

General Practitioner / Consultant

Date:

Dear Dr. _____

Re: ***Functional magnetic resonance imaging study of brain responses to food image viewing and food ingestion in insulin resistance (insulin sensitive volunteers)***

I am writing to inform you that your patient, _____ has consented to take part in a research study looking at the brain's responses to nutrient ingestion in healthy volunteers, using functional magnetic resonance imaging (fMRI), led by Professor Stephanie Amiel at King's College London and King's College Hospital.

Your patient has attended a screening visit and will undergo an oral glucose tolerance test to exclude the presence of diabetes. He will attend the Institute of Psychiatry's Centre for Neuroimaging Sciences on 2 separate occasions, no less than 24 hours apart. On each visit, after an overnight fast, he/she will receive in random order either ice cream or water whilst undergoing fMRI brain scans. Blood will also be taken to allow us to measure both brain, hormonal and metabolic responses to food/water ingestion. The results of these studies in healthy volunteers will allow us to make comparisons with people with insulin resistance and at risk of diabetes and obesity.

We do not anticipate that participation will place patients at risk. As your patient is healthy we do not anticipate that there will be any abnormal findings, but we will of course inform you of anything untoward that is detected during these studies.

If you have any questions, or require further information, or if you think that your patient should not participate in this study, please do not hesitate to contact me.

Yours sincerely,

Dr. Yee Seun Cheah MA MSc MRCP(UK)
NIHR BRC Clinical Research Fellow and Specialist Registrar in Diabetes & Endocrinology

Diabetes Research Group
Division of Gene & Cell Based Therapy
King's College London School of Medicine
Room 3.35, Weston Education Centre
Cutcombe Road
London SE5 9RJ
Tel: 020 7848 5654
Email: yee.cheah@kcl.ac.uk

General Practitioner / Consultant

Date:

Dear Dr. _____

Re: ***Functional magnetic resonance imaging study of brain responses to food image viewing and food ingestion in insulin resistance (insulin resistant volunteers)***

I am writing to inform you that your patient, _____ has consented to take part in a research study looking at the brain's responses to nutrient ingestion in healthy volunteers with insulin resistance, at risk of developing diabetes and obesity, using functional magnetic resonance imaging (fMRI), led by Professor Stephanie Amiel at King's College London and King's College Hospital.

Your patient has attended a screening visit which has identified the presence of insulin resistance. He will undergo an oral glucose tolerance test to exclude the presence of diabetes. He will then attend the Institute of Psychiatry's Centre for Neuroimaging Sciences on 2 separate occasions, no less than 24 hours apart. On each visit, after an overnight fast, he/she will receive in random order either ice cream or water whilst undergoing fMRI brain scans. Blood will also be taken to allow us to measure both brain, hormonal and metabolic responses to food/water ingestion.

After these initial neuroimaging studies, he will receive Glucophage SR (metformin hydrochloride), at a maximum dose of 2g once daily over 3 months. Lifestyle advice in the form of exercise and diet will also be provided. After completing this treatment he will then undergo the same neuroimaging studies described above, to determine the effect of improving insulin resistance on these processes.

We do not anticipate that participation will place patients at risk. As your patient is healthy we do not anticipate that there will be any abnormal findings, but we will of course inform you of anything untoward that is detected during these studies.

If you have any questions, or require further information, or if you think that your patient should not participate in this study, please do not hesitate to contact me.

Yours sincerely,

Dr. Yee Seun Cheah MA MSc MRCP(UK)
NIHR BRC Clinical Research Fellow and Specialist Registrar in Diabetes & Endocrinology